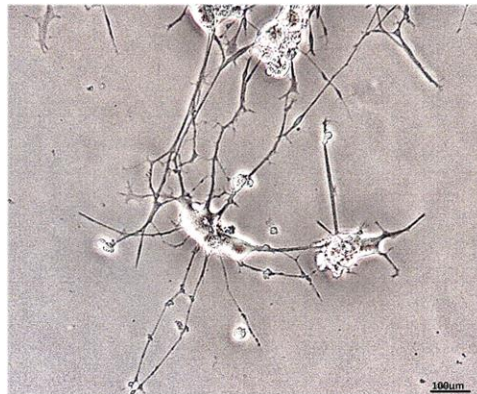




“The combined effects of plant polyphenols and fatty acids on protective cellular mechanisms associated with molecular perturbations of obesity and neurotoxicity”



Ellen Cassidy Joyce
(MSc, BSc Hons, PG cert)

A thesis submitted for the fulfilment of the degree of

Doctor of Philosophy in Biochemistry

2022

University of Worcester



Contents

Acknowledgements.....	5
List of Figures	6
List of Tables	10
Abbreviations.....	16
Abstract.....	24
Chapter 1 - Introduction	25
1.1 Major neurocognitive disorders (MND).....	25
1.2 MND - prevalence, incidence, cost, and trends	25
1.3 AD pathophysiology	28
1.4 Dementia and glucose transport	28
1.5 Obesity	29
1.6 Lipids	30
1.7 Fatty acids (FA).....	31
1.8 <i>De novo</i> fatty acid synthesis.....	34
1.9 Dietary Lipids.....	38
1.10 Triglycerides, diglycerides and monoglycerides	39
1.11 Cholesterol, cholesteryl esters and bile acids.....	41
1.12 Glycerophospholipids	44
1.13 Microbiome and fatty acid synthesis	47
1.14 Obesity and adipocyte function	48
1.15 Nuclear peroxisome proliferator-activated receptors (PPAR).....	54
1.16 Inflammation and fatty acids	59
1.17 Effect of western-style diet/high fat diet on intracellular signalling cascades	62
1.18 Polyphenols, obesity and inflammation	63
1.19 Aims and Objectives.....	74
Chapter 2 - Methods	76
2.1 Male Wistar rat animal study parameters	76
(a) Animal Care.....	76
(b) Phytotherapy treatment	76
2.2 Glassware	78
2.3 Lipid extraction	78
2.4 Solid phase extraction (SPE) for isolation of lipid classes by silica gel column chromatography	78
2.5 Acid-catalysed esterification of lipids to methyl esters (Methylation).....	79
2.6 Gas Chromatography – Flame Ionisation Detection (GC-FID)	81

2.6.1	Optimization of GC-FID	81
2.6.2	Final GC-FID method	85
2.7	Unsaturation Index (UI).....	89
2.8	Phospholipid analysis by HPLC.....	89
2.9	Cell culture	89
2.10	PC12 complete growth media.....	90
2.11	PC12 cell growth and subculturing	90
2.11.1	PC12 cells in suspension	90
2.11.2	Adherent PC12 cells	91
2.12	Cryopreservation of stocks	92
2.13	Coating of cell culture vessels.....	92
2.14	Preparation of collagen.....	92
2.15	Preparation of culture vessels	94
2.16	Differentiation.....	94
2.17	Differentiated PC12 experiments	94
2.18	GbE stocks	95
2.19	Fatty acid stocks.....	95
2.20	Cell imaging.....	95
2.21	MTT (3-[4,5-dimethylthiazol-2-yl]-2,5-diphenyltetrazolium bromide) cell viability assay ...	95
2.22	Annexin V/7-AAD cell viability/apoptosis assay.....	96
2.23	β -Tubulin III expression.....	97
2.24	Whole cell lysis.....	97
2.25	BCA (Bicinchoninic acid) protein concentration determination assay	98
2.26	Preparation of whole cell lysis for SDS-PAGE separation	98
2.27	SDS PAGE.....	99
2.28	Protein transfer to nitrocellulose.....	99
2.29	Western immunoblotting	99
Chapter 3 - Male Wistar rat study - Macronutrients and body metrics		101
3.1	Rat study macronutrient, food intake, efficiency, body metrics	101
3.2	Lipid profiles of NFD chow or HFD chow	103
3.3	Obesity induction period	105
3.4	GbE supplementation period	109
Chapter 4 – Liver		115
4.1	Introduction	115
4.2	Liver total fatty acids.....	118
4.3	Liver TAG	125

4.4	Liver CE.....	131
4.5	Liver MAG and DAG	137
4.6	Liver PPL.....	142
4.7	Discussion.....	148
4.8	Summary	152
Chapter 5 – Retroperitoneal (RET) and Mesenteric (MES) Adipose Tissue		153
5.1	Introduction	153
5.2	RET and MES total fatty acids	157
5.2.1	RET Total Fatty Acids – NFD vs HFD	157
5.2.2	MES total fatty acids – NFD vs HFD.....	158
5.2.3	RET - HFD GbE treatment.....	163
5.2.4	MES - HFD GbE treatment.....	163
5.3	RET and MES TAG.....	169
5.3.1	RET-TAG – NFD vs HFD	169
5.3.2	MES- TAG – NFD vs HFD	170
5.3.3	RET- TAG HFD GbE treatment	171
5.3.4	MES- TAG HFD GbE treatment.....	171
5.4	RET and MES CE	181
5.4.1	RET -CE– NFD vs HFD.....	181
5.4.2	MES-CE – NFD vs HFD	182
5.4.3	RET-CE HFD GbE treatment.....	185
5.4.4	MES-CE HFD GbE treatment	185
5.5	RET and MES MAG and DAG	195
5.5.1	RET- MAG + DAG - NFD Vs HFD	195
5.5.2	MES- MAG + DAG - NFD Vs HFD.....	196
5.5.3	RET-MAG + DAG- HFD GbE treatment	198
5.5.4	MES-MAG + DAG- HFD GbE treatment	199
5.6	RET and MES PPL.....	208
5.6.1	RES-PPL - NFD vs HFD.....	208
5.6.2	MES-PPL - NFD vs HFD.....	209
5.6.3	RET-PPL HFD GbE treatment	210
5.6.4	MES-PPL HFD GbE treatment.....	211
5.7	Discussion.....	221
5.8	Summary	237
Chapter 6 - Hippocampus and Hypothalamus		240
6.1	Introduction	240

6.2	Hypothalamus	245
6.3	Hippocampus	250
6.4	Discussion.....	255
6.5	Summary	265
Chapter 7 – PC12 rat pheochromocytoma cell neuronal model		266
7.1	Introduction	266
7.2	Growth curve	267
7.3	NGF neuronal differentiation.....	273
7.4	1% Horse Serum (HS) media differentiation.....	275
7.5	1% BSA media differentiation	279
7.6	Differentiation – β -Tubulin III	285
7.7	Neurofilament protein levels in NGF differentiation.....	287
7.8	Cell apoptosis in PC12 differentiation.....	289
7.9	<i>In vitro</i> model of oxidative stress injury in PC12 cells.....	293
7.10	GbE treatment in undifferentiated and differentiated PC12 cells	295
7.11	Cell viability of GbE treatments in oxidative stress induced neuronal injury	297
7.12	Cell viability of NFD, HFD and GbE treatments	299
7.13	Cell viability of NFD, HFD and GbE treatments in H ₂ O ₂ neuronal injury	303
7.14	NFD, HFD and GbE treatments and Akt activation	306
7.15	NFD, HFD and GbE treatments and Nrf2 protein expression	312
7.16	Effect of NFD, HFD and GbE treatment on neurofilament levels	316
7.17	The effect of PC12 differentiation on cellular total lipid profiles	319
7.18	The effect of NFD, HFD and GbE treatments on cellular total lipid profiles.....	323
7.19	Summary	327
Chapter 8 - Final conclusions		328
Publications and conferences		335
References		337
Appendix 1		436
Appendix 2		444
Appendix 3		454
Appendix 4		465
Appendix 5		477
Appendix 6		478

Acknowledgements

I would like to thank all the people who have helped and supported me along my PhD journey. Firstly, I want to sincerely thank my Director of Studies, Dr Allain Bueno for this fantastic opportunity and for all his help, guidance, and mentorship throughout the years. I have learned and gained so much from you. Thank you to the other members of my supervisory team Dr Steven Coles and Dr Amy Cherry for your additional pragmatic help and guidance in my research and for being an extra source of support along the way.

Thank you to Dr Monica Marques Telles, Dr Bruna Sousa Hirata, and Dr Valter Tadeu Boldarine from Universidade Federal de São Paulo (UNIFESP), Brazil, for the opportunity to be a part of a collaborative study and the additional help and support throughout this project.

Thank you to all the School of Science and the Environment staff and lab technicians that helped and supported me, particularly Dr Anne Sinnott, Noel Egginton, Mark Cook and Tracey Richards Pritchard. I would also like to thank the post-graduate students I have shared labs with, particularly Emma Wilde. Together, your day-to-day support and companionship really made a difference to me.

I would also like to thank you to the University of Worcester research school staff, in particular the SSE postgraduate co-ordinator Dr David Storey for all their support, guidance and on occasion just listening.

Last but by no means least, an immense thank you to my family (Andrée, Dermot, Eòin, Rory and Kristian) and my closest friends for their constant support and always championing my dreams. Without all of you, this would not have been possible.

Thank you very much / Go raibh míle maith agat.

List of Figures

Figure 1. Chemical structures of different lipid-based compounds	33
Figure 2. Illustration of transcriptional activation of <i>De novo</i> lipogenesis in adipocytes in response to high-sugar or high-fat diets	35
Figure 3. <i>De novo</i> Fatty Acid Synthesis from Acetyl CoA to Palmitic acid	35
Figure 4. <i>De novo</i> lipogenesis and fatty acid synthesis pathway for saturated (SFA) monounsaturated (MUFA) and n-6 and n-3 polyunsaturated (PUFA) fatty acids	37
Figure 5. The synthesis of diacylglycerols, triacylglycerols and the phospholipids phosphatidylcholine and phosphatidylethanolamine through common shared pathways	41
Figure 6. Lipid mediators enzymatically derived from n-6 and n-3 and polyunsaturated fatty acids (PUFAs) and their role in inflammation.	58
Figure 7. The chemical structures of polyphenols found in red wine (A-D) and Ginkgo biloba extract (GbE) (B-H)	65
Figure 8. Optimisation of FAME separation on gas chromatography flame ionisation detection	83
Figure 9. Food intake and energy intake in obesity induction	106
Figure 10. Food efficiency and energy efficiency	107
Figure 11. Body composition	108
Figure 12. Body weight and body weight gain after 14-day supplementation	111
Figure 13. Accumulated food intake, energy intake and food efficiency after 14-day supplementation	112
Figure 14. Mesenteric and retroperitoneal adipose tissue depot	155
Figure 15. Microphotograph of PC12 cells grown in suspension in RPMI complete media (15% serum) at low and high density	270
Figure 16. Microphotograph of PC12 cells grown as adherent cells on Type I collagen (10µg/cm ²) in RPMI complete media (15% serum)	271
Figure 17. Growth curve of PC12 cells grown in suspension and on type I collagen (10µg/cm ²) (adherent)	272
Figure 18. Formazan accumulation (dark colouration) in undifferentiated (round cells) and differentiated (cells with neurite outgrowth) PC12 cells following incubation with MTT	272

Figure 19. Viability (%) of PC12 cells after six days incubation with 1% horse serum (1% HS) media	276
Figure 20. Microphotographs of PC12 cell differentiation with RPMI media supplemented with 1% horse serum (1% HS) and nerve growth factor (NGF) for 144 hours	277
Figure 21. Microphotographs of PC12 cells treated with 50 and 100µg/ml GbE in 1% horse serum (HS) media for 144 hours	278
Figure 22. Viability (%) of PC12 cells after six days incubation with 1% bovine serum albumin (1% BSA) media	281
Figure 23. Microphotographs of PC12 cell differentiation with RPMI media supplemented with 1% bovine serum albumin (1% BSA) and nerve growth factor (NGF) for 7 days	282
Figure 24. Microphotographs of PC12 cells treated with 50 and 100µg/ml GbE in 1% BSA media for 144 hours	283
Figure 25. Microphotographs of replated differentiated PC12 cells	284
Figure 26. Effect of NGF treatment on Tubulin- β3 levels in PC12 cells	286
Figure 27. Detection of Neurofilament-L and Neurofilament-M by western blot analysis in undifferentiated (RPMI) PC12 cells and 7-Day NGF-differentiated (NGF) PC12 cells	288
Figure 28. Annexin-V/7-AAD FACS analysis of PC12 cell differentiation	292
Figure 29. Cell viability of PC12 cells incubated with H ₂ O ₂ (0-400 µM)	294
Figure 30. Cell viability of PC12 cells incubated with Ginkgo biloba (GbE) (12.5-400 µg/ml)	296
Figure 31. GbE attenuated the decrease in cell viability induced by H ₂ O ₂ in PC12 cells	298
Figure 32. Annexin-V/7-AAD FACS analysis of PC12 cells	302
Figure 33. Annexin-V/7-AAD FACS analysis of PC12 cells treated with 400µM H ₂ O ₂ for 24 hours	305
Figure 34. Effect of NGF treatment on expression of phosphorylated-Akt (Ser473) and Akt-Total in PC12 cells	309
Figure 35. Effect of normal fat diet (NFD) fatty acid supplementation and standardised Ginkgo biloba (GbE) treatment on expression of phosphorylated-Akt (Ser473) and Akt-Total	310
Figure 36. Effect of high fat diet (HFD) fatty acid supplementation and standardised Ginkgo biloba (GbE) treatment on expression of phosphorylated-Akt (Ser473) and Akt-Total	311
Figure 37. Effect of normal fat diet (NFD) fatty acid supplementation and standardised Ginkgo biloba (GbE) treatment on expression of NF-E2-related factor 2 (Nrf2)	314

Figure 38. Effect of high fat diet (HFD) fatty acid supplementation and standardised Ginkgo biloba (GbE) treatment on expression of NF-E2-related factor 2 (Nrf2)	315
Figure 39. Effect of normal fat diet (NFD) fatty acid supplementation and standardised Ginkgo biloba (GbE) treatment on expression of neurofilament-L (NF-L) and neurofilament-M (NF-M)	317
Figure 40. Effect of high fat diet (HFD) fatty acid supplementation and standardised Ginkgo biloba (GbE) treatment on expression of neurofilament-L (NF-L) and neurofilament-M (NF-M)	318
Figure 41. Summary of changes in liver, retroperitoneal and mesenteric tissue following 8 weeks of a HFD compared to a NFD	332
Figure 42. Summary of changes in liver, retroperitoneal and mesenteric tissue in rats fed a HFD and treated with Saline (S), pair-feeding (PF) and Ginkgo biloba (GbE) for 14 days	333
Figure 43. Summary of changes in hippocampus, hypothalamus and PC12 cells. Changes following 8 weeks of a HFD were compared to NFD	334
Figure 44. Comparison of differences in area%, area and height from minor changes in peak Integration of the same sample	443
Figure 45. Silica-based solid phase extraction of triglycerides (5mg) using varying solutions, expressed in area (μ V)	446
Figure 46. Silica-based solid phase extraction of Cholesteryl Stearate (5mg) using varying solutions, expressed in area (μ V)	447
Figure 47. Silica-based solid phase extraction of monoglycerides (1mg) using varying solutions, expressed in area (μ V)	447
Figure 48. Silica-based solid phase extraction of Heptadecanoic acid (5mg) using varying solutions, expressed in area (μ V)	449
Figure 49. Silica-based solid phase extraction of Erucic acid (5mg) using varying solutions, expressed in area (μ V)	449
Figure 50. Silica-based solid phase extraction of Phosphatidylethanolamine (100ug) using varying solutions, expressed in area (μ V)	450
Figure 51. Silica-based solid phase extraction of Phosphatidylserine (100ug) using varying solutions, expressed in area (μ V)	450
Figure 52. Silica-based solid phase extraction of Phosphatidylcholine (100ug) using varying solutions, expressed in area (μ V)	451
Figure 53. Silica-based solid phase extraction of Phosphatidylinositol (100ug) using varying solutions, expressed in area (μ V)	451
Figure 54. Silica-based solid phase extraction of Sphingomyelin (100ug) using varying solutions, expressed in area (μ V)	452

Figure 55. HILIC liquid chromatography separation of commercially available phospholipids and Folch-extracted egg yolk phospholipids using acetonitrile: ammonium format (90:10v/v) at a flow rate of 0.05ml/min	471
Figure 56. HILIC liquid chromatography separation of commercially available phospholipids and Folch-extracted egg yolk phospholipids using acetonitrile: ammonium format (90:10v/v) at a flow rate of 0.1ml/min	472
Figure 57. HILIC liquid chromatography separation of commercially available phospholipids and Folch-extracted egg yolk phospholipids using acetonitrile: ammonium format (90:10v/v) at a flow rate of 0.1ml/min	473
Figure 58. Sample percentage (%) of phospholipids classes separated in Folch-extracted egg yolk lipids by HILIC Liquid chromatography	474
Figure 59. Separation of phospholipid molecular species by C18 liquid chromatography using acetonitrile: ammonium format (90:10v/v) at a flow rate of 0.3ml/min	475
Figure 60. Separation of phospholipid molecular species by C18 liquid chromatography using acetonitrile: ammonium format (90:10v/v) under different flow rates of 0.2, 0.3 and 0.4ml/min	476
Figure 61. Viability (%) of PC12 cells after six days incubation with 1% horse serum (1% HS) media	480
Figure 62. Microphotographs of PC12 cell differentiation with RPMI media supplemented with 0.5% horse serum (0.5% HS) and nerve growth factor (NGF) for 7 days	481
Figure 63. Viability (%) of PC12 cells after six days incubation with 0.1% horse serum (0.1% HS) media	483
Figure 64. Microphotographs of PC12 cell differentiation with RPMI media supplemented with 0.1% horse serum (0.1% HS) and nerve growth factor (NGF) for 7 days	484

List of Tables

Table 1. The melting points of fatty acids and their corresponding methyl esters	31
Table 2. Preparation of solutions for the separation of solid phase separation of lipid classes	80
Table 3. Optimisation of Gas Chromatography – Flame Ionisation Detection (GC-FID)	82
Table 4. Final optimized FAME method for the Shimadzu GC-2010 plus	84
Table 5. No.1 Fatty acids standard mix (F.A.M.E. Mix, C4-C24) (Sigma-Aldrich (Merck KGaA, Darmstadt, Germany) used for the detection of fatty acid methyl esters by Gas Chromatography - Flame Ionisation Detection (GC-FID)	86
Table 6. Fatty acids standard mixes (PUFA No.3; Linolenic Acid Methyl Ester Isomer mix; Linoleic Acid Methyl Ester Isomer Mix; F.A.M.E. Mix, C20:1-C20:5 Unsaturates) used for the detection of fatty acid methyl esters by Gas Chromatography - Flame Ionisation Detection (GC-FID)	87
Table 7. Individual Fatty acids standard used for the detection of fatty acid methyl esters by Gas Chromatography - Flame Ionisation Detection (GC-FID)	88
Table 8. Summary of cell culture subculture guidelines for ATCC PC-12 cells (ATCC® CRL-1721™)	93
Table 9. Fatty acid percentage profiles of normal fat diet (NFD) and HFD (HFD) rat chow	104
Table 10. Liver total lipid fatty acid methyl esters (FAME) for normal fat diet (NFD) and high fat diet (HFD-S)	121
Table 11. Liver total lipid fatty acid methyl esters (FAME) ratios between normal fat diet (NFD) and high fat diet (HFD-S)	122
Table 12. Total Liver extract fatty acid methyl esters (FAME) for high fat diet groups; High fat diet with-saline (HFD-S), High fat diet -pair-fed (HFD-PF) and High fat diet- Ginkgo biloba (HFD-GbE)	123
Table 13. Total liver fatty acid methyl esters (FAME) ratios for high fat diet groups; High fat diet with-saline (HFD-S), High fat diet -pair-fed (HFD-PF) and High fat diet- Ginkgo biloba (HFD-GbE)	124
Table 14. Liver triglyceride fatty acid methyl esters (FAME) for normal fat diet (NFD) and high fat diet (HFD-S)	127
Table 15 Liver triglyceride fatty acid methyl esters (FAME) ratios between normal fat diet (NFD) and high fat diet (HFD-S)	128
Table 16. Liver triglyceride (TAG) fatty acid methyl esters (FAME) for high fat diet groups; High fat diet with-saline (HFD-S), High fat diet -pair-fed (HFD-PF) and High fat diet- Ginkgo biloba (HFD-GbE)	129
Table 17. Liver triglyceride (TAG) fatty acid methyl esters (FAME) ratios for high fat diet groups; High fat diet with-saline (HFD-S), High fat diet -pair-fed (HFD-PF) and High fat diet- Ginkgo biloba (HFD-GbE)	130

Table 18. Liver cholesteryl ester fatty acid methyl esters (FAME) for normal fat diet (NFD) and high fat diet (HFD-S)	133
Table 19 Liver cholesteryl ester fatty acid methyl esters (FAME) ratios between normal fat diet (NFD) and high fat diet (HFD-S)	134
Table 20. Liver cholesteryl ester (CE) fatty acid methyl esters (FAME) for high fat diet groups; High fat diet with-saline (HFD-S), High fat diet -pair-fed (HFD-PF) and High fat diet- Ginkgo biloba (HFD-GbE)	135
Table 21. Liver cholesteryl esters (CE) fatty acid methyl esters (FAME) ratios for high fat diet groups; High fat diet with-saline (HFD-S), High fat diet -pair-fed (HFD-PF) and High fat diet- Ginkgo biloba (HFD-GbE)	136
Table 22. Liver monoglyceride and diglyceride fatty acid methyl esters (FAME) for normal fat diet (NFD) and high fat diet (HFD-S)	138
Table 23 Liver monoglyceride and diglyceride fatty acid methyl esters (FAME) ratios between normal fat diet (NFD) and high fat diet (HFD-S)	139
Table 24. Liver monoglycerides and diglycerides (MAG+DAG) fatty acid methyl esters (FAME) for high fat diet groups; High fat diet with-saline (HFD-S), High fat diet -pair-fed (HFD-PF) and High fat diet- Ginkgo biloba (HFD-GbE)	140
Table 25. Liver monoglyceride and diglycerides (MAG+DAG) fatty acid methyl esters (FAME) ratios for high fat diet groups; High fat diet with-saline (HFD-S), High fat diet -pair-fed (HFD-PF) and High fat diet- Ginkgo biloba (HFD-GbE)	141
Table 26. Liver phospholipid fatty acid methyl esters (FAME) for normal fat diet (NFD) and high fat diet (HFD-S)	144
Table 27 Liver phospholipid fatty acid methyl esters (FAME) ratios between normal fat diet (NFD) and high fat diet (HFD-S)	145
Table 28. Liver phospholipid fatty acid methyl esters (FAME) for high fat diet groups; High fat diet with-saline (HFD-S), High fat diet -pair-fed (HFD-PF) and High fat diet- Ginkgo biloba (HFD-GbE)	146
Table 29. Liver phospholipid (PPL) fatty acid methyl esters (FAME) ratios for high fat diet groups; High fat diet with-saline (HFD-S), High fat diet -pair-fed (HFD-PF) and High fat diet- Ginkgo biloba (HFD-GbE)	147
Table 30. Retroperitoneal total lipid fatty acid methyl esters (FAME) for normal fat diet (NFD) and high fat diet (HFD-S)	159
Table 31 Retroperitoneal total lipid fatty acid methyl esters (FAME) ratios between normal fat diet (NFD) and high fat diet (HFD-S)	160
Table 32. Mesenteric total lipid fatty acid methyl esters (FAME) for normal fat diet (NFD) and high fat diet (HFD-S)	161
Table 33. Mesenteric total lipid fatty acid methyl esters (FAME) ratios between normal fat diet (NFD) and high fat diet (HFD-S)	162

Table 34. Retroperitoneal total lipid fatty acid methyl esters (FAME) for high fat diet groups; High fat diet with-saline (HFD-S), High fat diet -pair-fed (HFD-PF) and High fat diet- Ginkgo biloba (HFD-GbE)	165
Table 35. Retroperitoneal total lipid fatty acid methyl esters (FAME) ratios between high fat diet groups; High fat diet with saline (HFD-S), High fat diet pair-fed (HFD-PF) and High fat diet- Ginkgo biloba (HFD-GbE)	166
Table 36. Mesenteric total lipid fatty acid methyl esters (FAME) for high fat diet groups; High fat diet with-saline (HFD-S), High fat diet -pair-fed (HFD-PF) and High fat diet- Ginkgo biloba (HFD-GbE)	167
Table 37. Mesenteric total lipid fatty acid methyl esters (FAME) ratios between high fat diet groups; High fat diet with saline (HFD-S), High fat diet pair-fed (HFD-PF) and High fat diet- Ginkgo biloba (HFD-GbE)	168
Table 38. Retroperitoneal Triglyceride fatty acid methyl esters (FAME) for normal fat diet (NFD) and high fat diet (HFD-S)	173
Table 39. Retroperitoneal Triglyceride fatty acid methyl esters (FAME) ratios for normal fat diet (NFD) and high fat diet (HFD-S)	174
Table 40. Mesentery triglyceride fatty acid methyl esters (FAME) for normal fat diet (NFD) and high fat diet (HFD-S)	175
Table 41. Mesenteric triglyceride fatty acid methyl esters (FAME) ratios for normal fat diet (NFD) and high fat diet (HFD-S)	176
Table 42. Retroperitoneal Triglyceride fatty acid methyl esters (FAME) for high fat diet groups; High fat diet with-saline (HFD-S), High fat diet -pair-fed (HFD-PF) and High fat diet- Ginkgo biloba (HFD-GbE)	177
Table 43. Retroperitoneal Triglyceride fatty acid methyl esters (FAME) ratios for high fat diet groups; High fat diet with-saline (HFD-S), High fat diet -pair-fed (HFD-PF) and High fat diet- Ginkgo biloba (HFD-GbE)	178
Table 44. Mesenteric triglyceride fatty acid methyl esters (FAME) for normal fat diet (NFD) and high fat diet (HFD-S)	179
Table 45. Mesenteric triglyceride fatty acid methyl esters (FAME) ratios for normal fat diet (NFD) and high fat diet (HFD-S)	180
Table 46. Retroperitoneal Cholesteryl ester total lipid fatty acid methyl esters (FAME) for normal fat diet (NFD) and high fat diet (HFD-S)	187
Table 47. Retroperitoneal Cholesteryl ester fatty acid methyl esters (FAME) ratios for normal fat diet (NFD) and high fat diet (HFD-S)	188
Table 48. Mesenteric cholesteryl ester total lipid fatty acid methyl esters (FAME) for normal fat diet (NFD) and high fat diet (HFD-S)	189
Table 49. Mesenteric Cholesteryl ester fatty acid methyl esters (FAME) ratios for normal fat diet (NFD) and high fat diet (HFD-S)	190

Table 50. Retroperitoneal Cholesteryl ester fatty acid methyl esters (FAME) for high fat diet groups; High fat diet with-saline (HFD-S), High fat diet -pair-fed (HFD-PF) and High fat diet- Ginkgo biloba (HFD-GbE)	191
Table 51. Retroperitoneal Cholesteryl ester fatty acid methyl esters (FAME) ratios for high fat diet groups; High fat diet with-saline (HFD-S), High fat diet -pair-fed (HFD-PF) and High fat diet- Ginkgo biloba (HFD-GbE)	192
Table 52. Mesenteric cholesteryl ester fatty acid methyl esters (FAME) for high fat diet groups; High fat diet with-saline (HFD-S), High fat diet -pair-fed (HFD-PF) and High fat diet- Ginkgo biloba (HFD-GbE)	193
Table 53. Mesenteric cholesteryl esters (CE) fatty acid methyl esters (FAME) ratios for high fat diet groups; High fat diet with-saline (HFD-S), High fat diet -pair-fed (HFD-PF) and High fat diet- Ginkgo biloba (HFD-GbE)	194
Table 54. Retroperitoneal monoglyceride and diglyceride fatty acid methyl esters (FAME) for normal fat diet (NFD) and high fat diet (HFD-S)	200
Table 55. Retroperitoneal monoglyceride and diglyceride fatty acid methyl esters (FAME) ratios for normal fat diet (NFD) and high fat diet (HFD-S)	201
Table 56. Mesenteric monoglycerides and diglycerides fatty acid methyl esters (FAME) for normal fat diet (NFD) and high fat diet (HFD-S)	202
Table 57. Mesenteric monoglyceride and diglycerides (MAG+DAG) fatty acid methyl esters (FAME) ratios for normal fat diet (NFD) and high fat diet (HFD-S)	203
Table 58. Retroperitoneal monoglyceride and diglyceride fatty acid methyl esters (FAME) for high fat diet groups; High fat diet with-saline (HFD-S), High fat diet -pair-fed (HFD-PF) and High fat diet- Ginkgo biloba (HFD-GbE)	204
Table 59. Retroperitoneal monoglyceride and diglyceride fatty acid methyl esters (FAME) ratios for high fat diet groups; High fat diet with-saline (HFD-S), High fat diet -pair-fed (HFD-PF) and High fat diet- Ginkgo biloba (HFD-GbE)	205
Table 60. Mesenteric monoglycerides and diglycerides fatty acid methyl esters (FAME) for high fat diet groups; High fat diet with-saline (HFD-S), High fat diet -pair-fed (HFD-PF) and High fat diet- Ginkgo biloba (HFD-GbE)	206
Table 61. Mesenteric monoglyceride and diglycerides (MAG+DAG) fatty acid methyl esters (FAME) ratios for high fat diet groups; High fat diet with-saline (HFD-S), High fat diet -pair-fed (HFD-PF) and High fat diet- Ginkgo biloba (HFD-GbE)	207
Table 62. Retroperitoneal phospholipid fatty acid methyl esters (FAME) for normal fat diet (NFD) and high fat diet (HFD-S)	213
Table 63. Retroperitoneal phospholipid fatty acid methyl esters (FAME) ratios for high fat diet groups; High fat diet with-saline (HFD-S), High fat diet -pair-fed (HFD-PF) and High fat diet- Ginkgo biloba (HFD-GbE)	214
Table 64. Mesenteric phospholipid fatty acid methyl esters (FAME) for normal fat diet (NFD) and high fat diet (HFD-S)	215

Table 65. Mesenteric Phospholipids (PPL) fatty acid methyl esters (FAME) ratios for high fat diet groups; High fat diet with-saline (HFD-S), High fat diet -pair-fed (HFD-PF) and High fat diet- Ginkgo biloba (HFD-GbE)	216
Table 66. Retroperitoneal phospholipid fatty acid methyl esters (FAME) for high fat diet groups; High fat diet with-saline (HFD-S), High fat diet -pair-fed (HFD-PF) and High fat diet- Ginkgo biloba (HFD-GbE)	217
Table 67. Retroperitoneal phospholipid fatty acid methyl esters (FAME) ratios for high fat diet groups; High fat diet with-saline (HFD-S), High fat diet -pair-fed (HFD-PF) and High fat diet- Ginkgo biloba (HFD-GbE)	218
Table 68. Mesenteric phospholipid fatty acid methyl esters (FAME) for high fat diet groups; High fat diet with-saline (HFD-S), High fat diet -pair-fed (HFD-PF) and High fat diet- Ginkgo biloba (HFD-GbE)	219
Table 69. Mesenteric phospholipids (PPL) fatty acid methyl esters (FAME) ratios for high fat diet groups; High fat diet with-saline (HFD-S), High fat diet -pair-fed (HFD-PF) and High fat diet- Ginkgo biloba (HFD-GbE)	220
Table 70. Summary of retroperitoneal and mesenteric fatty acid profiles comparing the effects of a normal fat diet (NFD) and high fat diet (HFD) in total lipid sample, Triglycerides (TAG), Cholesteryl esters (CE), monoglycerides and diglycerides (MAG+DAG) and phospholipids (PPL)	238
Table 71. Summary of retroperitoneal and mesenteric fatty acid profiles comparing the effects of a high fat diet (HFD) and treatment with saline (HFD-S), pairfed (PF) and Ginkgo biloba (HFD-GbE) in total lipid sample, triglycerides (TAG), Cholesteryl esters (CE), monoglycerides and diglycerides (MAG+DAG) and phospholipids (PPL)	239
Table 72. Hypothalamus total fatty acid methyl esters (FAME) for normal fat diet (NFD) and high fat diet (HFD-S)	246
Table 73. Hypothalamus total fatty acid methyl esters (FAME) ratios for normal fat diet (NFD) and high fat diet (HFD-S)	247
Table 74. Hypothalamus total fatty acid methyl esters (FAME) for high fat diet groups; High fat diet with-saline (HFD-S), High fat diet -pair-fed (HFD-PF) and High fat diet- Ginkgo biloba (HFD-GbE)	248
Table 75. Hypothalamus total fatty acid methyl esters (FAME) ratios for high fat diet groups; High fat diet with-saline (HFD-S), High fat diet -pair-fed (HFD-PF) and High fat diet- Ginkgo biloba (HFD-GbE)	249
Table 76. Hippocampus total fatty acid methyl esters (FAME) for normal fat diet (NFD) and high fat diet (HFD-S)	251
Table 77. Hippocampus total fatty acid methyl esters (FAME) ratios for normal fat diet (NFD) and high fat diet (HFD-S)	252
Table 78. Hippocampus total fatty acid methyl esters (FAME) for high fat diet groups; High fat diet with-saline (HFD-S), High fat diet -pair-fed (HFD-PF) and High fat diet- Ginkgo biloba (HFD-GbE)	253

Table 79. Hippocampus total fatty acid methyl esters (FAME) ratios for high fat diet groups; High fat diet with-saline (HFD-S), High fat diet -pair-fed (HFD-PF) and High fat diet- Ginkgo biloba (HFD-GbE)	254
Table 80. PC12 fatty acid methyl esters (FAME) for RPMI complete media, 1% BSA media and 1%BSA media supplemented with nerve growth factor (NGF)	321
Table 81. PC12 fatty acid methyl ester (FAME) ratios for RPMI complete media, 1% BSA media and 1%BSA media supplemented with nerve growth factor (NGF)	322
Table 82. Fatty acid methyl esters of PC12 cells treated with a either NFD or HFD fatty acids, GbE (50µg/ml or 100µg/ml) or a combination of NFD, HFD and GbE	325
Table 83. Fatty acid methyl ester ratios of PC12 cells treated with a either NFD or HFD fatty acids, GbE (50µg/ml or 100µg/ml) or a combination of NFD, HFD and GbE	326
Table 84. Comparison of total solution volumes for method 1 or method 2 used for fatty acid (FA) extraction optimization	438
Table 85. Fatty acid (FA) composition of animal-based products, tissues, and cells	439
Table 86. Comparison Fatty acid (FA) composition of plant based culinary oils following two varying fatty acid extraction methods	440
Table 87. Comparison of fatty acid extraction methods on animal-based tissue fatty acid (FA) composition	441
Table 88. Lipid standards utilised for testing selective elution of lipid classes by solid phase	445
Table 89. Mobile phases and flow rates assessed for HILIC and C18 columns used for the separation of phospholipids by liquid chromatography	466
Table 90. Mass spectrometry acquisition conditions for the identification of phospholipid molecular species separated on a C18 column	467
Table 91. Flow rates and retention times of commercially available standards using HILIC liquid chromatography (Acetonitrile: ammonium formate (90:10v/v) separation of phospholipids	470
Table 92. Macronutrients, caloric value, and lipid profiles of normal fat diet (NFD) and high-fat diet (HFD) diet chow fed to male Wistar Rats	477

Abbreviations

11 β -HSD1	11-Beta-Hydroxysteroid-Dehydrogenase Type 1
24S-OH	24-Hydroxycholesterol
27-OH	27-Hydroxycholesterol
2-AG	2-Arachidonoylglycerol
3-KT	3-ketoacyl-CoA Thiolase
7-AAD	7-Amino-Actinomycin
α -MSH	Alpha-Melanocyte-Stimulating Hormone
AA	Arachidonic Acid
Abcd	Atp-Binding Cassette Sub-Family D Transporters
ACC	Acetyl CoA Carboxylase
ACAD	Acyl-CoA Dehydrogenase
ACAT2	Acyl-Coenzyme A: Cholesterol Acyltransferase 2
Acly	ATP-Citrate Lyase
ACN	Acetonitrile
ACOX1	Acyl-CoA Oxidase 1
ACSVL	Very Long-Chain Acyl-CoA Synthetases
AD	Alzheimer's Disease
AdA	Adrenic Acid
ADIPOR	Adiponectin Receptor
AEA	Anandamide
AGEs	Advanced Glycation End Products
AGPAT	E Acylglycerol-3-Phosphate Acyltransferases (AGPAT)
AgRP	Agouti-Related Protein
Akt	Protein Kinase B (PKB)
ALA	Alpha-Linoleic Acid
AmFm	Ammonium Formate
AMP	Adenosine Monophosphate
AMPK	AMP-Activated Protein Kinase
ADNIMERGE	Alzheimer's Disease Neuroimaging Initiative S
AP-1	Activator Protein 1
AP-2	Activator Protein 2
APA	American Psychiatric Association
apo B-100	Lipoprotein Apolipoprotein B-100
APPL1	Adaptor Protein
ARC	Arcuate Nucleus
ARE	Antioxidant Response Element
ASBP	Apical Sodium-Dependent Bile transporter
AST	Aspartate Aminotransferase
ATGL	Adipose Triglyceride Lipase
A β	Amyloid Beta
BA	Bile Acids
BBB	Blood Brain Barrier
Bcl-2	B-Cell Lymphoma 2
BDNF	Brain-Derived Neurotrophic Factor

BHT	Butylated Hydroxytoluene
BMI	Body Mass Index
BRP	Brain Reserve Potential
BSA	Bovine Serum Albumin
C/EBP α	CCAAT-Enhancer-Binding Protein Alpha
C:M	Chloroform: Methanol
C10:0	Capric acid / Hexanoic acid
C11:0	Undecylic acid / Undecanoic acid
C12:0	Lauric acid / Dodecanoic acid
C13:0	Tridecylic acid / Tridecanoic acid
C14:0	Myristic acid / Tetradecanoic acid
C14:1n7	Myristoleic acid / (9Z)-tetradecenoic acid
C15:0	Pentadecylic acid / Pentadecanoic acid
C15:1	(10Z)-Pentadecenoic Acid
C16:0	Palmitic acid / Hexadecanoic acid
C16:1n7	Palmitoleic acid / (9Z)-hexadecenoic acid
C17:0	Margaric acid / Heptadecanoic acid
C18	C18 Reversed Phase HPLC Column
C18:0	Stearic acid / Octadecanoic acid
C18:1n9	Oleic acid / (9Z)-octadecenoic acid
C18:1n9 <i>trans</i>	<i>trans</i> Oleic acid
C18:2n6	Linoleic acid / (9Z,12Z)-Octadecadienoic acid
C18:2n6 <i>trans</i>	<i>trans</i> Linoleic acid
C18:3n3	α -Linolenic acid / (9Z,12Z,15Z)-Octadecatrienoic acid
C18:3n6	γ -Linolenic acid / (6Z,9Z,12Z)-Octadecatrienoic acid
C18:4n-3	Stearidonic Acid / (6Z,9Z,12Z,15Z)-Octadecatetraenoic acid
C20:0	Arachidic acid / Eicosanoic acid
C20:1n9	Cetoleic acid / (11Z)-Eicosenoic acid
C20:2n6	(11Z,14Z)-Eicosadienoic Acid
C20:3n3	(11Z,14Z,17Z)-Eicosatrienoic Acid
C20:3n6	Dihomo-gamma-linolenic acid / (8Z,11Z,14Z)-Eicosatrienoic Acid
C20:4n6	Arachidonic acid / (5Z,8Z,11Z,14Z)-Eicosatetraenoic acid
C20:5n3	(5Z,8Z,11Z,14Z,17Z)-Eicosapentaenoic Acid
C21:0	Heneicosylic acid / Heneicosanoic acid
C22:0	Behenic acid / Docosanoic acid
C22:1n9	Erucic Acid / (13Z)-Docosenoic acid
C22:2n6	(13Z,16Z)-Docosadienoic Acid
C22:5n-3	(4Z,7Z,10Z,13Z,16Z)-Docosapentaenoic Acid
C22:6n3	(4Z,7Z,10Z,13Z,16Z,19Z)-Docosahexaenoic Acid
C23:0	Tricosylic acid / Tricosanoic acid
C24:0	Lignoceric acid / Tetracosanoic acid
C24:1n9	(15Z)-Tetracosenoic acid
C4:0	Butyric acid / Butanoic acid
C6:0	Caproic acid / Hexanoic acid
C8:0	Caprylic acid / Octanoic acid

cAMP	Cyclic AMP
CAV	Caveolin
CB1	Cannabinoid Receptor 1
CB2	Cannabinoid Receptor 2
CCK	Cholecystokinin
CDR	Clinical Dementia Rating
CE	Cholesteryl Ester
CERP	Cholesterol Efflux Regulatory Protein (ABCA1)
CFS	Cerebrospinal Fluid
CGI-58	Comparative Gene Identification-58
CHCl3	Chloroform
CHO	Chinese Hamster Ovary
ChREBP	Carbohydrate Response Element Binding Protein
CIC	Mitochondrial Citrate-Carrier
CNS	Central Nervous System
COX	Cyclooxygenases
cPLA2	Cytosolic Phospholipase A2
CPS	Cognitive Performance Scale
CPT-1	Carnitine Palmitoyltransferase-1
CR	Cognitive Reserve
CREB	Camp Responsive Element Binding Protein
CRP	C-Reactive Protein
CSF	Cerebral Spinal Fluid
CTRL	Control
CYP	Cytochrome P450 Enzyme
Cyt C	Cytochrome C
D9D	Fatty Acyl-CoA Delta-9 Desaturase / Stearoyl-CoA Desaturase 1 (SCD1)
DAG	Diacylglycerol / Diglycerides
DGAT	Diglyceride Acyl transferase
DGLA	Dihomo- γ -Linolenic Acid
DHA	Docosahexaenoic Acid
DHEA	Docosahexanoyl Ethanolamide
Diff	Differentiated
Dihomo-IsoPs	Dihomoisoprostanes
DiHOME	dihydroxyoctadecenoic acid
DMA 16:0	16:0 Dimethylacetal
DMA 18:0	18:0 Dimethylacetal
DMH	Dorsomedial Hypothalamic Nucleus
DMSO	Dimethyl Sulfoxide
DNA	Deoxyribonucleic Acid
DNL	<i>De novo</i> Lipogenesis
DSM-5	Statistical Manual of Mental Disorders
ECACC	European Collection of Authenticated Cell Cultures
ECM	Extracellular Matrix (ECM)
ECM	Extracellular Matrix
EDTA	Ethylenediamine Tetraacetic Acid

EET	Epoxyeicosatrienoic Acids
EFA	Essential Fatty Acids
E-FABP	Epidermal Fatty Acid-Binding Protein
Egb 761	Standardized Extract of <i>Ginkgo biloba</i>
ELOVL5	Elongase of Very Long Fatty Acid 5
ENIGMA	Elderly Nutritional Indicators For Geriatric Malnutrition Assessment
eNOS	Endothelial Nitric Oxide Synthase
EPA	Eicosapentaenoic Acid
EpDPAs	Epoxydocosapentaenoic Acid
EPEA	Eicosapentaenoyl Ethanolamide
EpETEs	Epoxyeicosatetraenoic Acids
EPI	Epididymal
EpOME	Epoxyoctadecamonoenoic acid
ER	Endoplasmic Reticulum
ERK	Extracellular Signal-Regulated Kinase
FA	Fatty Acid
FABP	Fatty Acid-Binding Proteins
FADS	Fatty Acid Desaturases
FAME	Fatty Acid Methyl Esters
FASN	Fatty Acid Synthase
FAT	FA Translocase
FATPs	FA Transport Proteins
FOXO1	Forkhead Box O1
FXR	Farnesoid X Receptor
G3P	Glycerophosphate
GAP-43	Growth-Associated Protein 43
GbE	Standardized Extract of <i>Ginkgo biloba</i>
GbE50	<i>Ginkgo biloba</i> extract 50µg
GbE100	<i>Ginkgo biloba</i> extract 100µg
GC-FID	Gas Chromatography – Flame Ionisation Detection
Gcg	Glucagon
GDP	Gross Domestic Product
GDS	Global Deterioration Scale
GI	Gastrointestinal
GLP-1	Glucagon-Like Peptide 1
GLUT	Sodium Independent Glucose transporter
GPAT	G3P acyltransferase
GPBAR1	G Protein-Coupled Bile Acid Receptor 1
GPCR	G Protein-Coupled Receptors
GSH	Glutathione
GSK3β	Glycogen Synthase Kinase 3 Beta
GU	Glucose Uptake
H ₂ O	Water
H ₂ O ₂	Hydrogen Peroxide
HbA1c	Glycated Haemoglobin
HDL	High Density Lipoprotein

HFCR	High Fat Caloric Restriction
HFD	High-Fat Lard-Enriched Diet
HFD100	High-Fat-Diet Fatty Acid Mix 100 μ M
HILIC	Hydrophilic Interaction Liquid Chromatography
HMG-CoA	3-Hydroxy-3-Methylglutaryl-CoA
HNF-4 α	Hepatocyte Nuclear Factor 4 α
HODE	Hydroxyoctadecadienoic Acid
HPLC-MS	High Performance Liquid Chromatography Mass Spectrometry
Hs-CRP	High-sensitivity C-Reactive Protein
HS	Horse Serum
HSL	Hormone-Sensitive Lipase
IBABP	Ileal Bile Acid Binding Protein
IDL	Intermediate-Density Lipoproteins
IGF-1	Insulin-Like Growth Factor 1
IGF-1R	Insulin-Like Growth Factor 1 Receptor
IKK β	I κ B kinase
IL	Interleukin
IMM	Inner Mitochondrial Membrane
Insig-2	Insulin Induced Gene 2
iNOS	Inducible Nitric Oxide Synthase
IPA	Isopropanol
IR	Insulin Resistance
IRS	Insulin Receptor Substrate
IsoPs	Isoprostanes
JAK	Janus Kinase
JNK	C-Jun N-Terminal Kinase
Keap1	Kelch-Like ECH-Associated Protein 1
KODE	Keto-Octadecadienoic Acid
LCAT	Lecithin-Cholesterol Acyltransferase
LCFA	Long Chain Fatty Acid
LD	Lipid Droplets
LDL	Low-Density Lipoproteins
LDLR	Low-Density Lipoprotein receptor
LEP-R	Leptin Receptor
LEP-Rb	Leptin Receptor Long Isoform
LD	Lipid droplet
LOX	Lipoxygenases
LOX-1	Reduced Lectin-Like Oxidized-Low Density Lipoprotein Receptor 1
LPA	Lysophosphatidic Acid (LPA)
LPC	Lysophosphatidylcholine
LPL	Lipoprotein Lipase
LPS	Lipopolysaccharide
LTS	Leukotrienes
LXR	Liver X Receptor
MAG	Monoacylglycerol / Monoglycerides

MAPK	Mitogen-Activated Protein Kinase
MCI	Mild Cognitive Impairment
MCR	Melanocortin Receptor
MDH	Malate Dehydrogenase
MEK	Mitogen-Activated Protein Kinase Kinase
MeOH	Methanol
MES	Mesenteric
MFP-2	Multifunctional Protein
MGAT	Monoglyceride Acyl Transferases
MGL/MgII	Monoglyceride Lipase
MHO	Metabolically Healthy Obesity
MMP	Matrix Metalloproteinase
MMSE	Mini Mental Status Examination
MND	Major Neurocognitive Disorders
mRNA	Messenger Ribonucleic Acid
MSD-COGS	Minimum Data Set Cognition Scale
mTOR	Mammalian Target Of Rapamycin
mTORC2	Rapamycin Complex 2
MTT	3-[4,5-dimethylthiazol-2-yl]-2,5-diphenyltetrazolium bromide
MUFA	Monounsaturated Fatty Acids
MUO	Metabolically Unhealthy Obesity
NaCl	Sodium Chloride
NADPH	Nicotinamide Adenine Dinucleotide Phosphate
NEFA	Non-Esterified Fatty Acids
NeuroPs	Neuroprostanes
NFD	Normal-fat-diet
NFD100	Normal-fat-diet fatty acid mix 100μM
NF-H	Neurofilament (Heavy)
NF-kβ	Nuclear Factor Kappa Beta
NF-L	Neurofilaments (Light)
NF-M	Neurofilaments (Medium)
NFTs	Neurofibrillary Tangles
NGF	Nerve Growth Factor
NHS	National Health Service
NPC1L1	Niemann-Pick C1-Like 1
NPY/AgRP	Neuropeptide Y/ Agouti-Related Protein
Nrf2	Nuclear Factor Erythroid-2 related factor 2
NSAID	Nonsteroidal Anti-Inflammatory Drug
ob	Obesity Gene
OFN	Oxygen Free Nitrogen
O ₂ ^{•-}	Superoxide Anion
•OH	Hydroxyl Radical
OS	Oxidative Stress
OxLDL	Oxidised Low-Density Lipoprotein
OXPPOS	Oxidative Phosphorylation
p38	P38 Mitogen-Activated Protein Kinase

p-Akt(S473)	Phosphorylated Akt (Serine 473)
p-Akt(T308)	Phosphorylated Akt (Threonine-308)
PA	1,2-Diacylglycerol Phosphate / Phosphatidic Acid
PAP1	Phosphatidate Phosphohydrolase (Pap1))
PC	Phosphatidylcholine
PC12	Rat Adrenal Phaeochromocytoma
PD	Parkinson's Disease
PDE	c-AMP-Phosphodiesterase
PDL	Poly-D-Lysine
PDK	Phosphoinositide-Dependent Protein Kinase
PE	Phosphatidylethanolamine
PexRAP	Peroxisomal Reductase Activating PPARy
PG	Prostaglandins
PGC1 α	Peroxisome Proliferator-Activated Receptor Gamma Coactivator 1-Alpha
PGE	Prostaglandin E
PGF	Prostaglandin F
PH	Pleckstrin Homology
PhytoPs	Phytosteranes
PI	Phosphatidylinositol
PI3-K	Phosphatidylinositol 3-Kinase
PIP ₂	Phosphatidylinositol 4,5-Bisphosphate
PIP ₃	Phosphatidylinositol 3,4,5-Trisphosphate
PKA	Protein Kinase A
PKB	Protein kinase B / Akt
Plin 1	Perilipin
PLL	Poly-L-Lysine
PNPLA2	Patatin Like Phospholipase Domain Containing 2
POMC	Neuropeptide Proopiomelanocortin
PPAR α/γ	Proliferator-Activated Receptors Alpha And Gamma
PPL	Phospholipids
PS	Phosphatidylserine
PTP-1B	Protein Tyrosine Phosphatase 1B
PTEN	Phosphatase and Tensin Homolog
PUFA	Polyunsaturated Fatty Acids
PYY	Gut-Hormone Peptide
RAGE	Receptors For Ages
RET	Retroperitoneal
ROS	Reactive Oxygen Species
RPMI	Roswell Park Memorial Institute
SAT	Subcutaneous Adipose Tissue
SCAP	Cleavage-Activating Protein
SCD1	Stearoyl-CoA Desaturase 1/ Fatty Acyl-CoA Delta-9 Desaturase (D9D)
SCFA	Short-Chain Fatty Acids
SCP-2	Sterol-Carrier Protein
SD	Standard Deviation

SEM	Standard Error Of Mean
SFA	Saturated Fatty Acids
SG	Sphingomyelin
SH-SY5Y	Sh-Sy5y Neuroblastoma Cells
SIBO	Small Intestinal Bacterial Overgrowth
SIRT1	Sirtuin 1
SM	Sphingomyelin
Soat2	Sterol O-Acyltransferase
Socs3	Suppressor Of Cytokine Signalling 3
SOD	Superoxide Dismutase
SPE	Solid Phase Extraction
SPM	Specialized Pro-Resolving Mediators
SREBP-1c	Sterol Regulatory Element Binding Protein 1c
SREBP-2	Sterol Regulatory Element-Binding Protein Isoform 2
STAT	Signal Transducer And Activator Of Transcription
T2DM	Type 2 Diabetes Mellitus
TAG	Triacylglycerol / Triglycerides
TGR5	Cell Surface Transmembrane G Protein-Coupled Receptor
TNF- α	Tumour Necrosis Factor-A
TrkB	Tropomyosin-Related Kinase B
TUBB3	PE Anti-Tubulin B3
TXs	Thromboxanes
UFA	Unsaturated Fatty Acids
UI	Unsaturation Index
UnDiff	Undifferentiated
UP2	Uncoupling protein 2
VAT	Visceral Adipose Tissue
VLCFA	Very Long Chain Fatty Acids
VLDL	Very Low-Density Lipoprotein
VLDL-TAG	Very Low-Density Lipoprotein - Triglyceride
VTA	Ventral Tegmental Area
WAT	White Adipose Tissue
WHO	World Health Organisation
Wnt	Wingless-Related Integration Site
WSD	"Western-Style" Diet

Abstract

A high-fat diet (HFD), typical of a “western-style” diet (WSD), is rich in lipids such as saturated fatty acids (SFA) and cholesterol and is associated with an increased risk of developing metabolic disorders, obesity and diabetes, cognitive impairment, anxiety, stress, and depression. *Ginkgo biloba* (GbE) has been shown to possess antioxidant, anti-inflammatory, and anti-obesogenic properties as well as neurological protection. GbE has been shown to reduce visceral adiposity, weight gain and food intake. In this study, male Wistar rats were fed either a normal fat diet (NFD) or HFD for 2 months to induce obesity. HFD-induced obese rats were then treated for 14 days with either GbE, saline or were calorically restricted. Retroperitoneal and mesenteric adipose tissues, liver, hippocampus, and hypothalamus tissues were analysed for total fatty acids, triglycerides, cholesteryl esters, monoglycerides, diglycerides and phospholipids profiles analysed by gas chromatography flame ionisation detection. A PC12 neuronal cell model was also established for in-house *in vitro* studies undergoing GbE, NFD and/or HFD treatment.

Key findings include that in all tissues except hippocampus and hypothalamus, a HFD increased SFA and decreased monounsaturated fatty acids (MUFA) and polyunsaturated fatty acids (PUFA) in total fatty acid profiles. More dynamic changes occurred across the cholesteryl esters, monoglycerides and diglycerides. Phospholipid profiles showed the most changes with GbE treatment. In PC12 neuronal cell treatment, HFD FA treatment increased Akt activation and neurofilament-L protein expression levels compared to NFD treatment. NFD treatment partially ameliorated decreased Nrf2 protein expression following hydrogen peroxide-induced oxidative stress while HFD treatment did not. GbE treatment increased levels of oleic acid and mead acid in PC12 cells. Future work would include longer treatment times, investigating other tissues and proteome analysis of tissues.

Chapter 1 - Introduction

1.1 Major neurocognitive disorders (MND)

The term Major Neurocognitive Disorders (MND) is used to describe a range of disorders that leads to significant decline in cognitive functional from previous levels (Sherman and Schnyer, 2016). The term was first used to replace the word Dementia in the fifth edition of Diagnostic and Statistical Manual of Mental Disorders (DSM-5) by the American Psychiatric Association (APA) (APA, 2013). Changes include memory decline and deterioration in emotional and intellectual abilities affecting reasoning and social skills (Sousa, Teixeira, *et al.*, 2020). Changes include memory decline and deterioration in emotional and intellectual abilities affecting reasoning and social skills (Sousa, Teixeira, *et al.*, 2020). MND can be categorised as either primary or secondary. Primary MND is associated with degenerative conditions such as Alzheimer's disease, vascular dementia, Lewy body dementia, frontotemporal dementia, and mild cognitive impairment (MCI). Secondary MND results from deterioration associated with other conditions such as infectious disease, stroke, and alcoholism (Emre, 2009).

1.2 MND - prevalence, incidence, cost, and trends

As of 2015, more than 900 million people worldwide are aged 60 years or more which is forecast to increase by a further 56% for high income countries and as much as 239% to lower income countries, respectively by 2050 (Prince, Ali, *et al.*, 2016; Prince, Comas-Herrera, *et al.*, 2016; Prince, Wimo, *et al.*, 2015). With an ever-increasing aging population comes an associated rise in chronic disease such as MND with the risk doubling for every 6.3 years increased age. The risk of MND starts at 3.9/1000 persons aged 60-64 and increases to 105/1000 persons aged 90+. As reported by Prince *et al.*, (2015), nearly 47 million people worldwide were estimated to be living with MND, with this number projected to reach 75 million by 2030, doubling nearly every 20 years. Higher incidents (58%) of MND are reported in low- or middle-income countries and is estimated to rise to 68% by 2050 driven by nearly 10 million new cases reported worldwide each year. When grouped by region, 49% of these 10 million cases are reported in Asia, 25% in Europe, 18% in the Americas and 8% in Africa. The global costs of dementia, which include direct medical costs, direct social care costs (paid professional care) and informal care (unpaid), have increased between 2010 and 2015 alone

by 35.4% rising from US\$ 604 billion to US\$ 818 respectively, the equivalent to 1.09% of the U.S.A global gross domestic product (GDP) (Prince, Wimo, *et al.*, 2015). MND symptoms are easily confused with common changes seen in ageing that may make identification of disease difficult to detect. Several assessment tools are used in a clinical setting for the identification of mild to severe cognitive decline assessing daily living and cognitive functioning. The most well-known scales are the global deterioration scale (GDS), the clinical dementia rating (CDR), the Mini Mental Status Examination (MMSE) the Cognitive Performance Scale (CPS) and the Minimum Data Set Cognition Scale (MSD-COGS) (Budson and Solomon, 2021; Plácido, Ferreira, *et al.*, 2021; Chen, Liu, *et al.*, 2014; Cohen-Mansfield, Taylor, *et al.*, 1999; Reisberg, Ferris, *et al.*, 1982). As reviewed by Sousa, Teixeira and Paúl (2020), predictive factors for MND can be categorised by sociodemographic factors, behavioural factors, and health factors. Sociodemographic factors include age, sex, education, and social isolation. Behavioural factors include physical activity, alcohol consumption and smoking. Health factors include some modifiable factors such as nutritional status, cholesterol levels, cardiovascular health, diabetes, obesity, and dyslipidaemia as well as hand-grip strength and cerebrovascular diseases (Prakash, Wang, *et al.*, 2021; Sousa, Teixeira, *et al.*, 2020; Tini, Scagliola, *et al.*, 2020; Mayeux and Stern, 2012; Skoog, Lernfelt, *et al.*, 1996). In addition to these factors both the cognitive reserve (CR) hypothesis and the brain reserve potential (BRP) also bridge both health and sociodemographic factors (Bartrés-Faz and Arenaza-Urquijo, 2011). The BRP hypotheses suggests that a larger brain volume or number of synapses helps with the tolerance of physiological insults on the brain and can extend the preclinical neuropathological stage before clinical deficits become evident (Bartrés-Faz and Arenaza-Urquijo, 2011). The CR hypothesis focuses on an individual's ability to effectively use cognitive processes and brain networks which may provide an increased ability to compensate for neuro-pathological damage and allowing maintenance of the patients' cognitive ability (Bartrés-Faz and Arenaza-Urquijo, 2011). Cognitive reserve is also positively correlated to education status with greater decline seen in people with low levels of education (Neth, Graff-Radford, *et al.*, 2020; van Loenhoud, Groot, *et al.*, 2018; Arenaza-Urquijo, Wirth, *et al.*, 2015; Stern, 2012; Whitwell, 2010). CR potential may also be used in conjunction with biomarkers for AD such as levels of cerebral glucose uptake (GU) and cerebrospinal fluid (CSF) β -amyloid ($A\beta_{42}$) and phosphorylated tau levels (Carapelle, Mundi, *et al.*, 2020). Combining the BRP and cognitive hypotheses, Prakash, and colleagues' (2021) analysis of the Alzheimer's Disease

Neuroimaging Initiative (ADNIMERGE) dataset identified 4 separable clinical AD sub-populations ranging from least severe disease, mid-severity to most severe disease, using “cognitive performance, brain volume” clustering. They identified that anti-hyperlipidaemia drugs were associated with the group known as cluster-0 that showed mid-severity of disease but with higher brain volume, while the higher antioxidant status of vitamins C and E were associated with the cluster-3 group of mid-severity disease that experienced higher cognition. Higher Vitamin D status was identified as protective in AD while anti-depressants were associated with most severe disease (cluster-2 group) (Prakash, Wang, *et al.*, 2021). Lu *et al.*, (2021), also found using the elderly nutritional indicators for geriatric malnutrition assessment (ENIGMA), may be used to identify populations at increased risk of neurocognitive disorders (NCD) and cognitive decline (Lu, Gwee, *et al.*, 2021). Of all the disorders categorised under MND, up to 70 per cent of these cases attributed to Alzheimer’s disease (AD), making AD a major public health concern with few treatment options or preventative interventions available (Prince, Wimo, *et al.*, 2015). Late-onset AD is categorized as symptoms occurring over the age of 65, while early-onset AD symptoms first appear between 30 and 65 years of age (Mendez, 2017). Genetics plays a large role in both late-onset and early-onset AD (Gatz, Reynolds, *et al.*, 2006). Analysis of collective data from 32 USA Alzheimer's Disease Centres maintained by the National Alzheimer's Coordinating Centre found a heritability of 69.8% (n=4302 participants) for late-onset AD and 92-100% heritability (n=702 participants) in early-onset AD, likely due to due to autosomal recessive causes (Wingo, Lah, *et al.*, 2012). More than 40 loci involved in immunity, endocytosis, cholesterol transport, ubiquitination, amyloid- β and tau processing are now associated for AD (Sims, Hill, *et al.*, 2020; Karch and Goate, 2015). As reviewed by Sims *et al.*, (2020) the earliest and most associated genes include mutations in the amyloid precursor protein (APP) and presenilin (PS) genes for early-onset AD and Apolipoprotein E (APOE) genes in late-onset AD associated with the amyloid cascade hypothesis of amyloid-beta (A β) misprocessing and deposition (McGirr, Venegas, *et al.*, 2020; Sims, Hill, *et al.*, 2020; Hardy and Selkoe, 2002; Rogaev, Sherrington, *et al.*, 1995; Sherrington, Rogaev, *et al.*, 1995; Corder, Saunders, *et al.*, 1994; Strittmatter, Saunders, *et al.*, 1993; Goate, Chartier-Harlin, *et al.*, 1991).

1.3 AD pathophysiology

AD is characterised by neurodegeneration influenced by a range of neuropathological abnormalities including Tau protein hyperphosphorylation, neurofibrillary tangles (NFTs), amyloid beta (A β) deposition and senile plaques (Singh, Kukreti, *et al.*, 2019; Singh, Srivastav, *et al.*, 2019; Kumar and Singh, 2015). More recently, neuro-inflammation, exacerbated oxidative stress (OS), activation of pro-apoptotic genes and abnormal glucose metabolism have also been associated with AD pathogenesis. Of these, neuro-inflammation and OS are two central issues that contribute to AD with each shown to contribute to A β deposition and NFTs (Massaad, 2011; Serrano-Pozo, Frosch, *et al.*, 2011; Gella and Durany, 2009). Preceding these issues however is abnormal glucose metabolism.

1.4 Dementia and glucose transport

A typical human brain consumes approximately 120 g of glucose daily, which is transported across the permeably restrictive blood brain barrier (BBB) mediated by astrocytes and a large family of sodium independent glucose transporters (GLUTs) and sodium-dependent glucose co-transporters (SGLT) (Shah, DeSilva, *et al.*, 2012). Most glucose in the brain is consumed *via* mitochondrial oxidative phosphorylation, converted to ATP and used to maintain normal neural function (Hall, Klein-Flügge, *et al.*, 2012). Normal glucose metabolism is rate limited by the enzyme cytochrome C oxidase and results in naturally occurring Reactive Oxygen Species (ROS) such as superoxide anion (O $_2^{\bullet-}$) hydrogen peroxide (H $_2$ O $_2$), and hydroxyl radical (\bullet OH) (Alzahrani, Alshammari, *et al.*, 2022) which when in excess leads to exacerbated OS (Perez-Pardo, Kliet, *et al.*, 2017; Nilsson and Busto, 1976). With age comes the decline in the efficiency of the highly regulated mitochondrial enzymatic process leading to increasing levels of ROS and OS (Ahmad, Ijaz, *et al.*, 2017; Pérez-Gracia, Torrejón-Escribano, *et al.*, 2008) supported by the finding of increased OS biomarkers in brain and peripheral blood tissues of AD sufferers (Sultana and Butterfield, 2010). A metabolic feature regularly seen in AD is a decline of approximately 50% in glucose based-ATP production, which tends to deteriorate as the disease progresses (Hoyer, 1992) with impaired glucose transport and ATP production correlated with increased levels of A β protein (Gella and Durany, 2009). Decreased levels of both GLUT-1 and GLUT-3 transporters have been reported in AD (Liu, Liu, *et al.*, 2008; Mooradian, Chung, *et al.*, 1997; Harr, Simonian, *et al.*, 1995; Simpson, Chundu, *et al.*, 1994) with each transporter respectively responsible for glucose transport across the BBB

(Brockmann, 2009) and into neurons (Augustin 2010; Shepherd *et al.* 1992). With decreased levels of these transporters correlating to abnormal hyperphosphorylation of tau (Liu, Liu, *et al.*, 2008), it is believed that such perturbations in GLUT transporter proteins levels, disrupts brain glucose homeostasis and mitochondrial function, which increases OS, neuro-inflammation and eventually neurodegeneration (Cong, Tao, *et al.*, 2011; Cunnane, Nugent, *et al.*, 2011; Hoyer, 2004). In contrast, increased levels of GLUT-2 (Liu *et al.*, 2008) and GLUT-12 (Pujol-Gimenez, Martisova, *et al.*, 2014) have been recently found in AD, and is thought to be a compensation mechanism, occurring as a result from the lack of glucose in neural tissue, and helps to continue a glucose supply. Glucose transported *via* GLUT-12 however enters anaerobic glycolytic metabolism, which further augments OS (Zawacka-Pankau, Grinkevich, *et al.*, 2011). Recent, compelling evidence has associated AD with Type 2 Diabetes Mellitus (T2DM) due to similar shared clinical, biochemical, and pathophysiological manifestations (Chen and Zhong, 2013) particularly OS (Rosales-Corral, Tan, *et al.*, 2015). Some researchers even suggest AD could be called Type 3 Diabetes (Kandimalla, Thirumala, *et al.*, 2017; Szablewski, 2017; Suzanne, 2014; Akter, Lanza, *et al.*, 2011).

1.5 Obesity

Obesity is a multifactorial chronic disease and a critical global issue. Spiralling increases in body mass index (BMI) has seen nearly 39 per cent of the global population classified as overweight (BMI \geq 25) with 13 per cent categorised as obese (BMI \geq 30) (World Health Organisation 2021). In the UK alone, the NHS costs attributed to elevated BMI is estimated to reach £8.3 billion in 2025 (Baker, 2019). Complications of obesity include a variety of non-communicable diseases such as coronary heart disease, hypertension, hypercholesterolemia, steatosis, cirrhosis, severe pancreatitis, and cancer. High incidences of metabolic disorders associated with obesity include insulin resistance (IR), metabolic syndrome, type II diabetes and atherogenic dyslipidaemia (Salamone and Bugianesi, 2010). The role of obesity in these metabolic disorders is discussed in detail in further sections. With regards to AD, one study reported a three-fold increased risk in people with high waist circumferences, and that the risk ratio of developing dementia increased for people suffering from obesity in the 30-40 years of age category compared to those that developed obesity in later years (Pugazhenth, Qin, *et al.*, 2017). A high-fat diet, typical of a “western-style” diet (WSD), is high in lipids such as saturated fatty acids (SFA) and cholesterol and is associated with an increased risk of

developing metabolic disorders including obesity, diabetes, cardiovascular disease as well as brain-related disorders related to hypothalamus-pituitary-adrenocortical axis dysregulation including cognitive impairment, anxiety, stress, and depression (López-Taboada, González-Pardo, *et al.*, 2020).

1.6 Lipids

Lipids are defined as a group of hydrophobic or amphipathic small molecules. Lipids are a diverse and ubiquitous group throughout the body and are utilized for many key biological functions (Fahy, Cotter, *et al.*, 2011). They act as a main structural component of cell membranes, are a major energy source for the body, provide insulation and protection when stored in adipocytes, as well as being involved in cell signalling, homeostasis, and cell membrane composition (Watson, 2015; Van Meer and de Kroon, 2011). The study of lipids is referred to as Lipidomics and is a subcategory of metabolomics alongside sugars, nucleic acids, and amino acids (Fahy, Cotter, *et al.*, 2011). Lipid molecules are diverse compounds, and they vary greatly by structure and complexity with their structure. Throughout the lipid biosynthesis pathway many different biochemical transformations occur that create unique structures that aid and facilitate their designated function. Due to the more complex nature of lipid structures as compared to nucleic acids, organisations such as LIPID MAPS, a global open access community-driven resource, has developed a comprehensive classification, nomenclature, and chemical representation system to accommodate the spectrum of lipids that exist (Lipid-Maps, 2022; Alves, Lamichhane, *et al.*, 2021; Fahy, Cotter, *et al.*, 2011; Fahy, Sud, *et al.*, 2007). Under this comprehensive classification, lipids are defined as being either hydrophobic or amphipathic small molecules originating from carbanion-based condensations of ketoacyl thioesters and/or by carbocation-based condensations of isoprene units (Fahy, Cotter, *et al.*, 2011). They are divided into eight categories: fatty acyls, glycerolipids, glycerophospholipids, sphingolipids, saccharolipids and polyketides, sterol lipids and prenol lipids (Fahy, Cotter, *et al.*, 2011). For this project, the main lipid categories focused on will be glycerolipids in the form of triglycerides, diglycerides, monoglycerides, sterol lipids in the form of cholesteryl esters and glycerophospholipids and sphingolipids in the form of phospholipids.

1.7 Fatty acids (FA)

Fatty acids belong to a group of compounds known as fatty acyls which also include alcohols, aldehydes, amines, and esters. Free fatty acids are carboxylic acids comprised of branched or unbranched aliphatic chain of hydrocarbon atoms, along with an acid group (COOH) at one end of the carbon chain and a Methyl Group (CH₃) at the other (See Figure 1 for structure). FA can be either saturated or unsaturated depending on the presence of double bonds. Saturated fatty acids (SFA) contain no carbon double bonds (C=C double bond) or other functional groups along the chain, but rather have one hydrogen attached to each carbon, producing a rigid structure that is usually solid at room temperature. A list of common fatty acids and their melting point can be seen in Table 1.

Table 1. The melting points of fatty acids and their corresponding methyl esters

	Fatty Acid	Melting Point (°C)	Methyl ester	Melting point (°C)
C12:0	Lauric acid	44	Methyl laurate	5
C14:0	Myristic acid	54	Methyl myristate	18.5
C16:0	Palmitic acid	63	Methyl palmitate	30.5
C18:0	Stearic acid	70	Methyl stearate	39.1
C16:1	Palmitoleic acid	0.5	Methyl palmitoleate	-0.5
C18:1	Oleic acid	16	Methyl oleate	-20
C18:2	Linoleic acid	-5	Methyl linoleate	-35
C18:3	Linolenic acid	-11	Methyl linolenate	-52
C20:1	Eicosenoic acid	24	Methyl <i>cis</i> -11-eicosenoate	-34
C22:1	Erucic acid	32	Methyl <i>cis</i> -13-docosenoate	-1
C24:1	Nervonic Acid	43	Methyl <i>cis</i> -15-tetracosenoate	14

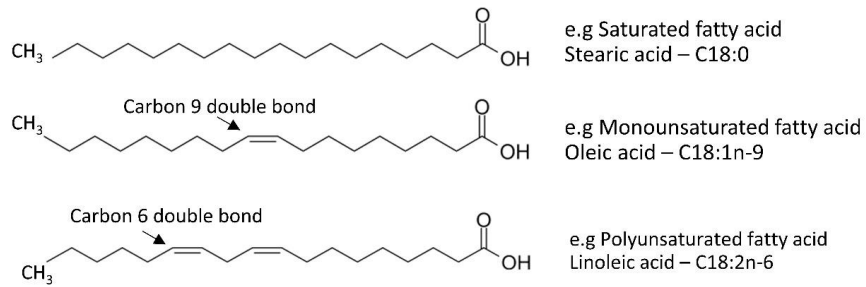
Adapted from Royal Society of Chemistry, 2022a, 2022b, 2022c, 2022d, 2022e; Chemical Book, 2017; Edith, Janius and Yunus, 2012; Knothe and Dunn, 2009; Gunstone, 1996).

Unsaturated FA contain at least one double bond along the carbon chain and are further divided into monounsaturated FA (MUFA) or polyunsaturated fatty acids (PUFA) with MUFA containing 1 double bond, and PUFA containing 2 or more double bonds. A *cis* double bond (as illustrated in Figure 1) describes when two hydrogen atoms are adjacent to the double bond and stick out on the same side of the chain creating a bend or a “kink” in the carbon chain influencing the structure and physical properties of the fatty acid molecule. Most often the kink caused by a FA double bond allows the FA to remain liquid at room temperature and prevents the FA packing tightly within biological structures (e.g., membranes), aiding flexibility and fluidity. A *trans* configuration at the double bond, where the adjacent two

hydrogen atoms lie on opposite sides of the chain, does not result in a kink, and the fatty acid functions like that of a saturated fatty acid. As a result, they do not cause the chain to bend much, and their shape is like rigid saturated fatty acids (Ridgway and McLeod, 2021; Panickar and Bhathena, 2010).

The nomenclature of fatty acid is derived from the number of carbons in the chain (e.g., C18), followed by the number of double bonds within the chain (e.g., C18:1), followed by an omega notation (ω - or n-) indicating the carbon number of the first double bond occurring from the methyl end of the chain (e.g., C18:1n-9, illustrated in Figure 1) (Ridgway and McLeod, 2021; Panickar and Bhathena, 2010). Fatty acids with two or more double bonds are known as polyunsaturated fatty acids and are further categorised into n-6 and n-3 fatty acids. Both n-6 and n-3 fatty acids, Linoleic acid (LA; C18:2n-6) and alpha-linolenic acid (ALA; 18:3n-3) may be converted by sequential desaturation and elongation to either C20-, C22- and C24- highly unsaturated n-6 and n-3 polyunsaturated fatty acids also referred to as long chain fatty acids (LCFA) (Shi and Tu, 2015). LCFA are a main source of energy for the body and are required for the synthesis of structural lipids (e.g., phospholipids and sphingolipids) (Schäffler and Schölmerich 2010) which are essential to reproduction, cell differentiation, inflammation, and cognition (Clarke and Nakamura, 2013; Harbige, 2003). LCFAs and derivatives, along with associated fatty acid enzymes (E.g., ELOVL5), can bind to several transcription factors such as peroxisome proliferator-activated receptor alpha (PPAR α), sterol regulatory element binding protein 1C (SREBP) (Takeuchi, Yahagi, *et al.*, 2010), Carbohydrate response element binding protein (ChREBP), Forkhead Box O1 (FOXO1), Peroxisome proliferator-activated receptor gamma coactivator 1-alpha (PGC1 α), liver X receptor (LXR) (Yoshikawa, Shimano, *et al.*, 2002), Hepatocyte nuclear factor 4 α (HNF-4 α) and Nuclear factor kappa B (NF- κ B) and regulate the expression of numerous downstream genes (Guan, Qu, *et al.*, 2011; Jump, 2011; Grimaldi, 2010; Vallim and Salter, 2010; Kennedy, Martinez, *et al.*, 2009).

Both LA and ALA are termed “essential fatty acids” (EFA) (Panickar and Bhathena, 2010; Chirala, Chang, *et al.*, 2003; Harbige, 2003; Simopoulos, 2002) as humans lack the necessary enzymes delta (Δ) 12 (D12D) and Δ 15 desaturase (D15D) that enable the introduction of the cis ‘n-3’ and ‘n-6’ double bonds at the carbon 2 methyl end of the fatty acid chain making linoleic acid (18: 2n-6) or ALA (C18:3n-3) (Lee, Lee, *et al.*, 2016). This makes both C18:2n-6 and C18:3n-3 essential fatty acids that must be acquired through the diet (Martin, 2015).



Free Fatty acids

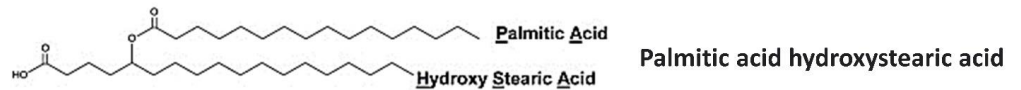
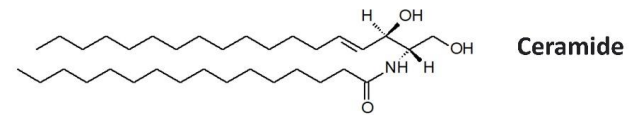
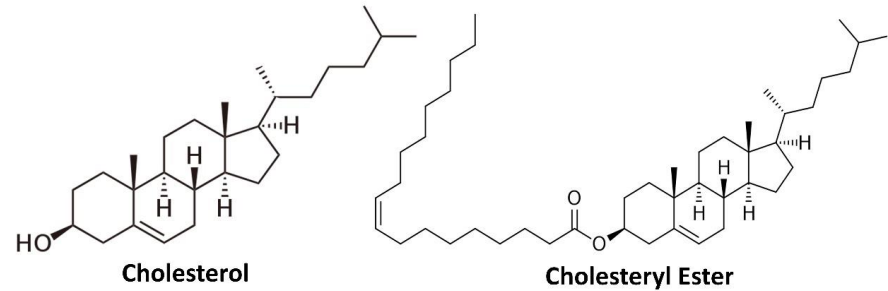
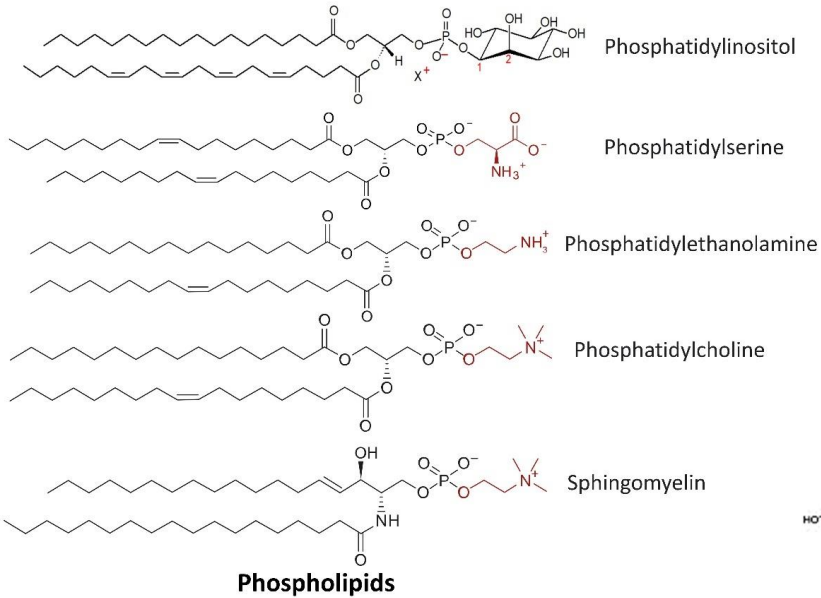
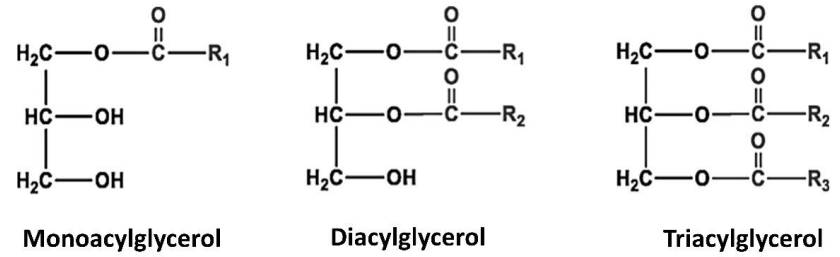


Figure 1. Chemical structures of different lipid-based compounds

Once ingested C18:2n-6 and C18:3n-3 can be converted *via* a series of elongase, desaturase and β -oxidation steps into long chain (LC) n-3 PUFA (Martin, 2015). Many desaturation and elongation fatty acid processes utilize, and therefore compete for, the same enzymes in both the n-6 and n-3 pathways (Martin, 2015). Both LA and ALA are abundant in plant-based oils such as nuts and seeds including flax, chia, walnut, rapeseed, and hemp. The human body is further limited in its ability to convert ω -3 ALA into longer chain n-3 eicosapentaenoic acid (EPA; C20:5n-3) and docosahexaenoic acid (DHA; C22:6n-3), as there is direct and preferential competition of enzyme activity for n-6 fatty acids for the conversion of LA to arachidonic acid (AA; C20:4n-6) (Santos, Price, *et al.*, 2020). Both EPA and DHA are predominantly obtained from fish and seafood in the diet, while AA is largely obtained from animal and dairy products (Kawashima 2019; Tallima and Ridi 2018). Fatty acids circulating in the body are obtained both through the diet as well as endogenously produced either through the liberation of stored fatty acid reserves or synthesised *de novo* (Stryer, Berg, *et al.*, 2019).

1.8 *De novo* fatty acid synthesis

Mammals can undergo *de novo* lipogenesis (DNL) to form fatty acids from Acetyl CoA and NADPH within the cytosol of the cell (illustrated in Figure 2.) primarily in the liver, adipose tissues, mammary glands (Ogunbona and Claypool, 2019; Stryer, Berg, *et al.*, 2019; Palmieri, Spera, *et al.*, 2015; Palmieri, 2004) and as well as some regions of the brain such as the hypothalamus (López, Tovar, *et al.*, 2005) DNL occurs when glucose is abundant and is controlled by several transcription-based steps (Hussain, 2014). Insulin levels within the plasma activate the endoplasmic reticulum (ER) membrane-bound transcription factor sterol regulatory element binding protein 1C (SREBP1c), the N-terminus of which translocates to the nucleus and upregulates all genes in the FA biosynthetic pathway (Song, Xiaoli, *et al.*, 2018). Uptake of excess plasma glucose promotes the nuclear translocation of the transcription factor carbohydrate response element binding protein (ChREBP), which upregulates both the transcription of pyruvate kinase facilitating the production of citrate from glucose derived Acetyl-CoA, as well as FA biosynthetic genes (Song, Xiaoli, *et al.*, 2018; Shi and Tu, 2015; Filhoulaud, Guilmeau, *et al.*, 2013; Lodhi, Wei, *et al.*, 2011; Postic, Dentin, *et al.*, 2007; Horton, Goldstein, *et al.*, 2002). Lipogenesis is more abundant and efficient in the liver than in adipose tissue (Lodhi, Wei, *et al.*, 2011).

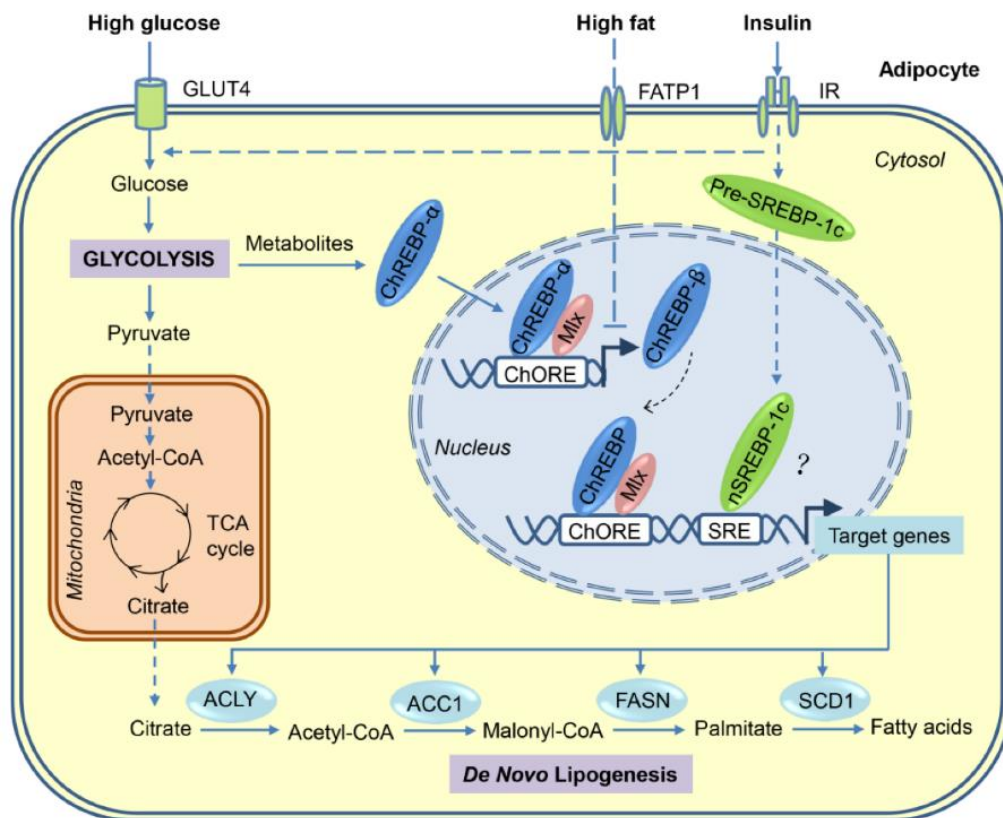


Figure 2. Illustration of transcriptional activation of de novo lipogenesis in adipocytes in response to high-sugar or high-fat diets (Song, Xiaoli and Yang, 2018)



Figure 3. De novo Fatty Acid Synthesis from Acetyl CoA to Palmitic acid

Acetyl CoA is obtained either from the mitochondrial irreversible oxidative decarboxylation of pyruvate obtained from carbohydrate and/or glucose metabolism *via* the glycolytic pathway or the β -oxidation of lipids within the mitochondria (Shi and Tu, 2015) . Acetyl CoA condenses with oxaloacetate to form citrate *via* the citric acid cycle, allowing it to be transported across the inner mitochondrial membrane (IMM), in exchange for cytosolic malate *via* the mitochondrial citrate- carrier (CIC), into the cytosol. Once in the cytosol, citrate is cleaved back to Acetyl CoA and oxaloacetate by ATP citrate lyase. Oxaloacetate is either utilized for gluconeogenesis or converted to malate and NADPH by malate dehydrogenase (MDH) and returned to the mitochondria *via* the CIC. Cytosolic Acetyl CoA is carboxylated to Malonyl-CoA by Acetyl CoA carboxylase (ACC), the rate-limiting step in the fatty acid synthesis

pathway. In animals, two isoforms of the enzyme ACC exist (ACC1 and ACC2), with ACC1 expressed more in lipogenic tissues (e.g., liver, adipose tissues, and mammary glands) while the ACC2 isoform is expressed more in highly metabolic organs (e.g., skeletal muscle, heart) (Chen, Duan, *et al.*, 2019; Shi and Tu, 2015; Barber, Price, *et al.*, 2005; Munday, 2002; Abu-Elheiga, Brinkley, *et al.*, 2000). ACC2 derived Malonyl-CoA is involved in the regulation of fatty acid β -oxidation by inhibiting the carnitine palmitoyl-CoA transferase-1. In times of energy demand, adenosine monophosphate (AMP)-activated protein kinase (AMPK) is activated, which phosphorylates both ACC1 and ACC2, inactivating them, leading to a decrease in fatty acid synthesis and an increase in fatty acid β - (Chen, Duan, *et al.*, 2019; Shi and Tu, 2015; Barber, Price, *et al.*, 2005; Munday, 2002; Abu-Elheiga, Brinkley, *et al.*, 2000). As shown in Figure 3, Malonyl-CoA is combined with Acetyl-CoA to produce the saturated fatty acid Palmitic acid (C16:0) *via* the rate limiting enzyme fatty acid synthase (FASN) (Christie, 2021; Ogunbona and Claypool, 2019; Stryer, Berg, *et al.*, 2019; Palmieri, Spera, *et al.*, 2015; Jensen-Urstad and Semenkovich, 2012; Palmieri, 2004).

As shown in Figure 4, C16:0 can be further converted into either C16:1n-7 or C18:1n-7 \rightarrow C18:1n-9 using the enzymes ELOVL6 and SCD1 (Delta-9-Desaturase) (Minville-Walz, Gresti, *et al.*, 2012). Also shown in Figure 4 and the fatty acid synthesis pathway, are some of the many enzymes utilized in fatty acid elongation and desaturation with some enzymes showing a preference for certain fatty acids. For example, the enzyme FADS2 catalyses Δ 4, Δ 6 and Δ 8 desaturation introducing cis double bonds in the fatty acid chain in fatty acids such as C16:0, C18:2n-6, and C18:3n-3 but not C14:0 or C18:0 (Wang, Park, *et al.*, 2020). When an excess amount of C16:0 occurs either through dietary ingestion or DNL, inhibited synthesis of highly unsaturated fatty acids EPA and DHA or AA from C18:2n-6 and C18:3n-3 is seen, indicating a preference of FADS2 for C16:0 (Park, Kothapalli, *et al.*, 2016). For cholesterol synthesis, two molecules of acetyl-CoA (also from citrate by ATP citrate lyase) are condensed to yield acetoacetyl-CoA which is then condensed with another acetyl-CoA to yield 3-hydroxy-3-methylglutaryl-CoA (HMG-CoA). The committed step in cholesterol synthesis is the reduction of cytosolic HMG-CoA to mevalonate. Fatty acid and cholesterol synthesis also requires NADPH and some of these are generated from cytosolic oxaloacetate *via* malate dehydrogenase and malic enzyme (Palmieri, 2004). Dysregulation of DNL contributes to diverse pathological conditions such as obesity, type 2 diabetes, and cardiovascular diseases (Ameer, Scandiuzzi, *et al.*, 2014).

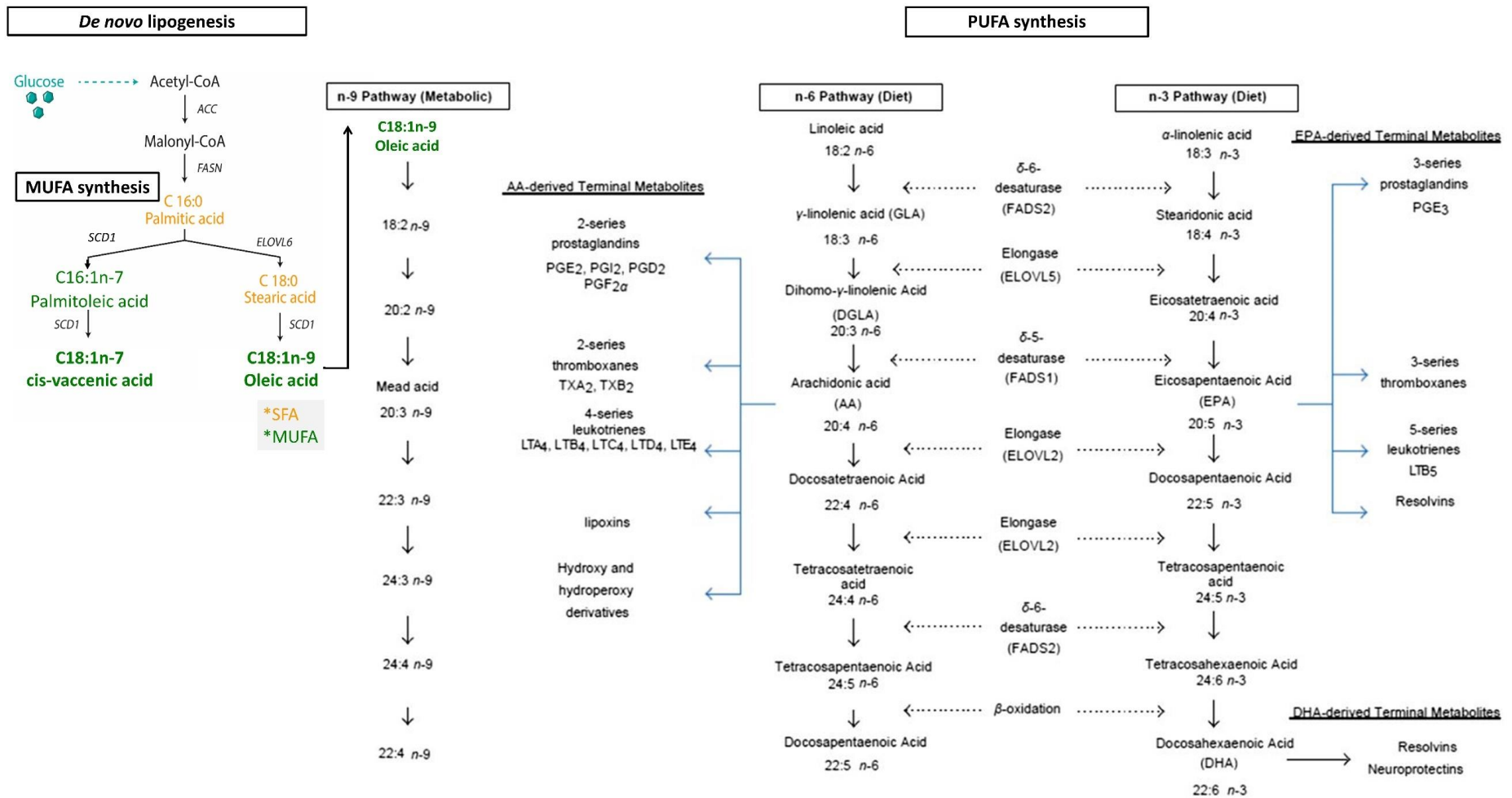


Figure 4. De novo lipogenesis and fatty acid synthesis pathway for saturated (SFA) monounsaturated (MUFA) and n-6 and n-3 polyunsaturated (PUFA) fatty acids; ACC—acetyl CoA carboxylase; FADS1 —fatty acid desaturase 1, FADS2 — fatty acid desaturase 2, FASN—fatty acid synthase; ELOVL2—fatty acid elongase 2, ELOVL5—fatty acid elongase 5, ELOVL6 — fatty acid elongase 6, SCD1 — Stearoyl-CoA desaturase-1 (Adapted from Piccinin et al. 2019; Martin 2015).

1.9 Dietary Lipids

Dietary lipids are utilized for energy or stored in the body, predominantly in adipose tissues with lipids primarily stored in the form of triglycerides/ triacylglycerols (TAG) composed of a glycerol molecule bound to three fatty acids (illustrated in Figure 1). They are transported around the body in the form of very low-density lipids (VLDL-TAG), cholesterol, cholesteryl esters and phospholipids and incorporated into cellular membranes in the form of phospholipids. Dietary sources of lipids, predominantly TAG, phospholipids (PPL), and cholesteryl esters (CE) are hydrolysed in the intestinal lumen by pancreatic lipase to form several lipid-based products including phosphatidylglycerols, monoacylglycerols (MAG), diacylglycerols (DAG), free fatty acids (FFAs), non-esterified cholesterol, and lysophospholipids (Bhutia and Ganapathy, 2021) and are structurally illustrated in Figure 1. These products are emulsified by bile acids and are absorbed by enterocytes by diffusion (FFA) and protein-mediated facilitated transport for larger lipid-based molecules. Cholesterol from the diet is absorbed by enterocytes by the Niemann-Pick C1-like 1 (NPC1L1) protein embedded in plasma membrane raft microdomains (Jia, Betters, *et al.*, 2011). Within the enterocyte, MAG, non-esterified cholesterol, and lysophospholipids are re-esterified in the smooth endoplasmic reticulum to generate mostly triglycerides as well as smaller amounts of cholesteryl esters, and phospholipids. Some FAs are converted to acyl-CoA for β -oxidation to produce fuel for the enterocyte (Kohlmeier, 2015). FFA, TAG, CE, and PPL are packed into chylomicrons, secreted into the lymphatic system and then to plasma to be transported to peripheral tissues such as adipose tissue and muscle (Bhutia and Ganapathy, 2021; Stryer, Berg, *et al.*, 2019). Lipoprotein lipase expressed on the luminal surfaces of capillary endothelial cells of peripheral tissues facilitates transported TAG breakdown and absorption. Any chylomicron remnants left in the plasma are transported to the liver taken up by receptor-mediated endocytosis and removed from circulation. Remaining FAs are released from the chylomicron during lysosomal processing of the particles (Hussain, 2014; Cohen and Fisher, 2013). The use of tissue fatty acid profiles and fatty acid metabolites are becoming more useful as biomarkers for the prediction and diagnosis of disease and its link to diet, including cardiometabolic disorders, hepatic and renal disorders and cognitive decline (Cisbani and Bazinet, 2021; Parry, Rosqvist, *et al.*, 2021; Song and Jensen, 2021; Koch, Furtado, *et al.*, 2020; Lee, Lai, *et al.*, 2020; Santos, Price, *et al.*, 2020; Alonso, Nouredin, *et al.*, 2019; De Aguilar, 2019; Marklund, Wu, *et al.*, 2019; Pranger, Corpeleijn, *et al.*, 2019; Leng, Winter, *et al.*, 2017; Del Gobbo, Imamura, *et al.*, 2016; Börgeson, Johnson, *et al.*, 2015; Loomba, Quehenberger, *et al.*, 2015; Malik, Chiuve, *et al.*, 2015; Ni, Zhao, *et al.*, 2015; Zarrouk, Riedinger, *et al.*, 2015; Huang and Mahley, 2014; Neuman, Cohen, *et al.*,

2014; Rauschert, Uhl, *et al.*, 2014; Mozaffarian, Lemaitre, *et al.*, 2013; Rönnemaa, Zethelius, *et al.*, 2012; Chajès, Jenab, *et al.*, 2011; Astorg, Bertrais, *et al.*, 2008; Sun, Ma, *et al.*, 2007; Lemaitre, King, *et al.*, 2003; Arab and Akbar, 2002; Baylin, Kabagambe, *et al.*, 2002). For instance, n-3 fatty acids are associated with decreased risk of cardiovascular disease, while higher SFA and n-6 fatty acids are more positively associated with obesity and inflammatory markers.

1.10 Triglycerides, diglycerides and monoglycerides

MAG, DAG and TAG (illustrated in Figure 1) may be absorbed from dietary sources in the intestines or endogenously produced as previously described in section 1.09. The synthesis of TAG occurs either through the monoglyceride pathway or the glycerophosphate pathway. In a well-fed state, dietary MAG and FFA are converted to DAG by monoglyceride acyl transferases (MGATs). DAG are converted to TAG by diglyceride acyl transferases (DGATs) in the smooth ER of enterocytes. This process utilizes fatty acyl CoA derived from the breakdown of the dietary LCFA by Acyl CoA synthetase activity (See Figure 5) (Stryer, Berg, *et al.*, 2019). In a fasting state, the glycerophosphate (G3P) pathway accounts for nearly 90% of all TAG synthesis and is utilized within the ER of the liver and adipose tissue (Alves-Bezerra and Cohen, 2017). FA used in TAG synthesis in the liver come from both dietary and endogenous sources. Endogenous sources include DNL derived fatty acids and those stored in tissues, transported to the liver by the bloodstream (Hussain, 2014). Glycerol used as the backbone of TAG is catalysed by glycerol kinase to form glycerol-3-phosphate (G3P). In TAG synthesis, FA are activated by acyl-CoA synthetases to acyl-CoA and are esterified to G3P, catalysed by mitochondrial and microsomal G3P acyltransferase (GPAT) enzymes and is a rate limiting step in TAG synthesis. GPAT gene expression is under the influence of the transcription factor ChREBP (King, 2014). This reaction produces lysophosphatidic acid (LPA), a monoacylglycerol phosphate structure, which can be acylated in the ER membrane by the acylglycerol-3-phosphate acyltransferases (AGPAT) to form 1,2-diacylglycerol phosphate otherwise known as phosphatidic acid (PA). PA produces cytidine diphosphate diacylglycerol (CDP-DG) and can either be dephosphorylated by lipin phosphatidate phosphohydrolase (PAP1) to form 1,2-DAG or be utilized as substrate for cardiolipins and glycerolphospholipids. DAG can then be acylated to TAG by DGAT catalysation (Stryer, Berg, *et al.*, 2019; Alves-Bezerra and Cohen, 2017; King, 2014). The formation of TAG for storage serves as a way of reducing the weight incurred by storing FA. When G3P is combined by esterification with 3 fatty acids to form TAG, the carboxyl end of a fatty acid chain (-COOH) is transferred to the hydroxyl group

(-OH) of glycerol-3-phosphate (G3P) by dehydration synthesis, a water molecule is released as a by-product making the TAG molecule lighter (Stryer, Berg, *et al.*, 2019). The majority of hepatic TAG and cholesteryl esters are secreted directed from the ER lipid bilayer into the bloodstream and transported to peripheral tissues, with TAG transported in the form of very low-density lipoprotein (VLDL-TAG), while a smaller quantity is stored in the liver localized to cytoplasmic lipid droplets (LDs) (Parry, Rosqvist, *et al.*, 2021; Roumans, Sagarminaga, *et al.*, 2021; Alves-Bezerra and Cohen, 2017; Martinez-Lopez and Singh, 2015; Bansal, Buring, *et al.*, 2007; Barrows and Parks, 2006).

TAG provides a neutral store of fatty acids in the body, predominantly stored in adipocytes that can later provide energy *via* β -oxidation. The breakdown of TAG both in liver, adipose tissues and other peripheral tissues produces DAG, MAG, FFA and glycerol molecules (Bhutia and Ganapathy, 2021; Alves-Bezerra and Cohen, 2017; Kohlmeier, 2015). During fasting states, plasma FA provides the main source of hepatic TAG. The daily rate of hepatic FA uptake and DNL is balanced by FA oxidation rates and the transportation of VLDL-TAG out of the liver, which results in less than 5% of steady state hepatic TAG (Bhutia and Ganapathy, 2021; Alves-Bezerra and Cohen, 2017; Kohlmeier, 2015). As plasma insulin levels drop during fasting, in response to energy demand in peripheral tissues, adipocytes undergo lipolysis through the catecholaminergic stimulation of the β -adrenergic receptors. This triggers the release of FFA and glycerol from TAG stored in intracellular lipid droplets of the adipocyte which can either enter the plasma in the form of bound-albumin FA or be used locally for energy supply or ketone body production (Alves-Bezerra and Cohen, 2017; Samuel and Shulman, 2016). The Liver is supplied with FA either by DNL, internalization of chylomicron remnants, or FAs secreted into the plasma from adipocytes and transported to the liver. They are transported across the hepatocyte plasma membrane either by passive or flip-flop diffusion (Barile *et al.* 2016) if in an unbound LCFA state (Kamp and Hamilton, 2006; Massey, Bick, *et al.*, 1997), or if bound to albumin, facilitated by a variety of plasma membrane-associated proteins including: plasma membrane FA-binding proteins (FABPs), FA transport proteins (FATPs), caveolin-1 (CAV-1), FA translocase (FAT)/CD36, and very long-chain acyl-CoA synthetases (ACSVL/ transport proteins) (Huang, Zhu, *et al.*, 2021; Ma, Nenkov, *et al.*, 2021; Amiri, Yousefnia, *et al.*, 2018; Glatz and Luiken, 2018; Schwenk, Holloway, *et al.*, 2010; Hamilton, 2007). An excess of hepatic TAG accumulation is associated with obesity, T2-diabetes, dyslipidaemia, and IR and can result in chronic liver disease (Caussy, Aubin, *et al.*, 2021; Birkenfeld and Shulman, 2014).

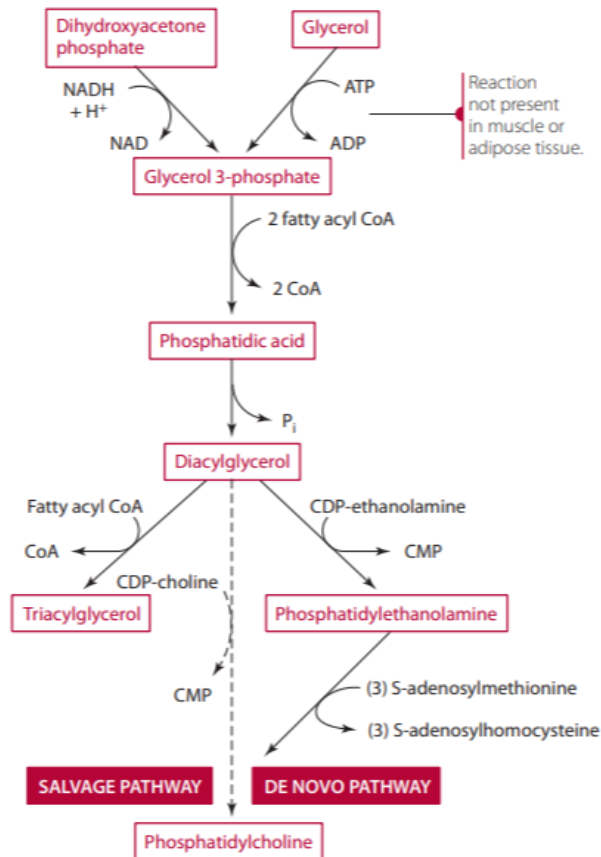


Figure 5. The synthesis of diacylglycerols, triacylglycerols and the phospholipids phosphatidylcholine and phosphatidylethanolamine through common shared pathways from the CoA-activated fatty acids and glycerol 3-phosphate precursors (Figure from Gropper, Smith and Groff, 2009).

1.11 Cholesterol, cholesteryl esters and bile acids

Cholesterol is an essential component of mammalian cell membrane, contributing to structural integrity, fluidity, thickness, and function of cell membranes and helps regulate membrane trafficking and signalling (Giudetti, Romano, *et al.*, 2016; Björkhem, Meaney, *et al.*, 2004). It is distributed throughout the membrane, predominately localized in cholesterol-rich microdomains (Anagnostopoulou, Camargo, *et al.*, 2020; Fridolfsson, Roth, *et al.*, 2014). Of the total levels of cholesterol in the body, the brain accounts for nearly 25% of bodily cholesterol levels (Giudetti, Romano, *et al.*, 2016; Björkhem, Meaney, *et al.*, 2004). Cholesterol homeostasis must be tightly regulated by maintaining dietary cholesterol absorption and excretion in the gastrointestinal tract and ubiquitous *de-novo* cholesterol synthesis, predominantly occurring in the liver and the brain, but also in nucleated cells (Nemes, Åberg, *et al.*, 2016). Due to the nature of the blood brain barrier (BBB), circulating cholesterol cannot cross the BBB. Levels of cholesterol in the brain which can be

synthesized *in situ* and accounts for 25% of total cholesterol found in the body must be tightly controlled through the conversion of cholesterol into its oxidized forms 24-S-hydroxycholesterol (24-OH-C) and 27-hydroxycholesterol (27-OHC). This allows these compounds to be imported into the brain across the BBB while 24S-HC can be exported (Giudetti, Romano, *et al.*, 2016).

The liver plays the main role in cholesterol biosynthesis, storage, and secretion. Cholesterol consists of a rigid planar tetracyclic ring with an angular methyl group on one side, an isooctyl chain attached to C17, and a small head group consisting of a β -hydroxyl group at C3 (Giudetti, Romano, *et al.*, 2016). The form cholesterol, acetyl CoA undergoes a complex 37-step process described in further detail elsewhere (Craig, Yarrarapu, *et al.*, 2021; Nemes, Åberg, *et al.*, 2016; Goldstein and Brown, 2015). To briefly summarize, the expression of genes for enzymes required in the synthesis of cholesterol are upregulated by sterol regulatory element-binding protein isoform 2 (SREBP-2), an ER membrane-bound transcription factor that also acts as a sterol sensor. Upon the depletion of cellular cholesterol, cleavage-activating protein (SCAP), a crucial ER membrane molecule, escorts SREBP-2 from the ER to the golgi apparatus, where it is cleaved by two proteases and is translocated to the nucleus, activating the transcription of cholesterol synthesis and Low-density lipoprotein receptor (LDLR) expression. Intracellular cholesterol levels are tightly controlled by the interaction of the cholesterol, the SCAP-SREBP complex with insulin induced gene 2 (INSIG-2), LDLR and intracellularly cholesterol levels (Islam, Hlushchenko, *et al.*, 2022; Craig, Yarrarapu, *et al.*, 2021; Nemes, Åberg, *et al.*, 2016; Radhakrishnan, Goldstein, *et al.*, 2008). When excess cholesterol is present, cholesterol synthesis is blocked by the SCAP-SREBP complex binding to the ER protein INSIG-2, resulting in SREBP-2 retention in the ER. LDLR expression is reduced lowering LDL/Cholesterol uptake. LDLR is a cell surface protein that binds to and mitigates endocytosis of VLDL/cholesterol into the cell. Endocytosed cholesterol is released by lysosomes and acts as a repressor of 3-hydroxy-3-methyl-glutaryl CoA reductase (Islam, Hlushchenko and Pfisterer, 2022). Both the enzymes 3-hydroxy-3-methyl-glutaryl CoA reductase and squalene monooxygenase act as rate-limiting factors in the cholesterol synthesis pathway (Craig, Yarrarapu, *et al.*, 2021; Nemes, Åberg, *et al.*, 2016). In hepatocytes, highly insoluble cholesterol is excreted into circulation in several ways; transformed into bile acids, excreted as neutral sterols within bile *via* biliary excretion, esterified into cholesteryl esters or converted to VLDL. While free cholesterol may be taken up by lipoproteins, it is confined to the outer surface of the lipoprotein particle. By converting cholesterol to cholesteryl esters which are much more hydrophobic it allows for higher partitioning of cholesterol into the hydrophobic inner core of lipoproteins, increasing the carrying capacity of the lipoproteins and facilitating more efficient cholesterol transport through the

blood stream (Freeman and Remaley, 2016; Chien, 2004). Dietary cholesterol absorbed by enterocytes is esterified by Sterol O-acyltransferase (SOAT2) in intestines and liver utilizing acyl-CoA as a source of acyl chains. The gradient of free cholesterol between lipoproteins and cell membranes is maintained by lecithin-cholesterol acyltransferase (LCAT) which produced by the liver and found abundantly in plasma HDL particles. LCAT utilizes phosphatidylcholine (PC) as a source of acyl chains to form CE. LCAT associates preferentially with the HDL lipoprotein and catalyses the transfer of the sn-2 fatty acid of PC to cholesterol to produce CE and lysophosphatidylcholine (LPC) (Nakamura, Kotite, *et al.*, 2004). Formed CE is then relocated from the surface of the HDL particle to the core facilitating the further uptake of cholesterol to the surface of the HDL particle (Feingold and Grunfeld, 2021). VLDL in the liver is assembled from cholesterol, cholesteryl esters (CE), TAG, PPL, and the lipoprotein apolipoprotein B-100 (apo B-100). VLDL-TAG may be further modified to intermediate-density lipoproteins (IDLs) and low-density lipoproteins (LDLs), by lipoprotein lipase and hepatic lipase, and transported to peripheral tissues (Craig, Yarrarapu, *et al.*, 2021; Nemes, Åberg, *et al.*, 2016; Hussain, 2014). In the reverse, cholesterol transport from peripheral tissues is mediated by high density lipoproteins (HDL), where cholesterol-poor pre- β HDL particles absorb free cholesterol *via* ABCA1 from peripheral tissues *via* cholesterol efflux regulatory protein (CERP) (also known as ABCA1). CE can be sequestered into HDL particle, partitioning into the bilayer midplane of the HDL particle which enlarges and matures into a spherical shape by progressive lipidation, where it is transported back to the liver (Nemes, Åberg, *et al.*, 2016; Hussain, 2014). CE can then be exchanged for TAG or other lipoproteins for recirculation (Nakamura, Kotite, *et al.*, 2004). HDL spheres returning to the liver release transported CE either by the action of hepatic scavenger receptor B1, or by LDL receptors in the liver after HDL-CE is transferred to apo B-100-containing proteins (Nemes, Åberg, *et al.*, 2016; Hussain, 2014).

Cholesterol is also converted to bile acids (BA) by both the classical pathway and alternative pathway and make up approximately 60-80% of bile solution (Craig, Yarrarapu, *et al.*, 2021). Primary BA are initially synthesised from cytochrome P450-mediated oxidation of cholesterol by hepatocytes and may be conjugated to at the carboxyl group glycine or taurine in the liver before secretion in the GI tract. Primary BA are or further hydrolysed to secondary BA in the lower gastrointestinal tract by commensal bacteria. Levels of BA are subject to age and diet, but of the 17 enzymes involved in BA synthesis 7 α -hydroxylase (CYP7A1) activity and the 12-hydroxylation of the steroid ring by CYP8B1 are rate limiting, controlling levels of BA synthesised (Ridlon, Kang, *et al.*, 2006). The enzymes CYP27A1, CYP7B1, and CYP46A1 are also found in the brain and facilitate brain cholesterol

homeostasis by converting cholesterol to the oxysterols 24- and 27-hydroxycholesterol (24S-HC and 27-OHC respectively) allowing them to be exported out of the brain across the blood brain barrier (Björkhem, Leoni, *et al.*, 2010; Björkhem, 2006). BA are amphiphilic structures with their hydrophobicity and solubility dependent on the presence, absence, or alterations of hydroxyl groups along the steroid backbone (Vallim, Tarling, *et al.*, 2013). BA act both as biological detergents creating a micellar surfactant interface between ingested dietary lipids and pancreatic enzymes such as lipases aiding fat metabolism and vitamin absorption as well as cell signalling actions including Farnesoid X receptor (FXR) and cell surface transmembrane G protein-coupled receptor (TGR5 /GPBAR1) (Kiriya and Nochi, 2021; Zhou and Hylemon, 2014; Vallim, Tarling, *et al.*, 2013). In their role as biological detergents used to solubilize dietary fats, BA are excreted from the liver and may be stored in the gallbladder. In response to dietary fat ingestion BA are released after stimulation by cholecystokinin (CCK) that promotes smooth muscle contraction in the gallbladder and the relaxation of the sphincter of Oddi allowing bile to enter the duodenum (Ridlon, Kang, *et al.*, 2014). The major bile acids are cholic acid (CA), chenodeoxycholic acid (CDCA), and deoxycholic acid (DCA) account for more than 90% of the total BA pool size and averages 40 $\mu\text{mol}\cdot\text{kg body wt}^{-1}$ in healthy subjects (Stellaard and Lütjohann, 2021) and is recycled between 4-12 times per day (Stellaard and Lütjohann, 2021; Chiang and Ferrell, 2018). This is achieved by numerous rounds of BA recycling *via* enterohepatic circulation, allowing for almost 90% of secreted bile acids to be absorbed *via* the apical sodium-dependent bile transporter (ASBP) and the cytosolic ileal bile acid binding protein (IBABP fatty acid-binding protein subclass 6/FABP6) (Ridlon, Kang, *et al.*, 2014). The remaining 10% of BA continues to the colon where they may be further microbially modified and either passively re-absorbed back into circulation or excreted through the faeces (Ridlon, Kang, *et al.*, 2006). Excess levels of bile acids may be toxic particularly to enterocytes and may promote small intestinal bacterial overgrowth (SIBO) (Zhou and Hylemon, 2014).

1.12 Glycerophospholipids

Glycerophospholipids (PPL) are composed of a glycerol backbone esterified to 2 fatty acids with a phosphate esterified to the *sn*-3 position esterified together by an alcohol group making the polar head phosphate group. PPL are hydrophilic at the negatively charged polar “head”, and hydrophobic at the fatty acid “tail”. Owing to their amphiphilic nature, when packaged together, PPL form the bulk of lipid bilayers, with oppositely oriented phospholipid molecules creating a hydrophobic inner core

of fatty acids, and hydrophilic exterior of phosphate heads, creating a sealed “envelope” around a cell. Of the fatty acids, for many phospholipids, one fatty acid may be saturated, while the other carries a double bond, allowing for fluidity when packaged together, affecting the fluidity of the membrane (Alberts, Johnson, *et al.*, 2002) as discussed earlier under fatty acids. The incorporation of ω -3 fatty acids into phospholipids such as EPA and DHA, mostly occurs in the sn-2 position of the phospholipid and changes the organization and size of lipid rafts (de Santis, Varela, *et al.*, 2018; Hou, McMurray, *et al.*, 2016; Schumann, 2016).

PPL make up approximately 50 per cent of cellular membrane. Glycolipids, cholesterol, and intercalated transmembrane proteins embedded in the bilayer structure account for the rest. In mammalian cells, the major PPL are phosphatidylcholine (PC), phosphatidylethanolamine (PE), phosphatidylserine (PS), phosphatidylinositol (PI), and sphingomyelin (SG) (illustrated in Figure 1) (Stryer, Berg, *et al.*, 2019). Cell membrane function is influenced by the fluidity and stability of the cell membrane, which is dependent of the type of fatty acids incorporated into the phospholipid structure, and the amount of cholesterol-rich microdomains. The membrane serves as a barrier and facilitator of ionic exchange and molecular transport in and out of the cell (Hulbert, Pamplona, *et al.*, 2007; Hulbert, Turner, *et al.*, 2005). If the membrane is rich in saturated fatty acid, the bilayer will become a more rigid gel-like structure, while a membrane rich in cis-unsaturated fatty acids will be more flexible. As an example, if phosphatidylcholine contains C18:0 acyl-chain in both the sn-1 and sn-2 position its melting point will be ~ 55 °C, which at body temperature would give it a solid rigid structure. If, however, the PUFA C18:2n-6 were instead attached at the sn-2 position, the phospholipid will now have a liquid crystalline state until ~ 15 °C, making it fluid at body temperature (Kahle, Schäfer, *et al.*, 2015; Lee, 1991).

The Unsaturation index (UI) is a measure of unsaturation that describes the fluidity of a biological membrane. It is useful in interpreting membrane and tissue fatty acid composition, fluidity, and basal metabolic rate (Weijers, 2012, 2015, 2016a; 2016b). Fatty acids can alter the physiochemical properties of cell membrane permeability by influencing cellular channels and G protein-coupled receptors (GPCRs) (Hussey, Lindley, *et al.*, 2017; Endo and Arita, 2016). As discussed, under cholesterol (Section 1.11), phospholipid membrane microdomains / lipid rafts are rich in cholesterol and sphingolipids. Lipid rafts enhance the permeability of the lipid bilayer and may regulate membrane bioactivity by facilitating protein interactions. Lipid rafts can concentrate proteins for transport in small vesicles or enable the proteins to function together such as GPCRs and transporters enabling the conversion of signals from extracellular to intracellular (Grouleff, Irudayam,

et al., 2015; Simons and Sampaio, 2011; Alberts, Johnson, *et al.*, 2002). Furthermore caveolae, which are formed from cholesterol, glycosphingolipids and proteins aided by CAV1 and CAV2 in a highly cholesterol-dependant process, act as distinct lipid-dense domains in the plasma membrane facilitating membrane transport including GLUT4 translocation and receptor signalling such as insulin (Haczeyni, Bell-Anderson, *et al.*, 2018). CAV1 is shown to be regulated by cholesterol, androgen and oestrogen (Haczeyni, Bell-Anderson, *et al.*, 2018; Breen, Camps, *et al.*, 2012). The orientation of the cholesterol hydroxyl groups to the PPL head group, allows for partial immobilization of the bilayer, and decreases the permeability of the bilayer to small water-soluble molecules (Simons and Sampaio, 2011; Alberts, Johnson, *et al.*, 2002). Membrane proteins and the lipids have bilateral compositional asymmetry. Certain phospholipids favour the inner leaflet such as PE, PE and PS and tend to be richer in PUFA and lower in SFA while PC and SG favour the outer leaflet and tend to be richer in SFA and lower in PUFA (Lorent, Levental, *et al.*, 2020; van IJendoorn, Agnetti, *et al.*, 2020; Rivel, Ramseyer, *et al.*, 2019; Simons and Sampaio, 2011; van Meer, 2011). Phospholipid unsaturation is similarly asymmetric, with a two-fold higher distribution of unsaturated fatty acids found in the cytoplasmic leaflet compared to the exoplasmic leaflet (Lorent, Levental, *et al.*, 2020).

The “triple cell membrane synergy” theory suggests that membrane phospholipids are protected from OS and lipid oxidation and peroxidation by protective antioxidants (Jové, Mota-Martorell, *et al.*, 2020; Pamplona, Barja, *et al.*, 2002). Cell membranes that undergo high and rapid activity such as axons, require a high membrane fluidity from DHA with the brain containing the highest levels of DHA and Na⁺/K⁺-ATPase. DHA incorporated into complexes with more phosphatidylethanolamine than phosphatidylcholine, is associated with increased protein kinase C (PKC) activity (Stillwell and Wassall, 2003). DHA levels in the membrane influences Na⁺-K⁺-ATPase pump with higher pump activity correlated with DHA levels, particularly in organs with high energy needs, such as in the heart and kidneys (Turner, Else, *et al.*, 2003). Conversely, the ‘membrane pacemaker’ hypothesis of metabolism, proposes that the FA composition of membranes, influences the peroxidation of lipids and if the membrane contains large amounts of unsaturated PUFA, this may lead to vulnerability and susceptibility to oxidative damage and decreasing longevity due to an increase in cellular metabolic rate (Hulbert, 2010).

The fluidity and flexibility of the cell membrane depends on the lipid types incorporated into the membrane structure; increased fluidity from incorporated unsaturated fatty acids (UFA) and decreased fluidity from incorporated SFA and cholesterol (Pilon, 2016). Consequently, a HFD rich in SFA may not only contribute to increased enlargement of fat depots but may also modulate tissue

and cell membrane lipid signatures. Altered membrane fluidity may also contribute to altered protein enrichment and localisation throughout the membrane, potentially affecting cellular function (Van Meer and de Kroon, 2011; Hulbert, Turner, *et al.*, 2005). One pertinent example of this is the association of decreased membrane fluidity with impaired insulin signalling and glucose uptake due to impaired insulin receptors and disrupted dispersion of GLUT4 glucose transporters respectively, throughout the cell membrane. This in turn may contribute to IR and the development of metabolic syndrome and diabetes, both co-morbidities of obesity (Pilon, 2016).

1.13 Microbiome and fatty acid synthesis

Along with the interplay of the gut microbiome and bile acid regulation, the microbiome also acts as a control of energy homeostasis and is strongly modulated by the diet. It has been reported that a high SFA, low fibre diet is associated with a greater abundance of *Anaerotruncus bacteria*, along with *Lachnospiraceae Flavonifractor*, *Campylobacter*, *Erysipelotrichaceae* and *Eisenbergiella* associated with an increased disease risk particularly related to obesity and pro-inflammatory disease (Bailén, Bressa, *et al.*, 2020). In obesity, an increased ratio of *Firmicutes/Bacteroidetes* ratio has been observed (Crovesy, Masterson, *et al.*, 2020). Similarly, a HFD has also been shown to modulate the composition and ratios of gastrointestinal microbiota, including an increased *Firmicutes/Bacteroidetes* ratio (Heiss, Mannerås-Holm, *et al.*, 2021; Gomes, Hoffmann, *et al.*, 2018). HFD has been shown to reduce microbial richness, while increasing Gram-negative bacteria that promote intestinal permeability and act as a source of lipopolysaccharide (LPS) that contributes to systemic inflammation and progression of metabolic diseases (Nakamura, 2012). These microbiota alterations affect gut-derived hormone levels impairing appetite regulation, enhance dietary energy harvest, increase intestinal permeability and lipopolysaccharides (LPS) circulating levels (Crovesy, Masterson, *et al.*, 2020; Gomes, Hoffmann, *et al.*, 2018; Nagpal, Newman, *et al.*, 2018; Trøseid, Nestvold, *et al.*, 2013; Turnbaugh, Ley, *et al.*, 2006). *Firmicutes* have a greater propensity for dietary carbohydrates (CHO) fermenting them into short chain fatty acids (SCFA's). A higher *Firmicutes/Bacteroidetes* ratio seen in high-fat diet may therefore contribute up to an additional 10% overall energy intake in the form of microbiota-derived SCFA's (Ibrahim, Anishetty, *et al.*, 2012). This may affect the expression of appetite-regulating hormone secretion, such as glucagon (*Gcg*) expression and GLP-1, PYY, and leptin levels (Gomes, Hoffmann, *et al.*, 2018; Nagpal, Newman, *et al.*, 2018) in response to intestinal energy availability (Tan, McKenzie, *et al.*, 2014).

Chronic levels of SCFA can lead to adverse effects and resistance to the anorexigenic hormones (Glucagon-like peptide (GLP-1), gut-hormone peptide (PYY), and leptin) effecting satiety and energy expenditure and a proclivity towards energy accumulation (Gomes, Hoffmann, *et al.*, 2018; Nagpal, Newman, *et al.*, 2018). A greater propensity for higher SCFA's in circulating plasma are reported to correspond to obesity-related gut microbiota communities that favour a higher *Firmicutes* to *Bacteroidetes* ratio (F/B) (Sonnenburg and Bäckhed, 2016; Turnbaugh, Ley, *et al.*, 2006). Excess SCFA's from the intestines are transported to the liver, converted to acetyl-CoA and propionyl-CoA and are fed into the tricarboxylic acid cycle for DNL and gluconeogenesis (Solinas, Borén, *et al.*, 2015). GbE supplementation also showed to improve insulin signalling/sensitivity in white adipose tissue and gastrocnemius muscle which is discussed in more detail further on (Hirata, Cruz *et al.*, 2019, Hirata, Pedroso *et al.*, 2019, Hirata *et al.*, 2015, Banin *et al.*, 2014). Owing to the reduced food intake associated with GbE supplementation, a pair-fed control group was also included for the microbiota study to account for caloric restriction. This group showed a similar microbiota phylum profile to that of the HFD only group, indicating that the quantity of SFA ingested may not account for the overall effect on the microbiota profiles. Interestingly, in a study by Heiss and colleagues, HFD-fed germ-free mice were protected from HFD-induced obesity hypothalamic inflammation and leptin resistance normally seen with an HFD. This was attributed to reduced fermentation and SCFA energy absorption from the intestine *via* a GLP-1 receptor-dependent mechanism (Heiss, Mannerås-Holm, *et al.*, 2021). Similarly, work by Wichmann and colleagues found that SCFA deficiency in germ-free mice increased glucagon (*Gcg*) expression and plasma GLP-1 levels, which was reversed by supplementing with SCFA or a HFD (Heiss, Mannerås-Holm, *et al.*, 2021; Wichmann, Allahyar, *et al.*, 2013). It also showed that GF-mice exhibit enhanced leptin sensitivity, independent of body weight and circulating leptin levels.

1.14 Obesity and adipocyte function

Levels of fat in westernised diet has led to higher caloric intake and increased levels of saturated fat (EFSA Panel on Dietetic Products and Allergies, 2010). A review of 28 clinical trials reported that there was a positive correlation with overweight and obesity and the proportion of fat-derived energy intake (Bray and Popkin, 1998). Obesity has a deleterious effect on metabolism and causes changes in adipose tissue physiology including adipocyte hypertrophy followed by hyperplasia caused by prolonged hypertrophy. Accompanying hypertrophy and hyperplasia is an increase in inflammatory immune cell infiltration and altered adipokine secretion (Chait and den Hartigh, 2020). Higher

incidences of metabolic disorders associated with obesity include IR (a major co-morbidity), metabolic syndrome, type II diabetes and atherogenic dyslipidaemia (Abdullah, Peeters, *et al.*, 2010; Salamone and Bugianesi, 2010) and an increased risk ratio of developing dementia in later years (Pugazhenthii, Qin, *et al.*, 2017).

Adipose tissue is classified into brown (BAT), beige and white (WAT), or with each possessing a different morphology. Brown adipose tissue is predominantly found in rodents but also in humans, particularly infants (Samuelson and Vidal-Puig, 2020; Carpentier, Blondin, *et al.*, 2018; Chusyd, Wang, *et al.*, 2016; Cypess, Weiner, *et al.*, 2015) and accounts for up to 2% of adipose tissue in humans (Cypess, Lehman, *et al.*, 2009). BAT gets its name from the high mitochondrion content and dense vascularization that appears brown when compared to WAT (Kwok, Lam, *et al.*, 2016). BAT functions to produce and dissipate heat derived from lipolysis through the activity of the uncoupled protein 1 (UCP-1) located in the inner membrane of the mitochondria (Carpentier, Blondin, *et al.*, 2018; Cypess, Lehman, *et al.*, 2009). Beige adipose tissue, a more recent addition to adipose tissue family, is where BAT tissue is found within WAT tissue (Shao, Wang, *et al.*, 2019; Harms and Seale, 2013; Sharp, Shinoda, *et al.*, 2012). WAT is confined to defined depot and subdivided into either subcutaneous (SAT), visceral (VAT) or ectopic. SAT is located under the skin, VAT located intra-abdominally, lining internal organs, and ectopic sequestered into locations not classically associated with adipose tissue storage. Tissues that produce WAT depots include the liver, the heart and pericardium, vascular tissue, omentum, mesentery, retroperitoneum, and epididymis (Chait and den Hartigh, 2020). Around 85% of WAT is subcutaneous and plays a major role in lipid storage in the form of TAG and supply of fatty acids to other tissues (Frayn and Karpe, 2013). Visceral WAT is confined predominantly to the mesentery, retroperitoneum and omentum and drains directly to the liver *via* portal circulation (Mittal, 2019). In body fat distribution from puberty, males tend to have more VAT, while females tend to have more SAT pre-menopause, while VAT may increase post-menopause (Chang, Varghese, *et al.*, 2018) with a strong genetic link to WAT distribution with a high degree of sex-heterogeneity which is stronger in females (Rask-Andersen, Karlsson, *et al.*, 2019).

Within adipose tissue, adipocytes make up around one third of all cells, with the rest of the tissue consisting of fibroblasts, endothelial cells, macrophages, stromal cells, immune cells, and pre-adipocytes (Chait and den Hartigh, 2020). Adipocytes are metabolic cells that aid whole-body energy homeostasis. In the postprandial phase, under the influence of insulin they store excess energy in the form of TAG. In times of need through hormonal signalling catecholamines trigger the breakdown of TAG resulting in lipolysis to glycerol and FA to provide energy substrate to the rest of the body

including muscle tissue, the brain, liver, kidneys, and heart (Vegiopoulos, Rohm, *et al.*, 2017). As such TAG are in a state of flux between storage and utilisation. Adipocytes respond to changes in the nutritional state, undergoing remodelling as necessary (Choe, Huh, *et al.*, 2016).

Obesity occurs when energy intake exceeds energy expenditure. Although adipocyte numbers are largely determined during childhood and tightly regulated in adults (Spalding, Arner, *et al.*, 2008), in times of excess energy intake, adipocytes continue to expand in size through hypertrophy to accommodate additional TAG molecules. Hypertrophic cells secrete adipokines that recruit adipose progenitor cells (pre-adipocytes) that mature into adipocytes, increasing the number of adipocytes available for TAG storage (hyperplasia) (Pyrina, Chung, *et al.*, 2020). If adipose tissue expansion becomes chronic, due to the limitation of hypertrophy and hyperphasia, changes in the quantity and quality of adipose tissue-resident cells may also occur, such as increased macrophage influx in response to IR as well as ectopic depositions of TAG into other tissues including visceral depots (Chait and den Hartigh, 2020; Alves-Bezerra and Cohen, 2017; Choe, Huh, *et al.*, 2016).

IR caused in overloaded or dysfunctional adipocytes in WAT leads to lipolysis and fatty acid mobilisation, continually releasing free fatty acids into circulation that bind to Toll-like receptors, further contributing to inflammation, dyslipidemia, and atherosclerosis (Koenen, Hill, *et al.*, 2021; Lopes, Corrêa-Giannella, *et al.*, 2016). Chronic low-level inflammation resulting from IR is associated with the activation of key signal transducers such as tumour necrosis factor- α (TNF- α), I κ B kinase β (IKK β) and c-Jun N-terminal kinase (JNK) (Lackey and Olefsky, 2016). This contrasts with metabolically healthy obesity (MHO) where people accumulate mostly subcutaneous depots, that is not accompanied with the same metabolic changes seen in metabolically unhealthy obesity (MUO), such as IR, inflammation, and hypertension (Barrea, Muscogiuri, *et al.*, 2021; Iacobini, Pugliese, *et al.*, 2019; Liu, Wang, *et al.*, 2019). Under normal circumstances, in the excess of energy intake, pancreatic insulin promotes DNL and the uptake and storage of excess glucose and TAG into the adipocyte lipid droplet, with secretion of TAG from functional adipocytes controlled by adipokines and lipokines (Vegiopoulos, Rohm, *et al.*, 2017). The secretion of adipokines varies depending on adipose tissues depots and adipocyte energy status. Adipokines FA oxidation and DNL as well as gluconeogenesis, glucose uptake, insulin signalling, and energy expenditure in the liver, brain, and skeletal muscle (Chait and den Hartigh, 2020). Metabolic changes in overloaded or dysfunctional adipocytes are associated with IR-related lipolysis and mobilisation of FA as well as the generation of lipotoxic DAG and ceramides (illustrated in Figure 1) and adverse adipokine profiles, low adiponectin, and high

leptin levels. Adverse adipokine levels secreted from adipose tissue, further contribute to systemic metabolic deterioration, affecting the liver, muscle, and brain (Vegiopoulos, Rohm, *et al.*, 2017).

Adiponectin is a systemic insulin sensitizing hormone and helps regulate lipid and glucose and lipid metabolism in adipocytes and other tissues such as the liver muscle and the pancreas. Adiponectin functions through two receptors, ADIPOR1 and ADIPOR2 facilitated by the docking of the adaptor protein (APPL1), highly expressed in adipose tissues, liver, and skeletal muscle. Signalling is mediated through peroxisome proliferator-activated receptors (PPAR) discussed in more detail later. Adiponectin increases hepatic fatty acid oxidation while decreasing hepatic gluconeogenesis and increases fatty acid oxidation and glucose uptake in skeletal muscle and WAT (Wang and Scherer, 2016). Adiponectin is also associated with anti-inflammatory properties in WAT, the pancreas and immune cells such as; regulating anti-inflammatory IL-10 production in macrophages; inhibiting tumour necrosis factor- α (TNF- α) induced NF- κ B pathways and monocyte adhesion in endothelial cells; inhibiting IL-2-induced Nuclear Factor Kappa Beta (NF- κ B) activation in natural killer cells; and inhibiting the production of ROS in neutrophils (Qiu, Wu, *et al.*, 2021; Esmaili, Hemmati, *et al.*, 2018; Kyriazi, Tsiotra, *et al.*, 2011; Robinson, Prins, *et al.*, 2011). Furthermore, adiponectin suppresses lipopolysaccharide (LPS)-induced NF- κ B activation in adipocytes and reduces the levels of lipotoxic ceramides and DAG levels in both WAT and B cells of the pancreas (Ye, Wang, *et al.*, 2015; Robinson, Prins, *et al.*, 2011; Ajuwon and Spurlock, 2005). Work by Bueno and colleagues have found that adiponectin gene expression was lowered in retroperitoneal WAT of mice fed a HFD enriched with either soybean oil, fish oil, coconut oil, or lard. Similarly, they also found that adiponectin expression was lowered in epididymal WAT of rats fed a HFD enriched with soybean or coconut oil. Adiponectin levels were also found to be lowered in 3T3-L1 cells treated with palmitic, LA, EPA, and DHA acids. Together this study indicated that the intake of certain fatty acids may affect adiponectin gene expression let specific (Bueno, Oyama, *et al.*, 2008).

Adiponectin expression and circulating levels are inversely proportional to adiposity levels. Increased visceral fat in overweight and obese subjects is associated with decreased total adiponectin levels, while weight loss is associated with improved adiponectin levels and significantly reduced inflammation (Gariballa, Alkaabi, *et al.*, 2019; Kishida, Kim, *et al.*, 2011). In dysfunctional adipocytes, adipose triglyceride lipase (ATGL/Pnpla2) increases the conversion of TAG to DAG. DAG activates protein kinase C which phosphorylates serine residues on insulin receptor substrate (IRS), thus inhibiting insulin Phosphatidylinositol 3-Kinase (PI3K)- Protein Kinase B (PKB/Akt) signalling. When IR occurs, both monoglyceride lipase (MGL/MgII) and hormone-sensitive lipase (HSL), normally

negatively regulated by insulin, promoting the conversion DAG to fatty acids, which are further converted to ceramides. Ceramides belong to the lipid class of sphingolipids and blocks insulin signalling by activating protein phosphatase 2A which in turn dephosphorylates Akt which in turn affects insulin signalling (Wali, Jarzebska, *et al.*, 2020). The increase in ceramides is directly linked to decreased adiponectin levels which mediates the activation of the adenosine monophosphate-activated protein kinase (AMPK) and promotes ceramide degradation responsible for the reduction of ceramide levels downstream of the AdipoR1 and AdipoR2 transmembrane adiponectin receptors (Sharma and Holland, 2017). Excess lipids that circulate along with lipid metabolites affect insulin sensitivity and glucose processing in the liver, reduce glucose uptake in muscle, and contribute to impaired glucose tolerance and T2DM (Vegiopoulos, Rohm, *et al.*, 2017; Samuel and Shulman, 2012). An increase in fatty acids mobilized from adipocytes also contributes to increased gluconeogenesis in the liver, which has been shown to be regulated more by adipocyte lipogenesis and FA transport to the liver where it is converted to acetyl-CoA, rather than by liver insulin levels (Titchenell, Quinn, *et al.*, 2016; Perry, Camporez, *et al.*, 2015). Interestingly, the fatty acid palmitoleate (C16:1) and palmitic acid-hydroxy-stearic acid (illustrated in Figure 1) which derive from adipocyte DNL, are associated with anti-diabetic and anti-inflammatory effects, and can improve systemic glucose metabolism. Their levels have been reported to be reduced in both serum and adipose tissue of high fat diet (HFD)-fed mice (Kellerer, Kleigrew, *et al.*, 2021; Hammarstedt, Syed, *et al.*, 2018; Syed, Lee, *et al.*, 2018).

The endocrine adipokine Leptin encoded by the obesity (*ob*) gene is expressed by adipocytes and regulates body weight by mediating food intake regulation and energy expenditure in the central nervous system (CNS). As adipocyte volume increases, leptin levels also increase. Leptin binds to the transmembrane leptin receptor (LEP-R) (a cognate receptor) and through a negative feedback loop between adipose tissue and the hypothalamus, inhibits the synthesis and release of neuropeptide Y/agouti-related protein (NPY/AgRP) in the arcuate nucleus (ARC) (Stephens, Basinski, *et al.*, 1995) and the dorsomedial hypothalamic nucleus (DMH) (Fei, Okano, *et al.*, 1997). Leptin receptor long isoform (LEP-Rb) inhibits the expression of NPY/AgRP an appetite stimulating protein. LEP-Rb also stimulate the expression of neuropeptide proopiomelanocortin (POMC), an appetite suppressing protein (Fruhwürth, Vogel, *et al.*, 2018), which stimulates the expression of alpha-melanocyte-stimulating hormone (α -MSH) which binds to the melanocortin receptor (MCR) (Münzberg, Flier, *et al.*, 2004; Cowley, *et al.*, *et al.*, 2001; Elias, Aschkenasi, *et al.*, 1999). This leads to appetite-suppression, inhibiting food intake and increasing energy expenditure (Obradovic, Sudar-Milovanovic, *et al.*, 2021;

Papathanasiou, Nolen-Doerr, *et al.*, 2019; Stern, Rutkowski, *et al.*, 2016; Park and Ahima, 2015). Leptin, together with hormones ghrelin and insulin induce acute responses in the melanocortin system of the hypothalamus in an opposing manner (Dietrich and Horvath, 2013). While Leptin enhances anorexigenic POMC/ α -MSH-expressing neuronal firing and decreases orexigenic NPY/AgRP neuronal firing (Izquierdo, Crujeiras, *et al.*, 2019; Moulton and Harvey, 2011). The stomach-derived hormone ghrelin enhances NPY/AgRP neuronal firing and decreases POMC cell firing (Lin, Hasegawa, *et al.*, 2016; Ueberberg, Unger, *et al.*, 2009; Kojima and Kangawa, 2005; Gauna, Meyler, *et al.*, 2004; Kojima, Hosoda, *et al.*, 1999). The insulin derived from the pancreas also affects ARC neuronal firing and has been shown to disrupt leptin mediated neuronal control (Nazarians-Armavil, Menchella, *et al.*, 2013) while ghrelin has been shown to improve insulin sensitivity as well as neurogenesis (Chung, Li, *et al.*, 2013; Li, Chung, *et al.*, 2013; Gauna, Meyler, *et al.*, 2004). Leptin works predominantly by inducing the Janus kinase (JAK)-signal transducer and activator of transcription (STAT) pathway (JAK-STAT3) pathway (Guo, Jiang, *et al.*, 2008). Insulin predominantly induces the Phosphatidylinositol 3-Kinase-AKT (PI3K-Akt) pathway (Hoy, Brandon, *et al.*, 2009; Liu, Hong, *et al.*, 2009; Vestergaard, Gormsen, *et al.*, 2008), while ghrelin induces JAK2/STAT3, PI3K-Akt and extracellular signal-regulated kinases (ERK1/2) pathways (Eid, Alkhateeb, *et al.*, 2018; Chung, Li, *et al.*, 2013; Li, Chung, *et al.*, 2013; Chung, Seo, *et al.*, 2008). Leptin also modulates lipid metabolism and lipolysis, proinflammatory immune responses and insulin sensitivity in several tissues (Stern, Rutkowski, *et al.*, 2016; Farr, Gavrieli, *et al.*, 2015). Circulating leptin serum levels strongly correlating to adiposity and body fat percentage. In a fasting state, plasma leptin levels decrease, promoting food intake, with feeding and overfeeding increasing *ob* gene expression and leptin levels (Kolaczynski, Considine, *et al.*, 1996; de Vos, Saladin, *et al.*, 1995). Leptin secretion displays a pulsatile-like circadian rhythm, with levels highest at midnight, and lowest in mid-afternoon, with a higher pulse amplitude in obesity where fat mass acts as an amplifier for leptin secretion (Koutkia, Canavan, *et al.*, 2003; Licinio, Negrão, *et al.*, 1998; Licinio, Mantzoros, *et al.*, 1997). Leptin resistance occurs due to defects in the leptin pathway including disruptions to leptin synthesis targeting cells, decreased LEP-R expression, and signalling (Izquierdo, Crujeiras, *et al.*, 2019). For example, decreased transport of leptin through LEP-R across the BBB has been reported, with excessive serum leptin levels contributing to decreased BBB permeability (di Spiezio, Sandin, *et al.*, 2018; Haddad-Tóvolli, Dragano, *et al.*, 2017; Burguera, Couce, *et al.*, 2000). This in turn affects hypothalamic control of satiety and appetite suppression, leading to excessive food intake and increase body weight, leading to obesity. Leptin levels have been found to be elevated in obesity without the proactive effects attributed to leptin on energy homeostasis

(Enriori, Evans, *et al.*, 2007; Münzberg, Flier, *et al.*, 2004; Heymsfield, Greenberg, *et al.*, 1999), with women more susceptible to resistance than men (Licio, Mantzoros, *et al.*, 1997). Leptin deficiency is also associated with obesity, hyperglycemia and IR (Obradovic, Sudar-Milovanovic, *et al.*, 2021). The consumption of a HFD can lead to leptin resistance in the ARC and ventral tegmental area (VTA) (Enriori, Evans, *et al.*, 2007; Münzberg, Flier, *et al.*, 2004; Heymsfield, Greenberg, *et al.*, 1999). Work from our group and others have shown that an HFD can stimulate suppressor of cytokine signalling 3 (SOCS3) expression and activation of STAT3 resistance by leptin in POMC, ARC and AgRP neurons in rodents while some compensatory mechanisms to leptin resistance may occur in both ARC and VTA regions (Machado, Banin, *et al.*, 2021; Machado, Pereira, *et al.*, 2021; Obradovic, Sudar-Milovanovic, *et al.*, 2021; Gamber, Huo, *et al.*, 2012; Münzberg, Flier, *et al.*, 2004; El-Haschimi, Pierroz, *et al.*, 2000).

1.15 Nuclear peroxisome proliferator-activated receptors (PPAR)

The nuclear peroxisome proliferator-activated receptors alpha and gamma (PPAR α/γ) are responsible for triggering gene transcription of lipid metabolism mediators involved in adipogenesis and β -oxidation, and contribute to the regulation of oxidative stress, inflammation, and neuroprotection (Han, Shen, *et al.*, 2017; Duvall and Levy, 2016; Echeverría, Ortiz, *et al.*, 2016; Motojima, Passilly, *et al.*, 1998; Martin, Schoonjans, *et al.*, 1997). PPAR α , stimulates β -oxidation lowering lipid levels by decreasing circulating TAG and free FAs, which in turn lowers the risk of hypertrophy and hyperplasia (Grygiel-Górniak, 2014). PPAR expression is ubiquitous but varies depending on the tissue. PPAR is predominantly expressed in tissues that undergo high rates of fatty acid catabolism, including the digestive tract, liver, heart, skeletal muscle, kidneys, and brain tissue, particularly in neurons and astrocytes (Tahri-Joutey, Andreoletti, *et al.*, 2021). A wide variety of lipophilic molecules/ligands activate PPAR α , which when bound, undergoes a conformational change triggering gene transcription involved in lipid metabolism and oxidation. Genes affected by PPAR α in the peroxisomal β -oxidation include acyl-CoA oxidase 1 (ACOX1), the enoyl-CoA hydratase/3-hydroxyacyl-CoA dehydrogenase (bifunctional proteins) and 3-ketoacyl-CoA Thiolase. ACOX1 is the rate-limiting step in the catabolism of long, very long, and branched FA (Moreno-Fernandez *et al.*, 2018) and affects mTOR localization affecting regulator of autophagy (He, Cui, *et al.*, 2021). As the PPAR α phosphorylation level increase, so does ACOX gene expression. The enoyl-CoA hydratase/3-hydroxyacyl-CoA dehydrogenase (bifunctional proteins) pathway that catalyses the hydration of short- and medium-chained FA and promotes mTOR activation (He, Cui, *et al.*, 2021). Finally, 3-

ketoacyl-CoA thiolase catalyses the cleavage of short and medium chain FA the final step in β -oxidation, generating acetyl-CoA and a fatty acyl-CoA ester (Adeva-Andany *et al.*, 2019). PPAR α also targets genes peroxisomal ATP-binding cassette sub-family D (ABCD) transporters (ABCD2 and ABCD3) (Rakhshandehroo, Knoch, *et al.*, 2010) with ABCD2 involved in the transport of VLCFA and LCFA and their Co-A derivatives into peroxisomes and ABCD3 involved in the transport of branched chain acyl-CoA into peroxisomes (Kawaguchi and Morita, 2016). Other mechanisms affected by PPAR include sterol-carrier proteins (SCP) and carnitine palmitoyltransferase 1A (CPT1) involved in the mitochondrial β -oxidation pathway (e.g., Acyl-CoA dehydrogenase (ACAD), the enoyl-CoA hydratase/3-hydroxyacyl-CoA dehydrogenase trifunctional proteins, subunit alpha and 3-ketoacyl-CoA Thiolase) and the cytochrome P450 enzyme CYP4A1 involved in microsomal ω -hydroxylation (Tahri-Joutey, Andreoletti, *et al.*, 2021).

Within the β -oxidation system, very long chain fatty acids (VLCFA) are shortened to LCFA in the peroxisome and participate in cellular thermogenesis and produce H_2O_2 (Cherkaoui-Malki, Surapureddi, *et al.*, 2012) while VLCFA and LCFA are further metabolised by mitochondrial β -oxidation for ATP synthesis *via* the oxidative phosphorylation pathway (Tahri-Joutey, Andreoletti, *et al.*, 2021). Two mammalian peroxisomal β -oxidation systems have been characterised to date. In the first β -oxidation system, four enzymes are involved in converting FA to acetyl-CoA and carbon-shortened acyl-CoA namely: ACOX1, multifunctional protein (MFP-1, a L-bifunctional protein consisting of the enzymes 2-Enoyl-CoA Hydratase And 3-Hydroxyacyl CoA Dehydrogenase), and 3-ketoacyl-CoA Thiolase (3-KT). Firstly, acyl-CoA is converted to 2-trans-enoyl-CoA by α , β -dehydrogenation by ACOX1. Next, enoyl-CoA is hydrated to L-3-hydroxyacyl-CoA by MFP-1, followed by dehydration to 3-ketoacyl-CoA. 3-ketoacyl-CoA is cleaved by 3-KT to produce one acetyl-CoA molecule and a two-carbon-shortened acyl-CoA (Tahri-Joutey, Andreoletti, *et al.*, 2021). MFP-1 is also be considered a trifunctional protein as it has auxiliary 3,2-trans-enoyl-CoA isomerase activity for the oxidation of UFA (Palosaari and Hiltunen, 1990). The second peroxisomal β -oxidation system is involved in the conversion of -methyl branched fatty carboxylates such as bile acid intermediates, involving 2-methylacyl-CoA-specific oxidases, the second multifunctional protein (MFP2, D-bifunctional protein consisting of the enzymes 2-Enoyl-CoA Hydratase And 3-Hydroxyacyl CoA Dehydrogenase) and the sterol-carrier protein (SCP-2) involved in thiolase activity (Tahri-Joutey *et al.*, 2021). During a mitochondrial β -oxidation cycle, 2 proteins are responsible the initial breakdown of VLCFA into long and medium chain FA. The first reaction involves the enzyme acyl-CoA dehydrogenase (ACAD). The three remaining reactions are carried out by a multifunctional protein

named trifunctional protein (TFP) which consists of two subunits. The first α -subunit contains the enzymes 2-enoyl-CoA hydratase (ECH) and 3-hydroxyacyl-CoA dehydrogenase (HAD) while the β -subunit encompasses the 3-KT enzymatic activity (Xia, Fu, *et al.*, 2019). Subsequent long and medium chain FA derived from VLCFA, are further degraded to Acetyl CoA by four separate reactions by individual acyl-CoA dehydrogenase (ACAD), 2-enoyl-CoA hydratase (ECH), 3-hydroxyacyl-CoA dehydrogenase (HAD) and 3-KT enzymes for use in the TCA cycle (Tahri-Joutey, Andreoletti, *et al.*, 2021; Wanders, Waterham, *et al.*, 2016). Fatty acids are activated outside the organelle by conjugation to either coenzyme A for peroxisomes or carnitine for mitochondria. LCFA must be actively transported into the peroxisome and mitochondria by ABC membrane transporters (ABCD subfamily) and very-long-chain acyl-CoA synthetases as they are unable to diffuse across the membrane. Shorter and medium chains may enter the mitochondria by diffusion before activation (Andreoletti, Raas, *et al.*, 2017; Schrader, Costello, *et al.*, 2015; Watkins and Ellis, 2012).

PPAR ligands include SFA, UFA and PUFAs, as well as their metabolites (Liput, Lepczyński, *et al.*, 2021; Chen, Shang, *et al.*, 2020; Forman, Chen, *et al.*, 1997; Kliewer, Sundseth, *et al.*, 1997). LC-PUFA are the natural ligands of PPAR α/γ , where n-3 PUFA, namely EPA (C20:5n-3) and DHA (C22:6n-3), bind with high affinity for activation (Duszka, Gregor, *et al.*, 2020; Kosgei, Coelho, *et al.*, 2020; Laleh, Yaser, *et al.*, 2019; Kersten and Stienstra, 2017; Pawar and Jump, 2003). n-6 LC-PUFA such as LA (C18:2n-6) and AA (C20:4n-6), n-3 DPA (C22:5n-3) and ω -9 erucic acid (C22:1n-9) have also been shown to stimulate PPAR activity (Chen, Shang, *et al.*, 2020; Laleh, Yaser, *et al.*, 2019; Duvall and Levy, 2016; Echeverría, Ortiz, *et al.*, 2016; Hostetler, Kier, *et al.*, 2006; Pawar and Jump, 2003). Endogenous FA metabolites also act as PPAR ligands including acyl CoAs, oxidised fatty acids, PPL, eicosanoids, endocannabinoid-like molecules and lipoprotein lipolytic products (Liput, Lepczyński, *et al.*, 2021). The effects of dietary n-3 and ω 6 PUFA in inflammation signalling is excellently reviewed by Liput and colleagues (2021) and pictorially represented in Figure 6. Bio-active oxylipins are derived from PUFA and may be released from phospholipid membranes and secreted, or remain cell bound and exert their biological function (e.g., oxidized phospholipids) (O'Donnell and Murphy, 2012, 2017; Hammond and O'Donnell, 2012). AA-derived oxylipins including prostaglandins, thromboxanes and leukotrienes are pro-inflammatory with prolonged production leading to chronic inflammation. Oxylipins derived from n-6 PUFA Dihomo- γ -linolenic acid (DGLA), Adrenic acid (AdA) and n-3 Eicosapentaenoic acid (EPA) produce less pro-inflammatory oxylipins. Oxylipins derived from n-3 PUFA Docosapentaenoic acid (DPA) and Docosahexaenoic acid (DHA) act as specialised pro-resolving

mediators (SPMs) and help to prevent chronic inflammation (Schebb, Kühn, *et al.*, 2022; Liput, Lepczyński, *et al.*, 2021).

It is reported that the oxidised form of EPA and LDL- cholesterol readily undergo oxidation and are more stimulatory of PPARs than native non-oxidised forms (Sethi, Ziouzenkova, *et al.*, 2002). Oxidized n-3 fatty acids have also been reported to inhibit NF- κ B activation *via* a PPAR α -dependent pathway (Mishra, Chaudhary, *et al.*, 2004). PPAR γ regulates adipogenesis, energy balance and lipid biosynthesis while PPAR β/δ participates in skeletal and cardiac fatty acid oxidation and helps regulate blood glucose and cholesterol levels (Grygiel-Górniak, 2014). Exogenous PPAR activators include dietary PUFA such as EPA and DHA and plant extracts such as polyphenolic flavonoids, isoflavonoids, terpenes, steroids, carotenoids, coumarins, lignans, and tannins (Liput, Lepczyński, *et al.*, 2021; Tahri-Joutey, Andreoletti, *et al.*, 2021; Ngoc, yen Man, *et al.*, 2019; Singh, 2018; den Besten, Bleeker, *et al.*, 2015; Dozsa, Dezso, *et al.*, 2014; Grygiel-Górniak, 2014; Wang, Waltenberger, *et al.*, 2014; Ko, Lee, *et al.*, 2010; Mueller and Jungbauer, 2009). The regulation of peroxisomal fatty acid β -oxidation by PPAR receptors by endogenous and exogenous sources is excellently reviewed by Tahri-Joutey *et al.*, (2021) and Grygiel-Górniak (2014). Synthetic PPAR α activators and PPAR γ agonists are used for the treatment of dyslipidemia and T2DM. PPAR α/γ dual agonist drugs work by reducing hyperlipidaemia and hypertension and act in an antiatherogenic, anti-inflammatory and anticoagulant capacity. Interestingly, the overexpression of PPAR β/δ prevents the development of obesity by diminished lipid accumulation in the presence of a HFD, while increasing glucose metabolism, protecting against ischemia-reperfusion injury (Yu, Chang, *et al.*, 2008).

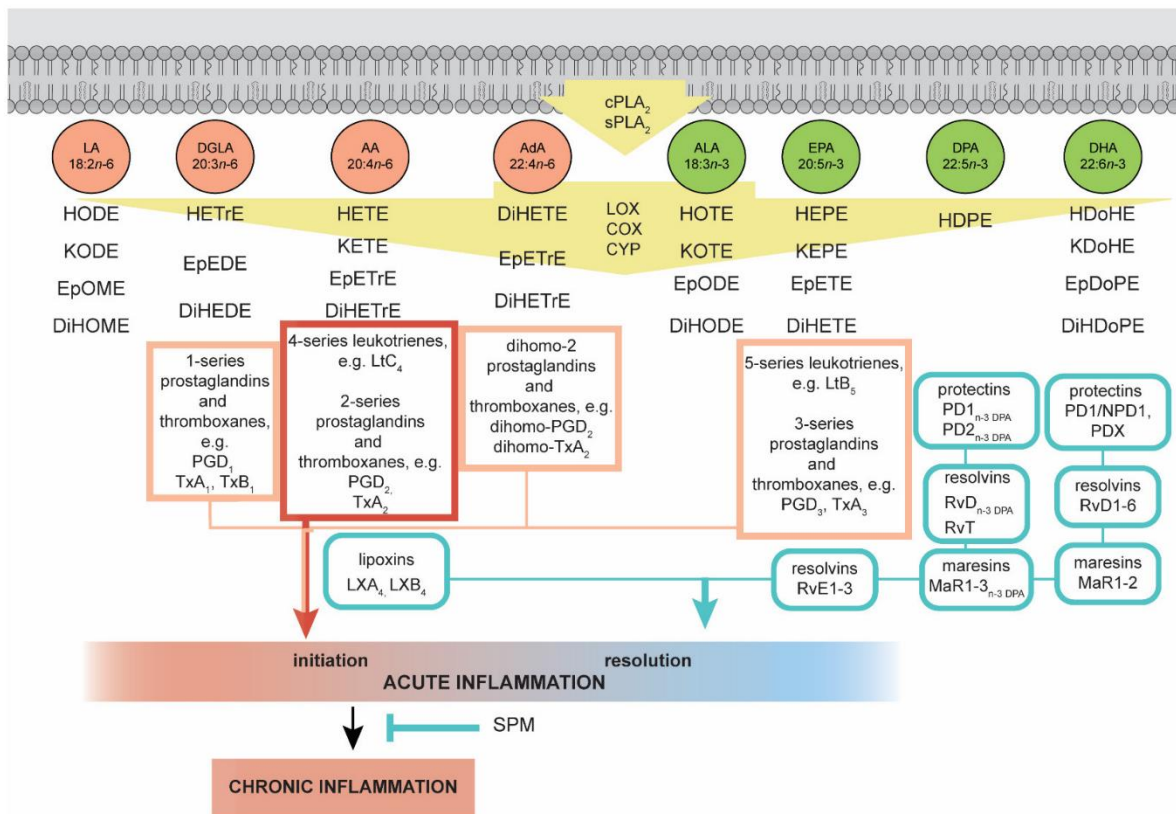


Figure 6. Lipid mediators enzymatically derived from n-6 and n-3 and polyunsaturated fatty acids (PUFAs) and their role in inflammation. Bio-active oxylipins are derived from PUFA released from phospholipid membranes. Arachidonic acid (AA)-derived oxylipins (marked in red) including prostaglandins, thromboxanes and leukotrienes are pro-inflammatory with prolonged production leading to chronic inflammation. Oxylipins derived from n-6 PUFA Dihomo- γ -linolenic acid (DGLA), Adrenic acid (AdA) and n-3 Eicosapentaenoic acid (EPA) produce less pro-inflammatory oxylipins. Oxylipins derived from n-3 PUFA Docosapentaenoic acid (DPA) and Docosahexaenoic acid (DHA) (marked in blue) function as specialised pro-resolving mediators (SPMs) and help to prevent chronic inflammation (Figure from Liput et al., 2021).

1.16 Inflammation and fatty acids

Inflammation is modulated by the levels of SFA, MUFA and n-6 and n-3 PUFA within the cell and membrane. Both n-6 linoleic acid (LA) and n-3 α -linolenic acid (ALA) are essential in mammals as they cannot be synthesised *de novo*, but when absorbed from the diet, can be converted to long-chain polyunsaturated fatty acids (LC-PUFAs), and serve as important regulators of inflammation. Both n-6 and n-3 PUFA utilize the same fatty acid pathway and enzymes to convert LA and ALA into LC-PUFA. In fact, the activity of $\Delta 6$ -desaturase that converts LA (C18:2n-6) to Gamma (γ)-LA (GLA; C18:3n-6) and ALA (C18:3n-3) to stearidonic acid (C18:4n-3) is limited during inflammatory conditions (Burdge and Calder, 2005; Calder and Grimble, 2002). As illustrated in Figure, SPMs are produced from both n-6 and n-3 PUFA, with the most significance influencers in inflammation being AA (C20:4n-6), Dihomo- γ -linolenic acid (DGLA; C20:3n-6) and EPA (C20:5n-3). Oxylipins derived from FA increase intercellular calcium concentrations, facilitating the translocation of cytosolic phospholipase A2 (cPLA2) to the cell membrane, that then cleaves PUFA from the sn-2 position of phospholipids (Yeung, Hawley, *et al.*, 2017). The enzymes cyclooxygenases (COX), lipoxygenases (LOX) and cytochrome P450 (CYP) oxidize the PUFA AA (C20:4n-6), DGLA (C20:3n-6) and EPA (C20:5n-3) creating the oxylipin subclass eicosanoids (Gabbs, Leng, *et al.*, 2015). PUFA derived oxylipins subclasses are referred to as octadecanoids if formed from LA (C18:2n-6) and ALA (C18:3n-3), and docosanoids if derived from Adrenic acid (AdA; C22:4n-6), DPA (C22:5n-3) and DHA (C22:6n-3) (Astarita, Kendall, *et al.*, 2015; Gabbs, Leng, *et al.*, 2015; Godessart, Camacho, *et al.*, 1996). Resolvins, protectins and maresins, are biosynthesized from n-3 PUFA and are more anti-inflammatory, while lipoxins biosynthesized from n-6 PUFA are more pro-inflammatory. SPMs regulate cytokine and chemokine production as well as vascular tone, blood pressure and the infiltration of neutrophils and their clearance of by macrophages (Duvall and Levy, 2016; Serhan and Petasis, 2011). Resolvin E-series are derived from EPA through the conversion of 18-hydroxyeicosapentaenoic acid (18-HEPE). DHA is the FA precursor of protectins, resolvin D-series and maresins (Endo and Arita, 2016). Higher n-3 PUFA levels are also associated with decreased tumour necrosis factor (TNF), interleukin-1 β (IL-1 β) and interleukin-6 (IL-6) cytokines. EPA and DHA are also converted by CYP450 monooxygenase to epoxyeicosatetraenoic acids (EpETEs) and epoxydocosapentaenoic acid (EpDPAs) (Endo and Arita, 2016) n-6 and n-3 FA are also precursors of endogenously produced cannabinoids, ligands of the cannabinoid receptor 1 and 2 (CB1 and CB2), with CB1 predominantly found in the CNS while CB2 is present predominantly in immune cells. Endogenous cannabinoids are metabolized by COX, LOX and CYP which can block pro-inflammatory IL-6. AA is also the precursor of the cannabinoids anandamide (AEA) and 2-

arachidonoylglycerol (2-AG) while EPA is the precursor for eicosapentaenoyl ethanolamide (EPEA) and DHA is the precursor for docosahexanoyl ethanolamide (DHEA) (Liput, Lepczyński, *et al.*, 2021). As well as enzymatically linked and controlled oxidation of phospholipid PUFA, PUFA are also susceptible to free radical-induced autoxidation and photodegradation, due to the presence of their double bonds. These have a similar bioactivity to enzymatically oxidised PUFA acting as pro-resolving mediators of inflammation (Campillo, Medina, *et al.*, 2021; Bosviel, Joumard-Cubizolles, *et al.*, 2017; Friedli and Freigang, 2017). Free radical-induced autoxidation and photodegradation creates non-enzymatic pro-resolving metabolites such as ALA-derived phytoprostanes (PhytoPs), EPA- and AA-derived isoprostanes (IsoPs), AdA-derived dihomoisoprostanes (dihomo-IsoPs) derived and DHA-derived neuroprostanes (NeuroPs) (Liput, Lepczyński, *et al.*, 2021; Galano, Lee, *et al.*, 2017). IsoPs, NeuroPs and PhytoPs are considered harmful biomarkers for uncontrolled oxidative damage (Liput, Lepczyński, *et al.*, 2021; Ahme, Galano, *et al.*, 2020; Hajeyah, Griffiths, *et al.*, 2020; Medina, Gil-Izquierdo, *et al.*, 2018; Galano, Lee, *et al.*, 2017; Milne, 2017), while NeuroPs are reported to have the same pre-resolving capacity as protectins (Bosviel, Joumard-Cubizolles, *et al.*, 2017).

Returning to eicosanoids, they are biologically active paracrine and autocrine signalling molecules and are subdivided into prostaglandins (PG), thromboxanes (TXs) and leukotrienes (LTS). They have a broad range of functions including inflammation, the immune response, cardiovascular homeostasis, and cell growth regulation (Evangelista, Cho, *et al.*, 2020; Djuric, Bassis, *et al.*, 2019; Djuric, Turgeon, *et al.*, 2017; Marion-Letellier, Savoye, *et al.*, 2016; Aldrovandi, Hammond, *et al.*, 2013; Node, Huo, *et al.*, 1999). AA-derived thromboxane A₂ is produced by the COX pathway, while AA-derived leukotriene B₄ is produced by the LOX pathway. These are proinflammatory and vasoconstrictive eicosanoids. Anti-inflammatory and anti-aggregatory eicosanoids are also produced from AA including prostacyclin, lipoxin A₄, lipoxin B₄ and epoxyeicosatrienoic acids (EETs) produced by cytochrome P450 epoxygenase which induce vasodilation and angiogenesis (Oni-Orisan, Edin, *et al.*, 2016; Harris, Mozaffarian, *et al.*, 2009; Serhan, 2005; Node, Huo, *et al.*, 1999). Prostaglandins (PG) belong to the prostanoid section of the oxylipin family and contain a five-membered ring encompassing carbons 8 to 12. Following the prefix "PG", a letter (A-K) is assigned depending on nature and the position of the substituents on the ring. For example, prostaglandin E₂ (PGE₂) contains a keto group, on the ring, while prostaglandin F (PGF) contains two hydroxyl groups. A numerical subscript (1-3) is also used to denote the number of double bonds in the alkyl substituents (Christie, 2006).

Of the three types of prostaglandins produced from eicosanoids, PGE1 is associated with reducing inflammation (Fang, Li, *et al.*, 2010), redness and swelling, while PGE2 works in reverse, promoting inflammation, vasoconstriction and is pro-aggregatory (Kawahara, Hohjoh, *et al.*, 2015). PGE3 works to mitigate inflammation caused by PGE2 (Nagy and Tiuca, 2017; Fan, Davidson, *et al.*, 2014; Yang, Chan, *et al.*, 2004). PGE1 is converted from DGLA. DGLA may also be converted to AA by $\Delta 5$ -desaturase, which can then be converted to inflammatory PGE2. $\Delta 5$ -desaturase whose activity is limited also serves to convert C20:4n-3 to C20:5n-3 (EPA), with preferential activity given to n-6 conversion when higher levels of n-6 and lower levels n-3 PUFA, as is common in WSD. Taken together this means that when dietary intake of n-3 FA is low, $\Delta 5$ -desaturase will convert DGLA to more pro-inflammatory AA, while if higher n-3 FA are ingested and available, $\Delta 5$ -desaturase will be used in the n-3 pathway. Due to the tight regulation of LA to AA however, it is reported that variations in LA intake may not lead to an increase in AA tissue content (Rett and Whelan, 2011).

Notwithstanding, the n-6/n-3 balance is therefore an important indicator and modulator of inflammation with recommendations of 6:1 or less for overall health, and a ratio of 1:1 for functional phospholipid and brain health as well as obesity (Husted and Bouzinova, 2016; Deckelbaum, 2010; Schmitz and Ecker, 2008; Harbige, 2003; Simopoulos, 2002; Broughton, Whelan, *et al.*, 1991). An unbalanced n-6/n-3-ratio upwards of 20+:1 is commonly found in a WSD. Although AA is normally associated with being pro-inflammatory, some studies have suggested that 5-10% of overall energy intake from n-6 fatty acid can be protective and help reduce inflammatory states in coronary heart disease when taken as part of a low SFA, low cholesterol diet (Harris, Mozaffarian, *et al.*, 2009). As n-6 PUFA generate more potent mediators of inflammation than that of n-3 PUFA, this results in an abnormally proinflammatory cellular environment (Simopoulos, 2001, 2008, 2016; Kang, 2003; Yam, Eliraz, *et al.*, 1996). EPA also competes with AA within the COX and LOX pathways in prostaglandin formation. A high n-6 PUFA dietary intake increases the levels of LA, DGLA and AA-derived oxylipins (Caligiuri, Love, *et al.*, 2013), while a n-3 PUFA intake increases ALA, EPA and DHA derived oxylipins (Hussey, Lindley, *et al.*, 2017). This was demonstrated *in vivo* when rats were fed a diet of either LA or LA+ALA for 6 weeks with the containing either approximately 18:1 or 8:1 LA/ALA ratio, respectively. The high n-6 /n-3-ratio of approximate 18:1 LA/ALA resulted in an increase in n-6/n-3 oxylipins in the liver compared with a lower ratio LA/ALA diet. Interestingly, the level of LA-derived tissue oxylipins was greater than the proportion of LA. Increased ingestion of LA, from both LA and LA+ALA diets resulted in increased LA and AA oxylipins in the kidney and liver, while the higher LA-only diet increased LA and AA oxylipins in serum (Leng, Winter, *et al.*, 2017).

1.17 Effect of western-style diet/high fat diet on intracellular signalling cascades

IR, predominantly associated with T2DM, chronic hyperglycaemia and obesity, has been positively correlated with decreased cognition in an ageing population (Cunnane, Nugent, *et al.*, 2011). IR appears to contribute to abnormal brain glucose metabolism, with upregulation of insulin receptors in AD (Frölich, Blum-Degen, *et al.*, 1998; Hoyer, 1992). Hyperglycaemia and hyperinsulinemia, more commonly associated with T2DM, metabolic syndrome and obesity have also been positively correlated with the pathogenesis of AD (Baker, Cross, *et al.*, 2011; Matsuzaki, Sasaki, *et al.*, 2010; Okereke, Kang, *et al.*, 2008). Microvascular complications of hyperglycaemia include low perfusion rates and increased vascular permeability attributed to abnormal proliferation of endothelial cells which can affect the BBB (Prasad, Sajja, *et al.*, 2014). These disturbances can also lead to an overproduction of mitochondrial superoxide leading to the exaggerated activation of intracellular signalling cascades, including PI3-K/Akt (Huang, Liu, *et al.*, 2018) lipid peroxidation and increased formation of advanced glycation end products (AGEs) (Dias and Griffiths, 2014). These master regulatory switches are involved in neural cell metabolism, survival, growth, differentiation, and apoptosis. Other downstream metabolic switches have all been recently implicated in AD, including the mammalian Target of Rapamycin (mTOR), glycogen synthase kinase 3 (GSK3), the predominantly antioxidant Nuclear Factor Erythroid-2 related factor 2 (Nrf2) and the predominantly pro-inflammatory NF- κ B (Ahmad, Ijaz, *et al.*, 2017; Mazzanti and Giacomo, 2016; Shen, Cheng, *et al.*, 2016; Csiszár, Csiszar, *et al.*, 2015). The activation of the Receptors for AGEs (RAGE) can activate - and be activated by NF- κ B. NF- κ B signalling can generate increasing and self-perpetuating levels of OS, amplifying inflammatory signalling and the transcription of pro-inflammatory proteins involved in cell differentiation and apoptosis. This can lead to synaptic instability and neural dysfunction (Weil, 2012). Nrf2 modulates cellular responses to OS, with Nrf2 levels moderated by the intensity of OS experienced. Nrf2 is activated by OS, allowing its translocation to the nucleus where it facilitates the transcription of antioxidant and Phase 2 detoxifying enzymes that combat OS (Villeneuve, Lau and Zhang 2010). The mTOR pathway helps regulates cell growth, proliferation, motility, survival, protein synthesis and gene transcription. While increased levels of mTOR are involved in a chronic pro-inflammatory state (Scannevin, Chollate, *et al.*, 2012), decreased mTOR activity improves response to OS and cell survival (LiCausi and Hartman, 2018).

There is evidence that specific nutrients such as FA can influence the activity of these molecular switches (Fiala, Kooij, *et al.*, 2017; Gardener, Gu, *et al.*, 2012) but the extent of how this can be achieved, and the molecular partners involved, remain largely unknown. As previously mentioned

PUFA play specific roles in modulating the inflammatory response, gene expression, synaptic stability, cell survival and apoptosis (Bazinet and Layé, 2014; Yates, Calder, *et al.*, 2014; Ledesma, Martin, *et al.*, 2012). With an approximate ratio of 1:1 of n-3 and n-6 PUFA in neural PPL of a healthy brain, neural tissue relies heavily on these for antioxidant protection and proper cell membrane function (Yates, Calder, *et al.*, 2014; Serhan, Dalli, *et al.*, 2012). Therefore, a fine balance between pro- and anti-inflammatory lipid mediation is necessary for optimum neural bioactivity and homeostasis (Fraser, Tayler, *et al.*, 2010; Crawford, 1992). An unbalanced n-6/n-3 ratio upwards of 20+:1, commonly found in WSD can lead to imbalanced PUFA ratios in the brain. With n-6 PUFA generating more potent mediators of inflammation than that of n-3, this results in an abnormally proinflammatory cellular environment (Simopoulos, 2001, 2008, 2016; Kang, 2003; Yam, Eliraz, *et al.*, 1996). Long term, this distorted fatty acid ratio can lead to abnormally increased NF- κ B activity contributing to neuro-inflammation and disturbed neural activity, both manifestations already attributed to AD (Simopoulos, 2008). Research also shows that rats treated with an SFA-HFD develop hyperinsulinaemia and hypothalamic IR (Dornellas, Watanabe, *et al.*, 2015). In contrast, a higher intake of n-3 PUFA is has been shown to be anti-inflammatory (Ghosh, DeCoffe, *et al.*, 2013) and improves insulin sensitivity in both men and women (Abbott, Burrows, *et al.*, 2016; Albert, Derraik, *et al.*, 2014; Tsitouras, Gucciardo, *et al.*, 2008). Supplementation with EPA and DHA in some studies improves IR and symptoms related to diabetes and metabolic syndrome (Park, Lim, *et al.*, 2016).

1.18 Polyphenols, obesity and inflammation

Lower nutritional status and obesity have both been reported to impact on the progression of AD (Abate, Marziano, *et al.*, 2017; Hu, Yu, *et al.*, 2013; Saragat, Buffa, *et al.*, 2012). Meta-analysis suggests that adherence to a Mediterranean diet has been linked to decreased risk of mild cognitive impairment and AD (Singh, Parsaik, *et al.*, 2014). The Mediterranean diet is based on high consumption of fruits and vegetables, pulses, seafood, olive oil and moderate wine consumption, which leads to better n-6/n-3 PUFA ratios, lower levels of saturated fat and an abundance of phytochemicals including plant antioxidants and polyphenolic compounds (Schwingshackl, Morze, *et al.*, 2020; Ditano-Vázquez, Torres-Peña, *et al.*, 2019; Román, Jackson, *et al.*, 2019). The consumption of red wine is one aspect associated with the “French paradox”. The “French Paradox” was first described in the 1980’s (Ferrières, 2004) where despite the French eating model containing higher dietary saturated fats, cholesterol and red wine, the diet is inversely associated with overweight and

obesity (Ducrot, Méjean, *et al.*, 2018) and affords cardiovascular and neurological protective properties (Obrenovich, Siddiqui, *et al.*, 2020; Obrenovich, Tabrez, *et al.*, 2020; Davies, Cillard, *et al.*, 2017; Sun, Simonyi, *et al.*, 2002) including lower levels of liver and cardiovascular disease and AD (Obrenovich, Siddiqui, *et al.*, 2020; Davies, Cillard, *et al.*, 2017; Ferrières, 2004). Polyphenols help prevent ROS damage by scavenging free radicals and (Yang *et al.*, 2016; Zhang and Tsao, 2016)al., 2016; Zhang and Tsao, 2016). Many polyphenolic compounds have been identified to offer neuroprotective properties against AD (Colizzi, 2019). Red wine contains a number of polyphenolic compounds, including resveratrol, quercetin, kaempferol and isorhamnetin (Obrenovich, Siddiqui, *et al.*, 2020; Kurin, Fakhruddin and Nagy, 2013) which are structurally similar (LaFoya, Munroe, *et al.*, 2019; Zamin, Filippi-Chiela, *et al.*, 2009) and are shown in Figure 7 A-D. Resveratrol is abundantly found in the Mediterranean diet, not just in red and purple grapes, but also tomatoes, berries and peanuts (Sebastià, Montoro, *et al.*, 2012, 2017; Burns, Yokota, *et al.*, 2002). It has been shown *via in vivo* animal studies that resveratrol is bioavailable (Vingtdeux *et al.*, 2010; Karuppagounder *et al.*, 2009). More recent clinical Phase 2 human trials with resveratrol have shown promising results for mild to moderate AD (Sawda, Moussa, *et al.*, 2017; Turner, Thomas, *et al.*, 2015). While resveratrol has limited bioavailability due to its fast metabolism, it has been successfully found in the CSF, indicating its ability to cross the BBB (Sawda, Moussa, *et al.*, 2017; Turner, Thomas, *et al.*, 2015). The results of Moussa *et al.*, (2017) and Turner *et al.*, (2015) also point to reduced permeability of the central nervous system (CNS) and BBB to pro-inflammatory agents through the reduction of matrix metalloproteinase-9 (MMP-9) in addition to lower accumulation of A β in the brain. Investigations into the role grape-derived polyphenols have on AD have reported moderation of A β neuropathology through inhibited A β generation and increased A β clearance. Similar modulation of tau neuropathology as also been reported through inhibition of abnormal tau phosphorylation and tau aggregation (Ho, Ferruzzi, *et al.*, 2013; Sun, Wang, *et al.*, 2010; Ho, Chen, *et al.*, 2009; Ono, Condrón, *et al.*, 2008; Vingtdeux, Dreses-Werringloer, *et al.*, 2008; Wang, Ho, *et al.*, 2008; Marambaud, Zhao, *et al.*, 2005).

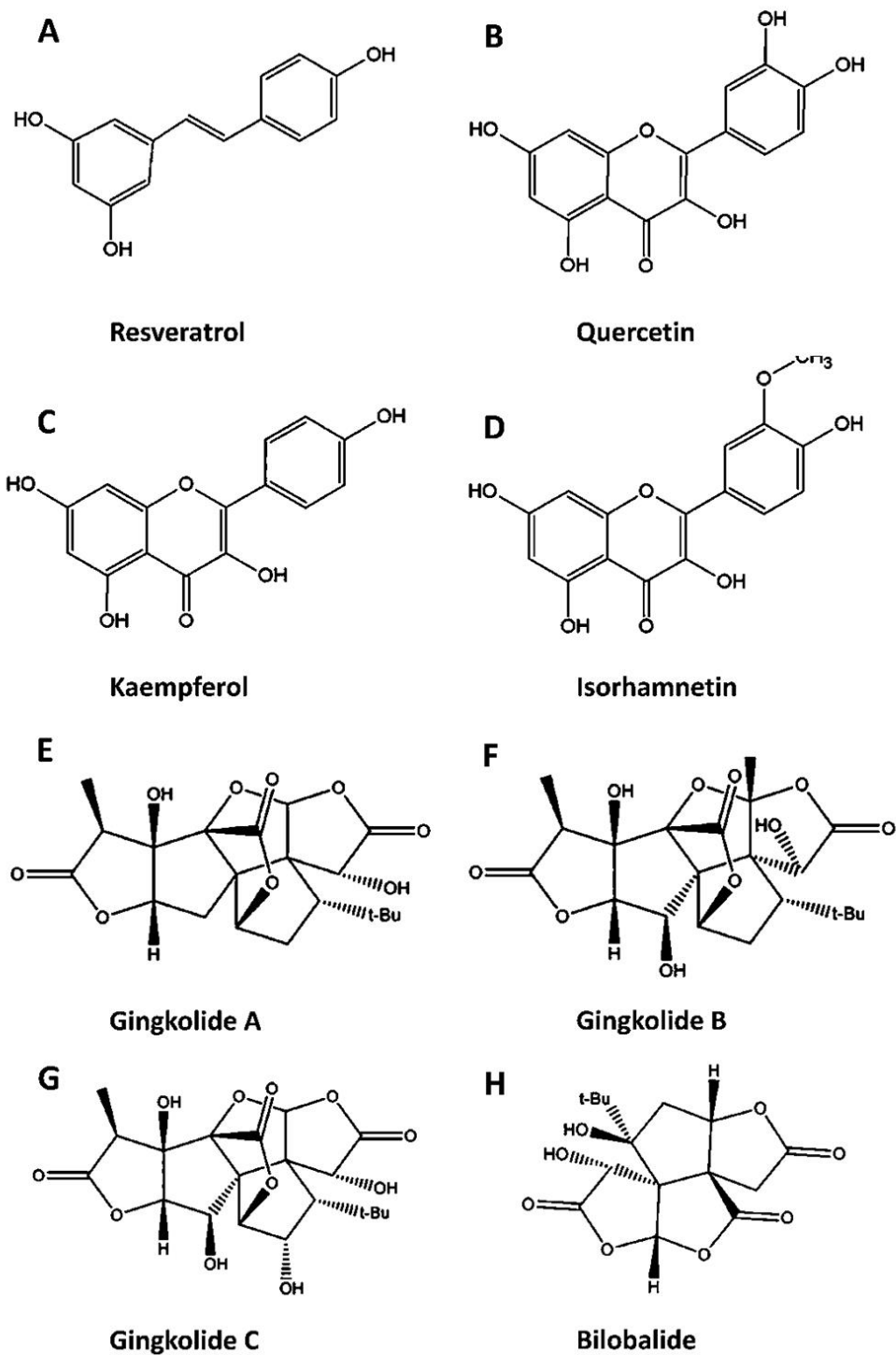


Figure 7. The chemical structures of polyphenols found in red wine (**A-D**) and Ginkgo biloba extract (GbE) (**B-H**) (Adapted from Hirata, Pedroso et al., 2019 and Kurin et al., 2013).

Ginkgo biloba extract (GbE) is another supplement rich in polyphenols and is one of the most widely used herbal supplements globally (Isah, 2015). Standardized extract of *Ginkgo biloba* leaves (EGb761) contains 24% flavonoid glycosides (including quercetin, kaempferol, isorhamnetin, also found in red wine) and 6% terpenoids divided into 3.1% ginkgolides and 2.9% bilobalides and approximately 10% low molecular weight organic acids (Hirata, Pedroso, *et al.*, 2019; Shi, Liu, *et al.*, 2010). The chemical structures of quercetin, kaempferol, isorhamnetin, ginkgolides and bilobalides are shown in Figure 7 B-H.

Owing to its reported neuroprotective properties (Singh, Srivastav, *et al.*, 2019; Rhein, Giese, *et al.*, 2010; Longpré, Garneau, *et al.*, 2006; Ramassamy, 2006; Ahlemeyer and Krieglstein, 2003a, 2003b; Ponto and Schultz, 2003). GbE is increasingly trialled for peripheral vascular disease treatment (Tian, Liu, *et al.*, 2017) and the treatment and prevention of neurodegenerative dementias associated with ageing and Alzheimer's Disease (Rhein, Giese, *et al.*, 2010; Zimmermann, Colciaghi, *et al.*, 2002; Luo, 2001). Like that of resveratrol, GbE it has been shown to protect against A β -induced neurotoxicity (Mango, Weisz, *et al.*, 2016; Shi, Zhao, *et al.*, 2009; Smith and Luo, 2003; Bastianetto, Ramassamy, *et al.*, 2000), preventing amyloidogenesis and fibril formation (Ramassamy, 2006; Colciaghi, Borroni, *et al.*, 2004; Luo, Smith, *et al.*, 2002) and inhibits metalloproteinase (MMP)-9 activity (Huang, Yang, *et al.*, 2013). In the hippocampus and cortex of mice, GbE has been shown to up-regulate expression of tau related proteins including microtubule-associated tau protein and neural protein phosphatase type 1 which dephosphorylates hyper-phosphorylated tau protein (Watanabe, Wolfram, *et al.*, 2001). Up-regulated expression of growth hormone, prolactin and nerve growth factor (Ahlemeyer and Krieglstein, 2003; Watanabe, Wolfram, *et al.*, 2001; Pierre, Jamme, *et al.*, 1999) responsible for proliferation, differentiation and growth of cells has also been reported, with the later shown to be altered in AD (Peng, Garzon, *et al.*, 2009; Pierre, Jamme, *et al.*, 1999; Scott, Mufson, *et al.*, 1995). The effects of GbE and the inhibition of amyloidogenesis has been linked to the lowering of circulating free cholesterol (Yao, Han, *et al.*, 2004). Neuronal degeneration sees an increase in liberated and exported cholesterol in the form of 24S-OH from the brain and is one of many potential emerging biomarkers for neurodegenerative diseases (Leoni and Caccia, 2011). In the brains of AD patients, a marked accumulation of 27-OHC has been found (Shafaati, Marutle, *et al.*, 2011) while plasma levels of 24S-HC have been found to be increased in AD patients (Lütjohann, Papassotiropoulos, *et al.*, 2000), decreased in PD patients (Lee, Seet, *et al.*, 2009) and unaffected in CSF of PD patients (Björkhem, Lövgren-Sandblom, *et al.*, 2013). GbE supplementation has been reported as comparable to cholinesterase inhibitor treatment in mild to moderate AD patients while providing additional

cognitive benefits (Canevelli, Adali, *et al.*, 2014; Lasaite, Spadiene, *et al.*, 2014; Yancheva, Ihl, *et al.*, 2009; Mazza, Capuano, *et al.*, 2006; Schulz, 2003; Wettstein, 2000). Intracellular levels of cholesterol have been shown to affect amyloid precursor protein (APP) processing and amyloidogenesis (Ramassamy, 2006; Yao, Han, *et al.*, 2004; Howland, Trusko, *et al.*, 1998; Simons, Keller, *et al.*, 1998; Bodovitz and Klein, 1996). Interestingly, in HFD-induced obese mice and rats, elevated cholesterol and triglyceride plasma levels were attenuated with GbE supplementation, with levels comparable to rats fed a normal fat diet (Yan, Fan, *et al.*, 2015; Banin, Hirata, *et al.*, 2014). Transcriptome profiling of liver from rats fed a high-fat diet supplemented with GbE showed repression of fatty acid biosynthesis and an enhancement of fatty acid metabolism (Gu, Xie, *et al.*, 2009) which may contribute to reduced lipid peroxidation (Yan, Fan, *et al.*, 2015; Huang, Yang, *et al.*, 2013; Spadiene, Savickiene, *et al.*, 2012), inhibited cellular lipogenesis and induced cellular lipolysis (Jeong, Kim, *et al.*, 2017).

Previously published work has shown that GbE possesses antioxidant, anti-inflammatory, and anti-obesogenic properties. This work has shown GbE reduces visceral adiposity, weight gain and food intake and reduce adipocyte hypertrophy in WAT. Furthermore, our group have shown that GbE modulates lipid metabolism, adipogenesis, inflammation and OS and improve insulin signalling and sensitivity (Machado, Banin, *et al.*, 2021; Machado, Pereira, *et al.*, 2021; Hirata, Cruz, *et al.*, 2019; Hirata, Pedroso, *et al.*, 2019; Hirata, Banin, *et al.*, 2015; Banin, Hirata, *et al.*, 2014). Previously published work has also shown that GbE plays an antioxidative role in the hippocampus of ovariectomized rats and restore serotonin and leptin receptor levels (Machado, Banin, *et al.*, 2021). Machado and colleagues (2021) hypothesised that the restoration of serotonin and leptin receptor levels were related to the restoration of serotonin levels in the ventro-medial hypothalamus, which in turn ameliorated the anorexigenic-serotonin response impaired by ovariectomy (Machado, Banin, *et al.*, 2021). In a 90-day clinical trial, patients with metabolic syndrome already on metformin were given GbE (120 mg capsule/day) or placebo. It was found in patients with metabolic syndrome that GbE significantly decreased HbA1c, fasting serum glucose, insulin levels and IR. BMI, waist circumference and visceral adiposity index also improved. Serum leptin and lipid profiles and the inflammatory markers highly sensitive C-reactive protein (hs-CRP), TNF- α , and IL-6 (Aziz, Hussain, *et al.*, 2018). Similarly, Isorhamnetin a bioactive compound found in GbE has been shown to improve insulin levels, glucose tolerance and energy expenditure in HFD-fed obese mice. It also reduced adipocyte size and increased hepatic IRS1 tyr-608 and S6 K thr-389 phosphorylation and diminished hepatic lipid content and mRNA expression of lipogenic enzymes and ER stress markers while

increasing mRNA expression of β -oxidation related genes. An increase in glucose transporter 2 (GLUT2) and PPAR γ mRNA content was also reported (Rodríguez-Rodríguez, Torres, *et al.*, 2015). Lipolysis is regulated by cyclic AMP (cAMP) levels through the inhibition of cAMP-phosphodiesterase (PDE) or by the by activation of adenylate cyclase (Saponara and Bosisio, 1998). Saponara and Bosisio (1998) reported that GbE biflavones inhibit cAMP-phosphodiesterase in rat adipose tissue, thereby reducing the catalytic breakdown of cAMP, thus promoting lipolysis. Alterations in PDE activity has also been reported in obesity, with BMI inversely correlated to total PDE and PDE3 activity in omentum WAT, but not SAT (Saponara and Bosisio, 1998). Further supporting this is a report that mice lacking the cGMP-phosphodiesterase, PDE9 were protected from diet-induced obesity and showed increased energy expenditure (Ceddia, Liu, *et al.*, 2021). Kaempferol, and other flavanol abundant in *GbE*, has been shown to protect against hyperglycaemic metabolic changes similar to that of insulin by ameliorating increased serum glucose levels and increased glucose uptake in rat soleus muscle *via* the PI3K and PKC pathway (Cazarolli, Folador, *et al.*, 2009; Jorge, Horst, *et al.*, 2004) as well as reduced caspase-3 activity in β -cells and islets, caused by hyperglycaemia, as well as IL-1 β and TNF- α levels (Al-Numair, Chandramohan, *et al.*, 2015; Abo-Salem, 2014; Zhang, Chopp, *et al.*, 2013). OS and cellular apoptosis were also reduced by the reduction of anti-apoptotic Akt and Bcl-2 protein expression (Al-Numair, Chandramohan, *et al.*, 2015; Zhang and Liu, 2011). These cellular changes improved cAMP levels, lipid peroxidation and β -cells synthesis and secretion of insulin (Al-Numair, Chandramohan, *et al.*, 2015; Zhang and Liu, 2011). Zang and colleagues (2015) found that in tallow-based HFD-fed mice, kaempferol treatment exhibited anti-obesity and anti-diabetic effects, reduced body weight, adipose tissue TAG levels and decreased fasting blood glucose, serum HbA1c (haemoglobin A(1c)) levels, while improving IR compared to HFD with no treatment (Zang, Zhang, *et al.*, 2015). While Zang and colleagues did not report whether food consumption was decreased with treatment, similar to some findings in epididymal WAT (Hirata, Cruz, *et al.*, 2019), they reported that epididymal, mesenteric and pararenal WAT as well as VAT tissue weights, were significantly lower than that of the HFD group. They also found that hepatic gene expression of PPAR- γ and SREBP-1c were down-regulated increasing lipid metabolism (Zang, Zhang, *et al.*, 2015). Recalling that abnormal glycaemic events that contribute to increased OS, which poses a risk factor for metabolic syndrome and AD, Bhatt *et al.*, (2012) reported improved glycaemic control and reduced levels of glycated haemoglobin (HbA1c) levels associated with hyperglycaemia in T2DM after a 3-month supplementation of resveratrol (Bhatt *et al.*, 2012). Similarly, resveratrol also decreased IR and delayed glucose peaks in diabetic

patients (Brasnyó, Molnár, *et al.*, 2011). Similar improvements to glycaemia, insulin levels, IR and reduced glycosylated HbA1c levels have also been reported with GbE supplementation in animal (Hirata, Banin, *et al.*, 2015; Banin, Hirata, *et al.*, 2014; Kudolo, Wang, *et al.*, 2006) and clinical studies (Aziz, Hussain, *et al.*, 2018; Lasaitte, Spadiene, *et al.*, 2014; Siegel, Ermilov, *et al.*, 2014; Kudolo, Wang, *et al.*, 2006; Kudolo, 2001). Several animal studies have also investigated the relationship between obesity induced by a HFD (which is shown to elevate cholesterol and TAG levels) and the effect of GbE supplementation. GbE shows similar results in relation to improved glycaemic control as well as improvements in cholesterol and triglyceride profiles (Jeong, Kim, *et al.*, 2017; Jeong, Jang, *et al.*, 2016; Hirata, Banin, *et al.*, 2015; Rhee, Lee, *et al.*, 2015; Yan, Fan, *et al.*, 2015; Banin, Hirata, *et al.*, 2014; Cong, Tao, *et al.*, 2011).

Similarly, the flavonoid Ginkgolide C, isolated from GbE leaves, has been shown to increase lipolysis and inhibit adipogenesis in adipocytes through increased phosphorylation of AMP-activated protein kinase (AMPK), resulting in decreased activity of acetyl-CoA carboxylase for fatty acid synthesis. Treatment also decreased the expression of PPAR and CCAAT/enhancer-binding protein, and increased lipolysis through enhanced adipose ATGL and hormone-sensitive lipase production (Liou, Lai, *et al.*, 2015). Quercetin, a polyphenolic flavonoid found in many plants including GbE has been reported to significantly upregulate PPAR α protein levels and β -oxidation (Sun, Yamasaki, *et al.*, 2015) and improve hepatic dyslipidaemia by downregulating SREBP-1c and FASN levels, and upregulating PPAR α , carnitine palmitoyl-transferase1 and medium-chain acyl-coenzyme A dehydrogenase expression, increasing lipolysis and β -oxidation (Wang, Zhang, *et al.*, 2016). Ginkgetin, a biflavone found in GbE leaves, blocked the differentiation of pre-adipocytes into adipocytes preventing hypertrophy in HFD fed mice white adipose tissue, by acting as a STAT5 inhibitor, inhibiting PPAR γ and the transcription factor CCAAT-enhancer-binding protein alpha (C/EBP α) expression (Cho, Park, *et al.*, 2019). GbE treatment has also been shown to inhibit adipocyte differentiation, downregulating the expression of adipogenesis genes, PPAR- γ and ap2 (Wu, Zhang, *et al.*, 2016). Similarly, GbE has been shown to modulate hepatic glucose transporter 2 (GLUT-2), PPAR- α and PGC1- α , improving hepatic dyslipidaemia, glucose metabolism and storage (Awad, Araby, *et al.*, 2021). GbE has also been shown to inhibit oxidised low-density lipoprotein (oxLDL), upregulation of matrix metalloproteinases (MMP1, MMP2, MMP3) associated with atherosclerotic lesions, which help suppress ROS generation. The same study by Tsai and colleagues (2016) also showed GbE reduced lectin-like ox-LDL receptor 1 (LOX-1) expression ameliorating oxLDL-inhibited PPAR- γ function (Tsai, Chang, *et al.*, 2016). Resveratrol has also been shown to interact with fatty acid β -oxidation and oxidative phosphorylation

in the mitochondrial metabolic pathways (Barone, Rizzo, *et al.*, 2019; Bastin and Djouadi, 2016). Resveratrol has been shown to significantly increase the expression of *Ppara* mRNA and PPAR protein levels in visceral adipose tissue of metabolic syndrome rats (Castrejón-Tellez, Rodríguez-Pérez, *et al.*, 2016). Similarly, resveratrol has also been shown to protect from renal lipotoxicity in a HFD mouse model by increasing PPAR α protein levels and AMP-activated protein kinase (AMPK) phosphorylation (Zhou, Lin, *et al.*, 2016) and has been shown to activate both PPAR α and the AMPK-Sirtuin 1 (SIRT1)-PGC-1 α signalling pathway *via* the adiponectin receptors in the renal cortex (Park, Lim, *et al.*, 2016). Significant decreases in OS and inflammatory markers such as hs-CRP, TNF- α , IL-6 and malondialdehyde levels have also been attributed to GbE supplementation (Yan, Li, *et al.*, 2020; Aziz, Hussain, *et al.*, 2018; Siegel, Ermilov, *et al.*, 2014; Thanoon, Abdul-Jabbar, *et al.*, 2012; Kudolo, Wang, *et al.*, 2006). In comparison, glutathione (GSH) and superoxide dismutase (SOD), both OS markers, were increased with GbE treatment (Yan, Li, *et al.*, 2020; Thanoon, Abdul-Jabbar, *et al.*, 2012; Bridi, Crossetti, *et al.*, 2001). It has also been shown that both resveratrol and GbE modulates the Akt insulin signalling pathway (Yan, Li, *et al.*, 2020; Lejri, Grimm, *et al.*, 2019; Brasnyó, Molnár, *et al.*, 2011). Akt activation requires a fine balance to moderate fluctuations between cell survival and apoptosis. Increased Akt phosphorylation (p-Akt) have modulating actions on the PI3K/Akt/mTOR and IGF-1R/Akt/Wingless-related integration site (Wnt) signalling pathways, responsible for regulating key aspects of cellular proliferation, differentiation, and apoptosis (Park, Lim, *et al.*, 2010; Vanamala, Reddivari, *et al.*, 2010). Both GbE and Ginkgolide B have been shown by Li and colleagues to promote cell cycle exit and neuronal differentiation in neural stem cells of the postnatal mammalian subventricular zone through the Wnt/ β -catenin pathway but not through the extracellular signal-regulated kinase (ERK) pathway (Li, Chang, *et al.*, 2018). GbE and resveratrol have also been shown to increase neurite outgrowth in PC12 and SH-SY5Y cells (Lejri, Grimm, *et al.*, 2019). Both GbE and resveratrol and GbE also increased the phosphorylation of phosphorylated insulin growth factor 1 receptor (IGF1R), Akt (Ser473), mTOR, Phosphatase and tensin homolog (PTEN) and Glycogen synthase kinase-3 beta (GSK3 β) (Tan, Sun, *et al.*, 2020; Lejri, Grimm, *et al.*, 2019). GbE was also able to inhibit H₂O₂-induced cell apoptosis in SH-SY5Y cells *via* inactivation of AKT, JNK, and caspase-3 (Shi, Zhao, *et al.*, 2009). GbE has also been shown to enhance hippocampal neurogenesis by restoring impaired phosphorylation of the transcription factor cAMP responsive element binding protein (CREB) and brain-derived neurotrophic factor (BDNF) expression, in β -amyloid-expressing neuroblastoma cells in a transgenic mouse model of AD (Xu, Cui, *et al.*, 2007). CREB is phosphorylated by Akt, and in turn, increases expression of BDNF (Esvald, Tuvikene, *et al.*, 2020; Dong, Pu, *et al.*,

2018). BDNF signalling involves the recruitment of Tropomyosin-related kinase B (TrkB), a receptor tyrosine kinase into cholesterol rich lipid rafts. BDNF can also stimulate the transcription of cholesterol pathway enzymes in neuronal cells (Suzuki, Numakawa, *et al.*, 2004). The downstream effectors of BDNF include the PI3-K and mitogen-activated protein kinase (MAPK) involved in survival signalling pathways, with both involved in the feedback loop of Akt signalling (Suzuki, Numakawa, *et al.*, 2004). This pathway may explain changes in cholesterol levels seen in GbE treatment, as mentioned earlier. Furthermore, down-regulation of the JNK/ Activator protein 1 (AP-1) signalling pathway by GbE, results in the inhibition of cytokines TNF α , IL-2, IL-4, and IFN- γ that are involved in the inflammatory process and cell death (Hirata, Banin, *et al.*, 2015; Cheng, Liang, *et al.*, 2012). Both the PI3K/Akt/mTOR (Wu and Liu, 2013) and IGF-1R/Akt/Wnt (Vanamala, Reddivari, *et al.*, 2010) signalling pathways are often over stimulated in hyperglycaemic events that can contribute to OS and increased risk of AD, cellular apoptosis, altered glucose uptake and mitochondrial dysfunction (Serrano-García, Pedraza-Chaverri, *et al.*, 2013).

Similar modulation of both resveratrol and GbE also seen on SIRT1 (Chung, Yao, *et al.*, 2010; Hou, Chong, *et al.*, 2010; Lagouge, Argmann, *et al.*, 2006) JNK, ERK, p38 and MAPKs (Hsu, Wu, *et al.*, 2009) and several nuclear factors, including downstream NF- κ B and the Nrf2- kelch-like ECH-associated protein 1 (Keap1)-Antioxidant Response Element (ARE) (Nrf2-Keap1-ARE) antioxidant cell defence signalling pathway (Singh, Srivastav, *et al.*, 2019; Ahmed, Javed, *et al.*, 2017; Huang, Yang, *et al.*, 2013; Serrano-García, Pedraza-Chaverri, *et al.*, 2013; Hsu, Wu, *et al.*, 2009; Liu, Goldring, *et al.*, 2007; Andreadi, Howells, *et al.*, 2006; Ishunina, Kamphorst, *et al.*, 2004). Nrf2, involved in regulating the transcription of detoxifying and antioxidant enzymes that counteract OS, binds to the ARE region of DNA, a binding region it competes with NF- κ B for. Nrf2 is a major regulator in cellular and organismal defence by regulating stress-inducible activation of multiple cytoprotective genes (Cuadrado, Manda, *et al.*, 2018; Yamamoto, Kensler, *et al.*, 2018; Ma, 2013). It is reported that Nrf2 may be upregulated by multiple polyphenols and reduces activity of pro-inflammatory NF- κ B (Wagner *et al.*, 2013) which is regulated by the Akt signalling pathways. Research suggests that resveratrol and GbE are both capable of upregulating the expression of Nrf2 (Liu, Wang, *et al.*, 2019; Hsu, Wu, *et al.*, 2009; Liu, Goldring, *et al.*, 2007; Yao, Nussler, *et al.*, 2007; Andreadi, Howells, *et al.*, 2006; Ishunina, Kamphorst, *et al.*, 2004) while resveratrol has been shown to restore Nrf2 levels in the brain (Kumar, Singh, *et al.*, 2011). Resveratrol has also been shown to attenuate cytotoxicity from A β 1-42 by upregulating Heme Oxygenase-1 *via* the PI3K/Akt/Nrf2 Pathway (Hui, Chengyong, *et al.*, 2018). Regarding SIRT1, GbE (Li, Zhang, *et al.*, 2017; Longpré, Garneau, *et al.*, 2006) have also been shown to increase SIRT1 activity,

a gene with protective effects against apoptosis caused by oxidative and toxic stress. SIRT1 is associated with AD development and is responsible for regulating epigenetic gene silencing that is often downregulated in IR (Ng, Wijaya, *et al.*, 2015; Pasinetti, Wang, *et al.*, 2015; Min, Sohn, *et al.*, 2013; Donmez, 2012; Yamakuchi and Lowenstein, 2009). The exact resveratrol/SIRT1 interaction, however, remains to be fully elucidated, with some data suggesting that the *in vivo* interactions between resveratrol and SIRT1 may occur artificially, with resveratrol potentially targeting other proteins that affect SIRT1 instead (Pacholec, Bleasdale, *et al.*, 2010; Baur and Sinclair, 2006; Borra, Smith, *et al.*, 2005). Other reports suggest that the neurological benefits, such as increased A β clearance associated with the consumption of grape juice products - a dietary supplier of resveratrol - is not limited to that of resveratrol alone. These results may be a result of a combination of other grape-derived polyphenolic components (Wang, Zhang, *et al.*, 2016; Marambaud, Zhao, *et al.*, 2005) with include quercetin, kaempferol and isorhamnetin also found in GbE. A clinical trial combining a high n-3 FA multi-nutrient supplement containing EPA and GbE along with other vitamins has showed promising results in improving cognition in elderly females (Strike, Carlisle, *et al.*, 2016).

While the exact mechanism of AD remains to be elucidated and new treatments slow to emerge, evidence suggests that specific nutrients can influence the activity of molecular switches that contribute to neuropathogenesis (Gardener, Gu, *et al.*, 2012; González-Gross, Marcos, *et al.*, 2001). What is known is that AD, Type 2 Diabetes Mellitus (T2DM) (Chen and Zhong, 2013) and obesity (Bondia-Pons, Ryan, *et al.*, 2012; Noeman, Hamooda, *et al.*, 2011; Furukawa, Fujita, *et al.*, 2004; Higdon and Frei, 2003) share some clinical, biochemical and pathophysiological manifestations through the induction of OS (Rosales-Corral, Tan, *et al.*, 2015). Furthermore, there is a higher risk of in older individuals who are overweight or obese of developing dementia (Ma, Ajnakina, *et al.*, 2020) as well as a three-fold increased risk of developing dementia with a high waist circumference (Pugazhenthii, Qin, *et al.*, 2017). An HFD rich in saturated fat common in westernized diets is also associated with obesity and brain-related disorders related to hypothalamus-pituitary-adrenocortical axis dysregulation including cognitive impairment, anxiety, stress and depression (López-Taboada, González-Pardo, *et al.*, 2020). The development of additional supporting strategies such as nutritional intervention and the use of natural products that can target specific molecular pathways affecting obesity, insulin resistance and neurodegeneration may offer promising new therapeutic avenues. With the evidence that the Mediterranean diet, which combines better PUFA ratios, and a plentiful abundance of plant-derived polyphenols can reduce the risk of developing AD (Schwingshackl, Morze, *et al.*, 2020; Shively, Appt, *et al.*, 2019; Singh, Parsaik, *et al.*, 2014; Gardener,

Gu, *et al.*, 2012; Babio, Bulló, *et al.*, 2009), a multifactorial approach to nutritional therapeutics for the prevention of OS, obesity and AD should be taken into consideration. The evidence for the use of PUFA and plant derived polyphenols such as those found in GbE and red wine that ameliorate the cellular risk factors associated with OS and consequently obesity and AD is promising. Published results from our group have already shown that HFD-induced obese rats supplemented with GbE improves insulin sensitivity and signalling, dyslipidaemia, body adiposity and that GbE possesses antioxidant, anti-inflammatory, and anti-obesogenic properties (Hirata, Cruz, *et al.*, 2019, Hirata *et al.*, 2015, Banin *et al.*, 2014). It has also been found that GbE supplementation was effective in reducing energy intake and decreasing weight gain in HFD-obese rats as well as reducing adipocyte hypertrophy to dimensions equivalent to adipocytes from non-obese rats. GbE also reduced the incorporation of acetate and oleate FA into epididymal adipocytes. Perilipin and *FASN* mRNA as well as *FASN* proteins levels were also reduced (Hirata, Cruz, *et al.*, 2019). It has also shown that in retroperitoneal WAT, GbE improves insulin signalling and increases both Adipo-R1 (an adiponectin receptor) and anti-inflammatory IL-10 gene expression. Increases in insulin receptor and Akt phosphorylation was also observed, while NF- κ B p65 phosphorylation and TNF- α levels were significantly reduced (Hirata, Banin, *et al.*, 2015). Following this, our group subsequently found within the retroperitoneal fat depot proteome, several proteins associated with carbon metabolism, adipogenesis (decorin), fatty acid metabolism and mitochondrial function (citrate synthase) were increased. Proteins involved in OS including peroxiredoxin and inflammatory response proteins such as complement C3, mast cell protease 1, and Ig gamma-2B chain C region were down-regulated. GbE also stimulated catalase activity, increased lactoylglutathione lyase levels and decreased lipid peroxidation indicated by reduced malondialdehyde levels (Hirata, Pedroso, *et al.*, 2019). Furthermore, our group have shown that GbE restores serotonin and leptin receptor levels in the hippocampus of ovariectomized rats (Machado, Banin, *et al.*, 2021) and that GbE can induce gene expression of hypothalamic anorexigenic effectors in male rats after a single dose (Machado, Pereira, *et al.*, 2021).

To build on previous findings this thesis will focus on examining the changes in tissue lipid profiles between normal fat diet (NFD) male Wistar rats and a HFD that induces obesity. The Effect of GbE supplementation on HFD-induced obesity male Wistar rats will also be examined. To date no reports have been published regarding the modulation of GbE on tissue lipid classes in a high-fat diet model. Further to this, the effect of a HFD and GbE supplementation will also be examined in an *in vitro* PC12 neuronal model which has not been looked at to date in the literature.

1.19 Aims and Objectives

Aims

This research project aims to investigate whether:

1. A HFD alters lipid profiles in various tissues of male Wistar rats compared to a normal fat diet (NFD).
2. The combined effects of a HFD coupled with GbE supplementation can modulate lipid class profiles in various tissues of HFD-obese male Wistar rats.
3. The effects of supplementation with GbE and FA mixes designed to represent the FA profiles found in both NFD a HFD rat chow used in the rat study from aim 1 and 2), on an *in vitro* PC12 neuronal model exposed to OS.

Objectives

1. Lipid profile analysis of the NFD and HFD rat chow used in the male Wistar rat study *via* lipid extraction and GC-FID separation.
2. Analysis of body weight, body weight gain, food intake, energy intake and food efficiency of rats fed a NFD, HFD, HFD supplemented with saline or HFD supplemented with GbE.
3. Tissue lipids from non-obese rats fed a NFD or HFD-induced obese rats will be analysed for total lipid profiles, neutral lipid classes including MAG, DAG, TAG, CE as well as phospholipid membrane profiles.
4. Tissue lipids from obese Wistar rats fed either HFD, HFD plus saline, or HFD plus GbE supplementation will be analysed for total lipid profiles, neutral lipid classes including MAG, DAG, TAG, CE as well as phospholipid membrane profiles.

Objectives 2 and 3 will be achieved by:

- a. Optimizing a silica column solid phase extraction (SPE) method for the separation of lipid classes from total lipid samples
- b. Optimizing a Gas Chromatography – Flame Ionization Detection (GC-FID) method for in-house fatty acid methyl ester (FAME) identification and analysis
- c. Analysing extracted lipids from various tissues (retroperitoneal and mesenteric adipose tissues, liver, hippocampus, and hypothalamus) collected from obese Wistar rats fed a high-saturated-fat diet supplemented with GbE.

- i. Total lipid profiles esterified to FAMES and analysed by GC-FID
 - ii. Total lipid samples separated into lipid classes SPE into MAG, DAG, TAG, CE and PPL, esterified to FAMES and analysed by gas chromatography – flame ionisation detection.
5. An *in vitro* PC12-neuronal cell model will be developed and optimised for in-house laboratory use. This will include:
 - a. Morphological observations.
 - b. Cell viability assays *via* 3-[4,5-dimethylthiazol-2-yl]-2,5-diphenyltetrazolium bromide) (MTT) assay.
 - c. Identification of neuronal markers using flow cytometry and western blotting techniques.
6. PC12 neuronal cells will be treated with a combination of the most abundant FA found in the NFD and HFD chow in the male Wistar rat study. NFD and HFD supplementation will also be combined with GbE supplementation. Treated cells will be analysed before and after exposure to OS.
 - Following cell treatments, cell toxicity will be analysed by MTT assay and Annexin V-7AAD flow cytometry.
7. Cell membrane phospholipid composition will be analysed *via* cellular total lipid extraction, esterification to FAMES and separation by GC-FID.
8. Western immunoblotting will be utilized to quantify the effect of cellular treatments on Intracellular signalling pathways including AKT, Nrf2 and neurofilament proteins.

Chapter 2 - Methods

2.1 Male Wistar rat animal study parameters

From our collaborator Dr Monica Telle's group at the Federal University of São Paulo, Brazil, tissue lipid extracts from a male Wistar rat phytotherapy study undertaken by Dr Bruna Hirata, were obtained. The animal study is summarised below.

(a) Animal Care

The Committee on Animal Research Ethics of the Federal University of São Paulo, Brazil approved all procedures for the care of the animals used in this study. All efforts were made to minimize suffering. Animal care has been standardised and previously published (Hirata, Cruz *et al.*, 2019, Hirata, Pedroso *et al.*, 2019). In brief, two-month-old male Wistar rats were purchased from the Multidisciplinary Center for Biological Investigation in Laboratory Animals Science (CEMIB - Campinas, Brazil). Rats were housed at 4 or 5 rats per cage. The rats were maintained at a controlled temperature ($23^{\circ}\text{C}\pm 1^{\circ}\text{C}$) and lighting was set to a 12:12-hr light/dark cycle with lights turned on at 6:00 a.m. Rats received *ad libitum* food and water.

For 8 weeks, male Wistar rats were fed either a standard chow diet (n=10) representing a normal fat diet (NFD), or a high-fat lard enriched (HFD) chow (28% lard) (n=30) to induce obesity. As previously standardised, the HFD chow was prepared by mixing 40% (w/w) standard chow with 28% (w/w) melted lard, 20% (w/w) casein powder (to standardise protein content to that of the NFD), 10% (w/w) sucrose, 2% (w/w) soybean oil, and 0.02% (w/w) butylated hydroxytoluene (5.0 kcal/g) (Hirata *et al.*, 2019, Hirata, Pedroso *et al.*, 2019, Hirata *et al.*, 2015, Banin *et al.*, 2014).

After 8 weeks of dietary intervention to induce obesity, the HFD-fed rats were randomly divided into three groups, while the non-obese NFD fed rats were assigned to a 4th group.

(b) Phytotherapy treatment

Ginkgo biloba extract (GbE) was obtained from Southern Anhui Dapeng (China). The main components of GbE are shown in Figure 7, with GbE standardised to contain 26.1% flavone glycosides, 6.7% terpenoids, 2.2% ginkgolide A, 1.1% ginkgolide B, 1.1% ginkgolide C and 2.5% bilobalide (2.50%). Phytotherapy treatment was performed for 14 days.

For the 14 days of phytotherapy treatment, each group received the following treatment:

- 1) **Group 1** (HFD+GbE) received a daily oral gavage of 500 mg/kg of GbE diluted in 2mL of 0.9% saline and HFD chow *ad libitum* (n=10)
- 2) **Group 2** (HFD+S) received a daily oral gavage of 2ml 0.9% saline only (as vehicle control for GbE) and HFD chow *ad libitum* (n=10)
- 3) **Group 3** (HFD+PF) received a daily oral gavage of 2ml 0.9% saline only (as vehicle control) and were calorie restricted (pairfed) equal to the amount of food consumed by the GbE supplemented group (n=10). Previous work has shown the GbE reduces food intake in male Wistar Rats (Hirata, Cruz, *et al.*, 2019, Hirata, Pedroso, *et al.*, 2019, Hirata *et al.*, 2015, Banin *et al.*, 2014).
- 4) **Group 4** (NFD) received a daily oral gavage of 2ml 0.9% saline only (as vehicle control) and continued to receive standard chow *ad libitum*.

During the phytotherapy supplementation period, 24-h food intake (calculated by the difference between food left from the food offered over a 24-hour period) and body weight (calculated by the difference between the first and last day of the 14-day period) was measured and collated by Dr Bruna Hirata. Following the 14-day treatment period, all the animals were fasted for 8 hours, anaesthetized (by barbiturate 80 mg/kg), and euthanized by decapitation. Retroperitoneal (RET) and mesenteric (MES) white adipose tissue, along with liver and brain tissue (hippocampus hypothalamus) was collected. Tissue lipids were extracted by Dr Bruna Hirata as previously described (Boldarine *et al.*, 2021; Hirata *et al.*, 2019; Bueno *et al.*, 2015; Dornellas *et al.*, 2015).

Samples were transported over dry ice to the University of Worcester along with raw samples of NFD and HFD rat chow samples for further analysis. Along with these samples, Dr Bruna Hirata also provided the raw data for food intake and body weight measurements for all animals in the study. From this raw data final body weight, body weight gain, food intake, energy intake and the food efficiency were calculated. All data are presented as Mean±SEM. For obesity-inducing period, the NFD and HFD groups were analysed by *Students t*-test. Body metric data from the 14-day phytotherapy treatment for the four groups (NFD, HFD+S, HFD+PF, HFD+GbE) was analysed by either One-way ANOVA with Tukey *post hoc* test or Two-way repeated measures ANOVA with Šídák *post hoc* test. The level of statistical significance was set at *p < 0.05.

2.2 Glassware

All glassware used for fatty acid samples was acid-etched in 10% nitric acid for a minimum of 2 hours, followed by a primary wash with 70°C wash with phosphate-free detergent, a secondary 70°C wash without detergent, followed by thorough rinsing in de-ionised water and left to dry in a drying cabinet.

2.3 Lipid extraction

Total lipids were extracted from samples (animal tissues and PC12 cells) using the double-pipette modified Folch *et al.*, (1957) method as previously described (Hirata, Cruz, *et al.*, 2019; Hirata *et al.*, 2015; Banin *et al.*, 2014). Optimization of fatty acid extraction methods can be seen in Appendix 1. In brief, 3 ml C:M (2:1, v/v +0.01%BHT) was added to each sample (100mg tissue or homogenised using a tissue homogeniser or 1×10^4 cells, sonicated) in a Pyrex borosilicate glass tube, flushed with oxygen-free N₂ (OFN), capped with glass stopper and stored at 4°C overnight (24 hours). After 24 hours, 25% v/v of 0.85% saline (1ml) was added to samples (CHCl₃: MeOH:Saline ratio of 8:4:3 (v/v/v)) vortexed and centrifuged at 1500 rpm for 5 minutes to separate the aqueous and organic layers. The lower lipid phase was recovered *via* a double pipette technique (Schreiner, 2006). In brief, one Pasteur pipette (150mm) was introduced into the lower phase by applying a little overpressure on the silicon pipette bulb. After penetrating the lower phase, the pipette bulb was removed allowing the lipid phase to enter the pipette without contamination by the upper phase. The lower lipid phase was recovered by a second longer pipette (230mm) inserted into the first pipette. The remaining upper phase was washed with 2 ml C: M 2:1, v/v+0.01% BHT and centrifuged for 5 minutes. The lower phase was recovered again by double pipette extraction. The recovered lower phases were pooled and reduced to dryness under OFN and stored at -20°C until needed.

2.4 Solid phase extraction (SPE) for isolation of lipid classes by silica gel column chromatography

A variety of methods exist for the separation of lipid classes (Adlof, 2003; Burdige *et al.*, 2000; Ingalls *et al.*, 1993). In this study the Ingalls *et al.*, (1993) method was selected for the separation of triglycerides (Fraction 1), cholesteryl esters (Fraction 2), monoglycerides and diglycerides (Fraction 3) and phospholipids (Fraction 6). Plastic HyperSep™ silica SPE columns (100 mg bed weight; 1 mL column volume, code:10563985), HPLC grade Isooctane, ethyl acetate, chloroform, methanol, and glacial acetic acid were obtained from Fisher Scientific (Cleveland, OH, USA). In-house optimization of this SPE method using commercially available standards is summarised in Appendix 2 and has been subsequently published (See Appendix 3) (Boldarine, Joyce *et al.*, 2021). The final SPE separation of

lipid samples were conducted using the following protocol. In brief, all SPE solvent elution mixtures were made fresh before extraction at a ratio specified by the Ingalls *et al.*, (1993) method (v/v), summarized in Table 2. HyperSep Columns were conditioned with 4 X 1 ml of isooctane (4 column volumes and allowed to drain under gravity. 5 mg of total dried lipid homogenate was loaded onto the pre-conditioned columns by two successive washes with 0.5 ml of isooctane-ethyl acetate (80: 1, v/v, Elution solution 1) and allowed to drain by gravity into a glass vial. Following the elution steps and solutions as set out in Table 2, each lipid fraction (TAG, DAG+MAG, CE, PPL) was eluted under gravity and the lipid fractions collected in separate glass vials. To avoid drying of the silica bed, each fraction solution was immediately loaded on to the column after the previous solution had finished draining. As recommended by Ingalls *et al.*, (1993) method, following the elution of fraction 1 and 2, the original sample vial was washed twice in succession with 0.5 ml of isooctane-ethyl acetate (75:25, v/v, Elution solution 3) to remove any remaining sample residue not dissolved in initial isooctane-ethyl acetate (80: 1, v/v). This solution 3 wash was loaded on to the silica gel columns, followed by elution with fraction solutions 3, 4 and 5 as per Table 2. Following fraction 5 elution and collection, the original sample vial was re-washed with 0.5 ml of methanol (Elution solution 6) to dissolve any remaining sample left behind from the solution 1 and 3 washes and applied to the silica gel columns. The final fraction elution was collecting using fraction 6 solution. Eluted samples were dried under OFN and acid-catalysed esterified as per the protocol outlined in Section 0. All samples were made up in 1 ml Heptane+BHT (100mg/ml) prior to injection. Samples were separated and analysed by GC-FID as outlines in Section 2.6.

2.5 Acid-catalysed esterification of lipids to methyl esters (Methylation)

To each sample 4ml Acetyl Chloride: Methanol (15:100) solution was added, flushed with OFN, sealed with a PTFE lined cap, and methylated at 70°C for three hours, with samples checked and mixed every hour. The resulting fatty acid methyl esters (FAMES) were extracted with 4 ml of petroleum spirit +0.01% BHT and 4 ml of 5% saline (to induce phase separation). The top layer of petrol spirit was collected and added to 2 ml of 2% potassium bicarbonate and vortexed to neutralize any remaining acid. The top petrol spirit layer was removed and added to 200 mg of anhydrous sodium sulphate to remove any residual water from the sample. Samples were dried under OFN at 37°C and stored at -20°C until needed. Methylated (FAME) samples were diluted in Heptane with 0.01% BHT.

Table 2. Preparation of solutions for the separation of solid phase separation of lipid classes

Solutions for SPE separation	Lipid class Elution	Total volume of solvent used (ml)		n-Octane	Ethyl Acetate	Glacial Acetic Acid	Methanol
Fraction 1	TAG	4.5	v/v	80	1	-	-
Fraction 2	CE	5	v/v	20	1	-	-
Fraction 3	MAG+DAG	4.5	v/v	75	25	-	-
Fraction 4	FFA	4	v/v	75	25	2	-
Fraction 5	-	8	v/v	75	25	2	-
Fraction 6	PPL	8	v/v	-	-	-	100
Total Solvent used per sample (ml)		36.0		23.3	2.5	0.2	8.0

2.6 Gas Chromatography – Flame Ionisation Detection (GC-FID)

2.6.1 Optimization of GC-FID

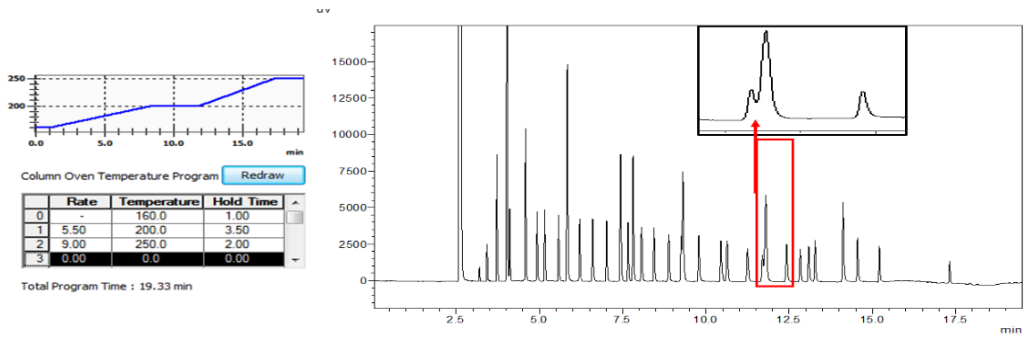
Method optimization was required for correct separation of fatty acid methyl esters (FAME) by GC-FID using a Shimadzu GC-2010 plus fitted with a Shimadzu – AOC-20S autosampler (Shimadzu, Kyoto, Japan), a Peak Scientific zero air precision compressor (Peak Scientific Instruments, Scotland, UK) and SGE Analytical Science™ BPX70 GC Capillary Column (120m x 0.25 mm x 0.25 µm – Code: 054624; Milton Keynes, United Kingdom). Various starting temperatures were explored including 130°C, 140°C, 150°C and 160°C, along with varying temperature increases and holds throughout the run (See Table 3). Shorter and longer final holding temperatures were also explored to minimize residual build up on the column between runs. In the FAME mix, overlapping of peaks, particularly of C18:3n3 and C20:0 as well as C20:3n3, C22:0 and C20:4n6 occurred at the higher start temperatures of 140°C, 150°C and 160°C (Figure 8). A final starting temperature of 130°C was sufficient to separate C18:3n3 and C20:0 into separate peaks. C20:3n3, C22:0 and C20:4n6 peaks were sufficiently separated to integrate them individually utilizing the split peak function of the Lab Solutions software (See Figure 8.D). Retention times of individual FAMES were also checked using this method. All individual FAMES separated sufficiently to give them unique retention times suitable for automated integration method (See Figure 8.D). The final optimized GC-FID FAME method is outlined in Table 4 with a run time of 26 mins. This method allows for easier post run analysis, with few misidentified peaks that require manual integration or correction.

Optimization of needle injection washing was also achieved by introducing 3 X 10ul washes of acetone followed by 6 X 10 µl washes of heptane, in place of 9 X 10 µl washes with heptane only. Acetone was chosen based on its polarity index of 5.1 and its miscibility of polar and non-polar substances as compared to the polar only nature of heptane with a polarity index of 0.1 (Harris, 2010). The use of acetone in the washing stage reduced any residual carry over and ghost peaking between runs. Washing with acetone first, followed by extensive washing of heptane afterword also allowed for complete removal of any acetone residue that might interfere with the sample run and profile.

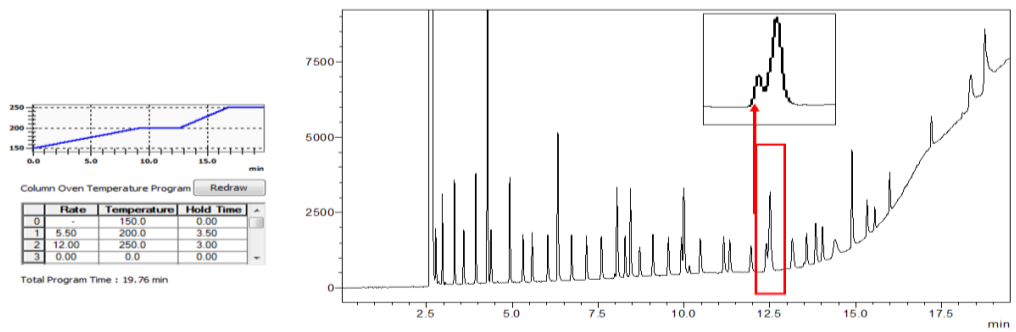
Table 3. Optimisation of Gas Chromatography – Flame Ionisation Detection (GC-FID)

GC-FID Method 1	<ul style="list-style-type: none"> • Starting temperature 160°C, hold 1 minute. • Increase by 5.5°C/min to 200°C, hold for 3.5 minutes. • Increase by 12°C/min to 250°C, hold for 2 minutes.
GC-FID Method 2	<ul style="list-style-type: none"> • Starting temperature 160°C, hold 1 minute. • Increase by 5.5°C/min to 200°C, hold for 3.5 minutes. • Increase by 9°C/min to 250°C, hold for 2 minutes.
GC-FID Method 3	<ul style="list-style-type: none"> • Starting temperature 150°C, hold 1 minute. • Increase by 5.5°C/min to 200°C, hold for 3.5 minutes. • Increase by 12°C/min to 250°C, hold for 3 minutes.
GC-FID Method 4	<ul style="list-style-type: none"> • Starting temperature 140°C, no hold. • Increase by 5.5°C/min to 200°C, hold for 3.5 minutes. • Increase by 12°C/min to 250°C, hold for 3 minutes.
GC-FID Method 5	<ul style="list-style-type: none"> • Starting temperature 130°C, hold 1 minute. • Increase by 5.5°C/min to 200°C, hold for 3.5 minutes. • Increase by 12°C/min to 250°C, hold for 4 minutes.
GC-FID Method 6 - Final optimized Method	<ul style="list-style-type: none"> • Starting temperature 130°C, hold 1 minute. • Increase by 5.5°C/min to 200°C, hold for 3.5 minutes. • Increase by 12°C/min to 250°C, hold for 3 minutes. • Increase by 10°C/min to 260°C, hold for 2 minutes.

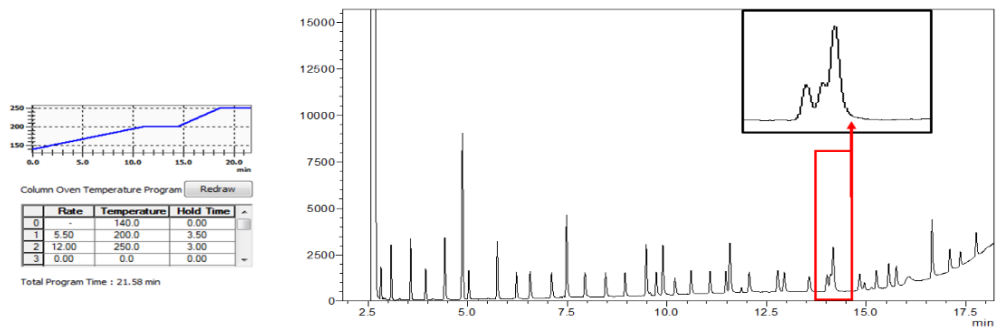
A. Starting temperature 160°C



B. Starting temperature 150°C



C. Starting temperature: 140°C



D. Starting temperature: 130°C

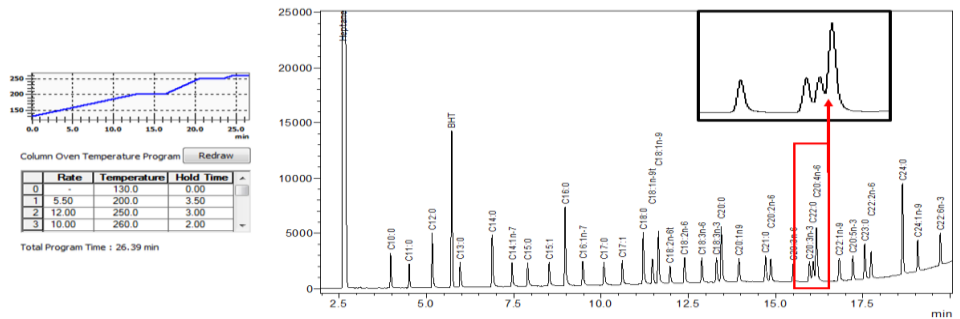


Figure 8. Optimisation of FAME separation on gas chromatography flame ionisation detection using various starting temperatures were explored from 130°C, 140°C, 150°C and 160°C and varying temperature hold times.

Table 4. Final optimized FAME method for the Shimadzu GC-2010 plus

Equipment
<ul style="list-style-type: none"> • Shimadzu GC-2010 plus – with flame ionisation detector • Shimadzu – AOC-20S autosampler • Peak Scientific zero air precision air compressor • Thermo Scientific TR FAME capillary column (60m x 0.32 mm x 0.25 µm – 260M155P) • Analysis Software: Lab Solutions, Shimadzu
Injection settings
<ul style="list-style-type: none"> • Injection port temperature: 230°C. • Injection volume: 1µl • Split ratio of 1:100 or 1:10 dependant on sample quantity • Purge flow: 3 ml/min • Injection needle rinse: 3 X 10ul Acetone, 6 X 10ul Heptane – Pre and post injection
Column Settings
<ul style="list-style-type: none"> • Thermo Scientific TR FAME (60m x 0.32 mm x 0.25 µm – Code:260M155P) • Equilibration time: 2 mins • Starting temperature 130°C, hold 1 minute. • Increase by 5.5°C/min to 200°C, hold for 3.5 minutes • Increase by 12°C/min to 250°C, hold for 3 minutes • Increase by 10°C/min to 260°C, hold for 2 minutes • Run time: 26 minutes
FID settings
<ul style="list-style-type: none"> • Temperature: 260°C • Makeup gas: Nitrogen (N2) at 30ml/min • Carrier gas: Hydrogen (H2) at 40ml/min • Air flow: 400ml/min

2.6.2 Final GC-FID method

For fatty acid identification, FAMES were separated by GC-FID using a Shimadzu GC-2010 plus fitted with a Shimadzu – AOC-20S autosampler (Shimadzu, Kyoto, Japan), a Peak Scientific zero air precision compressor (Peak Scientific Instruments, Scotland, UK) and SGE Analytical Science™ BPX70 GC Capillary Column (120m x 0.25 mm x 0.25 μ m – Code: 054624; Milton Keynes, United Kingdom). Nitrogen was used as a carrier gas with a flow rate of 30 mL/min, with air and hydrogen flow rates set at 400 mL/min and 40 mL/min respectively. Purge flow was set at 3 mL/min. The injection port temperature was set at 230°C and FID detector set at 260°C. A pre and post injection needle rinse (3 X 10ul Acetone, 6 X 10ul Heptane) was used. Sample injection volume was set at 1 μ l with a split ratio of 1:100. For samples of low quantity, a split ratio of 1:10 was utilized. As an additional control, heptane was injected after every 5 runs to test for ghost peaking. For maximum separation and complete elution of FAMES, the following ramp method was utilized over a 26 min run time: Starting temperature 130°C, hold 1 minute; Increase by 5.5°C/min to 200°C, hold for 3.5 minutes; Increase by 12°C/min to 250°C, hold for 3 minutes; Increase by 10°C/min to 260°C, hold for 2 minutes. A two-minute equilibration time was used in between runs. Samples were analysed using Shimadzu LabSolutions software (Shimadzu, Kyoto, Japan) against commercially available standards (Table 5, Table 6 and Table 7). Data was presented as mean percentage (%) of injected sample \pm SEM (Mean (%) \pm SEM). The unsaturation Index (UI) of the sample was also calculated outlined in the next section, as well as pertinent fatty acid ratios, when are presented as mean \pm SEM. Data was analysed by *Students t-test* when comparing two groups, or by One-way ANOVA with Tukey's *post hoc* test when comparing 3 or more groups. The level of statistical significance was set at *p < 0.05.

Table 5. No.1 Fatty acids standard mix (F.A.M.E. Mix, C4-C24) (Sigma-Aldrich (Merck KGaA, Darmstadt, Germany) used for the detection of fatty acid methyl esters by Gas Chromatography - Flame Ionisation Detection (GC-FID)

F.A.M.E. Mix, C4-C24 (Sigma-Aldrich (Merck KGaA, Darmstadt, Germany) – Code 18919	
C4:0	Methyl butyrate 4 wt. %
C6:0	Methyl hexanoate 4 wt. %
C8:0	Methyl octanoate 4 wt. %
C10:0	Methyl decanoate 4 wt. %
C11:0	Methyl undecanoate 2 wt. %
C12:0	Methyl dodecanoate 4 wt. %
C13:0	Methyl tridecanoate 2 wt. %
C14:0	Methyl myristate 4 wt. %
C14:1	Methyl myristoleate 2 wt. %
C15:0	Methyl pentadecanoate 2 wt. %
C15:1	Methyl <i>cis</i> -10-pentadecenoate 2 wt. %
C16:0	Methyl palmitate 6 wt. %
C16:1n7	Methyl palmitoleate 2 wt. %
C17:0	Methyl heptadecanoate 2 wt. %
C17:1	Methyl <i>cis</i> -10-heptadecenoate 2 wt. %
C18:0	Methyl stearate 4 wt. %
C18:1n9 <i>trans</i>	Methyl elaidate 2 wt. %
C18:1n9	Methyl oleate 4 wt. %
C18:2n6 <i>trans</i>	Methyl linolelaidate 2 wt. %
C18:2n6	Methyl linoleate 2 wt. %
C18:3n6	Methyl γ -linolenate 2 wt. %
C18:3n3	Methyl linolenate 2 wt. %
C20:0	Methyl arachidate 4 wt. %
C20:1n9	Methyl <i>cis</i> -11-eicosenoate 2 wt. %
C21:0	Methyl heneicosanoate 2 wt. %
C20:2n6	<i>cis</i> -11,14-Eicosadienoic acid methyl ester 2 wt. %
C20:3n6	<i>cis</i> -8,11,14-Eicosatrienoic acid methyl ester 2 wt. %
C20:4n6	Methyl arachidonate 2 wt. %
C20:3n3	<i>cis</i> -11,14,17-Eicosatrienoic acid methyl ester 2 wt. %
C22:0	Methyl behenate 4 wt. %
C22:1n9	Methyl <i>cis</i> -13-docosenoate 2 wt. %
C20:5n3	<i>cis</i> -5,8,11,14,17-Eicosapentaenoic acid methyl ester 2 wt. %
C23:0	Methyl tricosanoate 2 wt. %
C22:2n6	<i>cis</i> -13,16-Docosadienoic acid methyl ester 2 wt. %
C24:0	Methyl tetracosanoate 4 wt. %
C24:1n9	Methyl <i>cis</i> -15-tetracosenoate 2 wt. %
C22:6n3	<i>cis</i> -4,7,10,13,16,19-Docosahexaenoic acid methyl ester 2 wt. %

Table 6. Fatty acids standard mixes (PUFA No.3; Linolenic Acid Methyl Ester Isomer mix; Linoleic Acid Methyl Ester Isomer Mix; F.A.M.E. Mix, C20:1-C20:5 Unsaturates) used for the detection of fatty acid methyl esters by Gas Chromatography - Flame Ionisation Detection (GC-FID)

PUFA No.3 - From Menhaden Oil, analytical standard * - Code 47085-U	
C22:5n3	<i>cis</i> -4,7,10,13,16,19-Docosahexaenoic acid methyl ester
C20:3n3	<i>cis</i> -11,14,17-Eicosatrienoic acid methyl ester
C20:4n6	Methyl arachidonate
C22:5n3	Methyl all- <i>cis</i> -7,10,13,16,19-docosapentaenoate
C20:5n3	Methyl all- <i>cis</i> -5,8,11,14,17-eicosapentaenoate
20:1n11	Methyl <i>cis</i> -11-eicosenoate
C18:2n6	Methyl linoleate
C18:3n3	Methyl linolenate
C14:0	Methyl myristate
C18:1n9	Methyl oleate
C16:0	Methyl palmitate
C16:1n7	Methyl palmitoleate
C18:0	Methyl stearate
18:4n3	Methyl stearidonate
18:2n4	11,14-Octadecadienoic acid methyl ester
18:3n4	9,11,14-Octadecatrienoic acid methyl ester
C18:1n7	<i>cis</i> -11-Octadecenoic methyl ester
Linolenic Acid Methyl Ester Isomer mix - Code CRM47792	
	<i>cis</i> -9, <i>cis</i> -12, <i>cis</i> -15-Octadecatrienoic acid methyl ester 3% (w/w)
C18:3n3	<i>cis</i> -9, <i>cis</i> -12, <i>trans</i> -15-Octadecatrienoic acid methyl ester 7% (w/w)
(<i>cis</i> and	<i>cis</i> -9, <i>trans</i> -12, <i>cis</i> -15-Octadecatrienoic acid methyl ester 7% (w/w)
<i>trans</i>)	<i>cis</i> -9, <i>trans</i> -12, <i>trans</i> -15-Octadecatrienoic acid methyl ester 15% (w/w)
	<i>trans</i> -9, <i>cis</i> -12, <i>cis</i> -15-Octadecatrienoic acid methyl ester 7% (w/w)
	<i>trans</i> -9, <i>cis</i> -12, <i>trans</i> -15-Octadecatrienoic acid methyl ester 15% (w/w)
	<i>trans</i> -9, <i>trans</i> -12, <i>trans</i> -15-Octadecatrienoic acid methyl ester 30% (w/w)
Linoleic Acid Methyl Ester Isomer Mix - Code CRM47791	
	<i>cis</i> -9, <i>cis</i> -12-Octadecadienoic acid methyl ester 10 % (w/w)
C18:2n6	<i>cis</i> -9, <i>trans</i> -12-Octadecadienoic acid methyl ester 20 % (w/w)
(<i>Cis</i> and	<i>trans</i> -9, <i>cis</i> -12-Octadecadienoic acid methyl ester 20 % (w/w)
<i>trans</i>)	<i>trans</i> -9,12-Octadecadienoic acid methyl ester 50 % (w/w)
	<i>cis</i> -9, <i>cis</i> -12-Octadecadienoic acid methyl ester 10 % (w/w)
	<i>cis</i> -9, <i>trans</i> -12-Octadecadienoic acid methyl ester 20 % (w/w)
	<i>trans</i> -9, <i>cis</i> -12-Octadecadienoic acid methyl ester 20 % (w/w)
F.A.M.E. Mix, C20:1-C20:5 Unsaturates- Code 18913	
C20:1n9	<i>cis</i> -11-Eicosenoic acid methyl ester ~ 10 mg
C20:2n6	<i>cis</i> -11,14-Eicosadienoic acid methyl ester ~ 10 mg
C20:3n3	<i>cis</i> -11,14,17-Eicosatrienoic acid methyl ester ~ 10 mg
C20:4n6	<i>cis</i> -5,8,11,14-Eicosatetraenoic acid methyl ester ~ 10 mg
C20:5n3	<i>cis</i> -5,8,11,14,17-Eicosapentaenoic acid methyl ester ~ 10 mg

Table 7. Individual Fatty acids standard used for the detection of fatty acid methyl esters by Gas Chromatography - Flame Ionisation Detection (GC-FID)

C16:1n7	palmitoleic acid / <i>cis</i> -9-Hexadecenoic acid *	P9417
C17:0	Heptadecanoic acid *	H3500
C20:1n9	<i>cis</i> -11-Eicosenoic acid *	44878
C20:2n6	<i>cis</i> -11,14-Eicosadienoic acid methyl ester	E7477
C20:3n6	<i>cis</i> -8,11,14-Eicosatrienoic acid methyl ester	E3511
C20:4n6	Methyl arachidonate	A9298
C22:0	Docosanoic acid / Behenic acid *	216941
C22:1n9	<i>cis</i> -13-Docosenoic acid / Erucic acid *	45629
C20:5n3	<i>cis</i> -5,8,11,14,17-Eicosapentaenoic acid methyl ester	47571-U
C22:2n6	<i>cis</i> -13,16-Docosadienoic acid methyl ester	D4034
C24:1n9	<i>cis</i> -15-Tetracosenoic acid / Nervonic acid *	N1514
C22:6n3	<i>cis</i> -4,7,10,13,16,19-Docosahexaenoic acid *	D2534
DMA 16:0	16:0 dimethylacetal *	852446C
DMA 18:0	18:0 dimethylacetal *	852448C
DMA 18:1	18:1 dimethylacetal *	852449C
C18:1n7 <i>trans</i>	<i>trans</i> -Vaccenic acid / 11- <i>trans</i> -Octadecenoic acid *	V1131
C18:1n7	<i>cis</i> -vaccenic acid / <i>cis</i> -11-Octadecenoic acid *	V0384
C22:4n6	<i>cis</i> -7,10,13,16-Docosatetraenoic acid *	D3659
C22:5n3	<i>cis</i> -7,10,13,16,19-Docosapentaenoic methyl ester	47563-U
C20:3n9	<i>cis</i> -5,8,11-Eicosatrienoic acid, Mead acid	43059

*Fatty acid standards not purchased in methyl form, were subjected to methylation (as described in Section 2.5) prior to injection

2.7 Unsaturation Index (UI)

The Unsaturation index (UI), also known as the index of hydrogen deficiency (IHD), is a measure of unsaturation that describes the fluidity of a biological membrane. It is useful in interpreting membrane and tissue fatty acid composition, fluidity, and basal metabolic rate (Weijers 2016a, 2016b, 2015, 2012) is calculated as the mean number of *cis* double bonds per fatty-acid residue multiplied by 100.

$$\text{Unsaturation Index} = \text{Mean number of Cis double bonds} \times 100$$

For its use in interpreting membrane fluidity using fatty acid percentages (%) the following calculation is made:

$$\text{Unsaturation Index} = \text{Mean number of Cis double bonds} \times \% \text{ of fatty acid in sample}$$

2.8 Phospholipid analysis by HPLC

A HPLC method for the separation and characterization of PPL molecular species was explored utilizing a 2-dimensional (2D) LC (LC×LC; HILIC X C18) separation system. Initial method optimization data can be found in Appendix 4. Due to time constraints, this method of analysis was reassessed, and it was decided that total PPL fatty acid profiles were examined instead. Therefore, this additional analysis was not utilized for the further sample analysis of the PPL SPE fractions.

2.9 Cell culture

PC12 - Rat adrenal pheochromocytoma (ATCC® CRL-1721) hereafter referred to as PC12 cells were purchased through Public Health England from the European Collection of Authenticated Cell Cultures (ECACC) (PC-12 – 88022401). All reagents were obtained from Sigma-Aldrich and ThermoFisher Scientific unless otherwise indicated. Standardised *Ginkgo biloba* extract (GbE) was obtained from Southern Anhui Dapeng (China) and generously gifted by Dr M.M. Telles Group, Federal University of São Paulo, Brazil. All procedures were performed aseptically. PC12 cells grow satisfactory as small irregularly shaped cells in small multi-cell aggregates, floating in suspension but show poor adherence to plastic and non-coated surfaces. For adherence, cells are grown on either type I or type IV collagen-coated tissue culture vessels where they exhibit a varied profile of small epithelial-shaped cells, some stellate-shaped cells, some elongated cells and some rounded but attached cells and possess a high differentiation potential in response to NGF treatment (Kinarivala *et al.*, 2017; ATCC, 2014).

2.10 PC12 complete growth media

PC12 cells cultures were incubated in a humidified atmosphere containing 5% CO₂ at 37°C in complete growth media (Gibco™ Roswell Park Memorial Institute (RPMI) 1640 Medium (ATCC Modification) modified with 10% heat-inactivated horse serum, 5% fetal bovine serum and Penicillin/streptomycin solution at 100 I.U -100µg/ml. The reported doubling time of PC12 cells is 48 for suspension and 92 hours for adherent cells (ATCC, 2014). All data was collected between passages 9-13.

2.11 PC12 cell growth and subculturing

2.11.1 PC12 cells in suspension

The cell and media content of the flask were transferred to a plastic centrifuge tube and mixed thoroughly using a serological pipette to dissociate large aggregates into small clusters. Cell cultures were centrifuged at 21°C for 1 minute per ml at 200xg. The supernatant was removed and retained for use in the sub-culture media. The cell pellet was re-suspended in an initial 1 ml of complete growth media, thoroughly mixed 10 times using a 200µl pipette tip to breaks up cell clusters and counted by haemocytometer using trypan blue solution. Cultures were split every 2-3 days to a sub-cultivation to achieve 1 x 10⁵ to 1 x 10⁶ viable cells/ml. Appropriate aliquots of the cell suspension were added to a new culture vessel following appropriate volumes of growth media per culture vessel (See Type I collagen solution (Corning™ Collagen I, Rat 100mg, Cat no#11563550) was purchased from Fisher Scientific. Poly-L-lysine solution (0.01%, sterile-filtered, BioReagent, Cat no.#P4707) and type IV Collagen (from human placenta, Bornstein and Traub Type IV, powder, Cat no.#C5533) was purchased from Merck-Sigma-Aldrich. Type IV collagen solution was made up to a final solution of 1mg/ml (0.1% w/v collagen solution) in 0.1M glacial acetic acid stirred at room temperature for 1-3 hours as per Merck PC12 collagen coating protocol (Merck, 2020a). The solution was sterilised by incubating overnight at 4°C with 10% v/v chloroform. The top collagen layer was aseptically removed, aliquoted and stored at -20°C for up to 6 months. Aliquots were subsequently defrosted and diluted 10 times to obtain at 0.01% solution as needed.

Table 8). Sub-culturing growth media was comprised of 20% old, conditioned media and 80% new complete growth media warmed to 37°C prior to the addition of cells. Media was renewed every 2-3 days. Subculture was performed when cell density reached between $2-4 \times 10^6$ viable cells/ml or 70% confluency.

2.11.2 Adherent PC12 cells

Complete growth media was aspirated from the flask using a serological pipette and retained and the cells washed with 1X PBS. Cells were detached by 0.25% trypsin-EDTA at a ratio of 0.06-0.1ml/cm² and incubated for 3-5 minutes at 37°C in a humidified incubator. Trypsin-EDTA was neutralized by adding an equal volume of complete growth media to the flask and the contents gently triturated using a serological pipette to dissociate aggregates and remaining adherent cells. The contents were centrifuged at 21°C for 1 minute per ml at 200xg. The supernatant was removed and discarded. The cell pellet was re-suspended in an initial 1 ml of complete growth media gently triturated 5 times using a 200µl pipette tip to break up cell clusters and counted by haemocytometer using trypan blue staining. Cultures were split to a sub-cultivation ratio of 1:2 to 1:4 to achieve $1-2 \times 10^4$ cells/cm² viable cells. Appropriate aliquots of the cell suspension were added to a new culture vessel following appropriate volumes of growth media per culture vessel (See Table 8). Sub-culturing growth media was comprised of 80% new complete growth media and 20% of the old, conditioned media. Media was renewed every 2-3 days by gently pouring off 80% of old media and replacing with warmed (37°C) new complete media. Subculture was performed when cell density reached between $3-5 \times 10^4$ cells/cm² viable cells or 70% confluency.

2.12 Cryopreservation of stocks

Frozen stocks of a low passage number were prepared. Briefly, cell suspensions of 1×10^6 cells/ml were prepared in complete growth media supplemented with 10% dimethyl sulfoxide (DMSO) and aliquoted in to sterile cryostatic vials. Aliquots were frozen overnight to -80 using a CoolCell® Cell Freezing Container at a rate of $-1^\circ\text{C}/\text{minute}$ before transfer to liquid nitrogen for long term storage.

2.13 Coating of cell culture vessels

Recommendations for the concentrations of poly-L-lysine and collagen for coating tissue culture plates vary between suppliers and protocols. For this protocol Corning guidelines ($1\text{-}5\mu\text{g}/\text{cm}^2$) (Corning, 2019) and Sigma guidelines ($6\text{-}10\mu\text{g}/\text{cm}^2$) (Merck, 2020a) were chosen as recommended under the ATCC PC-12 (ATCC® CRL-1721™) protocol (ATCC, 2014). A final concentration of $10\mu\text{g}/\text{cm}^2$ was chosen.

2.14 Preparation of collagen

Type I collagen solution (Corning™ Collagen I, Rat 100mg, Cat no#11563550) was purchased from Fisher Scientific. Poly-L-lysine solution (0.01%, sterile-filtered, BioReagent, Cat no.#P4707) and type IV Collagen (from human placenta, Bornstein and Traub Type IV, powder, Cat no.#C5533) was purchased from Merck-Sigma-Aldrich. Type IV collagen solution was made up to a final solution of $1\text{mg}/\text{ml}$ (0.1% w/v collagen solution) in 0.1M glacial acetic acid stirred at room temperature for 1-3 hours as per Merck PC12 collagen coating protocol (Merck, 2020a). The solution was sterilised by incubating overnight at 4°C with 10% v/v chloroform. The top collagen layer was aseptically removed, aliquoted and stored at -20°C for up to 6 months. Aliquots were subsequently defrosted and diluted 10 times to obtain at 0.01% solution as needed.

Table 8. Summary of cell culture subculture guidelines for ATCC PC-12 cells (ATCC® CRL-1721™)(Thermo-Fisher 2020a; Orlowska et al. 2017; Merck 2020c, 2020a; Martin and Grishanin 2003; Kinarivala et al. 2017a; Corning 2019; ATCC 2014a).

Surface area (cm ²)			PC 12 cell - Suspension		Collagen type I solution (0.1mg/ml)	PC 12 cell - Adherent	
			Initial seeding density	Cells at confluency		Initial seeding density	Cells at confluency
			0.5 - 1 x 10 ⁶ viable cells/ml	2-4 x 10 ⁶ viable cells/ml	µl	1-2 x 10 ⁴ cells/cm ²	4-5 x 10 ⁴ cells/cm ²
Dishes Based on upper estimated recommendation							
35mm	8.8	2	1 x 10 ⁶	4 x 10 ⁶	20	0.18 x 10 ⁶	4.5 x 10 ⁵
60mm	21.5	5	2.5 x 10 ⁶	10 x 10 ⁶	880	0.43 x 10 ⁶	1.1 x 10 ⁶
100mm	56.7	12	6 x 10 ⁶	24 x 10 ⁶	2150	1.13 x 10 ⁶	2.8 x 10 ⁶
150mm	145	30	15 x 10 ⁶	60 x 10 ⁶	5670	2.9 x 10 ⁶	7.25 x 10 ⁶
Culture plates							
6-well	9.6	2	1 x 10 ⁶	4 x 10 ⁶	960	1.9 x 10 ⁵	4.8 x 10 ⁵
12-well	3.5	1	0.5 x 10 ⁶	2 x 10 ⁶	350	7 x 10 ⁴	1.75 x 10 ⁴
24-well	1.9	0.5	0.25 x 10 ⁶	1 x 10 ⁶	190	3.8 x 10 ⁴	9.5 x 10 ⁴
48-well	1.1	0.2	0.1 x 10 ⁶	0.4 x 10 ⁶	110	2.2 x 10 ⁴	5.5 x 10 ⁴
96-well	0.32	0.1	0.05 x 10 ⁶	0.2 x 10 ⁶	32	6.4 x 10 ³	1.6 x 10 ⁴
Flasks							
T-25	25	5	2.5 x 10 ⁶	10 x 10 ⁶	2500	5 x 10 ⁵	1.25 x 10 ⁶
T-75	75	10	5 x 10 ⁶	84 x 10 ⁶	7500	1.5 x 10 ⁶	3.75 x 10 ⁶
T-175	175	35	17.5 x 10 ⁶	70 x 10 ⁶	17500	3.5 x 10 ⁶	8.75 x 10 ⁶
T-225	225	45	22.5 x 10 ⁶	90 x 10 ⁶	22500	4.5 x 10 ⁶	11.5 x 10 ⁶

2.15 Preparation of culture vessels

Sufficient 0.01% solution of either PPL, type I or Type IV collagen was added to cover the surface of the tissue culture vessel of choice (as summarized in Table 8). The vessel was coated by gentle swirling and agitating of the applied solution around the vessel before being left to set in a sterile hood overnight at room temperature. The next day, the remaining solution was removed, and the culture vessels were washed three times in sterile PBS for 5 minutes. Culture vessels were sterilized by exposure to UV light and left to dry in a sterile culture hood, before being stored at 4°C until needed.

2.16 Differentiation

PC12 cells respond reversibly to nerve growth factor (NGF) by induction of the neuronal phenotype when plated on PPL and Collagen coated culture vessels. Nerve Growth Factor (NGF-2.5S from murine submaxillary gland, Cat. no# N6009) was purchased from Merck-Sigma-Aldrich. NGF was made up to a final concentration of 1×10^5 ng/ml stock solution in 0.85% NaCl, sterile filtered through a 0.2 µm pore PES membrane sterile filter, aliquoted and frozen and stored -20 °C for up to 6 months. Differentiation media was comprised of Gibco™ RPMI 1640 Medium (ATCC Modification) (code:11054566) modified with either 1%, 0.5% or 0.1% heat-inactivated horse serum (Sigma Cat. no# H1138) or 1% bovine serum albumin (Sigma Cat. no# A9418), Penicillin/streptomycin solution (100 I.U -100µg/ml; Gibco™ Penicillin-Streptomycin -10,000 U/mL, Cat no.# 11548876) and either 25, 50 or 100ng/ml NGF.

2.17 Differentiated PC12 experiments

Cells were seeded at 5×10^6 on T75-type I collagen-coated flasks with RPMI complete growth media and allowed to adhere for 24-36 hours. The media was changed to low-serum 1% bovine serum albumin (BSA) media supplemented with 25ng/ml NGF. Differentiation media was changed every 2 days. After 7 days, cells were trypsinized (Gibco™ Trypsin-EDTA (0.25%) Cat no.# 11560626) for 5 minutes at 37°C, an equal volume of RPMI complete media was added to neutralize the trypsin-EDTA and cells transferred to falcon tubes and centrifuged at 100xg for 1minute/ml. The supernatant was discarded, and cells were gently washed with 1X Sterile PBS, before being centrifuged again at 100xg for 1minute/ml to help remove dead cells. Cells were counted by haemocytometer and replated on type I collagen-coated culture vessels at desired concentrations for subsequent experiments in 1% BSA-25ng/ml NGF supplemented media. Differentiated cells were allowed to adhere and re-establish neurite outgrowth for 24 hours before further experimentation.

2.18 GbE stocks

GbE was made up to a main stock solution of $1 \times 10^5 \mu\text{g/ml}$ in sterile 0.85% NaCl and sterile filtered through a 0.2 μm pore PES membrane sterile filter. Further lower concentration stocks were made in RPMI 1640 media to produce the final concentrations required for treatment.

2.19 Fatty acid stocks

Fatty acids were obtained from Merck-Sigma-Aldrich (P5585-10G Palmitic acid BioXtra, $\geq 99\%$ - C16:0; S4751-10G Stearic acid - C18:0; O1383-5G Oleic acid - C18:1n9; L1012-5G Linoleic acid - C18:2n6; L2376-500MG Linolenic acid - C18:3n3). 100 mM stock solutions of each FA were prepared in ethanol, aliquoted into brown glass vials, flushed with N₂, capped, and frozen at -20°C . Each aliquot was used only once. For cell culture treatments a mixed FA stock solution was created based on fatty acid profiles of the normal and high fat diet rat chow used in the Wistar rat Study. Briefly, to mimic a normal fat diet (NFD) FA profile the following percentages of each 100 mM FA stock solution was mixed (C16:0 – 15%, C18:0 – 4%, C18:1n9 - 24%, C18:2n6 – 55%, C18:3n3 – 5%). To mimic a high fat diet (HFD) FA profile the following percentages of each 100 mM FA stock solution was mixed (C16:0 – 21%, C18:0 – 12%, C18:1n9 - 36%, C18:2n6 – 21%, C18:3n3 – 1%). These mixed FA stocks were aliquoted into brown glass vials, flushed with N₂, capped, and frozen at -20°C . Each aliquot was used only once. Prior to treatments, 100X stocks were made for both NFD and HFD FA treatments as a 4:1 molar complex with fatty acid-free BSA (100 mg/ml) (BSA - Sigma Aldrich, A8806, $\leq 0.02\%$ FA). 100 X stocks were diluted in RPMI 1640 media without serum substitute to give a final concentration of 1% BSA and 1X FA concentrations required for FA treatment. Control cells were exposed to 1% BSA media only.

2.20 Cell imaging

Images were taken using an inverted microscope, equipped with a 5MP Moticam 5 and processed on Motic Images Plus 3.0 - Image Analysis Software. Three representative fields of images were taken for each sample, and a total three replicate samples were tested for each group, corresponding to nine fields of images for each group.

2.21 MTT (3-[4,5-dimethylthiazol-2-yl]-2,5-diphenyltetrazolium bromide) cell viability assay

To determine cell viability of PC12 cell differentiation, cells were seeded in triplicate into 96 well plates at a density of 5×10^4 cells/cm² in 100 μl of RPMI complete media and allowed to adhere to

collagen coated surface for 24 hours. Plates were incubated at 37°C, 5% of CO₂. For differentiation experiments, after 24 hour adherence time, RPMI media was replaced with serum-reduced media (1%, 0.5% and 0.1% horse serum media or 1% BSA reduced-serum media) for 24 hours to synchronise the cell cycle followed by treatment with 25, 50 or 100ng/ml NGF (Sigma Aldrich, Nerve Growth Factor-2.5S from murine submaxillary gland, #N6009) or GbE 50 or 100µg/ml. Media was replaced every 48 hours. After 7 days of NGF treatment, culture media was aspirated slowly and carefully from the side of the well using a pipette tip to limit any disturbance of adherent cells. 10µL of 5mg/ml (final concentration 0.5 mg/ml) MTT labelling reagent (3-[4,5-dimethylthiazol-2-yl]-2,5-diphenyltetrazolium bromide (Sigma Aldrich # M2128)/1X PBS (Fisher scientific #BP2944-100)) was added to each well and incubated for 4 hours (37°C, 5% of CO₂). 100 µL of solubilization solution (10% SDS in 0.01M HCL) was added to each well, wrapped in tinfoil and incubated for 1 hour at room temperature. The wells were mixed for 30 seconds by shaking on a ThermoFisher Multiskan FC microplate photometer followed by measure of absorbance read at 590nm with a reference wavelength of 700 nm. The percentage viability was calculated by comparing the control absorbance values (cells without NGF treatment) against treatment samples. Proliferation/viability of each media was measured by MTT assay at 0, 48, 96 and 144 hrs of NGF treatment. Data was statistically analysed by One-way ANOVA with Tukey *post hoc* test. The level of statistical significance was set at *p < 0.05.

2.22 Annexin V/7-AAD cell viability/apoptosis assay

To determine the effect of 1% BSA-NGF treatment on PC12 differentiation, cellular viability/apoptosis was confirmed by flow cytometric analysis using 7AAD/ Annexin V FITC staining using the commercially available APC Annexin V Apoptosis Detection Kit with 7-AAD kit, as per the manufacturer's instructions (Biolegend 2020). Briefly, PC12 cells were treated for 7 days with 1% BSA media supplemented with 25ng/ml NGF. PC12 cells were trypsinized for 3 minutes to release them from the collagen-coated surface. Trypsin was then neutralized with an equal volume of RPMI-complete media, and the cell sample centrifuged (100xg) to pellet the cells. The supernatant was discarded. The cell pellet was washed with 1X PBS and centrifuged again, and the supernatant discarded. To 1 X 10⁵ cells, 100µl of cell staining buffer (Biolegend 420201) was added and 5µl each of Annexin (Biolegend 640945) and 7AAD (Biolegend 420404). Cells were gently vortexed before being incubated for 15 minutes in the dark at room temperature. A further 100µl of binding buffer was added to each sample and the sample vortexed immediately prior to running on a GuavaCyte

flow cytometer with Incyte software (Merck). Intact cells were separated from debris by Forward Scatter (FSC) / Side Scatter (SSC) gate. Bivariate analysis was conducted using the FL1 (Blue/Green) and FL3 (Blue/Red) channels to identify the percentage populations of apoptotic/non-apoptotic and viable/non-viable cells.

2.23 β -Tubulin III expression

To determine the effect of 1% BSA-NGF treatment on PC12 differentiation, levels of β -tubulin III were analysed by flow cytometry. PC12 cells were treated for 7 days with 1% BSA media supplemented with 25ng/ml NGF and compared against non-NGF treated cell grown in RPMI complete media. After 7 days cells were harvested by trypsinisation as described above. Cells underwent fixation and permeabilization with Biolegend Cyto-Fast™ Fix/Perm Buffer Set (Biolegend 426803) as per manufacturer's instructions (Biolegend 2018). Briefly, cells were analysed from 3 different passages (n=3) with a minimum of 4 replicates per passage. 75 μ l of Cyto-Fast™ Fix/Perm Buffer was added to each 1 X 10⁵ cells, gently vortexed and incubated at room temperature for 20 minutes. 1 ml of 1XCyto-Fast™ Perm Wash solution was added to each sample and centrifuged at 350xg for 5 minutes, discarding the supernatant. This wash step repeated. Antibodies were made up in 1XCytoFast™ Perm Wash Solution to a 100 μ l total volume. Cells were labelled with either Biolegend PE anti-Tubulin β 3 (TUBB3) Antibody (Biolegend 801222) or PE Mouse IgG2a, κ Isotype Ctrl Antibody (Biolegend 400212), as per manufacturer's instructions. Cells were separated and analysed by GuavaCyte flow cytometer with Incyte software (Merck) by Forward Scatter (FSC) / Yellow-blue channels and the mean fluorescence intensity (MFI) calculated. Data was presented as mean \pm SEM (n=3) analysed by one-way ANOVA with Tukey post-hoc test The level of statistical significance was set at *p < 0.05.

2.24 Whole cell lysis

Cell treatment plates were removed from the incubator and placed immediately on ice. All remaining steps were performed on ice. The culture media was aspirated from each plate well and cells gently washed with 1ml of ice-cold 1X PBS per well, followed by aspiration. Per million cells/well, 100 μ l of ice-cold RIPA lysis buffer (Thermo Scientific™ RIPA Lysis and Extraction Buffer, #10017003) supplemented with protease and phosphatase inhibitors (Thermo Scientific Pierce™ protease and phosphatase inhibitors 1 mini-tablet per 10ml buffer solution) was added. The cellular monolayer was scraped from the culture vessel surface by a flexible plastic scraper, and the cell/lysis solution was transferred to an Eppendorf tube, mixed thoroughly with a 200 μ l pipette tip and incubated on ice for 20 minutes. Lysates were centrifuged at 16,000 x g for 15 minutes at 4°C. The lysate

supernatant was transferred to a fresh Eppendorf tube and stored at -80°C for further use. A 10µl aliquot of the lysate was used for protein quantification *via* a Bicinchoninic Acid assay (BCA).

2.25 BCA (Bicinchoninic acid) protein concentration determination assay

Protein concentration was determined by Bicinchoninic acid assay (BCA). The BCA reagent was prepared as per manufacturer's instructions (ThermoFisher, Pierce™ BCA Protein Assay Kit, 23225). In brief, a 1:50 ratio working solution of BCA reagent: copper (II) sulphate pentahydrate (4% w/v) was made. 8 protein standards (0, 0.31, 0.061 0.125, 0.25, 0.5, 1, 2 µg/µL) were generated by serial dilution from a 10 mg/ml bovine serum albumin (BSA) protein standard to create a standard curve of known protein concentration. On ice, 25 µL of each standard was added in triplicate to a 96 well plate. A 1:10 dilution was made of each cell lysate by adding 2.5 µL of cell lysate to a fresh well followed by 22.5 µL of de-ionised water per well (1:10 dilution) and repeated in triplicate. 200 µL of BCA:4% cupric sulphate working solution was added to each well. The plate was wrapped in tinfoil and the wells mixed for 30 seconds by shaking on a ThermoFisher Multiskan FC microplate photometer followed by incubation at 37°C for 30 mins. Measurement of absorbance was read at λ 562nm on a ThermoFisher Multiskan FC microplate photometer. Cell lysate protein concentration was determined from the BSA protein standard curve equation.

2.26 Preparation of whole cell lysis for SDS-PAGE separation

Samples were prepared fresh for each experiment at a protein concentration of 1µg/µL as determined by BCA assay using the following formula:

$$\frac{\text{Desired concentration } 1\mu\text{g}/\mu\text{l}}{\text{Current concentration } \mu\text{g}/\mu\text{l}} \times \text{Total volume of sample needed}$$

On ice, and in a fume hood, an equal volume (1:1 ratio) of whole cell lysate was mixed with 2X loading buffer containing 3% β-mercaptoethanol (2XLB+6% BME- prepared in hood), and the mixture diluted with dH₂O to make a final volume of sample required. Samples were heat denatured at 95°C for 3 minutes.

2.27 SDS PAGE

Separation of whole cell lysates by SDS PAGE was carried out as described previously (O'Flanagan *et al.* 2014; Moloney *et al.* 2010). 10 µg (1µg/µL) of sample was loaded onto and separated by SDS-PAGE using 1X Running buffer (25mM Tris (trizma base), 192mM Glycine, 0.1% SDS). The samples were initially electrophoresed through a 5% stacking gel (69% H₂O, 17% Bis-acrylamide (30%), 13% 1.0M Tris PH 6.8, 1% SDS, 1% APS, 0.01% v/v TEMED) at 100 mv / 70 mA for 20 min until the loading buffer dye migrated to the 10% resolving gel (39 % H₂O, 33% Bis-acrylamide (30%), 25% 1.5M Tris PH 8.8, 0.1% SDS, 0.1% APS, 0.004% v/v TEMED). Electrophoresis was increased to 160 mV / 70 mA for a further 60-90 min.

2.28 Protein transfer to nitrocellulose

SDS-PAGE separated proteins were transferred electrophoretically to nitrocellulose membranes by cold wet transfer using ice cold transfer buffer (80% 48 mM Tris base, 39 mM glycine transfer solution mixed with 20% ethanol) for 1 hour at 100V 350 mA with stirring. The membrane was washed for 5 minutes with TBS-T (10mM Tris, 1.5 mM NaCl, 0.1% Tween) and blocked in 1% BSA in TBS-T for a minimum of 1 hour at room temperature or overnight at 4°C.

2.29 Western immunoblotting

Following nitrocellulose membrane blocking, the membrane was incubated with primary antibodies made in 1% BSA/TBS-T on a see-saw rocker for a minimum of 1 hour at room temperature or at 4°C overnight on a see-saw rocker. Following antibody incubation, membranes underwent three 10-minute washes with 1X TBS-T to remove any residual primary antibody. Membranes were then incubated with an HRP-linked secondary antibody for 1 hour at room temperature (RT) followed by three 5-minute washes in 1X TBS-T. Immunoreactive proteins were detected with enhanced chemiluminescence (ECL) ECL Prime Western Blotting System, Amersham Biosciences, Cyvita, Little Chalfont, Buckinghamshire, UK) as per the manufacturer's instructions. Chemiluminescent signal was captured using Syngene PXi-gel-doc-system (Cambridge, UK). Semi-quantification of results was performed by densitometry (Syngene Genetools software, Cambridge, UK) and normalized to control protein (β-actin), as shown in equation below. Results were shown as percentage (%) of control sample. Data was statistically analysed by One-way ANOVA with Tukey *post hoc* test. The level of statistical significance was set at *p < 0.05.

$$\text{Lane normalisation factor} = \frac{\text{Observed signal of housekeeping protein for each lane}}{\text{Highest observed signal of housekeeping protein on the blot}}$$

The following primary antibodies, dilutions and sources were used:

Neurofilament-L (C28E10) Rabbit mAb (1:2000) (Cell Signalling #2837), Neurofilament-M (E7L2T) Rabbit mAb (1:2000) (Cell Signalling #67255), Nrf2 (D1Z9C) XP[®] Rabbit mAb (Cell Signalling #12721), β -Actin (D6A8) Rabbit mAb (1:10000) (Cell Signalling #8457), Akt total (1: 2,000) (Cell Signalling #9272), p-AktSer473 (1:1000) (Cell Signalling #4060), GAPDH Direct-Blot™ HRP anti-GAPDH Antibody (Biolegend #607904). Primary antibodies were detected by anti-rabbit IgG, horseradish peroxidase (HRP)-linked secondary antibody (1:1000, Cell signalling #7074).

Chapter 3 - Male Wistar rat study - Macronutrients and body metrics

3.1 Rat study macronutrient, food intake, efficiency, body metrics

More than 50 per cent of the adult population in both the United States of America and Europe are classified as either overweight or obese (Eurostat, 2021; Fryar, Carroll and Afful, 2020). Of the wide-ranging factors that contribute to obesity and metabolic disease that include genetic susceptibility, hormone disorders, socioeconomic status, and physical activity, a HFD is considered a major but modifiable contributor (Wali *et al.*, 2020; Hochberg, 2018). Levels of fat in the western diet has led to higher caloric intake and increased dietary intakes of saturated fat (EFSA Panel on Dietetic Products and Allergies, 2010). A review of 28 clinical trials reported that there was a positive correlation with overweight and obesity and the proportion of fat-derived energy intake. Furthermore, it was also reported that a reducing dietary fat intake by 16g/day could reduce energy intake by up to 10 per cent, closing the gap between energy intake and energy expenditure (Bray and Popkin, 1998).

It is also known that a HFD leads to deleterious metabolic effects such as IR, T2DM and metabolic syndrome as discussed in chapter 1. Consequences of a HFD include abnormal adipocyte hypertrophy and subsequent hypoxia, OS and low-grade chronic inflammation, especially in the visceral white adipose tissue depots (Hirata, Cruz *et al.*, 2019; Hirata *et al.*, 2015). Rodent studies based on a HFD have been used for decades as a model for western diet intake in humans and have been shown to contribute to IR and cardiometabolic disease in both humans and rodents (Kumar *et al.*, 2021; Canfora *et al.*, 2019; Greenhill, 2018; von Frankenberg *et al.*, 2017).

In the male Wistar rat study, rats were fed either standard rat chow (NuvilabR, Brazil, 2.7 kcal/g), or a supplemented high fat chow prepared by mixing 40% (w/w) ground standard chow with 28% (w/w) melted lard, 20% (w/w) casein powder, 10% (w/w) sucrose, 2% (w/w) soybean oil, and 0.02% (w/w) butylated hydroxytoluene (5.0 kcal/g) as standardized previously and used in previous studies (Hirata, Cruz, *et al.*, 2019; Hirata, Pedroso, *et al.*, 2019).

The macronutrients of the rat chow have been previously standardised and published (Hirata, Cruz *et al.*, 2019) and can be seen in Appendix 5. The macronutrients of most interest include Lipids (NFD-4.5%; HFD - 31.6%); Protein (NFD-22.7%; HFD-27%); Carbohydrate (NFD-35.9%; HFD-27.5%); and Fibre (NFD-18.9%; HFD-8.6%). Lipids in the HFD (HFD) chow were 8 times higher than that of a normal fat diet chow, while carbohydrate percent is decreased by 25% from 36% in NFD to 27.5% in HFD.

The HFD chow provides 19.5% of energy from carbohydrate, 23.2% from protein, and 57.3% from fat, and is demonstrated to induce obesity in a rat model (Hirata *et al.*, 2015, Banin *et al.*, 2014). The energy supply of 57% from fat in the HFD, is nearly double that recommended by the world health organisation (WHO) (FAO, 2010). The supplementation of lard in the rat chow for a HFD also resulted in a 2-fold decrease in total fibre and a 2-fold increase (gram for gram) in the calculated energy (kcal/g) supplied by the HFD chow. Fibre content is important for gut health acting as a gut microbiota regulator aiding and microbiome balance that utilize fibre for energy. Heinritz *et al.*, (2016) found that when comparing pigs fed either an isocaloric diets of either low-fat/high-fibre (LF), or a high-fat/low-fibre (HF) diet for seven weeks the HFD produced a significant increase hypertrophy on digestive organs. The diet *also* increasing the intestinal gene copy numbers of *Bacteroides* and *Enterobacteriaceae* and increased concentration of short chain fatty acids acetate and butyrate associated with obesity (Heinritz *et al.*, 2016). Glucose levels was higher in HF animals, while CRP levels (an acute-phase marker for systemic inflammation) were lower in LF animals (Heinritz *et al.*, 2016). Furthermore, higher fibre intake lowers risk of cardiometabolic disease, hypertension, diabetes, obesity, and certain gastrointestinal diseases, lowers blood pressure, improves glycemia and insulin sensitivity in both diabetic and non-diabetic individuals and enhances weight loss in obese individuals. Increased fibre intake also lowers serum cholesterol levels by aiding the binding and excretion excess dietary cholesterol and bile acids (Anderson *et al.*, 2009). Bailén *et al* (2020) has reported that a high saturated fat/low fibre diet is also associated with a greater sequence abundance of butyrate producing *Anaerotruncus* bacteria, along with alterations in *Lachnospiraceae* *Flavonifractor*, *Campylobacter*, *Erysipelotrichacea* and *Eisenbergiella* associated with increased disease risk particularly with obesity and other pro-inflammatory diseases (Bailén *et al.*, 2020).

3.2 Lipid profiles of NFD chow or HFD chow

Lipids from both NFD and HFD chows were extracted by the Folch method, as described in Chapter 2, and analysed by GC-FID. This data has been published as part of another study (See Appendix 5 for published Table) (Hirata, Cruz *et al.*, 2019). As illustrated in Table 9 the lipid profiles of the HFD chow contains a 2-fold increase in saturated fatty acids (SFA), and nearly 50 percent increase in monounsaturated fatty acids (MUFA) compared to the NFD. The amounts of SFA (~34%) and MUFA (~40%) in the HFD chow are consistent with other reports of western style diet ratios (33% SFA and 36% MUFA) based on a typical American diet (Shively *et al.* 2019; U.S. Department of Agriculture 2016). The levels of n-6 PUFA decreased by nearly 60 percent, while n-3 PUFA decreased by two thirds. Overall PUFA levels decreased by nearly 50 percent in the HFD chow, with a greater decrease in n-3 PUFA. A high intake of dietary saturated fatty acids (SFAs) is associated with higher levels of low-density lipoprotein (LDL) in serum and elevated OS (Kris-Etherton, Petersen and van Horn, 2018) leading to increased risk of obesity and inflammation which may only be attenuated by the replacement of SFA with unsaturated fats and unrefined carbohydrates (Bailén *et al.* 2020; Chiu, Williams and Krauss 2017). Both diets, while providing the essential n-6 (LA) and n-3 PUFA (ALA), does not provide any n-3 LCFA such as EPA and DHA associated with increased anti-inflammatory resolution. A high n-6 PUFA intake is also associated with increased levels of LA, DGLA and AA derived oxylipins, with LA and AA associated with being more pro-inflammatory (Caligiuri *et al.*, 2013), while a n-3 PUFA intake increases ALA, EPA, and DHA derived oxylipins, associated with being anti-inflammatory (Hussey, Lindley & Sarabjit and Mastana, 2017). This was demonstrated well when a diet with a high n-6/n-3-ratio of approximate 18:1 LA/ALA resulted in an increase in n-6/n-3 oxylipins in the liver compared to a lower n-6/n-3 ratio diet (approx. 8:1) (Leng, Winter and Aukema, 2017). The rat chow in our study consisted of a n-6 /n-3-ratio of 12:1 in NFD and 17:1 ratio in the HFD. Extrapolating from the results of Leng and colleagues (2017), it is likely that an increase in n-6/n-3 oxylipins may also occur between our two baseline diet groups.

Table 9. Fatty acid percentage profiles of normal fat diet (NFD) and HFD (HFD) rat chow. Data was analysed by Students t test. The level of statistical significance was set at * $p < 0.05$. Replicated with permission from Hirata, Cruz et al., 2019.

	Standard chow / Normal Fat Diet			Lard enriched Chow / High Fat diet			T test
	Mean %	±	SEM	Mean %	±	SEM	p value
C14:0				1.1	±	<0.1	-
C16:0	13.8	±	0.3	21.4	±	0.1	<0.001
C18:0	3.5	±	0.1	11.6	±	0.1	<0.001
C20:0	0.3	±	<0.1	0.3	±	<0.1	0.98
ΣSFA	17.6	±	0.4	34.4	±	0.2	<0.001
C16:1n7	-		-	1.7	±	<0.1	-
C18:1n7	1.2	±	0.4	2.3	±	<0.1	0.01
C18:1n9	22.2	±	0.3	35.5	±	0.2	<0.001
C20:1n9	0.3	±	0.1	0.6	±	<0.1	0.79
ΣMUFA	23.6	±	0.5	40.1	±	0.1	<0.001
C18:2n6	51.0	±	0.6	21.4	±	0.1	<0.001
C20:2n6	-		-	0.6	±	<0.1	-
C20:3n6	-		-	0.2	±	0.1	-
C20:4n6	-		-	0.3	±	<0.1	-
ΣPUFA n-6	51.0	±	0.6	22.6	±	<0.1	<0.001
C18:3n3	4.3	±	0.1	1.3	±	<0.1	<0.001
ΣPUFA n-3	4.3	±	0.1	1.3	±	<0.1	<0.001
ΣPUFA Total	55.4	±	0.7	23.9	±	<0.1	<0.001
n-6/n-3	11.8	±	0.2	17.7	±	0.2	<0.001
LA/ALA	11.8	±	0.2	16.8	±	0.3	<0.001

ΣSFA = Total Saturated Fatty acids; ΣMUFA= Total monounsaturated fatty acids;

ΣPUFA = Total polyunsaturated fatty acids

3.3 Obesity induction period

For the development of obesity, 2-month-old Wistar rats received either standard chow (NFD, n=10, control group) or a lard-enriched HFD chow (HFD, n=30, obesity induction) *ad libitum* over an 8-week period, as described in Section 2.1.

All rats were weighed weekly. Food (g/100 g/24 h) and energy intake kcal/100 g/24 h were calculated in grams per 24 hrs and by the difference between the food left after 24 hours and that offered 24 h before. Food efficiency was calculated by the ratio of body weight gain (g) to food ingestion (g) weekly. The body weight, food and energy intake, food efficiency, body weight gain data set pertaining to this study has been included in a larger data set previously published (Hirata, Cruz *et al.*, 2019). As illustrated in Figure 9.A, except in the first week of feeding, where HFD animals consumed nearly 23% extra food intake in grams (g/100 g/24 h) ($p=0.0004$) compared to NFD animals, HFD animals consumed significantly less food in grams between weeks 3-9, decreasing steadily from 18% less in week 3 (0.001) to 34% less by week 9 ($p<0.0001$). Energy intake in grams per 24 hrs (kcal/100 g/24 h) as illustrated in Figure 9.B was 125% more in the HFD group in week one ($p<0.0001$) compared to NFD, but halved to 70% more by week 2 and steadily decreased over weeks 3-9 ($p<0.0001$), remaining significantly higher than that of the NFD group, until week 9 ($p=0.054$) where a 20% increase was observed.

Food efficiency [BW gain (g) / food ingestion (g)] as illustrated in Figure 10.A was significantly higher in HFD (10.64 ± 0.37) when compared to NFD (5.09 ± 0.21) ($p<0.0001$). Although energy efficiency (Body mass increase/caloric intake (Kcal/24 hours)) was higher in the HFD group (2.34 ± 0.26) compared to the NFD group (1.86 ± 0.08) as illustrated in Figure 10.B no other significant differences were seen. In Figure 11.A from Week 2-9 of obesity-induction period, both groups showed continued body weight increase. From weeks 2 to 9, the HFD group steadily gained more weight than the NFD group, gaining 8% more in week 2 ($p=0.0005$) up to 28% more by week 9 ($p<0.0001$) with an average extra 158g per HFD animal compared to NFD (Figure 11.Figure 10B.)

Overall, during the obesity development period, it was demonstrated that even when food and energy intake significantly decrease when consuming a HFD (that contributes 57% of calories from fat), food efficiency increases, and contributes to nearly 30% higher weight gain when compared to an NFD.

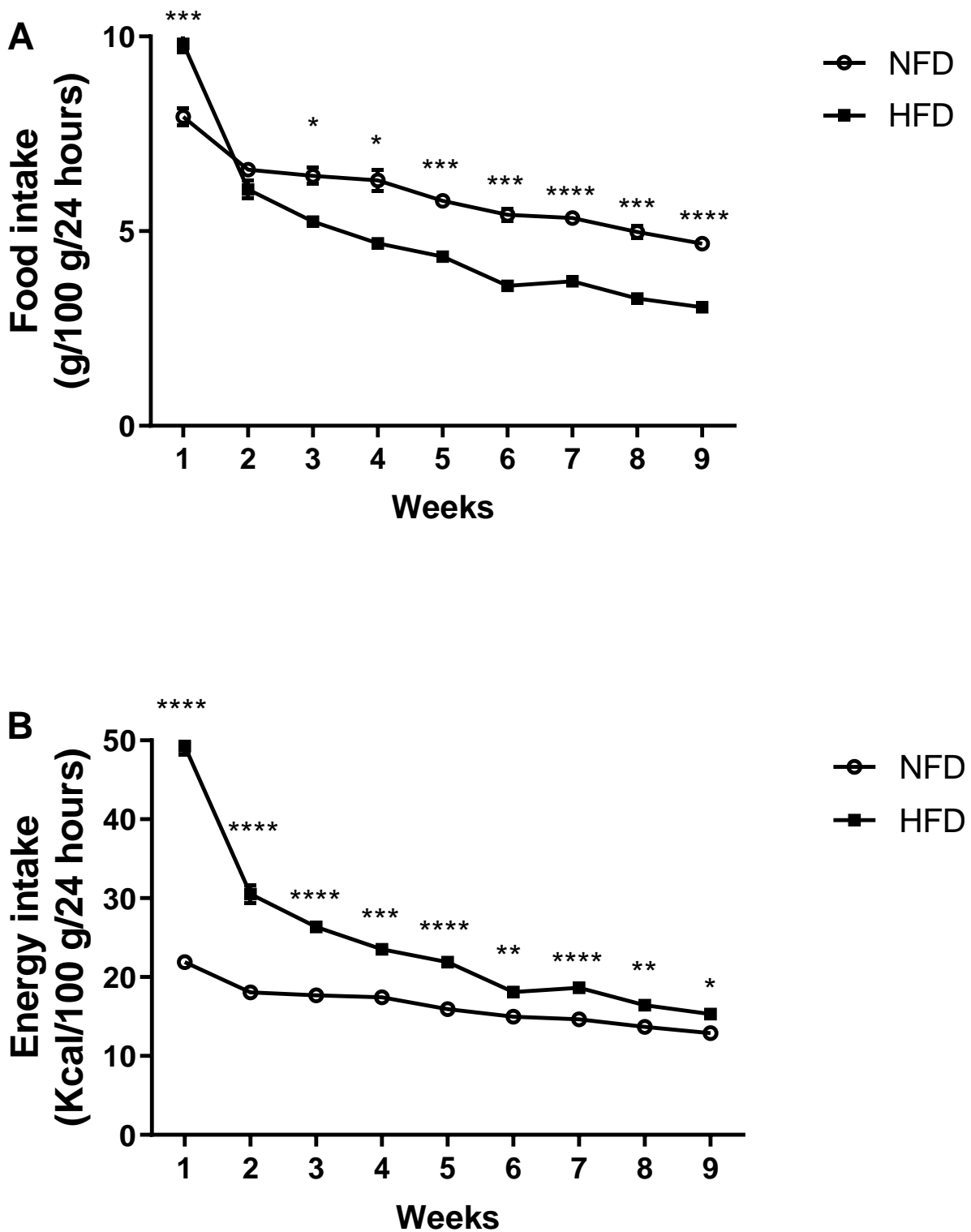


Figure 9. Food intake and energy intake in obesity induction. Food intake (g/100 g/24 h) (A), energy intake (kcal/100 g/24 h) (B), of normal-fat diet (NFD; $n = 5$) and high-fat diet (HFD; $n = 13$) groups during the obesity induction period. $*p < 0.05$, $**p < 0.01$, $***p < 0.001$, $****p < 0.0001$ vs. NFD (Two-way repeated measure ANOVA with Šídák post hoc test). Data previously published as part of a larger data set and replicated with permission from Hirata, Cruz et al., (2019).

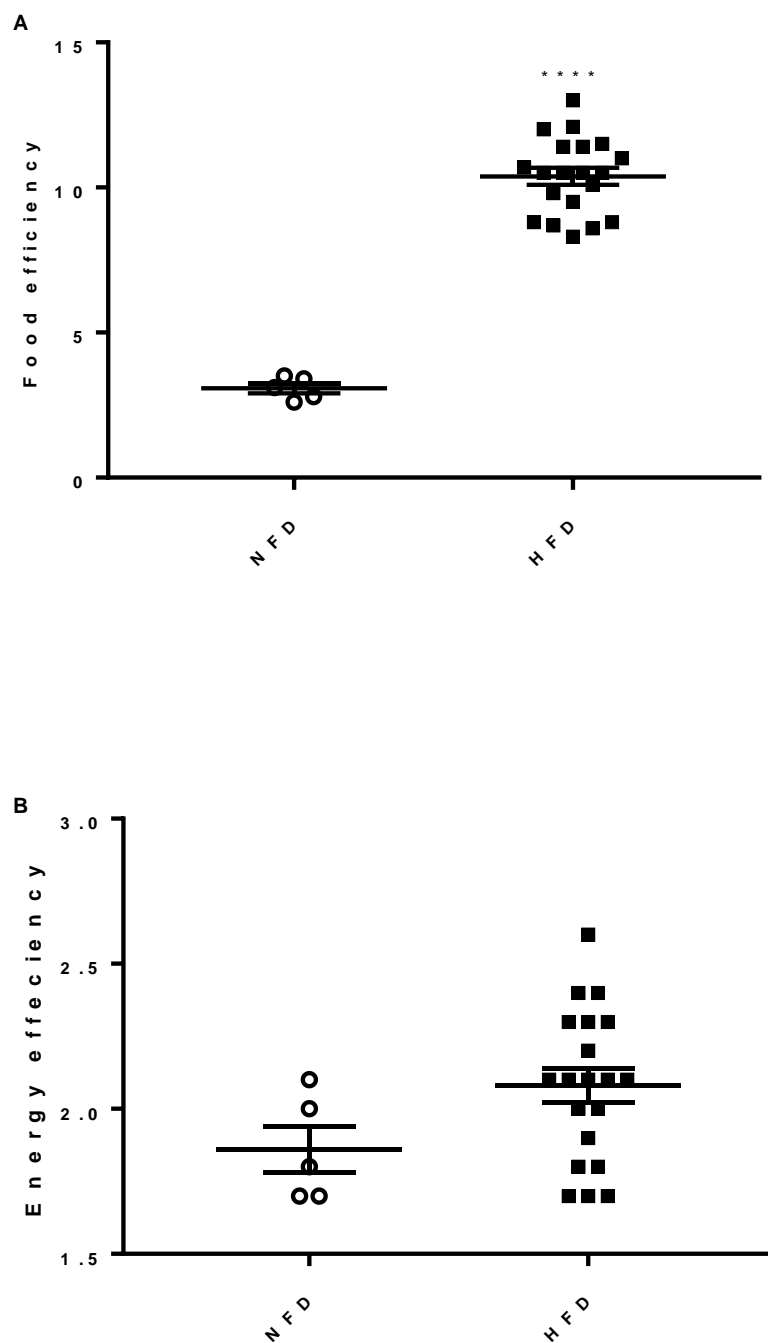


Figure 10. Food efficiency and energy efficiency. [BW gain (g)/food ingestion(g)] (A), Energy efficiency intake [BW gain (g)/Energy intake (kcal/100 g/24 h)] (B), of normal-fat diet (NFD; n = 5) and high-fat diet (HFD; n = 13) groups during the obesity induction period. ****p < 0.0001 vs. NFD (Student's t-test). Data previously published as part of a larger data set and replicated with permission from Hirata, Cruz et al., 2019.

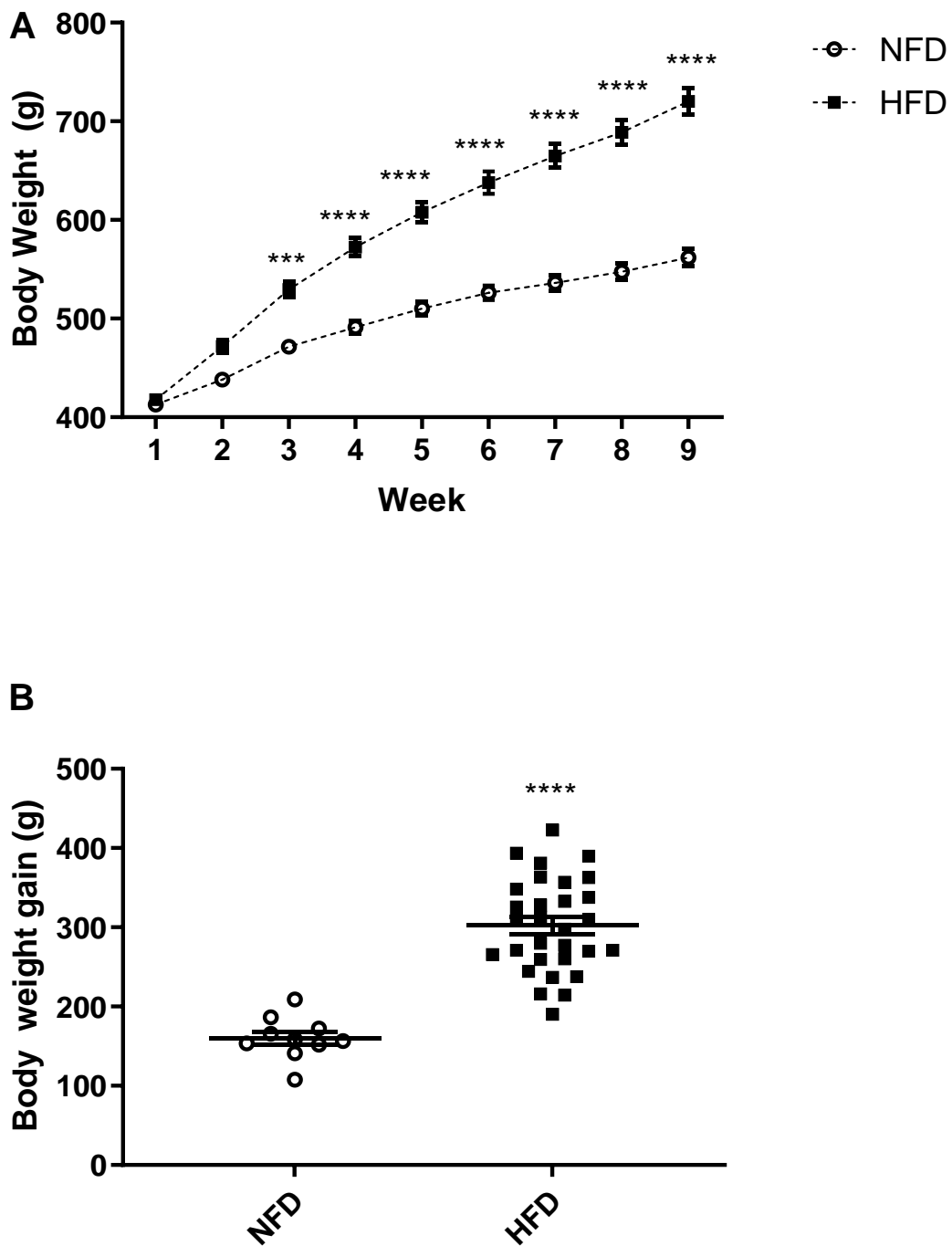


Figure 11. Body composition. Body weight (g) during the obesity induction period A) and body weight gain (difference between initial and final BW) (g) (B) of normal-fat diet (NFD; n = 10) and high-fat diet (HFD; n = 30). Statistically analysed by A) Two-way repeated ANOVA with Šídák *post hoc* test B) Student's t-test. ***p < 0.001, ****p < 0.0001 vs. NFD; Data previously published and replicated with permission from Hirata, Cruz *et al.*, 2019.

3.4 GbE supplementation period

In accordance with previous studies in similar conditions (Hirata, Cruz *et al.*, 2019), after the 8-week obesity induction period, the HFD group (n=30) was randomly sorted into 3 subsets (n=10 each). The first group received 1mL 0.9% saline by gavage daily for 2 weeks (HFD-S). The second HFD subset was orally gavaged with GbE (500 mg/kg) in a 0.9% Saline vehicle (HFD+GbE). Due to previous findings that GbE decreases food intake in rats (Hirata, Cruz *et al.*, 2019, Hirata, *et al.*, 2015, Banin *et al.*, 2014), an additional subset was included with matched pair-feeding (HFD-PF) to levels seen in the HFD-GbE group (HFD-PF). The NFD group continued with standard chow only.

As described in the methods section, GbE was obtained from Huacheng Biotech Inc. (China), with the major bioactive compounds being flavone glycosides (25.21%), terpenoids (6.62%), ginkgolides A, B, C (3.09%), and bilobalides (2.73%) (shown in Figure 7.f) (Hirata, Cruz *et al.*, 2019, Hirata, *et al.*, 2015, Banin *et al.*, 2014). Food and energy intake was measured daily for the 14 days of supplementation. Body weight gain was calculated by the difference between the first and the last day of the 2 weeks period. All three HFD groups showed a significant increase body weight as compared to the NFD group as shown in Figure 11.A, where the HFD-S group gained an extra 150.4g (p= 0.0005), HFD-PF gain 136.3g (p=0.002) and HFD-GbE gained 147.2g (p=0.0007). For body weight gain however, both HFD-GbE and HFD-PF gained little body weight as compared to the NFD and HFD-S groups. Compared to NFD, HFD-GbE gained just 1.5g (p=0.09), while HFD-PF of experienced a net loss of nearly 10 g, resulting in a significant body weight gain difference of 26.5g between the HFD-PF group and NFD group (p= 0.006).

As shown in Figure 13.A, the mean differences in daily food intake levels (g/100 g/24 h) in the NFD group was significantly higher compared to all three HFD (HFDS, HFD-PF and HFD-GbE) groups. The exception was on day 14 where the rats were fasted for the final 8 hours before being anaesthetized and euthanized, with significantly less food intake seen in the HFD-PF (p=0.03) and HFD-GbE (p=0.003) but not in HFD-S (p=0.33) (Figure 12.B) compared to the NFD group.

As shown in Figure 13.B the mean differences in energy intake in grams per 24 hrs (kcal/100 g/24 h) did not significantly differ for more groups across the 14-day period. Changes of note include the significant increase in energy intake on day 4 in the NFD group compared to the HFD-S (p=0.03), HFD-PF (p=0.03) and HFD-GbE (0.02) group. Day 10 also showed a significantly decreased difference in the HFD-PF (p=0.03) and HFD-GbE (0.01) groups compared to the NFD group.

As shown in Figure 13.C food efficiency (Body weight/food intake (g/24 hrs) was significantly different between the NFD vs. HFD-PF (1.16, $p=0.04$) groups but between any other group. The food efficiency profiles for all groups were like that of body weight gain. The results reported above are in keeping with previous results from our group and others, looking into the effects of NFD and HFD intake in a rodent model. Similarly, GbE treatment results are also in keeping with previous studies conducted (Hirata, Cruz *et al.*, 2019, Hirata, Pedroso *et al.*, 2019, Hirata, *et al.*, 2015, Banin *et al.*, 2014).

During the 14-day treatment window, it is interesting to note that all three HFD subsets, continued to gain weight compared to the NFD while no differences were seen between the HFD subsets. This is most likely due to the nature of a HFD particularly those high in SFA that promote weight gain and obesity (Bray and Popkin 1998; Hochberg 2018; Wali *et al.* 2020). Interestingly, the changes in body weight gain that were seen when comparing the NFD and HFD subsets, show that NFD gained most over the 14-day period, while HFD-PF and HFD GbE groups gained least, significantly so for the HFD-PF group. Interestingly, the HFD-S, HFD-PF and HFD-GbE groups did not significantly differ in food intake (Figure 13.A), energy intake (Figure 13.B) or energy efficiency (Figure 13.C) compared to each other over the 14-day treatment period. Only the HFD-PF group showed less significant energy efficiency compared to the NFD after the 14-day treatment (Figure 13.C).

A clinical study by Viguerie *et al.*, (2005) looked at adipose tissue gene expression in obese patients during low-fat and high-fat hypocaloric diets. They took two groups of 25 obese patients and placed them on a 10-week hypocaloric diet with either 20–25 or 40–45% of total energy derived from fat, the latter like the HFD profile in our study. They measured the mRNA levels of 38 genes, including ten genes regulated by energy restriction but did not find any significant changes between the groups. Viguerie *et al.*, (2005) did find however that levels of PPAR γ and PPAR1 α mRNA were increased, while the expression of the genes encoding leptin, osteonectin, phosphodiesterase 3B, HSL, receptor A for natriuretic peptide, fatty acid translocase, lipoprotein lipase (LPL), uncoupling protein 2 and PPAR γ was decreased (Viguerie *et al.*, 2005).

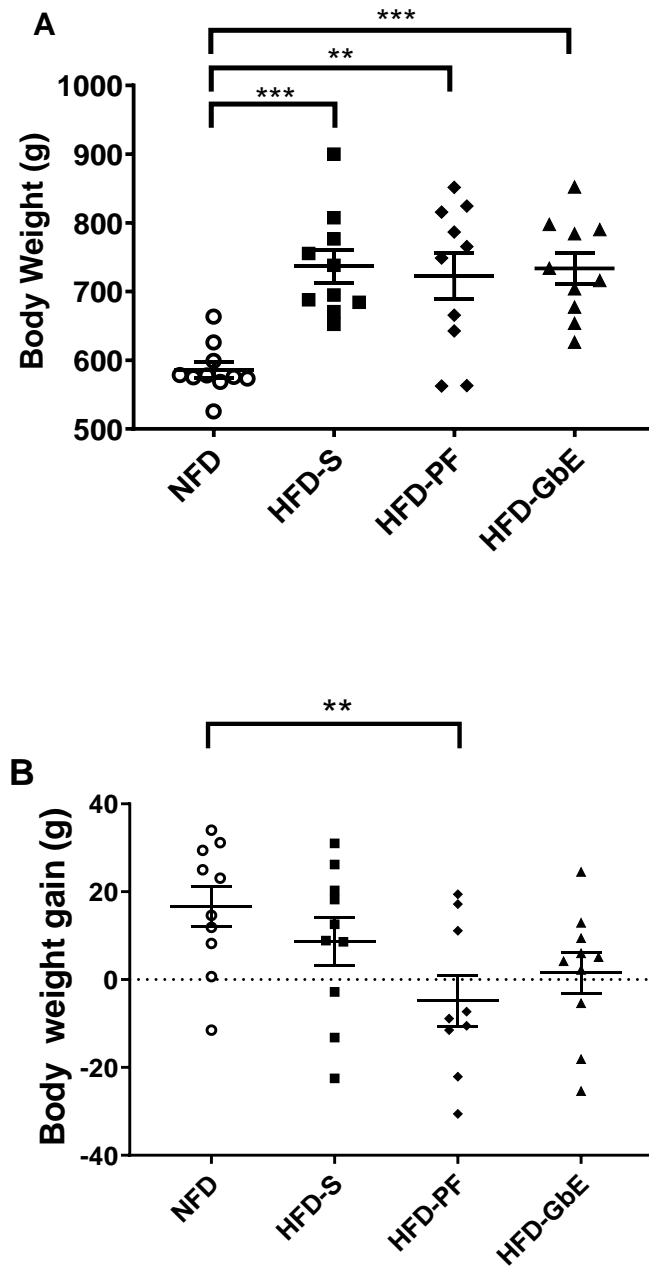


Figure 12. Body weight and body weight gain after 14-day supplementation. Body weight (g) (A) and Body weight gain (g) (B) of normal-fat diet (NFD; n = 10), high-fat diet (HFD-S; n = 10), high-fat diet with pair-feeding (HFD-PF; n = 10) and high-fat diet. Data presented as mean±SEM. Data analysed by Two-way ANOVA with Tukey *post-hoc* test. Statistical significance was set at **p < 0.01, ***p < 0.001.

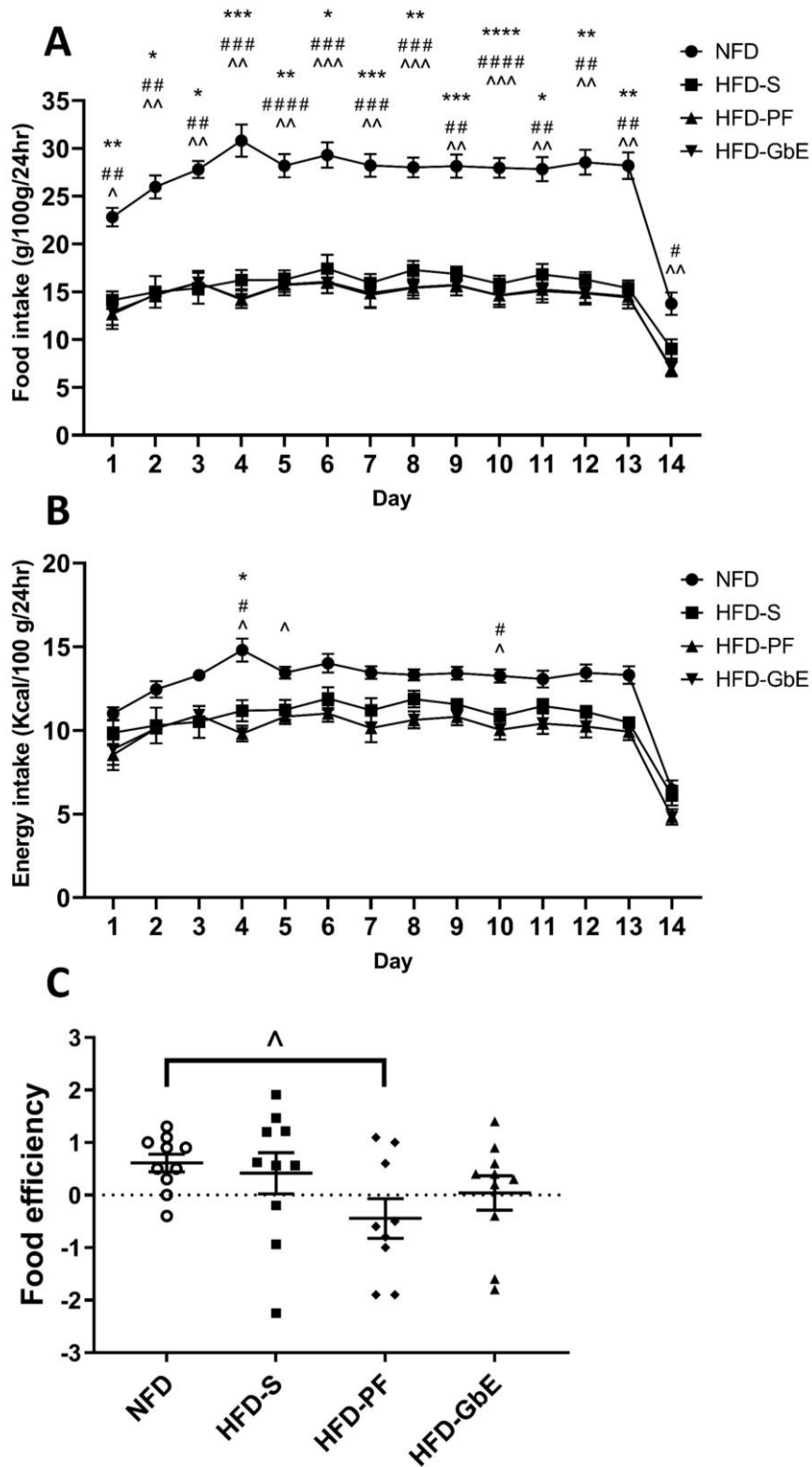


Figure 13. Accumulated food intake, energy intake and food efficiency after 14-day supplementation (A) food intake (g/100g body weight /24hr) (B) energy intake (Kcal/100g body weight/24hr) (C) food efficiency [BW gain (g)/food ingestion(g)]. Data presented as mean±SEM. Data analysed by: Panel A & B; Three-way repeat measures ANOVA with Tukey *post hoc* test, Panel C; Two-way ANOVA with Tukey *post hoc* test. Statistical significance was set at NFD Vs HFD-S, *p<0.05, **p<0.01, ***p<0.001, ****p<0.0001; NFD Vs HFD-PF, #p<0.05, ##p<0.01, ###p<0.001, ####p<0.0001; NFD Vs HFD-GbE, ^p<0.05, ^^p<0.01, ^^p<0.001 for each day between groups.

As both groups lost 7kg during the programme, Viguerie and colleagues concluded that it was energy restriction and/or weight loss not the fat: carbohydrate ratio in a low-energy diet that played the highest role in modifying the expression of genes in human adipose tissue. Parks and colleagues (2012) also found that calorie restriction with a HFD was effective at attenuating inflammatory responses and oxidative stress-related markers in obese tissues of the high fat diet fed rats (Park *et al.*, 2012). They found that high fat caloric restriction (HFCR) affected a variety of metabolites known to be altered in inflammation and OS caused by obesity. Parks *et al.*, (2012) also reported lowered hepatic triglyceride and total cholesterol levels and a return to normal levels in the plasma leptin/adiponectin ratio. HFCR also improved glucose tolerance and normalized adipocyte size and morphology. Expression levels of CRP and manganese superoxide dismutase were suppressed in adipose tissue. Lipid peroxidation was reduced and a decrease in the expression of inducible nitric oxide synthetase, cyclooxygenase-2, NF-E2-related factor, and heme oxygenase-1 in the liver (Park *et al.*, 2012). Previous work from our group comparing NFD and HFD diets and GbE supplementation in male Wistar rats has shown when comparing adipocyte size and morphology or epididymal adipose tissue, the adipocyte volume was significantly larger by 114% ($p=0.01$) in an HFD-S compared to NFD group, but GbE supplementation reduced this by 42.5% ($p=0.03$) and was of a statistically similar volume in HFD+GbE compared to NFD (Hirata, Cruz, *et al.*, 2019). Perilipin (Plin 1), FASN mRNA, and FASN protein levels were also reduced following GbE treatment along with acetate accumulation. GbE treatment also showed a tendency to reduce oleate incorporation into lipids by 43% ($p= 0.06$) compared to a HFD alone, which was found to have a 130% higher oleate incorporation ($p = 0.01$) in HFD cells compared to NFD (Hirata, Cruz *et al.*, 2019). Although not shown here, previous work from our group has shown that GbE treatment causes rats to consume less food without the need for limiting food availability (Hirata, Cruz *et al.*, 2019) is encouraging and points to metabolic alterations that may promote more satiety with less food. This could be useful given that the main tactics deployed for weight-loss in a medical setting often focus on restricting energy intake while the main mechanism for success is found with bariatric surgery (Beaulac and Sandre, 2017; Wolfe, Kvach and Eckel, 2016). As an example, in laparoscopic sleeve gastrectomy, a significant decrease in BMI and serum TAG was reported after surgery, while HDL-C levels were increased and significantly correlated to an increase in pre-heparin LPL and TAG levels and weight loss (Ohira *et al.*, 2021). Despite the good results being achieved in the short run however, a large subset of the clinical group was prone to weight re-gain within 2 years of bariatric surgery (Cadena-Obando *et al.*, 2020). This may be partially attributed to pre-existing metabolic conditions that may have contributed to weight re-gain as well

as the type of surgery and subsequent dietary lifestyle (Nauli and Matin, 2019). If GbE can reduce food intake in a 14-day period, further studies focusing on longer GbE treatment times might provide more insight into the underlying mechanisms involved in reduced food intake. Following these observations in the body composition, food and energy intake and food efficiency, next we proceeded to explore the fatty acid profiles of several tissues collected from the subset including retroperitoneal and mesenteric adipose tissues, liver, hypothalamus, and hippocampus tissues.

Chapter 4 – Liver

4.1 Introduction

The liver is a dynamic organ that plays a part in most organs in the body. It aids digestion and metabolism and acts as storage for fat soluble vitamins and TAG. It is involved in cholesterol synthesis and homeostasis. The liver plays a key role in the synthesis and breakdown of TAG and PPL. The liver also plays a key role in drug metabolism and plays a role in breaking down heme into bilirubin released during red blood cell breakdown. The liver blood supply primarily comes from the portal vein (Kalra *et al.*, 2022). *Via* the portal vein, the liver is exposed to FA, cholesterol, and TAG daily from both endogenous circulating forms of lipids and exogenous forms taken from the diet and absorbed by the gastrointestinal tract (Mattace Raso *et al.*, 2013). The liver is involved in both DNL and lipolysis through FA β -oxidation. While DNL and FA β -oxidation operate through different pathways, both may occur at the same time within a cell (Solinas, Borén and Dulloo, 2015). Lipogenesis in the liver is more abundant and efficient than in adipose tissue (Lodhi, Wei and Semenkovich, 2011). The daily rate of hepatic FA uptake and DNL is balanced by FA oxidation rates and the transportation of VLDL-TAG out of the liver (Bhutia *et al.*, 2021; Alves-Bezerra *et al.*, 2017; Kohlmeier, 2015). When TAG levels in the liver drop, adipocyte FA lipolysis and metabolism increase to liberate FA for energy production (Bhutia *et al.*, 2021; Alves-Bezerra *et al.*, 2017; Kohlmeier, 2015).

As discussed in more detail in Chapter 1 Section, 1.8 and 1.10, the liver is capable of synthesizing TAG from dietary and endogenous sources of MAG, DAG and FFA by acyl transferases. Fatty acyl CoA is used in these reactions which is derived from the breakdown of the dietary LCFA by Acyl CoA synthetase activity. TAG is synthesised by the liver as a means of long- term lipid storage for the body (Stryer *et al.*, 2019). An excess of hepatic TAG accumulation is associated with obesity, T2DM, dyslipidaemia, and IR and can result in chronic liver disease (Caussy, Aubin and Loomba, 2021; Birkenfeld and Shulman, 2014). As discussed in more detail in Chapter 1 section 1.11, the liver also plays the predominant role in cholesterol biosynthesis, storage, and secretion. To form cholesterol, acetyl CoA undergo a complex 37 step process involving SREBP-2, SCAP, 3-hydroxy-3-methyl-glutaryl CoA reductase and squalene monooxygenase (Craig, Yarrarapu and Dimri, 2021; Nemes *et al.*, 2016).

While a small quantity of TAG is stored in the liver and localized to cytoplasmic lipid droplets (LDs), the majority of hepatic VLDL-TAG and CE are secreted into the bloodstream from the ER lipid bilayer and transported to peripheral tissues (Parry *et al.*, 2021; Roumans *et al.*, 2021; Alves-Bezerra and Cohen, 2017; Martinez-Lopez and Singh, 2015; Bansal *et al.*, 2007; Barrows and Parks, 2006). Highly insoluble cholesterol is excreted into circulation either in the form of bile acids, CE or converted to VLDL for efficient cholesterol transport through the blood stream (Freeman and Remaley, 2016; Chien, 2004). VLDL in the liver is assembled from cholesterol, CE, TAG, PPL, and the lipoprotein apolipoprotein B-100 (apo B-100) (Craig, Yarrarapu and Dimri, 2021; Nemes *et al.*, 2016; Hussain, 2014). Secreted circulating TAG and CEs are predominantly stored in adipocytes to provide a localized energy supply from β -oxidation. During fasting states, plasma insulin levels drop and signal to tissues, especially the liver and adipocytes, to begin lipolysis through the catecholaminergic stimulation of the β -adrenergic receptors. TAG molecules are β -oxidized to release DAG, MAG, FFA and glycerol molecules and can either be used locally for energy production or secreted into circulating plasma in the form of bound-albumin FA, unbound LCFA and as part of HDL particles largely comprised of PPL, TAG and CE-bound FA (Nemes *et al.* 2016; Hussain 2014; Kamp and Hamilton 2006; Massey, Bick and Pownall 1997). These are transported back to the liver (Alves-Bezerra *et al.*, 2017; Samuel and Shulman, 2016). Cholesterol in the form of CE also is sequestered into HDL particles and transported back to the liver (Nemes *et al.*, 2016; Hussain, 2014). CE can then be exchanged for TAG or other lipoproteins for recirculation (Nakamura *et al.*, 2004). HDL spheres returning to the liver release the transported CE either by the action of hepatic scavenger receptor B1, or by LDL receptors in the liver after HDL CE are transferred to apo B-100-containing lipoproteins such as VLDL, IDL, and LDL by the cholesterol-ester transfer proteins (Nemes *et al.*, 2016; Hussain, 2014). Circulating FA are transported into the hepatocyte by diffusion if in an unbound state (Kamp and Hamilton, 2006; Massey, Bick and Pownall, 1997), or by a variety of plasma membrane-associated proteins in bound to albumin including: plasma membrane FABPs, FATPs, CAV-1, FAT/CD36, and ACSVL (Huang, Zhu and Shi, 2021; Ma *et al.*, 2021; Amiri *et al.*, 2018; Glatz and Luiken, 2018; Schwenk *et al.*, 2010; Hamilton, 2007). PPAR α/γ receptors are responsible for triggering gene transcription of lipid metabolism mediators involved in β -oxidation. PPAR expression is ubiquitous but is predominantly expressed in tissues that undergo high rates of fatty acid catabolism, including the liver, as well as muscle and brain tissues (Tahri-Joutey *et al.*, 2021).

As discussed in previous chapters, a HFD is a dietary risk factor for multiple diseases including hypertension, vascular diseases, insulin resistance, metabolic syndrome, T2DM, obesity and Non-

alcoholic fatty liver disease (NAFLD) (Kumar *et al.* 2021; Malesza *et al.* 2021; Wang, Hwang *et al.* 2021; Gao *et al.* 2020; von Frankenberg *et al.* 2017; Besten *et al.* 2015; Abu-Elheiga *et al.* 2012; Inoue *et al.* 2012; Holloway *et al.* 2011; Hariri 2010; Hancock *et al.* 2008; Buettner, Schölmerich and Bollheimer 2007; Yang *et al.* 2007). NAFLD may be considered an indicator of metabolic syndrome in the liver as it is associated with inflammation, OS, IR, disrupted FA metabolism and mitochondrial dysfunction (Katsiki, Mikhailidis and Mantzoros 2016; Hebbard and George 2011; Jou, Choi and Diehl 2008). NAFLD is associated with several liver pathologies including dysregulated cytokines including elevated TNF- α (Greco *et al.*, 2008; Crespo *et al.*, 2001), hepatic steatosis and fibrosis, advanced non-alcoholic steatohepatitis (NASH), and cirrhosis (Katsiki *et al.*, 2016).

Dietary fats are involved in hepatic lipogenesis and the inducement and study of NAFLD in animal models often focuses on dietary causes of NAFLD predominantly in the form of either a HFD, high-carbohydrate/fructose or high-cholesterol diet or a combination of either (Radhakrishnan *et al.*, 2022; Lian *et al.*, 2020; Aydos *et al.*, 2019; Jensen *et al.*, 2018; Mells *et al.*, 2015; Eccleston *et al.*, 2011; Alkhouri, Dixon and Feldstein, 2009). Jensen and colleagues (2018) found in Sprague-Dawley rats, the development of NAFLD is driven more by a HFD than high fructose, with the later effecting the circulating lipid pool more (Jensen *et al.*, 2018). The balance between *n*-3 and *n*-6 PUFAs are important in NAFLD as a higher *n*-6/*n*-3 ratio is associated with a pro-inflammatory state, hepatic lipid metabolism dysregulation, increased liver fat percentage and insulin homeostasis (Mäkelä *et al.*, 2022; Cui *et al.*, 2021; Luo *et al.*, 2021; Bogl, Kaprio and Pietiläinen, 2020; van Name *et al.*, 2020; da Silva *et al.*, 2014; Valenzuela and Videla, 2011; Pachikian *et al.*, 2008; Araya *et al.*, 2004; Videla *et al.*, 2004)

As detailed in Section 1.14, hormones play a key role in liver function and energy homeostasis. When there is excess energy intake, pancreatic insulin promotes DNL and the uptake and storage of excess glucose in the form of TAG to be transported to adipocytes for storage (Vegiopoulos, Rohm and Herzig, 2017). When adipocytes become overburdened and dysfunction, ATGL increases the conversion of TAG to DAG (Reid *et al.*, 2008), which is further converted to toxic ceramides. See Section 1.14. for more detail. Ceramides block insulin signalling and decrease adiponectin levels (Sharma and Holland, 2017). Adiponectin is a key systemic insulin sensitizing hormone that helps regulate lipid and glucose metabolism in the liver, pancreas, muscle and adipocyte. Adiponectin increases hepatic FA oxidation while decreasing hepatic gluconeogenesis. Adiponectin also increasing fatty oxidation and glucose uptake in skeletal muscle and WAT (Wang and Scherer, 2016). Adiponectin expression and circulating levels are inversely proportional to adiposity levels. Increased

VAT in overweight and obese subjects is associated with decreased total adiponectin levels, while weight loss is associated with improved adiponectin levels and significantly reduced inflammation (Gariballa *et al.*, 2019; Kishida *et al.*, 2011). Previously work has found that adiponectin gene expression decreased in retroperitoneal WAT of mice fed a HFD enriched with either soybean oil, fish oil, coconut oil, or lard (Bueno *et al.*, 2008).

In keeping with previous RET and MES chapter this chapter liver tissue lipid profiles following NFD and HFD fed male Wistar rats will be discussed. The effect of 14 days of GbE phytotherapy on total lipid profiles, neutral lipid classes (TAG, DAG, MAG, FFA, CE) and total PPL lipid FA will also be discussed.

4.2 Liver total fatty acids

Adipocytes respond to changes in the nutritional state, undergoing remodelling as necessary (Choe *et al.*, 2016). When obesity occur, adipocytes continue to expand in size through hypertrophy to accommodate additional TAG molecules transported from the liver. Hypertrophic cells secrete adipokines that recruit adipose progenitor cells (pre-adipocytes) that mature into adipocytes, increasing the number of adipocytes available for TAG storage (hyperphasia) (Pyrina *et al.*, 2020). In chronic adipose tissue expansion, due to the limitations of hypertrophy and hyperphasia, changes in the quantity and quality of adipose tissue-resident cells may occur, such as increased macrophage influx in response to IR (Chait *et al.*, 2020; Alves-Bezerra *et al.*, 2017; Choe *et al.*, 2016). Metabolic changes including changes in adipokine secretion in overloaded or dysfunctional adipocytes is often associated with IR-related lipolysis, FA oxidation and the generation of lipotoxic DAG and ceramides (Chait and den Hartigh, 2020). Changes in adipokines with a HFD include lowered adiponectin, and higher leptin levels (covered in section 1.14) and contribute to systemic metabolic deterioration in the liver (Vegiopoulos, Rohm and Herzig, 2017).

Total sample fatty acid profiles were subjected to acid-catalysed esterification to methyl esters and analysed by GC-FID. Several changes were seen in total fatty acids profiles between the NFD and HFD-S groups when comparing baseline effects of each diet. This data is summarised in Table 10 and Table 11 as mean±SEM of fatty acid percentages. Despite the significant increase in SFA in the HFD rat chow ($p<0.001$) no significant changes in total SFA percentage (%) levels were seen between the NFD (38%) and HFD (35%) groups ($p=0.62$). An increase of nearly 11% was seen in total MUFA levels between the NFD (9.9%) and HFD (20.8%) group ($p=0.002$), predominantly in the form of oleic acid (C18:1n9) (NFD 6.8%; HFD 18.5%, $p=0.002$) (Table 10). Oleic acid is also associated with the promotion of

steatosis in an *in vitro* model (Li *et al.*, 2021; Rafiei, Omidian and Bandy, 2019; Samovski and Abumrad, 2019; Liao *et al.*, 2014; Ziamajidi *et al.*, 2013; Cui, Chen and Hu, 2010) with high circulating plasma levels of oleic acid associated with NAFLD and NASH (Araya *et al.*, 2004). In a cell model, oleic acid steatosis is associated with lipid peroxidation *via* decreased SOD-1, apoptosis *via* increase caspase-9, and decreased proliferation *via* increased production of p27 with unchanged alanine transaminase (ALT) levels (Cui, Chen and Hu, 2010). Oleic acid is also reported to induce the expression of mRNA lipogenesis and FA oxidation enzymes (FAS and CPT1A) and is associated with impaired indices of aerobic energy metabolism including PPAR γ mRNA expression, mitochondrial membrane potential (MMP), and galactose-supported ATP production (Rafiei, Omidian and Bandy, 2019). Cui and colleagues (2010) also reported that oleic acid-induced steatosis is associated with increased lipid peroxidation *via* decreased SOD-1, apoptosis *via* increase caspase-9, and decreased proliferation *via* increased production of p27 with unchanged alanine transaminase (ALT) levels (Cui, Chen and Hu, 2010).

Total PUFA % levels decreased by 8.2% from 58.9% in NFD and 42.7% in HFD ($p < 0.0001$), while total UFA levels remained at similar levels between the groups at 60.8% in NFD and 63.4% in HFD ($p = 0.66$), balanced by the increase in total MUFA (Table 10). This change in PUFA and MUFA is seen in the significant change in the MUFA/PUFA ratios (Table 11) that increased from 0.2 in NFD, to 0.49 in HFD ($p = 0.003$). Total n-6 PUFA decreased significantly by nearly 7% in the HFD group (38.8%) compared to NFD (45.6%) ($p = 0.0001$), predominantly in the form of the AA (C20:4n6) that dropped 10.4% from 24.1% in NFD to 13.7% in the HFD group ($p = 0.01$). Total n-3 PUFA also decreased by 1.4%, from 5.3% in NFD to 3.9% in HFD ($p = 0.01$) the equivalent of a 25% decrease in total n-3 PUFA. This was largely associated with the 33% decrease in C22:6n-3 from 3.8% in NFD, to 2.6% in HFD. As previously mentioned in earlier sections, n-3 FA are associated more with anti-inflammatory eicosanoids and inflammation mitigation while n-6 PUFAs, such (Table 10) as C20:4n-6 are associated more with proinflammatory eicosanoid mitigation (Hussey, Lindley & Sarabjit and Mastana, 2017; Monteiro *et al.*, 2014). The significant decrease in C20:4n-6 could suggest its utilization in pro-inflammatory mitigation, but this would need to be further investigated. For example, liquid chromatography mass spectrometry LC-MS could be used to measure oxylipin levels in tissues and in circulation (Fu, Yin, Wu, *et al.*, 2022; Liakh, Pakiet, Sledzinski, *et al.*, 2020; Tans, Bande, van Rooij, *et al.*, 2020; Wang, Yutuc and Griffiths, 2020; Hinz, Liggi, Mocciano, *et al.*, 2019; Hewawasam, Liu, Jeffery, *et al.*, 2018). n-3 FA have been shown to positively affect inflammation and steatosis induced by a HFD through the upregulation of PPAR- α and preventing NF- $\kappa\beta$ binding (Tapia *et al.*, 2014). n-3 FA have also been

shown to limit hepatic TAG storage (Ferramosca and Zara, 2014). The decrease in n-3 FA may negatively affect the inflammatory process associated with steatosis. The balance between n-3 and n-6 PUFAs are important in NAFLD as a higher n-6/n-3 ratio is associated with a pro-inflammatory state, hepatic lipid metabolism dysregulation, increased liver fat percentage and insulin homeostasis (Mäkelä *et al.*, 2022; Cui *et al.*, 2021; Luo *et al.*, 2021; Bogl, Kaprio and Pietiläinen, 2020; van Name *et al.*, 2020; da Silva *et al.*, 2014; Valenzuela and Videla, 2011; Pachikian *et al.*, 2008; Araya *et al.*, 2004; Videla *et al.*, 2004). Despite the decrease in n-6 and n-3 in the HFD, the n-6/n-3 was relatively consistent between both the NFD (8.7) and HFD groups (10) ($p=0.66$) (Table 11). As high levels of oleic acid can induce lipid peroxidation, this may contribute to the decrease in total PUFA levels seen here as higher unsaturation index PUFA are more susceptible to peroxidation, particularly those PUFA with a higher unsaturation index such as C20:4n-6 and C22:6n-3 (Hulbert *et al.*, 2007). This is also reflected in the decrease seen in the unsaturation index that decreased from 178.8 in NFD to 146.9 in HFD ($p=0.001$) (Table 11), due to the changes in the MUFA and PUFA ratios, it indicates an overall decrease in the fluidity of liver-derived FA following the 2-month HFD-induced obesity stage.

Interestingly, treatment with HFD-GbE or pair feeding (HFD-PF) did not significantly alter the total fatty acid profiles of the liver compared to a HFD alone (HFD-S) (Table 12 and Table 13). This is like that seen in RET and MES total fatty acids profiles in this study, as well as findings from a recent study from our group looking at HFD and induced menopause and their influence on RET adipose tissue (Boldarine *et al.*, 2021), where any changes in lipid class profiles were masked when analysing total lipid profiles only. Next, Liver samples were separated into TAG, CE, MAG+DAG and PPL and analysed further.

Table 10. Liver total lipid fatty acid methyl esters (FAME) for normal fat diet (NFD) and high fat diet (HFD-S) (N=10 per group). Fatty acid results are presented as area % percentage mean and standard error of the mean (SEM), and statistically analysed by Students t-test. The level of statistical significance was set at * $p < 0.05$.

	NFD			HFD-S			p value
	MEAN %	SEM		MEAN %	SEM		
C14:0	0.16	± 0.02		0.20	± 0.00		0.98
C16:0	20.44	± 0.38		22.47	± 0.28		0.03
C18:0	15.94	± 1.11		11.36	± 0.80		0.21
C20:0	0.05	± 0.02		0.04	± 0.02		>0.99
C22:0	0.14	± 0.02		0.11	± 0.01		>0.99
C24:0	0.28	± 0.01		0.27	± 0.15		>0.99
ΣSFA.DMA	0.48	± 0.05		0.40	± 0.03		>0.99
ΣSFA	38.04	± 0.89		35.13	± 0.65		0.62
C16:1n7	0.41	± 0.09		0.37	± 0.03		>0.99
C18:1n7	2.08	± 0.14		1.32	± 0.05		0.01
C18:1n9	6.76	± 1.76		18.45	± 0.92		0.002
C20:1n9	0.13	± 0.02		0.22	± 0.01		0.14
C24:1n9	0.10	± 0.01		0.05	± 0.02		0.84
DMA18:1	0.26	± 0.02		0.15	± 0.02		0.06
ΣC18:1	2.18	± 0.14		1.43	± 0.06		0.01
Σω7	0.48	± 0.09		0.40	± 0.04		>0.99
Σω9	7.03	± 1.76		18.82	± 0.92		0.001
ΣMUFA	9.87	± 1.67		20.75	± 0.98		0.002
C18:2n6	19.69	± 1.26		23.00	± 0.77		0.84
C18:3n6	0.16	± 0.02		0.18	± 0.01		>0.99
C20:2n6	0.40	± 0.02		0.31	± 0.01		0.08
C20:3n6	0.29	± 0.03		0.38	± 0.01		0.62
C20:4n6	24.10	± 1.87		13.72	± 0.87		0.01
C22:2n6	0.03	± 0.02		0.01	± 0.01		>0.99
C22:4n6	0.77	± 0.10		1.27	± 0.06		0.04
Σn-6 PUFA	45.56	± 0.76		38.77	± 0.59		0.0001
Σn-6 metabolites	25.76	± 1.76		15.74	± 0.89		0.01
C18:3n3	0.46	± 0.04		0.47	± 0.03		>0.99
C20:3n3	0.30	± 0.04		0.28	± 0.05		>0.99
C20:5n3	0.17	± 0.02		0.10	± 0.00		0.23
C22:5n3	0.72	± 0.03		0.72	± 0.03		>0.99
C22:6n3	3.78	± 0.26		2.55	± 0.15		>0.05
Σn-3 PUFA	5.32	± 0.22		3.92	± 0.15		0.01
Σn-3 metabolites	4.85	± 0.26		3.46	± 0.17		0.02
ΣPUFA	50.86	± 0.89		42.69	± 0.63		<0.0001
ΣUFA	60.74	± 0.84		63.42	± 0.65		0.66

Table 11. Liver total lipid fatty acid methyl esters (FAME) ratios between normal fat diet (NFD) and high fat diet (HFD-S) (N=10 per group). Results presented as mean and standard error of the mean (SEM), and statistically analysed by Students t-test. The level of statistical significance was set at * $p < 0.05$.

	NFD			HFD-S			t test
	MEAN	±	SEM	MEAN	±	SEM	p value
ΣMUFA/ΣPUFA	0.20	±	0.05	0.49	±	0.02	0.003
ΣMUFA/ΣSFA	4.51	±	0.46	1.75	±	0.12	0.002
ΣPUFA/ΣSFA	1.33	±	0.02	1.22	±	0.02	0.21
ΣUFA/ΣSFA	1.61	±	0.07	1.81	±	0.05	0.82
C18:0/C16:0	0.78	±	0.07	0.50	±	0.04	0.12
C16:1n7/C16:0	0.01	±	0.01	0.00	±	0.00	>0.99
C18:1n9/C16:0	0.33	±	0.08	0.81	±	0.03	0.002
C18:1n9/C16:1n7	19.03	±	4.42	53.43	±	3.93	0.002
C18:1n7/C18:0	0.12	±	0.01	0.13	±	0.02	>0.99
C18:1/C18:0	0.13	±	0.02	0.14	±	0.02	>0.99
n-6/n-3	8.70	±	0.34	9.99	±	0.38	0.66
n-6/n-3 metabolites	5.28	±	0.23	4.54	±	0.18	0.64
C18:2n6/C18:3n3	43.96	±	2.67	51.47	±	2.25	0.88
C20:4n6/C20:3n6	85.05	±	9.99	37.75	±	3.07	0.02
C20:4n6/C22:6n3	6.33	±	0.27	5.43	±	0.22	0.64
C20:4n6/C20:5n3	144.77	±	16.72	152.01	±	14.78	>0.99
C20:4n6/C18:2n6	1.32	±	0.17	0.60	±	0.05	0.046
C20:4n6/C18:3n3	60.53	±	11.22	32.05	±	3.88	0.75
C20:3n3/C18:3n3	0.44	±	0.15	0.27	±	0.12	>0.99
C20:5n3/C18:3n3	0.41	±	0.05	0.21	±	0.02	0.10
C22:5n3/C18:3n3	1.69	±	0.24	1.65	±	0.13	>0.99
C22:6n3/C18:3n3	9.51	±	1.82	5.91	±	0.69	0.97
C22:6n3/C22:5n3	5.38	±	0.43	3.50	±	0.19	0.06
C18:2n6/C16:0	0.94	±	0.05	1.04	±	0.03	0.99
C18:3n6/C18:2n6	0.01	±	0.00	0.01	±	0.00	>0.99
C20:3n6/C18:3n6	2.23	±	0.33	2.23	±	0.20	>0.99
C22:5n3/C20:5n3	4.27	±	0.32	8.09	±	0.64	0.004
C22:4n6/C20:4n6	35.49	±	3.99	11.22	±	1.09	0.003
1 (% monoenoics)	8.00	±	1.47	17.23	±	0.89	0.004
2 (% dienoics)	40.40	±	2.51	46.70	±	1.56	0.88
3 (% trienoics)	3.77	±	0.27	4.09	±	0.14	>0.99
4 (% tetraenoics)	99.53	±	7.09	59.49	±	3.61	0.01
5 (% pentaenoics)	4.46	±	0.21	4.11	±	0.11	>0.99
6 (% hexaenoics)	22.63	±	1.54	15.25	±	0.90	0.046
Unsaturation Index	178.78	±	4.52	146.85	±	2.32	0.001

Table 12. Total Liver extract fatty acid methyl esters (FAME) for high fat diet groups; High fat diet with-saline (HFD-S), High fat diet -pair-fed (HFD-PF) and High fat diet- Ginkgo biloba (HFD-GbE) (N=10 per group). Fatty acid results are presented as area % percentage mean and standard error of the mean (SEM), and statistically analysed by one-way ANOVA with Tukey's Post-hoc test. The level of statistical significance was set at * $p < 0.05$.

	HFD-S			HFD-PF			HFD-GbE			S Vs PF	S Vs PF	S Vs GbE
	MEAN	SEM		MEAN	SEM		MEAN	SEM		p value	p value	p value
C14:0	0.20	± 0.00		0.17	± 0.02		0.21	± 0.01		0.81	0.51	0.86
C16:0	22.47	± 0.28		22.09	± 0.43		22.57	± 0.37		0.68	0.98	0.98
C18:0	11.36	± 0.80		11.06	± 1.36		10.63	± 0.92		0.60	0.94	0.80
C20:0	0.04	± 0.02		0.02	± 0.01		0.01	± 0.01		0.38	0.86	0.16
C22:0	0.11	± 0.01		0.09	± 0.02		0.10	± 0.02		0.34	0.57	0.94
C24:0	0.27	± 0.15		0.34	± 0.20		0.13	± 0.02		0.96	0.58	0.72
DMA 16:0	0.01	± 0.01		0.03	± 0.02		0.01	± 0.01		0.93	0.60	0.79
DMA18:0	0.38	± 0.03		0.41	± 0.07		0.31	± 0.05		>0.99	0.45	0.45
∑SFA.DMA	0.40	± 0.03		0.42	± 0.07		0.34	± 0.06		>0.99	0.60	0.60
∑SFA	35.13	± 0.65		31.14	± 3.58		34.22	± 0.74		0.28	0.53	0.91
C16:1n7	0.37	± 0.03		0.36	± 0.04		0.32	± 0.03		0.93	0.34	0.52
C16:1n9	0.02	± 0.02		0.05	± 0.02		0.03	± 0.02		0.52	0.98	0.63
C18:1n7	1.32	± 0.05		1.50	± 0.08		1.37	± 0.03		0.42	0.36	0.99
C18:1n9	18.45	± 0.92		18.23	± 2.10		19.63	± 0.78		0.75	0.94	0.54
C20:1n9	0.22	± 0.01		0.27	± 0.03		0.28	± 0.01		0.17	>0.99	0.17
C24:1n9	0.05	± 0.02		0.03	± 0.02		0.03	± 0.02		0.31	0.94	0.48
∑DMA18:1	0.15	± 0.02		0.17	± 0.04		0.17	± 0.02		0.99	0.99	0.99
∑C18:1	1.43	± 0.06		1.43	± 0.17		1.46	± 0.03		0.92	0.99	0.98
∑ω7	0.40	± 0.04		0.34	± 0.05		0.40	± 0.03		0.93	0.99	0.97
∑ω9	18.82	± 0.92		16.73	± 2.65		19.99	± 0.76		>0.99	0.60	0.66
∑MUFA	20.75	± 0.98		18.67	± 2.79		21.96	± 0.80		0.99	0.62	0.68
C18:2n6	23.00	± 0.77		23.23	± 1.06		23.69	± 0.88		0.53	0.98	0.63
C18:3n6	0.18	± 0.01		0.20	± 0.02		0.18	± 0.02		0.50	0.44	0.99
C20:2n6	0.31	± 0.01		0.31	± 0.03		0.31	± 0.02		0.97	0.58	0.43
C20:3n6	0.38	± 0.01		0.34	± 0.02		0.36	± 0.03		0.50	0.78	0.90
C20:4n6	13.72	± 0.87		13.97	± 1.92		12.44	± 0.92		0.67	0.98	0.55
C22:4n6	1.27	± 0.06		1.10	± 0.09		1.37	± 0.06		0.19	0.07	0.80
∑n-6 PUFA	38.77	± 0.59		35.16	± 4.00		38.36	± 0.22		0.42	0.59	0.96
∑n-6 metabolites	15.74	± 0.89		14.25	± 2.30		14.67	± 0.84		0.33	0.85	0.67
C18:3n3	0.47	± 0.03		0.47	± 0.04		0.43	± 0.05		0.84	0.15	0.35
C20:3n3	0.28	± 0.05		0.27	± 0.03		0.26	± 0.03		0.77	0.97	0.86
C20:5n3	0.10	± 0.00		0.11	± 0.01		0.10	± 0.00		0.42	0.44	>0.99
C22:5n3	0.72	± 0.03		0.64	± 0.04		0.69	± 0.04		0.52	0.97	0.39
C22:6n3	2.55	± 0.15		2.62	± 0.26		2.52	± 0.13		0.73	0.99	0.80
∑n-3 PUFA	3.92	± 0.15		3.65	± 0.50		4.01	± 0.13		0.57	0.78	0.94
∑n-3 metabolites	3.46	± 0.17		3.24	± 0.47		3.54	± 0.14		0.58	0.76	0.96
∑PUFA	42.69	± 0.63		38.81	± 4.45		42.34	± 0.20		0.42	0.61	0.96
∑UFA	63.42	± 0.65		57.46	± 6.44		64.28	± 0.77		0.61	0.49	0.97

Table 13. Total liver fatty acid methyl esters (FAME) ratios for high fat diet groups; High fat diet with-saline (HFD-S), High fat diet -pair-fed (HFD-PF) and High fat diet- Ginkgo biloba (HFD-GbE)(N=10 per group). Results presented as mean and (SEM), and statistically analysed by one-way ANOVA with Tukey's Post-hoc test. The level of statistical significance was set at * $p < 0.05$.

	HFD-S		HFD-PF		HFD-GbE		S Vs PF	S Vs PF	S Vs GbE
	MEAN	SEM	MEAN	SEM	MEAN	SEM	p value	p value	P Value
Σ MUFA/ Σ PUFA	0.49	± 0.02	0.51	± 0.06	0.51	± 0.03	0.60	0.98	0.71
Σ MUFA/ Σ SFA	1.75	± 0.12	1.97	± 0.41	1.59	± 0.10	0.85	0.81	0.48
Σ PUFA/ Σ SFA	1.22	± 0.02	1.24	± 0.02	1.26	± 0.03	0.76	0.95	0.56
Σ UFA/ Σ SFA	1.81	± 0.05	1.86	± 0.08	1.90	± 0.06	0.48	0.99	0.41
C18:0/C16:0	0.50	± 0.04	0.52	± 0.07	0.48	± 0.04	0.80	0.99	0.87
C18:1n9/C16:0	0.81	± 0.03	0.81	± 0.09	0.88	± 0.03	0.74	0.78	0.34
C18:1n9/C16:1n7	53.43	± 3.93	54.76	± 5.96	61.49	± 4.63	0.99	0.21	0.14
C18:1n7/C18:0	0.13	± 0.02	0.16	± 0.02	0.13	± 0.02	0.59	0.43	0.95
C18:1/C18:0	0.14	± 0.02	0.17	± 0.02	0.13	± 0.02	0.15	0.09	0.95
n-6/n-3	9.99	± 0.38	9.96	± 0.50	9.64	± 0.31	0.90	0.98	0.97
n-6/n-3 metabolite	4.54	± 0.18	4.34	± 0.24	4.10	± 0.18	0.35	>0.99	0.39
C18:2n6/C18:3n3	51.47	± 2.25	54.02	± 4.76	56.73	± 3.86	0.96	0.11	0.06
C20:4n6/C20:3n6	37.75	± 3.07	40.46	± 6.36	38.84	± 4.94	0.77	>0.99	0.80
C20:4n6/C22:6n3	5.43	± 0.22	5.23	± 0.27	4.94	± 0.28	0.67	0.95	0.48
C20:4n6/C20:5n3	152.0	± 14.8	144.73	± 24.3	167.68	± 24.9	0.68	0.24	0.67
C20:4n6/C18:2n6	0.60	± 0.05	0.63	± 0.11	0.54	± 0.07	0.72	0.97	0.58
C20:4n6/C18:3n3	32.05	± 3.88	35.18	± 7.03	32.60	± 6.04	0.85	0.86	>0.99
C20:3n3/C18:3n3	0.27	± 0.12	0.46	± 0.13	0.66	± 0.13	0.32	0.83	0.11
C20:5n3/C18:3n3	0.21	± 0.02	0.23	± 0.02	0.19	± 0.01	0.99	0.35	0.38
C22:5n3/C18:3n3	1.65	± 0.13	1.58	± 0.20	1.76	± 0.20	0.88	0.53	0.80
C22:6n3/C18:3n3	5.91	± 0.69	6.48	± 1.14	6.46	± 1.13	0.90	0.68	0.91
C22:6n3/C22:5n3	3.50	± 0.19	3.93	± 0.27	3.60	± 0.23	0.87	0.85	>0.99
C18:2n6/C16:0	1.04	± 0.03	1.06	± 0.03	1.07	± 0.03	0.44	>0.99	0.44
C20:3n6/C18:3n6	2.23	± 0.20	1.97	± 0.16	2.08	± 0.18	0.60	0.82	0.94
C22:5n3/C20:5n3	8.09	± 0.64	6.80	± 0.69	9.03	± 0.72	0.72	0.10	0.34
C22:4n6/C20:4n6	11.22	± 1.09	14.76	± 3.39	9.34	± 0.98	0.97	0.62	0.47
1 (% monoenoics)	17.23	± 0.89	15.30	± 2.32	18.37	± 0.74	0.99	0.58	0.64
2 (% dienoics)	46.70	± 1.56	42.41	± 5.09	48.01	± 1.78	0.91	0.66	0.89
3 (% trienoics)	4.09	± 0.14	3.99	± 0.51	4.37	± 0.24	0.96	0.99	0.91
4 (% tetraenoics)	59.49	± 3.61	53.88	± 9.08	55.28	± 3.48	0.35	0.86	0.68
5 (% pentaenoics)	4.11	± 0.11	3.45	± 0.44	3.98	± 0.19	0.41	0.86	0.74
6 (% hexaenoics)	15.25	± 0.90	14.13	± 2.13	15.13	± 0.81	0.39	0.71	0.86
Unsaturation Index	146.85	± 2.32	133.15	± 15.60	145.13	± 1.53	0.35	0.58	0.93

4.3 Liver TAG

Next TAG fatty acid profiles were examined. As previously mentioned in earlier sections excess TAG accumulation associated with obesity, T2DM, dyslipidaemia, and IR and can result in chronic liver disease (Caussy, Aubin and Loomba, 2021; Birkenfeld and Shulman, 2014).

When comparing the effects of 2 months of HFD-induced obesity to that of a NFD TAG FA levels, no significant changes were seen in total SFA % levels between the either group ($p=0.44$) (Table 14). When compared to liver total fatty acid profiles (SFA, NFD, 38%; HFD 35.1%), TAG percentage levels are nearly 10% lower in TAG SFA for both NFD and HFD groups (NFD 28%; HFD 25.7%) compared to total liver FAME (NFD, 38%; HFD 35.1%) (Table 14). This is an interesting finding and shows that total fatty profiles do not necessarily represent TAG profiles in the liver. There is a significant increase in HFD total MUFA (28.5%) compared to NFD (21.1%; $p=0.001$). Like that seen in total fatty acid profiles, this is largely due to C18:1n-9 (NFD 17.5%, HFD 28.5%; $p<0.0001$) (Table 14).

In contrast to the 10% decrease in SFA levels seen between total FA profiles and that of TAG, an approximate inverse increase in MUFA % levels were seen for both NFD and HFD-S group, compared to TAG levels. Similarly, again to total FAME, n-6 PUFA decreased from 45.6% in NFD to 28.8% in HFD ($p=0.0001$), largely due to the decreased in C20:4n-6 from 24.1% in NFD to 13.7% in HFD ($p=0.01$). n-3 PUFA % levels also decreased by 1.5% between the groups (NFD 3.2%; HFD 1.7%, $p<0.0001$), largely due to a decrease in C18:3n-3 (Table 14). Overall total PUFA decreased from 48.9% in NFD to 33.6% in HFD ($p=0.001$), but overall UFA levels remained comparable ($p=0.27$) (Table 14). As was seen in the total FAMES, the MUFA/PUFA ratio doubled from 0.4 in NFD to 0.8 in HFD ($p<0.0001$) while the MUFA/SFA decreased from 1.4 in NFD to 0.9 in HFD ($p<0.0001$) (Table 15). This was accompanied by a decrease in the unsaturation index from 134.1 in NFD to 105.5 in HFD ($p=0.03$). The n-6/n-3 ratio increased from 14.3 in NFD to 18.5 in HFD ($p<0.0001$) (Table 15) which was not observed when analysing total liver extract FAMES. The changes seen between NFD and HFD in TAG are largely similar to total FA profiles for the same reasons outlined in the previous section, including the effects of oleic acid on liver inflammation. What differs most between total FAME and TAG is that the n-6/n-3 ratio increased, mostly due to the decrease in n-3, which may be a result from the decrease found in the rat chow diet, or from the potential use of n-3 in inflammation mitigation.

Similar to that seen in Total fatty acid profiles, little changes in the FA profiles arose following phytotherapy (HFD-GbE) or caloric restriction (HFD-PF) compared to the HFD-S group as shown in Table 16 and Table 17. Treatment with GbE did lead to a significant increase in n-3 metabolites from 1.1% in the HFD-S group to 1.7% in HFD-GbE group ($p=0.04$), which is comparable to the levels in the

NFD group (1.8%) (Table 16). Caloric restriction in the form of pairfeeding (HFD-PF) partially ameliorated the decrease in n-3 metabolites that arose from an HFD, with levels increasing to 1.4%. The change in n-3 metabolites was largely seen in the levels of C22:6n3 that increased significantly from 0.5% in HFD-S, to 0.7% in HFD-PF ($p=0.004$) and 1% in HFD-GbE ($p=0.0001$) (Table 16). As the rat chow does not contain C22:6n3, this change indicates either DNL of VLCFA in the liver or the delivery of C22:6n3 to the liver from peripheral tissues may be occurring due to caloric restriction (HFD-PF) and increased further with GbE treatment. These changes were also reflected in the change of the n-6/n-3 ratio that significantly decreased to 13.9 in HFD-GbE compared to 18.5 in HFD-S ($p=0.001$). Caloric restriction (HFD-PF) did not sufficiently alter the n-6/n-3 ratio which remained comparable to HFD-S at 17 ($p=0.34$) (Table 17). An increase in n-3 FA may positively affect the inflammatory process associated with steatosis and help mitigate the pro-inflammatory state in the liver associated with a HFD, that can lead to hepatic lipid metabolism and insulin dysregulation (Mäkelä *et al.*, 2022; Cui *et al.*, 2021; Luo *et al.*, 2021; Bogl, Kaprio and Pietiläinen, 2020; van Name *et al.*, 2020; da Silva *et al.*, 2014; Valenzuela and Videla, 2011; Pachikian *et al.*, 2008; Araya *et al.*, 2004; Videla *et al.*, 2004). Overall, similar changes in TAG profiles were seen as those in the total fatty acid profiles. Most changes occurred in MUFA and PUFA. MUFA increased with HFD feeding and remained elevated despite caloric restriction and GbE treatment. PUFA levels decreased following an HFD, in both n-6 and n-3 PUFA compared to a NFD. Both caloric restriction (HFD-PF) and GbE treatment resulted in a significant increase in C22:6n-3, more so with GbE. Overall PUFA levels however remained similar in all three HFD groups.

Table 14. Liver triglyceride fatty acid methyl esters (FAME) for normal fat diet (NFD) and high fat diet (HFD-S) (N=10 per group). Fatty acid results are presented as area % percentage mean and standard error of the mean (SEM), and statistically analysed by Students t-test. The level of statistical significance was set at * $p < 0.05$.

	NFD			HFD-S			p value
	MEAN	±	SEM	MEAN	±	SEM	
C14:0	0.2	±	0.02	0.3	±	0.04	0.12
C16:0	25.5	±	0.41	25.4	±	0.34	0.91
C18:0	1.6	±	0.16	2.3	±	0.10	0.01
C20:0	0.1	±	0.02	0.0	±	0.03	0.57
DMA18:0	0.1	±	0.01	0.2	±	0.03	0.02
∑S.DMA	0.1	±	0.01	0.2	±	0.03	0.02
∑SFA	28.0	±	0.45	25.7	±	2.87	0.44
C16:1n7	0.9	±	0.20	0.6	±	0.17	0.43
C17:1	0.03	±	0.02	0.1	±	0.02	0.049
C18:1n7 <i>trans</i>	0.01	±	0.01	0.0	±	0.01	0.88
C18:1n7	1.9	±	0.10	1.7	±	0.13	0.49
C18:1n9	17.5	±	1.21	28.5	±	0.44	<0.0001
C20:1n9	0.3	±	0.03	0.4	±	0.02	0.32
C22:1n9	0.1		0.02	0.1		0.02	0.69
∑DMA18:1	0.3	±	0.03	0.2	±	0.04	0.27
∑C18:1	2.0	±	0.11	1.7	±	0.23	0.34
∑ω7	0.9	±	0.20	0.7	±	0.17	0.34
∑ω9	17.9	±	1.21	26.1	±	2.92	0.02
∑MUFA	21.1	±	1.20	28.5	±	3.20	0.04
C18:2n6	39.4	±	1.07	29.6	±	0.60	<0.0001
C18:3n6	0.3	±	0.01	0.3	±	0.04	0.78
C20:2n6	0.3	±	0.01	0.4	±	0.03	0.01
C20:3n6	0.3	±	0.03	0.3	±	0.01	0.30
C20:4n6	4.2	±	0.17	3.2	±	0.09	0.0001
∑n-6 PUFA	45.7	±	1.14	31.9	±	3.58	0.002
∑n-6 metabolites	6.3	±	0.19	5.2	±	0.59	0.08
C18:3n3	1.5	±	0.10	0.7	±	0.04	<0.0001
C20:3n3	0.1	±	0.01	0.1	±	0.03	0.30
C20:5n3	0.3	±	0.03	0.1	±	0.01	0.0003
C22:5n3	0.5	±	0.04	0.5	±	0.03	0.86
C22:6n3	0.9	±	0.06	0.5	±	0.04	<0.0001
∑n-3 PUFA	3.2	±	0.11	1.7	±	0.20	<0.0001
∑n-3 metabolites	1.8	±	0.08	1.1	±	0.14	0.001
∑PUFA	48.9	±	1.16	33.6	±	3.78	0.001
∑UFA	69.9	±	0.41	62.1	±	6.91	0.27

Table 15 Liver triglyceride fatty acid methyl esters (FAME) ratios between normal fat diet (NFD) and high fat diet (HFD-S) (N=10 per group). Results presented as mean and standard error of the mean (SEM), and statistically analysed by Students t-test. The level of statistical significance was set at * $p < 0.05$.

	NFD			HFD-S			p value
	MEAN	±	SEM	MEAN	±	SEM	
ΣMUFA/ΣPUFA	0.4	±	0.03	0.8	±	0.03	<0.0001
ΣMUFA/ΣSFA	1.4	±	0.08	0.9	±	0.01	<0.0001
ΣPUFA/ΣSFA	1.7	±	0.06	1.3	±	0.02	<0.0001
ΣUFA/ΣSFA	2.5	±	0.05	2.4	±	0.03	0.15
C18:0/C16:0	0.1	±	0.02	0.1	±	0.01	0.08
C16:1n7/C16:0	0.0	±	0.01	0.0	±	0.01	0.94
C18:1n9/C16:0	0.7	±	0.05	1.1	±	0.03	<0.0001
C18:1n9/C16:1n7	27.1	±	4.67	57.0	±	7.49	0.003
C18:1n7/C18:0	1.3	±	0.19	0.8	±	0.07	0.03
C18:1/C18:0	1.3	±	0.20	0.8	±	0.07	0.04
n-6/n-3	14.3	±	0.52	18.5	±	0.60	<0.0001
n-6/n-3 metabolites	3.6	±	0.20	4.7	±	0.24	0.003
C18:2n6/C18:3n3	28.4	±	2.33	44.8	±	2.55	0.0002
C20:4n6/C20:3n6	16.5	±	1.57	10.3	±	0.84	0.01
C20:4n6/C22:6n3	4.9	±	0.30	6.1	±	0.39	0.02
C20:4n6/C20:5n3	16.9	±	1.82	44.2	±	9.08	0.005
C20:4n6/C18:2n6	0.1	±	0.01	0.1	±	0.01	>0.99
C20:4n6/C18:3n3	3.1	±	0.30	4.9	±	0.35	0.001
C20:3n3/C18:3n3	0.1	±	0.02	0.2	±	0.04	0.01
C20:5n3/C18:3n3	0.2	±	0.01	0.1	±	0.03	0.01
C22:5n3/C18:3n3	0.4	±	0.08	0.8	±	0.04	0.001
C22:6n3/C18:3n3	0.7	±	0.09	0.8	±	0.06	0.14
C22:6n3/C22:5n3	1.7	±	0.10	1.1	±	0.04	<0.0001
C18:2n6/C16:0	1.6	±	0.06	1.2	±	0.04	<0.0001
C18:3n3/C16:0	0.1	±	0.01	0.01	±	0.01	<0.0001
C18:3n6/C18:2n6	0.0	±	0.01	0.0	±	0.01	0.31
C20:3n6/C18:3n6	0.9	±	0.12	1.0	±	0.16	0.72
C22:5n3/C20:5n3	2.2	±	0.42	7.2	±	1.45	0.002
C22:4n6/C20:4n6	3.6	±	0.20	2.1	±	0.04	<0.0001
1 (% monoenoics)	16.4	±	1.24	24.0	±	2.68	0.02
2 (% dienoics)	79.4	±	2.13	54.1	±	6.10	0.001
3 (% trienoics)	7.4	±	0.31	4.7	±	0.60	0.001
4 (% tetraenoics)	21.6	±	0.74	17.1	±	1.96	0.05
5 (% pentaenoics)	4.0	±	0.23	2.7	±	0.34	0.004
6 (% hexaenoics)	5.3	±	0.30	2.9	±	0.37	<0.0001
Unsaturation Index	134.1	±	1.32	105.5	±	11.77	0.03

Table 16. Liver triglyceride (TAG) fatty acid methyl esters (FAME) for high fat diet groups; High fat diet with-saline (HFD-S), High fat diet -pair-fed (HFD-PF) and High fat diet- Ginkgo biloba (HFD-GbE) (N=10 per group). Fatty acid results are presented as area % percentage mean and standard error of the mean (SEM), and statistically analysed by one-way ANOVA with Tukey's Post-hoc test. The level of statistical significance was set at * $p < 0.05$.

	HFD-S		HFD-PF		HFD-GbE		S Vs PF	S Vs GbE	PF Vs GbE
	MEAN %	SEM	MEAN %	SEM	MEAN %	SEM	<i>p value</i>	<i>p value</i>	<i>p value</i>
C14:0	0.3	± 0.04	0.2	± 0.02	0.3	± 0.02	0.50	0.96	0.68
C16:0	25.4	± 0.34	24.6	± 0.38	24.3	± 0.39	0.51	0.29	0.29
C17:0	0.2	± 0.01	0.2	± 0.01	0.2	± 0.02	0.45	0.78	0.82
C18:0	2.3	± 0.10	3.0	± 0.38	3.8	± 0.55	0.36	0.02	0.35
C20:0	0.0	± 0.03	0.2	± 0.12	0.1	± 0.02	0.19	0.92	0.36
C21:0	0.1	± 0.01	0.1	± 0.02	0.2	± 0.02	0.64	0.13	0.53
C24:0	1.6	± 0.05	1.4	± 0.11	1.7	± 0.07	0.23	0.27	0.01
DMA18:0	0.2	± 0.03	0.4	± 0.07	0.5	± 0.09	0.03	0.01	0.88
∑SFA	25.7	± 2.87	28.8	± 0.54	26.5	± 2.98	0.67	0.97	0.79
C16:1n7	0.6	± 0.17	0.6	± 0.07	0.5	± 0.05	0.87	0.51	0.83
C17:1	0.1	± 0.02	0.1	± 0.01	0.1	± 0.02	0.58	0.71	0.24
C18:1n7	1.7	± 0.13	0.1	± 0.02	1.9	± 0.07	<0.0001	0.50	<0.0001
C18:1n9 <i>trans</i>	0.0	± 0.02	1.9	± 0.19	0.1	± 0.02	<0.0001	0.99	<0.0001
C18:1n9	28.5	± 0.44	28.0	± 1.54	27.1	± 0.76	0.95	0.60	0.79
C20:1n9	0.4	± 0.02	0.4	± 0.01	0.4	± 0.03	0.79	0.33	0.74
DMA18:1	0.2	± 0.04	0.4	± 0.10	0.5	± 0.10	0.38	0.03	0.38
∑C18:1	1.7	± 0.23	2.0	± 0.19	1.8	± 0.21	0.30	0.06	0.68
∑ω7	0.7	± 0.17	0.6	± 0.09	0.4	± 0.07	0.68	0.96	0.83
∑ω9	26.1	± 2.92	30.3	± 1.45	24.8	± 2.84	0.89	0.41	0.71
∑MUFA	28.5	± 3.20	31.3	± 1.32	27.4	± 3.14	0.49	0.93	0.31
C18:2n6	29.6	± 0.60	29.5	± 1.24	27.6	± 0.59	0.77	0.95	0.60
C18:3n6	0.3	± 0.04	0.3	± 0.04	0.2	± 0.03	>0.99	0.24	0.27
C20:2n6	0.4	± 0.03	0.4	± 0.03	0.4	± 0.02	0.89	0.38	0.64
C20:3n6	0.3	± 0.01	0.3	± 0.02	0.3	± 0.02	0.60	0.60	0.15
C20:4n6	3.2	± 0.09	3.5	± 0.22	5.0	± 0.64	0.93	0.45	0.66
∑n-6 PUFA	31.9	± 3.58	35.4	± 1.26	31.8	± 3.55	0.71	>0.99	0.70
∑n-6 metabolites	5.2	± 0.59	5.8	± 0.33	7.0	± 0.94	0.79	0.18	0.51
C18:3n3	0.7	± 0.04	0.8	± 0.11	0.7	± 0.03	0.54	0.99	0.48
C20:3n3	0.1	± 0.03	0.2	± 0.02	0.2	± 0.03	0.26	0.15	0.94
C20:5n3	0.1	± 0.01	0.1	± 0.03	0.1	± 0.01	0.90	0.89	>0.99
C22:5n3	0.5	± 0.03	0.5	± 0.04	0.6	± 0.04	0.68	0.16	0.03
C22:6n3	0.5	± 0.04	0.7	± 0.07	1.0	± 0.09	0.27	0.0001	0.004
∑n-3 PUFA	1.7	± 0.20	2.2	± 0.20	2.3	± 0.29	0.43	0.19	0.87
∑n-3 metabolites	1.1	± 0.14	1.4	± 0.11	1.7	± 0.23	0.60	0.04	0.29
∑PUFA	33.6	± 3.78	37.5	± 1.44	34.1	± 3.82	0.69	0.99	0.75
∑UFA	62.1	± 6.91	68.8	± 0.68	61.6	± 6.86	0.71	>0.99	0.67

Table 17. Liver triglyceride (TAG) fatty acid methyl esters (FAME) ratios for high fat diet groups; High fat diet with-saline (HFD-S), High fat diet -pair-fed (HFD-PF) and High fat diet- Ginkgo biloba (HFD-GbE)(N=10 per group). Results presented as mean an (SEM), and statistically analysed by one-way ANOVA with Tukey's Post-hoc test. The level of statistical significance was set at * $p < 0.05$.

	HFD-S			HFD-PF			HFD-GbE			S Vs PF	S Vs GbE	PF Vs GbE
	MEAN %	SEM		MEAN %	SEM		MEAN %	SEM		<i>p value</i>	<i>p value</i>	<i>p value</i>
ΣMUFA/ΣPUFA	0.8	± 0.03		0.8	± 0.06		0.8	± 0.03		>0.99	0.84	0.84
ΣMUFA/ΣSFA	0.9	± 0.01		1.0	± 0.06		1.0	± 0.05		0.87	0.78	0.98
ΣPUFA/ΣSFA	1.3	± 0.02		1.3	± 0.06		1.3	± 0.03		0.93	0.98	0.84
ΣUFA/ΣSFA	2.4	± 0.03		2.4	± 0.06		2.3	± 0.06		0.99	0.53	0.62
C18:0/C16:0	0.1	± 0.01		0.1	± 0.01		0.2	± 0.03		0.90	0.04	0.09
C16:1n7/C16:0	0.0	± 0.01		0.01	± 0.01		0.01	± 0.01		0.45	0.45	>0.99
C18:1n9/C16:0	1.1	± 0.03		1.2	± 0.08		1.1	± 0.03		0.89	>0.99	0.89
C18:1n9/C16:1n7	57.0	± 7.49		56.5	± 8.31		66.3	± 6.74		>0.99	0.65	0.64
C18:1n7/C18:0	0.8	± 0.07		0.01	± 0.01		0.6	± 0.07		<0.0001	0.03	<0.0001
C18:1/C18:0	0.8	± 0.07		0.7	± 0.14		0.6	± 0.08		0.72	0.23	0.63
n-6/n-3	18.5	± 0.60		17.0	± 0.96		13.9	± 0.64		0.34	0.001	0.02
n-6/n-3 metabolites	4.7	± 0.24		4.4	± 0.27		4.0	± 0.14		0.58	0.11	0.51
C18:2n6/C18:3n3	44.8	± 2.55		41.6	± 3.82		42.2	± 1.74		0.72	0.80	0.99
C20:4n6/C20:3n6	10.3	± 0.84		11.0	± 0.94		14.9	± 2.29		0.94	0.12	0.19
C20:4n6/C22:6n3	6.1	± 0.39		5.4	± 0.43		4.7	± 0.24		0.37	0.02	0.33
C20:4n6/C20:5n3	44.2	± 9.08		48.6	± 9.75		66.3	± 10.1		0.95	0.26	0.41
C20:4n6/C18:2n6	0.1	± 0.01		0.1	± 0.01		0.2	± 0.03		0.90	0.04	0.09
C20:4n6/C18:3n3	4.9	± 0.35		4.9	± 0.52		7.8	± 1.25		>0.99	0.046	0.048
C20:3n3/C18:3n3	0.2	± 0.04		0.2	± 0.06		0.3	± 0.07		0.85	0.24	0.52
C20:5n3/C18:3n3	0.1	± 0.03		0.1	± 0.02		0.1	± 0.01		>0.99	0.92	0.92
C22:5n3/C18:3n3	0.8	± 0.04		0.6	± 0.07		0.9	± 0.06		0.37	0.10	0.005
C22:6n3/C18:3n3	0.8	± 0.06		0.9	± 0.12		1.6	± 0.19		0.80	0.001	0.004
C22:6n3/C22:5n3	1.1	± 0.04		1.5	± 0.06		1.7	± 0.11		0.003	<0.0001	0.09
C18:2n6/C16:0	1.2	± 0.04		1.2	± 0.05		1.1	± 0.03		0.70	0.70	0.26
C20:3n6/C18:3n6	1.0	± 0.16		1.1	± 0.12		1.5	± 0.10		0.82	0.04	0.15
C22:5n3/C20:5n3	7.2	± 1.45		6.5	± >0.99		8.1	± 0.71		0.89	0.84	0.56
C22:4n6/C20:4n6	2.1	± 0.04		2.6	± 0.21		2.9	± 0.45		0.39	0.10	0.70
1 (% monoenoics)	24.0	± 2.68		26.4	± 0.72		22.2	± 2.54		0.73	0.84	0.41
2 (% dienoics)	54.1	± 6.10		59.8	± 2.48		50.4	± 5.71		0.73	0.87	0.43
3 (% trienoics)	4.7	± 0.60		5.8	± 0.26		5.0	± 0.58		0.32	0.90	0.55
4 (% tetraenoics)	17.1	± 1.96		19.4	± 1.20		24.1	± 3.48		0.81	0.12	0.38
5 (% pentaenoics)	2.7	± 0.34		2.7	± 0.30		3.1	± 0.39		0.98	0.61	0.73
6 (% hexaenoics)	2.9	± 0.37		4.0	± 0.40		5.7	± 0.81		0.39	0.005	0.12
Unsaturation Index	105.5	± 11.77		118.1	± 2.87		110.6	± 12.4		0.67	0.93	0.87

4.4 Liver CE

As mentioned in the previous RET section 4.3, CE may be reflective of FA from dietary sources, or a reflection of PPL FA liberated for CE production in the cell. When comparing a NFD and HFD CE FA profiles, total SFA increased to 25.6% of the CE HFD FA sample compared to 16.9% in NFD ($p < 0.0001$) (Table 18). This contrasts with the decrease seen in that of the HFD-TAG fraction. The increase in CE SFA levels in the HFD is predominantly caused by the increase of C16:0 from 12% in NFD to 19% in HFD ($p = 0.03$), and to a lesser degree C18:0 ($p = 0.0001$) (Table 18).

In keeping with changes seen in TAG-MUFA, total CE-MUFA also increased from 11% in NFD to 15.5% in the HFD ($p < 0.0001$) group compared to the NFD control group, again largely due to the increase in C18:1n-9 which increased from 7% in NFD to 13.8% in HFD ($p < 0.0001$).

Like that of TAG profiles, CE-n-6 PUFA decreased from 51.5% in NFD to 48.4% in HFD ($p = 0.03$), represented mostly from the 3% decrease in C18:2n-6 ($p = 0.001$). n-3 PUFA also decreased from 15.7% in NFD to 10.5% in HFD ($p < 0.0001$), largely represented by the 2% decrease in C18:3n-3 ($p < 0.0001$) and the 2% decrease in C22:6n-3 ($p < 0.0001$). The n-6/n-3 ratio also increased from 3.3 in NFD to 4.6 in HFD ($p < 0.0001$), largely due to the decrease in n-3 % levels (Table 19). These CE n-6/n-3 ratios are much lower to the ratios seen in of TAG that had a n-6/n-3 ratio of 14.3 in NFD and 18.5 in the HFD group. This indicates that more n-3 PUFA are being utilized for CE production than n-6 PUFA. The increase in the n-6/n-3 ratio from 3.3 in NFD to 4.6 in the HFD group may indicate that less n-3 PUFA is available from either the diet or endogenous stores for the esterification of cholesterol for transportation. This is possibly due to the decrease in n-3 PUFA found in the HFD chow compared to the NFD. HFD rat chow consists of 21.4% C18:2n-6 compared to 51% in the NFD chow ($p < 0.001$), and while C18:3n-3 levels in NFD are 4.3% compared to 1.3% in the HFD chow (Table 18). This indicates that both C18:2n-6 and C18:3n-3 are either being preferentially esterified to CE from the diet or are being liberated from the plasma membrane. As discussed in earlier chapters, esterification of Chol to CE in the liver occurs in the endoplasmic reticulum, catalysed by an ACAT where a LCFA, liberated from the PPL PC, is esterified to CHOL to form CE (Nakamura *et al.*, 2004). These changes resulted in an overall 8% decrease in total PUFA dropping from 67.1% in NFD, to 58.9% in HFD ($P < 0.0001$) (Table 18). This is also reflected in the MUFA/PUFA ratio that increase from 0.17 in NFD to 0.26 in HFD ($p = 0.0009$) and the PUFA/SFA ratio that decreased from 4.7 in NFD to 2.7 in HFD ($p < 0.0001$) (Table 19). The UFA also significantly decreased from by 3.7% from 78.2% in NFD to 74.45% in HFD ($p = 0.0002$) (Table 18). These changes were reflected in the decrease of the

unsaturation index from 202 in NFD to 185 in HFD ($p=0.0002$). Together these changes in FA % levels indicate that less n-3 is available either from the diet or from within the PPL membrane or less is being transported from adipose tissues back to the liver and is being replaced with more SFA within the CE fraction.

When comparing the HFD groups, while no changes were seen in total SFA, total MUFA levels increased significantly to 23.1% in GbE treatment compared to 15.5% in NFD ($p=0.0001$) and to 17.2% in caloric restriction (HFD-S vs HFD-PF, $p=0.002$) indicating a direct response to GbE treatment (Table 20). This is largely attributable to the increase seen in C18:1n-9 to 19.1% in the GbE group compared to the 13.8% in HFD-S ($p=0.01$) and 14.1% in HFD-PF ($p=0.01$) groups. n-6 PUFA also decreased significantly from 48.4% in NFD to 44.7% in HFD-PF ($p=0.12$) and 40.2% in GbE ($p=0.0003$) (Table 20). This is largely attributable to the decrease in both C18:2n-6 ($p=0.01$) and C20:4n-6 ($p=0.001$) in the GbE group compared to HFD-S (Table 20). The decrease in GbE n-6 PUFA levels was also significantly decreased compared to HFD-PF ($p=0.02$), again indicating the GbE treatment is likely responsible for this change. In contrast, n-3 PUFA continued to decrease from 10.5% in the NFD group to 6.4% in the GbE group ($p=0.01$), which was not seen in the HFD-PF group (9.9% which was comparable to the HFD-S group ($p=0.87$)) and significantly higher than that in the GbE group ($p=0.03$). This was reflected in the n-6/n-3 ratio that doubled to 8.2 in the HFD-GbE group compared to 4.6 ($p=0.01$) in the HFD-S group and 4.6 ($p=0.01$) in the HFD-PF group (Table 21). Despite the increase in MUFA, the decrease in PUFA resulted in a decrease of UFA % levels from 74.5% in the HFD-S group down to 69.7% in the HFD-GbE group ($p=0.05$). This resulted in a decrease in the unsaturation index from 184.7 to 143.7 in the HFD-GbE group ($p=0.0003$) (Table 20). Again, this indicates that either less n-3 is available either from the diet or from within the PPL membrane or less is being transported from adipose tissues back to the liver with more MUFA being used in the GbE group to form CE.

Table 18. Liver cholesteryl ester fatty acid methyl esters (FAME) for normal fat diet (NFD) and high fat diet (HFD-S) (N=10 per group). Fatty acid results are presented as area % percentage mean and standard error of the mean (SEM), and statistically analysed by Students t-test. The level of statistical significance was set at * $p < 0.05$.

	NFD			HFD-S			p value
	MEAN	±	SEM	MEAN	±	SEM	
C14:0	0.08	±	0.02	0.26	±	0.02	<0.0001
C15:0	0.10	±	0.03	0.10	±	0.00	>0.99
C16:0	12.00	±	0.46	18.97	±	0.40	<0.0001
C17:0	0.14	±	0.02	0.10	±	0.00	0.03
C18:0	1.29	±	0.13	1.98	±	0.10	0.001
C20:0	0.24	±	0.04	0.15	±	0.02	0.054
C24:0	2.59	±	0.22	3.89	±	0.18	0.0003
DMA18:0	0.10	±	0.00	0.11	±	0.02	0.61
ΣSFA	16.9	±	0.5	25.6	±	0.4	<0.0001
C16:1n7	0.59	±	0.15	0.45	±	0.03	0.35
C18:1n7	0.71	±	0.09	0.83	±	0.03	0.19
C18:1n9	7.12	±	0.72	13.77	±	0.42	<0.0001
C20:1n9	0.82	±	0.07	0.17	±	0.02	<0.0001
C22:1n9	0.07	±	0.02	0.05	±	0.02	0.43
ΣDMA18:1	1.03	±	0.09	0.19	±	0.03	<0.0001
ΣC18:1	0.77	±	0.08	0.88	±	0.02	0.20
Σω7	0.59	±	0.15	0.46	±	0.03	0.38
Σω9	8.01	±	0.68	14.04	±	0.42	<0.0001
ΣMUFA	11.03	±	0.66	15.51	±	0.44	<0.0001
C18:2n6	38.90	±	0.90	35.03	±	0.51	0.001
C18:3n6	0.74	±	0.03	0.73	±	0.04	0.78
C20:2n6	0.26	±	0.02	0.30	±	0.03	0.18
C20:3n6	0.86	±	0.05	1.14	±	0.05	0.001
C20:4n6	8.18	±	0.32	7.31	±	0.27	0.054
Σn-6 PUFA	51.50	±	1.11	48.43	±	0.67	0.03
Σn-6 metabolites	12.60	±	0.44	13.40	±	0.47	0.23
C18:3n3	4.91	±	0.29	3.10	±	0.12	<0.0001
C20:3n3	0.17	±	0.02	0.17	±	0.02	>0.99
C20:5n3	1.72	±	0.17	0.64	±	0.04	<0.0001
C22:5n3	2.81	±	0.17	2.70	±	0.11	0.58
C22:6n3	6.08	±	0.33	3.92	±	0.15	<0.0001
Σn-3 PUFA	15.66	±	0.48	10.50	±	0.31	<0.0001
Σn-3 metabolites	10.77	±	0.48	7.42	±	0.24	<0.0001
ΣPUFA	67.14	±	1.04	58.92	±	0.75	<0.0001
ΣUFA	78.16	±	0.69	74.45	±	0.40	0.0002

Table 19 Liver cholesteryl ester fatty acid methyl esters (FAME) ratios between normal fat diet (NFD) and high fat diet (HFD-S) (N=10 per group). Results presented as mean and standard error of the mean (SEM), and statistically analysed by Students t-test. The level of statistical significance was set at * $p < 0.05$.

	NFD		HFD-S		p value
	MEAN	SEM	MEAN	SEM	
Σ MUFA/ Σ PUFA	0.17	± 0.02	0.26	± 0.02	0.0009
Σ MUFA/ Σ SFA	1.32	± 0.06	1.40	± 0.04	0.27
Σ PUFA/ Σ SFA	4.73	± 0.17	2.71	± 0.08	<0.0001
Σ UFA/ Σ SFA	5.49	± 0.16	3.45	± 0.08	<0.0001
C18:0/C16:0	0.11	± 0.01	0.10	± <0.01	0.31
C16:1n7/C16:0	0.03	± 0.02	<0.01	± <0.01	0.0495
C18:1n9/C16:0	0.59	± 0.04	0.71	± 0.03	0.03
C18:1n9/C16:1n7	15.61	± 3.09	31.75	± 1.89	0.0003
C18:1n7/C18:0	0.62	± 0.10	0.43	± 0.03	0.07
C18:1/C18:0	0.64	± 0.10	0.47	± 0.03	0.09
n-6/n-3	3.32	± 0.14	4.63	± 0.14	<0.0001
n-6/n-3 metabolites	1.19	± 0.07	1.83	± 0.09	<0.0001
C18:2n6/C18:3n3	8.22	± 0.59	11.47	± 0.45	0.0004
C20:4n6/C20:3n6	9.96	± 0.86	6.52	± 0.35	0.001
C20:4n6/C22:6n3	1.37	± 0.11	1.89	± 0.10	0.002
C20:4n6/C20:5n3	5.22	± 0.60	11.90	± 1.03	<0.0001
C20:4n6/C18:2n6	0.20	± <0.01	0.21	± 0.01	0.36
C20:4n6/C18:3n3	1.74	± 0.16	2.40	± 0.12	0.005
C20:3n3/C18:3n3	0.02	± 0.01	0.04	± 0.02	0.43
C20:5n3/C18:3n3	0.36	± 0.03	0.21	± 0.02	0.001
C22:5n3/C18:3n3	0.61	± 0.09	0.90	± 0.04	0.01
C22:6n3/C18:3n3	1.30	± 0.13	1.29	± 0.05	0.94
C22:6n3/C22:5n3	2.22	± 0.15	1.48	± 0.07	0.0003
C18:2n6/C16:0	3.27	± 0.16	1.84	± 0.05	<0.0001
C18:3n3/C16:0	0.42	± 0.03	0.18	± 0.01	<0.0001
C18:3n6/C18:2n6	0.02	± <0.01	0.02	± <0.01	>0.99
C20:3n6/C18:3n6	1.16	± 0.07	1.56	± 0.08	0.002
C22:5n3/C20:5n3	1.77	± 0.25	4.33	± 0.25	<0.0001
C22:4n6/C20:4n6	3.28	± 0.21	1.88	± 0.04	<0.0001
1 (% monoenoics)	-0.34	± 1.39	12.99	± 0.38	<0.0001
2 (% dienoics)	78.26	± 1.80	70.67	± 1.03	0.002
3 (% trienoics)	22.43	± 1.04	15.89	± 0.39	<0.0001
4 (% tetraenoics)	43.08	± 1.76	44.79	± 1.78	0.50
5 (% pentaenoics)	22.56	± 1.25	16.73	± 0.64	0.001
6 (% hexaenoics)	36.47	± 2.02	23.59	± 0.91	<0.0001
Unsaturation Index	202.41	± 3.21	184.67	± 2.18	0.0002

Table 20. Liver cholesteryl ester (CE) fatty acid methyl esters (FAME) for high fat diet groups; High fat diet with-saline (HFD-S), High fat diet -pair-fed (HFD-PF) and High fat diet- Ginkgo biloba (HFD-GbE) (N=10 per group). Fatty acid results are presented as area % percentage mean and standard error of the mean (SEM), and statistically analysed by one-way ANOVA with Tukey's Post-hoc test. The level of statistical significance was set at * $p < 0.05$.

	HFD-S			HFD-PF			HFD-GbE			S Vs PF	S Vs GbE	PF Vs GbE
	MEAN %	SEM		MEAN %	SEM		MEAN %	SEM		<i>p value</i>	<i>p value</i>	<i>p value</i>
C14:0	0.26	± 0.02		0.29	± 0.03		0.30	± 0.02		0.51	0.33	0.93
C16:0	18.97	± 0.40		17.79	± 0.54		19.90	± 1.05		0.27	0.51	0.51
C17:0	0.10	± <0.01		0.12	± 0.01		0.19	± 0.01		0.30	<0.0001	0.001
C18:0	1.98	± 0.10		2.58	± 0.57		2.05	± 0.16		0.41	0.99	0.50
C20:0	0.15	± 0.02		0.14	± 0.04		0.18	± 0.09		0.99	0.88	0.85
C21:0	0.00	± <0.01		0.02	± 0.02		0.10	± <0.01		0.71	0.0007	0.0001
C22:0	0.13	± 0.06		0.14	± 0.02		0.05	± 0.03		0.97	0.42	0.39
C24:0	3.89	± 0.18		3.19	± 0.24		2.92	± 0.29		0.13	0.02	0.72
DMA18:0	0.11	± 0.02		0.51	± 0.07		0.37	± 0.04		<0.0001	0.001	0.10
∑SFA	25.6	± 0.4		24.9	± 0.8		26.0	± 1.0		>0.99	0.52	0.54
C16:1n7	0.45	± 0.03		0.47	± 0.06		0.44	± 0.04		0.96	>0.99	0.94
C18:1n7	0.83	± 0.03		1.26	± 0.05		1.32	± 0.10		0.0003	0.0001	0.77
C18:1n9 <i>trans</i>	0.02	± 0.01		0.03	± 0.02		0.02	± 0.01		0.96	0.99	0.92
C18:1n9	13.77	± 0.42		14.07	± 1.06		19.12	± 1.63		0.98	0.01	0.01
C20:1n9	0.17	± 0.02		0.30	± 0.03		0.75	± 0.20		0.75	0.01	0.04
C22:1n9	0.05	± 0.02		0.11	± 0.01		0.10	± 0.03		0.06	0.19	0.89
DMA18:1	0.19	± 0.03		0.66	± 0.13		1.08	± 0.33		0.28	0.01	0.35
∑C18:1	0.88	± 0.02		1.32	± 0.04		1.25	± 0.16		0.01	0.03	0.86
∑ω7	0.46	± 0.03		0.48	± 0.05		0.45	± 0.07		0.97	0.99	0.93
∑ω9	14.04	± 0.42		14.51	± 1.06		19.94	± 1.55		0.95	0.002	0.01
∑MUFA	15.51	± 0.44		17.16	± 0.99		23.08	± 1.49		0.54	0.0001	0.002
C18:2n6	35.03	± 0.51		32.70	± 1.49		30.72	± 0.89		0.25	0.01	0.37
C18:3n6	0.73	± 0.04		0.91	± 0.12		0.48	± 0.06		0.23	0.07	0.002
C20:2n6	0.30	± 0.03		0.33	± 0.04		0.36	± 0.03		0.833	0.31	0.69
C20:3n6	1.14	± 0.05		0.73	± 0.04		0.51	± 0.06		0.0001	<0.0001	0.02
C20:4n6	7.31	± 0.27		6.88	± 0.33		5.09	± 0.51		0.72	0.001	0.01
∑n-6 PUFA	48.43	± 0.67		44.70	± 1.49		40.19	± 1.54		0.12	0.0003	0.05
∑n-6 metabolites	13.40	± 0.47		11.98	± 0.56		9.32	± 0.87		0.31	0.0004	0.02
C18:3n3	3.10	± 0.12		2.83	± 0.37		1.62	± 0.23		0.74	0.0008	0.01
C20:3n3	0.17	± 0.02		0.29	± 0.03		0.20	± 0.02		0.003	0.48	0.03
C20:5n3	0.64	± 0.04		0.72	± 0.18		0.31	± 0.08		0.87	0.12	0.049
C22:5n3	2.70	± 0.11		2.08	± 0.18		1.60	± 0.27		0.09	0.001	0.23
C22:6n3	3.92	± 0.15		4.00	± 0.44		2.77	± 0.65		0.99	0.19	0.17
∑n-3 PUFA	10.50	± 0.31		9.87	± 0.94		6.42	± 1.19		0.87	0.01	0.03
∑n-3 metabolites	7.42	± 0.24		7.02	± 0.77		4.82	± 0.97		0.92	0.04	0.10
∑PUFA	58.92	± 0.75		54.56	± 2.01		46.63	± 2.56		0.27	0.0003	0.02
∑UFA	74.45	± 0.40		71.71	± 1.67		69.68	± 1.66		0.35	0.047	0.55

Table 21. Liver cholesteryl esters (CE) fatty acid methyl esters (FAME) ratios for high fat diet groups; High fat diet with-saline (HFD-S), High fat diet -pair-fed (HFD-PF) and High fat diet- Ginkgo biloba (HFD-GbE) (N=10 per group). Results presented as mean an (SEM), and statistically analysed by one-way ANOVA with Tukey's Post-hoc test. The level of statistical significance was set at * $p < 0.05$.

	HFD-S		HFD-PF		HFD-GbE		S Vs PF	S Vs GbE	PF Vs GbE
	MEAN %	SE M	MEAN %	SE M	MEAN %	SE M	<i>p value</i>	<i>p value</i>	<i>p value</i>
ΣMUFA/ΣPUFA	0.26 ± 0.02		0.32 ± 0.02		0.52 ± 0.06		0.54	0.0003	0.01
ΣMUFA/ΣSFA	1.40 ± 0.04		1.31 ± 0.10		1.01 ± 0.04		0.60	0.001	0.01
ΣPUFA/ΣSFA	2.71 ± 0.08		2.56 ± 0.17		2.09 ± 0.20		0.78	0.03	0.12
ΣUFA/ΣSFA	3.45 ± 0.08		3.37 ± 0.18		3.11 ± 0.21		0.94	0.33	0.54
C18:0/C16:0	0.10 ± 0.01		0.14 ± 0.03		0.10 ± 0.01		0.22	>0.99	0.22
C18:1n9/C16:0	0.71 ± 0.03		0.81 ± 0.06		0.96 ± 0.05		0.30	0.002	0.08
C18:1n9/C16:1n7	31.75 ± 1.89		35.08 ± 5.43		47.27 ± 6.06		0.87	0.06	0.19
C18:1/C18:0	0.47 ± 0.03		0.60 ± 0.06		0.61 ± 0.07		0.24	0.18	0.99
n-6/n-3	4.63 ± 0.14		4.83 ± 0.45		8.23 ± 1.21		0.98	0.01	0.01
n-6/n-3 metabolites	1.83 ± 0.09		1.87 ± 0.18		2.41 ± 0.29		0.99	0.12	0.17
C18:2n6/C18:3n3	11.47 ± 0.45		12.96 ± 1.52		22.80 ± 2.80		0.85	0.001	0.003
C20:4n6/C20:3n6	6.52 ± 0.35		9.62 ± 0.48		10.55 ± 1.09		0.02	0.002	0.65
C20:4n6/C22:6n3	1.89 ± 0.10		1.89 ± 0.21		2.56 ± 0.36		>0.99	0.16	0.17
C20:4n6/C20:5n3	11.90 ± 1.03		13.03 ± 2.01		20.97 ± 3.05		0.92	0.01	0.04
C20:4n6/C18:2n6	0.21 ± 0.01		0.23 ± 0.02		0.15 ± 0.02		0.61	0.047	0.01
C20:4n6/C18:3n3	2.40 ± 0.12		2.70 ± 0.30		3.39 ± 0.19		0.58	0.01	0.07
C20:3n3/C18:3n3	0.04 ± 0.02		0.08 ± 0.01		0.14 ± 0.02		0.24	0.0003	0.03
C20:5n3/C18:3n3	0.21 ± 0.02		0.24 ± 0.03		0.17 ± 0.03		0.60	0.48	0.11
C22:5n3/C18:3n3	0.90 ± 0.04		0.79 ± 0.08		0.96 ± 0.04		0.35	0.72	0.10
C22:6n3/C18:3n3	1.29 ± 0.05		1.53 ± 0.19		1.55 ± 0.18		0.50	0.43	>0.99
C22:6n3/C22:5n3	1.48 ± 0.07		1.92 ± 0.09		1.56 ± 0.13		0.01	0.84	0.049
C18:2n6/C16:0	1.84 ± 0.05		1.84 ± 0.12		1.57 ± 0.11		>0.99	0.12	0.13
C18:3n3/C16:0	0.18 ± 0.01		0.14 ± 0.02		0.06 ± 0.02		0.44	0.001	0.02
C18:3n6/C18:2n6	0.02 ± 0.01		0.03 ± 0.01		0.01 ± 0.01		0.40	>0.99	0.40
C20:3n6/C18:3n6	1.56 ± 0.08		0.88 ± 0.09		1.13 ± 0.07		<0.0001	0.004	0.11
C22:5n3/C20:5n3	4.33 ± 0.25		3.60 ± 0.34		5.50 ± 0.51		0.36	0.09	0.005
C22:4n6/C20:4n6	1.88 ± 0.04		2.21 ± 0.15		1.76 ± 0.05		0.04	0.60	0.004
1 (% monoenoics)	12.99 ± 0.38		13.09 ± 1.07		12.81 ± 3.36		>0.99	>0.99	>0.99
2 (% dienoics)	70.67 ± 1.03		66.00 ± 3.01		62.48 ± 1.77		0.26	0.02	0.45
3 (% trienoics)	15.89 ± 0.39		14.98 ± 1.47		10.37 ± 1.17		0.83	0.003	0.02
4 (% tetraenoics)	44.79 ± 1.78		40.26 ± 2.13		32.02 ± 3.19		0.41	0.003	0.07
5 (% pentaenoics)	16.73 ± 0.64		13.92 ± 1.67		9.34 ± 1.59		0.33	0.002	0.07
6 (% hexaenoics)	23.59 ± 0.91		24.07 ± 2.65		16.64 ± 3.83		0.99	0.18	0.16
Unsaturation Index	184.67 ± 2.18		172.29 ± 6.66		143.66 ± 8.73		0.39	0.0003	0.01

4.5 Liver MAG and DAG

In the MAG and DAG fraction, as shown in Table 22 and Table 23 total SFA increased from 37.8% in NFD to 40.8% in HFD ($p=0.02$) (Table 22). Total MUFA also increase from 16.1% in NFD to 21.5% in HFD ($p=0.0002$), again largely attributable to the increase in C18:1n-9 ($p=0.001$). n-6 PUFA decreased from 39% in NFD to 29.3% in HFD ($p<0.0001$), a drop of 10%, again largely attributable to decreased C18:2n-6 levels ($p<0.0001$) (Table 22). In contrast to the other neutral lipid fractions, n-3PUFA increased from 5.2% in NFD to 6.9% in HFD ($p=0.003$) (Table 22). This is reflected in the change in the n-6/n-3 ratio that decreased from 7.5 in NFD, to 4.5 in HFD ($p<0.0001$), although the opposite was noted in the n-6/n-3 metabolite ratio that increased from 3.4 in NFD to 4.4 in HFD ($p=0.008$) (Table 23). These changes resulted in a decrease of total PUFA from 44.2% in NFD to 36.2% in HFD ($p<0.0001$), which resulted in a decrease in the total UFA from 60.2% in NFD to 57.7% in HFD ($p=0.04$). This was reflected in the decreased unsaturation index that dropped from 134.7 in NFD to 118.8 in HFD ($p=0.0002$) (Table 22).

When comparing the HFD group, as shown in Table 24 and Table 25, the total SFA levels return to NFD levels with both HFD-PF (36.2%, $p=0.01$) and HFD-GbE (35.6%, $p=0.003$) treatment. In contrast, MUFA levels continued to increase from 21.5% in HFD-S to 26.1% in HFD-PF ($p=0.01$) and HFD-GbE (27%, $p=0.001$) (Table 24). While overall n-6 PUFA level did not change between either of the groups, n-6 metabolites did decrease further from 10.6% in HFD-S to 8.1% in HFD-PF ($p=0.01$) and 7.1% in HFD-GbE ($p=0.0003$) (Table 24), indicating that less n-6 may be available from dietary sources, or that it is being utilized in pro-inflammation. In contrast, n-3 metabolites did not change, but n-3 PUFA did decrease from 6.9% in HFD-S to 4.5% in HFD-PF ($p=0.003$) and 4.2% in HFD-GbE ($p=0.001$) (Table 24). Overall UFA % levels increase from 57.7% in HFD-S to 63.4% in HFD-PF ($p=0.004$) and 63.5% in HFD-GbE ($p=0.003$) (Table 24). Overall, as most significant changes occurred in both the HFD-PF and HFD-GbE groups, this might indicate that this was more attributable to caloric restriction which occurred in both groups, rather than treatment with GbE.

Table 22. Liver monoglyceride and diglyceride fatty acid methyl esters (FAME) for normal fat diet (NFD) and high fat diet (HFD-S) (N=10 per group). Fatty acid results are presented as area % percentage mean and standard error of the mean (SEM), and statistically analysed by Students t-test. The level of statistical significance was set at * $p < 0.05$.

	NFD		HFD		p value
	MEAN	SEM	MEAN	SEM	
C14:0	0.2	± 0.02	0.5	± 0.03	<0.0001
C15:0	0.2	± 0.02	0.1	± 0.02	0.02
C16:0	26.5	± 0.53	26.4	± 0.32	0.84
C17:0	0.3	± 0.01	0.3	± 0.01	0.62
C18:0	9.7	± 0.28	11.6	± 0.57	0.01
C20:0	0.3	± 0.03	0.8	± 0.11	0.0003
C22:0	0.2	± 0.02	0.1	± 0.01	0.15
C23:0	0.1	± 0.02	0.2	± 0.02	0.25
C24:0	1.4	± 0.19	1.4	± 0.19	>0.99
∑DMA18:0	0.3	± 0.03	0.6	± 0.05	0.0001
∑S.DMA	0.3	± 0.03	0.7	± 0.07	0.0001
∑SFA	37.8	± 0.89	40.8	± 0.66	0.02
C16:1n7	0.5	± 0.10	0.4	± 0.03	0.23
C18:1n7	1.9	± 0.10	1.4	± 0.10	0.006
C18:1n9	11.7	± 0.92	16.2	± 0.62	0.001
C20:1n9	0.3	± 0.04	0.5	± 0.10	0.02
C22:1n9	1.1	± 0.10	2.1	± 0.36	0.01
C24:1n9	0.1	± 0.02	0.2	± 0.05	0.20
∑DMA18:1	0.3	± 0.04	0.5	± 0.15	0.26
∑C18:1	2.0	± 0.10	1.6	± 0.10	0.01
∑ω7	0.6	± 0.10	0.4	± 0.04	0.29
∑ω9	13.3	± 0.92	19.1	± 0.71	0.0001
∑MUFA	16.1	± 0.87	21.5	± 0.67	0.0002
C18:2n6	27.7	± 0.93	18.8	± 0.83	<0.0001
C18:3n6	0.3	± 0.02	0.5	± 0.05	0.005
C20:2n6	0.3	± 0.05	0.3	± 0.01	0.86
C20:3n6	1.0	± 0.06	1.9	± 0.20	0.0001
C20:4n6	8.2	± 0.37	5.9	± 0.24	0.0001
C22:2n6	0.1	± 0.01	0.1	± 0.02	0.61
∑n-6 PUFA	39.0	± 1.10	29.3	± 0.81	<0.0001
∑n-6 metabolites	11.2	± 0.38	10.6	± 0.26	0.20
C18:3n3	1.9	± 0.12	4.4	± 0.54	0.0002
C20:3n3	0.2	± 0.02	0.2	± 0.03	0.03
C20:5n3	0.3	± 0.03	0.1	± 0.02	<0.0001
C22:5n3	0.8	± 0.03	0.7	± 0.10	0.72
C22:6n3	1.9	± 0.08	1.5	± 0.08	0.0009
∑n-3 PUFA	5.2	± 0.13	6.9	± 0.50	0.003
∑n-3 metabolites	3.3	± 0.08	2.5	± 0.18	0.0005
∑PUFA	44.2	± 1.14	36.2	± 0.66	<0.0001
∑UFA	60.2	± 0.83	57.7	± 0.78	0.04

Table 23 Liver monoglyceride and diglyceride fatty acid methyl esters (FAME) ratios between normal fat diet (NFD) and high fat diet (HFD-S) (N=10 per group). Results presented as mean and standard error of the mean (SEM), and statistically analysed by Students t-test. The level of statistical significance was set at * $p < 0.05$.

	NFD		HFD		p value
	MEAN	SEM	MEAN	SEM	
Σ MUFA/ Σ PUFA	0.4	± 0.03	0.6	± 0.03	<0.0001
Σ MUFA/ Σ SFA	2.4	± 0.12	1.9	± 0.09	0.01
Σ PUFA/ Σ SFA	1.2	± 0.05	0.9	± 0.03	0.0002
Σ UFA/ Σ SFA	1.6	± 0.06	1.4	± 0.04	0.02
C18:0/C16:0	0.4	± 0.01	0.4	± 0.02	0.01
C18:1n9/C16:0	0.5	± 0.04	0.6	± 0.03	0.003
C18:1n9/C16:1n7	27.6	± 4.50	44.3	± 4.30	0.02
C18:1n7/C18:0	0.2	± 0.01	0.1	± 0.02	0.01
C18:1/C18:0	0.2	± 0.01	0.1	± 0.02	0.03
n-6/n-3	7.5	± 0.23	4.5	± 0.37	<0.0001
n-6/n-3 metabolites	3.4	± 0.09	4.4	± 0.34	0.008
C18:2n6/C18:3n3	15.1	± 1.05	4.8	± 0.57	<0.0001
C20:4n6/C20:3n6	8.8	± 0.81	3.3	± 0.31	<0.0001
C20:4n6/C22:6n3	4.2	± 0.13	4.0	± 0.25	0.51
C20:4n6/C20:5n3	25.4	± 3.38	49.4	± 6.09	0.002
C20:4n6/C18:2n6	0.3	± 0.01	0.3	± 0.01	0.49
C20:4n6/C18:3n3	4.5	± 0.37	1.5	± 0.15	<0.0001
C20:3n3/C18:3n3	0.1	± 0.02	0.0	± 0.01	<0.0001
C20:5n3/C18:3n3	0.2	± 0.02	0.0	± 0.01	<0.0001
C22:5n3/C18:3n3	0.4	± 0.03	0.2	± 0.02	<0.0001
C22:6n3/C18:3n3	1.1	± 0.10	0.4	± 0.03	<0.0001
C22:6n3/C22:5n3	2.6	± 0.16	1.8	± 0.06	0.001
C20:3n6/C18:3n6	3.1	± 0.11	4.2	± 0.28	0.003
C22:5n3/C20:5n3	2.6	± 0.55	5.6	± 1.08	0.02
C22:4n6/C20:4n6	5.6	± 0.52	3.2	± 0.16	0.0004
1 (% monoenoics)	11.8	± 0.94	13.8	± 1.84	0.34
2 (% dienoics)	56.2	± 1.85	38.4	± 1.66	<0.0001
3 (% trienoics)	11.2	± 0.63	22.4	± 2.44	0.0002
4 (% tetraenoics)	38.2	± 1.60	31.0	± 1.20	0.002
5 (% pentaenoics)	5.7	± 0.21	4.3	± 0.54	0.02
6 (% hexaenoics)	11.7	± 0.48	8.9	± 0.51	0.001
Unsaturation Index	134.7	± 2.63	118.8	± 2.03	0.0002

Table 24. Liver monoglycerides and diglycerides (MAG+DAG) fatty acid methyl esters (FAME) for high fat diet groups; High fat diet with-saline (HFD-S), High fat diet -pair-fed (HFD-PF) and High fat diet- Ginkgo biloba (HFD-GbE) (N=10 per group). Fatty acid results are presented as area % percentage mean and standard error of the mean (SEM), and statistically analysed by one-way ANOVA with Tukey's Post-hoc test. The level of statistical significance was set at * $p < 0.05$.

	HFD-S		HFD-PF		HFD-GbE		S Vs PF	S Vs GbE	PF Vs GbE
	MEAN %	SEM	MEAN %	SEM	MEAN %	SEM	<i>p value</i>	<i>p value</i>	<i>p value</i>
C14:0	0.53	± 0.03	0.27	± 0.03	0.29	± 0.02	<0.0001	<0.0001	0.87
C16:0	26.41	± 0.32	23.99	± 0.28	24.33	± 0.39	0.88	0.0001	0.75
C17:0	0.29	± 0.01	0.22	± 0.01	0.23	± 0.02	0.004	0.01	0.86
C18:0	11.63	± 0.57	8.30	± 1.21	7.32	± 0.83	0.048	0.01	0.73
C20:0	0.76	± 0.11	0.31	± 0.10	0.25	± 0.05	0.01	0.002	0.88
C22:0	0.11	± 0.01	0.11	± 0.01	0.17	± 0.03	>0.99	0.16	0.14
C24:0	1.38	± 0.19	1.88	± 0.09	2.19	± 0.33	0.56	0.22	0.76
DMA 16:0	0.09	± 0.02	0.09	± 0.05	0.05	± 0.02	>0.99	0.72	0.69
DMA18:0	0.61	± 0.05	0.58	± 0.09	0.53	± 0.06	0.95	0.71	0.87
∑DMA C16:0+C18:0	0.70	± 0.07	0.67	± 0.13	0.56	± 0.07	0.97	0.57	0.69
∑SFA	40.78	± 0.66	36.24	± 1.11	35.63	± 1.03	0.01	0.003	0.89
C16:1n7	0.39	± 0.03	0.40	± 0.04	0.34	± 0.03	0.80	0.91	0.54
C17:1	0.02	± 0.01	0.01	± 0.01	0.03	± 0.02	0.58	0.41	0.95
C18:1n9 <i>trans</i>	0.09	± 0.01	0.10	± 0.01	0.06	± 0.02	0.85	0.36	0.14
C18:1n9	16.19	± 0.62	21.04	± 1.76	22.82	± 0.72	0.02	0.002	0.53
C20:1n9	0.54	± 0.10	0.83	± 0.17	0.48	± 0.04	0.22	0.92	0.10
C22:1n9	2.14	± 0.36	1.14	± 0.35	0.94	± 0.19	0.07	0.03	0.89
C24:1n9	0.18	± 0.05	0.08	± 0.02	0.17	± 0.03	0.11	0.99	0.14
DMA18:1	0.48	± 0.15	0.96	± 0.25	0.57	± 0.07	0.15	0.93	0.27
∑C18:1	1.56	± 0.10	1.66	± 0.11	1.68	± 0.05	0.71	0.61	0.99
∑ω7	0.43	± 0.04	0.40	± 0.04	0.37	± 0.03	0.83	0.52	0.85
∑ω9	19.12	± 0.71	23.17	± 1.47	24.45	± 0.58	0.03	0.003	0.64
∑MUFA	21.47	± 0.67	26.08	± 1.38	27.02	± 0.61	0.01	0.001	0.77
C18:2n6	18.79	± 0.83	24.62	± 1.61	25.15	± 0.87	0.01	0.002	0.94
C18:3n6	0.47	± 0.05	1.07	± 0.23	0.61	± 0.11	0.03	0.80	0.11
C20:2n6	0.30	± 0.01	0.34	± 0.02	0.37	± 0.02	0.21	0.01	0.39
C20:3n6	1.93	± 0.20	1.56	± 0.34	0.40	± 0.04	0.50	0.0002	0.004
C20:4n6	5.87	± 0.24	5.53	± 0.68	5.42	± 0.20	0.85	0.73	0.98
C22:2n6	0.10	± 0.02	0.02	± 0.01	0.04	± 0.02	0.003	0.03	0.63
∑n-6 PUFA	29.33	± 0.81	32.77	± 1.33	32.28	± 0.82	0.07	0.13	0.94
∑n-6 metabolites	10.58	± 0.26	8.13	± 0.82	7.07	± 0.27	0.01	0.0003	0.34
C18:3n3	4.38	± 0.54	2.39	± 0.57	1.81	± 0.24	0.02	0.002	0.65
C20:3n3	0.16	± 0.03	0.18	± 0.02	0.18	± 0.02	0.77	0.77	>0.99
C20:5n3	0.12	± 0.02	0.16	± 0.04	0.14	± 0.02	0.65	0.91	0.88
C22:5n3	0.73	± 0.10	0.45	± 0.04	0.56	± 0.05	0.02	0.18	0.47
C22:6n3	1.48	± 0.08	1.35	± 0.13	1.51	± 0.09	0.66	0.97	0.51
∑n-3 PUFA	6.89	± 0.50	4.54	± 0.53	4.17	± 0.24	0.003	0.001	0.82
∑n-3 metabolites	2.49	± 0.18	2.16	± 0.20	2.38	± 0.13	0.38	0.90	0.63
∑PUFA	36.23	± 0.66	37.34	± 1.21	36.45	± 0.73	0.68	0.99	0.77
∑UFA	57.69	± 0.78	63.42	± 1.24	63.46	± 1.21	0.004	0.003	>0.99

Table 25. Liver monoglyceride and diglycerides (MAG+DAG) fatty acid methyl esters (FAME) ratios for high fat diet groups; High fat diet with-saline (HFD-S), High fat diet -pair-fed (HFD-PF) and High fat diet- Ginkgo biloba (HFD-GbE) (N=10 per group). Results presented as mean an (SEM), and statistically analysed by one-way ANOVA with Tukey's Post-hoc test. The level of statistical significance was set at * $p < 0.05$.

	HFD-S		HFD-PF		HFD-GbE		S Vs PF	S Vs GbE	PF Vs GbE
	MEAN %	SEM	MEAN %	SEM	MEAN %	SEM	<i>p value</i>	<i>p value</i>	<i>p value</i>
ΣMUFA/ΣPUFA	0.59	± 0.03	0.70	± 0.05	0.72	± 0.01	0.07	0.03	0.90
ΣMUFA/ΣSFA	1.93	± 0.09	1.44	± 0.13	1.33	± 0.07	0.01	0.001	0.72
ΣPUFA/ΣSFA	0.90	± 0.03	1.05	± 0.05	1.04	± 0.06	0.10	0.13	0.99
ΣUFA/ΣSFA	1.42	± 0.04	1.77	± 0.08	1.80	± 0.09	0.01	0.004	0.96
C18:0/C16:0	0.44	± 0.02	0.33	± 0.06	0.31	± 0.04	0.16	0.09	0.94
C18:1n9/C16:0	0.62	± 0.03	0.88	± 0.07	0.95	± 0.03	0.003	0.0003	0.57
C18:1n9/C16:1n7	44.27	± 4.30	60.92	± 7.43	68.73	± 4.09	0.11	0.01	0.58
C18:1n7/C18:0	0.13	± 0.02	0.24	± 0.03	0.23	± 0.03	0.03	0.049	0.96
C18:1/C18:0	0.14	± 0.02	0.26	± 0.03	0.24	± 0.03	0.03	0.09	0.88
n-6/n-3	4.47	± 0.37	8.05	± 0.84	8.06	± 0.60	0.002	0.002	>0.99
n-6/n-3 metabolites	4.41	± 0.34	4.01	± 0.56	3.03	± 0.18	0.76	0.06	0.20
C18:2n6/C18:3n3	4.81	± 0.57	15.33	± 2.88	16.70	± 2.36	0.01	0.003	0.90
C20:4n6/C20:3n6	3.30	± 0.31	4.16	± 0.83	14.72	± 1.68	0.86	<0.0001	<0.0001
C20:4n6/C22:6n3	4.02	± 0.25	3.58	± 0.48	3.70	± 0.20	0.64	0.79	0.97
C20:4n6/C20:5n3	49.41	± 6.09	34.16	± 6.61	40.44	± 3.89	0.16	0.50	0.69
C20:4n6/C18:2n6	0.32	± 0.01	0.22	± 0.04	0.22	± 0.01	0.04	0.04	>0.99
C20:4n6/C18:3n3	1.48	± 0.15	2.87	± 0.62	3.51	± 0.48	0.12	0.02	0.60
C20:3n3/C18:3n3	0.02	± 0.01	0.09	± 0.02	0.11	± 0.02	0.03	0.004	0.68
C20:5n3/C18:3n3	0.01	± 0.01	0.09	± 0.02	0.08	± 0.01	0.002	0.01	0.88
C22:5n3/C18:3n3	0.17	± 0.02	0.27	± 0.06	0.36	± 0.06	0.36	0.04	0.44
C22:6n3/C18:3n3	0.37	± 0.03	0.80	± 0.13	0.98	± 0.13	0.03	0.002	0.50
C22:6n3/C22:5n3	1.81	± 0.06	3.13	± 0.29	2.85	± 0.23	0.002	0.01	0.66
C18:2n6/C16:0	0.71	± 0.03	1.03	± 0.06	1.03	± 0.04	0.0001	0.0001	>0.99
C18:3n3/C16:0	0.14	± 0.02	0.10	± 0.03	0.09	± 0.01	0.32	0.19	0.94
C18:3n6/C18:2n6	0.03	± <0.01	0.05	± 0.02	0.03	± 0.01	0.19	0.64	0.63
C20:3n6/C18:3n6	4.16	± 0.28	1.52	± 0.07	0.93	± 0.18	<0.0001	<0.0001	0.08
C22:5n3/C20:5n3	5.60	± 1.08	3.08	± 0.43	3.90	± 0.17	0.02	0.15	0.60
1 (% monoenoics)	13.78	± 1.84	14.35	± 3.01	20.31	± 0.87	0.98	0.10	0.13
2 (% dienoics)	38.41	± 1.66	50.02	± 3.25	51.26	± 1.77	0.01	0.002	0.93
3 (% trienoics)	22.44	± 2.44	18.07	± 3.95	10.38	± 1.16	0.52	0.01	0.14
4 (% tetraenoics)	30.96	± 1.20	20.66	± 2.86	22.62	± 1.13	0.003	0.02	0.75
5 (% pentaenoics)	4.29	± 0.54	3.08	± 0.38	3.43	± 0.25	0.10	0.30	0.80
6 (% hexaenoics)	8.92	± 0.51	8.14	± 0.73	9.00	± 0.53	0.64	>0.99	0.57
Unsaturation Index	118.80	± 2.03	114.31	± 4.10	116.9	± 2.34	0.56	0.91	0.80

4.6 Liver PPL

Phospholipids are synthesised and metabolised predominantly in hepatic tissue *via* glycolysis/glyceroneogenesis or glycerol phosphorylation (Nguyen *et al.*, 2008). Phospholipid FA profiles are influenced by many factors, including dietary intake, availability of FA and oxidative stress. PPL FA modulate membrane flexibility and fluidity and affect protein signalling and trafficking such as GLUT transportation (Ranković *et al.*, 2017; Popović *et al.*, 2014).

When comparing the effect of a HFD on PPL total fatty acid profiles compared to a NFD (Table 26 and Table 27, total SFA levels increased from 43% in NFD to 66% in HFD ($p=0.01$) an increase of 23% of the sample percentage total (Table 26). Though not significant different, total MUFA levels decreased by 1% from 5.2% in NFD to 4.1% in HFD ($p=0.06$). n-6 PUFA decreased from 44.1% in NFD to just 14.4% in HFD ($p<0.0001$), a decrease of 30%. This was attributable to a 7.5% decrease in C18:2n-6 from 12% in NFD to 4.5% in HFD ($p<0.0001$) and a 21% decrease in C20:4n-6 that decreased from 30.1% in NFD to 9.3% in HFD ($p<0.0001$) (Table 26). In contrast, C18:3n-3 increased from 0.35% in NFD to 2.2% in HFD ($p=0.01$), however C22:6n-3 decreased from 4.3% in NFD to 1.2% in HFD ($p<0.0001$). This resulted in a 1.8 % overall decrease in n-3PUFA from 5.7% in NFD to 3.9% in HFD ($p=0.02$) (Table 26). Combined, this resulted in a decrease in the n-6/n-3 ratio from 8% in NFD to 3.3% in HFD ($p<0.0001$), while the decreased n-6/n-3 metabolite ratio trending towards significance ($p=0.07$), decreased from 6.2% to 4.8% ($p<0.0001$) (Table 27). Overall total PUFA levels decreased by 31.5% in the PPL fraction dropping from 49.8% in NFD to 18.3% in HFD ($p<0.0001$). This decrease in PUFA levels was reflected in the MUFA/PUFA ratios that increased from 0.1 in NFD to 0.3 in HFD ($p=0.03$), while PUFA/SFA decreased from 1.2 in NFD to 0.3 in HFD ($p<0.0001$) (Table 27). This drop in PUFA affected the total UFA levels which also decreased by 32.6% from 55% in NFD to 22.4% in HFD ($p<0.0001$). These changes also resulted in a near 3-fold decrease in the unsaturation index of the PPL fraction which dropped from 185 in NFD to 67 in the HFD ($p<0.0001$) (Table 27).

In the HFD groups (Table 28 and Table 29), compared to HFD-S, both HFD-PF ($p<0.0001$) and HFD-GbE ($p<0.0001$) total SFA levels decreased from 66% to 40% and 41% respectively, comparable those seen in the NFD (43%) (Table 28). No changes occurred in total MUFA levels between the groups. The largest change occurred in n-6 PUFA levels, that increased to 37.9% in HFD-PF and 37.3% in HFD-GbE compared to the 14.4% observed in HFD-S, indicating a partial amelioration of n-6 PUFA levels compared to the 49% levels seen in NFD. This is attributable to the 5.4% and 5.7% increase in C18:2n-6 in both HFD-PF (9.9%, $p<0.0001$) and HFD-GbE (10.2%, $p<0.0001$) compared to the 4.5% in the HFD-S (Table 26). Similarly, C20:4n-6 also increased from 9.3% in HFD-S to 26.6% ($p<0.0001$) and

25.5% ($p < 0.0001$). Similarly, n-3 PUFA levels also increased from 3.9% in HFD-S to 6.4% in both HFD-PF ($p < 0.0001$) and HFD-GbE ($p < 0.0001$) (Table 26). This increase in n-3 PUFA was seen in the major n-3 FA found along the n-3 PUFA pathway including C20:3n-3, C22:5n-3 but largely due to the increase of C22:6n-3 that increased 3-fold from 1.2% in HFD-S to 4.6% in HFD-PF ($p < 0.0001$) and 4.7% in HFD-GbE ($p < 0.0001$) (Table 28). This increase in n-3 metabolites was accompanied by a decrease in C18:3n-3 from the elevated 2.3% seen in HFD-S down to 0.7% and in HFD-PF ($p < 0.0001$) and 0.8% in HFD-GbE ($p < 0.0001$). The n-6/n-3 ratios increased from 3.3 in HFD-S to 5.4 in HFD-PF ($p = 0.01$), and 5.3 in HFD-GbE ($p = 0.01$) (Table 28). This change was not seen however in the n-6/n-3 metabolites ratio, which were comparable ranging from 4.5-4.8 (Table 29). Overall, total PUFA levels increase from 18.3% in HFD-S to 44.4% in HFD-PF ($p < 0.0001$) and 43.7% in HFD-GbE ($p < 0.0001$), with a similar increase in overall UFA levels (Table 28). This was reflected in the unsaturation index that increased from 67 in HFD-S to 167.5 in HFD-PF ($p < 0.0001$) and 164.4 in HFD-GbE ($p < 0.0001$), moving back towards the unsaturation of 185 seen in NFD (Table 29). The changes in levels between C18:2n-6 and C18:3n-3 compared to the increase in n-6 and n-3 metabolites, do not equal each other, suggesting that an alternative source of n-6 and n-3 metabolites is occurring in the liver. This could be from either from DNL, or alternatively from n-6 and n-3 PUFA transported from peripheral adipose tissues back to the liver. As most changes seen between the PPL HFD groups occurred in both the HFD-PF and HFD-GbE groups, this suggests changes may have occurred more so due to caloric restriction rather than GbE treatment.

Table 26. Liver phospholipid fatty acid methyl esters (FAME) for normal fat diet (NFD) and high fat diet (HFD-S) (N=10 per group). Fatty acid results are presented as area % percentage mean and standard error of the mean (SEM), and statistically analysed by Students t-test. The level of statistical significance was set at * $p < 0.05$.

	NFD			HFD-S			p value
	MEAN	±	SEM	MEAN	±	SEM	
C14:0	0.02	±	0.01	0.10	±	0.01	0.0008
C16:0	17.34	±	0.58	23.68	±	3.09	0.06
C18:0	23.99	±	1.08	39.72	±	4.96	0.01
C20:0	0.15	±	0.02	0.48	±	0.14	0.04
C22:0	0.21	±	0.01	0.25	±	0.03	0.28
C24:0	0.40	±	0.05	0.59	±	0.11	0.12
DMA 16:0	0.01	±	0.01	0.02	±	0.01	0.56
DMA18:0	0.28	±	0.05	0.67	±	0.21	0.09
∑SFA.DMA	0.29	±	0.05	0.69	±	0.21	0.08
∑SFA	43.02	±	0.80	66.12	±	8.28	0.01
C16:1n7	0.21	±	0.08	0.12	±	0.02	0.29
C16:1n9	0.01	±	0.01	<0.01	±	<0.01	0.33
C18:1n7	2.02	±	0.19	0.89	±	0.10	<0.0001
C18:1n9 <i>trans</i>	0.01	±	0.01	0.08	±	0.02	0.01
C18:1n9	2.05	±	0.06	2.36	±	0.29	0.31
C20:1n9	0.20	±	0.02	0.08	±	0.01	0.0001
C22:1n9	0.05	±	0.02	0.23	±	0.06	0.02
C24:1n9	0.20	±	<0.01	0.20	±	0.03	0.99
DMA18:1	0.35	±	0.05	0.13	±	0.03	0.0008
∑C18:1	2.12	±	0.20	0.97	±	0.11	<0.0001
∑ω7	0.26	±	0.09	0.13	±	0.02	0.16
∑ω9	2.54	±	0.05	2.93	±	0.37	0.30
∑MUFA	5.19	±	0.26	4.07	±	0.49	0.06
C18:2n6	12.05	±	0.46	4.53	±	1.15	<0.0001
C18:3n6	0.11	±	0.01	0.12	±	0.05	0.84
C20:2n6	0.38	±	0.01	0.11	±	0.03	<0.0001
C20:3n6	0.32	±	0.04	0.29	±	0.05	0.65
C20:4n6	30.72	±	0.58	9.29	±	2.95	<0.0001
C22:4n6	0.42	±	0.05	0.06	±	0.06	0.001
∑n-6 PUFA	44.10	±	0.77	14.39	±	4.11	<0.0001
∑n-6 metabolites	31.93	±	0.58	9.85	±	2.98	<0.0001
C18:3n3	0.35	±	0.05	2.23	±	0.62	0.01
C20:3n3	0.29	±	0.03	0.16	±	0.04	0.02
C20:5n3	0.08	±	0.01	<0.01	±	<0.01	<0.0001
C22:5n3	0.63	±	0.04	0.26	±	0.08	0.0005
C22:6n3	4.28	±	0.23	1.23	±	0.37	<0.0001
∑n-3 PUFA	5.67	±	0.26	3.90	±	0.66	0.02
∑n-3 metabolites	5.30	±	0.28	1.66	±	0.48	<0.0001
∑PUFA	49.76	±	0.80	18.29	±	4.46	<0.0001
∑UFA	54.95	±	0.86	22.35	±	4.63	<0.0001

Table 27 Liver phospholipid fatty acid methyl esters (FAME) ratios between normal fat diet (NFD) and high fat diet (HFD-S) (N=10 per group). Results presented as mean and standard error of the mean (SEM), and statistically analysed by Students t-test. The level of statistical significance was set at * $p < 0.05$.

	NFD			HFD-S			p value
	MEAN	±	SEM	MEAN	±	SEM	
ΣMUFA/ΣPUFA	0.10	±	<0.01	0.32	±	0.10	0.03
ΣMUFA/ΣSFA	8.52	±	0.54	14.85	±	1.95	0.006
ΣPUFA/ΣSFA	1.16	±	0.04	0.29	±	0.08	<0.0001
ΣUFA/ΣSFA	1.28	±	0.04	0.35	±	0.08	<0.0001
C18:0/C16:0	1.41	±	0.12	1.53	±	0.18	0.59
C18:1n9/C16:0	0.10	±	<0.01	0.09	±	0.01	0.33
C18:1n9/C16:1n7	13.70	±	2.10	17.51	±	2.67	0.29
C18:1n7/C18:0	0.10	±	0.01	<0.01	±	<0.01	<0.0001
C18:1/C18:0	0.10	±	0.01	<0.01	±	<0.01	<0.0001
n-6/n-3	7.96	±	0.41	3.25	±	0.78	<0.0001
n-6/n-3 metabolites	6.17	±	0.31	4.81	±	0.66	0.07
C18:2n6/C18:3n3	42.38	±	7.09	2.86	±	0.93	<0.0001
C20:4n6/C20:3n6	107.40	±	12.00	27.59	±	7.55	<0.0001
C20:4n6/C22:6n3	7.32	±	0.38	6.26	±	0.86	0.26
C20:4n6/C18:2n6	2.58	±	0.11	1.58	±	0.25	0.002
C20:4n6/C18:3n3	108.43	±	18.25	6.12	±	2.33	<0.0001
C20:3n3/C18:3n3	1.01	±	0.17	0.11	±	0.03	<0.0001
C20:5n3/C18:3n3	0.24	±	0.07	<0.01	±	<0.01	0.004
C22:5n3/C18:3n3	2.41	±	0.58	0.19	±	0.06	0.001
C22:6n3/C18:3n3	15.34	±	2.74	0.81	±	0.28	<0.0001
C22:6n3/C22:5n3	6.69	±	0.25	3.82	±	0.54	0.0001
C18:2n6/C16:0	0.70	±	0.03	0.20	±	0.06	<0.0001
C18:3n3/C16:0	<0.01	±	<0.01	0.10	±	0.03	0.001
C18:3n6/C18:2n6	0.01	±	<0.01	0.14	±	0.13	0.32
C20:3n6/C18:3n6	3.51	±	0.66	2.13	±	0.55	0.15
C22:4n6/C20:4n6	69.07	±	3.87	2.15	±	2.15	<0.0001
1 (% monoenoics)	2.54	±	0.45	3.00	±	0.35	0.43
2 (% dienoics)	25.14	±	0.96	9.28	±	2.34	<0.0001
3 (% trienoics)	3.79	±	0.27	8.67	±	2.04	0.03
4 (% tetraenoics)	124.45	±	2.28	37.40	±	11.73	<0.0001
5 (% pentaenoics)	3.56	±	0.22	1.33	±	0.37	<0.0001
6 (% hexaenoics)	25.77	±	1.34	7.39	±	2.24	<0.0001
Unsaturation Index	185.23	±	3.17	67.03	±	16.47	<0.0001

Table 28. Liver phospholipid fatty acid methyl esters (FAME) for high fat diet groups; High fat diet with-saline (HFD-S), High fat diet -pair-fed (HFD-PF) and High fat diet- Ginkgo biloba (HFD-GbE) (N=10 per group). Fatty acid results are presented as area % percentage mean and standard error of the mean (SEM), and statistically analysed by one-way ANOVA with Tukey's Post-hoc test. The level of statistical significance was set at * $p < 0.05$.

	HFD-S		HFD-PF		HFD-GbE		S Vs PF	S Vs GbE	PF Vs GbE
	MEAN	SEM	MEAN	SEM	p value	SEM	p value	p value	p value
C16:0	23.68	± 3.09	14.85	± 1.70	14.22	± 1.61	<0.0001	<0.0001	1.0
C18:0	39.72	± 4.96	23.49	± 2.67	24.88	± 2.77	<0.0001	<0.0001	0.75
C20:0	0.48	± 0.14	0.17	± 0.03	0.21	± 0.04	0.06	0.07	0.99
C22:0	0.25	± 0.03	0.22	± 0.03	0.22	± 0.03	0.45	0.45	>0.99
C24:0	0.59	± 0.11	<0.01	± <0.01	<0.01	± <0.01	0.02	0.001	0.54
DMA 16:0	0.02	± 0.01	0.01	± 0.01	0.05	± 0.02	0.52	0.89	0.64
DMA18:0	0.67	± 0.21	0.95	± 0.13	0.50	± 0.07	0.26	0.60	0.04
∑SFA.DMA	0.69	± 0.21	0.96	± 0.13	0.53	± 0.07	0.28	0.63	0.05
∑SFA	66.12	± 8.28	40.11	± 4.46	40.49	± 4.52	<0.0001	<0.0001	0.99
C16:1n7	0.12	± 0.02	0.10	± 0.01	0.09	± 0.01	0.38	0.12	0.78
C18:1n7	0.89	± 0.10	0.90	± 0.15	0.88	± 0.11	0.99	0.99	0.98
C18:1n9 <i>trans</i>	0.08	± 0.02	0.07	± 0.02	0.02	± 0.01	0.84	0.005	0.02
C18:1n9	2.36	± 0.29	2.24	± 0.28	2.23	± 0.25	0.73	0.69	>0.99
C20:1n9	0.08	± 0.01	0.20	± 0.03	0.21	± 0.03	0.002	0.001	0.93
C22:1n9	0.23	± 0.06	0.08	± 0.04	0.02	± 0.02	0.79	0.01	0.13
C24:1n9	0.20	± 0.03	0.11	± 0.02	0.17	± 0.03	0.001	0.35	0.02
∑DMA18:1	0.13	± 0.03	0.31	± 0.05	0.31	± 0.05	0.001	0.001	>0.99
∑C18:1	0.97	± 0.11	0.94	± 0.15	0.92	± 0.12	0.95	0.88	0.98
∑ω7	0.13	± 0.02	0.10	± 0.01	0.09	± 0.01	0.14	0.04	0.79
∑ω9	2.93	± 0.37	2.69	± 0.34	2.65	± 0.30	0.44	0.34	0.98
∑MUFA	4.07	± 0.49	4.09	± 0.48	4.08	± 0.46	>0.99	>0.99	>0.99
C18:2n6	4.53	± 1.15	9.91	± 1.14	10.22	± 1.27	<0.0001	<0.0001	0.95
C18:3n6	0.12	± 0.05	0.10	± 0.03	0.10	± 0.02	0.52	0.31	0.93
C20:2n6	0.11	± 0.03	0.18	± 0.03	0.24	± 0.04	0.49	0.02	0.15
C20:3n6	0.29	± 0.05	0.32	± 0.04	0.40	± 0.06	0.83	0.11	0.29
C20:4n6	9.29	± 2.95	26.62	± 2.97	25.54	± 2.85	<0.0001	<0.0001	0.89
C22:4n6	0.06	± 0.06	0.79	± 0.09	0.84	± 0.10	<0.0001	<0.0001	0.92
∑n-6 PUFA	14.39	± 4.11	37.95	± 4.24	37.34	± 4.18	<0.0001	<0.0001	0.98
∑n-6 metabolites	9.85	± 2.98	28.01	± 3.13	27.09	± 3.02	<0.0001	<0.0001	0.92
C18:3n3	2.23	± 0.62	0.74	± 0.11	0.81	± 0.16	0.01	0.02	0.99
C20:3n3	0.16	± 0.04	0.40	± 0.08	0.22	± 0.03	0.003	0.78	0.01
C22:5n3	0.26	± 0.08	0.59	± 0.07	0.64	± 0.08	0.001	0.0001	0.73
C22:6n3	1.23	± 0.37	4.64	± 0.58	4.71	± 0.60	<0.0001	<0.0001	0.99
∑n-3 PUFA	3.90	± 0.66	6.40	± 0.75	6.40	± 0.75	0.0001	0.0001	>0.99
∑n-3 metabolites	1.66	± 0.48	5.65	± 0.69	5.60	± 0.69	<0.0001	<0.0001	0.99
∑PUFA	18.29	± 4.46	44.36	± 4.94	43.74	± 4.89	<0.0001	<0.0001	0.98
∑UFA	22.35	± 4.63	48.46	± 5.40	47.84	± 5.34	<0.0001	<0.0001	0.98

Table 29. Liver phospholipid (PPL) fatty acid methyl esters (FAME) ratios for high fat diet groups; High fat diet with-saline (HFD-S), High fat diet -pair-fed (HFD-PF) and High fat diet- Ginkgo biloba (HFD-GbE) (N=10 per group). Results presented as mean an (SEM), and statistically analysed by one-way ANOVA with Tukey's Post-hoc test. The level of statistical significance was set at * $p < 0.05$.

	HFD-S		HFD-PF		HFD-GbE		S Vs PF	S Vs GbE	PF Vs GbE
	MEAN	SEM	MEAN	SEM	MEAN	SEM	p value	p value	p value
Σ MUFA/ Σ PUFA	0.32	± 0.10	0.09	± 0.01	0.09	± 0.01	0.01	0.01	>0.99
Σ MUFA/ Σ SFA	14.9	± 1.95	8.90	± 1.05	8.98	± 1.02	<0.0001	<0.0001	>0.99
Σ PUFA/ Σ SFA	0.29	± 0.08	>0.99	± 0.11	0.97	± 0.11	<0.0001	<0.0001	0.89
Σ UFA/ Σ SFA	0.35	± 0.08	1.09	± 0.12	1.06	± 0.12	<0.0001	<0.0001	0.89
C18:0/C16:0	1.53	± 0.18	1.44	± 0.17	1.58	± 0.18	0.51	0.81	0.21
C18:1n9/C16:0	0.09	± 0.01	0.13	± 0.02	0.15	± 0.02	0.08	0.01	0.51
C18:1n9/C16:1n7	17.5	± 2.67	24.9	± 4.03	21.7	± 2.67	0.05	0.36	0.54
C18:1n7/C18:0	<0.01	± <0.01	0.01	± 0.01	<0.01	± <0.01	0.45	>0.99	0.45
C18:1/C18:0	<0.01	± <0.01	0.01	± 0.01	0.01	± 0.01	0.67	0.67	>0.99
n-6/n-3	3.25	± 0.78	5.41	± 0.65	5.30	± 0.62	0.01	0.01	0.98
n-6/n-3 metabolites	4.81	± 0.66	4.55	± 0.55	4.49	± 0.58	0.45	0.36	0.99
C18:2n6/C18:3n3	2.86	± 0.93	12.66	± 1.79	13.71	± 2.73	0.0004	0.0001	0.88
C18:3n6/C18:2n6	0.14	± 0.13	0.01	± <0.01	0.01	± <0.01	0.45	0.45	>0.99
C20:3n6/C18:3n6	2.13	± 0.55	2.39	± 0.50	4.18	± 0.76	0.95	0.03	0.04
C20:4n6/C20:3n6	27.6	± 7.55	76.6	± 9.88	63.1	± 9.03	<0.0001	0.0009	0.27
C20:4n6/C22:6n3	6.26	± 0.86	5.32	± 0.67	5.09	± 0.68	0.13	0.05	0.88
C20:4n6/C18:2n6	1.58	± 0.25	2.43	± 0.28	2.32	± 0.29	0.0005	0.002	0.84
C20:4n6/C18:3n3	6.12	± 2.33	34.32	± 4.96	32.94	± 5.31	<0.0001	<0.0001	0.95
C20:3n3/C18:3n3	0.11	± 0.03	0.50	± 0.08	0.27	± 0.04	<0.0001	0.02	0.001
C20:5n3/C18:3n3	<0.01	± <0.01	0.01	± 0.01	0.01	± 0.01	0.67	0.67	>0.99
C22:5n3/C18:3n3	0.19	± 0.06	0.78	± 0.13	0.85	± 0.15	0.0004	0.0001	0.85
C22:6n3/C18:3n3	0.81	± 0.28	6.11	± 1.04	6.30	± 1.17	0.0001	0.0001	0.98
C22:6n3/C22:5n3	3.82	± 0.54	7.14	± 0.91	6.64	± 0.79	<0.0001	<0.0001	0.56
C18:2n6/C16:0	0.20	± 0.06	0.61	± 0.07	0.65	± 0.09	<0.0001	<0.0001	0.81
C18:3n3/C16:0	0.10	± 0.03	0.03	± 0.02	0.04	± 0.02	0.03	0.08	0.92
1 (% monoenoics)	3.00	± 0.35	1.41	± 0.35	1.34	± 0.33	0.0007	0.0004	0.98
2 (% dienoics)	9.28	± 2.34	20.25	± 2.33	21.0	± 2.63	0.0001	<0.0001	0.93
3 (% trienoics)	8.67	± 2.04	5.31	± 0.69	5.17	± 0.79	0.10	0.09	>0.99
4 (% tetraenoics)	37.4	± 11.73	109.6	± 12.24	105.44	± 11.77	<0.0001	<0.0001	0.89
5 (% pentaenoics)	1.33	± 0.37	3.07	± 0.39	3.32	± 0.40	0.0001	<0.0001	0.76
6 (% hexaenoics)	7.39	± 2.24	27.90	± 3.51	28.18	± 3.59	<0.0001	<0.0001	0.99
Unsaturation Index	67.1	± 16.47	167.5	± 18.69	164.42	± 18.35	<0.0001	<0.0001	0.97

4.7 Discussion

As discussed in Chapter 3 high fat caloric restriction (HFCR) which occurred in both the HFD-PF and HFD-GbE group can affect a variety of metabolites known to be altered in inflammation and OS caused by obesity. To quickly recap, in a 30% HFD model, 12 weeks of caloric restriction has a vast influence on gene regulation involved in lipid metabolism and mitochondrial functioning (Duivenvoorde *et al.*, 2011). Significant upregulation of all genes occurred related to cholesterol synthesis (*Cyp51, Fdps, Hmgcr, Insig1, Lss, Mvd, Sqle, and Tm7sf2*), fatty acid synthesis and elongation (*Acaca, Acly, Elovl3, Elovl6, and Pecn*). *Stard4* and *Stard5*, encoding for cholesterol transfer proteins that regulate transfer between different cellular compartments (e.g., endoplasmic reticulum, Golgi apparatus) were also upregulated, as was NADPH-producing *Me1* that plays a central role in adipose metabolism, linking gluconeogenesis and fatty acid metabolism (Duivenvoorde *et al.*, 2011). *Rdh11* and *Sorl1* which help reduce short-chain (fatty) aldehydes and limit the uptake of proteases and lipoproteins were also upregulated. *BC005764*, involved in triglycerides formation was also downregulated. The transcription of *Ppara* and *Ppar γ* , key regulators of lipid metabolism, were not altered (Duivenvoorde *et al.*, 2011). Lowered hepatic triglyceride levels and total cholesterol levels have been reported in HFCR by Parks *et al.* (2021) along with a return to normal plasma leptin/adiponectin ratio levels. HFCR also improved glucose tolerance and normalized adipocyte size and morphology, suggesting that adipocyte TAG storage was mobilised out of the adipose tissue and utilized. Parks *et al.* (2021) also found that lipid peroxidation was reduced in HFCR along with a decrease in inducible NOS, OS, Nrf2 and heme oxygenase-1 expression in the liver (Park *et al.*, 2012). Similarly, previous work from our group comparing NFD and HFD diet and GbE supplementation in rats has shown that adipocyte volume was significantly larger in the HFD-S group (increased by 114%, $p=0.01$) compared to the NFD group. With GbE supplementation, adipocyte volume reduced by 42.5% ($p=0.03$) to a statistically similar volume to that seen in the NFD (Hirata *et al.*, 2019). Perilipin (Plin 1), fatty acid synthase (FASN) mRNA and FAS protein levels were also reduced in the adipocyte following GbE treatment (Hirata, Cruz *et al.*, 2019). An increase in C18:1n-9 was also observed in total FAME, TAG, CE, MAG+DAG and PPL fractions of the HFD-S groups. Previously reported s, there was a 130% higher oleic acid incorporation ($p=0.01$) in HFD adipocyte cells compared to NFD, while GbE treatment trended towards a 43% ($p=0.06$) reduction in oleic acid incorporation into adipocyte lipids compared to HFD-S alone (Hirata, Cruz *et al.*, 2019). In contrast to this, in the liver samples, oleic acid did not change in the liver TAG fraction, remaining similar between HFD-S, HFD-PF and HFD-GbE groups at 27-28% of the sample. Similarly, it also did not change in the PPL fraction, remaining

comparable between 2.2 - 2.4% between all HFD groups. Changes were seen however in the CE fraction, where GbE treatment resulted in a further significant increase in oleic acid (19%, $p=0.01$) compared to HFD-S (13.8%) and HFD-PF (14.1%), while C16:0 levels remaining the same. Similarly, oleic acid also increased in the MAG+DAG fraction, increasing from 16.2% in HFD-S to 21% in HFD-PF ($p=0.02$), and 22.8% in HFD-GbE ($p=0.002$), while C16:0 levels remaining the same. In Chapter 5, regarding retroperitoneal lipids, oleic acid is also shown to decrease in the TAG fraction of HFD-PF ($p=0.004$) and HFD-GbE ($p=0.0002$) compared to HFD-S. It also decreased significantly in the CE fraction in both HFD-PF ($p<0.0001$) and HFD-GbE ($p=0.0006$), as well as decreasing in the PPL fraction (HFD-PG, $p<0.0001$; HFD-GbE, $p=0.01$, Vs HFD-S). Taken together, as GbE has been shown to reduce in oleic acid incorporation into adipocyte lipids (Hirata, Cruz, de Sá, *et al.*, 2019), this may explain the increases in oleic acid seen in the liver CE and MAG+DAG fraction following GbE treatment, and the decrease in oleic acid in retroperitoneal lipids.

As outlined in chapter 1, section 1.8 animals undergo DNL to form fatty acids from Acetyl CoA and NADPH to palmitic acid (C16:0) within the cytosol of the cell, more abundantly in the liver, adipose tissues, mammary glands (Ogunbona *et al.*, 2019; Stryer *et al.*, 2019; Palmieri *et al.*, 2015; Palmieri, 2004). C16:0 can be converted into either C16:1n-7 or C18:1n-7 \rightarrow C18:1n-9 using the enzymes ELOVL6 and SCD1 (Delta-9-Desaturase) (Minville-Walz *et al.*, 2012). Oleic acid is also more abundant in the HFD rat chow, accounting for 35% of total lipids in HFD compared to 22% in the NFD.

Research shows that rats treated with a diet rich in saturated fat develop hyperinsulinaemia and hypothalamic insulin resistance (Dornellas *et al.*, 2015a). Insulin levels within the plasma activate the endoplasmic reticulum (ER) membrane-bound transcription factor sterol regulatory element binding protein 1C (SREBP1c), the N-terminus of which translocates to the nucleus and upregulates all genes in the FA biosynthetic pathway (Song *et al.*, 2018). Oleic acid has been shown to induce liver X-receptor alpha mRNA synthesis and SREBP1c expression as well as decreased intracellular lipid levels and inflammation markers in human neutrophils (Reyes-Quiroz *et al.*, 2014). Oleic acid has also been shown in an *in vitro* hepatic cell model to protect against palmitic acid induced ER stress that increased expression of inflammasome marker NLRP3, Caspase-1 and IL-1beta which resulted in pyroptosis and cell death due to inflammation and proinflammatory signalling (Zeng *et al.*, 2020). Oleic acid is associated with TAG accumulation, and shuttling palmitic acid, normally poorly incorporated, into TAG, protecting from palmitic acid induced apoptosis (Listenberger *et al.*, 2003). Palmitic acid has also been negatively shown to be impact the expression of the insulin signalling pathway, and low-level inflammation resulting from IR is associated with the activation of key signal

transducers such as tumour necrosis factor- α (TNF- α), IKK β and c-Jun N-terminal kinase (JNK) (Lackey *et al.*, 2016). In contrast however, oleic acid has been shown to protect against IR in adipocytes by regulating fatty acid-induced regulation of genes related to the IRS1/PI3K pathway (López-Gómez *et al.*, 2020). Work from our group have shown that GbE has been shown to modulate lipid metabolism, adipogenesis, inflammation and OS and improve insulin signalling and sensitivity (Hirata, Cruz *et al.*, 2019, Hirata, Pedroso *et al.*, 2019, Hirata *et al.*, 2015, Banin *et al.*, 2014).

The increase in oleic acid after both caloric restriction and GbE found in the liver CE and MAG+DAG fractions, may contribute to this. In a 90-day clinical trial, patients with metabolic syndrome already on metformin were given GbE (120 mg capsule/day) or placebo. In patients with metabolic syndrome, it was found that *Ginkgo biloba* significantly decreased HbA1c, fasting serum glucose, insulin levels and insulin resistance. BMI, waist circumference and visceral adiposity index were all improved. Serum leptin and lipid profiles and the inflammatory markers (hsCRP), (TNF- α), and IL-6 all improved compared to baseline values (Aziz *et al.*, 2018). Similarly, Isorhamnetin a bioactive compound found in *Ginkgo biloba* has been shown to improve insulin levels, glucose tolerance and energy expenditure in HFD-fed obese mice. It also reduced adipocyte size and increased hepatic IRS1 tyr-608 and S6 K thr-389 phosphorylation and diminished hepatic lipid content and mRNA expression of lipogenic enzymes and ER stress markers while increasing mRNA expression of β -oxidation related genes. An increase in glucose transporter 2 (GLUT2) and PPAR γ mRNA content was also reported (Rodríguez-Rodríguez *et al.*, 2015). Lipolysis is regulated by cyclic AMP (cAMP) levels through the inhibition of Phosphodiesterase (PDE) or by the by activation of adenylate cyclase (Saponara *et al.*, 1998).

In contrast to this, however, are reports that chronic oleic acid treatment is associated with the promotion of steatosis in an *in vitro* model (Li *et al.*, 2021; Rafiei, Omidian and Bandy, 2019; Samovski and Abumrad, 2019; Liao *et al.*, 2014; Ziamajidi *et al.*, 2013; Cui, Chen and Hu, 2010). Oleic acid is reported to induce the expression of mRNA lipogenesis and fatty acid oxidation enzymes (*FAS* and *CPT1A*), and impaired indices of aerobic energy metabolism *PPAR γ* mRNA expression, MMP, and galactose-supported ATP production (Rafiei, Omidian and Bandy, 2019). In a cell model, oleic acid steatosis is associated with lipid peroxidation *via* decreased SOD-1, increased apoptosis *via* increased caspase-9, and decreased proliferation *via* increased production of p27 with unchanged alanine transaminase (ALT) levels (Cui, Chen and Hu, 2010). High circulating plasma levels of oleic acid is also associated with NAFLD and NASH (Araya *et al.*, 2004). In future studies, a longer treatment period than 2 weeks with GbE may be required to fully explore the impact on oleic acid levels in the liver.

With regards to PUFA, while no significant changes occurred in the total sample levels of PUFA for n-6 PUFA or n-3 PUFA, a slight increase in DHA was seen in TAG following GbE treatment, while both n-6 PUFA and n-3 PUFA decreased in the CE and MAG+DAG fractions after GbE treatment while they significantly increased in the PPL fraction for both HFD-PF and HFD-GBE treatment. This may suggest an influence of GbE on PUFA inflammation mitigation or the liberation of PUFA from adipocytes back to the liver. This is supported by the findings that show while n-6 PUFA increase by approximately 5-6% in HFD-PF and HFD-GbE, n-6 metabolites increase by over 20% in both groups, compared to HFD-S alone.

While C18:3n-3 decreased in HFD-HF and HFD-GbE liver PPL fractions, n-3 metabolites increased significantly by approximately 4%. As HFD rat chow does not contain decreased amounts of both n-6 and n-3 PUFA, any may not account for the increases seen here, the liver PPL data suggests an additional source of PUFA are being transported to the liver from peripheral tissues or being manufactured *in situ* by DNL. This is supported by the decrease in PUFA in the retroperitoneal and mesenteric PPL fractions of both HFD-PF and HFD-GbE groups shown in chapter 5. n-3 FA have been shown to positively affect inflammation and steatosis induced by a HFD through the upregulation of PPAR- α and preventing NF- κ B binding (Tapia *et al.*, 2014). n-3 FA have also been shown to limit hepatic TAG storage (Ferramosca and Zara, 2014). As previously mentioned in earlier sections, n-3 FA are associated more with anti-inflammatory eicosanoids and inflammation mitigation while n-6 PUFAs are associated more with proinflammatory eicosanoid mitigation (Hussey, Lindley & Sarabjit and Mastana, 2017; Monteiro *et al.*, 2014). The balance between n-3 and n-6 PUFAs are important in NAFLD as a higher n-6/n-3 ratio is associated with a pro-inflammatory state, hepatic lipid metabolism dysregulation, increased liver fat percentage and insulin homeostasis (Mäkelä *et al.*, 2022; Cui *et al.*, 2021; Luo *et al.*, 2021; Bogl, Kaprio and Pietiläinen, 2020; van Name *et al.*, 2020; da Silva *et al.*, 2014; Valenzuela and Videla, 2011; Pachikian *et al.*, 2008; Araya *et al.*, 2004; Videla *et al.*, 2004). Interestingly, while the n-6/n-3 ratio increased following GbE treatment in the CE, MAG+DAG and PPL fractions, it decreased in the TAG fraction, indicating a better n-6/n-3 profile for long term lipid storage in TAG and PPL that are higher in PUFA that can be utilized for LDL transport of TAG, that can then be transported and sequestered into adipose tissues. This is important as PPL metabolism and maintenance is essential for the formation of lipoproteins such as VLDL that are involved in the transportation of lipids around that body (van der Veen *et al.*, 2017). They are also important in the formation of lipid droplets, whereby excess FA are converted to TAG and sequestered into cytosolic lipid droplets to protect against lipotoxicity (Listenberger *et al.*, 2003). They are also a supply of FA

for cholesterol esterification to cholesteryl esters for transportation out of the cell around the body and a source of FA for PUFA oxylipin production and inflammation mitigation. Due to this a continual replacement of phospholipids is necessary for the membrane. As discussed in more detail in Chapter 1, under 1.12 phospholipids, cell membrane function is influenced by the fluidity and stability of the cell membrane which is dependent of the type of fatty acids incorporated into the phospholipid structure, and the amount of cholesterol-rich microdomains (Di Miceli *et al.* 2020). The membrane serves as a barrier and facilitator of ionic exchange and molecular transport in and out of the cell (Hulbert *et al.*, 2005, 2007). If the membrane is rich in saturated fatty acid, the bilayer will become a more rigid gel-like structure, while a membrane rich in cis-unsaturated fatty acids will be more flexible and protective against inflammation.

4.8 Summary

Following a HFD consumption to induce obesity, the most notable change was a decrease in n-6 and n-3 PUFA compared to a NFD. This decrease was quite dramatic in the PPL fraction which experienced a 30% decrease in PUFA levels (14.4%) following a HFD compared to the NFD group (41.1%). MUFA levels also significantly increased in total FA profiles compared to a NFD. This was largely due to increase in oleic acid (C18:1n-9). MUFA also remained elevated in the total FA and TAG profiles, remained elevated despite caloric restriction and GbE treatment. GbE treatment increased MUFA levels further in the CE fraction compared to the pair-fed and Saline only HFD groups. This may have a positive effect on IR, DNL and protection from palmitate inflammation.

Both caloric restriction (HFD-PF) and GbE treatment resulted in a significant increase in n-3 PUFA in total FA, TAG and PPL profiles. In contrast, n-3 PUFA decreased in the CE fraction following GbE treatment. This finding may indicate the mobilization of PUFA from peripheral tissues back towards the liver, or some additional protection against PUFA utilization for inflammation mitigation.

Chapter 5 – Retroperitoneal (RET) and Mesenteric (MES) Adipose Tissue

5.1 Introduction

As outlined in the Chapter 1 and chapter 4, a HFD, typical of a WSD, can lead to a higher caloric intake and increased levels of saturated fat and cholesterol (EFSA Panel on Dietetic Products and Allergies, 2010) which have been widely identified as a major contributor to increased energy intake weight gain and obesity (Bray and Popkin, 1998). Adipose tissue is a key endocrine organ, maintaining energy homeostasis through excess fatty acid storage and secretion. Through the secretion of bioactive peptides and proteins known as adipokines, adipose tissues function as an endocrine organ influencing a host of other organs including the brain, liver, skeletal muscle, kidneys, and pancreas. While three types of adipose tissues exist, namely white, beige, and brown, WAT is most linked to metabolic disturbances particularly when combined with a high fat diet (Hung *et al.*, 2014; Jialal, Kaur and Devaraj, 2014; Abete *et al.*, 2011; Costa *et al.*, 2011; Mittendorfer, 2011; Fang *et al.*, 2008; Furukawa *et al.*, 2004). Obesity is caused by hypertrophy and hyperplasia when of adipocytes. Obesity is closely linked to many metabolic disturbances including to WAT functioning that include hyperglycaemia, IR, metabolic syndrome, T2DM, atherogenic dyslipidaemia, OS, and low-grade inflammation (Wali *et al.*, 2020; Hochberg, 2018). WAT is sub-divided into either sub-cutaneous (SAT) or visceral adipose tissue (VAT), with VAT considering more pathogenic and metabolically disturbing with greater risk of disease (Gealekman *et al.*, 2011).

The composition of adipose tissues is considered a reflection of previous food intake and metabolic health, with adipose tissue reflecting the long-term intake of dietary lipids while blood lipids may reflect short term intake. The analysis and profiling of lipids offers the potential to understanding obesity, T2DM and metabolic disturbances (Al-Sari *et al.*, 2020). Of particular interest is the study of VAT, the fat that surrounds the internal organs, which when in excess are considered risk factors and indicators of metabolic disease and mortality (Koster *et al.*, 2015; Kuk *et al.*, 2006). From puberty, sex differences occur between males and females in fat accumulation, with women more prone to SAT accumulation pre-menopause, while men tend to acquire more VAT depots (Liu *et al.*, 2021; A. M. Nauli and Matin, 2019; Rask-Andersen *et al.*, 2019). Both Retroperitoneal (RET) and Mesenteric (MES) adipose tissue is categorised as visceral white adipose tissue (VAT). It is reported that around 6% and 21% of dietary fat is store in RET and MES tissue of men respectively, while only 5% is stored in RET

tissue of women, favouring subcutaneous depots (Votruba *et al.*, 2007; Votruba and Jensen, 2006; Mårin *et al.*, 1996). This thesis focuses will look at both MES and RET VAT, as they both contribute to abdominal VAT (Hung *et al.*, 2014; Wolk, Furuheim and Vessby, 2001).

This chapter focuses on both on RET VAT and MES VAT. In more recent years, the mesentery has been renamed as a standalone organ in the gastrointestinal system, with its continuous collection of tissues that includes the greater omentum, lesser omentum, mesentery proper, and mesocolon (Nauli and Matin, 2019). The mesentery connects and is continuous with the gastrointestinal organs located within the abdominal cavity predominantly to the posterior wall of the abdominal cavity and is host to nervous tissue, blood vessels, and lymphatic vessels of the GI tract (Byrnes *et al.*, 2021; Calvin Coffey *et al.*, 2020). It not only stores energy as TAG to be later released as free fatty acids, but also secretes a variety of endocrine molecules including adiponectin, leptin, and resistin. Due to the intricate nature of the mesentery with the GI tract, it is an organ of interest in many GI diseases associated with inflammation including obesity, Crohn's disease, insulin resistance, T2DM and cardiovascular disease (Lam *et al.*, 2012; Foster *et al.*, 2011; Catalano, Stefanovski and Bergman, 2010; Schäffler and Schölmerich, 2010; Schäffler, Schölmerich and Büchler, 2005; Bjorntorp, 1990). Intraperitoneal/mesenteric fat depots are made up of VAT depots of the mesentery organ (Nauli and Matin, 2019; Hung *et al.*, 2014), with up to 21% of dietary fat stored in mesenteric tissue (Votruba and Jensen, 2006; Mårin *et al.*, 1996). Increased large-sized mesenteric adipocytes have been reported in obesity (Lam *et al.*, 2012; Wueest *et al.*, 2012). An increase in mesenteric fat depots is also associated with increased risk of metabolic syndrome, inflammation, and oxidative damage in vascular tissue (Booth, Magnuson and Foster, 2014; Hung *et al.*, 2014; Konrad and Wueest, 2014; Foster and Pagliassotti, 2012; Lam *et al.*, 2012; Catalano, Stefanovski and Bergman, 2010; Panagiotakos *et al.*, 2005). The mesentery connects gastrointestinal organs located on the anterior side of the abdominal cavity (Lee, Wu and Fried, 2013), as shown in the Figure 14 below. RET organs are located to the posterior of the abdominal cavity and include the pancreas, duodenum, ascending and descending colon and kidneys. RET VAT surrounds the RET organs, while intraperitoneal fat depots are made up of VAT depots of the mesentery organs, which include greater omentum, lesser omentum, mesentery proper, and mesocolon (Nauli and Matin, 2019).

As outlined in the introductory sections 1.7, 1.8, 1.10, 1.11, 1.11, 1.12, dietary sources of lipids, are hydrolysed in the intestinal lumen and absorbed by GI enterocytes either by diffusion (FFA) for smaller molecules or protein-mediated facilitated transport for larger molecules. Once absorbed, FFA, TAG, CE and PPL are packed into chylomicrons, secreted into the lymphatic system, and

transported to the liver for further processing and then onto peripheral tissues such as adipose tissue and muscle (Stryer *et al.*, 2019; Bhutia and Ganapathy, 2015).

The lymph fluid containing absorbed dietary fats drains first through smaller mesenteric lymph vessels before entering the larger lymphatic system including the retroperitoneal cisterna chyli, and finally entering the blood circulation *via* the portal vein (Williams and Rabbani, 2011). Once drained into the portal vein for circulation, fatty acid and mesenteric cytokines can act locally or systemically, with circulating cytokines shown to stimulate inflammation and impair insulin signalling and steatohepatitis in the liver especially (Booth, Magnuson and Foster, 2014; Hung *et al.*, 2014; Foster and Pagliassotti, 2012; Stanton *et al.*, 2011). As the lymphatics from the GI tract are present in both the mesentery and the retroperitoneum, both RET and MES VAT receive the same supply of dietary lipids. As mentioned earlier, men tend to accumulate more visceral depots than women. This is in part related to hormones with pre-menopausal women tending to carry more SAT as a source of energy for pregnancy (Gavin *et al.*, 2013; Terry *et al.*, 1991). It is thought that postprandially, as chylomicrons tend to be larger in size and quantity in males than in females (Knuth and Horowitz, 2006), they may congest the lamina propria and low-pressure lymphatics in males. This may allow the enzyme LPL an opportunity to hydrolyse TAG in the chylomicrons, with liberated fatty acids stored in nearby abdominal VAT (Nauli and Matin, 2019; Palmisano *et al.*, 2018; Escobedo *et al.*, 2016; Wang, Magkos and Mittendorfer, 2011; Knuth and Horowitz, 2006; Staprans *et al.*, 1990).

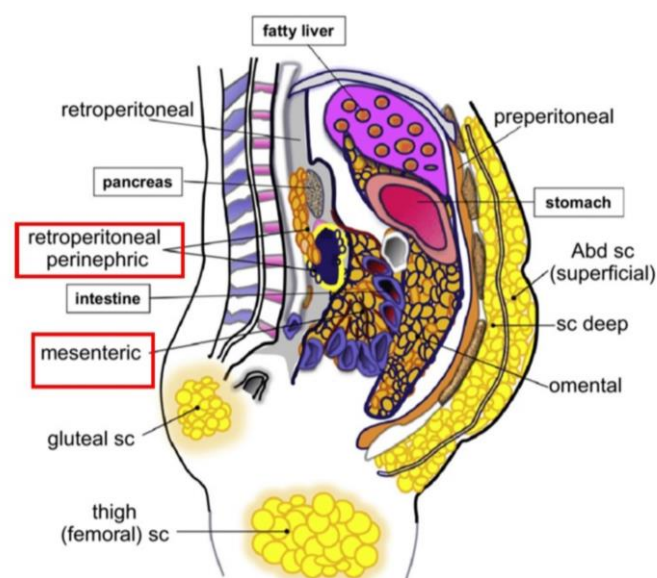


Figure 14. Mesenteric and retroperitoneal adipose tissue depot (Adapted from Lee, Wu and Fried, 2013).

VAT levels are higher in overweight and obese individuals and linked to a HFD (Bueno *et al.*, 2011; Caricilli *et al.*, 2008). The increase in visceral depots is accompanied by hyperinsulinemia and IR and additional metabolic changes such as dyslipidemia and atherosclerosis associated with metabolic syndrome (Koenen *et al.*, 2021; Lopes *et al.*, 2016). These metabolic changes are termed metabolically unhealthy obesity (MUO) (Iacobini *et al.*, 2019) and include impaired insulin signalling, immune cell infiltration, increased inflammation, cytokine production (e.g., CRP, IL-6, and TNF-alpha) and vasoconstriction (Li *et al.*, 2015, 2016; Wali *et al.*, 2020). Furthermore, cytokines from macrophages inhibit insulin signalling by phosphorylating serine residues of insulin receptor substrate (IRS) proteins (Wali *et al.*, 2020). This leads to increased lipolysis and liberation of FA from adipose tissue into circulation (Samuel and Shulman, 2016). It has been observed that thigh subcutaneous adipose tissue has a different lipid profile compared to back, abdomen and breast tissues, that largely contain similar lipid profiles to each other (Al-Sari *et al.*, 2020). This is interesting as SAT is supplied by circulated dietary and hepatic lipids, facilitated by lipoprotein lipase expressed on the luminal surfaces of capillary endothelial cells of peripheral tissues facilitating breakdown and absorption of the circulating lipids. Tissue lipid profiles can therefore differ due to supply and availability and proximity of the tissue to the origin of the circulating lipids, namely the intestines and liver.

In this present study, Male Wistar rats were fed from two to 4-months-old with a high-fat lard enriched diet (HFD) (28% lard) to induce obesity. The rats were randomly divided into groups of 10 and by daily oral gavage received either: 500 mg/kg of GbE (HFD-GbE) diluted in 2mL of 0.9% saline (vehicle) (n=10); Saline (NaCl) vehicle only (HFD-S) (n=10); or NaCl vehicle only with rats' pair-fed to that of the GbE supplemented group (HFD-PF) (n=10) to control for changes in food intake. A control group fed a normal fed diet (NFD) rats was also used. Following 14 days of supplementation the rats were euthanized and RET and MES WAT were collected. Tissue lipids were extracted as previously described (Schreiner, 2006). Total sample fatty acid profiles were subjected to acid-catalysed esterification to methyl esters and analysed by GC-FID. As demonstrated in Al-Sari (2020), in subcutaneous adipose tissue, lipid classes consist of around 65% TAG, around 32% are PPL and the rest represented by MAG, DAG, CE and other lipid-based molecules. Firstly, the total lipid profile of the collected samples was analysed. The samples were then separated into TAG, CE, MAG+DAG and PPL lipid classes as previously described (Boldarine, Joyce *et al.*, 2021). Data was presented as FA percentages (mean FA% \pm SEM) or as ratio means (mean \pm SEM).

5.2 RET and MES total fatty acids

5.2.1 RET Total Fatty Acids – NFD vs HFD

Both NFD and HFD-S groups were compared for baseline effects of each corresponding diet (NFD and HFD). To review, the NFD and HFD chow consisted of 4.5% and 31.6% lipids, respectively, with the HFD providing 57% of calories from fat, nearly double the recommended daily intake of SFA by the world health organisation (WHO). In Table 30 and Table 31, the effect of NFD and HFD on the total RET fatty acid profiles is summarised as mean \pm SEM of fatty acid percentages. A significant increase of 16% in total SFA (Σ SFA) was seen in HFD (28.4 \pm 0.27%), compared to NFD (24.1 \pm 0.6%) ($p=0.0004$) most notably in C18:0 (NFD 3.1 \pm 0.03%; HFD 6.3 \pm 0.2%, ($p<0.0001$)) (See Table 30). Total monounsaturated fatty acids (Σ MUFA) significantly increased by 60% in HFD (47.28 \pm 0.32%) compared to NFD (29.59 \pm 0.44%; $p<0.0001$), most notably in C18:1n9 (NFD 24.9 \pm 0.1%; HFD 42.6 \pm 0.3%, ($p<0.0001$)). Total polyunsaturated fatty acids Σ PUFA decreased by 48% in HFD (23.51 \pm 0.12%) compared to NFD (45.2 \pm 1%; $p<0.0001$) which can be further divided into a 46% decrease of Σ n-6 PUFA (22.9 \pm 0.1%) compared to NFD (42.7 \pm 1%; $p<0.0001$) and a 74% decrease in a Σ n-3 PUFA HFD levels (0.66 \pm 0.01%) compared to NFD (2.5 \pm 0.04%; $p<0.0001$). These results are in keeping with other studies that show that a HFD changes fatty acid composition (Boldarine *et al.*, 2021; Hirata, Cruz, *et al.*, 2019; Hirata, Pedroso, *et al.*, 2019; Hirata *et al.*, 2015; Banin *et al.*, 2014; Fujiwara and Amisaki, 2013). Meanwhile nearly a 2-fold decrease of total PUFA is seen in HFD-RET-VAT compared to NFD-RET VAT (23.5% and 45.2%, respectively), with the 2-fold difference largely due to C18:2n-6, which is significantly decreased in HFD-RET-VAT. The n-6/n-3 ratio of the NFD-RET-VAT tissues is 17:1, the n-6/n-3 ratio in HFD-RET-VAT is double this at 34:1. (Table 31). The changes in MUFA and PUFA levels in both groups also significantly affected the unsaturation index of the tissues. The overall NFD-RET-VAT unsaturation index decreased by 31% in HFD-RET-VAT (Table 31), indicating a higher degree of unsaturation present in lipids stored in NFD-RET-VAT, which may influence the availability of PUFA to PPLs to maintain membrane fluidity. This will be explored in more detail under PPL.

5.2.2 MES total fatty acids – NFD vs HFD

Similar differences in MES total FA profiles compared to RET total FA profiles. A significant increase of 28% in total SFA (Σ SFA; NFD, 22.10 \pm 0.49%; HFD-S, 28.23 \pm 0.20%, p <0.001), represented largely by the 15% increase in C16:0 (C16:0 ; NFD, 17.58 \pm 0.46%; HFD-S, 20.21 \pm 0.12%, P =0.001) and the 128% increase in C18:0 (C18:0; NFD, 2.94 \pm 0.04%; HFD-S, 6.57 \pm 0.16 %, p <0.001) (Table 32). Total monounsaturated fatty acids (Σ MUFA) in the HFD-S group significantly increased by 60% in HFD (Σ MUFA; NFD,29.59 \pm 0.39%;HFD-S,47.27 \pm 0.35%, p <0.001), most notably from the 69% increase in C18:1n-9 (C18:1n-9; NFD, 25.28 \pm 0.09%; HFD-S, 42.71 \pm 0.31 %, p <0.001) (Table 32).

Total polyunsaturated fatty acids Σ PUFA in the HFD-S group decreased by 48% in HFD (Σ PUFA; NFD,46.89 \pm 0.84%; HFD-S,23.66 \pm 0.18%, p <0.001), largely by the changes in n-6 PUFA C18:2n-6 which decreased by 48% (C18:2n-6; NFD,43.01 \pm 0.84%; HFD-S,22.45 \pm 0.16%, p <0.001) (Table 32). C20:4n-6 also decreased by 69% (C20:4n-6; NFD,0.65 \pm 0.04%; HFD-S,0.20 \pm 0.01%, p <0.001), while C22:4n-6 decreased by 64% (C22:4n-6; NFD,0.23 \pm 0.03%; HFD-S,0.08 \pm 0.01%, P =0.003). Levels of C18:3n-3 decreased by 70%. This was reflected in the n-6/n-3 ratio that doubled from \sim 18.5 to \sim 36.8 in the HFD (n-6/n-3; NFD, 18.51 \pm 0.36; HFD-S 36.76 \pm 1.07, p <0.001) higher than that seen in RET tissue. Overall UFA levels in the HFD-S group decreased by 7% (Σ UFA; NFD,76.48 \pm 0.48%; HFD-S,70.93 \pm 0.22%, p <0.001) (Table 32). Changes between the SFA, PFA and MUFA percentage levels were also reflected in their respective ratios (Table 33) where MUFA/PUFA ratio increased by 215%; MUFA/SFA ratio increased by 152%, PUFA/SFA ratio decreased by 68% and UFA/SFA decreased by 28%. These overall changes between saturated and unsaturated FA are reflected in the unsaturation index of the total FA sample which decreased by 25% (Unsaturation Index; NFD,128.52 \pm 1.33%; HFD-S,95.88 \pm 0.22%, p <0.001)., less than the 28% decreased seen in RET tissue (Table 33).

Leng and colleagues (2017) have demonstrated that when a diet with a high n-6/n-3-ratio of approximate 18:1 LA/ALA, as seen in this study in the HFD-chow, this resulted in an increase in n-6/n-3 oxylipins in the liver compared to a lower ratio diet (approx. 8:1) (Leng *et al.* 2017). A high n-6 PUFA intake increases the levels of LA, DGLA and AA derived oxylipins which are predominantly pro-inflammatory (Caligiuri *et al.*, 2013), while a n-3 PUFA oxylipins from ALA, EPA and DHA are predominantly anti-inflammatory (Hussey *et al.*, 2017).

Table 30. Retroperitoneal total lipid fatty acid methyl esters (FAME) for normal fat diet (NFD) and high fat diet (HFD-S) (N=10 per group). Fatty acid results are presented as area % percentage mean and standard error of the mean (SEM), and statistically analysed by Students t-test. The level of statistical significance was set at *p < 0.05.

Name	NFD			HFD-S			p value
	Mean	±	SEM	Mean	±	SEM	
C10:0	0.02	±	0.01	0.01	±	0.01	0.13
C12:0	0.07	±	0.01	0.04	±	0.01	0.009
C14:0	0.75	±	0.05	0.67	±	0.01	0.807
C15:0	0.26	±	0.01	0.11	±	0.01	<0.0001
C16:0	19.42	±	0.55	20.74	±	0.12	0.47
C17:0	0.30	±	0.01	0.32	±	0.01	0.03
C18:0	3.12	±	0.03	6.33	±	0.17	<0.0001
C20:0	0.08	±	0.01	0.08	±	0.01	0.97
C21:0	0.07	±	0.01	0.10	±	0.01	0.006
C22:0	0.02	±	0.01	0.01	±	0.01	0.70
ΣSFA	24.09	±	0.61	28.42	±	0.27	0.0004
C14:1n7	0.02	±	0.01	0.01	±	0.01	0.06
C15:1	0.05	±	0.01	0.02	±	0.01	0.001
C16:1n7	1.85	±	0.26	1.54	±	0.07	0.91
C17:1	0.14	±	0.01	0.21	±	0.01	0.001
C18:1n7	2.38	±	0.11	2.44	±	0.02	0.97
C18:1n9 <i>trans</i>	0.05	±	0.01	0.09	±	0.01	0.13
C18:1n9	24.90	±	0.14	42.64	±	0.27	<0.0001
C20:1n9	0.23	±	0.01	0.34	±	0.01	<0.0001
ΣC18:1	27.32	±	0.21	45.17	±	0.28	<0.0001
Σn-7	2.53	±	0.12	2.46	±	0.02	0.97
Σn-9	25.15	±	0.14	42.98	±	0.27	<0.0001
ΣMUFA	29.59	±	0.44	47.28	±	0.32	<0.0001
C18:2n6 <i>trans</i>	0.03	±	0.01	0.05	±	0.01	0.54
C18:2n6	41.32	±	0.01	22.27	±	0.14	<0.0001
C18:3n6	0.09	±	0.01	0.01	±	0.01	<0.0001
C20:2n6	0.28	±	0.01	0.21	±	0.01	<0.0001
C20:3n6	0.12	±	0.01	0.06	±	0.01	0.001
C20:4n6	0.63	±	0.03	0.22	±	0.02	<0.0001
C22:4n6	0.24	±	0.02	0.07	±	0.01	<0.0001
Σn-6 PUFA	42.69	±	0.99	22.85	±	0.12	<0.0001
Σn-6 metabolites	1.36	±	0.04	0.57	±	0.03	<0.0001
C18:3n3	2.23	±	0.03	0.64	±	0.01	<0.0001
C22:5n3	0.12	±	0.01	0.02	±	0.01	0.0002
C22:6n3	0.15	±	0.01	0.02	±	0.01	0.002
Σn-3 PUFA	2.51	±	0.04	0.66	±	0.01	<0.0001
Σn-3 metabolites	0.28	±	0.02	0.02	±	0.01	<0.0001
ΣPUFA	45.20	±	0.99	23.51	±	0.12	<0.0001
ΣUFA	74.79	±	0.58	70.79	±	0.27	0.76

Table 31 Retroperitoneal total lipid fatty acid methyl esters (FAME) ratios between normal fat diet (NFD) and high fat diet (HFD-S) (N=10 per group). Results presented as mean and standard error of the mean (SEM), and statistically analysed by Students t-test. The level of statistical significance was set at * $p < 0.05$.

Name	NFD			HFD-S			p value
	Mean	SEM		Mean	SEM		
Σ MUFA/ Σ PUFA	0.66	±	0.03	2.01	±	0.02	<0.0001
MUFA/SFA	1.19	±	0.02	1.63	±	0.03	<0.0001
Σ PUFA/ Σ SFA	1.90	±	0.09	0.83	±	0.01	<0.0001
Σ UFA/ Σ SFA	3.13	±	0.10	2.49	±	0.03	0.001
C18:0/C16:0	0.16	±	0.01	0.30	±	0.01	<0.0001
C16:1n-7/C16:0	0.09	±	0.01	0.07	±	0.01	0.76
C18:1n-9/C16:0	1.29	±	0.03	2.06	±	0.02	<0.0001
C18:1n-9/C16:1n-7	16.05	±	2.19	28.06	±	1.14	0.007
C18:1n-7/C18:0	0.76	±	0.03	0.39	±	0.01	<0.0001
C18:1/C18:0	8.75	±	0.07	7.19	±	0.23	0.0002
n-6/n-3	17.02	±	0.44	34.67	±	0.45	<0.0001
C20:4n-6/C22:6n-3	4.42	±	0.22	15.74	±	1.39	<0.0001
C22:4n-6/C20:4n-6	2.74	±	0.17	3.65	±	0.45	0.5
C20:4n-6/C20:3n-6	5.67	±	0.35	3.80	±	0.29	0.02
C20:4n-6/C18:2n-6	0.02	±	0.01	0.01	±	0.01	0.009
C20:4n-6/C18:3n-3	0.28	±	0.01	0.34	±	0.03	0.650
C20:3n-3/C18:3n-3	0.01	±	0.01	0.01	±	0.01	0.97
C20:5n-3/C18:3n-3	0.01	±	0.01	0.01	±	0.01	0.02
C22:5n-3/C18:3n-3	0.05	±	0.01	0.02	±	0.01	0.003
C22:6n-3/C18:3n-3	0.07	±	0.01	0.01	±	0.01	<0.0001
C22:6n-3/C22:5n-3	1.27	±	0.07	0.51	±	0.22	0.03
C18:3n-6/C18:2n-6	0.01	±	0.01	0.01	±	0.01	<0.0001
C20:3n-6/C18:3n-6	1.44	±	0.26	4.60	±	0.33	<0.0001
1 (% monoenoics)	29.61	±	0.42	42.56	±	4.49	0.21
2 (% dienoics)	83.23	±	1.90	40.49	±	4.27	<0.0001
3 (% trienoics)	7.31	±	0.10	1.93	±	0.21	<0.0001
4 (% tetraenoics)	3.48	±	0.14	1.04	±	0.14	<0.0001
5 (% pentaenoics)	0.65	±	0.04	0.05	±	0.02	<0.0001
6 (% hexaenoics)	0.88	±	0.06	0.03	±	0.01	<0.0001
Unsaturation Index	125.17	±	1.43	86.08	±	9.08	0.02

Table 32. Mesenteric total lipid fatty acid methyl esters (FAME) for normal fat diet (NFD) and high fat diet (HFD-S) (N=10 per group). Fatty acid results are presented as area % percentage mean and standard error of the mean (SEM), and statistically analysed by Students t-test. The level of statistical significance was set at * $p < 0.05$.

Name	NFD			HFD-S			p value
	Mean%	±	SEM	Mean%	±	SEM	
C12:0	0.08	±	<0.01	0.06	±	0.01	0.32
C14:0	0.61	±	0.05	0.68	±	0.01	0.97
C15:0	0.27	±	0.01	0.12	±	<0.01	<0.001
C16:0	17.58	±	0.46	20.21	±	0.12	0.001
C17:0	0.34	±	0.01	0.33	±	<0.01	>0.99
C18:0	2.94	±	0.04	6.57	±	0.16	<0.001
C20:0	0.13	±	0.01	0.11	±	0.01	0.5
C21:0	0.08	±	0.01	0.13	±	0.01	0.4
C22:0	0.02	±	0.01	0.01	±	0.01	0.98
C23:0	<0.01	±	<0.01	<0.01	±	<0.01	0.82
C24:0	0.03	±	0.01	0.01	±	<0.01	0.17
ΣSFA	22.10	±	0.49	28.23	±	0.20	<0.001
C14:1n-7	0.01	±	0.01	<0.01	±	<0.01	0.92
C15:1	0.02	±	0.01	<0.01	±	<0.01	0.9
C16:1n-7	1.38	±	0.24	1.45	±	0.07	>0.99
C17:1	0.13	±	0.01	0.21	±	0.01	<0.001
C18:1n7	2.43	±	0.11	2.42	±	0.02	>0.99
C18:1n-9 <i>trans</i>	0.06	±	0.02	0.09	±	0.01	0.98
C18:1n-9	25.28	±	0.09	42.71	±	0.31	<0.001
C20:1n9	0.28	±	0.02	0.38	±	0.01	0.001
C22:1n-9	0.01	±	<0.01	<0.01	±	<0.01	0.02
ΣC18:1	27.77	±	0.17	45.22	±	0.32	<0.001
Σn-7	2.46	±	0.11	2.43	±	0.02	>0.99
Σn-9	25.57	±	0.08	43.10	±	0.30	<0.001
ΣMUFA	29.59	±	0.39	47.27	±	0.35	<0.001
C18:2n-6 <i>trans</i>	0.05	±	0.01	0.02	±	0.01	0.59
C18:2n-6	43.01	±	0.84	22.45	±	0.16	<0.001
C18:3n-6	0.09	±	0.01	0.02	±	0.01	<0.001
C20:2n-6	0.28	±	0.02	0.20	±	0.01	0.02
C20:3n-6	0.16	±	0.02	0.06	±	0.01	0.009
C20:4n-6	0.65	±	0.04	0.20	±	0.01	<0.001
C22:2n-6	0.01	±	0.01	<0.01	±	<0.01	0.96
C22:4n-6	0.23	±	0.03	0.08	±	0.01	0.003
Σn-6 PUFA	44.48	±	0.83	23.03	±	0.17	<0.001
Σn-6 metabolites	1.42	±	0.06	0.56	±	0.04	<0.001
C18:3n-3	2.11	±	0.03	0.62	±	0.02	<0.001
C20:5n-3	0.03	±	0.01	-	±	-	
C22:5n-3	0.11	±	0.01	0.01	±	0.01	<0.001
C22:6n-3	0.15	±	0.01	-	±	-	
Σn-3 PUFA	2.41	±	0.03	0.63	±	0.02	<0.001
Σn-3 metabolites	0.30	±	0.01	0.01	±	<0.01	<0.001
ΣPUFA	46.89	±	0.84	23.66	±	0.18	<0.001
ΣUFA	76.48	±	0.48	70.93	±	0.22	<0.001

Table 33. Mesenteric total lipid fatty acid methyl esters (FAME) ratios between normal fat diet (NFD) and high fat diet (HFD-S) (N=10 per group). Results presented as mean and standard error of the mean (SEM), and statistically analysed by Students t-test. The level of statistical significance was set at * $p < 0.05$.

Name	NFD			HFD-S			p value
	Mean%	SEM		Mean%	SEM		
Σ MUFA/ Σ PUFA	0.63	±	0.02	2.00	±	0.03	<0.001
Σ MUFA/ Σ SFA	0.47	±	0.02	1.19	±	0.01	<0.001
Σ PUFA/ Σ SFA	1.59	±	0.05	0.50	±	0.01	<0.001
Σ UFA/ Σ SFA	3.48	±	0.10	2.51	±	0.03	<0.001
C18:0/C16:0	0.17	±	0.01	0.33	±	0.01	<0.001
C16:1n-7/C16:0	0.08	±	0.01	0.07	±	0.00	>0.99
C18:1n-9/C16:0	1.45	±	0.04	2.11	±	0.02	<0.001
C18:1n-9/C16:1n-7	23.09	±	3.52	30.05	±	1.37	0.87
C18:1n-7/C18:0	0.83	±	0.05	0.37	±	0.01	<0.001
C18:1/C18:0	9.46	±	0.19	6.93	±	0.21	<0.001
n-6/n-3	18.51	±	0.36	36.76	±	1.07	<0.001
C18:2n-6/C18:3n-3	20.44	±	0.40	36.36	±	1.02	<0.001
C20:4n-6/C20:3n-6	4.52	±	0.48	4.06	±	0.45	>0.99
C20:4n-6/C22:6n-3	4.23	±	0.13	20.17	±	6.40	0.001
C20:4n-6/C18:2n-6	0.02	±	0.00	0.01	±	0.00	<0.001
C20:4n-6/C18:3n-3	0.31	±	0.02	0.32	±	0.02	>0.99
C22:5n-3/C18:3n-3	0.05	±	0.01	0.01	±	0.00	0.002
C22:6n-3/C22:5n-3	1.27	±	0.05	0.33	±	0.19	0.001
C18:2n6/C16:0	2.47	±	0.11	1.11	±	0.01	<0.001
C18:3n3/C16:0	0.12	±	0.00	0.03	±	0.00	<0.001
C20:3n-6/C18:3n-6	2.38	±	0.62	3.43	±	0.56	0.98
C22:4n-6/C20:4n-6	2.49	±	0.10	2.66	±	0.30	>0.99
1 (% monoenoics)	29.59	±	0.39	47.27	±	0.35	<0.001
2 (% dienoics)	86.71	±	1.67	45.34	±	0.33	<0.001
3 (% trienoics)	7.07	±	0.10	2.10	±	0.07	<0.001
4 (% tetraenoics)	3.52	±	0.19	1.13	±	0.08	<0.001
5 (% pentaenoics)	0.71	±	0.04	0.03	±	0.01	<0.001
6 (% hexaenoics)	0.92	±	0.04	0.02	±	0.01	<0.001
Unsaturation Index	128.52	±	1.33	95.88	±	0.22	<0.001

5.2.3 RET - HFD GbE treatment

In Table 34 and Table 35, the three subsets of HFD fed mice (HFD-S, HFD-PF and HFD-GbE) were compared. Almost no changes in fatty acid profiles occurred between any group, despite changes in body weight occurring in the HFD-PF and HFD-GbE groups. One of the only notable changes was an increase in n-3 metabolites in the HFD-GbE group compared to HFD-S ($p=0.03$) and HFD-PF ($p=0.02$).

5.2.4 MES - HFD GbE treatment

Comparing the MES HFD subsets (HFD-S, HFD-PF and HFD-GbE) (Table 36 and Table 37), the only significant difference that occurred across the groups was a slight significant decrease in total SFA in the HFD-GbE group compared to the HFD-PF group ($p=0.03$) (Σ SFA; HFD-S, $28.23\pm 0.20\%$; HFD, PF, $8.59\pm 0.21\%$; HFD-GbE, $27.84\pm 0.18\%$) that was not seen between the HFD-S and HFD-PF group ($p=0.42$) (Table 36). This change also increased the Σ UFA/ Σ SFA ratio in the HFD-GbE group ($p=0.03$) compared to the HFD-PF group, with no differences seen between the HFD-S and HFD-PF group ($p=0.49$) (Table 37). When comparing the C18:1/C18:0 ratios, although not significant the C18:1/C18:0 ratio increased in the GbE Group, compared to HFD-PF ($p=0.08$), while no changes occurred between the HFD-S and HFD-PF group ($p=0.32$).

It has been shown that when a diet contains a higher n-6/n-3-ratio of approximate 18:1 or more, then an increase in n-6/n-3 oxylipins may also occur. Given that the n-6/n-3 ratio doubled from ~ 18.5 to ~ 36.7 in the MES HFD-S group, this may indicate the potential for a more pro-inflammatory environment in the HFD-S group (Leng *et al.*, 2017). Oxylipins that are derived from n-6 PUFA such as LA, DGLA and AA are predominantly pro-inflammatory (Caligiuri *et al.*, 2013) and are more likely to increase the greater the difference between n-6 PUFA and n-3 PUFA levels are. As n-3 PUFA levels drop substantially in the HFD-S group, less anti-inflammatory oxylipins from ALA, EPA and DHA may occur (Hussey *et al.*, 2017). This may also indicate that in GbE treatment, less n-3 LCFA are required for inflammation mediation in the form of pre-resolving mediators such as eicosanoids (Liput *et al.*, 2021; Astarita *et al.*, 2015; Gabbs *et al.*, 2015; Godessart *et al.*, 1996).

The similarities between the RET and MES total FA percentage levels are in keeping with the idea both tissues were exposed to similar levels of fatty acids from dietary sources from the lymphatic vessels of the GI tract, thus these tissues store similar levels to each other. Although adipose tissue profiles are used as an indicator of dietary intake of fats, the levels in both RET and MES tissue differ slightly to the profiles of the rat chow. For example, SFA levels were ~18% SFA and ~34% in NFD-chow and HFD-chow (Table 9), respectively, compared to 22% (NFD) and 28% (HFD-S) in both RET and MES tissues which suggests some regulation of adipocyte storage at least in RET and MES tissue. Similarly, while MUFA levels were ~24% and ~40% in NFD-chow and HFD-chow respectively, levels in RET and MES tissues were ~30% (NFD) and ~47% (HFD-S) suggesting that *de novo* lipogenesis of MUFA is occurring in the HFD-S group. This is also evident from the 46% increase in HFD-S C18:1n-9/C16:0 ratio indicating an increase in SCD-1 (Delta-9-Desaturase) activity (Heras-Molina *et al.*, 2020) which facilitates the synthesis of C18:1n-9 from C16:0 (C18:1n-9/C16:0; NFD, 1.45±0.04%; HFD-S, 2.11±0.02%, p<0.001) (Table 37).

Next, total lipid profiles were separated by solid phase extraction into the lipid classes: TAG, CE, MAG and DAG and PPL.

Table 34. Retroperitoneal total lipid fatty acid methyl esters (FAME) for high fat diet groups; High fat diet with-saline (HFD-S), High fat diet -pair-fed (HFD-PF) and High fat diet- Ginkgo biloba (HFD-GbE) (N=10 per group). Fatty acid results are presented as area % percentage mean and standard error of the mean (SEM), and statistically analysed by one-way ANOVA with Tukey's Post-hoc test. The level of statistical significance was set at * $p < 0.05$.

	HFD-S		HFD-PF		HFD-GbE		p value		
	MEAN %	SEM	MEAN %	SEM	MEAN %	SEM	S Vs PF	S Vs GbE	PF Vs GbE
C10:0	0.01 ±	0.01	0.02 ±	0.01	0.01 ±	0.01	0.04	0.59	0.23
C12:0	0.04 ±	0.01	0.05 ±	0.01	0.05 ±	0.01	0.23	0.65	0.65
C14:0	0.67 ±	0.01	0.71 ±	0.02	0.68 ±	0.02	0.68	0.16	0.16
C15:0	0.11 ±	0.01	0.11 ±	0.01	0.11 ±	0.01	0.89	0.83	0.99
C16:0	20.74 ±	0.12	20.69 ±	0.21	20.79 ±	0.17	0.97	0.98	0.90
C17:0	0.32 ±	0.01	0.33 ±	0.01	0.32 ±	0.01	0.67	>0.99	0.71
C18:0	6.33 ±	0.17	6.84 ±	0.11	6.52 ±	0.14	0.04	0.59	0.23
C20:0	0.08 ±	0.01	0.08 ±	0.01	0.07 ±	0.01	0.98	0.82	0.71
C21:0	0.10 ±	0.01	0.10 ±	0.01	0.10 ±	0.01	>0.99	0.99	0.99
ΣSFA	28.42 ±	0.27	28.93 ±	0.25	28.68 ±	0.29	0.39	0.78	0.78
C14:1n7	0.01 ±	0.01	0.01 ±	0.01	0.01 ±	0.01	0.93	0.87	0.63
C15:1	0.02 ±	0.01	0.01 ±	0.01	0.01 ±	0.01	0.17	0.31	0.92
C16:1n7	1.54 ±	0.07	1.48 ±	0.06	1.50 ±	0.04	0.75	0.88	0.96
C17:1	0.21 ±	0.01	0.20 ±	0.01	0.21 ±	0.01	0.19	>0.99	0.20
C18:1n7	2.44 ±	0.02	2.39 ±	0.01	2.39 ±	0.01	0.12	0.11	>0.99
C18:1n9 <i>trans</i>	0.09 ±	0.01	0.09 ±	0.01	0.08 ±	0.01	>0.99	0.73	0.70
C18:1n9	42.64 ±	0.27	42.57 ±	0.20	42.72 ±	0.24	0.98	0.97	0.89
C20:1n9	0.34 ±	0.01	0.37 ±	0.01	0.36 ±	0.01	0.23	0.45	0.88
ΣC18:1	45.17 ±	0.28	44.81 ±	0.34	44.95 ±	0.27	0.69	0.87	0.94
Σn-7	2.46 ±	0.02	2.17 ±	0.24	2.17 ±	0.24	0.58	0.58	>0.99
Σn-9	42.98 ±	0.27	42.94 ±	0.19	43.08 ±	0.23	0.99	0.95	0.90
ΣMUFA	47.28 ±	0.32	46.87 ±	0.33	47.04 ±	0.28	0.63	0.85	0.92
C18:2n6	22.27 ±	0.14	22.29 ±	0.14	22.27 ±	0.11	0.99	>0.99	0.99
C18:3n6	0.01 ±	0.01	0.01 ±	0.01	0.01 ±	0.01	0.18	0.75	0.50
C20:2n6	0.21 ±	0.01	0.21 ±	0.02	0.21 ±	0.01	>0.99	0.98	0.97
C20:3n6	0.06 ±	0.01	0.06 ±	0.01	0.05 ±	0.01	0.89	0.82	0.99
C20:4n6	0.22 ±	0.02	0.19 ±	0.02	0.21 ±	0.01	0.37	0.93	0.57
C22:4n6	0.07 ±	0.01	0.05 ±	0.01	0.08 ±	0.01	0.46	0.84	0.19
Σn-6 PUFA	22.85 ±	0.12	22.80 ±	0.17	22.84 ±	0.11	0.96	>0.99	0.98
Σn-6 metabolites	0.57 ±	0.03	0.51 ±	0.05	0.56 ±	0.03	0.52	>0.99	0.56
C18:3n3	0.64 ±	0.01	0.64 ±	0.02	0.63 ±	0.01	0.99	0.78	0.84
C22:5n3	0.02 ±	0.01	0.01 ±	0.01	0.02 ±	0.01	0.51	0.78	0.83
C22:6n3	0.02 ±	0.01	0.02 ±	0.01	0.01 ±	0.01	0.98	0.97	0.90
Σn-3 PUFA	0.59 ±	0.07	0.65 ±	0.02	0.67 ±	0.01	0.56	0.45	0.98
Σn-3 metabolites	0.01 ±	0.01	0.01 ±	0.01	0.04 ±	0.01	0.99	0.03	0.02
ΣPUFA	21.16 ±	2.35	23.45 ±	0.18	23.50 ±	0.12	0.47	0.46	>0.99
ΣUFA	63.71 ±	7.08	70.33 ±	0.25	70.55 ±	0.29	0.50	0.47	>0.99

Table 35. Retroperitoneal total lipid fatty acid methyl esters (FAME) ratios between high fat diet groups; High fat diet with saline (HFD-S), High fat diet pair-fed (HFD-PF) and High fat diet- Ginkgo biloba (HFD-GbE) (N=10 per group). Results presented as mean and standard error of the mean (SEM), and statistically analysed by one-way ANOVA with Tukey's Post-hoc test. The level of statistical significance was set at * $p < 0.05$.

	HFD-S		HFD-PF		HFD-GbE		p value		
	Mean	SEM	Mean	SEM	Mean	SEM	S Vs PF	S Vs GbE	PF Vs GbE
Σ MUFA/ Σ PUFA	2.01 ± 0.02		2.00 ± 0.03		2.00 ± 0.02		0.93	0.95	>0.99
MUFA/SFA	1.63 ± 0.03		1.60 ± 0.02		1.62 ± 0.02		0.60	0.92	0.82
Σ PUFA/ Σ SFA	0.83 ± 0.01		0.81 ± 0.01		0.82 ± 0.01		0.44	0.85	0.76
Σ UFA/ Σ SFA	2.49 ± 0.03		2.43 ± 0.03		2.46 ± 0.04		0.41	0.80	0.79
C18:0/C16:0	0.30 ± 0.01		0.33 ± 0.01		0.31 ± 0.01		0.02	0.61	0.12
C16:1n-7/C16:0	0.07 ± 0.01		0.07 ± 0.01		0.07 ± 0.01		0.79	0.88	0.98
C18:1n-9/C16:0	2.06 ± 0.02		2.06 ± 0.03		2.06 ± 0.03		0.99	>0.99	0.99
C18:1n-9/C16:1n-7	28.06 ± 1.14		29.18 ± 1.33		28.56 ± 0.66		0.75	0.94	0.91
C18:1n-7/C18:0	0.39 ± 0.01		0.32 ± 0.04		0.33 ± 0.04		0.27	0.43	0.94
C18:1/C18:0	7.19 ± 0.23		6.57 ± 0.13		6.93 ± 0.18		0.06	0.57	0.33
n-6/n-3	34.67 ± 0.45		35.15 ± 1.12		34.41 ± 0.60		0.91	0.97	0.79
C18:2n-6/C18:3n-3	34.68 ± 0.60		35.00 ± 0.99		35.39 ± 0.51		0.95	0.78	0.92
C20:4n-6/C20:3n-6	3.80 ± 0.29		3.84 ± 0.36		3.97 ± 0.16		>0.99	0.91	0.94
C20:4n-6/C22:6n-3	15.74 ± 1.39		16.90 ± 0.60		15.47 ± 1.21		0.91	0.99	0.83
C20:4n-6/C18:2n-6	0.01 ± 0.01		0.01 ± 0.01		0.01 ± 0.01		0.35	0.91	0.56
C20:4n-6/C18:3n-3	0.34 ± 0.03		0.29 ± 0.02		0.33 ± 0.02		0.29	0.96	0.40
C20:3n-3/C18:3n-3	0.01 ± 0.01		0.01 ± 0.01		0.01 ± 0.01		0.95	0.01	0.01
C22:5n-3/C18:3n-3	0.02 ± 0.01		0.01 ± 0.01		0.02 ± 0.01		0.84	0.55	0.24
C22:6n-3/C18:3n-3	0.01 ± 0.01		0.01 ± 0.01		0.02 ± 0.01		0.74	0.18	0.04
C22:6n-3/C22:5n-3	0.51 ± 0.22		0.31 ± 0.19		0.82 ± 0.12		0.72	0.39	0.08
C18:2n6/C16:0	1.07 ± 0.01		1.08 ± 0.01		1.07 ± 0.01		0.96	0.99	0.91
C18:3n3/C16:0	0.03 ± 0.01		0.03 ± 0.01		0.03 ± 0.01		>0.99	0.70	0.73
C18:3n-6/C18:2n-6	0.01 ± 0.01		0.01 ± 0.01		0.01 ± 0.01		0.52	0.91	0.77
C20:3n-6/C18:3n-6	4.60 ± 0.33		5.20 ± 1.14		4.62 ± 0.33		0.84	>0.99	0.84
C22:4n-6/C20:4n-6	3.65 ± 0.45		4.39 ± 0.60		2.97 ± 0.34		0.52	0.56	0.10
C18:3n-6/C20:3n-6	42.56 ± 4.74		46.88 ± 0.33		47.05 ± 0.28		0.51	0.49	>0.99
C18:3n6/C22:4n6	40.49 ± 4.51		45.00 ± 0.29		44.98 ± 0.22		0.45	0.45	>0.99
1 (% monoenoics)	42.56 ± 4.74		46.88 ± 0.33		47.05 ± 0.28		0.51	0.49	>0.99
2 (% dienoics)	40.49 ± 4.51		45.00 ± 0.29		44.98 ± 0.22		0.45	0.45	>0.99
3 (% trienoics)	1.93 ± 0.22		2.12 ± 0.07		2.09 ± 0.03		0.59	0.69	0.98
4 (% tetraenoics)	1.04 ± 0.14		0.94 ± 0.11		1.14 ± 0.07		0.82	0.79	0.42
5 (% pentaenoics)	0.05 ± 0.02		0.04 ± 0.01		0.07 ± 0.01		0.99	0.38	0.31
6 (% hexaenoics)	0.03 ± 0.02		0.02 ± 0.01		0.07 ± 0.01		0.91	0.10	0.04
Unsaturation Index	86.08 ± 9.57		95.00 ± 0.32		95.40 ± 0.35		0.50	0.47	>0.99

Table 36. Mesenteric total lipid fatty acid methyl esters (FAME) for high fat diet groups; High fat diet with-saline (HFD-S), High fat diet -pair-fed (HFD-PF) and High fat diet- Ginkgo biloba (HFD-GbE) (N=10 per group). Fatty acid results are presented as area % percentage mean and standard error of the mean (SEM), and statistically analysed by one-way ANOVA with Tukey's Post-hoc test. The level of statistical significance was set at * $p < 0.05$.

	HFD-S			HFD-PF			HFD-GbE			S Vs PF	S Vs GbE	PF Vs GbE
	Mean%	SEM		Mean%	SEM		Mean %	SEM		<i>p value</i>	<i>p value</i>	<i>p value</i>
C12:0	0.06	± 0.01		0.06	± 0.01		0.06	± 0.01		0.91	>0.99	0.93
C14:0	0.68	± 0.01		0.72	± 0.02		0.68	± 0.02		0.93	0.28	0.28
C15:0	0.12	± 0.01		0.12	± 0.01		0.11	± 0.01		0.18	0.97	0.97
C16:0	20.21	± 0.12		20.17	± 0.21		19.89	± 0.11		0.98	0.32	0.41
C17:0	0.33	± 0.01		0.35	± 0.01		0.34	± 0.01		0.34	0.81	0.71
C18:0	6.57	± 0.16		6.92	± 0.18		6.48	± 0.15		0.29	0.92	0.15
C20:0	0.11	± 0.01		0.11	± 0.01		0.10	± 0.01		0.92	0.99	0.87
C21:0	0.13	± 0.01		0.12	± 0.01		0.14	± 0.01		0.83	0.74	0.40
C24:0	0.01	± 0.01		-	± -		0.03	± 0.01		-	<0.0001	-
∑SFA	28.23	± 0.20		28.59	± 0.21		27.84	± 0.18		0.42	0.34	0.03
C16:1n-7	1.45	± 0.07		1.46	± 0.10		1.44	± 0.06		0.99	>0.99	0.98
C17:1	0.21	± 0.01		0.21	± 0.01		0.22	± 0.01		0.81	0.86	0.50
C18:1n7	2.42	± 0.02		2.37	± 0.01		2.41	± 0.02		0.08	0.82	0.24
C18:1n-9 <i>trans</i>	0.09	± 0.01		0.09	± 0.00		0.06	± 0.01		0.99	0.17	0.13
C18:1n-9	42.71	± 0.31		42.68	± 0.37		43.47	± 0.11		>0.99	0.17	0.15
C20:1n9	0.38	± 0.01		0.35	± 0.04		0.39	± 0.01		0.65	0.98	0.54
∑C18:1	45.22	± 0.32		45.14	± 0.38		45.94	± 0.12		0.98	0.21	0.15
∑n-7	2.43	± 0.02		2.37	± 0.01		2.41	± 0.02		0.09	0.87	0.24
∑n-9	43.10	± 0.30		43.04	± 0.35		43.86	± 0.11		0.99	0.14	0.11
∑MUFA	47.27	± 0.35		47.16	± 0.34		47.99	± 0.10		0.96	0.19	0.12
C18:2n-6t	0.02	± 0.01		0.01	± 0.01		0.01	± 0.01		0.51	0.70	0.95
C18:2n-6	22.45	± 0.16		22.37	± 0.14		22.26	± 0.11		0.90	0.57	0.83
C18:3n-6	0.02	± 0.01		0.01	± 0.01		0.02	± 0.01		0.17	0.67	0.59
C20:2n-6	0.20	± 0.01		0.20	± 0.02		0.20	± 0.01		>0.99	0.99	0.99
C20:3n-6	0.06	± 0.01		0.05	± 0.02		0.07	± 0.01		0.98	0.71	0.60
C20:4n-6	0.20	± 0.01		0.20	± 0.02		0.19	± 0.01		0.99	0.81	0.89
C22:4n-6	0.08	± 0.01		0.07	± 0.02		0.06	± 0.01		0.63	0.42	0.93
∑n-6 PUFA	23.03	± 0.17		22.90	± 0.18		22.79	± 0.12		0.84	0.55	0.88
∑n-6 metabolites	0.56	± 0.04		0.53	± 0.06		0.53	± 0.03		0.87	0.89	>0.99
C18:3n-3	0.62	± 0.02		0.62	± 0.03		0.60	± 0.02		>0.99	0.72	0.72
C22:5n-3	0.01	± 0.01		0.01	± 0.01		0.01	± 0.01		>0.99	0.96	0.98
C22:6n-3	0.01	± 0.01		0.01	± 0.01		0.01	± 0.01		0.34	0.87	0.64
∑n-3 PUFA	0.63	± 0.02		0.63	± 0.03		0.61	± 0.02		>0.99	0.76	0.81
∑n-3 metabolites	0.01	± 0.01		0.01	± 0.01		0.01	± 0.01		0.89	0.97	0.78
∑PUFA	23.66	± 0.18		23.53	± 0.20		23.40	± 0.13		0.86	0.55	0.86
∑UFA	70.93	± 0.22		70.69	± 0.22		71.39	± 0.16		0.69	0.25	0.05

Table 37. Mesenteric total lipid fatty acid methyl esters (FAME) ratios between high fat diet groups; High fat diet with saline (HFD-S), High fat diet pair-fed (HFD-PF) and High fat diet- Ginkgo biloba (HFD-GbE) (N=10 per group). Results presented as mean and standard error of the mean (SEM), and statistically analysed by one-way ANOVA with Tukey's Post-hoc test. The level of statistical significance was set at * $p < 0.05$.

	HFD-S		HFD-PF		HFD-GbE		S Vs PF	S Vs GbE	PF Vs GbE
	Mean	SEM	Mean	SEM	Mean	SEM	<i>p value</i>	<i>p value</i>	<i>p value</i>
ΣMUFA/ΣPUFA	2.00	± 0.03	2.01	± 0.03	2.05	± 0.01	0.98	0.31	0.42
ΣMUFA/ΣSFA	1.19	± 0.01	1.22	± 0.01	1.19	± 0.01	0.39	0.98	0.29
ΣPUFA/ΣSFA	0.50	± 0.01	0.50	± 0.01	0.49	± <0.01	0.98	0.31	0.40
ΣUFA/ΣSFA	2.51	± 0.03	2.47	± 0.03	2.57	± 0.02	0.49	0.30	0.03
C18:0/C16:0	0.33	± 0.01	0.34	± 0.01	0.33	± 0.01	0.99	0.99	>0.99
C16:1n-7/C16:0	0.07	± <0.01	0.07	± <0.01	0.07	± <0.01	0.99	0.99	>0.99
C18:1n-9/C16:0	2.11	± 0.02	2.12	± 0.04	2.19	± 0.02	0.99	0.17	0.21
C18:1n-9/C16:1n-7	30.05	± 1.37	30.61	± 2.47	30.61	± 1.29	0.97	0.97	>0.99
C18:1n-7/C18:0	0.37	± 0.01	0.34	± 0.01	0.37	± 0.01	0.14	0.99	0.11
C18:1/C18:0	6.93	± 0.21	6.56	± 0.17	7.13	± 0.16	0.32	0.72	0.08
n-6/n-3	36.76	± 1.07	37.24	± 1.75	37.86	± 1.08	0.96	0.83	0.94
C15:0/C17:0	0.33	± 0.01	0.34	± 0.01	0.33	± 0.01	0.34	>0.99	0.36
C18:2n-6/C18:3n-3	36.36	± 1.02	36.72	± 1.72	37.57	± 1.03	0.98	0.79	0.89
C20:4n-6/C20:3n-6	4.06	± 0.45	4.33	± 0.61	2.97	± 0.37	0.92	0.25	0.14
C20:4n-6/C22:6n-3	20.17	± 6.40	-	± -	24.56	± 3.44	-	<0.0001	-
C20:4n-6/C18:3n-3	0.32	± 0.02	0.31	± 0.02	0.31	± 0.02	0.93	0.96	0.99
C22:6n-3/C22:5n-3	0.33	± 0.19	-	± -	0.18	± 0.12	-	<0.0001	-
C18:2n6/C16:0	1.11	± 0.01	1.11	± 0.01	1.12	± 0.01	>0.99	0.88	0.84
C18:3n3/C16:0	0.03	± <0.01	0.03	± <0.01	0.03	± <0.01	>0.99	0.86	0.87
C20:3n-6/C18:3n-6	3.43	± 0.56	3.59	± 0.88	6.30	± 1.20	0.99	0.08	0.13
C22:4n-6/C20:4n-6	2.66	± 0.30	3.58	± 0.64	3.49	± 0.47	0.38	0.43	0.99
1 (% monoenoics)	47.27	± 0.35	47.16	± 0.34	47.99	± 0.10	0.96	0.19	0.12
2 (% dienoics)	45.34	± 0.33	45.15	± 0.30	44.92	± 0.23	0.89	0.57	0.84
3 (% trienoics)	2.10	± 0.07	2.05	± 0.12	2.05	± 0.07	0.94	0.93	>0.99
4 (% tetraenoics)	1.13	± 0.08	1.05	± 0.15	0.99	± 0.05	0.85	0.58	0.89
5 (% pentaenoics)	0.03	± 0.01	0.03	± 0.02	0.04	± 0.01	>0.99	0.96	0.98
6 (% hexaenoics)	0.02	± 0.01	<0.01	± <0.01	0.01	± 0.01	0.34	0.87	0.64
Unsaturation Index	95.88	± 0.22	95.46	± 0.29	96.00	± 0.30	0.52	0.95	0.35

5.3 RET and MES TAG

As mentioned in the Chapter 1, TAG is an integral part of the adipocyte, where excess fatty acids are converted to TAG in the liver and transported to peripheral tissues as very low-density lipoprotein (VLDL-TAG) *via* the bloodstream (Roumans *et al.*, 2021; Parry *et al.*, 2021; Alves-Bezerra and Cohen, 2017; Martinez-Lopez and Singh, 2015; Bansal *et al.*, 2007; Barrows and Parks, 2006). TAG provides a neutral store of fatty acids in the body, predominantly stored in adipocytes that can later provide energy substrate other organs that break the fatty acids down into energy *via* β -oxidation. The daily rate of hepatic FA uptake and DNL is balanced by FA oxidation rates and the transportation of VLDL-TAG out of the liver, which results in less than 5% of steady state hepatic TAG. As such, when TAG levels in the liver drop, such as caloric restriction or a fasting state, FA lipolysis and metabolism in the adipocyte increases to liberate FA to be transported to the liver for energy production (Bhutia and Ganapathy, 2021; Alves-Bezerra and Cohen, 2017; Kohlmeier, 2015). An excess of hepatic TAG accumulation is associated with obesity, T2DM, dyslipidaemia, and IR and can result in chronic liver disease (Caussy, Aubin and Loomba, 2021; Birkenfeld and Shulman, 2014). After SPE elution, RET and MES TAG samples were subjected to acid-catalysed esterification to produce fatty acid methyl esters and analysed by GC-FID.

5.3.1 RET-TAG – NFD vs HFD

As shown in Table 38, total SFA significantly increased by 18% in HFD-RET-TAG compared to NFD-RET-TAG (NFD $23.45 \pm 0.66\%$; HFD-S $27.63 \pm 0.24\%$, $p=0.0007$). This is like total RET lipid profiles that saw an increase of 16% in the HFD group (NFD, $24.1 \pm 0.6\%$; HFD, $28.4 \pm 0.27\%$, $p=0.0004$). Total MUFA increased by 67% in HFD-S compared to NFD (NFD $28.95 \pm 0.45\%$; HFD-S $48.33 \pm 0.29\%$, $p<0.0001$), while total lipid profiles showed a 60% increase (NFD, $29.59 \pm 0.44\%$; HFD, $47.28 \pm 0.32\%$, $p<0.0001$). Total PUFA decreased in HFD by 49% compared to NFD (NFD $45.77 \pm 0.99\%$; HFD-S $23.42 \pm 0.14\%$, $p<0.0001$), like total lipid profiles that showed a 48% decrease (NFD, $23.51 \pm 0.12\%$; HFD, $45.2 \pm 1\%$, $p<0.0001$). In the PUFA fraction, the changes in RET-TAG are largely attributable to the 48% decrease in total n-6 PUFA, notably in C18:2n-6 (NFD $42.95 \pm 1.09\%$; HFD-S $22.34 \pm 0.14\%$, $p<0.0001$) and a 72% decrease in C20:4n-6 (NFD $0.54 \pm 0.03\%$; HFD $0.15 \pm 0.01\%$, $p<0.0001$) (Table 38). This is very similar to the C18:2n-6 in RET total lipid profiles (NFD, $41.32 \pm 1\%$; HFD, $22.27 \pm 0.1\%$, $p<0.0001$) and C20:4n6 (NFD $0.63 \pm 0.03\%$; HFD $0.22 \pm 0.02\%$, $p<0.0001$) (Table 30). Though total n-3 PUFA decreased by 63%

this was not significant (HFD-S, 0.61±0.01%; NFD, 1.66±0.32%, p=0.15) (Table 38), it is similar to C18:3n-3 changes seen in total RET lipids (NFD 2.23±0.03%, HFD 0.64±0.01%; p<0.0001) (Table 30). Similar profile changes for C22:6n-3 are seen in RET TAG (NFD 0.13±0.02; HFD-S 0.01±0.01%, p=0.002) (Table 38), compared to total RET profiles (NFD 0.15±0.01%; HFD 0.02±0.01%, p=0.002) (Table 30).

5.3.2 MES- TAG – NFD vs HFD

When comparing MES NFD and HFD-S TAG profiles, several FA levels changes, summarised in Table 40 and Table 41. In the HFD-S group, total SFA significantly increased by 28% (Σ SFA; 21.68±0.50%; 27.69±0.23%, p<0.0001). This was largely due to an 15% increase in C16:0 (C16:0; 17.57±0.48%; 20.23±0.15%, p=0.002), and the 129% increase in C18:0 (C18:0; 2.63±0.05%; 6.02±0.17%, p<0.0001) (Table 40). Total MUFA levels in TAG are identical to that of total FA profiles. Total MUFA increased by 63% in HFD-S compared to NFD (Σ MUFA; 29.55±0.42%; 48.30±0.32%, p<0.0001) largely attributable to the 73% increase in C18:1n-9 (C18:1n-9; NFD, 25.27±0.13%; HFD-S, 43.80±0.27%, p<0.0001) (Table 40). This increase was also notable compared to C16:0 levels, as the C18:1n-9/C16:0 ratio decreased by 50% (C18:1n-9/C16:0; NFD, 1.45±0.04; HFD-S, 2.17±0.03, p<0.0001) (Table 41). Similarly, the levels of C18:1 increased more relative to C18:0 (C18:1/C18:0; NFD, 9.82±0.23; HFD-s, 7.48±0.25, p<0.0001). Total PUFA decreased in HFD-S by 51% compared to NFD (Σ PUFA; NFD, 47.96±0.86%; HFD-S, 23.31±0.19%, p<0.0001), in keeping with findings from the total fatty acid profiles. This is largely attributed to the 50% decrease in C18:2n-6 (C18:2n-6; 44.64±0.85%; HFD-S, 22.34±0.19%, p<0.0001) and 63% decrease in higher Σ n-6 metabolites (Σ n-6 metabolites; NFD, 1.12±0.04%; HFD, 0.41±0.03%, p<0.0001), including a 74% decrease in C20:4n-6 (C20:4n-6; NFD, 0.52±0.03%; HFD-S, 0.14±0.01%, p<0.0001) (Table 40). n-3PUFA also decreased by 74%, (Σ n-3 PUFA; 2.19±0.03%; HFD-S, 0.56±0.02%, p<0.0001), most notable from the 72% decrease in C18:3n-3 (C18:3n-3; NFD, 1.95±0.03%; HFD-S, 0.55±0.02%, p<0.0001), but also the 93% decrease in higher n-3PUFA metabolites (Σ n-3 metabolites; NFD, 0.24±0.01%; HFD-S, 0.02±0.01%, p<0.0001) (Table 40). These changes dramatically increased the n-6/n-3 ratio by 95% (n-6/n-3; 20.95±0.42; 40.82±1.02, p<0.0001) (Table 41). This suggests that less n-3 will be available for inflammation mediation. Furthermore, as C18:2n-6 and C18:3n-3 compete for the same enzymes for the synthesis of higher metabolites used for oxylipin formation, and with n-6 metabolites favoured over n-3, it is likely that more pro-inflammatory n-6 oxylipins will be produced, further exasperating an already pro-inflammatory state. This hypothesis is further supported by the decrease of 51% in

UFA in HFD-S group compared to NFD (Σ UFA; NFD, 77.51 \pm 0.50%; HFD-S, 71.60 \pm 0.19%, $p < 0.0001$) (Table 40) and the 26% decrease in the unsaturation index (Unsaturation Index; 129.83 \pm 1.36; 95.97 \pm 0.21, $p < 0.0001$) (Table 41).

5.3.3 RET- TAG HFD GbE treatment

Interestingly, when comparing the RET HFD subsets (Table 42 and Table 43), like total lipid profiles few changes in the TAG lipid profiles was seen. The only notable change occurred in C18:1n9, with a significant 5% decrease seen between both HFD-S and HFD-PF ($p = 0.0004$) and HFD-S and HFD-GbE ($p = 0.0002$), while HFD-PF and HFD-GbE showed no difference at all ($p = 0.98$) (HFD-S 46.07, \pm 0.29%; HFD-PF 43.81 \pm 0.26%, HFD-GbE 43.71 \pm 0.48%) (Table 42). This change in C18:1n-9 profile was not seen in RET total lipid profiles, which showed similar percentage area means across all three HFD subsets of 42.57-42.72% (Table 34). Overall, only a significant decrease in the Σ PUFA/ Σ SFA ratio was seen between HFD-S and HFD-PF ($p = 0.03$) (HFD-S 0.85 \pm 0.01; HFD-PF 0.82 \pm 0.01; HFD-GbE 0.83 \pm 0.01) (Table 43). Taken together, these results suggest that when analysing RET total tissue lipid profiles, it is likely that overall, the TAG profile is represented.

5.3.4 MES- TAG HFD GbE treatment

When comparing the MES HFD subsets (Table 44 and Table 45), few changes in FA percentage levels occurred. There was a decrease of 11% in C18:0 levels between the HFD-PF and HFD-GbE groups ($p = 0.02$) (C18:0 HFD-S, 6.02 \pm 0.17%; HFD-PF 6.30 \pm 0.21%; HFD-GbE, 5.64 \pm 0.10%) (Table 44). Interestingly, this decrease was not seen in the total fatty acid profile, further supporting the need for lipid classes separation when analysing FA profiles. While total SFA remaining similar between the HFD-S and HFD-PF groups, a significant decrease was seen between the HFD-S and HFD-GbE groups ($p = 0.04$), and was similarly reflected, although not significantly, between the HFD-PF and HFD-GbE groups ($p = 0.07$) (MES-TAG- Σ SFA; HFD-S, 27.69 \pm 0.23%; HFD-PF, 27.65 \pm 0.16%; HFD-GbE, 27.04 \pm 0.14%) (Table 44). In contrast, an increase in C18:1n-9 was seen between the HFD-GbE group compared to HFD-S ($p = 0.04$), although this change was not significantly different to the HFD-PF group ($p = 0.12$) (C18:1n-9; HFD-S, 43.80 \pm 0.27%; HFD-PF, 43.94 \pm 0.30%, HFD-GbE, 44.65 \pm 0.12%) (Table 44).

Finally, the C18:2n-6/C18:3n-3 ratio significantly increased in the HFD-GbE group compared to both the HFD-S ($p=0.05$) and HFD-PF ($p=0.05$) groups (C18:2n-6/C18:3n-3; 41.25 ± 1.07 ; 41.25 ± 1.70 ; 45.58 ± 0.90) (Table 45), although these changes were not reflected entirely in the n-6/n-3 ratio where the changes did not reach significance (S vs PF, $p>0.99$; S vs GbE, $p=0.09$; PF vs GbE, $p=0.1$) (n-6/n-3; HFD-S, 40.82 ± 1.02 ; HFD-PF, 40.86 ± 1.71 ; HFD-GbE, 44.62 ± 0.91 ; S vs PF, $p>0.99$; S vs GbE, $p=0.09$; PF vs GbE, $p=0.1$). This is an interesting finding as it suggests that an even bigger increase in the gap between n-6 and n-3 is occurring in the adipocyte. This may be because n-3 FA are being mobilized into other areas or that n-3 PUFA are utilised within the cell in a pro-inflammatory mediated way. Interestingly, it has been reported that in an obese phenotype and in a fasting state, the mobilization of FA from adipose tissue to circulating FA favours the liberation and circulation of PUFA, while SFA less likely to be mobilized out of the adipocyte (Raclot, 2003; Connor, Lin and Colvis, 1996).

Table 38. Retroperitoneal Triglyceride fatty acid methyl esters (FAME) for normal fat diet (NFD) and high fat diet (HFD-S) (N=10 per group). Fatty acid results are presented as area % percentage mean and standard error of the mean (SEM), and statistically analysed by Students t-test. The level of statistical significance was set at * $p < 0.05$.

	NFD			HFD-S			p value
	Mean %	±	SEM	Mean %	±	SEM	
C12:0	0.06	±	0.01	0.04	±	0.01	0.0004
C14:0	0.68	±	0.05	0.58	±	0.01	0.85
C15:0	0.22	±	0.01	0.09	±	0.01	<0.0001
C16:0	19.37	±	0.60	20.83	±	0.11	0.61
C17:0	0.26	±	0.01	0.27	±	0.01	0.51
C18:0	2.63	±	0.03	5.65	±	0.15	<0.0001
C20:0	0.07	±	0.01	0.06	±	0.01	0.31
C21:0	0.05	±	0.01	0.08	±	0.01	0.0001
∑DMA18:0	0.09	±	0.01	0.02	±	0.01	0.01
∑SFA	23.45	±	0.66	27.63	±	0.24	0.0007
C16:1n7	1.68	±	0.24	1.36	±	0.05	0.98
C17:1	0.12	±	0.01	0.16	±	0.01	0.51
C18:1n7t	0.05	±	0.01	0.04	±	0.01	0.96
C18:1n9 <i>trans</i>	0.03	±	0.01	0.29	±	0.22	>0.99
C18:1n9	24.73	±	0.15	46.07	±	0.29	<0.0001
∑DMA18:1	0.11	±	0.01	0.09	±	0.01	>0.99
∑C18:1	26.94	±	0.22	46.43	±	0.27	<0.0001
∑n-7	3.87	±	0.33	1.43	±	0.08	<0.0001
∑n-9	24.78	±	0.15	46.36	±	0.28	<0.0001
∑MUFA	28.95	±	0.45	48.33	±	0.29	<0.0001
C18:2n6 <i>trans</i>	0.05	±	0.01	0.07	±	0.04	>0.99
C18:2n6	42.95	±	1.09	22.34	±	0.14	<0.0001
C18:3n6	0.08	±	0.01	0.05	±	0.01	0.07
C20:2n6	0.24	±	0.01	0.16	±	0.01	<0.0001
C20:3n6	0.09	±	0.01	0.04	±	0.01	<0.0001
C20:4n6	0.54	±	0.03	0.15	±	0.01	<0.0001
C22:4n6	0.18	±	0.01	0.05	±	0.01	<0.0001
∑n-6 PUFA	44.12	±	1.07	22.81	±	0.14	<0.0001
∑n-6 metabolites	1.13	±	0.04	2.69	±	2.26	>0.99
C18:3n-3 <i>trans</i>	0.04	±	0.01	0.05	±	0.01	0.97
C18:3n3	1.57	±	0.29	0.53	±	0.01	0.06
C20:3n3	0.04	±	0.01	0.02	±	0.01	0.38
C22:5n3	0.09	±	0.01	0.01	±	0.01	<0.0001
C22:6n3	0.13	±	0.02	0.01	±	0.01	0.002
∑n-3 PUFA	1.66	±	0.32	0.61	±	0.01	0.15
∑n-3 metabolites	0.23	±	0.02	0.08	±	0.05	0.38
∑PUFA	45.77	±	0.99	23.42	±	0.14	<0.0001
∑UFA	74.72	±	0.56	71.75	±	0.26	0.01

Table 39. Retroperitoneal Triglyceride fatty acid methyl esters (FAME) ratios for normal fat diet (NFD) and high fat diet (HFD-S) (N=10 per group). Results presented as mean an (SEM), and statistically analysed by one-way ANOVA with Tukey's Post-hoc test. The level of statistical significance was set at * $p < 0.05$.

Fatty acid ratios	NFD			HFD-S			p value
	Mean	SEM		Mean	SEM		
Σ MUFA/ Σ PUFA	0.64	±	0.02	2.06	±	0.02	<0.0001
Σ MUFA/ Σ SFA	0.81	±	0.01	0.57	±	0.01	<0.0001
Σ PUFA/ Σ SFA	1.98	±	0.09	0.85	±	0.01	<0.0001
Σ UFA/ Σ SFA	3.21	±	0.11	2.60	±	0.03	0.002
C18:0/C16:0	0.14	±	0.01	0.50	±	0.23	0.97
C16:1n-7/C16:0	0.08	±	0.01	1.69	±	1.63	>0.99
C18:1n-9/C16:0	1.29	±	0.04	45.81	±	43.60	>0.99
C18:1n-9/C16:1n-7	17.59	±	2.41	34.37	±	1.35	0.001
C18:1n-7/C18:0	0.82	±	0.03	0.58	±	0.58	>0.99
C18:1/C18:0	10.25	±	0.11	25.62	±	17.47	>0.99
n-6/n-3	36.97	±	18.00	37.74	±	0.82	0.98
C18:2n-6/C18:3n-3	128.10	±	107.23	41.91	±	0.74	0.98
C20:4n-6/C20:3n-6	6.24	±	0.34	3.27	±	0.36	0.001
C20:4n-6/C22:6n-3	4.70	±	0.40	17.10	±	1.93	0.0004
C20:4n-6/C18:3n-3	2.64	±	1.60	0.35	±	0.07	0.97
C20:3n-3/C18:3n-3	0.43	±	0.41	2.96	±	2.93	>0.99
C22:5n-3/C18:3n-3	0.45	±	0.27	0.02	±	0.01	0.97
C22:6n-3/C22:5n-3	1.56	±	0.33	0.94	±	0.12	0.96
C18:2n6/C16:0	2.25	±	0.12	1.07	±	0.01	<0.0001
C18:3n3/C16:0	0.08	±	0.02	0.07	±	0.04	>0.99
C18:3n-6/C18:2n-6	0.01	±	0.01	0.01	±	0.01	>0.99
C20:3n-6/C18:3n-6	1.05	±	0.07	1.11	±	0.15	>0.99
C22:4n-6/C20:4n-6	3.03	±	0.08	3.34	±	0.12	0.78
C18:3n6/C22:4n6	86.46	±	2.17	45.07	±	0.29	<0.0001
1 (% monoenoics)	28.90	±	0.43	48.33	±	0.28	<0.0001
2 (% dienoics)	86.46	±	2.06	45.07	±	0.27	<0.0001
3 (% trienoics)	4.93	±	0.89	1.99	±	0.05	<0.0001
4 (% tetraenoics)	2.86	±	0.13	0.73	±	0.08	0.02
5 (% pentaenoics)	0.49	±	0.03	0.05	±	0.01	<0.0001
6 (% hexaenoics)	0.77	±	0.12	0.05	±	0.01	0.0002
Unsaturation Index	124.41	±	1.49	96.23	±	0.24	<0.0001

Table 40. Mesentery triglyceride fatty acid methyl esters (FAME) for normal fat diet (NFD) and high fat diet (HFD-S) (N=10 per group). Fatty acid results are presented as area % percentage mean and standard error of the mean (SEM), and statistically analysed by Students t-test. The level of statistical significance was set at * $p < 0.05$.

	NFD			HFD-S			p value
	Mean %	±	SEM	Mean %	±	SEM	
C12:0	0.07	±	0.01	0.05	±	<0.01	0.42
C14:0	0.59	±	0.05	0.65	±	0.01	>0.99
C15:0	0.24	±	0.01	0.10	±	<0.01	<0.0001
C16:0	17.57	±	0.48	20.23	±	0.15	0.002
C17:0	0.29	±	0.01	0.30	±	<0.01	0.89
C18:0	2.63	±	0.05	6.02	±	0.17	<0.0001
C20:0	0.12	±	0.01	0.08	±	0.01	0.04
C21:0	0.05	±	0.01	0.11	±	0.01	0.08
C22:0	0.03	±	<0.01	<0.01	±	<0.01	0.001
DMA18:0	0.11	±	0.02	0.16	±	0.02	0.77
∑SFA	21.68	±	0.50	27.69	±	0.23	<0.0001
C16:1n-7	1.33	±	0.23	1.36	±	0.06	>0.99
C17:1	0.10	±	0.01	0.19	±	<0.01	0.0001
C18:1n7 <i>trans</i>	0.02	±	0.02	0.04	±	0.01	>0.99
C18:1n7	2.39	±	0.11	2.48	±	0.02	>0.99
C18:1n9	25.27	±	0.13	43.80	±	0.27	<0.0001
C20:1n9	0.25	±	<0.01	0.32	±	0.01	<0.0001
DMA18:1	0.19	±	0.03	0.03	±	0.01	0.002
∑C18:1	25.73	±	0.24	44.62	±	0.52	<0.0001
∑n-7	3.75	±	0.34	3.88	±	0.07	>0.99
∑n-9	25.52	±	0.13	44.19	±	0.27	<0.0001
∑MUFA	29.55	±	0.42	48.30	±	0.32	<0.0001
C18:2n-6t	0.01	±	0.01	<0.01	±	<0.01	0.92
C18:2n-6	44.64	±	0.85	22.34	±	0.19	<0.0001
C18:3n-6	0.09	±	0.01	0.02	±	<0.01	<0.0001
C20:2n-6	0.22	±	0.01	0.16	±	0.01	0.001
C20:3n-6	0.09	±	<0.01	0.03	±	<0.01	<0.0001
C20:4n-6	0.52	±	0.03	0.14	±	0.01	<0.0001
C22:4n-6	0.20	±	0.01	0.07	±	0.01	<0.0001
∑n-6 PUFA	45.77	±	0.85	22.75	±	0.18	<0.0001
∑n-6 metabolites	1.12	±	0.04	0.41	±	0.03	<0.0001
C18:3n-3	1.95	±	0.03	0.55	±	0.02	<0.0001
C20:3n-3	0.02	±	0.01	<0.01	±	<0.01	0.26
C22:5n-3	0.10	±	<0.01	0.01	±	<0.01	<0.0001
C22:6n-3	0.12	±	0.01	0.01	±	<0.01	<0.0001
∑n-3 PUFA	2.19	±	0.03	0.56	±	0.02	<0.0001
∑n-3 metabolites	0.24	±	0.01	0.02	±	<0.01	<0.0001
∑PUFA	47.96	±	0.86	23.31	±	0.19	<0.0001
∑UFA	77.51	±	0.50	71.60	±	0.19	<0.0001

Table 41. Mesenteric triglyceride fatty acid methyl esters (FAME) ratios for normal fat diet (NFD) and high fat diet (HFD-S) (N=10 per group). Results presented as mean an (SEM), and statistically analysed by one-way ANOVA with Tukey's Post-hoc test. The level of statistical significance was set at **p* < 0.05.

	NFD			HFD-S			p value
	Mean	±	SEM	Mean	±	SEM	
ΣMUFA/ΣPUFA	0.62	±	0.02	2.07	±	0.03	<0.0001
ΣMUFA/ΣSFA	0.46	±	0.02	1.19	±	0.01	<0.0001
ΣPUFA/ΣSFA	1.63	±	0.05	0.48	±	0.01	<0.0001
ΣUFA/ΣSFA	3.60	±	0.11	2.59	±	0.03	<0.0001
C18:0/C16:0	0.15	±	0.01	0.30	±	0.01	<0.0001
C16:1n-7/C16:0	0.07	±	0.01	0.07	±	0.01	>0.99
C18:1n-9/C16:0	1.45	±	0.04	2.17	±	0.03	<0.0001
C18:1n-9/C16:1n-7	24.03	±	3.75	32.72	±	1.41	0.64
C18:1n-7/C18:0	0.92	±	0.06	0.42	±	0.01	<0.0001
C18:1/C18:0	9.82	±	0.23	7.48	±	0.25	<0.0001
n-6/n-3	20.95	±	0.42	40.82	±	1.02	<0.0001
C15:0/C17:0	0.15	±	0.01	0.30	±	0.01	<0.0001
C18:2n-6/C18:3n-3	22.91	±	0.46	41.25	±	1.07	<0.0001
C20:4n-6/C20:3n-6	6.04	±	0.30	4.91	±	0.33	0.45
C20:4n-6/C22:6n-3	4.46	±	0.20	16.88	±	1.82	0.0001
C20:4n-6/C18:2n-6	0.01	±	0.01	0.01	±	0.01	0.0001
C20:4n-6/C18:3n-3	0.27	±	0.01	0.25	±	0.02	>0.99
C20:3n-3/C18:3n-3	0.01	±	0.01	<0.01	±	0.01	0.25
C20:5n-3/C18:3n-3	<0.01	±	0.01	<0.01	±	0.01	>0.99
C22:5n-3/C18:3n-3	0.05	±	0.01	0.01	±	0.01	<0.0001
C22:6n-3/C18:3n-3	0.06	±	0.01	0.02	±	0.01	<0.0001
C22:6n-3/C22:5n-3	1.22	±	0.13	1.28	±	0.24	>0.99
C18:2n6/C16:0	2.57	±	0.12	1.10	±	0.01	<0.0001
C18:3n3/C16:0	0.11	±	0.01	0.03	±	0.01	<0.0001
C18:3n-6/C18:2n-6	<0.01	±	0.01	<0.01	±	0.01	0.03
C20:3n-6/C18:3n-6	1.13	±	0.17	2.09	±	0.32	0.39
C22:4n-6/C20:4n-6	2.59	±	0.11	2.92	±	0.70	>0.99
1 (% monoenoics)	29.55	±	0.42	48.30	±	0.32	<0.0001
2 (% dienoics)	89.75	±	1.70	44.99	±	0.37	<0.0001
3 (% trienoics)	6.41	±	0.08	1.77	±	0.05	<0.0001
4 (% tetraenoics)	2.88	±	0.15	0.82	±	0.07	<0.0001
5 (% pentaenoics)	0.51	±	0.02	0.03	±	0.01	<0.0001
6 (% hexaenoics)	0.72	±	0.06	0.05	±	0.01	<0.0001
Unsaturation Index	129.83	±	1.36	95.97	±	0.21	<0.0001

Table 42. Retroperitoneal Triglyceride fatty acid methyl esters (FAME) for high fat diet groups; High fat diet with-saline (HFD-S), High fat diet -pair-fed (HFD-PF) and High fat diet- Ginkgo biloba (HFD-GbE) (N=10 per group). Fatty acid results are presented as area % percentage mean and standard error of the mean (SEM), and statistically analysed by one-way ANOVA with Tukey's Post-hoc test. The level of statistical significance was set at * $p < 0.05$.

	HFD-S		HFD-PF		HFD-GbE		p value		
	Mean %	SEM	Mean %	SEM	Mean %	SEM	S Vs PF	S Vs GbE	PF Vs GbE
C12:0	0.04	± <0.01	0.05	± <0.01	0.04	± <0.01	0.03	0.05	0.05
C14:0	0.58	± 0.01	0.65	± 0.01	0.61	± 0.01	0.20	0.01	0.01
C16:0	20.83	± 0.11	20.93	± 0.16	20.85	± 0.14	0.87	>0.99	0.90
C18:0	5.65	± 0.15	6.28	± 0.11	5.96	± 0.15	0.01	0.27	0.26
C20:0	0.06	± <0.01	0.07	± <0.01	0.06	± <0.01	0.21	0.85	0.46
C22:0	0.01	± <0.01	0.01	± <0.01	0.01	± <0.01	0.44	0.56	>0.99
∑SFA	27.63	± 0.24	28.42	± 0.15	28.02	± 0.27	0.05	0.44	0.44
C16:1n7	1.36	± 0.05	1.33	± 0.06	1.35	± 0.03	0.92	>0.99	0.95
C17:1	0.16	± 0.01	0.17	± 0.01	0.18	± <0.01	0.75	0.48	0.89
C18:1n7t	0.04	± <0.01	0.04	± <0.01	0.03	± <0.01	>0.99	0.86	0.92
C18:1n7	0.30	± <0.01	1.96	± 0.21	2.27	± 0.01	0.72	0.94	0.48
C18:1n9 <i>trans</i>	0.29	± 0.22	0.09	± 0.01	0.08	± <0.01	0.51	0.47	>0.99
C18:1n9	46.07	± 0.29	43.81	± 0.26	43.71	± 0.48	0.0004	0.0002	0.98
C20:1n9	0.29	± 0.01	0.30	± 0.01	0.30	± 0.01	0.67	0.78	0.98
∑DMA18:1	0.09	± 0.01	0.09	± 0.02	0.25	± 0.23	>0.99	0.66	0.66
∑C18:1	46.43	± 0.27	45.88	± 0.20	45.86	± 0.45	0.46	0.44	>0.99
∑n-7	1.43	± 0.08	3.32	± 0.22	11.74	± 5.40	0.90	0.07	0.16
∑n-9	46.36	± 0.28	44.11	± 0.25	44.02	± 0.48	0.0003	0.0002	0.99
∑MUFA	48.33	± 0.29	47.78	± 0.19	47.96	± 0.29	0.31	0.59	0.87
C18:2n6 <i>trans</i>	0.07	± 0.04	0.06	± <0.01	0.06	± <0.01	0.76	0.77	>0.99
C18:2n6	22.34	± 0.14	22.04	± 0.13	22.24	± 0.08	0.20	0.82	0.48
C18:3n6	0.05	± 0.01	0.03	± <0.01	0.03	± <0.01	0.69	0.28	0.75
C20:2n6	0.16	± 0.01	0.16	± 0.01	0.17	± 0.01	>0.99	0.84	0.87
C20:3n6	0.04	± <0.01	0.03	± <0.01	0.04	± <0.01	0.22	>0.99	0.23
C20:4n6	0.15	± 0.01	0.14	± 0.01	0.15	± 0.01	0.66	0.99	0.60
C22:4n6	0.05	± <0.01	0.03	± 0.01	0.04	± <0.01	0.01	0.54	0.06
∑n-6 PUFA	22.81	± 0.14	22.49	± 0.16	22.72	± 0.09	0.22	0.89	0.43
∑n-6 metabolites	2.69	± 2.26	0.39	± 0.04	0.43	± 0.03	0.44	0.45	>0.99
C18:3n-3 <i>trans</i>	0.05	± <0.01	0.05	± <0.01	0.05	± <0.01	0.60	0.78	0.95
C18:3n3	0.53	± 0.01	0.55	± 0.02	0.54	± 0.01	0.77	0.98	0.88
C20:3n3	0.02	± <0.01	0.02	± <0.01	0.01	± <0.01	0.67	0.95	0.84
C22:5n3	0.01	± <0.01	0.01	± <0.01	0.01	± <0.01	0.67	0.95	0.84
C22:6n3	0.01	± <0.01	0.09	± 0.08	0.01	± <0.01	0.32	>0.99	0.30
∑n-3 PUFA	0.61	± 0.01	0.68	± 0.06	0.60	± 0.01	0.39	0.99	0.34
∑n-3 metabolites	0.08	± 0.05	0.08	± 0.06	0.02	± <0.01	>0.99	0.62	0.61
∑PUFA	23.42	± 0.14	23.17	± 0.15	23.33	± 0.10	0.39	0.88	0.68
∑UFA	71.75	± 0.26	70.95	± 0.15	71.29	± 0.28	0.06	0.37	0.57

Table 43. Retroperitoneal Triglyceride fatty acid methyl esters (FAME) ratios for high fat diet groups; High fat diet with-saline (HFD-S), High fat diet -pair-fed (HFD-PF) and High fat diet- Ginkgo biloba (HFD-GbE) (N=10 per group). Results presented as mean an (SEM), and statistically analysed by one-way ANOVA with Tukey's Post-hoc test. The level of statistical significance was set at * $p < 0.05$.

	HFD-S		HFD-PF		HFD-GbE		p value		
	Mean	SEM	Mean	SEM	Mean	SEM	S Vs PF	S Vs GbE	PF Vs GbE
Σ MUFA/ Σ PUFA	2.06	± 0.02	2.06	± 0.02	2.06	± 0.02	>0.99	0.95	0.97
Σ MUFA/ Σ SFA	0.57	± 0.01	0.59	± 0.01	0.58	± 0.01	0.11	0.48	0.62
Σ PUFA/ Σ SFA	0.85	± 0.01	0.82	± 0.01	0.83	± 0.01	0.03	0.44	0.33
Σ UFA/ Σ SFA	2.60	± 0.03	2.50	± 0.02	2.55	± 0.03	0.05	0.42	0.46
C18:0/C16:0	0.50	± 0.23	0.30	± 0.01	0.29	± 0.01	0.53	0.49	>0.99
C16:1n-7/C16:0	1.69	± 1.63	0.06	± <0.01	0.06	± <0.01	0.45	0.45	>0.99
C18:1n-9/C16:0	45.81	± 43.6	2.09	± 0.02	2.12	± 0.03	0.45	0.45	>0.99
C18:1n-9/C16:1n-7	34.37	± 1.35	33.47	± 1.59	32.27	± 0.77	0.94	0.23	0.38
C18:1n-7/C18:0	0.58	± 0.58	0.31	± 0.03	1.65	± 0.85	0.99	0.23	0.16
C18:1/C18:0	25.62	± 17.47	7.33	± 0.13	7.75	± 0.25	0.42	0.43	>0.99
n-6/n-3	37.74	± 0.82	35.01	± 2.27	37.80	± 0.39	0.37	>0.99	0.36
C18:2n-6/C18:3n-3	41.91	± 0.74	40.67	± 1.37	41.35	± 0.52	0.63	0.91	0.87
C20:4n-6/C20:3n-6	3.27	± 0.36	4.42	± 0.41	3.73	± 0.16	0.04	0.55	0.27
C20:4n-6/C22:6n-3	17.10	± 1.93	17.55	± 4.43	18.92	± 1.30	0.99	0.89	0.96
C20:4n-6/C18:2n-6	0.01	± <0.01	0.01	± <0.01	0.01	± <0.01	0.69	0.99	0.63
C20:4n-6/C18:3n-3	0.35	± 0.07	0.25	± 0.02	0.29	± 0.02	0.23	0.55	0.81
C20:3n-3/C18:3n-3	2.96	± 2.93	0.04	± <0.01	0.02	± <0.01	0.41	0.40	>0.99
C22:5n-3/C18:3n-3	0.02	± 0.01	0.01	± <0.01	0.02	± <0.01	0.56	0.99	0.64
C22:6n-3/C18:3n-3	0.04	± 0.02	0.16	± 0.15	0.02	± <0.01	0.64	0.97	0.50
C22:6n-3/C22:5n-3	0.94	± 0.12	12.71	± 11.57	0.91	± 0.07	0.44	>0.99	0.42
C18:2n6/C16:0	1.07	± 0.01	1.05	± 0.01	1.07	± 0.01	0.34	0.91	0.57
C18:3n3/C16:0	0.07	± 0.04	0.03	± <0.01	0.03	± <0.01	0.46	0.45	>0.99
C20:3n-6/C18:3n-6	1.11	± 0.15	1.08	± 0.16	1.22	± 0.15	0.92	0.35	0.19
C22:4n-6/C20:4n-6	3.34	± 0.12	5.97	± 0.64	3.74	± 0.16	<0.0001	0.67	0.0002
C18:3n6/C22:4n6	45.07	± 0.29	44.53	± 0.28	44.93	± 0.17	0.29	0.91	0.50
1 (% monoenoics)	48.33	± 0.28	47.78	± 0.18	47.96	± 0.27	0.82	0.79	0.42
2 (% dienoics)	45.07	± 0.27	44.53	± 0.26	44.93	± 0.16	0.99	0.38	0.31
3 (% trienoics)	1.99	± 0.05	1.99	± 0.06	1.96	± 0.03	0.91	0.10	0.04
4 (% tetraenoics)	0.73	± 0.08	0.65	± 0.08	0.78	± 0.06	0.50	0.47	>0.99
5 (% pentaenoics)	0.05	± 0.01	0.03	± 0.01	0.05	± 0.01	0.34	0.68	0.82
6 (% hexaenoics)	0.05	± 0.01	0.38	± 0.32	0.05	± 0.01	0.91	>0.99	0.90
Unsaturation Index	96.23	± 0.24	95.35	± 0.35	95.73	± 0.29	0.59	0.69	0.98

Table 44. Mesenteric triglyceride fatty acid methyl esters (FAME) for normal fat diet (NFD) and high fat diet (HFD-S) (N=10 per group). Fatty acid results are presented as area % percentage mean and standard error of the mean (SEM), and statistically analysed by Students t-test. The level of statistical significance was set at *p < 0.05.

	HFD-S		HFD-PF		HFD-GbE		p value		
	Mean %	SEM	Mean %	SEM	Mean %	SEM	S Vs PF	S Vs GbE	PF Vs GbE
C12:0	0.05 ±	<0.01	0.04 ±	0.01	0.04 ±	0.01	0.92	0.79	0.97
C14:0	0.65 ±	0.01	0.65 ±	0.02	0.60 ±	0.02	0.97	>0.99	>0.99
C16:0	20.23 ±	0.15	20.01 ±	0.18	19.92 ±	0.11	0.55	0.30	0.91
C17:0	0.30 ±	0.01	0.30 ±	0.01	0.28 ±	0.01	>0.99	0.002	0.002
C18:0	6.02 ±	0.17	6.30 ±	0.21	5.64 ±	0.10	0.44	0.22	0.02
C20:0	0.08 ±	0.01	0.01 ±	0.01	0.09 ±	0.01	<0.0001	0.45	<0.0001
C21:0	0.11 ±	0.01	0.08 ±	0.01	0.08 ±	0.01	0.20	0.16	>0.99
DMA18:0	0.16 ±	0.02	0.16 ±	0.03	0.29 ±	0.06	0.96	0.10	0.05
∑SFA	27.69 ±	0.23	27.65 ±	0.16	27.04 ±	0.14	0.98	0.04	0.07
C16:1n-7	1.36 ±	0.06	1.35 ±	0.09	1.27 ±	0.05	>0.99	0.57	0.64
C17:1	0.19 ±	0.01	0.18 ±	0.01	0.15 ±	0.02	0.85	0.08	0.24
C18:1n7 <i>trans</i>	0.04 ±	0.01	0.11 ±	0.02	0.04 ±	0.01	0.0002	>0.99	0.0003
C18:1n7	2.48 ±	0.02	2.56 ±	0.03	2.46 ±	0.04	0.18	0.93	0.09
C18:1n-9t	0.07 ±	0.01	0.08 ±	0.01	0.08 ±	0.01	0.35	0.30	>0.99
C18:1n-9	43.80 ±	0.27	43.94 ±	0.30	44.65 ±	0.12	0.91	0.04	0.12
C20:1n9	0.32 ±	0.01	0.33 ±	0.01	0.31 ±	0.01	0.75	0.70	0.31
∑DMA18:1	0.03 ±	0.01	0.05 ±	<0.01	0.03 ±	0.01	<0.0001	<0.0001	<0.0001
∑C18:1	44.62 ±	0.52	44.03 ±	0.30	44.73 ±	0.12	0.48	0.97	0.36
∑n-7	3.88 ±	0.07	4.02 ±	0.08	3.77 ±	0.08	0.38	0.55	0.06
∑n-9	44.19 ±	0.27	44.36 ±	0.30	45.04 ±	0.12	0.88	0.04	0.13
∑MUFA	48.30 ±	0.32	48.61 ±	0.28	48.99 ±	0.12	0.65	0.13	0.54
C18:2n-6 <i>trans</i>	0.01 ±	0.01	0.01 ±	0.01	0.05 ±	0.01	0.37	<0.0001	0.0001
C18:2n-6	22.34 ±	0.19	22.27 ±	0.19	22.27 ±	0.11	0.96	0.96	>0.99
C18:3n-6	0.02 ±	0.01	0.01 ±	0.01	0.04 ±	0.01	0.55	<0.0001	<0.0001
C20:2n-6	0.16 ±	0.01	0.15 ±	0.01	0.14 ±	0.01	0.84	0.29	0.62
C20:3n-6	0.03 ±	0.01	0.03 ±	0.01	0.03 ±	0.01	0.81	>0.99	0.76
C20:4n-6	0.14 ±	0.01	0.12 ±	0.01	0.12 ±	0.01	0.46	0.34	0.98
C22:4n-6	0.07 ±	0.01	0.02 ±	0.01	0.06 ±	0.01	0.004	0.74	0.02
∑n-6 PUFA	22.75 ±	0.18	22.62 ±	0.20	22.71 ±	0.12	0.86	0.99	0.92
∑n-6 metabolites	0.41 ±	0.03	0.33 ±	0.03	0.38 ±	0.01	0.10	0.75	0.34
C18:3n-3	0.55 ±	0.02	0.55 ±	0.02	0.49 ±	0.01	>0.99	0.07	0.07
C22:5n-3	0.01 ±	0.01	0.01 ±	0.01	0.01 ±	0.01	0.87	0.28	0.13
C22:6n-3	0.01 ±	0.01	0.01 ±	0.01	0.01 ±	0.01	>0.99	0.63	0.61
∑n-3 PUFA	0.56 ±	0.02	0.56 ±	0.02	0.51 ±	0.01	0.54	0.61	0.99
∑n-3 metabolites	0.02 ±	0.01	0.01 ±	0.01	0.02 ±	0.01	0.74	0.33	0.09
∑PUFA	23.31 ±	0.19	23.18 ±	0.22	23.23 ±	0.12	0.42	>0.99	0.44
∑UFA	71.60 ±	0.19	71.79 ±	0.16	72.22 ±	0.14	0.47	0.99	0.41

Table 45. Mesenteric triglyceride fatty acid methyl esters (FAME) ratios for normal fat diet (NFD) and high fat diet (HFD-S) (N=10 per group). Results presented as mean an (SEM), and statistically analysed by one-way ANOVA with Tukey's Post-hoc test. The level of statistical significance was set at * $p < 0.05$.

	HFD-S		HFD-PF		HFD-GbE		p value		
	Mean %	SEM	Mean %	SEM	Mean %	SEM	S Vs PF	S Vs GbE	PF Vs GbE
Σ MUFA/ Σ PUFA	2.07 ± 0.03		2.10 ± 0.03		2.11 ± 0.01		0.95	0.28	0.18
Σ MUFA/ Σ SFA	1.19 ± 0.01		1.19 ± 0.01		1.16 ± 0.01		0.95	0.28	0.18
Σ PUFA/ Σ SFA	0.48 ± 0.01		0.48 ± 0.01		0.47 ± 0.01		0.78	0.53	0.92
Σ UFA/ Σ SFA	2.59 ± 0.03		2.60 ± 0.02		2.67 ± 0.02		0.95	0.04	0.08
C18:0/C16:0	0.30 ± 0.01		0.32 ± 0.01		0.28 ± 0.01		0.36	0.52	0.05
C16:1n-7/C16:0	0.07 ± 0.01		0.07 ± 0.01		0.06 ± 0.01		>0.99	0.70	0.68
C18:1n-9/C16:0	2.17 ± 0.03		2.20 ± 0.03		2.24 ± 0.02		0.64	0.09	0.45
C18:1n-9/C16:1n-7	32.72 ± 1.41		33.83 ± 2.67		35.85 ± 1.55		0.91	0.47	0.74
C18:1n-7/C18:0	0.42 ± 0.01		0.41 ± 0.01		0.44 ± 0.01		0.95	0.43	0.30
C18:1/C18:0	7.48 ± 0.25		7.05 ± 0.22		7.96 ± 0.14		0.33	0.24	0.01
n-6/n-3	40.82 ± 1.02		40.86 ± 1.71		44.62 ± 0.91		>0.99	0.09	0.10
C18:2n-6/C18:3n-3	41.25 ± 1.07		41.25 ± 1.70		45.58 ± 0.90		>0.99	0.05	0.05
C20:4n-6/C20:3n-6	4.91 ± 0.33		5.56 ± 0.44		4.38 ± 0.32		0.44	0.56	0.08
C20:4n-6/C22:6n-3	16.88 ± 1.82		15.79 ± 2.02		13.25 ± 1.42		0.90	0.31	0.57
C20:4n-6/C18:2n-6	0.01 ± 0.01		0.01 ± 0.01		0.01 ± 0.01		0.46	0.23	0.90
C20:4n-6/C18:3n-3	0.25 ± 0.02		0.22 ± 0.01		0.24 ± 0.01		0.31	0.93	0.50
C22:5n-3/C18:3n-3	0.01 ± 0.01		0.01 ± 0.01		0.02 ± 0.01		0.78	0.12	0.03
C22:6n-3/C18:3n-3	0.02 ± 0.01		0.02 ± 0.01		0.02 ± 0.01		0.98	0.42	0.34
C22:6n-3/C22:5n-3	1.28 ± 0.24		1.06 ± 0.18		1.16 ± 0.24		0.83	0.92	0.96
C18:2n6/C16:0	1.10 ± 0.01		1.11 ± 0.01		1.12 ± 0.01		0.82	0.65	0.96
C18:3n3/C16:0	0.03 ± 0.01		0.03 ± 0.01		0.02 ± 0.01		0.91	0.08	0.04
C18:3n-6/C18:2n-6	<0.01 ± 0.01		<0.01 ± 0.01		<0.01 ± 0.01		0.61	0.02	0.002
C20:3n-6/C18:3n-6	2.09 ± 0.32		1.92 ± 0.34		0.85 ± 0.13		0.90	0.01	0.03
C22:4n-6/C20:4n-6	2.92 ± 0.70		6.32 ± 0.51		1.98 ± 0.05		0.0002	0.38	<0.0001
1 (% monoenoics)	48.30 ± 0.32		43.75 ± 4.87		48.99 ± 0.12		0.50	0.98	0.40
2 (% dienoics)	44.99 ± 0.37		40.39 ± 4.50		44.94 ± 0.22		0.44	>0.99	0.45
3 (% trienoics)	1.77 ± 0.05		1.58 ± 0.19		1.67 ± 0.03		0.48	0.80	0.86
4 (% tetraenoics)	0.82 ± 0.07		0.52 ± 0.08		0.72 ± 0.03		0.01	0.49	0.09
5 (% pentaenoics)	0.03 ± 0.01		0.03 ± 0.01		0.05 ± 0.01		0.71	0.29	0.07
6 (% hexaenoics)	0.05 ± 0.01		0.05 ± 0.01		0.07 ± 0.01		0.89	0.65	0.38
Unsaturation Index	95.97 ± 0.21		86.31 ± 9.59		96.43 ± 0.26		0.45	>0.99	0.41

5.4 RET and MES CE

The significance and importance of CE changes has been covered already Chapter 1 and Chapter 4. CE represent FA's either available from the diet or FA that have been liberated from the phospholipid membrane to transport cholesterol around the body (Nakamura *et al.*, 2004).

5.4.1 RET -CE– NFD vs HFD

Significant changes occur across SFA, MUFA and PUFA % levels in the CE fatty acid profile following an HFD, summarised in Table 46 and Table 47. Total SFA increased in HFD-S by 20% (CE, HFD-S $24.86 \pm 0.29\%$; NFD $20.76 \pm 0.63\%$, $p=0.001$), largely due to the increase in C18:0 (CE, HFD-S $5.36 \pm 0.11\%$; NFD $2.67 \pm 0.07\%$, $p<0.0001$) (Table 46). This is around 4% less in area percentage than the amount of SFA found within the TAG fractions of both NFD and HFD (TAG, HFD-S $27.63 \pm 0.24\%$; NFD $23.45 \pm 0.66\%$, $p=0.0007$). This increased the C18:0/C16:0 ratio in the NFD by 83% (HFD-S 0.29 ± 0.00 ; NFD 0.16 ± 0.00 , $p<0.0001$) (Table 47). Total MUFA increased in HFD-S by 74% (HFD-S $44.02 \pm 0.2\%$; NFD $25.24 \pm 0.38\%$, $p<0.0001$), mostly due to the increase in C18:1n-9 (CE, HFD-S $41.75 \pm 0.22\%$; NFD $21.10 \pm 0.22\%$, $p<0.0001$) (Table 46). This is an additional increase of 7% compared to MUFA levels in the TAG fraction which increased by 67% in HFD-S compared to NFD (TAG, HFD-S $48.33 \pm 0.29\%$; NFD $28.95 \pm 0.45\%$, $p<0.0001$) (Table 46) but does not explain the difference lower 60% increase in total RET lipid profiles (Total-FA, HFD, $47.28 \pm 0.32\%$, NFD, $29.59 \pm 0.44\%$, $p<0.0001$) (Table 30). Total PUFA in CE decreased in HFD-S by 42% (CE, HFD-S $29.70 \pm 0.28\%$; NFD $52.08 \pm 1.06\%$, $p<0.0001$) (Table 46). These PUFA levels are approximately 6% higher for both the NFD and HFD groups compared to TAG levels (TAG-PUFA decreased in HFD by 49% compared to NFD (HFD-S $23.42 \pm 0.14\%$; NFD $45.77 \pm 0.99\%$, $p<0.0001$), like total lipid profiles that showed a 48% decrease (RET -Total-FA PUFA; NFD, $23.51 \pm 0.12\%$, HFD, $45.2 \pm 1\%$; $p<0.0001$) (Table 30). This CE PUFA change included a decrease of 41% in n-6 PUFA (HFD-S $28.2 \pm 0.21\%$; NFD $47.95 \pm 1.05\%$, $p<0.0001$) largely attributable to C18:2n-6 (HFD-S $27.35 \pm 0.16\%$; NFD $46.14 \pm 1.08\%$, $p<0.0001$) but also n-6 metabolites (HFD-S $0.85 \pm 0.09\%$; NFD $1.76 \pm 0.11\%$, $p=0.0003$) (Table 46). Similarly, n-3 PUFA decreased in HFD-S by 64% (HFD-S $1.5 \pm 0.07\%$; NFD $4.14 \pm 0.18\%$, $p<0.0001$) with a 79% decrease in n-6 metabolites (HFD-S $1.5 \pm 0.07\%$; NFD $4.14 \pm 0.18\%$, $p<0.0001$) (

Table 46). These changes were reflected in the n-6/n-3 ratio which increased by 63% in the HFD group (HFD-S 19.19 ± 0.88 ; NFD 11.78 ± 0.55 , $p < 0.0001$) (Table 47). The changes in the SFA, MUFA and PUFA were also reflected in the CE fatty acid % ratios of the HFD-S subset (Table 47) such as a 204% increase in the $\Sigma\text{MUFA}/\Sigma\text{PUFA}$ (HFD-S 1.48 ± 0.02 ; NFD 0.49 ± 0.02 , $p < 0.0001$), a 31% decrease in the $\Sigma\text{MUFA}/\Sigma\text{SFA}$ ratio (HFD-S 0.56 ± 0.01 ; NFD 0.82 ± 0.01 , $p < 0.0001$) and a 53% decrease in the $\Sigma\text{PUFA}/\Sigma\text{SFA}$ ratio (HFD-S 1.20 ± 0.02 ; NFD 2.54 ± 0.12 , $p < 0.0001$). Overall, a 21% decrease in the $\Sigma\text{UFA}/\Sigma\text{SFA}$ ratio (HFD-S 2.97 ± 0.04 ; NFD 3.76 ± 0.15 , $P = 0.003$) was seen. Ultimately this resulted in a decrease of 22% in the unsaturation index of the HFD group (HFD-S 106.31 ± 0.69 ; NFD 136.10 ± 1.87 , $p < 0.0001$) (Table 47).

5.4.2 MES-CE – NFD vs HFD

When comparing MES NFD and HFD-S CE, significant changes occur across SFA, MUFA and PUFA % levels, as well as their ratios (Table 48 and Table 49). In the HFD-S group, total SFA levels increased by 48% compared to the NFD group (ΣSFA ; NFD, $14.96 \pm 0.51\%$; HFD-S, $22.19 \pm 0.38\%$, $p < 0.0001$). This was due to the 35% and 172% significant increase in both C16:0 (C16:0; NFD, $12.20 \pm 0.46\%$; HFD-S, $16.46 \pm 0.27\%$, $p < 0.0001$) and C18:0 (C18:0; NFD, $1.63 \pm 0.05\%$; HFD-S, $4.43 \pm 0.16\%$, $p < 0.0001$), respectively (Table 48). The increase in SFA in MES-CE for the HFD-S is much higher than that found in the RET-CE fraction, that increased by 20% (RET-CE, NFD $20.76 \pm 0.63\%$; HFD-S $24.86 \pm 0.29\%$, $p = 0.001$) (Table 48). This was due to SFA represents a lower percentage of the CE fraction in the NFD MES VAT (~21%), compared to NFD RET-VAT (~14%). In contrast, SFA represented ~22% of the MES-CE-profile, compared to ~25% in RET-CE. Furthermore, in the MES HFD-S group, total MUFA increased by 88% compared to the NFD group (ΣMUFA ; NFD, $22.74 \pm 0.51\%$; HFD-S, $42.84 \pm 0.47\%$, $p < 0.0001$). This was attributed to the 25% and 100% increases in C18:1n-7 (C18:1n-7; NFD, $1.83 \pm 0.10\%$; HFD-S, $2.29 \pm 0.03\%$, $p = 0.007$) and C18:1n-9 (C18:1n-9; NFD, $19.27 \pm 0.27\%$; HFD-S, $38.44 \pm 0.45\%$, $p < 0.0001$), respectively (Table 48). These percentages for total MUFA are slightly lower than that seen in RET-CE-MUFA (NFD 25.24 ± 0.38 ; HFD-S $44.02 \pm 0.2\%$, $p < 0.0001$) (Table 46) although both RET and MES MUFA percentages increased relatively consistently following a HFD in both tissues, with a MUFA NFD/HFD ratio of 0.53 in MES tissue, and 0.57 in RET tissue. The increase of 47% in the C18:1n-9/C16:0 ratio of the HFD-S group (C18:1n-9/C16:0; NFD, 1.59 ± 0.04 ; HFD-S, 2.34 ± 0.04 , $p < 0.0001$) (Table 49) suggests that more C18:1n-9 is either more available or is being liberated into the CE fraction in the HFD group. To explore this further, when looking at the overall difference in C18:1n-9

between the NFD and the HFD, we see that in TAG, the NFD/HFD C18:1n-9 ratio is 0.58 (NFD/HFD=0.58), while in CE, the ratio is 0.5, which suggests that more overall C18:1n-9 is being incorporated into the CE fraction in an HFD, compared to that stored in TAG. As C18:1n-9 levels are higher in both TAG and CE compared to that available from the respective rat chows, this again points to DNL occurring either at a local level within the adipocyte, or in the liver and further stored in the adipocyte.

MES CE PUFA levels also decreased in the HFD-S group compared to the NFD group by 44% (Σ PUFA; NFD,60.13 \pm 1.02%; HFD-S,33.55 \pm 0.63%, p <0.0001) (Table 48). This is very similar to the 42% decrease also seen in RET tissue. MES-CE n-6 PUFA decreased by 42% (Σ n-6 PUFA; NFD,55.37 \pm 0.96%; HFD-S,31.96 \pm 0.57%, p <0.0001), predominantly from the 42% decrease in C18:2n-6 (C18:2n-6; NFD,53.60 \pm 0.95%; HFD-S,31.19 \pm 0.56%, p <0.0001) but also in the 56% decrease in n-6 metabolites (Σ n-6metabolites; NFD,1.73 \pm 0.06%; HFD-S,0.76 \pm 0.05%, p <0.0001) (Table 48). Similarly, n-3PUFA also decreased by 67% (MES-CE- Σ n-3 PUFA; NFD,4.76 \pm 0.12%; HFD-S,1.59 \pm 0.08%, p <0.0001), predominantly from the 64% decrease in C18:3n-3 (C18:3n-3; NFD,4.22 \pm 0.11%; HFD-S,1.50 \pm 0.08%, p <0.0001), as well as the 83% decrease in n-3 metabolites (Σ n-3 metabolites; NFD,0.54 \pm 0.02%; HFD-S,0.09 \pm 0.01%, p <0.0001) (Table 48). The n-6/n-3 ratio in HFD-S also increased by 74% (n-6/n-3; NFD,11.68 \pm 0.26; HFD-S,20.47 \pm 0.86, p <0.0001) compared to NFD (Table 49).

Overall, total UFA represented ~83% and ~76% of NFD and HFD-S CE fatty acids, respectively, with a significant decrease of 8% seen in the HFD-S group (Σ UFA; NFD,82.87 \pm 0.56%; HFD-S,76.38 \pm 0.35%, p <0.0001) (Table 48). This, along with the increase in SFA saw a decrease in the UFA/SFA ratio by 38% (Σ UFA/ Σ SFA; NFD,5.60 \pm 0.21; HFD-S,3.45 \pm 0.07, p <0.0001) (Table 49). This suggests that mostly UFA are being liberated from the sn2-position of phospholipids for the synthesis of CE, but the availability of UFA is decreased by 8% in the HFD-S group, which may indicate that more SFA are being incorporated at the sn2- position of the phospholipid PC, which may result in a more rigid membrane in an HFD. This hypothesis is also backed up by the 26% decrease in the unsaturation index following a HFD (Unsaturation Index; NFD,151.73 \pm 1.69; HFD-S,112.65 \pm 1.01, p <0.0001) (Table 49). Furthermore, the MUFA/PUFA ratio increased by 237% (Σ MUFA/ Σ PUFA; NFD, 0.38 \pm 0.02; HFD-S, 1.28 \pm 0.04, p <0.0001) (Table 49) which shows that much less PUFA are available for CE synthesis, indicating that a much larger portion of fatty acids at the sn2-position of the PC in the phospholipid membrane is made from MUFA. Firstly, this suggests that less PUFA are available for incorporation into the membrane following a HFD, which makes sense owing to the increase in MUFA and decrease

in PUFA in HFD rat chow. Secondly utilized from the membrane for the synthesis of other molecules such as oxylipins and are being replaced by MUFA rather than PUFA.

The CE FA data from RET tissue for the NFD and HFD groups suggests that higher amounts and ratios of SFA and MUFA and lower amounts of PUFA, both in n-6 and n-3 form are being incorporated to and/or cleaved from the sn-2 bonding site of PC of the lipid membrane. This may indicate that the lipid membrane of the adipocyte is less fluid in the HFD group compared to the NFD group. This may occur due to lower amounts of PUFA and double bonds, or oxidation and utilization of PUFA in another pathway such as pro-resolving mediation of inflammation. As previously mentioned, in peripheral tissues CE are predominantly synthesised by LCAT which utilizes PC as a source of acyl chains. LCAT associates preferentially with the HDL lipoprotein and catalyses the transfer of the sn-2 fatty acid of PC to cholesterol to produce CE and LPC (Nakamura *et al.*, 2004). It should therefore be considered pragmatic to also consider PPL fatty acids as a source of CE when analysing CE profile levels. Of the fatty acids incorporated into PPLs, one fatty acid may be saturated, while the other generally carries a double bond, allowing for fluidity when packaged together, affecting the fluidity of the membrane (Alberts *et al.*, 2002). The incorporation of ω -3 fatty acids into PPLs such as EPA and DHA, mostly occurs in the sn-2 position of the PPL and changes the organization and size of lipid rafts (De-Santis *et al.*, 2018; Hou, McMurray and Chapkin, 2016; Schumann, 2016). Certain PPLs favour the inner leaflet such as PE, PS and PI and tend to be richer in PUFA and lower in SFA while P and sphingomyelin favour the outer leaflet and tend to be richer in SFA and lower in PUFA (Lorent *et al.*, 2020; van IJendoorn, Agnetti and Gassama-Diagne, 2020; Rivel, Ramseyer and Yesylevskyy, 2019; Simons and Sampaio, 2011; van Meer, 2011). PPL unsaturation is similarly asymmetric, with a two-fold higher distribution of unsaturated fatty acids in the cytoplasmic leaflet compared to the exoplasmic leaflet (Lorent *et al.*, 2020). As covered in Chapter 1, PUFA are used to produce inflammation molecules including resolvins, protectins and maresins, lipoxins and eicosanoids (Schebb *et al.*, 2022; Liput *et al.* 2021; Astarita *et al.* 2015; Gabbs *et al.* 2015; Godessart *et al.* 1996). The significantly decreased amounts of RET-CE n-6 PUFA ($p < 0.0001$), VLCFA n-6 metabolite ($p = 0.0003$), n-3 PUFA ($p < 0.0001$), and VLCFA n-3 metabolite levels ($p < 0.0001$) in the HFD-S group further suggest an increased inflammatory state. Looking into the PPL fraction may provide more insight.

5.4.3 RET-CE HFD GbE treatment

Looking at the RET-CE of the three HFD subsets (Table 50 and Table 51), in a similar trend to that of Total and TAG FA levels, fewer significant changes occurred between the groups. With that said, however, some changes of note include the significant increase in C18:1n-7 in both the HFD-PF and HFD-GbE groups compared to HFD-S. Very little C18:1n-7 (vaccenic acid) occurred in the HFD-S group (~0.01%), but this increase to 2% in HFD-PF and 2.25% in HFD-GbE (Table 50). This coincided with significantly lower amounts of C18:1n-9 in both HFD-PF (~38.7%, $p < 0.0001$) and HFD-GbE groups (~39.8%, $p = 0.0006$) compared to HFD-S (~42.1%) (Table 50). The C18:1n-9/C16:0 that did not change between the HFD-S and HFD-GbE group but did decrease in HFD-PF compared to both ($p = 0.04$, $p = 0.01$, respectively) (Table 51). C18:1n-7 levels in both the PF and GbE group returned to levels comparable to the NFD group.

5.4.4 MES-CE HFD GbE treatment

Very few changes in FA levels occurred in the HFD subsets treated with GbE or calorie restricted (HFD-PF) (Table 52 and Table 53). Interestingly, both the UFA level and unsaturation index remained completely the same for all three groups. This was also seen in the MUFA/SFA, MUFA/PUFA, PUFA/SFA, UFA/SFA and n-6/n-3 ratios (Table 53). As previously described, MAG and DAG are both pre-cursors and by-products of TAG synthesis and lysis, respectively. This occurs in liver, adipose tissues and other peripheral tissues, by a variety of enzymes. There was a small decrease in C18:0 levels in the HFD-GbE group compared to HFD-PF, though no changes occurred between HFD-S and HFD-PF ($p = 0.16$), or HFD-S and HFD-GbE ($p = 0.77$) (Table 52). C18:1n-7 levels increased significantly in the HFD-PF group ($p = 0.001$) and non-significantly in the HFD-GbE ($p = 0.12$) compared to HFD-S. While no significant differences occurred in total PUFAs, both in total n-6 PUFA and total n-3PUFA, a decrease in C18:3n-6 levels were seen for HFD-PF ($p = 0.01$) and an increase in HFD-GbE ($p = 0.09$), compared to the HFD-S group. The decrease in HFD-PF was also significant compared to HFD-GbE ($p < 0.0001$) (Table 52).

Together this may suggest that calorie restriction may be responsible for the change rather than GbE treatment. C18:1n-7 is a major component of the PPL cardiolipin (CL) found in mitochondrial membranes, with CL accounting for up to 20% of mitochondrial PPL membrane (Bueno *et al.*, 2015). Mainly located in the inner mitochondrial membrane (IMM), CL is an important co-factor for

cholesterol translocation from the outer mitochondrial membrane to the IMM, playing an important role in the importing of proteins (Schlattner *et al.*, 2014). Adenylate cyclase activity is reported to be enhanced with the incorporation of C18:1n-7 in erythrocytes (Henis, Rimonl and Felderl, 1982; Orly and Schramm, 1975). Adenylate cyclase is an important molecule facilitating lipolysis and is explored further in the chapter (Nielsen, Jessen, *et al.*, 2014; Reid *et al.*, 2008). As shown in Figure 10, although body weight did not decrease in the PF and GbE groups, body weight gain did decrease after 14 days of treatment, significantly so in the PF group. It is possible that in both groups, the rats began to under lipolysis, and this may correspond with C18:1n-7 levels although this would need to be further explored. No significant differences in CE PUFA levels were seen between the three HFD subsets.

Table 46. Retroperitoneal Cholesteryl ester total lipid fatty acid methyl esters (FAME) for normal fat diet (NFD) and high fat diet (HFD-S) (N=10 per group). Fatty acid results are presented as area % percentage mean and standard error of the mean (SEM), and statistically analysed by Students t-test. The level of statistical significance was set at * $p < 0.05$.

	NFD			HFD-S			p value
	Mean %	±	SEM	Mean %	±	SEM	
C14:0	0.55	±	0.04	0.54	±	0.03	>0.99
C15:0	0.19	±	0.01	0.09	±	<0.01	<<0.0101
C16:0	16.83	±	0.57	18.36	±	0.20	0.38
C17:0	0.25	±	<0.01	0.27	±	<0.01	0.36
C18:0	2.67	±	0.07	5.36	±	0.11	<0.0001
C20:0	0.08	±	<0.01	0.09	±	0.01	0.99
C21:0	0.09	±	0.01	0.12	±	<0.01	0.003
DMA18:0	0.06	±	<0.01	0.03	±	0.01	0.39
ΣSFA	20.76	±	0.63	24.86	±	0.29	0.001
C14:1n7	0.04	±	0.01	<0.01	±	<0.01	<0.0001
C15:1	0.04	±	<0.01	<0.01	±	<0.01	<0.0001
C16:1n7	1.56	±	0.22	1.48	±	0.06	>0.99
C17:1	0.11	±	0.01	0.22	±	0.01	<0.0001
C18:1n7 <i>trans</i>	0.04	±	<0.01	0.02	±	0.01	0.33
C18:1n7	1.93	±	0.09	0.01	±	0.01	<0.0001
C18:1n9 <i>trans</i>	0.03	±	<0.01	0.08	±	<0.01	<0.0001
C18:1n9	21.10	±	0.22	41.75	±	0.22	<0.0001
C20:1n9	0.21	±	0.01	0.33	±	0.01	<0.0001
C20:3n-9	0.11	±	0.01	<0.01	±	<0.01	<0.0001
C22:1n9	0.01	±	0.01	<0.01	±	<0.01	0.99
C24:1n9	0.01	±	0.01	0.06	±	0.02	0.81
DMA18:1	0.07	±	0.01	0.07	±	0.01	>0.99
ΣC18:1	23.10	±	0.25	41.86	±	0.22	<0.0001
Σn-7	3.54	±	0.31	1.50	±	0.06	0.0003
Σn-9	21.45	±	0.21	42.14	±	0.22	<0.0001
ΣMUFA	25.24	±	0.38	44.02	±	0.20	<0.0001
C18:2n6 <i>trans</i>	0.05	±	0.01	<0.01	±	<0.01	<0.0001
C18:2n6	46.14	±	1.08	27.35	±	0.16	<0.0001
C18:3n6	0.16	±	0.01	0.10	±	0.01	0.02
C20:2n6	0.24	±	0.01	0.20	±	0.01	0.02
C20:3n6	0.18	±	0.01	0.12	±	0.01	0.17
C20:4n6	0.90	±	0.08	0.33	±	0.05	0.0004
C22:2n6	0.03	±	0.01	<0.01	±	<0.01	0.33
C22:4n6	0.25	±	0.01	0.10	±	0.04	0.04
ΣMUFA	25.24	±	0.38	44.02	±	0.20	<0.0001
Σn-6 PUFA	47.95	±	1.05	28.20	±	0.21	<0.0001
Σn-6 metabolites	1.76	±	0.11	0.85	±	0.09	0.0003
C18:3n-3 <i>trans</i>	0.07	±	0.02	0.13	±	0.01	0.59
C18:3n3	3.50	±	0.13	1.25	±	0.05	<0.0001
C20:3n3	0.04	±	0.01	<0.01	±	<0.01	0.0009
C20:5n3	0.09	±	0.01	<0.01	±	<0.01	<0.0001
C22:5n3	0.19	±	0.02	0.04	±	0.01	<0.0001
C22:6n3	0.24	±	0.03	0.08	±	0.04	0.09
Σn-6 PUFA	47.95	±	1.05	28.20	±	0.21	<0.0001
Σn-3 PUFA	4.14	±	0.18	1.50	±	0.07	<0.0001
Σn-3 metabolites	0.57	±	0.05	0.12	±	0.04	<0.0001
ΣPUFA	52.08	±	1.06	29.70	±	0.28	<0.0001
ΣUFA	77.32	±	0.70	73.72	±	0.23	0.01

Table 47. Retroperitoneal Cholesteryl ester fatty acid methyl esters (FAME) ratios for normal fat diet (NFD) and high fat diet (HFD-S) (N=10 per group). Results presented as mean an (SEM), and statistically analysed by one-way ANOVA with Tukey's Post-hoc test. The level of statistical significance was set at *p < 0.05.

	NFD			HFD-S			p value
	Mean %	±	SEM	Mean %	±	SEM	
ΣMUFA/ΣPUFA	0.49	±	0.02	1.48	±	0.02	<0.0001
ΣMUFA/ΣSFA	0.82	±	0.01	0.56	±	0.01	<0.0001
ΣPUFA/ΣSFA	2.54	±	0.12	1.20	±	0.02	<0.0001
ΣUFA/ΣSFA	3.76	±	0.15	2.97	±	0.04	0.003
C18:0/C16:0	0.16	±	<0.01	0.29	±	<0.01	<0.0001
C16:1n-7/C16:0	0.09	±	0.01	0.08	±	<0.01	0.99
C18:1n-9/C16:0	1.26	±	0.04	2.28	±	0.02	<0.0001
C18:1n-9/C16:1n-7	16.22	±	2.29	28.82	±	1.37	0.01
C18:1/C18:0	8.69	±	0.20	7.83	±	0.16	0.11
n-6/n-3	11.78	±	0.55	19.19	±	0.88	<0.0001
C18:2n-6/C18:3n-3	13.33	±	0.54	22.21	±	0.94	<0.0001
C20:4n-6/C20:3n-6	5.13	±	0.26	2.65	±	0.34	0.0009
C20:4n-6/C22:6n-3	3.85	±	0.16	7.68	±	1.55	0.39
C20:4n-6/C18:2n-6	0.02	±	<0.01	0.01	±	<0.01	0.23
C20:4n-6/C18:3n-3	0.25	±	0.01	0.26	±	0.04	>0.99
C22:5n-3/C18:3n-3	0.06	±	<0.01	0.03	±	<0.01	0.02
C22:6n-3/C18:3n-3	0.07	±	0.01	0.07	±	0.03	>0.99
C22:6n-3/C22:5n-3	1.23	±	0.07	2.45	±	1.14	0.99
C18:2n6/C16:0	2.79	±	0.15	1.49	±	0.02	<0.0001
C18:3n3/C16:0	0.21	±	0.01	0.07	±	<0.01	<0.0001
C20:3n-6/C18:3n-6	1.12	±	0.09	1.27	±	0.06	0.94
C22:4n-6/C20:4n-6	3.58	±	0.19	4.43	±	0.78	0.99
1 (% monoenoics)	23.66	±	0.41	44.02	±	0.20	<0.0001
2 (% dienoics)	92.92	±	2.14	55.11	±	0.33	<0.0001
3 (% trienoics)	12.06	±	0.45	4.80	±	0.26	<0.0001
4 (% tetraenoics)	4.60	±	0.35	1.72	±	0.29	0.0004
5 (% pentaenoics)	1.42	±	0.13	0.18	±	0.03	<0.0001
6 (% hexaenoics)	1.45	±	0.17	0.48	±	0.22	0.09
Unsaturation Index	136.10	±	1.87	106.31	±	0.69	<0.0001

Table 48. Mesenteric cholesteryl ester total lipid fatty acid methyl esters (FAME) for normal fat diet (NFD) and high fat diet (HFD-S) (N=10 per group). Fatty acid results are presented as area % percentage mean and standard error of the mean (SEM), and statistically analysed by Students t-test. The level of statistical significance was set at * $p < 0.05$.

	NFD			HFD-S			p value
	Mean	±	SEM	Mean	±	SEM	
C14:0	0.42	±	0.04	0.54	±	0.01	0.13
C15:0	0.16	±	0.01	0.08	±	0.01	<0.0001
C16:0	12.20	±	0.46	16.46	±	0.27	<0.0001
C17:0	0.26	±	0.01	0.28	±	0.01	0.72
C18:0	1.63	±	0.05	4.43	±	0.16	<0.0001
C20:0	0.07	±	0.01	0.09	±	0.01	0.31
C21:0	0.09	±	0.01	0.14	±	0.01	0.0033
C22:0	0.02	±	0.01	0.02	±	0.01	0.58
ΣSFA.DMA	0.08	±	0.01	0.14	±	0.02	0.05
ΣSFA	14.96	±	0.51	22.19	±	0.38	<0.0001
C16:1n-7	1.22	±	0.22	1.50	±	0.07	0.94
C17:1	0.10	±	0.01	0.19	±	0.01	0.0006
C18:1n-7 <i>trans</i>	0.04	±	0.01	0.04	±	0.01	0.99
C18:1n-7	1.83	±	0.10	2.29	±	0.03	0.007
C18:1n-9t	0.02	±	0.01	0.10	±	0.01	<0.0001
C18:1n-9	19.27	±	0.27	38.44	±	0.45	<0.0001
C20:1n-9	0.17	±	0.01	0.28	±	0.01	<0.0001
DMA 18:1	0.06	±	0.01	0.01	±	0.01	0.002
C18:1 Total	19.65	±	0.41	38.99	±	0.56	<0.0001
Σn-7	3.1	±	0.30	2.33	±	0.03	0.014
Σn-9	19.49	±	0.28	38.81	±	0.44	<0.0001
ΣMUFA	22.74	±	0.51	42.84	±	0.47	<0.0001
C18:2n-6 <i>trans</i>	0.05	±	0.01	0.01	±	0.01	0.002
C18:2n-6	53.60	±	0.95	31.19	±	0.56	<0.0001
C18:3n-6	0.15	±	0.01	0.09	±	0.01	0.0001
C20:2n-6	0.20	±	0.01	0.18	±	0.01	0.57
C20:3n-6	0.15	±	0.01	0.10	±	0.01	0.0021
C20:4n-6	0.92	±	0.05	0.31	±	0.03	<0.0001
C22:4n-6	0.29	±	0.01	0.07	±	0.01	<0.0001
Σn-6 PUFA	55.37	±	0.96	31.96	±	0.57	<0.0001
Σn-6metabolites	1.73	±	0.06	0.76	±	0.05	<0.0001
C18:3n-3	4.22	±	0.11	1.50	±	0.08	<0.0001
C20:3n-3	0.03	±	0.01	0.02	±	0.01	0.98
C20:5n-3	0.07	±	0.01	0.01	±	0.01	<0.0001
C22:5n-3	0.21	±	0.01	0.04	±	0.01	<0.0001
C22:6n-3	0.23	±	0.02	0.03	±	0.01	<0.0001
Σn-3 PUFA	4.76	±	0.12	1.59	±	0.08	<0.0001
Σn-3 metabolites	0.54	±	0.02	0.09	±	0.01	<0.0001
ΣPUFA	60.13	±	1.02	33.55	±	0.63	<0.0001
ΣUFA	82.87	±	0.56	76.38	±	0.35	<0.0001

Table 49. Mesenteric Cholesteryl ester fatty acid methyl esters (FAME) ratios for normal fat diet (NFD) and high fat diet (HFD-S) (N=10 per group). Results presented as mean an (SEM), and statistically analysed by one-way ANOVA with Tukey's Post-hoc test. The level of statistical significance was set at *p < 0.05.

	NFD			HFD-S			p value
	Mean	SEM		Mean	SEM		
ΣMUFA/ΣPUFA	0.38	±	0.02	1.28	±	0.04	<0.0001
ΣMUFA/ΣSFA	0.25	±	0.01	0.66	±	0.02	<0.0001
ΣPUFA/ΣSFA	2.66	±	0.10	0.79	±	0.02	<0.0001
ΣUFA/ΣSFA	5.60	±	0.21	3.45	±	0.07	<0.0001
C18:0/C16:0	0.13	±	0.01	0.27	±	0.01	<0.0001
C16:1n-7/C16:0	0.10	±	0.01	0.09	±	0.01	0.99
C18:1n-9/C16:0	1.59	±	0.04	2.34	±	0.04	<0.0001
C18:1n-9/C16:1n-7	20.24	±	3.19	26.17	±	1.23	0.72
C18:1n-7/C18:0	1.13	±	0.07	0.52	±	0.02	<0.0001
C18:1/C18:0	12.10	±	0.20	8.90	±	0.35	<0.0001
C15:0/C17:0	0.13	±	0.01	0.27	±	0.01	<0.0001
n-6/n-3	11.68	±	0.26	20.47	±	0.86	<0.0001
C18:2n-6/C18:3n-3	12.77	±	0.29	21.23	±	0.91	<0.0001
C20:4n-6/C20:3n-6	6.17	±	0.25	3.02	±	0.14	<0.0001
C20:4n-6/C22:6n-3	4.01	±	0.11	13.74	±	1.27	<0.0001
C20:4n-6/C18:2n-6	0.02	±	0.01	0.01	±	0.01	0.001
C20:4n-6/C18:3n-3	0.22	±	0.01	0.21	±	0.02	0.99
C20:3n-3/C18:3n-3	0.01	±	0.01	0.02	±	0.01	0.08
C20:5n-3/C18:3n-3	0.02	±	0.01	0.01	±	0.01	<0.0001
C22:5n-3/C18:3n-3	0.05	±	0.01	0.03	±	0.01	0.001
C22:6n-3/C18:3n-3	0.06	±	0.01	0.02	±	0.01	<0.0001
C22:6n-3/C22:5n-3	1.09	±	0.06	0.60	±	0.04	<0.0001
C18:2n6/C16:0	4.47	±	0.23	1.90	±	0.06	<0.0001
C18:3n3/C16:0	0.35	±	0.02	0.09	±	0.01	<0.0001
C20:3n-6/C18:3n-6	1.02	±	0.04	1.15	±	0.05	0.53
C22:4n-6/C20:4n-6	3.20	±	0.13	4.44	±	0.20	0.003
1 (% monoenoics)	22.74	±	0.51	42.84	±	0.47	<0.0001
2 (% dienoics)	107.75	±	1.89	62.76	±	1.11	<0.0001
3 (% trienoics)	13.62	±	0.33	5.15	±	0.27	<0.0001
4 (% tetraenoics)	4.81	±	0.24	1.54	±	0.14	<0.0001
5 (% pentaenoics)	1.41	±	0.05	0.21	±	0.03	<0.0001
6 (% hexaenoics)	1.39	±	0.10	0.15	±	0.03	<0.0001
Unsaturation Index	151.73	±	1.69	112.65	±	1.01	<0.0001

Table 50. Retroperitoneal Cholesteryl ester fatty acid methyl esters (FAME) for high fat diet groups; High fat diet with-saline (HFD-S), High fat diet -pair-fed (HFD-PF) and High fat diet- Ginkgo biloba (HFD-GbE) (N=10 per group). Fatty acid results are presented as area % percentage mean and standard error of the mean (SEM), and statistically analysed by one-way ANOVA with Tukey's Post-hoc test. The level of statistical significance was set at *p < 0.05.

	HFD-S		HFD-PF		HFD-GbE		S Vs PF	S Vs GbE	PF Vs GbE
	Mean %	SEM	Mean %	SEM	Mean %	SEM			
C14:0	0.54 ± 0.03	0.55 ± 0.01	0.40 ± 0.02	0.99	0.0005	0.0004			
C15:0	0.09 ± <0.01	0.08 ± <0.01	0.07 ± <0.01	0.0004	0.19	0.19			
C16:0	18.36 ± 0.20	18.17 ± 0.44	17.28 ± 0.32	0.20	0.92	0.92			
C17:0	0.27 ± <0.01	0.25 ± 0.01	0.26 ± 0.01	0.29	0.48	0.93			
C18:0	5.36 ± 0.11	5.28 ± 0.31	5.14 ± 0.30	0.97	0.81	0.92			
C20:0	0.09 ± 0.01	0.08 ± 0.01	0.07 ± 0.01	0.62	0.54	0.99			
C21:0	0.12 ± <0.01	0.13 ± <0.01	0.14 ± 0.01	0.85	0.11	0.28			
DMA18:0	0.03 ± 0.01	<0.01 ± <0.01	0.09 ± 0.02	0.45	0.02	0.0008			
ΣSFA	24.86 ± 0.29	24.56 ± 0.72	23.47 ± 0.59	0.92	0.21	0.38			
C16:1n7	1.48 ± 0.06	1.45 ± 0.07	1.41 ± 0.05	0.95	0.75	0.90			
C17:1	0.22 ± 0.01	0.20 ± 0.01	0.21 ± 0.01	0.07	0.31	0.71			
C18:1n7t	0.02 ± 0.01	0.01 ± <0.01	0.03 ± 0.01	0.81	0.53	0.22			
C18:1n7	0.01 ± 0.01	2.03 ± 0.02	2.25 ± 0.05	<0.0001	<0.0001	0.0001			
C18:1n9 trans	0.08 ± <0.01	0.10 ± 0.01	0.10 ± 0.01	0.39	0.46	0.99			
C18:1n9	41.75 ± 0.22	38.71 ± 0.41	39.79 ± 0.31	<0.0001	0.0006	0.06			
C20:1n9	0.33 ± 0.01	0.30 ± 0.02	0.30 ± 0.02	0.44	0.57	0.97			
C24:1n9	0.06 ± 0.02	0.04 ± 0.01	0.02 ± 0.01	0.76	0.24	0.61			
DMA18:1	0.07 ± 0.01	0.11 ± 0.02	0.01 ± <0.01	0.13	0.01	<0.0001			
ΣC18:1	41.86 ± 0.22	40.85 ± 0.41	42.17 ± 0.33	0.09	0.79	0.02			
Σn-7	1.50 ± 0.06	3.50 ± 0.06	3.69 ± 0.04	<0.0001	<0.0001	0.04			
Σn-9	42.14 ± 0.22	39.09 ± 0.40	40.15 ± 0.31	<0.0001	0.0004	0.07			
ΣMUFA	44.02 ± 0.20	42.99 ± 0.38	44.16 ± 0.32	0.06	0.94	0.03			
C18:2n6	27.35 ± 0.16	28.66 ± 0.75	28.77 ± 0.71	0.30	0.24	0.99			
C18:3n6	0.10 ± 0.01	0.07 ± 0.01	0.08 ± 0.01	0.06	0.12	0.94			
C20:2n6	0.20 ± 0.01	0.19 ± 0.02	0.21 ± 0.01	0.77	0.61	0.25			
C20:3n6	0.12 ± 0.01	0.11 ± 0.01	0.11 ± 0.01	0.70	0.63	0.99			
C20:4n6	0.33 ± 0.05	0.30 ± 0.04	0.36 ± 0.03	0.87	0.89	0.60			
C22:4n6	0.10 ± 0.04	0.06 ± 0.01	0.06 ± 0.01	0.37	0.41	>0.99			
Σn-6 PUFA	28.20 ± 0.21	29.44 ± 0.78	29.65 ± 0.70	0.49	0.99	0.58			
Σn-6 metabolites	0.85 ± 0.09	0.73 ± 0.07	0.83 ± 0.05	0.49	0.99	0.58			
C18:3n-3 trans	0.13 ± 0.01	0.09 ± 0.01	0.11 ± 0.01	0.10	0.55	0.52			
C18:3n3	1.25 ± 0.05	1.26 ± 0.08	1.29 ± 0.06	>0.99	0.93	0.95			
C22:5n3	0.04 ± 0.01	0.03 ± 0.01	0.04 ± <0.01	0.65	>0.99	0.60			
C22:6n3	0.08 ± 0.04	0.10 ± 0.04	0.03 ± <0.01	0.91	0.44	0.24			
Σn-3 PUFA	1.50 ± 0.07	1.50 ± 0.12	1.47 ± 0.07	>0.99	0.97	0.97			
Σn-3 metabolites	0.12 ± 0.04	0.16 ± 0.04	0.07 ± 0.01	0.69	0.62	0.20			
ΣPUFA	29.70 ± 0.28	30.94 ± 0.81	31.12 ± 0.73	0.38	0.29	0.98			
ΣUFA	73.72 ± 0.23	73.93 ± 0.66	75.28 ± 0.57	0.96	0.11	0.18			

Table 51. Retroperitoneal Cholesteryl ester fatty acid methyl esters (FAME) ratios for high fat diet groups; High fat diet with-saline (HFD-S), High fat diet -pair-fed (HFD-PF) and High fat diet- Ginkgo biloba (HFD-GbE) (N=10 per group). Results presented as mean an (SEM), and statistically analysed by one-way ANOVA with Tukey's Post-hoc test. The level of statistical significance was set at * $p < 0.05$.

	HFD-S		HFD-PF		HFD-GbE		S Vs PF	S Vs GbE	PF Vs GbE
	Mean	SEM	Mean	SEM	Mean	SEM	p value		
Σ MUFA/ Σ PUFA	1.48	± 0.02	1.40	± 0.05	1.43	± 0.04	0.25	0.53	0.86
Σ MUFA/ Σ SFA	0.56	± 0.01	0.57	± 0.02	0.53	± 0.01	0.93	0.18	0.09
Σ PUFA/ Σ SFA	1.20	± 0.02	1.28	± 0.07	1.34	± 0.07	0.59	0.19	0.70
Σ UFA/ Σ SFA	2.97	± 0.04	3.04	± 0.11	3.23	± 0.11	0.86	0.14	0.33
C18:0/C16:0	0.29	± 0.00	0.29	± 0.01	0.30	± 0.01	0.98	0.96	0.89
C16:1n-7/C16:0	0.08	± 0.00	0.08	± 0.01	0.08	± 0.00	>0.99	0.97	0.96
C18:1n-9/C16:0	2.28	± 0.02	2.14	± 0.05	2.31	± 0.04	0.04	0.82	0.01
C18:1n-9/C16:1n-7	28.82	± 1.37	27.31	± 1.45	28.46	± 0.99	0.69	0.98	0.80
C18:1n-7/C18:0	0.01	± 0.01	0.39	± 0.02	0.45	± 0.02	<0.0001	<0.0001	0.07
C18:1/C18:0	7.83	± 0.16	7.97	± 0.44	8.47	± 0.52	0.97	0.51	0.65
n-6/n-3	19.19	± 0.88	20.60	± 1.64	20.45	± 0.78	0.67	0.73	>0.99
C18:2n-6/C18:3n-3	22.21	± 0.94	23.54	± 1.50	22.70	± 0.85	0.69	0.95	0.86
C20:4n-6/C20:3n-6	2.65	± 0.34	2.75	± 0.22	3.27	± 0.19	0.96	0.23	0.35
C20:4n-6/C22:6n-3	7.68	± 1.55	7.67	± 1.60	14.92	± 1.67	>0.99	0.01	0.01
C20:4n-6/C18:2n-6	0.01	± 0.00	0.01	± 0.00	0.01	± 0.00	0.79	0.85	0.46
C20:4n-6/C18:3n-3	0.26	± 0.04	0.23	± 0.02	0.28	± 0.02	0.0001	0.35	0.004
C20:3n-3/C18:3n-3	0.00	± 0.00	0.02	± 0.00	0.01	± 0.00	0.52	0.85	0.84
C20:5n-3/C18:3n-3	0.00	± 0.00	0.00	± 0.00	0.00	± 0.00	0.45	0.98	0.34
C22:5n-3/C18:3n-3	0.03	± 0.00	0.02	± 0.00	0.03	± 0.00	0.96	0.38	0.26
C22:6n-3/C22:5n-3	2.45	± 1.14	3.35	± 1.15	0.72	± 0.08	0.78	0.41	0.14
C18:2n6/C16:0	1.49	± 0.02	1.59	± 0.08	1.68	± 0.07	0.50	0.11	0.61
C18:3n3/C16:0	0.07	± 0.00	0.07	± 0.01	0.07	± 0.00	0.98	0.59	0.71
C18:3n-6/C18:2n-6	0.00	± 0.00	0.00	± 0.00	0.00	± 0.00	0.04	0.08	0.95
C20:3n-6/C18:3n-6	1.27	± 0.06	1.61	± 0.20	1.47	± 0.10	0.19	0.56	0.73
C22:4n-6/C20:4n-6	4.43	± 0.78	5.32	± 0.43	5.28	± 0.15	0.46	0.52	>0.99
1 (% monoenoics)	44.02	± 0.20	42.87	± 0.37	43.85	± 0.34	0.04	0.92	0.09
2 (% dienoics)	55.11	± 0.33	57.79	± 1.51	58.09	± 1.40	0.27	0.21	0.98
3 (% trienoics)	4.80	± 0.26	4.61	± 0.29	4.81	± 0.23	0.86	>0.99	0.86
4 (% tetraenoics)	1.72	± 0.29	1.44	± 0.18	1.67	± 0.13	0.62	0.98	0.73
5 (% pentaenoics)	0.18	± 0.03	0.16	± 0.03	0.19	± 0.01	0.81	0.98	0.71
6 (% hexaenoics)	0.48	± 0.22	0.58	± 0.22	0.16	± 0.02	0.91	0.44	0.24
Unsaturation Index	106.3	± 0.69	107.5	± 1.49	108.7	± 1.28	0.78	0.33	0.72

Table 52. Mesenteric cholesteryl ester fatty acid methyl esters (FAME) for high fat diet groups; High fat diet with-saline (HFD-S), High fat diet -pair-fed (HFD-PF) and High fat diet- Ginkgo biloba (HFD-GbE) (N=10 per group). Fatty acid results are presented as area % percentage mean and standard error of the mean (SEM), and statistically analysed by one-way ANOVA with Tukey's Post-hoc test. The level of statistical significance was set at * $p < 0.05$.

	HFD-S		HFD-PF		HFD-GbE		S Vs PF	S Vs GbE p Value	PF Vs GbE
	Mean	SEM	Mean	SEM	Mean	SEM			
C14:0	0.54 ± 0.01	0.57 ± 0.02	0.53 ± 0.02	0.61	0.78	0.25			
C15:0	0.08 ± 0.01	0.07 ± 0.01	0.07 ± 0.01	0.25	0.08	0.08			
C16:0	16.46 ± 0.27	16.54 ± 0.25	15.82 ± 0.29	0.65	0.97	0.97			
C17:0	0.28 ± 0.01	0.27 ± 0.01	0.26 ± 0.01	0.75	0.17	0.50			
C18:0	4.43 ± 0.16	4.89 ± 0.17	4.27 ± 0.17	0.16	0.77	0.04			
C20:0	0.09 ± 0.01	0.08 ± 0.01	0.09 ± 0.01	0.91	0.99	0.84			
C21:0	0.14 ± 0.01	0.11 ± 0.01	0.12 ± 0.01	0.02	0.25	0.40			
DMA18:0	0.14 ± 0.02	0.19 ± 0.03	0.13 ± 0.14	0.89	>0.99	0.85			
∑SFA	22.19 ± 0.38	22.72 ± 0.35	21.79 ± 0.62	0.70	0.82	0.35			
C16:1n-7	1.50 ± 0.07	1.55 ± 0.10	1.46 ± 0.07	0.87	0.95	0.70			
C17:1	0.19 ± 0.01	0.15 ± 0.01	0.20 ± 0.01	0.05	0.74	0.01			
C18:1n-7 trans	0.04 ± 0.01	0.05 ± 0.01	0.03 ± 0.01	0.50	0.28	0.03			
C18:1n-7	2.29 ± 0.03	2.65 ± 0.10	2.46 ± 0.05	0.001	0.16	0.12			
C18:1n-9 trans	0.10 ± 0.01	0.09 ± 0.01	0.09 ± 0.01	0.81	0.66	0.97			
C18:1n-9	38.44 ± 0.45	38.82 ± 0.51	38.21 ± 0.48	0.85	0.94	0.65			
C20:1n9	0.28 ± 0.01	0.29 ± 0.04	0.33 ± 0.02	0.95	0.39	0.58			
C22:1n-9	0.01 ± 0.01	0.01 ± 0.01	0.07 ± 0.04	<0.0001	<0.0001	<0.0001			
C24:1n-9	0.01 ± 0.01	0.01 ± 0.01	0.02 ± 0.01	<0.0001	<0.0001	<0.0001			
C18:1 Total	38.99 ± 0.56	39.47 ± 0.67	38.77 ± 0.62	0.84	0.97	0.70			
∑n-7	2.33 ± 0.03	2.70 ± 0.10	2.49 ± 0.04	0.001	0.17	0.08			
∑n-9	38.81 ± 0.44	39.19 ± 0.52	38.72 ± 0.47	0.84	0.99	0.76			
∑MUFA	42.84 ± 0.47	43.60 ± 0.45	42.88 ± 0.45	0.47	>0.99	0.51			
C18:2n-6t	0.01 ± 0.01	0.01 ± 0.01	0.08 ± 0.01	0.92	<0.0001	<0.0001			
C18:2n-6	31.19 ± 0.56	30.77 ± 0.50	30.87 ± 0.76	0.88	0.93	0.99			
C18:3n-6	0.09 ± 0.01	0.05 ± 0.01	0.12 ± 0.01	0.01	0.09	<0.0001			
C20:2n-6	0.18 ± 0.01	0.18 ± 0.02	0.16 ± 0.01	0.96	0.52	0.38			
C20:3n-6	0.10 ± 0.01	0.08 ± 0.01	0.08 ± 0.01	0.08	0.23	0.84			
C20:4n-6	0.31 ± 0.03	0.32 ± 0.03	0.30 ± 0.01	0.99	0.95	0.90			
C22:2n-6	0.01 ± 0.01	0.01 ± 0.01	0.01 ± 0.00	0.63	0.70	0.99			
C22:4n-6	0.07 ± 0.01	0.06 ± 0.01	0.09 ± 0.01	0.57	0.39	0.06			
∑n-6 PUFA	31.96 ± 0.57	31.47 ± 0.55	31.71 ± 0.80	0.85	0.96	0.96			
∑n-6metabolites	0.76 ± 0.05	0.69 ± 0.07	0.76 ± 0.05	0.66	>0.99	0.62			
C18:3n-3	1.50 ± 0.08	1.50 ± 0.10	1.45 ± 0.10	>0.99	0.93	0.92			
C20:3n-3	0.02 ± 0.01	0.01 ± 0.01	0.04 ± 0.02	0.18	0.49	0.02			
C20:5n-3	0.01 ± 0.01	0.01 ± 0.01	0.01 ± 0.00	0.85	0.67	0.35			
C22:5n-3	0.04 ± 0.01	0.02 ± 0.01	0.04 ± 0.01	0.24	>0.99	0.26			
C22:6n-3	0.03 ± 0.01	0.12 ± 0.04	0.10 ± 0.06	0.29	0.44	0.95			
∑n-3 PUFA	1.59 ± 0.08	1.63 ± 0.12	1.63 ± 0.13	0.96	0.96	>0.99			
∑n-3 metabolites	0.09 ± 0.01	0.13 ± 0.04	0.18 ± 0.07	0.90	0.98	0.97			
∑PUFA	33.55 ± 0.63	33.10 ± 0.65	33.34 ± 0.89	0.90	0.98	0.97			
∑UFA	76.38 ± 0.35	76.70 ± 0.34	76.22 ± 0.88	0.92	0.98	0.83			

Table 53. Mesenteric cholesteryl esters (CE) fatty acid methyl esters (FAME) ratios for high fat diet groups; High fat diet with-saline (HFD-S), High fat diet -pair-fed (HFD-PF) and High fat diet- Ginkgo biloba (HFD-GbE) (N=10 per group). Results presented as mean an (SEM), and statistically analysed by one-way ANOVA with Tukey's Post-hoc test. The level of statistical significance was set at * $p < 0.05$.

	HFD-S		HFD-PF		HFD-GbE		S Vs PF	S Vs GbE	PF Vs GbE
	Mean	SEM	Mean	SEM	Mean	SEM	p value	p value	p value
ΣMUFA/ΣPUFA	1.28 ± 0.04		1.32 ± 0.04		1.30 ± 0.04		0.74	0.97	0.86
ΣMUFA/ΣSFA	0.66 ± 0.02		0.69 ± 0.02		0.66 ± 0.04		0.81	>0.99	0.77
ΣPUFA/ΣSFA	0.79 ± 0.02		0.76 ± 0.02		0.78 ± 0.03		0.74	0.98	0.85
ΣUFA/ΣSFA	3.45 ± 0.07		3.39 ± 0.07		3.53 ± 0.13		0.86	0.83	0.53
C18:0/C16:0	0.27 ± 0.01		0.30 ± 0.01		0.27 ± 0.01		0.12	>0.99	0.13
C16:1n-7/C16:0	0.09 ± 0.01		0.09 ± 0.01		0.09 ± 0.01		0.91	0.96	0.99
C18:1n-9/C16:0	2.34 ± 0.04		2.35 ± 0.04		2.42 ± 0.03		0.98	0.29	0.39
C18:1n-9/C16:1n-7	26.17 ± 1.23		26.28 ± 2.26		26.71 ± 1.37		>0.99	0.97	0.98
C18:1n-7/C18:0	0.52 ± 0.02		0.55 ± 0.03		0.59 ± 0.03		0.77	0.23	0.58
C18:1/C18:0	8.90 ± 0.35		8.15 ± 0.25		9.20 ± 0.35		0.24	0.79	0.07
C15:0/C17:0	0.27 ± 0.01		0.30 ± 0.01		0.27 ± 0.01		0.12	>0.99	0.13
n-6/n-3	20.47 ± 0.86		20.19 ± 1.52		20.27 ± 1.24		0.99	0.99	>0.99
C18:2n-6/C18:3n-3	21.23 ± 0.91		21.30 ± 1.37		21.92 ± 1.08		>0.99	0.91	0.92
C20:4n-6/C20:3n-6	3.02 ± 0.14		4.39 ± 0.55		3.78 ± 0.29		0.04	0.32	0.48
C20:4n-6/C22:6n-3	13.74 ± 1.27		5.97 ± 2.01		9.95 ± 2.53		0.03	0.38	0.36
C20:4n-6/C20:5n-3	27.00 ± 0.01				27.97 ± 14.18		-	<0.0001	-
C20:4n-6/C18:2n-6	0.01 ± 0.01		0.01 ± 0.01		0.01 ± 0.01		0.98	0.97	0.90
C20:4n-6/C18:3n-3	0.21 ± 0.02		0.21 ± 0.01		0.21 ± 0.01		>0.99	>0.99	0.98
C20:3n-3/C18:3n-3	0.02 ± 0.01		0.01 ± 0.01		0.03 ± 0.02		0.42	0.46	0.05
C22:5n-3/C18:3n-3	0.03 ± 0.01		0.01 ± 0.01		0.03 ± 0.01		0.17	>0.99	0.20
C22:6n-3/C18:3n-3	0.02 ± 0.01		0.08 ± 0.03		0.07 ± 0.04		0.32	0.46	0.96
C22:6n-3/C22:5n-3	0.60 ± 0.04		11.84 ± 8.33		1.76 ± 0.34		0.08	0.96	0.12
C18:2n6/C16:0	1.90 ± 0.06		1.87 ± 0.05		1.96 ± 0.08		0.91	0.81	0.56
C18:3n3/C16:0	0.09 ± 0.01		0.09 ± 0.01		0.09 ± 0.01		>0.99	0.99	0.99
C18:3n-6/C18:2n-6	0.01 ± 0.01		0.01 ± 0.01		0.01 ± 0.01		<0.0001	<0.0001	<0.0001
C20:3n-6/C18:3n-6	1.15 ± 0.05		1.91 ± 0.30		0.75 ± 0.10		0.02	0.29	0.001
C22:5n-3/C20:5n-3	4.92 ± 0.01				5.01 ± 1.58		<0.0001	<0.0001	<0.0001
C22:4n-6/C20:4n-6	4.44 ± 0.20		5.74 ± 1.16		3.69 ± 0.48		0.36	0.69	0.10
1 (% monoenoics)	42.84 ± 0.47		43.60 ± 0.45		42.88 ± 0.45		0.47	>0.99	0.51
2 (% dienoics)	62.76 ± 1.11		61.93 ± 1.03		62.22 ± 1.54		0.89	0.95	0.99
3 (% trienoics)	5.15 ± 0.27		4.88 ± 0.32		5.09 ± 0.32		0.80	0.99	0.88
4 (% tetraenoics)	1.54 ± 0.14		1.50 ± 0.17		1.58 ± 0.10		0.97	0.98	0.90
5 (% pentaenoics)	0.21 ± 0.03		0.09 ± 0.04		0.22 ± 0.08		0.28	>0.99	0.24
6 (% hexaenoics)	0.15 ± 0.03		0.69 ± 0.25		0.59 ± 0.34		0.29	0.44	0.95
Unsaturation Index	112.7 ± 1.01		112.7 ± 1.12		112.6 ± 1.92		>0.99	>0.99	>0.99

5.5 RET and MES MAG and DAG

As reviewed at the beginning of the chapter and in chapter 1, the breakdown of TAG both in liver, adipose tissues and other peripheral tissues produces DAG, MAG, FFA and glycerol molecules. The levels of MAG and DAG are therefore a reflection in the breakdown of TAG in the adipocyte, either for the incorporation of fatty acids into the PPLs for the cellular membrane, or for energy production.

5.5.1 RET- MAG + DAG - NFD Vs HFD

As summarised in (Table 54 and Table 55), several changes occurred in the fatty acid profiles of the MAG and DAG fraction in the HFD-S group compared to the NFD group in RET tissue. While no significant difference occurred in total SFA (NFD $23.69 \pm 0.67\%$, HFD-S $25.95 \pm 0.40\%$; $p=0.38$), a significant increase of 90% in C18:0 was seen in HFD-S (NFD $2.77 \pm 0.07\%$, HFD-S $5.28 \pm 0.14\%$; $p < 0.0001$) (Table 54)) which suggests that DNL might be occurring. This is supported by the increase in total MUFA which increased by 76% in HFD-S (NFD $26.48 \pm 0.51\%$, HFD-S $46.62 \pm 0.42\%$; $p < 0.0001$), largely attributed to the increase in C18:1n-9 (NFD $21.75 \pm 0.25\%$, HFD-S $44.14 \pm 0.42\%$; $p < 0.0001$) (Table 54)). This is partially explained by 50% increase in C18:1n-9 of the HFD-chow, although SFA levels of chow are not reflected in MAG and DAG levels. The idea that C16:0 is being utilized for MUFA synthesis rather than being converted to C18:0 is supported by the following ratio changes; C18:0/C16:0 ratio increased by 89% (NFD 0.14 ± 0.01 ; HFD-S 0.27 ± 0.00 , $p < 0.0001$); C18:1n-9/C16:0 ratio increased by 102% (NFD 1.13 ± 0.03 ; HFD-S 2.28 ± 0.05 , $p < 0.0001$); C18:1n-9/C16:1n-7 ratio increased by 139% (NFD 14.06 ± 1.96 ; HFD-S 33.60 ± 0.88 , $p < 0.0001$); MUFA/ Σ SFA ratio decreased by 38% (NFD 0.89 ± 0.01 ; HFD-S 0.56 ± 0.01 , $p < 0.0001$) (Table 55). In the HFD-S group an increase of 224% in the MUFA/ Σ PUFA ratio occurred (NFD 0.56 ± 0.03 ; HFD-S 1.82 ± 0.03 $p < 0.0001$) indicating a significant change between the two FA groups (Table 55). Of note is the decrease of C18:1n-7 to undetectable levels in the HFD. Total PUFA decreased by 46% (NFD $47.66 \pm 1.32\%$, HFD-S $25.68 \pm 0.22\%$; $p < 0.0001$), mostly attributed to the 45% decrease in n-6 fatty acids C18:2n-6 (NFD $43.30 \pm 1.40\%$, HFD-S $23.86 \pm 0.25\%$; $p < 0.0001$), and 59% decrease in C22:4n-6 (NFD $0.30 \pm 0.02\%$, HFD-S $0.12 \pm 0.01\%$; $p < 0.0001$) (Table 54). This is again largely representative of the PUFA levels seen in the rat chow for both NFD and HFD groups, further corroborating that adipocyte serve as storage vesicles for dietary lipids. In the n-3 fatty acids, C18:3n-3 decreased by 72% (NFD $2.09 \pm 0.08\%$, HFD-S $0.57 \pm 0.01\%$; $p < 0.0001$) (Table 54), with levels representing approximately half of the levels found in the diet. A decrease of 82% in n-3 metabolites (NFD $0.48 \pm 0.09\%$, HFD-S $0.08 \pm 0.01\%$; $p=0.04$) was also

seen (Table 54). As the diet only provides n-3 FA in the form of C18:3n-3, n-3 metabolites must be synthesised *de novo*. The n-3 metabolites levels found between the NFD and HFD groups suggest that either the fatty metabolism pathway is either affected by the levels of fatty acids available from the diet and in the tissue, or that higher n-3 metabolites from MAG and DAG are being liberated and utilized in other pathways, such as oxylipin mediation of inflammation. The increase in the n-6/n-3 ratio 83% in the HFD group (NFD 17.05±1.04; HFD-S 31.22±0.91, p<0.0001), largely attributed to the nearly 2-fold change in the C18:2n-6/C18:3n-3 ratio (NFD 20.88±0.73; HFD-S 41.73± 0.93, p<0.0001) (Table 55), suggests that larger abundance of C18:2n-6 may be outcompeting C18:3n-3 for synthesis pathway enzymes. This is similarly reflected in the unsaturation index that decreased by 21% (NFD 126.53±2.27; HFD-S 100.29± 0.53, p<0.0001) (Table 55).

The synthesis of n-6 and n-3 VLCFA utilizes the same desaturation and elongation enzymes in both the n-6 and n-3 pathways, with higher levels of C18:2n-6 favoured in the pathway (Kim, Jo and Chung, 2018; Martin, 2015). Likewise, the enzyme FADS2 which introduces a double bond at the Δ6, Δ4 and Δ8 positions is utilized on the fatty acids C16:0, C18:2n-6, and C18:3n-3. Higher levels of C16:0 can inhibit the synthesis of highly unsaturated fatty acids EPA and DHA or AA from C18:2n-6 and C18:3n-3 (Park *et al.*, 2016). In this MAG+DAG a drop in C16:0 levels are seen accompanied by an increase in MUFA levels within the HFD group, which suggest that C16:0 might be utilized in MUFA synthesis pathway activity.

5.5.2 MES- MAG + DAG - NFD Vs HFD

Comparing the NFD group to the HFD-S group (Table 56 and Table 57), total SFA decreased by 35% (Σ SFA; NFD,44.28±6.57%; HFD-S, 28.57±0.35%, p=0.03). This was due to the 25% decrease in C16:0 (NFD,27.44±3.1%; HFD-S, 20.7±0.21%,p=0.03) and the 53% decrease in C18:0 (C18:0; NFD,13.17±3.06%; HFD-S, 6.18±0.21%, p=0.04) as well as a 90% in C24:0 (C24:0;NFD,1.84±0.47%;HFD-S, 0.19±0.02%, p=0.003) (Table 56). This was also noted in the decrease in the C18:0/C16:0 ratio (C18:0/C16:0; NFD,0.43±0.07; HFD-S,0.30±0.01, p=0.02) (Table 57). Taking these changes within context however, it is seen that the NFD MAG+DAG SFA levels are nearly double that found in MES-TAG (Σ SFA;21.68±0.50%;27.69±0.23%, p<0.0001) (Table 40) while no changes occurred between TAG and MAG+DAG HFD-S SFA levels. This suggests that more UFA are being liberated from the NFD TAG depot than that of the HFD group. This is also supported by the near 4-fold decrease in the MUFA/SFA ratio seen in MAG+DAG between the groups (Σ MUFA/ Σ SFA; NFD,3.98±2.39; HFD-S,1.10±0.02, p<0.0001) (Table 57), showing that a greater disparity between SFA

and MUFA occurs in the NFD compared to HFD. Regarding MUFA percentage levels, total MUFA increased in HFD-S by 110% (Σ MUFA; NFD, 21.25 \pm 1.94%; HFD-S, 44.66 \pm 0.46%, $p < 0.0001$) (Table 56). When comparing SFA and MUFA results, MES MAG+DAG profiles for NFD and HFD are opposite reflections of each other; with higher SFA (44.3%) and lower MUFA (21.2%) seen in NFD, and lower SFA (28.6%) and higher MUFA (44.6%) seen in HFD-S (Table 56). These profiles are like the MES CE fractions for the same groups. MAG+DAG MUFA levels (MES-MAG+DAG- Σ MUFA; NFD, 21.25 \pm 1.94%; HFD-S, 44.66 \pm 0.46%, $p < 0.0001$) are lower for both NFD and HFD groups than levels seen in TAG fraction (MES-TAG; Σ MUFA; NFD, 29.55 \pm 0.42%; HFD-S, 48.30 \pm 0.32%, $p < 0.0001$) (Table 40) indicating that MUFA are being mobilized out of TAG potentially for other uses such as phospholipid membrane turnover due to CE or oxylipin production. As UFA are the main FA that were found in the CE fraction, largely represented by MUFA, it stands to reason that a replacement of UFA into the phospholipid membrane may be warranted, with the nearest available supply coming from TAG storage. C18:1n-9 levels however decreased twice as much in NFD MAG+DAG compared to TAG (NFD, C18:1n-9 TAG; 29.6%; MAG+DAG, 29.6%) compared to the HFD (HFD-S, C18:1n-9 TAG; 43.8%; MAG+DAG, 39.7%) (Table 40). Furthermore, a substantial decrease of 26% from 77.6% to 50.9% in UFA levels can be seen between the TAG and MAG+DAG of the NFD, compared to almost no decrease in MAG+DAG (70.4%) compared to TAG (71.6%) in the HFD group (Table 56). This might indicate DNL occurring in the HFD group where C18:1n-9 is being replaced at a faster pace within the adipocyte depot compared to an NFD. PUFA levels decreased from 47.96% in the NFD group in TAG, to 29.6% in HFD-S (Table 56) indicating a substantial mobilization of PUFA out of TAG. Interestingly though is the increase in overall PUFA in the HFD-S group which increase from 23.31% in TAG, to 26.08% in MAG+TAG. These changes explain why the MAG+DAG PUFA levels decreased by only 12 % the HFD group (Σ PUFA; NFD, 29.60 \pm 5.08%; HFD-S, 26.08 \pm 0.40%, $p = 0.01$) (Table 56) compared to the NFD. Despite this decrease in PUFA however, the unsaturation index increased by 18% in the HFD-S group (Unsaturation Index; NFD, 84.70 \pm 12.23; HFD-S, 100.27 \pm 0.99, $p = 0.004$) (Table 57), likely reflecting the changes in the MUFA levels, but also suggesting dynamic changes are occurring in HFD MUFAs, perhaps from DNL. No significant differences were seen overall for n-6 PUFA, n-3 PUFA levels or the n-6/n-3 ratio. n-6 metabolites however did decrease in the HFD-S group by 12% (Σ n-6 metabolites; NFD, 1.57 \pm 0.19%; HFD-S, 0.98 \pm 0.10%, $p = 0.01$) (Table 56), which may indicate an increased need for n-6 metabolites within the membrane for pro-inflammatory mediation which have been shown to be increased following an HFD.

5.5.3 RET-MAG + DAG- HFD GbE treatment

Between the HFD subsets (Table 58 and Table 59), several changes can be seen between the MAG and DAG fraction of lipids. The total SFA levels increased in the HFD-PF compared to the HFD-S and HFD-GbE groups ($P=0.001$) (HFD-S $25.95\pm 0.40\%$; HFD-PF $28.73\pm 0.58\%$; HFD-GbE $25.92\pm 0.44\%$), with no changes seen between HFD-S and HFD-GbE (Table 58). C16:0 increased in HFD-PF compared to HFD-GbE ($p=0.01$), while HFD-GbE decreased compared to HFD-S ($p=0.01$), although not by a large percentage (Table 58). HFD-PF C18:0 levels are significantly increased compared to both the S and HFD-GbE groups ($p=0.0002$ and $p=0.003$, respectively) (HFD-S $5.28\pm 0.14\%$; HFD-PF $6.63\pm 0.24\%$; HFD-GbE $5.59\pm 0.20\%$) (Table 58). An increase in the $\Sigma\text{MUFA}/\Sigma\text{SFA}$ ratio was also seen in HFD-PF compared to both HFD-S and HFD-GbE ($p=0.0006$ and $p=0.0006$, respectively) (HFD-S 0.56 ± 0.01 ; HFD-PF 0.65 ± 0.02 ; HFD-GbE 0.56 ± 0.01) (Table 59). An increase in the C18:0/C16:0 ratio also occurred in HFD-PF compared to HFD-S ($p=0.0004$) and HFD-GbE ($p=0.046$) (HFD-S 0.27 ± 0.01 , HFD-PF 0.32 ± 0.01 ; HFD-GbE 0.29 ± 0.01) (Table 59) suggesting that changes in C18:0/C16:0 metabolism may be occurring. Changes in total MUFA included a decrease in the HFD-PF group compared to both HFD-S and HFD-GbE groups ($p=0.001$) (HFD-S $46.62\pm 0.42\%$; HFD-PF $44.32\pm 0.46\%$; HFD-GbE $46.49\pm 0.23\%$) (Table 58). This is largely attributed to decrease in HFD-PF C18:1n-9 (HFD-S $44.14\pm 0.42\%$; HFD-PF $39.85\pm 0.47\%$; HFD-GbE $42.24\pm 0.25\%$), although n-7 fatty acids increase in both the HFD-PF group ($p<0.0001$) and HFD-GbE group (<0.0001) compared to the saline group, most notably due to the increase in C18:1n-7 (Table 58). This is reflected in the decrease seen in the HFD-PF group for the C18:1/C18:0 ratios compared to HFD-S ($p=0.0001$) and HFD-GbE ($p=0.001$) (HFD-S 8.45 ± 0.30 ; HFD-PF 6.41 ± 0.27 ; HFD-GbE 8.05 ± 0.29) as well as the HFD-PF C18:1n-9/C16:0 ratios compared to HFD-S (<0.0001) and HFD-GbE (0.0001) (Table 59). The return of C18:1n-7 levels in the HFD-PF ($2.03\pm 0.04\%$, $p<0.0001$) and HFD-GbE group ($2.13\pm 0.03\%$, $p<0.0001$) (Table 58), to similar levels in the NFD group, further suggest a shift in MUFA DNL. Moreover, this is like C18:1n-7 level changes in the CE fraction.

While total PUFA decreased in the HFD-PF group compared to HFD-S ($p=0.02$), they increased in the HFD-GbE group compared to HFD-PF ($p=0.001$), similar to levels seen in the HFD-S group ($p=0.64$), that largely correspond with changing n-6 PUFA levels (Table 58). Overall, the total UFA decreased in the HFD-PF group compared to HFD-S ($p=0.0006$) and the HFD-GbE group ($p=0.0002$), but no changes were seen between HFD-S and HFD-GbE ($p=0.93$) (HFD-S $72.30\pm 0.38\%$; HFD-PF $68.56\pm 0.80\%$; HFD-GbE $72.61\pm 0.52\%$) (Table 58). A decrease was seen in the $\Sigma\text{PUFA}/\Sigma\text{SFA}$ ratios between HFD-PF and HFD-S ($p=0.002$) and HFD-GbE ($p=0.0003$) (HFD-S 0.99 ± 0.02 ; HFD-PF 0.85 ± 0.03 ; HFD-GbE 1.01 ± 0.03).

A similar change also occurred in the $\sum\text{UFA}/\sum\text{SFA}$ ratio where HFD-PF decreased compared to HFD-S ($p=0.0006$) and HFD-GbE ($p=0.0003$) (HFD-S 2.79 ± 0.06 ; HFD-PF 2.40 ± 0.07 ; HFD-GbE 2.81 ± 0.06) (Table 59). Lastly these changes were reflected in the unsaturation Index that decreased in the HFD-PF group compared to HFD-S ($p=0.0007$) and HFD-GbE ($p=0.0001$) (Table 59). To summarise, following an HFD, MUFA levels increase and PUFA levels decreased in the MAG and DAG fraction. Of note C18:1n-7 decreased to undetectable levels in the HFD MAG and DAG fraction.

5.5.4 MES-MAG + DAG- HFD GbE treatment

Between the MES -CE HFD subsets that received GbE treatment (HFD-GbE), caloric restriction (HFD-PF) of saline only (HFD-S), as summarised in Table 60 and Table 61, the total percentage levels of SFA increased in the HFD-PF compared to HFD-S ($p=0.02$), while HFD-GbE decreased compared to both HFD-S ($p=0.09$) and HFD-PF ($p=0.0001$) ($\sum\text{SFA}$; HFD-S, $28.57\pm0.35\%$; HFD-PF, $29.92\pm0.30\%$; HFD-GbE, $27.56\pm0.33\%$) (Table 60). These changes occurred in both C16:0 and C18:0 levels between the group, with levels increasing for both FA in the HFD-PF group but decreasing in the HFD-GbE group. No changes of note occurred between the groups regarding MUFA levels, PUFA levels or the n-6/n-3 ratio levels. Changes that occur from either treatment may instead occur from influences of DNL activity instead which has been shown to be increased following calorie restriction, and decreased with GbE compound treatment (Hirata, Cruz, *et al.*, 2019; Sun *et al.*, 2015). This is very interesting considering that both PF and GbE groups underwent calorie restriction, while the HFD-GbE group received GbE treatment that caused decreased food intake (caloric restriction). An increase in n-6 metabolites however did occur in HFD-GbE compared to HFD-S ($p=0.04$) although not significantly compared to HFD-PF ($p=0.1$) ($\sum\text{n-6 metabolites}$; HFD-S, $0.98\pm0.10\%$; HFD-PF, $1.02\pm0.05\%$; HFD-GbE, $1.24\pm0.06\%$) (Table 60). The increase n-6 metabolites may suggest less need for pro-inflammatory mediation, allowing for less need for n-6 PUFA mobilisation into the phospholipid membrane. This will be explored in the next section.

Table 54. Retroperitoneal monoglyceride and diglyceride fatty acid methyl esters (FAME) for normal fat diet (NFD) and high fat diet (HFD-S) (N=10 per group). Fatty acid results are presented as area % percentage mean and standard error of the mean (SEM), and statistically analysed by Students t-test. The level of statistical significance was set at * $p < 0.05$.

	NFD			HFD-S			p value
	Mean %	±	SEM	Mean %	±	SEM	
C14:0	0.65	±	0.05	0.48	±	0.02	0.36
C16:0	19.41	±	0.60	19.37	±	0.26	>0.99
C17:0	0.24	±	0.01	0.25	±	<0.01	0.85
C18:0	2.77	±	0.07	5.28	±	0.14	<0.0001
C20:0	0.07	±	0.01	0.06	±	0.01	>0.99
C22:0	0.04	±	<0.01	0.04	±	0.01	>0.99
C24:0	0.12	±	0.03	0.16	±	0.01	0.98
DMA18:0	0.11	±	0.01	0.07	±	0.02	0.95
ΣSFA	23.69	±	0.67	25.95	±	0.40	0.38
C16:1n7	1.79	±	0.23	1.32	±	0.04	0.91
C17:1	0.08	±	0.02	0.18	±	<0.01	0.04
C18:1n7	1.97	±	0.09	0.01	±	0.01	<0.0001
C18:1n9 <i>trans</i>	0.02	±	0.01	0.11	±	0.01	<0.0001
C18:1n9	21.75	±	0.25	44.14	±	0.42	<0.0001
C20:1n9	0.23	±	0.02	0.36	±	0.01	0.002
C22:1n9	0.41	±	0.05	0.38	±	0.05	>0.99
C24:1n9	0.01	±	0.01	0.07	±	0.01	0.06
ΣDMA18:1	0.05	±	0.01	0.05	±	0.02	>0.99
ΣC18:1	23.75	±	0.30	44.25	±	0.42	<0.0001
Σn-7	3.78	±	0.32	1.32	±	0.04	<0.0001
Σn-9	22.53	±	0.23	44.95	±	0.41	<0.0001
ΣMUFA	26.48	±	0.51	46.62	±	0.42	<0.0001
C18:2n6	43.30	±	1.40	23.86	±	0.25	<0.0001
C18:3n6	0.10	±	0.02	0.07	±	0.01	0.97
C20:2n6	0.23	±	0.02	0.21	±	0.02	>0.99
C20:3n6	0.18	±	0.01	0.11	±	0.02	0.25
C20:4n6	0.71	±	0.04	0.50	±	0.05	0.25
C22:2n6	0.10	±	0.01	0.01	±	0.01	<0.0001
C22:4n6	0.30	±	0.02	0.12	±	0.01	<0.0001
Σn-6 PUFA	44.97	±	1.34	24.87	±	0.21	<0.0001
Σn-6 metabolites	1.62	±	0.10	1.01	±	0.07	0.01
C18:3n-3 <i>trans</i>	0.13	±	0.03	0.14	±	0.02	>0.99
C18:3n3	2.09	±	0.08	0.57	±	0.01	<0.0001
C20:3n3	0.01	±	0.01	0.02	±	0.01	0.96
C20:5n3	0.02	±	0.01	<0.01	±	<0.01	0.13
C22:5n3	0.17	±	0.01	0.03	±	<0.01	<0.0001
C22:6n3	0.28	±	0.09	0.04	±	<0.01	0.45
Σn-3 PUFA	2.69	±	0.14	0.80	±	0.02	<0.0001
Σn-3 metabolites	0.48	±	0.09	0.08	±	0.01	0.04
ΣPUFA	47.66	±	1.32	25.68	±	0.22	<0.0001
ΣUFA	74.14	±	0.89	72.30	±	0.38	0.93

Table 55. Retroperitoneal monoglyceride and diglyceride fatty acid methyl esters (FAME) ratios for normal fat diet (NFD) and high fat diet (HFD-S) (N=10 per group). Results presented as mean an (SEM), and statistically analysed by one-way ANOVA with Tukey's Post-hoc test. The level of statistical significance was set at * $p < 0.05$.

Name	NFD			HFD-S			p value
	Mean	±	SEM	Mean	±	SEM	
ΣMUFA/ΣPUFA	0.56	±	0.03	1.82	±	0.03	<0.0001
ΣMUFA/ΣSFA	0.89	±	0.01	0.56	±	0.01	<0.0001
ΣPUFA/ΣSFA	2.04	±	0.11	0.99	±	0.02	<0.0001
ΣUFA/ΣSFA	3.16	±	0.13	2.79	±	0.06	0.52
C18:0/C16:0	0.14	±	0.01	0.27	±	<0.01	<0.0001
C16:1n-7/C16:0	0.09	±	0.01	0.07	±	<0.01	0.78
C18:1n-9/C16:0	1.13	±	0.03	2.28	±	0.05	<0.0001
C18:1n-9/C16:1n-7	14.06	±	1.96	33.60	±	0.88	<0.0001
C18:1/C18:0	8.62	±	0.27	8.45	±	0.30	>0.99
n-6/n-3	17.05	±	1.04	31.22	±	0.91	<0.0001
C18:2n-6/C18:3n-3	20.88	±	0.73	41.73	±	0.93	<0.0001
C20:4n-6/C20:3n-6	4.16	±	0.33	3.88	±	0.36	>0.99
C20:4n-6/C22:6n-3	3.43	±	0.37	15.11	±	1.69	0.0003
C20:4n-6/C18:2n-6	0.02	±	<0.01	0.02	±	<0.01	0.97
C20:4n-6/C18:3n-3	0.34	±	0.02	0.87	±	0.10	0.01
C20:3n-3/C18:3n-3	0.02	±	<0.01	0.06	±	<0.01	0.01
C22:5n-3/C18:3n-3	0.08	±	0.01	0.05	±	0.01	0.52
C22:6n-3/C18:3n-3	0.14	±	0.04	0.06	±	0.01	0.97
C22:6n-3/C22:5n-3	1.61	±	0.45	1.35	±	0.15	>0.99
C18:2n6/C16:0	2.26	±	0.14	1.23	±	0.02	<0.0001
C18:3n3/C16:0	0.11	±	0.01	0.03	±	<0.01	<0.0001
C20:3n-6/C18:3n-6	1.96	±	0.36	1.66	±	0.10	>0.99
C22:4n-6/C20:4n-6	2.40	±	0.08	3.95	±	0.16	<0.0001
1 (% monoenoics)	24.63	±	0.61	46.62	±	0.42	<0.0001
2 (% dienoics)	87.35	±	2.77	48.15	±	0.49	<0.0001
3 (% trienoics)	7.88	±	0.36	2.68	±	0.09	0.02
4 (% tetraenoics)	4.04	±	0.22	2.49	±	0.26	<0.0001
5 (% pentaenoics)	0.96	±	0.07	0.14	±	0.02	0.45
6 (% hexaenoics)	1.66	±	0.53	0.21	±	0.03	<0.0001
Unsaturation Index	126.53	±	2.27	100.29	±	0.53	<0.0001

Table 56. Mesenteric monoglycerides and diglycerides fatty acid methyl esters (FAME) for normal fat diet (NFD) and high fat diet (HFD-S) (N=10 per group). Fatty acid results are presented as area % percentage mean and standard error of the mean (SEM), and statistically analysed by Students t-test. The level of statistical significance was set at * $p < 0.05$.

	NFD			HFD-S			p value
	Mean	±	SEM	Mean	±	SEM	
C14:0	0.65	±	0.08	0.52	±	0.03	0.12
C15:0	0.18	±	0.04	0.07	±	0.01	0.02
C16:0	27.44	±	3.01	20.70	±	0.21	0.04
C17:0	0.18	±	0.04	0.29	±	0.02	0.02
C18:0	13.17	±	3.06	6.18	±	0.21	0.04
C20:0	0.09	±	0.02	0.08	±	0.02	0.68
C21:0	0.07	±	0.02	0.14	±	0.02	0.02
C22:0	0.24	±	0.08	0.04	±	0.01	0.03
C24:0	1.84	±	0.47	0.19	±	0.02	0.003
DMA18:0	0.36	±	0.16	0.36	±	0.04	0.99
∑SFA	44.28	±	6.57	28.57	±	0.35	0.03
C16:1n-7	0.88	±	0.26	1.58	±	0.11	0.02
C17:1	0.02	±	0.01	0.10	±	0.02	0.01
C18:1n-7	2.97	±	0.33	1.23	±	0.41	0.004
C18:1n-9	14.77	±	2.28	39.66	±	0.51	<0.0001
C20:1n-9	1.89	±	0.45	0.39	±	0.02	0.004
C22:1n-9	0.47	±	0.14	0.15	±	0.06	0.05
C24:1n-9	0.25	±	0.07	0.01	±	0.01	0.004
DMA 18:1 Total	0.01	±	0.01	1.44	±	0.48	0.01
C18:1 Total	15.21	±	2.44	40.23	±	0.65	<0.0001
∑n-7	3.84	±	0.36	2.84	±	0.36	0.08
∑n-9	17.37	±	1.79	40.28	±	0.50	<0.0001
∑MUFA	21.25	±	1.94	44.66	±	0.46	<0.0001
C18:2n-6	26.28	±	4.85	23.56	±	0.32	0.58
C18:3n-6	0.32	±	0.13	0.18	±	0.06	0.35
C20:2n-6	0.14	±	0.04	0.15	±	0.02	0.86
C20:3n-6	0.47	±	0.12	0.19	±	0.01	0.03
C20:4n-6	0.41	±	0.13	0.39	±	0.03	0.93
C22:2n-6	0.13	±	0.05	0.01	±	0.01	0.02
C22:4n-6	0.11	±	0.04	0.06	±	0.01	0.33
∑n-6 PUFA	27.85	±	4.93	24.54	±	0.36	0.51
∑n-6 metabolites	1.57	±	0.19	0.98	±	0.10	0.01
C18:3n-3	1.47	±	0.17	1.30	±	0.18	>0.99
C22:5n-3	0.09	±	0.03	0.08	±	0.03	0.82
C22:6n-3	0.17	±	0.06	0.15	±	0.06	0.49
∑n-3 PUFA	1.75	±	0.20	1.55	±	0.21	0.79
∑n-3 metabolites	0.28	±	0.08	0.25	±	0.09	0.50
∑PUFA	29.60	±	5.08	26.08	±	0.40	0.01
∑UFA	50.85	±	6.84	70.74	±	0.43	<0.0001

Table 57. Mesenteric monoglyceride and diglycerides (MAG+DAG) fatty acid methyl esters (FAME) ratios for normal fat diet (NFD) and high fat diet (HFD-S) (N=10 per group). Results presented as mean an (SEM), and statistically analysed by one-way ANOVA with Tukey's Post-hoc test. The level of statistical significance was set at * $p < 0.05$.

	NFD			HFD-S			p value
	Mean	±	SEM	Mean	±	SEM	
ΣMUFA/ΣPUFA	0.92	±	0.15	1.72	±	0.04	0.24
ΣMUFA/ΣSFA	3.98	±	2.39	1.10	±	0.02	<0.0001
ΣPUFA/ΣSFA	1.29	±	0.15	0.59	±	0.01	0.11
ΣUFA/ΣSFA	1.63	±	0.40	2.48	±	0.04	0.08
C18:0/C16:0	0.43	±	0.07	0.30	±	0.01	0.02
C16:1n-7/C16:0	0.04	±	0.01	0.08	±	0.01	<0.0001
C18:1n-9/C16:0	0.67	±	0.14	1.92	±	0.03	0.10
C18:1n-9/C16:1n-7	17.73	±	4.48	26.12	±	1.72	0.15
C18:1n-7/C18:0	0.40	±	0.10	0.22	±	0.07	0.005
C18:1/C18:0	3.10	±	1.04	6.60	±	0.30	0.40
C15:0/C17:0	0.43	±	0.07	0.30	±	0.01	0.61
n-6/n-3	16.30	±	2.24	20.06	±	3.75	0.31
C18:2n-6/C18:3n-3	17.78	±	2.61	22.64	±	3.83	0.37
C20:4n-6/C20:3n-6	1.52	±	0.59	2.09	±	0.19	0.12
C20:4n-6/C18:3n-3	0.22	±	0.07	0.39	±	0.08	0.93
C20:3n-3/C18:3n-3	0.01	±	0.01	0.01	±	0.01	0.80
C20:5n-3/C18:3n-3	0.01	±	0.01	0.01	±	0.01	0.95
C22:5n-3/C18:3n-3	0.06	±	0.03	0.06	±	0.03	<0.0001
C22:6n-3/C18:3n-3	0.15	±	0.07	0.14	±	0.07	0.57
C18:2n6/C16:0	1.22	±	0.30	1.14	±	0.02	0.75
C18:3n3/C16:0	0.06	±	0.01	0.06	±	0.01	0.77
1 (% monoenoics)	21.25	±	1.94	44.66	±	0.46	>0.05
2 (% dienoics)	53.09	±	9.78	47.43	±	0.63	0.24
3 (% trienoics)	6.83	±	0.43	5.06	±	0.65	0.13
4 (% tetraenoics)	2.04	±	0.68	1.81	±	0.18	0.0002
5 (% pentaenoics)	0.47	±	0.16	0.40	±	0.16	0.91
6 (% hexaenoics)	1.02	±	0.34	0.91	±	0.35	0.06
Unsaturation Index	84.70	±	12.23	100.27	±	0.99	0.004

Table 58. Retroperitoneal monoglyceride and diglyceride fatty acid methyl esters (FAME) for high fat diet groups; High fat diet with-saline (HFD-S), High fat diet -pair-fed (HFD-PF) and High fat diet- Ginkgo biloba (HFD-GbE) (N=10 per group). Fatty acid results are presented as area % percentage mean and standard error of the mean (SEM), and statistically analysed by one-way ANOVA with Tukey's Post-hoc test. The level of statistical significance was set at * $p < 0.05$.

	HFD-S			HFD-PF			HFD-GbE			<i>p value</i>		
	Mean	±	SEM	Mean	±	SEM	Mean	±	SEM	S Vs PF	S Vs GbE	PF Vs GbE
C14:0	0.48	±	0.02	0.46	±	0.02	0.33	±	0.02	0.84	0.0001	0.0004
C15:0	0.09	±	<0.01	0.09	±	0.01	0.08	±	0.01	0.0004	0.99	0.99
C16:0	19.37	±	0.26	20.74	±	0.34	19.04	±	0.25	0.42	0.01	0.01
C17:0	0.25	±	<0.01	0.28	±	0.01	0.26	±	<0.01	0.01	0.95	0.02
C18:0	5.28	±	0.14	6.63	±	0.24	5.59	±	0.20	0.0002	0.53	0.003
C20:0	0.06	±	0.01	0.08	±	0.01	0.03	±	0.01	0.50	0.14	0.01
C21:0	0.14	±	<0.01	0.16	±	<0.01	0.18	±	0.01	0.09	0.001	0.14
C22:0	0.04	±	0.01	0.03	±	0.01	0.03	±	0.01	0.78	0.64	0.97
C23:0	0.02	±	0.01	0.04	±	0.01	0.03	±	0.01	0.46	0.73	0.89
C24:0	0.16	±	0.01	0.22	±	0.02	0.19	±	0.02	0.06	0.35	0.58
∑DMA18:0	0.07	±	0.02	0.00	±	<0.01	0.18	±	0.02	0.01	<0.0001	<0.0001
∑SFA	25.95	±	0.40	28.73	±	0.58	25.92	±	0.44	0.001	>0.99	0.001
C15:1	0.01	±	0.01	0.00	±	<0.01	0.00	±	<0.01	0.40	0.40	>0.990
C16:1n7	1.32	±	0.04	1.26	±	0.04	1.26	±	0.04	0.57	0.50	0.992
C17:1	0.18	±	<0.01	0.18	±	<0.01	0.18	±	0.01	0.49	>0.99	0.52
C18:1n7	0.01	±	0.01	2.03	±	0.04	2.13	±	0.03	<0.0001	<0.0001	0.10
C18:1n9 <i>trans</i>	0.11	±	0.01	0.09	±	<0.01	0.11	±	0.02	0.39	0.99	0.43
C18:1n9	44.14	±	0.42	39.85	±	0.47	42.24	±	0.25	<0.0001	0.01	0.001
C20:1n9	0.36	±	0.01	0.41	±	0.02	0.34	±	0.02	0.16	0.61	0.02
C22:1n9	0.38	±	0.05	0.34	±	0.06	0.16	±	0.04	0.87	0.01	0.03
C24:1n9	0.07	±	0.01	0.07	±	0.01	0.07	±	0.01	0.99	0.95	0.90
DMA18:1	0.05	±	0.02	0.04	±	0.02	0.00	±	<0.01	0.94	0.09	0.16
∑C18:1	44.25	±	0.42	41.98	±	0.47	44.47	±	0.25	0.001	0.92	0.0003
∑n-7	1.32	±	0.04	3.29	±	0.06	3.38	±	0.05	<0.0001	<0.0001	0.43
∑n-9	44.95	±	0.41	40.72	±	0.45	42.81	±	0.23	<0.0001	0.00	0.001
∑MUFA	46.62	±	0.42	44.32	±	0.46	46.49	±	0.23	0.001	0.97	0.001
C18:2n6 <i>trans</i>	<0.01	±	<0.01	0.01	±	0.01	0.03	±	0.01	0.85	0.05	0.13
C18:2n6	23.86	±	0.25	22.54	±	0.39	24.32	±	0.37	0.03	0.64	0.003
C18:3n6	0.07	±	0.01	0.05	±	0.01	0.04	±	0.01	0.66	0.25	0.71
C20:2n6	0.21	±	0.02	0.19	±	0.01	0.21	±	0.01	0.60	>0.99	0.57
C20:3n6	0.11	±	0.02	0.17	±	0.03	0.13	±	0.01	0.07	0.62	0.33
C20:4n6	0.50	±	0.05	0.39	±	0.05	0.52	±	0.05	0.30	0.95	0.16
C22:2n6	0.01	±	0.01	0.01	±	0.01	0.00	±	<0.01	>0.99	0.48	0.42
C22:4n6	0.12	±	0.01	0.10	±	0.01	0.08	±	0.01	0.24	0.04	0.62
∑n-6 PUFA	24.87	±	0.21	23.44	±	0.40	25.32	±	0.37	0.02	0.65	0.002
∑n-6 metabolites	1.01	±	0.07	0.90	±	0.08	0.98	±	0.09	0.59	0.95	0.77
C18:3n-3 <i>trans</i>	0.14	±	0.02	0.13	±	0.03	0.15	±	0.01	0.84	0.99	0.75
C18:3n3	0.57	±	0.01	0.59	±	0.02	0.60	±	0.01	0.84	0.54	0.86
C20:3n3	0.02	±	0.01	0.00	±	<0.01	0.00	±	<0.01	0.0001	0.0001	>0.99
C22:5n3	0.03	±	<0.01	0.03	±	0.01	0.03	±	<0.01	>0.99	0.80	0.74
C22:6n3	0.04	±	<0.01	0.06	±	0.03	0.04	±	0.01	0.78	>0.99	0.78
∑n-3 PUFA	0.80	±	0.02	0.79	±	0.04	0.80	±	0.02	0.98	>0.99	0.98
∑n-3 metabolites	0.08	±	0.01	0.10	±	0.04	0.07	±	0.02	0.60	0.89	0.32
∑PUFA	25.68	±	0.22	24.24	±	0.39	26.12	±	0.37	0.02	0.64	0.001
∑UFA	72.30	±	0.38	68.56	±	0.80	72.61	±	0.52	0.0006	0.93	0.0002

Table 59. Retroperitoneal monoglyceride and diglyceride fatty acid methyl esters (FAME) ratios for high fat diet groups; High fat diet with-saline (HFD-S), High fat diet -pair-fed (HFD-PF) and High fat diet- Ginkgo biloba (HFD-GbE) (N=10 per group). Results presented as mean an (SEM), and statistically analysed by one-way ANOVA with Tukey's Post-hoc test. The level of statistical significance was set at * $p < 0.05$.

	HFD-S			HFD-PF			HFD-GbE			p value		
	Mean	±	SEM	Mean	±	SEM	Mean	±	SEM	S Vs PF	S Vs GbE	PF Vs GbE
ΣMUFA/ΣPUFA	1.82	±	0.03	1.83	±	0.02	1.78	±	0.02	0.91	0.54	0.30
ΣMUFA/ΣSFA	0.56	±	0.01	0.65	±	0.02	0.56	±	0.01	0.0006	>0.99	0.0005
ΣPUFA/ΣSFA	0.99	±	0.02	0.85	±	0.03	1.01	±	0.03	0.002	0.84	0.0003
ΣUFA/ΣSFA	2.79	±	0.06	2.40	±	0.07	2.81	±	0.06	0.0006	0.98	0.0003
C18:0/C16:0	0.27	±	<0.01	0.32	±	0.01	0.29	±	0.01	0.0004	0.13	0.0457
C16:1n-7/C16:0	0.07	±	<0.01	0.06	±	<0.01	0.07	±	<0.01	0.12	0.78	0.34
C18:1n-9/C16:0	2.28	±	0.05	1.93	±	0.05	2.23	±	0.04	<0.0001	0.71	0.0001
C18:1n-9/C16:1n-7	33.60	±	0.88	31.89	±	1.11	33.91	±	1.08	0.45	>0.99	0.46
C18:1/C18:0	8.45	±	0.30	6.41	±	0.27	8.05	±	0.29	0.0001	0.59	0.001
n-6/n-3	31.22	±	0.91	30.34	±	1.81	31.73	±	0.91	0.89	0.96	0.73
C18:2n-6/C18:3n-3	41.73	±	0.93	38.86	±	1.50	40.67	±	0.57	0.17	0.77	0.46
C20:4n-6/C20:3n-6	3.88	±	0.36	2.68	±	0.44	4.00	±	0.46	0.16	0.98	0.09
C20:4n-6/C22:6n-3	15.11	±	1.69	15.15	±	3.65	22.34	±	3.78	>0.99	0.24	0.27
C20:4n-6/C18:2n-6	0.02	±	<0.01	0.02	±	<0.01	0.02	±	<0.01	0.44	0.99	0.34
C20:4n-6/C18:3n-3	0.87	±	0.10	0.66	±	0.08	0.87	±	0.09	0.23	>0.99	0.22
C22:5n-3/C18:3n-3	0.05	±	0.01	0.07	±	0.01	0.06	±	0.01	0.99	0.90	0.94
C22:6n-3/C18:3n-3	0.06	±	0.01	0.12	±	0.07	0.07	±	0.03	0.52	>0.99	0.50
C22:6n-3/C22:5n-3	1.35	±	0.15	3.38	±	2.66	1.24	±	0.50	0.53	0.99	0.47
C18:2n6/C16:0	1.23	±	0.02	1.09	±	0.03	1.28	±	0.03	0.004	0.47	0.0001
C18:3n3/C16:0	0.03	±	<0.01	0.03	±	<0.01	0.03	±	<0.01	0.56	0.35	0.05
C20:3n-6/C18:3n-6	1.66	±	0.10	2.33	±	0.32	1.91	±	0.21	0.06	0.64	0.40
C22:4n-6/C20:4n-6	3.95	±	0.16	4.02	±	0.48	6.05	±	0.16	0.99	0.0002	0.0002
1 (% monoenoics)	46.62	±	0.42	43.71	±	0.56	46.49	±	0.23	0.0002	0.97	0.0002
2 (% dienoics)	48.15	±	0.49	45.48	±	0.79	49.10	±	0.74	0.03	0.61	0.003
3 (% trienoics)	2.68	±	0.09	2.93	±	0.21	2.75	±	0.07	0.44	0.93	0.6386
4 (% tetraenoics)	2.49	±	0.26	1.92	±	0.22	2.40	±	0.26	0.26	0.97	0.35
5 (% pentaenoics)	0.14	±	0.02	0.19	±	0.04	0.17	±	0.02	0.83	0.75	0.99
6 (% hexaenoics)	0.21	±	0.03	0.42	±	0.23	0.24	±	0.09	0.32	0.99	0.36
Unsaturation Index	100.29	±	0.53	94.51	±	1.22	101.12	±	0.92	0.0007	0.82	0.0001

Table 60. Mesenteric monoglycerides and diglycerides fatty acid methyl esters (FAME) for high fat diet groups; High fat diet with-saline (HFD-S), High fat diet -pair-fed (HFD-PF) and High fat diet- Ginkgo biloba (HFD-GbE) (N=10 per group). Fatty acid results are presented as area % percentage mean and standard error of the mean (SEM), and statistically analysed by one-way ANOVA with Tukey's Post-hoc test. The level of statistical significance was set at * $p < 0.05$.

	HFD-S		HFD-PF		HFD - GbE		S Vs PF	S Vs GbE	PF Vs GbE
	Mean	SEM	Mean	SEM	Mean	SEM		p value	
C14:0	0.52 ± 0.03	0.56 ± 0.02	0.45 ± 0.02	0.39	0.08	0.003			
C15:0	0.07 ± 0.01	0.08 ± 0.01	0.07 ± 0.01	0.003	0.69	0.69			
C16:0	20.70 ± 0.21	21.52 ± 0.19	19.93 ± 0.14	0.86	0.01	0.01			
C17:0	0.29 ± 0.02	0.28 ± 0.01	0.25 ± 0.01	0.96	0.07	0.12			
C18:0	6.18 ± 0.21	6.84 ± 0.18	5.98 ± 0.19	0.06	0.75	0.01			
C20:0	0.08 ± 0.02	0.11 ± 0.02	0.10 ± 0.02	0.57	0.83	0.90			
C21:0	0.14 ± 0.02	0.17 ± 0.01	0.17 ± 0.01	0.28	0.31	>0.99			
C24:0	0.19 ± 0.02	0.03 ± 0.01	0.03 ± 0.01	<0.0001	<0.0001	0.99			
DMA18:0	0.36 ± 0.04	0.27 ± 0.03	0.40 ± 0.07	0.38	0.83	0.15			
ΣSFA	28.57 ± 0.35	29.92 ± 0.30	27.56 ± 0.33	0.02	0.09	0.0001			
C16:1n-7	1.58 ± 0.11	1.40 ± 0.08	1.23 ± 0.05	0.29	0.02	0.36			
C17:1	0.10 ± 0.02	0.16 ± 0.01	0.16 ± 0.01	0.04	0.04	>0.99			
C18:1n-7	1.23 ± 0.41	2.53 ± 0.03	2.63 ± 0.10	0.002	0.001	0.95			
C18:1n-9	39.66 ± 0.51	39.60 ± 0.35	39.03 ± 0.42	>0.99	0.57	0.62			
C20:1n9	0.39 ± 0.02	0.41 ± 0.02	0.53 ± 0.03	0.83	0.001	0.01			
C22:1n-9	0.15 ± 0.06	0.04 ± 0.03	0.68 ± 0.06	0.24	<0.0001	<0.0001			
C24:1n-9	0.01 ± 0.01	0.06 ± 0.01	0.23 ± 0.04	0.23	<0.0001	<0.0001			
ΣC18:1	40.23 ± 0.65	40.19 ± 0.57	39.65 ± 0.63	>0.99	0.79	0.81			
Σn-7	2.84 ± 0.38	4.01 ± 0.10	3.90 ± 0.11	0.002	0.001	0.99			
Σn-9	40.28 ± 0.50	40.17 ± 0.32	40.59 ± 0.36	0.98	0.84	0.73			
ΣMUFA	44.66 ± 0.46	44.35 ± 0.28	44.65 ± 0.35	0.82	>0.99	0.83			
C18:2n-6	23.56 ± 0.32	22.54 ± 0.19	19.56 ± 2.19	0.84	0.09	0.24			
C18:3n-6	0.18 ± 0.06	0.11 ± 0.02	0.15 ± 0.03	0.43	0.84	0.78			
C20:2n-6	0.15 ± 0.02	0.17 ± 0.01	0.13 ± 0.01	0.80	0.52	0.21			
C20:3n-6	0.19 ± 0.01	0.18 ± 0.01	0.14 ± 0.01	0.31	0.00	0.01			
C20:4n-6	0.39 ± 0.03	0.36 ± 0.02	0.30 ± 0.02	0.71	0.04	0.20			
C22:2n-6	0.01 ± 0.01	0.03 ± 0.01	0.03 ± 0.01	0.04	0.05	0.99			
C22:4n-6	0.06 ± 0.01	0.17 ± 0.01	0.49 ± 0.03	0.001	<0.0001	<0.0001			
Σn-6 PUFA	24.54 ± 0.36	23.56 ± 0.20	20.96 ± 2.19	0.85	0.14	0.34			
Σn-6 metabolites	0.98 ± 0.10	1.02 ± 0.05	1.24 ± 0.06	0.91	0.04	0.10			
C18:3n-3	1.30 ± 0.18	1.30 ± 0.18	1.29 ± 0.18	>0.99	>0.99	>0.99			
C22:5n-3	0.08 ± 0.03	0.08 ± 0.03	0.08 ± 0.03	>0.99	>0.99	>0.99			
C22:6n-3	0.15 ± 0.06	0.15 ± 0.06	0.15 ± 0.06	>0.99	>0.99	>0.99			
Σn-3 PUFA	1.55 ± 0.21	1.55 ± 0.21	1.54 ± 0.21	>0.99	>0.99	>0.99			
Σn-3 metabolites	0.25 ± 0.09	0.25 ± 0.09	0.25 ± 0.09	>0.99	>0.99	>0.99			
ΣPUFA	26.08 ± 0.40	25.11 ± 0.29	22.50 ± 2.10	0.85	0.12	0.32			
ΣUFA	70.74 ± 0.43	69.45 ± 0.44	67.15 ± 2.19	0.77	0.15	0.44			

Table 61. Mesenteric monoglyceride and diglycerides (MAG+DAG) fatty acid methyl esters (FAME) ratios for high fat diet groups; High fat diet with-saline (HFD-S), High fat diet -pair-fed (HFD-PF) and High fat diet- Ginkgo biloba (HFD-GbE) (N=10 per group). Results presented as mean an (SEM), and statistically analysed by one-way ANOVA with Tukey's Post-hoc test. The level of statistical significance was set at *p < 0.05.

	HFD-S		HFD-PF		HFD - GbE		S Vs PF	S Vs GbE	PF Vs GbE
	Mean	SEM	Mean	SEM	Mean	SEM	p value		
ΣMUFA/ΣPUFA	1.72	± 0.04	1.77	± 0.02	2.80	± 0.98	>0.99	0.38	0.41
ΣMUFA/ΣSFA	1.10	± 0.02	1.19	± 0.02	3.98	± 2.39	>0.99	0.32	0.34
ΣPUFA/ΣSFA	0.59	± 0.01	0.57	± 0.01	0.50	± 0.05	0.89	0.12	0.28
ΣUFA/ΣSFA	2.48	± 0.04	2.32	± 0.04	2.44	± 0.09	0.17	0.88	0.37
C18:0/C16:0	0.30	± 0.01	0.32	± 0.01	0.30	± 0.01	0.31	>0.99	0.35
C16:1n-7/C16:0	0.08	± <0.01	0.06	± <0.01	0.06	± <0.01	0.10	0.03	0.85
C18:1n-9/C16:0	1.92	± 0.03	1.84	± 0.03	1.96	± 0.03	0.19	0.60	0.03
C18:1n-9/C16:1n-7	26.12	± 1.72	29.48	± 2.17	32.14	± 1.41	0.39	0.06	0.56
C18:1n-7/C18:0	0.22	± 0.07	0.37	± 0.01	0.44	± 0.02	0.05	0.003	0.50
C18:1/C18:0	6.60	± 0.30	5.92	± 0.19	6.70	± 0.27	0.16	0.95	0.10
C15:0/C17:0	0.30	± 0.01	0.32	± 0.01	0.30	± 0.01	0.12	>0.99	0.13
n-6/n-3	20.06	± 3.75	19.13	± 3.51	18.33	± 4.10	0.98	0.94	0.99
C18:2n-6/C18:3n-3	22.64	± 3.83	21.64	± 3.65	19.98	± 4.16	0.98	0.88	0.95
C20:4n-6/C20:3n-6	2.09	± 0.19	2.06	± 0.09	2.18	± 0.21	0.99	0.93	0.86
C20:4n-6/C18:3n-3	0.39	± 0.08	0.36	± 0.08	0.30	± 0.06	>0.99	>0.99	0.98
C22:5n-3/C18:3n-3	0.06	± 0.03	0.06	± 0.03	0.06	± 0.03	0.32	0.46	0.96
C22:6n-3/C18:3n-3	0.14	± 0.07	0.15	± 0.07	0.15	± 0.07	0.08	0.96	0.12
C18:2n6/C16:0	1.14	± 0.02	1.05	± 0.02	0.98	± 0.11	0.91	0.81	0.56
C18:3n3/C16:0	0.06	± 0.01	0.06	± 0.01	0.07	± 0.01	>0.99	0.99	0.99
1 (% monoenoics)	44.66	± 0.46	44.35	± 0.28	44.65	± 0.35	0.47	>0.99	0.51
2 (% dienoics)	47.43	± 0.63	45.48	± 0.40	39.76	± 4.35	0.89	0.95	0.99
3 (% trienoics)	5.06	± 0.65	4.80	± 0.58	4.80	± 0.57	0.80	0.99	0.88
4 (% tetraenoics)	1.81	± 0.18	2.13	± 0.08	3.17	± 0.14	0.97	0.98	0.90
5 (% pentaenoics)	0.40	± 0.16	0.40	± 0.16	0.39	± 0.16	0.28	>0.99	0.24
6 (% hexaenoics)	0.91	± 0.35	0.92	± 0.35	0.91	± 0.35	0.29	0.44	0.95
Unsaturation Index	100.27	± 0.99	98.08	± 0.94	93.68	± 4.18	>0.99	>0.99	>0.99

5.6 RET and MES PPL

As covered in the introduction, PPLs (PPL) make up approximately 50 per cent of cellular membrane with glycolipids, cholesterol, and intercalated transmembrane proteins embedded in the bilayer structure accounting for the rest. In mammalian cells, the major PPL are PC, PE, PS, PI and SM (Stryer *et al.*, 2019). Cell membrane function is influenced by the fluidity and stability of the cell membrane, which is dependent of the type of FA incorporated into the PPL structure, and the amount of cholesterol-rich microdomains. The membrane serves as a barrier and facilitator of ionic exchange and molecular transport in and out of the cell. If the membrane is rich in SFA, the bilayer will become a more rigid gel-like structure, while a membrane rich in cis-UFA will be more flexible (Weijers, 2012, 2015b, 2015a; Hulbert *et al.*, 2005, 2007). Fatty acids can alter the physiochemical properties of cell membrane permeability by influencing cellular channels and G protein-coupled receptors (GPCR) (Endo and Arita, 2016).

5.6.1 RES-PPL - NFD vs HFD

As summarized in Table 62 and Table 63, a significant increase in total SFA occurred in the PPL fraction of HFD-S compared to the NFD, largely due to the 48% increase in C18:0 (NFD $13.82 \pm 1.05\%$; HFD-S $20.46 \pm 0.59\%$, $p = 0.002$) and a 2-fold increase in C24:0 (NFD $1.01 \pm 0.20\%$; HFD-S $2.10 \pm 0.10\%$, $p = 0.01$). Table 62). Total PUFA decreased in the HFD-S group by 29% (NFD $34.29 \pm 1.15\%$; HFD-S $24.28 \pm 1.57\%$, $p = 0.01$), mostly due to the 37% decrease in n-6 PUFA (NFD, $30.06 \pm 1.37\%$; HFD-S, $19.06 \pm 0.34\%$, $p < 0.0001$), predominantly from C18:2n-6 (NFD, $24.91 \pm 1.65\%$; HFD-S, $13.87 \pm 0.44\%$, $p = 0.0003$) (Table 62). This is in keeping with the other fractions that also saw decreases in PUFA following an HFD. Interestingly, PUFA levels in TAG were ~23% for HFD-S, compared to ~45% for NFD. Similar PUFA % level of 24% for HFD rats was also seen in the PPL fraction while NFD-PUFA was around ~34%. Interestingly, n-3 PUFA levels did not decrease in line with n-6 PUFA as was generally seen in the other fractions, remaining relatively comparable between both NFD and HFD in the PPL fraction. When comparing fatty acid ratios, summarised in Table 63, a decrease of 45% was seen $\sum\text{PUFA}/\sum\text{SFA}$ in the HFD-S group compared to NFD (NFD, 0.91 ± 0.06 ; HFD-S, 0.50 ± 0.04 , $P = 0.002$). SFA and PUFA in PPLs are of similar ratios resulting in a ratio of 0.91 in an NFD, but this ratio decreases to 0.5 in the HFD, with double the amount of SFA incorporated into PPL than PUFA. A similar decrease of 35% was also seen in $\sum\text{UFA}/\sum\text{SFA}$ in HFD-S compared to NFD (NFD, 1.55 ± 0.09 ; HFD-S, $>0.99 \pm 0.03$, $P = 0.002$) Table 63). These results would suggest that the levels of unsaturation would decrease in the PPLs.

But this was not reflected in the unsaturation index between the NFD and HFD-S (NFD, 105.58±4.26; HFD-S 94.66±9.25, $P > 0.99$) (Table 63) where no changes occurred. The unsaturation index (UI) describes the fluidity of a biological membrane (Weijers, 2012). This suggests that while overall PUFA % levels decrease, the level of unsaturation within the membrane remains the same, meaning a similar level of fluidity exists between the biological membrane of the two groups. This is an interesting result as HFDs have been associated with decreased membrane fluidity, affecting insulin signalling (Parrish *et al.*, 1997; Storlien *et al.*, 1991).

5.6.2 MES-PPL - NFD vs HFD

When comparing the HFD-S group compared to the NFD group, shown in Table 64 and Table 65, the total SFA in HFD-S decreased by 16% (Σ SFA; NFD, 59.50±2.95%; HFD-S, 50.22±>0.99%, $p=0.002$), predominantly influenced by the 24% decrease in C16:0 (C16:0; NFD, 27.38±1.53%; HFD-S, 20.74±0.52%, $p=0.0001$) (Table 64). This resulted in an increase in the C18:0/C16:0 ratio (C18:0/C16:0; NFD, 1.03±0.04; HFD-S, 1.31±0.04, $p=0.002$) (Table 65). Total MUFA levels increased by 84% in the HFD-S group (Σ MUFA; NFD, 10.47±0.47%; HFD-S, 19.30±1.02%, $p<0.0001$) with 117% and 89% increases seen in both n-7 (Σ ω 7NFD, 2.43±0.07%; HFD-S, 5.27±0.74%, $p=0.0002$) and n-9 MUFA (n-9; NFD, 7.43±0.42%; HFD-S, 14.03±0.52%, $p<0.0001$) (Table 64), respectively. This increase was largely associated with the increase in C18:1 (C18:1 Total; NFD, 8.28±0.50%; HFD-S, 14.82±0.52%, $p=0.06$) (Table 64). Furthermore, a 71% increase in the C18:1n-9/C16:1n-7 ratio was seen (C18:1n-9/C16:1n-7; NFD, 27.55±3.04; HFD-S, 47.08±.83, $p=0.001$) (Table 65). n-3 PUFA decreasing by 32% compared to NFD (Σ n-3 PUFA; NFD, 1.57±0.07%; HFD-S, 2.89 ±0.04%, $p.01$) (Table 64). This caused the n-6/n-3 ratio to increase by 56% (n-6/n-3; NFD, 17.04±0.92; HFD-S, 26.54±1.01, $p<0.001$). The PUFA/SFA ratio also decreased (Σ PUFA/ Σ SFA; NFD, 2.72±0.17; HFD-S, 1.55±0.09, $p<0.001$) (Table 65).

5.6.3 RET-PPL HFD GbE treatment

In the HFD subsets, several significant changes occurred in the PPL fraction (Table 66 and Table 67). When compared to S group, total SFA decreased in the PF group by only 6% ($p=0.79$) but while not significant, SFA in the GbE group increased by 20% ($p=0.09$) (Table 66). When comparing PF to GbE, GbE SFA levels increased by 27% ($p=0.02$) (HFD-S, $49.24\pm 0.95\%$; HFD-PF, $46.36\pm 4.44\%$; HFD-GbE, $58.87\pm 2.90\%$). DMA18:0 decreased by 65% in PF ($p=0.0002$) and by 32% in GbE group ($p=0.01$) compared to the S group, while no significant difference occurred between the PF and GbE group (HFD-S, $1.63\pm 0.28\%$; HFD-PF, $0.33\pm 0.20\%$; HFD-GbE, $0.70\pm 0.06\%$) (Table 66). A dramatic increase in MUFA in PF rats and the decrease in GbE treatment is an interesting finding. The greatest change is seen in metabolites in the MUFA group. A 40% increase in PF ($p=0.01$) and a 20% decrease in GbE ($p=0.27$) was seen as compared to HFD-S in total MUFA levels, while GbE was significantly decreased by 43% compared to PF ($p=0.0002$) (HFD-S, $24.81\pm 1.26\%$; HFD-PF, $34.78\pm 3.14\%$; HFD-GbE, $19.78\pm 1.87\%$) (Table 66). Several dynamic changes in the MUFA pathway occurred from C16:1n-7 through to C24:1n-9. C16:1n-7, a recognised lipokine, increased by 235% in PF ($p<0.0001$) and but not significantly so in GbE ($p=0.11$) compared to HFD-S, although GbE levels were 45% than the PF group ($p=0.002$) (HFD-S, $0.48\pm 0.09\%$; HFD-PF, $1.61\pm 0.20\%$; HFD-GbE, $0.88\pm 0.08\%$) (Table 66). A dramatic 48% and 52% decrease of C18:1n-9 in PF ($p=0.003$) and GbE ($p=0.001$), respectively was seen compared to HFD-S, while PF and GbE levels remaining relatively similar ($p=0.95$) (HFD-S $20.93\pm 1.12\%$; HFD-PF, $10.96\pm 2.92\%$; HFD-GbE, $10.10\pm 1.07\%$) (Table 66). In the PF group, this was accompanied by a significant increase in C20:1n-9, C22:1n-9 and C24:1n-9, which were also increased in the GbE group compared HFD-S, but not to the extent of the PF group. C24:1n-9 increase by nearly 4568% in PF ($p<0.0001$) compared to HFD-S, while GbE was 84% less than PF ($p<0.0001$) (HFD-S $0.07\pm 0.03\%$; HFD-PF, $3.26\pm 0.57\%$; HFD-GbE, $0.54\pm 0.06\%$) (Table 66). This led to an overall n-7 increase of 86% in PF compared to HFD-S ($p=0.001$) and HFD-GbE ($p=0.001$). n-9 levels did not significantly change in PF ($p=0.23$) compared to HFD-S it did decrease by 24% in GbE ($p=0.04$), while GbE levels were 43% less than PF ($p=0.001$) (HFD-S, $1.94\pm 0.22\%$; HFD-PF, $3.62\pm 0.40\%$; HFD-GbE, 1.99 ± 0.19) (Table 66). Conversely, as PPL-MUFA percentage levels dropped to ~20% following GbE treatment, this drop in GbE MUFA was accompanied by an increase in SFA to nearly 59% of total sample levels compared to PF (~46%) and S (49%). In the previous section, lipolysis and DNL following calorie restriction was discussed. DNL produces C16:0 that can then be converted to C18:0 or MUFA. In the PF group, we see a decrease in C16:0 and an increase in C18:0, followed by increased varieties

of MUFA compared to the S group. These changes were also accompanied by a decrease in total PUFA by 37% in PF ($p=0.001$), but only 19% in GbE ($p=0.1$), compared to HFD-S, while GbE was 29% higher than the PF group (0.1) (HFD-S $24.28\pm 1.57\%$: HFD-PF, $15.37\pm 1.65\%$; 1 HFD-GbE, $19.76\pm 1.17\%$) (Table 66). n-6 PUFA decreased by 38% in PF ($p<0.0001$), and 21% in GbE, ($p=0.02$) compared to HFD-S, although GbE was 48% higher than the PF group (0.09) (HFD-S $19.06\pm 0.34\%$: HFD-PF, $11.77\pm 1.58\%$; HFD-GbE, $14.98\pm 0.77\%$) (Table 66). In contrast, for n-6 metabolites no differences were seen between the PF and HFD-S group, while GbE was 33% ($p=0.02$) and 48 % higher ($p=0.003$) than HFD-S and HFD-PF (Table 66), respectively.

5.6.4 MES-PPL HFD GbE treatment

A dynamic range of changes occurred in MES PPL HFD subset groups that received GbE treatment (HFD-GbE), caloric restriction (HFD-PF) of saline only (HFD-S) (Table 68 and Table 69). Compared to HFD-S, total SFA percentage levels increased by 36% in HFD-GbE ($p=0.001$) but decreased by 26% in HFD-PF ($p=0.05$) (Table 68). Due to these changes, HFD-GbE increased by 84% compared to HFD-PF ($p<0.0001$) (Σ SFA; HFD-S, $50.22\pm 1.01\%$: HFD-PF, $33.04\pm 1.86\%$: HFD-GbE, $60.81\pm 1.42\%$) (Table 68). These changes were largely due to the 7% and 42% decrease in C16:0 ($p=0.01$) and C18:0 ($p=0.0001$), respectively in HFD-PF, and a 59% increase in C16:0 ($p=0.0002$) in HFD-GbE, compared to HFD-S (C16:0; HFD-S, $20.74\pm 0.52\%$:HFD-PF, $16.60\pm 1.41\%$:HFD-GbE, $28.43\pm 1.67\%$) (C18:0;HFD-S, $26.94\pm 0.68\%$:HFD-PF, $13.91\pm 0.98\%$:HFD-GbE, $26.55\pm 0.91\%$) (Table 68). While no overall difference occurred between HFD-S and HFD-GbE C18:0 levels, a 91% increase in C18:0 in the GbE group occurred compared to HFD-PF ($p=0.0001$) (Table 68). Total MUFA levels increased 2-fold in the HFD-PF group accounted for 35% of the total sample ($p<0.0001$) but only decreased by 12% in HFD-GbE to 14% of the sample ($p=0.25$), compared to 16% in the HFD-S (Σ MUFA; HFD-S, $32.49\pm 0.89\%$: HFD-PF, $33.46\pm 1.84\%$: HFD-GbE, $14.11\pm 0.63\%$) (Table 68). Dynamic changes occurred across most individual MUFA, dominated by overall increases in HFD-PF levels compared to both HFD-S and HFD-GbE. Overall, in HFD-PF, n-7 MUFA increased over 5-fold compared to HFD-S ($p<0.0001$) and (HFD-GbE ($p<0.0001$)) (Σ n-7; HFD-S, $4.53\pm 0.74\%$: HFD-PF, $1.17\pm 1.17\%$: HFD-GbE, $<0.53\pm 0.01\%$). Similarly, n-9 PUFA increased 2-fold in HFD-PF compared to HFD-S ($p<0.0001$) and HFD-GbE ($p<0.0001$) (Σ n-9; HFD-S, $13.93\pm 0.52\%$: HFD-PF, $25.96\pm 1.76\%$: HFD-GbE, $10.89\pm 0.82\%$) (Table 68), while levels remained relatively similar between HFD-S and HFD-GbE. These changes were also reflected in the C18:1/C18:0 ratio that increased in HFD-PF, compared to both HFD-S ($p=0.03$) and HFD-GbE ($p=0.02$), but with levels remaining similar between HFD-S and HFD-GbE ($p=0.99$) (C18:1/C18:0; HFD-S, 0.39 ± 0.03 ; HFD-

PF, 0.89 ± 0.42 ; HFD-GbE, 0.36 ± 0.04) (Table 69). Overall total PUFA decreased by 52% in HFD-PF ($p < 0.0001$) and 17% in HFD-GbE ($p < 0.0001$), compared to HFD-S, although HFD-GbE PUFA levels remained 74% higher than HFD-PF ($p = 0.008$) (Σ PUFA; HFD-S, $29.90 \pm 0.89\%$; HFD-PF, $9.53 \pm 0.05\%$; HFD-GbE, $18.33 \pm 0.1\%$) (Table 68). These changes are largely attributed to the 61% and 25% decrease in n-6 PUFA seen in the HFD-PF ($p < 0.0001$) and HFD-GbE group ($p < 0.0001$) compared to HFD-S (Σ n-6 PUFA; HFD-S, $28.11 \pm 0.05\%$; HFD-PF, $9.23 \pm 0.07\%$; HFD-GbE, $17.90 \pm 0.13\%$) and the 82% and 29% decrease in HFD-PF ($p < 0.0001$) and HFD-GbE ($p < 0.0001$) n-6 metabolites compared to HFD-S, although n-6 metabolites levels remained 3 times higher in HFD-GbE compared to HFD-PF ($p = 0.0003$) (Σ n-6 metabolites; HFD-S, $13.64 \pm 0.28\%$; HFD-PF, $2.19 \pm 0.28\%$; HFD-GbE, $8.86 \pm 0.42\%$) (Table 68). n-3 PUFA levels decreased in both HFD-PF ($p < 0.0001$) and HFD-GbE ($p < 0.0001$) compared to HFD-S, but not between the HFD-PF and HFD-GbE groups (HFD-S, $1.79 \pm 0.04\%$; HFD-PF, $0.30 \pm 0.04\%$; HFD-GbE, $0.43 \pm 0.07\%$) (Table 68). Interestingly, the C18:2n-6/C18:3n-3 ratio increased in both HFD-PF ($p = 0.01$) and HFD-GbE ($p = 0.01$) compared to HFD-S (C18:2n-6/C18:3n-3; HFD-S, 66.97 ± 11.53 ; HFD-PF, 84.72 ± 25.90 ; HFD-GbE, 76.26 ± 26.37) (Table 69) although the opposite was seen in the n-6/n-3 ratio that decreased in HFD-PF ($p = 0.01$), and increased in HFD-GbE (0.02) compared to HFD-S, but still remained similar between the HFD-PF and HFD-GbE group (n-6/n-3; HFD-S, 41.25 ± 3.31 ; HFD-PF, 23.90 ± 8.42 ; HFD-GbE, 59.95 ± 10.25) (Table 69). Overall total UFA increased by 7% in the HFD-PF group ($p = 0.27$) but decreased significantly in the HFD-GbE group ($p < 0.0001$) compared to HFD-S (Σ UFA; HFD-S, $62.39 \pm 0.47\%$; HFD-PF, $42.99 \pm 0.95\%$; HFD-GbE, $32.44 \pm 0.36\%$) (Table 68). UFA levels were 35% less in HFD-GbE compared to HFD-PF ($p < 0.0001$). despite this, the unsaturation index decreased more in the HFD-PF group ($p < 0.0001$) than the HFD-GbE group ($p = 0.002$) compared to HFD-S (Unsaturation Index; HFD-S, 81.39 ± 9.67 ; HFD-PF, 61.36 ± 3.74 ; HFD-GbE, 66.79 ± 3.17) (Table 69). This change is reflected in the MUFA/PUFA ratio that increased in the HFD-PF group ($p < 0.0001$) but not in the HFD-GbE group ($p = 0.66$) when compared to HFD-S (Σ MUFA/ Σ PUFA; HFD-S, 0.67 ± 0.05 ; HFD-PF, 2.57 ± 0.23 ; HFD-GbE, 0.85 ± 0.09) (Table 69) indicating more change between MUFA and PUFA levels occurred in HFD-PF compared to the other two groups. Similarly, looking at the PUFA/SFA ratio, more changes occurred in the HFD-PF group with a decrease in the ratio seen compared to both HFD-S (< 0.0001) and HFD-GbE (< 0.0001), although HFD-GbE levels did decrease as well compared to HFD-S although not significantly ($p = 0.07$) (Σ PUFA/ Σ SFA; HFD-S, 1.53 ± 0.12 ; HFD-PF, 0.30 ± 0.04 ; HFD-GbE, 1.34 ± 0.09) (Table 69).

Table 62. Retroperitoneal phospholipid fatty acid methyl esters (FAME) for normal fat diet (NFD) and high fat diet (HFD-S) (N=10 per group). Fatty acid results are presented as area % percentage mean and standard error of the mean (SEM), and statistically analysed by Students t-test. The level of statistical significance was set at *p < 0.05.

	NFD			HFD-S			p value
	Mean	±	SEM	Mean	±	SEM	
C14:0	0.24	±	0.07	0.32	±	0.03	0.24
C16:0	21.90	±	0.74	24.26	±	0.65	0.74
C17:0	0.13	±	0.04	0.17	±	0.04	0.5
C18:0	13.82	±	1.05	20.46	±	0.59	0.002
C20:0	0.08	±	0.03	0.07	±	0.02	0.91
C22:0	0.07	±	0.03	0.20	±	0.04	0.66
C24:0	1.01	±	0.20	2.10	±	0.10	0.01
DMA 16:0	0.02	±	0.02	0.00	±	0.00	0.32
DMA 18:0	1.17	±	0.16	1.63	±	0.28	0.18
∑SFA.DMA	1.19	±	0.16	1.63	±	0.28	0.20
∑SFA	38.43	±	1.36	49.24	±	0.95	0.0004
C15:1	0.52	±	0.15	0.00	±	0.00	0.12
C16:1n7	0.77	±	0.11	0.48	±	0.09	0.94
C17:1	<0.01	±	0.00	0.05	±	0.03	0.17
C18:1n7	1.90	±	0.20	1.46	±	0.17	0.99
C18:1n9	14.91	±	1.33	20.93	±	1.12	0.18
C20:1n9	1.30	±	0.43	0.66	±	0.15	0.16
C20:3n9	0.22	±	0.22	0.00	±	0.00	0.31
C22:1n9	2.05	±	0.85	0.27	±	0.08	0.85
C24:1n9	0.85	±	0.42	0.07	±	0.03	0.95
DMA18:1	1.90	±	0.19	0.80	±	0.13	0.01
∑C18:1	16.81	±	1.51	22.48	±	1.22	0.42
n-7	2.67	±	0.21	1.94	±	0.22	0.74
n-9	19.33	±	0.86	21.93	±	1.07	0.96
∑MUFA	24.42	±	0.77	24.81	±	1.26	0.80
C18:2n6	24.91	±	1.65	13.87	±	0.44	0.0003
C20:2n6	0.02	±	0.02	0.11	±	0.02	0.05
C20:3n6	0.32	±	0.10	0.76	±	0.06	0.09
C20:4n6	3.39	±	0.30	3.53	±	0.28	>0.99
C22:2n6	0.01	±	0.01	0.31	±	0.04	<0.0001
C22:4n6	0.19	±	0.10	0.11	±	0.06	>0.99
∑ n-6 PUFA	30.06	±	1.37	19.06	±	0.34	<0.0001
∑ n-6 metabolites	5.16	±	0.40	4.82	±	0.29	0.51
C18:3n-3 trans	2.37	±	0.46	2.22	±	0.20	0.76
C18:3n3	0.95	±	0.16	0.31	±	0.08	0.13
C22:6n3	0.22	±	0.05	2.67	±	1.76	0.21
∑ n-3PUFA	4.23	±	0.80	5.21	±	1.72	0.62
∑ n-3 metabolites	0.91	±	0.70	2.68	±	1.77	0.38
∑PUFA	34.29	±	1.15	24.28	±	1.57	0.01
∑UFA	58.72	±	1.34	49.09	±	0.75	0.001

Table 63. Retroperitoneal phospholipid fatty acid methyl esters (FAME) ratios for high fat diet groups; High fat diet with-saline (HFD-S), High fat diet -pair-fed (HFD-PF) and High fat diet- Ginkgo biloba (HFD-GbE) (N=10 per group). Results presented as mean an (SEM), and statistically analysed by one-way ANOVA with Tukey's Post-hoc test. The level of statistical significance was set at * $p < 0.05$.

	NFD			HFD-S			p value
	Mean	SEM	SEM	Mean	SEM	SEM	
Σ MUFA/ Σ PUFA	0.72	±	0.04	1.07	±	0.09	0.22
Σ MUFA/ Σ SFA	1.60	±	0.10	2.03	±	0.10	0.42
Σ PUFA/ Σ SFA	0.91	±	0.06	0.50	±	0.04	0.002
Σ UFA/ Σ SFA	1.55	±	0.09	>0.99	±	0.03	0.002
C18:0/C16:0	0.64	±	0.05	0.85	±	0.03	0.18
C16:1n-7/C16:0	0.04	±	0.01	0.02	±	0.00	0.74
C18:1n-9/C16:0	0.68	±	0.06	0.86	±	0.03	0.53
C18:1n-9/C16:1n-7	18.32	±	3.00	38.80	±	4.56	0.15
C18:1n-7/C18:0	0.15	±	0.03	0.07	±	0.01	0.36
C18:1/C18:0	1.34	±	0.21	1.11	±	0.07	>0.99
n-6/ n-3	11.22	±	3.98	6.45	±	1.11	>0.99
C18:2n-6/C18:3n-3	26.58	±	3.27	55.74	±	10.46	0.70
C20:4n-6/C20:3n-6	8.12	±	1.80	4.87	±	0.51	0.89
C20:4n-6/C22:6n-3	11.02	±	0.68	22.62	±	9.89	>0.99
C20:4n-6/C18:2n-6	0.15	±	0.02	0.26	±	0.02	0.24
C20:4n-6/C18:3n-3	3.68	±	0.89	14.41	±	3.50	0.53
C20:5n-3/C18:3n-3	0.68	±	0.68	0.00	±	0.00	>0.99
C22:5n-3/C18:3n-3	<0.01	±	0.00	0.09	±	0.07	>0.99
C22:6n-3/C18:3n-3	0.19	±	0.06	14.28	±	12.27	>0.99
C18:2n6/C16:0	1.14	±	0.07	0.57	±	0.01	<0.0001
C18:3n3/C16:0	0.04	±	0.01	0.01	±	0.00	0.11
C22:4n-6/C20:4n-6	5.19	±	0.52	8.89	±	1.68	0.99
1 (% monoenoics)	21.35	±	3.00	24.81	±	1.26	>0.99
2 (% dienoics)	49.87	±	3.29	29.33	±	0.76	0.001
3 (% trienoics)	15.26	±	1.83	9.87	±	0.76	0.50
4 (% tetraenoics)	14.33	±	1.16	14.56	±	1.14	>0.99
5 (% pentaenoics)	3.43	±	3.43	0.06	±	0.04	>0.99
6 (% hexaenoics)	1.35	±	0.29	16.03	±	10.58	>0.99
Unsaturation Index	105.58	±	4.26	94.66	±	9.25	>0.99

Table 64. Mesenteric phospholipid fatty acid methyl esters (FAME) for normal fat diet (NFD) and high fat diet (HFD-S) (N=10 per group). Fatty acid results are presented as area % percentage mean and standard error of the mean (SEM), and statistically analysed by Students t-test. The level of statistical significance was set at * $p < 0.05$.

	NFD			HFD-S			p value
	Mean	SEM		Mean	SEM		
C14:0	0.23	±	0.02	0.58	±	0.03	0.001
C16:0	27.38	±	1.53	20.74	±	0.52	0.0001
C18:0	27.86	±	1.39	26.94	±	0.68	0.24
C20:0	0.22	±	0.01	0.12	±	0.02	<0.0001
C21:0	0.03	±	0.01	0.04	±	0.01	0.03
C23:0	0.24	±	0.02	0.11	±	0.02	0.0001
C24:0	0.77	±	0.05	0.11	±	0.02	<0.0001
∑SFA.DMA	2.13	±	0.13	1.58	±	0.13	<0.0001
∑SFA	59.50	±	2.95	50.22	±	>0.99	0.002
C16:1n-7	0.24	±	0.02	0.23	±	0.02	0.70
C18:1n7	2.09	±	0.07	4.30	±	0.24	0.0002
C18:1n-9	6.14	±	0.46	10.41	±	0.57	0.02
C20:1n9	0.75	±	0.04	3.22	±	0.30	<0.0001
C22:1n-9	0.25	±	0.07	0.10	±	0.03	0.97
C24:1n-9	0.24	±	0.02	0.20	±	0.01	0.12
C18:1 Total	8.28	±	0.50	14.82	±	0.52	0.06
∑n-7	2.43	±	0.07	5.27	±	0.74	0.0002
∑n-9	7.43	±	0.42	14.03	±	0.52	<0.0001
∑MUFA	10.47	±	0.47	19.30	±	1.02	<0.0001
C18:2n-6	14.36	±	1.52	14.47	±	0.67	>0.99
C18:3n-6	0.27	±	0.07	0.12	±	0.02	0.0004
C20:2n-6	0.40	±	0.08	0.21	±	0.02	0.36
C20:3n-6	0.46	±	0.04	0.54	±	0.02	0.98
C20:4n-6	10.62	±	1.19	12.14	±	0.44	>0.99
C22:2n-6	0.13	±	0.01	0.08	±	0.01	0.02
C22:4n-6	0.88	±	0.13	0.55	±	0.07	<0.0001
∑n-6 PUFA	27.28	±	2.55	28.11	±	0.88	>0.99
∑n-6 metabolites	12.75	±	1.36	13.64	±	0.47	>0.99
C18:3n-3	1.13	±	0.10	1.3	±	0.14	>0.99
C20:5n-3	0.32	±	0.03	0.2	±	0.02	0.33
C22:5n-3	0.25	±	0.04	0.32	±	0.02	0.96
C22:6n-3	0.55	±	0.05	1.07	±	0.03	0.02
∑n-3 PUFA	1.57	±	0.07	2.89	±	0.04	0.01
∑n-3 metabolites	1.25	±	0.07	0.86	±	0.03	0.02
∑PUFA	28.86	±	2.62	29.17	±	0.89	0.96
∑UFA	39.33	±	3.02	62.39	±	0.47	0.01

Table 65. Mesenteric Phospholipids (PPL) fatty acid methyl esters (FAME) ratios for high fat diet groups; High fat diet with-saline (HFD-S), High fat diet -pair-fed (HFD-PF) and High fat diet- Ginkgo biloba (HFD-GbE) (N=10 per group). Results presented as mean an (SEM), and statistically analysed by one-way ANOVA with Tukey's Post-hoc test. The level of statistical significance was set at * $p < 0.05$.

	NFD			HFD-S			p value
	Mean	SEM		Mean	SEM		
Σ MUFA/ Σ PUFA	0.38	±	0.02	0.67	±	0.05	0.008
Σ MUFA/ Σ SFA	0.38	±	0.02	0.67	±	0.05	0.008
Σ PUFA/ Σ SFA	2.72	±	0.17	1.55	±	0.09	<0.001
Σ UFA/ Σ SFA	0.70	±	0.09	0.97	±	0.04	0.44
C18:0/C16:0	1.03	±	0.04	1.31	±	0.04	>0.99
C18:1n-9/C16:0	0.24	±	0.03	0.51	±	0.04	0.001
C18:1n-9/C16:1n-7	27.55	±	3.04	47.08	±	2.83	0.01
C18:1/C18:0	0.31	±	0.03	0.56	±	0.03	0.003
n-6/n-3	17.04	±	0.92	26.54	±	1.01	<0.001
C18:2n-6/C18:3n-3	45.92	±	3.94	67.27	±	3.85	0.07
C20:4n-6/C20:3n-6	23.35	±	2.19	22.84	±	1.49	>0.99
C20:4n-6/C22:6n-3	19.24	±	0.83	39.94	±	2.97	0.99
C20:4n-6/C18:2n-6	0.76	±	0.07	0.85	±	0.04	0.93
C20:3n-3/C18:3n-3	1.56	±	0.19	1.56	±	0.09	0.99
C22:5n-3/C18:3n-3	0.86	±	0.18	0.91	±	0.04	0.67
C22:6n-3/C18:3n-3	1.87	±	0.27	1.37	±	0.06	>0.99
C22:6n-3/C22:5n-3	2.46	±	0.24	1.71	±	0.22	0.99
C18:2n6/C16:0	0.57	±	0.09	0.71	±	0.05	>0.99
C18:3n-6/C18:2n-6	0.02	±	0.01	0.01	±	0.00	0.88
C20:3n-6/C18:3n-6	3.58	±	1.29	5.57	±	0.94	>0.99
C22:4n-6/C20:4n-6	12.69	±	0.76	24.63	±	2.33	0.96
1 (% monoenoics)	10.47	±	0.47	19.30	±	1.02	<0.001
2 (% dienoics)	30.11	±	3.03	29.52	±	1.31	>0.99
3 (% trienoics)	4.52	±	0.25	3.65	±	0.14	0.29
4 (% tetraenoics)	45.98	±	5.25	50.73	±	1.91	>0.99
5 (% pentaenoics)	1.24	±	0.19	0.98	±	0.06	>0.99
6 (% hexaenoics)	3.30	±	0.33	1.91	±	0.14	0.07
Unsaturation Index	95.62	±	8.30	106.10	±	2.04	>0.99

Table 66. Retroperitoneal phospholipid fatty acid methyl esters (FAME) for high fat diet groups; High fat diet with-saline (HFD-S), High fat diet -pair-fed (HFD-PF) and High fat diet- Ginkgo biloba (HFD-GbE) (N=10 per group). Fatty acid results are presented as area % percentage mean and standard error of the mean (SEM), and statistically analysed by one-way ANOVA with Tukey's Post-hoc test. The level of statistical significance was set at * $p < 0.05$.

Name	HFD-S		HFD-PF		HFD-GbE		S Vs PF	S Vs GbE	PF Vs GbE
	Mean	SEM	Mean	SEM	Mean	SEM	p value		
C16:0	24.26	± 0.65	19.53	± 2.07	24.43	± 2.19	0.15	0.01	0.01
C17:0	0.17	± 0.04	0.03	± 0.02	0.13	± 0.03	0.19	0.01	0.27
C18:0	20.46	± 0.59	24.83	± 2.54	28.69	± 1.49	0.89	0.96	0.74
C20:0	0.07	± 0.02	0.09	± 0.04	0.06	± 0.02	0.002	0.92	0.001
C22:0	0.20	± 0.04	0.02	± 0.02	0.22	± 0.04	0.47	0.01	0.0007
C24:0	2.10	± 0.10	1.28	± 0.18	4.21	± 0.82	0.02	0.15	0.0002
∑DMA18:0	1.63	± 0.28	0.33	± 0.20	0.70	± 0.06	0.0002	0.01	0.40
∑SFA	49.24	± 0.95	46.36	± 4.44	58.87	± 2.90	0.79	0.09	0.02
C16:1n7	0.48	± 0.09	1.61	± 0.20	0.88	± 0.08	<0.0001	0.11	0.002
C18:1n7	1.46	± 0.17	0.90	± 0.21	0.68	± 0.10	0.07	0.01	0.61
C18:1n9	20.93	± 1.12	10.96	± 2.92	10.10	± 1.07	0.003	0.001	0.95
C20:1n9	0.66	± 0.15	2.35	± 0.21	1.33	± 0.16	<0.0001	0.03	0.001
C22:1n9	0.27	± 0.08	8.54	± 0.95	1.72	± 0.20	<0.0001	0.18	<0.0001
C24:1n9	0.07	± 0.03	3.26	± 0.57	0.54	± 0.06	<0.0001	0.59	<0.0001
∑DMA18:1	0.80	± 0.13	3.79	± 0.27	2.68	± 0.35	<0.0001	0.0001	0.02
∑C18:1	22.48	± 1.22	11.86	± 3.12	10.81	± 1.14	0.003	0.001	0.93
∑n-7	1.94	± 0.22	3.62	± 0.40	1.99	± 0.19	0.001	0.99	0.001
∑n-9	21.93	± 1.07	26.78	± 3.03	14.43	± 1.45	0.23	0.04	0.001
∑MUFA	24.81	± 1.26	34.78	± 3.14	19.78	± 1.87	0.01	0.27	0.0002
C18:2n6	13.87	± 0.44	7.43	± 1.47	8.56	± 0.50	0.0001	0.001	0.67
C18:3n6	-	± -	1.42	± 0.17	0.66	± 0.14	-	-	0.001
C20:2n6	0.11	± 0.02	-	± -	0.03	± 0.02	-	0.0002	-
C20:3n6	0.76	± 0.06	0.30	± 0.07	0.43	± 0.04	<0.0001	0.001	0.26
C20:4n6	3.53	± 0.28	2.62	± 0.33	4.72	± 0.25	0.09	0.02	0.0001
C22:2n6	0.31	± 0.04	-	± -	0.26	± 0.02	-	0.31	-
C22:4n6	0.11	± 0.06	-	± -	0.32	± 0.05	0.20	0.01	0.0001
∑n-6 PUFA	19.06	± 0.34	11.77	± 1.58	14.98	± 0.77	0.0001	0.02	0.09
∑n-6 metabolites	4.82	± 0.29	4.34	± 0.52	6.42	± 0.35	0.68	0.02	0.003
C18:3n-3 trans	2.22	± 0.20	3.06	± 0.26	4.09	± 0.50	0.22	0.002	0.11
C18:3n3	0.31	± 0.08	0.11	± 0.06	0.20	± 0.04	0.09	0.43	0.61
C22:5n3	0.01	± 0.01	-	± -	0.09	± 0.02	-	0.0001	-
C22:6n3	2.67	± 1.76	0.42	± 0.16	0.35	± 0.04	0.28	0.26	>0.99
∑n-3 PUFA	5.21	± 1.72	3.60	± 0.22	4.78	± 0.51	0.53	0.95	0.71
∑n-3 metabolites	2.68	± 1.77	0.42	± 0.16	0.49	± 0.07	0.06	0.04	>0.99
∑PUFA	24.28	± 1.57	15.37	± 1.65	19.76	± 1.17	0.001	0.10	0.11
∑UFA	49.09	± 0.75	50.15	± 4.42	39.54	± 2.97	0.97	0.09	0.06

Table 67. Retroperitoneal phospholipid fatty acid methyl esters (FAME) ratios for high fat diet groups; High fat diet with-saline (HFD-S), High fat diet -pair-fed (HFD-PF) and High fat diet- Ginkgo biloba (HFD-GbE) (N=10 per group). Results presented as mean an (SEM), and statistically analysed by one-way ANOVA with Tukey's Post-hoc test. The level of statistical significance was set at * $p < 0.05$.

Name	HFD-S		HFD-PF		HFD-GbE		S Vs PF	S Vs GbE p value	PF Vs GbE
	Mean	SEM	Mean	SEM	Mean	SEM			
Σ MUFA/ Σ PUFA	1.07 ± 0.09	2.35 ± 0.17	0.98 ± 0.05	<0.0001	0.84	<0.0001			
Σ MUFA/ Σ SFA	2.03 ± 0.10	1.56 ± 0.30	3.52 ± 0.66	0.72	0.05	0.01			
Σ PUFA/ Σ SFA	0.50 ± 0.04	0.39 ± 0.07	0.35 ± 0.03	0.33	0.13	0.85			
Σ UFA/ Σ SFA	1.00 ± 0.03	1.28 ± 0.24	0.71 ± 0.08	0.39	0.35	0.03			
C18:0/C16:0	0.85 ± 0.03	1.31 ± 0.12	1.22 ± 0.07	0.002	0.01	0.72			
C16:1n-7/C16:0	0.02 ± <0.01	0.10 ± 0.02	0.04 ± 0.01	0.004	0.71	0.02			
C18:1n-9/C16:0	0.86 ± 0.03	0.72 ± 0.22	0.47 ± 0.07	0.76	0.12	0.39			
C18:1n-9/C16:1n-7	38.80 ± 4.56	9.92 ± 4.81	11.35 ± 0.74	<0.0001	0.0001	0.96			
C18:1n-7/C18:0	0.07 ± 0.01	0.05 ± 0.02	0.02 ± <0.01	0.80	0.07	0.26			
C18:1/C18:0	1.11 ± 0.07	0.75 ± 0.35	0.40 ± 0.05	0.47	0.06	0.47			
n-6/n-3	6.45 ± 1.11	3.36 ± 0.54	3.34 ± 0.25	0.01	0.01	>0.99			
C18:2n-6/C18:3n-3	55.74 ± 10.46	33.89 ± 8.90	37.36 ± 4.82	0.38	0.28	0.97			
C20:4n-6/C20:3n-6	4.87 ± 0.51	7.23 ± 0.57	11.56 ± 1.13	0.16	<0.0001	0.01			
C20:4n-6/C22:6n-3	22.62 ± 9.89	7.07 ± 2.42	14.46 ± 1.42	0.07	0.40	0.39			
C20:4n-6/C18:2n-6	0.26 ± 0.02	0.48 ± 0.08	0.56 ± 0.03	0.02	0.001	0.53			
C20:4n-6/C18:3n-3	14.41 ± 3.50	7.81 ± 3.26	20.64 ± 3.32	0.57	0.40	0.15			
C22:6n-3/C18:3n-3	14.28 ± 12.27	0.42 ± 0.21	1.35 ± 0.12	0.55	0.31	>0.99			
C18:2n6/C16:0	0.57 ± 0.01	0.47 ± 0.12	0.38 ± 0.04	0.60	0.18	0.67			
C18:3n3/C16:0	0.01 ± <0.01	0.01 ± <0.01	0.01 ± <0.01	0.23	0.68	0.08			
1 (% monoenoics)	24.81 ± 1.26	11.29 ± 7.59	9.44 ± 1.46	0.11	0.06	0.95			
2 (% dienoics)	29.33 ± 0.76	14.87 ± 2.94	17.71 ± 1.04	<0.0001	0.0004	0.53			
3 (% trienoics)	9.87 ± 0.76	19.71 ± 1.99	18.37 ± 1.95	0.001	0.004	0.84			
4 (% tetraenoics)	14.56 ± 1.14	10.49 ± 1.34	20.15 ± 1.02	0.05	0.01	<0.0001			
6 (% hexaenoics)	16.03 ± 10.58	2.54 ± 0.97	2.12 ± 0.22	0.06	0.03	0.99			
Unsaturation Index	94.66 ± 9.25	58.90 ± 8.44	68.45 ± 4.19	0.01	0.06	0.65			

Table 68. Mesenteric phospholipid fatty acid methyl esters (FAME) for high fat diet groups; High fat diet with-saline (HFD-S), High fat diet -pair-fed (HFD-PF) and High fat diet- Ginkgo biloba (HFD-GbE) (N=10 per group). Fatty acid results are presented as area % percentage mean and standard error of the mean (SEM), and statistically analysed by one-way ANOVA with Tukey's Post-hoc test. The level of statistical significance was set at * $p < 0.05$.

	HFD-S		HFD-PF		HFD - GbE		S Vs PF	S Vs GbE	PF Vs GbE
	Mean	SEM	Mean	SEM	Mean	SEM		p value	
C14:0	0.58	± 0.03	0.75	± 0.08	1.36	± 0.22	0.06	<0.0001	0.01
C16:0	20.74	± 0.52	16.60	± 1.41	28.43	± 1.67	0.01	0.0002	0.003
C18:0	26.94	± 0.68	13.91	± 0.98	26.55	± 0.91	0.0001	>0.99	0.0001
C20:0	0.12	± 0.02	0.01	± 0.01	0.23	± 0.07	0.85	0.004	0.02
C21:0	0.04	± 0.01	0.01	± 0.01	0.01	± 0.01	0.004	>0.99	0.004
C22:0	0.11	± 0.02	0.34	± 0.05	0.32	± 0.05	<0.0001	<0.0001	<0.0001
C24:0	0.53	± 0.05	0.54	± 0.14	2.02	± 0.25	0.03	0.03	>0.99
∑SFA.DMA	1.58	± 0.13	0.66	± 0.11	1.32	± 0.26	0.09	0.01	0.46
∑SFA	50.22	± >0.99	33.04	± 1.86	60.81	± 1.42	0.05	0.001	<0.0001
C16:1n-7	0.23	± 0.02	0.18	± 0.09	0.26	± 0.07	0.0001	<0.0001	0.74
C18:1n-7	4.30	± 0.24	0.99	± 0.19	0.27	± 0.08	<0.0001	<0.0001	<0.0001
C18:1n-9	10.41	± 0.57	9.73	± 3.24	9.03	± 0.97	0.81	0.02	0.01
C20:1n-9	3.22	± 0.30	7.50	± 0.96	1.37	± 0.26	<0.0001	0.44	<0.0001
C22:1n-9	0.10	± 0.03	8.49	± 1.12	0.20	± 0.02	0.02	0.85	0.07
C24:1n-9	0.20	± 0.01	0.24	± 0.08	0.29	± 0.03	0.36	0.17	0.89
DMA 18:1	14.03	± 0.52	6.33	± 0.75	2.69	± 0.37	<0.0001	<0.0001	<0.0001
C18:1 Total	14.82	± 0.52	9.98	± 3.22	9.30	± 0.94	0.001	0.77	0.0002
∑n-7	4.53	± 0.74	1.17	± 1.17	0.53	± 0.07	<0.0001	0.01	<0.0001
∑n-9	13.93	± 0.52	25.96	± 1.76	10.89	± 0.82	<0.0001	0.86	0.0001
∑MUFA	32.49	± 0.89	33.46	± 1.84	14.11	± 0.63	<0.0001	0.25	<0.0001
C18:2n-6	14.47	± 0.67	7.04	± 1.52	9.04	± 0.66	0.002	0.004	0.96
C18:3n-6	0.12	± 0.02	0.01	± 0.01	1.33	± 0.19	0.08	<0.0001	<0.0001
C20:2n-6	0.21	± 0.02	0.16	± 0.05	0.27	± 0.07	0.93	0.001	0.003
C20:3n-6	0.54	± 0.02	0.44	± 0.07	0.73	± 0.06	0.85	0.0004	0.002
C20:4n-6	12.14	± 0.44	1.36	± 0.46	5.77	± 0.57	<0.0001	<0.0001	0.01
C22:2n-6	0.08	± 0.01	0.16	± 0.03	0.33	± 0.04	0.002	<0.0001	<0.0001
C22:4n-6	0.55	± 0.07	0.07	± 0.03	0.43	± 0.15	0.01	>0.99	0.02
∑n-6 PUFA	28.11	± 0.05	9.23	± 0.07	17.90	± 0.13	<0.0001	<0.0001	0.01
∑n-6 metabolites	13.64	± 0.28	2.19	± 0.28	8.86	± 0.42	<0.0001	<0.0001	0.0003
C18:3n-3	0.20	± 0.02	0.06	± 0.03	0.05	± 0.02	0.01	<0.0001	0.02
C20:5n-3	0.20	± 0.01	0.09	± 0.09	0.01	± 0.01	0.03	0.59	0.20
C22:5n-3	0.32	± 0.02	0.02	± 0.01	0.01	± 0.01	<0.0001	<0.0001	<0.0001
C22:6n-3	1.07	± 0.03	0.13	± 0.03	0.37	± 0.10	<0.0001	0.002	0.02
∑n-3 PUFA	1.79	± 0.04	0.30	± 0.04	0.43	± 0.07	<0.0001	<0.0001	0.15
∑n-3 metabolites	1.59	± 0.04	0.24	± 0.08	0.38	± 0.08	<0.0001	<0.0001	0.61
∑PUFA	29.90	± 0.04	9.53	± 0.05	18.33	± 0.10	<0.0001	<0.0001	0.008
∑UFA	62.39	± 0.47	42.99	± 0.95	32.44	± 0.36	<0.0001	<0.0001	0.0007

Table 69. Mesenteric phospholipids (PPL) fatty acid methyl esters (FAME) ratios for high fat diet groups; High fat diet with-saline (HFD-S), High fat diet -pair-fed (HFD-PF) and High fat diet- Ginkgo biloba (HFD-GbE) (N=10 per group). Results presented as mean an (SEM), and statistically analysed by one-way ANOVA with Tukey's Post-hoc test. The level of statistical significance was set at **p* < 0.05.

	HFD-S		HFD-PF		HFD - GbE		S Vs PF	S Vs GbE	PF Vs GbE
	Mean	SEM	Mean	SEM	Mean	SEM		p value	
ΣMUFA/ΣPUFA	0.67	± 0.05	2.57	± 0.23	0.85	± 0.09	<0.0001	0.66	<0.0001
ΣMUFA/ΣSFA	1.74	± 0.07	3.13	± 0.25	3.14	± 0.24	0.51	0.19	0.02
ΣPUFA/ΣSFA	1.53	± 0.12	0.30	± 0.04	1.34	± 0.09	<0.0001	0.07	<0.0001
ΣUFA/ΣSFA	0.91	± 0.05	1.42	± 0.12	0.54	± 0.03	0.09	0.005	<0.0001
C18:0/C16:0	1.34	± 0.05	0.88	± 0.08	0.96	± 0.06	0.0002	0.002	0.58
C16:1n-7/C16:0	0.01	± <0.01	0.01	± <0.01	0.01	± <0.01	0.001	0.01	0.49
C18:1n-9/C16:0	0.52	± 0.05	0.53	± 0.14	0.33	± 0.04	0.98	0.01	0.004
C18:1n-9/C16:1n-7	66.53	± 4.27	41.56	± 3.98	26.54	± 1.88	<0.0001	<0.0001	0.0003
C18:1n-7/C18:0	0.02	± <0.01	0.08	± 0.02	<0.01	± <0.01	<0.0001	<0.0001	<0.0001
C18:1/C18:0	0.39	± 0.03	0.89	± 0.42	0.36	± 0.04	0.03	0.99	0.02
n-6/n-3	41.25	± 3.31	23.90	± 8.42	59.95	± 10.25	0.01	0.02	0.93
C18:2n-6/C18:3n-3	66.97	± 11.53	84.72	± 25.90	76.26	± 26.37	0.01	0.01	0.96
C20:4n-6/C20:3n-6	26.98	± 1.95	3.78	± 1.10	8.92	± 1.76	<0.0001	<0.0001	0.88
C20:4n-6/C22:6n-3	44.39	± 2.66	8.29	± 3.62	27.05	± 6.29	<0.0001	<0.0001	0.97
C20:4n-6/C18:2n-6	0.84	± 0.05	0.22	± 0.08	0.65	± 0.06	<0.0001	<0.0001	<0.0001
C20:4n-6/C18:3n-3	65.44	± 6.86	21.06	± 15.05	40.80	± 9.71	<0.0001	0.02	0.06
C20:3n-3/C18:3n-3	<0.01	± <0.01	2.32	± 2.32	<0.01	± <0.01	<0.0001	<0.0001	0.34
C22:5n-3/C18:3n-3	0.94	± 0.09	0.33	± 0.31	<0.01	± <0.01	0.36	0.87	0.24
C22:6n-3/C18:3n-3	1.47	± 0.15	1.59	± 0.60	1.21	± 0.64	<0.0001	<0.0001	<0.0001
C22:6n-3/C22:5n-3	1.63	± 0.13	3.33	± 0.60	5.12	± <0.01	<0.0001	0.001	0.18
C18:2n6/C16:0	0.65	± 0.10	0.41	± 0.07	0.33	± 0.03	0.84	0.77	0.49
C18:3n-6/C18:2n-6	0.04	± 0.01	<0.01	± <0.01	0.16	± 0.03	0.88	0.74	0.45
C22:4n-6/C20:4n-6	16.23	± 0.80	21.50	± 12.65	9.68	± 2.22	0.0007	0.0001	0.61
1 (% monoenoics)	14.50	± 1.70	35.12	± 2.05	14.10	± 0.91	0.99	0.27	0.33
2 (% dienoics)	20.94	± 3.65	14.72	± 3.02	19.30	± 1.25	0.05	<0.0001	0.001
3 (% trienoics)	2.64	± 0.38	4.42	± 1.46	6.31	± 0.64	0.01	0.0001	0.21
4 (% tetraenoics)	41.27	± 4.97	5.73	± 1.90	24.79	± 2.60	0.15	0.03	0.71
5 (% pentaenoics)	0.70	± 0.09	0.59	± 0.45	0.07	± 0.07	<0.0001	<0.0001	<0.0001
6 (% hexaenoics)	1.34	± 0.16	0.78	± 0.17	2.21	± 0.62	<0.0001	<0.0001	<0.0001
Unsaturation Index	81.39	± 9.67	61.36	± 3.74	66.79	± 3.17	<0.0001	0.25	<0.0001

5.7 Discussion

A high fat diet is associated with metabolic disturbances including inflammation, IR and dyslipidaemia (Koenen *et al.* 2021; Lopes *et al.* 2016). Increased VAT which includes RET and MES WAT is considered more pathogenic and metabolically disturbing with greater risk of disease than SAT (Mittal, 2019; Hung *et al.*, 2014; Jialal, Kaur and Devaraj, 2014; Abete *et al.*, 2011; Costa *et al.*, 2011; Gealekman *et al.*, 2011; Mittendorfer, 2011; Ibrahim, 2010; Fang *et al.*, 2008; Yim *et al.*, 2007; Furukawa *et al.*, 2004; Wajchenberg, 2000). The use of tissue fatty acid profiles and fatty acid metabolites are becoming more useful as biomarkers for the prediction and diagnosis of disease and its link to diet including cardiometabolic, hepatic and renal disorders, obesity as well as cognitive dysfunction (Cisbani and Bazinet, 2021; Parry *et al.*, 2021; Song and Jensen, 2021; Koch *et al.*, 2020; Santos, Price and Bueno, 2020).

Overall, the MES results are consistent with the findings in RET tissue with RET and MES have very similar adipocyte lipid profiles. Of the lipid classes explored, the greatest differences were seen in the PPL fraction in both RET and MES. PPL are responsible for the fluidity and stability of the cell membrane which is dependent of the type of FA incorporated into the PPL structure (Weijers, 2012, 2015b, 2015a; Hulbert *et al.*, 2005, 2007). Intestinal phospholipid remodelling has also been reported in a high-fat diet (Wang *et al.* 2016). Higher SFA incorporation in cellular membranes is generally associated with decreased membrane fluidity, insulin resistance (IR) and impaired GLUT4 trafficking (Pilon, 2016; van Meer, 2011; van Meer and de Kroon, 2011). Interestingly, the UI levels were opposite in RET and MES PPL. While the UI decreased in RET-PPL from 105.6 (NFD) to 94.7 (HFD-S) it increased from 95.6 (NFD) to 106.1 (HFD-S) in MES-PPL. This indicates that changes in the membrane fluidity may be occurring due to the HFD diet. The MES-PPL UI decreased significantly further in both the HFD-PF and HFD-GbE group to 77.2 and 72.8, respectively, lower than that of the NFD group. A similar decrease in unsaturation occurred in the RET-PPL fraction, both in the HFD-PF (58.9) and HFD-GbE (68.6) groups. This would suggest that the membrane is becoming less fluid in the HFD-PF and HFD-GbE groups. When taking into consideration that previous results from our group under the same experimental conditions have shown that disordered insulin signalling was recovered following GbE treatment, another explanation may lie in the fluid nature of PPL lipid raft microdomain formation to facilitate cell signalling. For example, caveolae vesicles contain cholesterol and C16:0/C18:0-rich lipid raft microdomain and create small pits in the plasma membrane participating

in endocytosis and exocytosis, associated with regulating lipid trafficking, storage, and metabolism, known to positively activate insulin receptors (Parton, 2018). An increase in caveolae within the membrane to facilitate signalling will also be accompanied with an increase in the SFA C16:0 and C18:0 as they make up some of the integral structure of the caveolae molecule. The increased levels of SFA following GbE treatment to levels like that of a NFD and may explain IR changes observed previously in our HFD obese rat study, particularly as IR are anchored across the phospholipid membrane (Hirata *et al.*, 2015).

In nutrient excess, caveolin-1 (CAV1), a protein related to caveolae formation in the membrane, is upregulated in the aorta of HFD-obese rats (Yang *et al.*, 2007) along with increased phosphorylation of PKB/Akt and eNOS (Ser1177) which negatively regulates eNOS expression (Ju *et al.*, 1997; Michel and Feron, 1997). As reviewed by Sansbury & Hill (2014), the NO-producing activity of eNOS is diminished in metabolic disease. With a decrease in eNOS shown in obese humans and rodent models (Enos, Velázquez and Murphy, 2014; Sansbury *et al.*, 2012; Zhang *et al.*, 2012; Georgescu *et al.*, 2011; Perez-Matute *et al.*, 2009; Valerio *et al.*, 2006). eNOS increases fat oxidation and lipid synthesis in adipose tissue, liver and skeletal muscle and is associated with anti-obesity, increased insulin-sensitivity, and glucose metabolism rate (Kashiwagi *et al.*, 2013; Sansbury *et al.*, 2012). Similarly, ceramides, formed from metabolic changes in overloaded or dysfunctional adipocytes is associated with IR-related lipolysis and mobilisation of FA (Vegiopoulos, Rohm and Herzig, 2017), decreases eNOS activity by disrupting the eNOS-Akt complex from HSP90 (Zhang *et al.*, 2012). Cav-1 phosphorylation has also been shown to be increased in inflammatory macrophages, activated microglia and endothelial cells in the spinal cord injury (Shin, 2007). Structural studies have shown that caveolae are the primary location of insulin receptors within the cell membrane (Karlsson *et al.*, 2002; Gustavsson *et al.*, 1999). As eNOS is primarily found in the perinuclear region of cells and must be trafficked to from the golgi to plasma membranes, García-Cardena and colleagues (1996) showed that palmitoylation of eNOS, is necessary for its targeting into caveolae within the membrane. Furthermore, Shaul and colleagues (1996) showed that both myristoylation and palmitoylation are required to target the enzyme to caveolae and that each acylation process enhances targeting by 10-fold (Shaul *et al.*, 1996). Palmitoylation is where cysteine (and to a lesser degree serine and threonine) residues of proteins are covalently attached to FA such as palmitic acid (C16:0) while myristoylation is that addition of myristic acid (C14:0) to the N-terminal glycine of proteins (Jennings and Linder, 2010). Reports have shown that N-myristoylation of eNOS is a prerequisite to palmitoylation of membrane-bound eNOS where palmitoylation helps stabilize the membrane bound protein

(Udenwobele *et al.*, 2017; Prabhakar, Cheng and Michel, 2000; Liu, García-Cardena and Sessa, 1996). Once eNOS localizes to the caveolae of the plasma membrane, it binds to caveolin-1. eNOS bound to Caveolin-1 prevents the binding of Calmodulin (CaM) and renders eNOS inactive, however increased calcium influx activates the calcium/CaM complex which displaces CAV-1 turning eNOS active (Udenwobele *et al.*, 2017; Ju *et al.*, 1997; Michel and Feron, 1997; Michel *et al.*, 1997).

In the phospholipid fraction of MES-HFD-GbE treated rats in this study, the levels of C16:0 returned to a similar level (27%) seen in the NFD group (28%), while both HFD-S and HFD-PF showed decreased levels of 21% and 17%, respectively. GbE treatment over 7 days has been shown to increase eNOS mRNA levels and protein expression and NO release in mesenteric arterioles of senile rats (Chen *et al.*, 2019). Similar studies with GbE treatment for 1- 2 days showed similar increased eNOS promoter activity and eNOS expression in endothelial cells (Chiu *et al.*, 2020; Koltermann *et al.*, 2007). In cardiac hypertrophy, GbE treatment for 8 days restored eNOS protein expression which was decreased by chronic β -adrenergic receptor stimulation and consequent autonomic imbalance and baroreflex dysfunction (Mesquita *et al.*, 2017). A similar activation of Akt/eNOS was seen following Bilobalide treatment, a compound within GbE, in Cerebral Ischemia Reperfusion (Zheng *et al.*, 2018). Taken together, the fact that GbE treatment has been shown to increase eNOS expression and protein levels, and that eNOS is trafficked to plasma membrane-bound caveolae by the covalent bonding of C14:0 and C16:0 to eNOS by myristoylation palmitoylation, the increase in C14:0 and C16:0 seen in the PPL fraction of the GbE-treated group may be attributed to increase trafficking of eNOS to the plasma membrane. Furthermore, as insulin signalling has been shown to be restored following GbE treatment and caveolae are known to be the main location of insulin receptors, and that eNOS is known to increase insulin-sensitivity, the trafficking of C14:0/C16:0-bound-eNOS to caveolae may also play a role in the recovery of insulin signalling seen following GbE treatment. This may also explain the increase in C14:0 and C16:0 levels within the PPL fraction of the GbE treated group that is not seen in the other HFD-S and HFD-PF groups.

In the RET-PPL fraction, SFA increased and PUFA decreased in the HFD-S group compared to the NFD. In the RET HFD treatment groups, several significant changes occurred in the PPL fraction following treatment. Following GbE treatment SFA increased again by 20% ($p=0.09$) compared to HFD-S only, an increase not seen in the PF group. This was similarly seen in the MES PPL fraction. A dramatic increase in RET MUFA was seen in the PF group, while GbE treatment decreased levels. This may be linked to changes in DNL Acetyl-CoA to C16:0 to C18:0 conversion. The enzymes ACC and FASN that are responsible for initial Acetyl-CoA to C16:0 conversion, have been shown to be upregulated in

calorie restriction (Ameer *et al.*, 2014; Bruss *et al.*, 2010) and downregulated by GbE as shown previously (Hirata, Cruz, *et al.*, 2019), which may explain the changes seen RET PPL. Interestingly, this increase of MUFA in the PF group was not seen in the MES fraction.

Total PUFA in RET-PPL also decreased by 37% in PF and 19% in GbE compared to HFD-S. Specifically, n-6 PUFA decreased by 38% in PF and 21% in GbE, compared to HFD-S. Interestingly n-6 metabolites following GbE treatment were 33% and 48% higher compared to HFD-S and HFD-PF. The changes in PUFA may be a result of calorie restriction. Alternatively, PUFAs may be cleaved and utilized for other purposes such as inflammation mediation. In comparison, the RET-PPL GbE group has more n-6 metabolites compared to the other groups, and the decreased levels of C18:2n-6 following caloric restriction is partially ameliorated. Interestingly, n-3 metabolites levels did not differ between PF and GbE RET PPL but did similarly decrease by 84% in PF and 82% in GbE groups compared to HFD-S. Together, as both PF and GbE received the same quantity of food and availability of PUFA, this might suggest that GbE may not influence n-3 DNL or the production of n-3-derived oxylipins but may influence n-6 PUFA oxylipin production following calorie restriction. As oxidised PPLs are utilized directly for pro-resolving mediation or their FA cleaved for oxylipin production, a continual replacement of PPLs is necessary for the membrane.

A similar change occurred in the MES-PPL fraction. In the MES-PPL fraction, n-6 PUFA decreased by 61% and 25% in HFD-PF and HFD-GbE group compared to HFD-S. This decrease brings levels close to that seen in the NFD group for both the HFD-PF and HFD-GbE groups. An even more dramatic decrease in n-6 metabolites was seen in the HFD-PF group, compared to HFD-S ($p < 0.0001$) and HFD-GbE ($p = 0.0003$) (Σ n-6 metabolites; HFD-S, $13.64 \pm 0.88\%$: HFD-PF, $2.20 \pm 0.50\%$: HFD-GbE, $8.85 \pm 0.71\%$), although it appears that GbE treatment was able to partially ameliorate the dramatic effects of caloric restriction on PUFA levels within the membrane that can be seen in the HFD-PF group. The decrease in MES-PPL Σ n-6 PUFA especially C18:2n-6 in both PF and GbE groups may also suggest a switch to increased n-6 PUFA mobilization/utilization for metabolic activities such as inflammatory-mitigating cytokine production involved in intracellular and intercellular signalling. As levels of n-6 metabolites did not decrease as much in the GbE group, compared to caloric restriction (PF) alone, this suggests GbE has some influence on the utilization of n-6 metabolites from the PPL membrane, perhaps owing to the antioxidant capacity of GbE. The fact that n-3PUFA levels significantly decreased in HFD-PF ($p < 0.0001$) and HFD-GbE ($p < 0.0001$) compared to HFD-S (Σ n-3 PUFA; HFD-S, $1.79 \pm 0.04\%$: HFD-PF, $0.3 \pm 0.04\%$: HFD-GbE, $0.43 \pm 0.07\%$) but to lesser extent following GbE treatment, with an increase in n-3 metabolites seen following GbE treatment comparing to either HFD-S or HFD-PF (Σ n-3

metabolites; HFD-S, $0.20 \pm 0.02\%$:HFD-PF, $0.24 \pm 0.04\%$:HFD-GbE, $0.38 \pm 0.11\%$) further supports the partial protection of GbE on PUFA in PPL membrane.

Metabolic changes associated with metabolically unhealthy obesity (MUO) associated with visceral VAT (Iacobini *et al.*, 2019) and a HFD include impaired insulin signalling, immune cell infiltration, increased proinflammatory cytokines (e.g., CRP, IL-1 β , IL-6, and TNF- α) and vasoconstriction (Wali *et al.*, 2020; Li *et al.*, 2015; Bigornia *et al.*, 2012; Lam *et al.*, 2012). Inflammation in the GI tract resulting from an HFD, is likely caused by the transport of lipids across the intestinal barrier causing lymphoid cell recruitment and consequent epithelial cellular injury. Gut-associated lymphoid tissue (GALT) contains a multitude of immune cells responsible for defending against pathogenic substances from the intestines. A high SFA diet has been shown to stimulate chronic inflammation disrupting the intestinal barrier and further proliferating inflammation (Rohr *et al.*, 2020; Lam *et al.*, 2012, 2015).

As reviewed by Rohr and colleagues (2020), a HFD affects multiple cytokines involved in increasing intestinal barrier permeability. These includes HFD-related increase in NF- κ β and as well as increased proinflammatory and barrier disrupting cytokines; IL-1 β , IL-4, IL-13, IL-6, IL-12, IL-23, IL-18, IFN γ , TNF α , perforin and Granzyme B; and a decrease in barrier-forming cytokines IL-10, IL-17 and IL-22 (Rohr *et al.*, 2020; Magnuson *et al.*, 2018; Zou *et al.*, 2018; Ng *et al.*, 2017; Robles *et al.*, 2017; Kawano *et al.*, 2016; Luck *et al.*, 2015; Teixeira *et al.*, 2011). Furthermore, a HFD is shown to disrupt the gut microbiota profiles, in favour of short-chain-FA (SCFA)-producing *Firmicutes* bacteria (Overby and Ferguson, 2021; den Besten *et al.*, 2015; Murugesan *et al.*, 2015; Rahat-Rozenbloom *et al.*, 2014; Samuel *et al.*, 2008). SCFAs regulate the production of leukocyte-derived cytokines (TNF- α , IL-2, IL-6 and IL-10) as well as eicosanoids and chemokines such as monocyte chemoattractant protein-1 (MCP-1) and cytokine-induced neutrophil chemoattractant (CINC-2) further enhancing immune cell recruitment and activation (Vinolo *et al.*, 2011). An increase in macrophage specific proteins (F4/80+ and CD68) in perigonadal, perirenal, mesenteric, and subcutaneous adipose tissue is positively correlated with body mass, with macrophages largely responsible for the increase in TNF- α , iNOS and IL-6 expression involved in inflammatory pathways (Weisberg *et al.*, 2003). The infiltration of macrophages into mesenteric tissue is also associated with inflammatory diseases such as colitis and Crohn's disease (Yin *et al.*, 2021; Scoville *et al.*, 2018; Sideri *et al.*, 2015). It has been shown in vitro by Yoshida and colleagues (2001) that epithelial cells release IL-6 and growth-related oncogene/cytokine-induced neutrophil chemoattractant-1 (GRO/CINC-1) in the presence of the LCFA LA and AA, stimulating locomotion and activation of neutrophils. They also reported that the secretion of IL-6 and GRO/CINC-1 was further enhanced in the presence of IL-1 β or TGF- β .

Furthermore, they found that MAPK activity, involved in survival signalling pathways and Akt signalling was also significantly enhanced following LCFA treatment (Yoshida *et al.*, 2001). Macrophage-derived cytokines have been reported to inhibit insulin signalling by phosphorylating serine residues of insulin receptor substrate (IRS) proteins (Wali *et al.*, 2020). This leads to increased lipolysis and liberation of FA from adipose tissue into circulation (Samuel and Shulman, 2016). Furthermore, Magnuson and colleagues (2018) also reported that following a high fat diet for 7 weeks, C57BL/6 mice had increased immune cell numbers in visceral lymph nodes, most likely recruited from immune cells from the intestines and retained by cytokine secretion from VAT (Magnuson *et al.*, 2018)

Interestingly, under the same experimental conditions, previously published work has shown that an HFD-S group experienced elevated glycemia compared to an NFD, which was ameliorated with GbE treatment. Likewise, while IRS-1 levels were decreased in an HFD, compared to an NFD, GbE treatment ameliorated IRS-1 levels, above that of baseline (Banin *et al.*, 2014). Likewise, GbE treatment increased insulin-induced IR phosphorylation levels 2.81-fold, in retroperitoneal WAT depot compared to HFD-S nontreated obese rats. GbE also significantly reduced the phosphorylation of NF- κ B p65 by 60% along with TNF- α levels, while increasing the gene expression of the anti-inflammatory cytokine IL-10 in comparison to the nontreated obese rats (Hirata *et al.*, 2015). It has also been shown in vitro in a HFD guinea pig model that the phospholipids of proliferating lymphoid cells in immune-stimulated lymph nodes are most likely obtained from and reflect the TAG profiles of close surrounding adipocytes (Pond and Mattacks, 2003). If this is assumed, then local immune cell phospholipid membranes in the HFD model will contain a greater abundance of SFA and MUFA, compared to PUFA, of which the majority will be n-6 PUFA with levels 36 times higher than that of n-3 PUFA, leading to much more pro-inflammatory oxylipin and cytokine production (Khalili, Valdes-Ramos and Harbige, 2021; Malesza *et al.*, 2021; von Frankenberg *et al.*, 2017). These metabolic and pro-inflammatory disturbances can lead to chronic low-grade inflammation, oxidative stress, obesity, insulin resistance, metabolic syndrome, T2DM and cardiovascular disease (Malesza *et al.*, 2021). Dynamic changes occurred across most individual MUFA in MES-PPL, dominated by overall increases in HFD-PF levels compared to both HFD-S and HFD-GbE. The dramatic increase in MUFA in the HFD-PF group suggests that a greater phospholipid turnover may be occurring in this group, with a need to utilize more abundantly available MUFA rather than PUFA in the membrane. This is further supported by the overall total PUFA decrease of 52% in HFD-PF ($p < 0.0001$) and but only 17% in HFD-GbE ($p = 0 < 0.0001$), compared to HFD-S, while HFD-GbE PUFA levels remained 74% higher than HFD-

PF ($p=0.008$) (MES-PPL Σ PUFA; HFD-S, $29.17\pm 0.89\%$: HFD-PF, $10.51\pm 1.41\%$: HFD-GbE, $18.34\pm 0.97\%$). This suggests that following GbE treatment, the PUFAs within the phospholipid membrane are being partially spared either from CE or oxylipin production, or perhaps being oxidized less in situ compared to caloric restriction alone. This may have occurred due to the antioxidant capacity attributed to GbE. Furthermore, considering that both HFD-PF and HFD-GbE both experienced the same level of caloric restriction, the vast difference between groups regarding MUFA and PUFA is most likely due to GbE treatment. Throughout the lipid fraction of the HFD-PF group, there have been indicators of DNL from the changes in the SFA and MUFA levels. MUFA levels increased 3.5 times in the MES-PPL HFD-PF group compared to the other groups but no comparable changes occurred in any of the HFD groups in MES-TAG total MUFA levels ($\sim 48-49\%$ for all group), MES-CE MUFA levels ($\sim 42-43\%$ for all groups), or the MES-MAG+DAG group ($\sim 44\%$ for all groups), firmly suggested that DNL is occurring in the HFD-PF group allowing for MUFA synthesis and supply into the phospholipid membrane. This is further supported by SFA levels also remaining similar in all fractions for all HFD groups (TAG $\sim 27\%$; CE- $\sim 22\%$; MAG+DAG 28-29%) but decreased from 50% in HFD-S to 33% in HFD-PF, while returning to 61% in HFD-GbE, which is comparable to NFD PPL levels. Results also suggest that DNL may be occurring in the RET-PPL PF group, producing MUFA that are being incorporated into the PPL membrane, with percentage levels nearly 10% higher in PF ($\sim 34\%$) compared to HFD-S ($\sim 25\%$) or NFD ($\sim 24\%$). The increase in C16:0, C18:0 and total SFA in the RET PPL PF group as well as the drop in C18:1n-9 and total n-9 levels and increase n-7 levels suggests that calorie restriction may influence DNL and MUFA synthesis pathways. As total SFA goes up, total MUFA levels decrease. Also, as n-7 levels increase, this may suggest that the conversion of C16:0 to C18:1n-7 MUFA may be promoted rather than that of C18:1n-9 that showed decreased levels. This may suggest that SCD1-mediated conversion of C16:0 to C16:1n-7 and C18:1n-7 is favoured, rather than the conversion of C18:0 to C18:1n-9. Conversely, as the PF group is in a reduced caloric state compared to S and GbE groups, it is more likely that lipolysis may occur which should restrict DNL through endocrine and paracrine negative feedback including adiponectin, leptin or oxylipin signalling. Studies have identified that adipose tissue DNL produces cytokine-like lipids known as lipokines that function as endocrine signallers affecting distant organs and controlling metabolic homeostasis. C16:1n-7 (Palmitoleate) can function as a lipokines and has been shown to stimulate muscle insulin action, suppress hepatic steatosis and reduce inflammation (Yore *et al.*, 2014; Cao *et al.*, 2008). Lipokines act on fatty acid binding proteins (FABPs) that function as lipid chaperones controlling the partitioning of lipids inside the cell. Cao and colleagues (2008) observed that C16:1n-7 was the most enriched and significantly regulated lipid

species in adipose tissue of FABP^{-/-} mice. Mice lacking the FABPs are resistant to diet-induced obesity, fatty liver disease, insulin resistance, and T2DM (Maeda *et al.*, 2005). Cao and colleagues (2008) found that C16:1n-7 was increased in plasma in both regular and high-fat diet fed FABP^{-/-} mice. They also found that C16:1n-7 was reduced by 50% in WT mice adipose tissue after an HFD, but only decreased by 10% in FABP^{-/-} mice. They also found that C16:1n7 functioned as an insulin-sensitizing hormone improving glucose metabolism. Cao and colleagues (2008) found TAG-C16:1n-7 potentiated the entire hepatic proximal insulin-signalling pathway including insulin receptor activation and phosphorylation of insulin receptor substrate 1, 2 and Akt (Cao *et al.*, 2008). LXR receptors control the expression of several genes including SREBP1c through insulin levels within the plasma, with SREBP1c upregulates all genes in the FA biosynthetic pathway including DNL (Song *et al.* 2018). In *ob/ob* mice (LOKO mice) which lack LXR, DNL glucose utilization shifts from the liver to adipose tissue, which acts as a sink for glucose, improving insulin sensitivity and protects from hepatic steatosis. Unfortunately, in the study adipose tissue inflammatory markers became elevated compared to the control group, perhaps from adipocyte hypertrophic growth due to excess glucose uptake and DNL as in the seen in *ob/ob* mice (Beaven *et al.*, 2013). Overnight fasting has been shown to suppress DNL enzymes and FA desaturation and elongase activity, particularly involving ELOVL6. The Loss of ELOVL6 function has been shown *in vivo* to increase C16:0 and C16:1n-7 and reduce C18:0 and C18:1n-9 (Matsuzaka *et al.*, 2007) like that observed in the RET – PPL PF and GbE groups. ELOVL6, SCD1, and FASN mRNA levels show similar changes in hepatic SREBP-1c mRNA and protein levels (Wang *et al.*, 2006) after fasting which can be decreased by up to 60% (Gosmain *et al.*, 2005; Shimomura *et al.*, 1999; Horton *et al.*, 1998). One clinical study involving impaired fasting glycemia showed that higher activities of ELOVL6 accompanied lower percentage levels of C18:1n-7 (MacÁšek *et al.*, 2021). This makes the increase of C18:1n-7 levels in both the RET – PPL PF and GbE group, comparable to the NFD group, particularly interesting, especially when ELOVL6 activity is purported to decrease with fasting, which both groups essentially underwent. C18:1n-7 is a major component of the PPL cardiolipin (CL) found in mitochondrial membranes with CL accounting for up to 20% of mitochondrial PPL membranes (Bueno *et al.*, 2015). Mainly located in the inner mitochondrial membrane (IMM), CL is an important co-factor for cholesterol translocation from the outer mitochondrial membrane to the IMM, playing an important role in the importing of proteins (Schlattner *et al.*, 2014). Adenylate cyclase activity is reported to be enhanced with the incorporation of C18:1n-7 in erythrocytes (Henis, Rimoni and Felderl, 1982; Orly and Schramm, 1975). Adenylate cyclase catalyses the conversion of ATP (Seifert *et al.*, 2012) (c-AMP) (Seifert *et al.*, 2012). Increased

c-AMP levels result in the activation of protein kinase A/ cAMP-dependent protein kinase (PKA). PKA phosphorylates cytosolic lipid droplets (LDs)-protein PLIN1 and cytoplasmic HSL. PLIN1 stimulates the release of comparative gene identification-58 (CGI-58), which in turn activates ATGL. This stimulates lipolysis and the conversion of TAG to DAG (Nielsen, Jessen, Jens *et al.*, 2014; Reid *et al.*, 2008). Phosphorylated/activated HSL translocate from the cytosol to the surface of the LDs, where it docks with activated PLIN1 and thus able to interact with ATGL-generated DAG promoting lipolysis. DAG also activates PKC which phosphorylates serine residues on IRS and inhibits insulin PI3K-Akt signaling. Normally the activation of Akt leads to the degradation of cAMP back to 5'-AMP, which leads to the deactivation of PLIN1 and HSL thus suppressing lipolysis. Therefore, the production of DAG through PLIN1 and ATGL activity by further promotes lipolysis (Saponara and Bosisio, 1998; Nielsen *et al.*, 2014). Alterations in PDE activity has also been reported in obesity, with body mass index BMI inversely correlated to total PDE activity in omentum WAT (Omar *et al.*, 2011). Adenylate cyclase activity has been shown to be significantly lower in women living with obesity compared to normal-weight women. From the same study by Martin and colleagues, they also showed that in post-obesity women that had undergone weight loss by gastric stapling, levels of hormone-stimulated cAMP matched that of normal-weight women (Martin *et al.*, 1990). Furthermore, GbE biflavones have been shown to inhibit PDE activity in rat adipose tissue thereby reducing the catalytic breakdown of cAMP and promoting lipolysis (Saponara and Bosisio, 1998b). Additionally, quercetin, a polyphenolic flavonoid found in GbE has been reported to improve hepatic dyslipidaemia by downregulating SREBP-1c and FAS levels and significantly upregulate PPAR α protein levels involved in β -oxidation (Sun *et al.*, 2015) as well as carnitine palmitoyl-transferase1 and medium-chain acyl-coenzyme A dehydrogenase expression (Wang *et al.*, 2016). Kaempferol, and other flavanol abundant in GbE has been shown to protect against hyperglycaemic metabolic changes similar to that of insulin by ameliorating increased serum glucose levels and increased glucose uptake in rat soleus muscle *via* the PI3K-Akt pathway (Cazarolli *et al.*, 2009; Jorge *et al.*, 2004), as well as reduced caspase-3 activity in β -cells and islets caused by hyperglycaemia and IL-1 β and TNF- α levels (Al-Numair *et al.*, 2015; Abo-Salem, 2014; Zhang *et al.*, 2013). OS and cellular apoptosis were also reduced by the reduction of anti-apoptotic Akt and Bcl-2 protein expression (Al-Numair *et al.*, 2015; Zhang and Liu, 2011). These cellular changes improved cAMP levels, lipid peroxidation and β -cells synthesis and secretion of insulin and plasma glucose levels (Al-Numair *et al.*, 2015; Zhang and Liu, 2011). Zang and colleagues (2015) found that in HFD-fed mice, kaempferol treatment exhibited anti-obesity and anti-diabetic effects, reducing body weight, adipose tissue TAG levels and decreased fasting blood glucose, serum

HbA1c (haemoglobin A(1c)) levels while improving insulin resistance compared to HFD with no treatment. They found that hepatic gene expression of peroxisome proliferator-activated receptor (PPAR- γ) and sterol regulatory element-binding protein (SREBP-1c) were down-regulated, increasing lipid metabolism (Zang *et al.*, 2015). Ginkgetin, a biflavone found in GbE blocked the differentiation of preadipocytes into adipocytes preventing hypertrophy in HFD-fed mice WAT, by acting as a STAT5 inhibitor, inhibiting PPAR γ and C/EBP α expression (Cho *et al.*, 2019). GbE treatment has also been shown to inhibit adipocyte differentiation, downregulating the expression of adipogenesis genes PPAR- γ and Ap2 (Wu *et al.*, 2016). Similarly, GbE has been shown to modulate hepatic GLUT-2 (glucose transporter 2), PPAR- α (Peroxisome proliferator-activated receptor alpha), and PGC1- α (The peroxisome proliferator-activated receptor gamma (PPAR γ) coactivator-1), improving hepatic dyslipidaemia, glucose metabolism and storage (Awad, Araby and Albaiomy, 2021). Although body weight did not decrease in the PF and GbE groups, body weight gain did decrease after 14 days of treatment, significantly so in the PF group. It is possible that in both PF and GbE groups, the rats began to undergo lipolysis, and this may correspond with C18:1n-7 levels although this would need to be further explored. Bruss and colleagues (2010) found that caloric-restricted mice oxidized four times as much fat per day compared to *ad libitum*-fed control mice despite a reduction in energy intake from fat. This FA oxidation was accompanied by alternating diurnal periods of FA synthesis which was increased threefold in the caloric-restricted mice that received 70% of food compared to the control group, from day 2 of calorie deficit. They reported that CR mice gorged when presented with food, consuming all of it within 1 hour, which left them in a state of fasting for 23 hours post food ingestion. During this time of gorging, they ate 10 times the number of calories to that of the control group that were fed *ad-libitum* and consumed food over the course of the day. They found that before gorging, energy expenditure was lower in the CR mice, but energy expenditure levels increased rapidly post-gorging to levels seen in the control group for approximately 6 hours but returned to pre-gorging levels by 10 hours post-feeding (Bruss *et al.*, 2010). They found that that respiratory quotient values increase from 0.7, indicating FA oxidation, to 1, indicating DNL in the 6 hours post feeding, with DNL highest in the thermogenic response post-feeding. They also demonstrated newly synthesised lipids occurring both in the liver and adipose tissue following gorging. Accompanying this was an increased expression of FAS and ACC mRNA levels in adipose tissue, reduced FAS levels in the liver of the CR group while pre-gorging FAS and ACC levels increased beyond that of the control group post-feeding. The elevated ACC and FAS levels seen in adipose tissue suggested that DNL occurs first to adipose tissue, followed by the liver, and acted as a protective

mechanism to protect against excess glucose and calorie levels after a gorging feed (Bruss *et al.*, 2010). Duivenvoorde and colleagues (2011), also showed that in an HFD model, 12 weeks of caloric restriction has a vast influence on gene regulation involved in lipid metabolism and mitochondrial functioning. Interestingly the transcription of *Ppara* and *Pparg*, key regulators of lipid metabolism, were not altered. However, significant upregulation of all genes involved in cholesterol synthesis (*Cyp51*, *Fdps*, *Hmgcr*, *Insig1*, *Lss*, *Mvd*, *Sqle* and *Tm7sf2*), FAS and elongation (*Acaca*, *Acly*, *Elovl3*, *Elovl6*, and *Pecr*) were reported. NADPH-producing *Me1* was also upregulated which has been shown to play a central role in adipose metabolism, linking gluconeogenesis and fatty acid metabolism. Both *Aspg* and *Lpcat3*, encoding for lipolysis-related proteins were upregulated as were *Stard4* and *Stard5* encoding for cholesterol transfer proteins that regulate transfer between different cellular compartments (e.g., endoplasmic reticulum, Golgi apparatus). *Rdh11* and *Sorl1* were also upregulated which help reduce short-chain (fatty) aldehydes as well as the uptake of proteases and lipoproteins. The downregulation of *BC005764* that is involved in TAGs formation was also reported (Duivenvoorde *et al.*, 2011). Additionally, a study by Viguerie *et al.*, (2005) looked at adipose tissue gene expression in patients living with obesity undergoing low-fat and high-fat hypocaloric diets. They took two groups of 25 subjects each and placed them on a 10-week hypocaloric diet with either 20–25 or 40–45% of total energy derived from fat, the later like that of the HFD chow in our study. They measured the mRNA levels of 38 genes, including ten genes regulated by energy restriction but did not find any significant changes. They did find however that levels of PPAR1 α mRNA were increased, while the expression of the genes encoding leptin, osteonectin, phosphodiesterase 3B, hormone-sensitive lipase, receptor A for natriuretic peptide, fatty acid translocase, lipoprotein lipase, uncoupling protein 2 and PPAR γ were decreased (Viguerie *et al.*, 2005). Viguerie and colleagues concluded that it was energy restriction and/or weight loss and not the ratio of fat: carbohydrate in a low-energy diet that played the highest role in modifying the expression of genes in human adipose tissue., as both groups lost weight despite difference nutrient profiles of the diets. Parks and colleagues 2012 also found that calorie restriction with a HFD was effective at attenuating inflammatory response and oxidative stress-related markers in obese tissues of the HFD-fed rats (Park *et al.*, 2012). They found that high fat caloric restriction (HFCR) affected a variety of metabolites known to be altered in inflammation and OS caused by obesity. Parks and colleagues reported lowered hepatic triglyceride levels and total cholesterol levels and a return to normal levels in the plasma leptin/adiponectin ratio. HFCR also improved glucose tolerance and normalized adipocyte size and morphology. Expression levels of CRP and manganese superoxide

dismutase was also suppressed in adipose tissue. Lipid peroxidation was reduced and a decrease in the expression of inducible NOS, COX-2, Nrf2, and heme oxygenase-1 in the liver (Park *et al.*, 2012). GbE treatment has been shown to downregulate lipogenesis and upregulate lipolysis, while significantly decreasing OS and inflammatory markers such as highly sensitive C-reactive protein (Hs-CRP), tumour necrosis factor- α (TNF- α), interleukin-6 (IL-6) and malondialdehyde levels (Aziz, Hussain, Mahwi, Ahmed, *et al.*, 2018; Aziz, Hussain, Mahwi and Ahmed, 2018; Siegel *et al.*, 2014; Thanoon, Abdul-Jabbar and Taha, 2012; Kudolo *et al.*, 2006). The flavonoid Ginkgolide C, isolated from GbE leaves, has been shown to increase lipolysis and inhibit adipogenesis in adipocytes through increased phosphorylation of AMP-activated protein kinase (AMPK), resulting in decreased activity of acetyl-CoA carboxylase for fatty acid synthesis. Treatment also decreased the expression of PPAR and CCAAT/enhancer-binding protein, and increased lipolysis through enhanced adipose triglyceride lipase and HSL production (Liou *et al.*, 2015). Quercetin, a polyphenolic flavonoid found in GbE has been shown to significantly upregulate PPAR α protein levels and FA β -oxidation (Sun *et al.*, 2015) and improve hepatic dyslipidaemia by downregulating SREBP-1c and fatty acid synthase (FASN) levels, and upregulating PPAR α , carnitine palmitoyl-transferase1 and medium-chain acyl-coenzyme A dehydrogenase expression, increasing lipolysis and β -oxidation (Wang *et al.*, 2016). Ginkgetin, a biflavone from GbE leaves, blocked the differentiation of preadipocytes into adipocytes preventing hypertrophy in HFD-fed mic white adipose tissue, by acting as a STAT5 inhibitor, inhibiting PPAR γ and C/EBP α expression (Cho *et al.*, 2019). Wu *et al.*, (2016) reported a similar finding that GbE treatment inhibited adipocyte differentiation and downregulated the expression of adipogenesis genes PPAR- γ and Ap2 (Wu *et al.*, 2016). Similarly, GbE has been shown to modulate hepatic GLUT-2, PPAR- α and PGC1- α improving hepatic dyslipidaemia, glucose metabolism and storage (Awad, Araby and Albaiomy, 2021). Finally, GbE has also been shown to inhibit oxidised low-density lipoprotein (oxLDL) upregulation of matrix metalloproteinases (MMP1, MMP2, MMP3) associated with atherosclerotic lesions, suppressing ROS generation. The same study by Tsai and colleagues (2016) also showed GbE reduced lectin-like ox-LDL receptor 1 (LOX-1) expression ameliorating oxLDL-inhibited PPAR- γ function (Tsai *et al.*, 2016).

Increased adipocyte volume and cytokine production associated with obesity is also associated with increased 11-beta-hydroxysteroid-dehydrogenase type 1 (11 β -HSD1, encoding gene, HSD11B1). 11 β -HSD1 is expressed in all BAT, SAT, and WAT adipose depots in both preadipocytes and adipocytes with 11 β -HSD1 activity induced during adipogenesis to assist in differentiation and maturation (Vargovic *et al.*, 2011; Paulsen *et al.*, 2007; Goedecke *et al.*, 2006). SFA are particularly associated

with increased 11 β -HSD1 expression (Petrus *et al.*, 2015) which have been shown to be increased here in mesenteric and retroperitoneal depots. Generally, glucocorticoids facilitate both lipogenesis and lipolysis and may be dependent on dosage and circulating levels (Gathercole *et al.*, 2011). They are thought to have a more significant impact at a local tissue level, rather than in circulation, with a slow turnover rate in tissues such as adipose tissue controlled by 11 β -HSD1 activity (Hughes *et al.*, 2010). They stimulate the uptake of fatty acids by stimulating lipoprotein lipase and increase hepatic *de novo* lipogenesis *via* increased FAS expression, although this has been shown to be suppressed following low exogenous glucocorticoid treatment. Furthermore, insulin-stimulated lipogenesis has also been shown to be augmented by glucocorticoids (Gathercole *et al.*, 2011). Counteractively, while glucocorticoids have an acute antilipolytic effect on adipocytes, they also stimulate lipolysis *via* hormone-sensitive lipase and adipose triglyceride lipase, but only after 48 hours of exposure (Chapman, Holmes and Seckl, 2013; Gathercole *et al.*, 2011; Peckett, Wright and Riddell, 2011). While 11 β -HSD1 regenerates cortisol from cortisone within both adipose tissue and liver, it has been shown that in obesity, 11 β -HSD1 levels can increase up to 3-fold in SAT tissue accompanied by leptin deficiency as well as decreased 11 β -HSD1 activity in the liver (Chapman, Holmes and Seckl, 2013; Mlinar *et al.*, 2011; Paulsen *et al.*, 2007; Sandeep *et al.*, 2005; Livingstone and Walker, 2003; Paulmyer-Lacroix *et al.*, 2002; Rask *et al.*, 2002). Interestingly, quercetin, a compound found in GbE has been shown to dock and inhibit 11 β -HSD1 (Zhu *et al.*, 2018; Torres-Piedra *et al.*, 2010). Under similar experimental conditions to this study GbE treatment decreased Protein tyrosine phosphatase 1B (PTP-1B) expression levels (Banin *et al.*, 2014). Similarly, quercetin has also been shown to bind to and decrease mRNA levels of PTP-1B affecting the downstream activation of protein kinase B (PKB) and MAPK that trigger the GLUT4 transporter translocation to the plasma membrane (Chuang *et al.*, 2010; Zheng, Kar and Quirion, 2002) which is enhanced by LCFAs (Yoshida *et al.*, 2001). In mesenteric WAT, 11 β -HSD1 inhibition has been shown to decrease lipid synthesis and fatty acid cycling gene expression and increase fatty acid oxidation *via* CPT-1, while having the opposite effect in epididymal WAT (Hirata, Cruz *et al.*, 2019; Hirata, Pedrosa *et al.*, 2019; Chapman, Holmes and Seckl, 2013; Berthiaume *et al.*, 2007).

Hypertrophy is associated with reduced adiponectin production, macrophage infiltration, hypoxia and the secretion of pro-inflammatory cytokines (e.g., TNF- α , IL-6, IL-1 β). Together these contribute to low-grade inflammation and insulin resistance. As well as providing fatty acids for CE synthesis, PPL-PUFA also function as precursors for inflammation-mediating oxylipins such as eicosanoids. LA derived n-6 metabolites include 1 and 2 series prostaglandins (PGs), 2 series thromboxanes (TXs), 4

series leukotrienes (LTs) and lipoxins, and n-3 ALA derived n-3 metabolites include 3 series PGs and TXs, 5-series LTs along with resolvins and neuroprotectins (Nakamura *et al.*, 2001, Ratnayake and Galli, 2009, Bhagat *et al.*, 2015, Martin, 2015.) As mentioned before, there is a significant decrease in Ret-PPL C18:2n-6 in the HFD group (NFD, 24.91±1.65%; HFD-S, 13.87±0.44%, p=0.0003). This is in keeping with decreases in C18:2n-6 seen across all fractions; TAG, CE and MAG+DAG fractions. C18:2n-6 levels seen in the HFD-PPL fraction however fall below levels found in the HFD rat chow while levels in TAG, CE and MAG+DAG all sit above the 21% of HFD-chow C18:2n-6. The 29% decrease in RET-PPL PUFA levels in the HFD-S group may suggest that these are being utilized in an inflammation-mediated capacity, being cleaved to produce pro-resolving mediators. C18:2n-6 derived oxylipins include hydroxyoctadecadienoic acid (HODE), keto-octadecadienoic acid (KODE), epoxyoctadecamonoenoic acid (EpOME), and dihydroxyoctadecenoic acid (DiHOME) (Liput *et al.*, 2021) and have been shown to be both pro- and anti-inflammatory (Caligiuri *et al.*, 2013; Choque *et al.*, 2014; Cole *et al.*, 2020). Under the same experimental conditions previously published comparing NFD, HFD diet and GbE supplementation in rats, when comparing adipocyte size and morphology, the adipocyte volume was significantly larger by 114% (p=0.01) in an HFD-S compared to NFD group, but GbE supplementation reduced this by 42.5% (p=0.03) and was of a statistically similar volume in HFD+GbE compared to NFD (Hirata, Cruz *et al.*, 2019). PLIN1, FASN mRNA, and FASN protein levels were also reduced following GbE treatment along with acetate accumulation and oleate incorporation. GbE treatment also showed a tendency to reduce oleate incorporation into lipids by 43% (p= 0.06) compared to a HFD alone, which was found to have a 130% higher oleate incorporation (p = 0.01) in HFD cells compared to NFD (Hirata, Cruz, *et al.*, 2019)). Similarly, again under the same experimental conditions but in the retroperitoneal fat depot proteome, GbE treatment caused a 30% significant increase in catalase activity and a 40% decrease in Malondialdehyde (MDA) levels between HFD-S and HFD-GbE groups of diet-induced obese rats. GbE treatment also resulted in the RET adipocyte volume decreasing by 56% (p=0.04) compared to HFD-S treatment, along with a 30% significant increase in catalase activity and a 40% decrease in Malondialdehyde (MDA) levels. Both catalase and MDA levels suggest an upregulation in antioxidant activity following GbE treatment. Following proteomic analysis by mass spectrometry, 605 proteins were found to have altered expression between the two groups. These were narrowed down to 198 proteins, of which, 20 were downregulated following GbE treatment, 5 upregulated following GbE treatment while 10 were no longer detectable following GbE treatment and were only detectable in the HFD-S group. Of those identified as significantly different in expression levels were proteins involved in lipid and carbon

metabolism, inflammation, and OS. This is in keeping with other findings that GbE bilobalides protected against H₂O₂-induced oxidative damage in melanocytes (Lu *et al.*, 2016), hippocampus (Kaur *et al.* 2013), renal nephropathy (Chang *et al.*, 2021; Yu *et al.*, 2021) and colitis (Zhou *et al.*, 2006). Firstly, GbE treatment significantly reduced the protein expression levels of peroxiredoxin, an enzyme involved regulating endogenous H₂O₂ levels, resulting in a 0.54-fold change (GbE/S) compared to HFD-S. This was in keeping with the increased catalase activity and reduced MDA levels, further supporting the antioxidant and OS modulating capacity of GbE. Those proteins altered and involved in fatty acid metabolism were 3-Ketoacyl-CoA thiolase B, Trifunctional enzyme subunit alpha and citrate synthase. 3-Ketoacyl-CoA thiolase B was decreased beyond detection in HFD-GbE. 3-ketoacyl-CoA thiolase is part of the PPAR activated peroxisomal FA β -oxidation pathway, and is the last step involved in converting FA to one acetyl-CoA molecule and a two-carbon-shortened acyl-CoA for energy synthesis in the Krebs cycle (Tahri-Joutey *et al.*, 2021). A 0.58-fold decrease was seen in trifunctional enzyme subunit alpha with GbE which catalyses the later reactions in the mitochondrial β -oxidation pathway. A 1.98-fold increase in citrate synthase was seen with GbE which is the first of the eight enzymes involved in the Krebs cycle. These finding suggest that in GbE treatment, an increase in energy production due to citrate synthase activity as the first enzymatic step of energy production in the Krebs cycle may take place, while 3-Ketoacyl-CoA thiolase B and trifunctional enzyme subunit alpha, involved in the last steps in peroxisomal β -oxidation and mitochondrial β -oxidation pathway, respectively, appear to be down regulated. The decrease in aspartate aminotransferase (AST), an indicator of liver damage or disease, also found in the RET proteome study (Hirata, Pedroso, *et al.*, 2019) following GbE treatment is consistent with findings from Yan and colleagues (2015) that reported GbE attenuated HFD-induced liver injury through reducing hepatic steatosis, TAG accumulation, serum AST, Alanine transaminase (ALT), Aspartate transaminase and Alkaline phosphatase (ALP) (Yan *et al.*, 2015). The 1.65-fold increase in Decorin following GbE treatment is also consistent with other findings. The extracellular matrix (ECM) of the adipose tissue has been implicated in insulin resistance with decorin, a proteoglycan and component of the ECM, associated with glucose tolerance. Svärd and colleagues looked at decorin knockout (DcnKO) mice fed either a low fat or high fat diet for 10 weeks. They found that DcnKO mice had greater food efficiency during overfeeding. They also exhibited impaired glucose tolerance, elevated expression and circulation of leptin, downregulated TAG biosynthesis genes and an upregulation of adipose genes involved in complement and coagulation cascades (Svärd *et al.*, 2019). While GbE treatment did not cause weight loss in this study over the 14-day treatment, it did reduce weight gain, which

was more notable in the caloric-restricted PF group. Interestingly CAV2 showed a 0.4-fold decrease following GbE treatment in the RET proteome study (Hirata, Pedroso *et al.*, 2019). Caveolae within the lipid rafts of membranes, are formed from cholesterol, glycosphingolipids and other proteins which are aided by CAV1 and CAV2 in a highly cholesterol-dependant process. CAV1 and CAV2 are the main structural components of caveolae (He, Cui and Zhu, 2021; Gámez-Ruiz *et al.*, 2011; Le Lay and Kurzchalia, 2005). Cav-1 is abundantly expressed in terminally differentiated cells such as adipocytes, while CAV2 is co-expressed with CAV1. Caveolae have a characteristic scaffolding domain in the plasma membrane due to CAV1 and CAV2 that allows interaction with signalling molecules, facilitating membrane transport including GLUT4 translocation and receptor signalling such as insulin (He, Cui and Zhu, 2021; Haczeyni, Bell-Anderson and Farrell, 2018; Gámez-Ruiz *et al.*, 2011; Le Lay and Kurzchalia, 2005). Gámez-Ruiz and colleagues (2011) found that caveolin expression did not change in RET adipocytes of rats fed with a control or high-fat (HF) diet for 72 days, although they did find that HFD subcutaneous adipocytes exhibited a reduction. For the control diet rat, food intake decreased CAV-1 phosphorylation in RET adipocytes and increased in subcutaneous adipocytes. CAV-2 phosphorylation increased in both RET and subcutaneous adipocytes in non-fasting rats, irrespective of the type of diet (Gámez-Ruiz *et al.*, 2011). This may suggest that the 0.4-fold decrease in CAV2 in GbE treatment, may be caused by decreased food intake.

5.8 Summary

In summary, a HFD causes an increase in SFA and MUFA and a decrease in PUFA in total lipid profiles is seen in TAG, CE, MAG+DAG and PPL fractions compared to a NFD in both MES and RET adipose tissue. Table 70 and Table 71 shows the key changes that occurred in both Ret and MES tissues across all diets and treatment groups. No changes in SFA, MUFA or PUFA are seen in total lipid profiles following caloric restriction or GbE treatment. Higher SFA and lower PUFA, would indicate a risk for a pro-inflammatory environment. When MES and RET adipose tissue is separated into separate lipid classes, more dynamic changes can be seen with caloric restriction and GbE treatments. RET-TAG fatty acid profiles showed increased SFA and MUFA and decreased PUFA levels while MES-TAG showed reduced levels of SFA in TAG but no changes MUFA or PUFA. Following either caloric restriction (PF) or GbE treatment, no overall changes were seen in RET-TAG SFA, MUFA or PUFA levels compared to saline-only treated (HFD-S) group while reduced levels of SFA in TAG-HFD-GbE are seen in MES-TAG. In the both the MES- and RET-CE fraction increased SFA and MUFA levels and decreased PUFA levels occurred in HFD-S like the changes seen in total lipid profiles and TAG. In both MES and RET three HFD groups, few significant changes occurred in the caloric restricted (PF) group and the GbE treatment groups compared to the HFD-S group. Changes of note include a significant increase in C18:1n-7 in both the RET-HFD-PF and RET-HFD-GbE groups compared to RET-HFD-S coinciding with significantly lower levels of C18:1n-9 RET-HFD-PF and RET-HFD-GbE groups compared to RET-HFD-S. This may indicate changes in fatty acid enzyme activity involved in DNL and lipolysis.

The most notable change was seen in the PPL fraction for both MES and RET where increased SFA and decreased MUFA and n-6 PUFA occurred following an HFD, compared to a NFD. In HFD-fed animals, when compared to the HFD-saline only group, SFA levels increased further in PPL fatty acids following GbE treatment. MUFA levels significantly increased and PUFA decreased following caloric restriction. With GbE treatment MUFA levels decreased in contrast to the PF group, while PUFA levels also decreased but not to the extent seen in the PF group. Moreover, the changes seen in GbE treatment are often contradictory to those seen in the HFD-PF calorically restricted group, despite both groups receiving the same amount of food for 14 days. This indicates that GbE may have some protective effect on over lipid profiles despite caloric restriction, such as that seen with PPL PUFA and UI levels when compared to the PF group. These findings may suggest changes in enzyme activity involved in DNL and lipogenesis such as HSL, PLIN1, FAS and ELOVL6 and/or CAV related lipid trafficking and oxylipin production associated with inflammation mediation.

Table 70. Summary of retroperitoneal and mesenteric fatty acid profiles comparing the effects of a normal fat diet (NFD) and high fat diet (HFD) in total lipid sample, Triglycerides (TAG), Cholesteryl esters (CE), monoglycerides and diglycerides (MAG+DAG) and phospholipids (PPL). ↑=increased Vs NFD, ↓=decreased Vs NFD

	Retroperitoneal			Mesenteric		
	NFD	HFD	HFD Vs NFD	NFD	HFD	HFD Vs NFD
	Sample %	Sample %		Sample %	Sample %	
Total Sample						
SFA	24.1	28.4	↑ p=0.0004	22.1	28.2	↑ p <0.001
MUFA	29.6	47.3	↑ p<0.0001	29.6	47.3	↑ p<0.001
PUFA	45.2	23.5	↓ p<0.0001	46.9	23.7	↓ p<0.001
n-6	42.7	22.9	↓ p<0.0001	44.5	23.0	↓ p<0.001
n-3	2.5	0.7	↓ p<0.0001	2.1	0.6	↓ p<0.001
n-6/n-3	17.0	34.7	↑ p<0.0001	18.5	36.8	↑ p<0.001
TAG						
∑SFA	23.5	27.6	↑ p=0.0007	21.7	27.7	↑ p<0.0001
∑MUFA	29.0	48.3	↑ p<0.0001	29.6	48.3	↑ p<0.0001
∑PUFA	45.8	23.4	↓ p<0.0001	48.0	23.3	↓ p<0.0001
∑n-6 PUFA	44.1	22.8	↓ p<0.0001	45.8	22.8	↓ p<0.0001
∑n-3PUFA	1.7	0.6	p=0.2	2.2	0.6	↓ p<0.0001
n-6/n-3	37.0	37.7	p>0.99	21.0	40.8	↑ p<0.0001
CE						
∑SFA	20.8	24.9	↑ p=0.001	15.0	22.2	↑ p<0.0001
∑MUFA	25.2	44.0	↑ p<0.0001	22.7	42.8	↑ p<0.0001
∑PUFA	52.1	29.7	↓ p<0.0001	60.1	33.6	↓ p<0.0001
∑n-6 PUFA	48.0	28.2	↓ p<0.0001	55.4	32.0	↓ p<0.0001
∑n-3PUFA	0.6	0.1	↓ p<0.0001	4.8	1.6	↓ p<0.0001
n-6/n-3	11.8	19.2	↑ p<0.0001	11.7	20.5	↑ p<0.0001
MAG+DAG						
∑SFA	23.7	26.0	p=0.38	44.3	28.6	↓ p=0.03
∑MUFA	26.5	46.6	↑ p<0.0001	21.3	44.7	↑ p<0.0001
∑PUFA	47.7	25.7	↓ p<0.0001	29.6	26.1	↓ p=0.01
∑n-6 PUFA	45.0	24.9	↓ p<0.0001	27.9	24.5	p=0.5
∑n-3PUFA	2.7	0.8	↓ p<0.0001	1.8	1.6	p=0.8
n-6/n-3	17.1	31.2	↑ p<0.0001	16.3	20.1	p=0.3
PPL						
∑SFA	38.4	49.2	↑ p=0.0004	59.5	50.2	↓ p=0.002
∑MUFA	24.4	24.8	p=0.80	10.5	19.3	↑ p<0.0001
∑PUFA	34.3	24.3	↓ p=0.01	28.9	29.2	p=0.96
∑ n-6 PUFA	30.1	19.1	↓ p<0.0001	27.3	28.1	p>0.99
∑ n-3PUFA	4.2	5.2	p=0.62	1.6	2.9	↑ p=0.01
n-6/ n-3	11.2	6.5	p>0.99	17.0	26.5	↑ p<0.001

Table 71. Summary of retroperitoneal and mesenteric fatty acid profiles comparing the effects of a high fat diet (HFD) and treatment with saline (HFD-S), pairfed (PF) and Ginkgo biloba (HFD-GbE) in total lipid sample, triglycerides (TAG), Cholesteryl esters (CE), monoglycerides and diglycerides (MAG+DAG) and phospholipids (PPL).

↑=increased Vs NFD, ↓=decreased Vs NFD

	HFD-S	HFD-PF	HFD-GbE	S Vs PF	S Vs GbE	PF Vs GbE	HFD-S	HFD-PF	HFD-GbE	S Vs PF	S Vs GbE	PF Vs GbE
	Sample %			p Value			Sample %			p Value		
Total sample												
∑SFA	28.4	28.9	28.7	0.39	0.78	0.78	28.2	28.6	27.8	0.42	0.34	↓0.03
∑MUFA	47.3	46.9	47.0	0.63	0.85	0.92	47.3	47.2	48.0	0.96	0.19	0.12
∑PUFA	21.2	23.5	23.5	0.47	0.46	>0.99	23.7	23.5	23.4	0.86	0.55	0.86
∑n-6 PUFA	22.9	22.8	22.8	0.96	>0.99	0.98	23.0	22.9	22.8	0.84	0.55	0.88
∑n-3 PUFA	0.6	0.7	0.7	0.56	0.45	0.98	0.6	0.6	0.6	>0.99	0.76	0.81
n-6/n-3	34.7	35.2	34.4	0.91	0.97	0.79	36.8	37.2	37.9	0.96	0.83	0.94
TAG												
∑SFA	27.6	28.4	28.0	0.05	0.44	0.44	27.7	27.7	27.0	0.98	↓0.04	0.07
∑MUFA	48.3	47.8	48.0	0.31	0.59	0.87	48.3	48.6	49.0	0.65	0.13	0.54
∑PUFA	23.4	23.2	23.3	0.39	0.88	0.68	23.3	23.2	23.2	0.42	>0.99	0.44
∑n-6 PUFA	22.8	22.5	22.7	0.22	0.89	0.43	22.8	22.6	22.7	0.86	0.99	0.92
∑n-3 PUFA	0.6	0.7	0.6	0.39	0.99	0.34	0.6	0.6	0.5	0.54	0.61	0.99
n-6/n-3	37.7	35.0	37.8	0.37	>0.99	0.36	40.8	40.9	44.6	>0.99	0.09	0.1
CE												
∑SFA	24.9	24.6	23.5	0.92	0.21	0.38	22.2	22.7	21.8	0.7	0.82	0.35
∑MUFA	44.0	43.0	44.2	0.06	0.94	↑0.03	42.8	43.6	42.9	0.47	>0.99	0.51
∑PUFA	29.7	30.9	31.1	0.38	0.29	0.98	33.6	33.1	33.3	0.9	0.98	0.97
∑n-6 PUFA	28.2	29.4	29.7	0.49	0.99	0.58	32.0	31.5	31.7	0.85	0.96	0.96
∑n-3 PUFA	1.5	1.5	1.5	>0.99	0.97	0.97	1.6	1.6	1.6	0.96	0.96	>0.99
n-6/n-3	19.2	20.6	20.5	0.67	0.73	>0.99	20.5	20.2	20.3	0.99	0.99	>0.99
MAG+DAG												
∑SFA	26.0	28.7	25.9	↑0.001	>0.99	↓0.001	28.6	29.9	27.6	↑0.02	0.09	↓0.0001
∑MUFA	46.6	44.3	46.5	↓0.001	0.97	↑0.001	44.7	44.4	44.7	0.82	>0.99	0.83
∑PUFA	25.7	24.2	26.1	↓0.02	0.64	↑0.001	26.1	25.1	22.5	0.85	0.12	0.32
∑n-6 PUFA	24.9	23.4	25.3	↓0.02	0.65	↑0.002	24.5	23.6	21.0	0.85	0.14	0.34
∑n-3 PUFA	0.8	0.8	0.8	0.98	>0.99	0.98	1.6	1.6	1.5	>0.99	>0.99	>0.99
n-6/n-3	31.2	30.3	31.7	0.89	0.96	0.73	20.1	19.1	18.3	0.98	0.94	0.99
PPL												
∑SFA	49.2	46.4	58.9	0.79	0.09	↑0.02	50.2	33.0	60.8	↓0.05	↑0.001	↑<0.0001
∑MUFA	24.8	34.8	19.8	↑0.01	0.27	↓0.0002	32.5	33.5	14.1	↑<0.0001	0.25	↓<0.0001
∑PUFA	24.3	15.4	19.8	↓0.001	0.1	0.11	29.9	9.5	18.3	↓<0.0001	↓<0.0001	↑0.008
∑n-6 PUFA	19.1	11.8	15.0	↓0.0001	↓0.02	0.09	28.1	9.2	17.9	↓<0.0001	↓<0.0001	↑0.01
∑n-3 PUFA	5.2	3.6	4.8	0.53	0.95	0.71	1.8	0.3	0.4	↓<0.0001	↓<0.0001	0.15
n-6/n-3	6.5	3.4	3.3	↓0.01	↓0.01	>0.99	41.3	23.9	60.0	↓0.01	↑0.02	0.93

Chapter 6 - Hippocampus and Hypothalamus

6.1 Introduction

Obesity is related to a number of comorbidities, which include metabolic syndrome, cardiovascular disease and cognitive dysfunction (Balasubramanian *et al.*, 2021; Karunathilaka and Rathnayake, 2021; Buie *et al.*, 2019; Forny-Germano, de Felice and do Nascimento Vieira, 2019; Hovens, Dalenberg and Small, 2019; Salama *et al.*, 2018; Dye *et al.*, 2017; Prickett, Brennan and Stolwyk, 2015; André *et al.*, 2014; Miller and Spencer, 2014; Nguyen, Killcross and Jenkins, 2014; Riggs, 2012; Kanoski and Davidson, 2011; Cserjesi, 2009; Braet, 2003). Obesity occurs from chronic over ingestion of calories, in excess of energy output. The association between obesity and a high-fat Western-style diet (WD) are well established (Victorio *et al.*, 2021). As previously discussed in other chapters, a HFD and obesity is also associated with impaired glucose processing and the development of metabolic disease. In contrast to a HFD are studies that suggest that a higher adherence to the Mediterranean diet is associated with significantly lower odds of developing metabolic syndrome (Babio *et al.* 2009) along with lower incidence of mortality and cardiovascular disease (Giroli *et al.* 2021; Menotti and Puddu 2015). A Mediterranean diet is associated with reduced risk of developing mild cognitive impairment and AD (Singh *et al.*, 2014; Gardener *et al.*, 2012) with adherence to the diet reported to reduce disease progression by up to 33% (Singh *et al.*, 2014). A Mediterranean diet boasts of lower levels of saturated fat, better omega-6:3 PUFA ratios, and an abundance of phytochemicals including plant antioxidants and polyphenolic compounds (Menotti and Puddu, 2015; Estruch and Salas-Salvadó, 2013; Babio *et al.*, 2009).

As discussed in more detail in the Chapter 1 Section 1.1, major neurocognitive disorders (MND) such as AD are associated with a significant decline in cognitive functioning (Sherman *et al.*, 2016). Predictive factors for MND can be categorised by sociodemographic factors, bio-behavioural factors, and health factors (Sousa, Teixeira and Paúl, 2020). Health factors used to determine MND include some modifiable factors such as nutritional status, cholesterol levels, cardiovascular health, diabetes, obesity and dyslipidemia as well as handgrip strength and cerebrovascular diseases (Prakash *et al.*, 2021; Sousa, Teixeira and Paúl, 2020; Tini *et al.*, 2020; Mayeux and Stern, 2012; Skoog *et al.*, 1996). With regards to AD and the effect of obesity, recent reports have shown that there is a higher risk of developing dementia in an older population who are overweight or obese (Ma *et al.* 2020) although late-life obesity has been suggested as protective against AD (Fitzpatrick *et al.* 2009). Obesity in

middle-age is also identified as a risk factor for MND, particularly AD (Anstey *et al.*, 2011; Fitzpatrick *et al.*, 2009; Calle *et al.*, 1999, 2003). It has been reported that there is a three-fold increased risk in developing AD in people with high waist circumferences, and that the risk ratio of developing dementia increased for people suffering obesity in the 30-40 years-old category compared to those that developed obesity in later years (Pugazhenti, Qin and Reddy, 2017). Interestingly, while studying the effect of late life obesity and weight loss on brain structure, with weight loss categorised as 5% loss of weight between clinical visits, Pegueroles and colleagues (2018), found atrophy in occipital, inferior temporal, precuneus and frontal brain regions of weight stable individuals. In contrast they found increased cortical thickness in the weight-loss group suggesting a reverse causation for atrophy due to weight loss (Pegueroles *et al.*, 2018).

The brain contains high levels of lipids, essential for structure and function. Lipids make up 50% of the dry weight of the brain, while the brain contains the second highest concentration of lipids within the body, second only to adipose tissue (Dyall, 2015; Singh, 2005; Youdim, Martin and Joseph, 2000; Edmond *et al.*, 1998; Robinson *et al.*, 1992). While adipocytes store FA predominantly in TAG, brain lipids are mostly contained within the phospholipids of the cell membrane (Bruce, Zsombok and Eckel, 2017; Hamilton *et al.*, 2007). Brain lipids are rich in LC-PUFA, particularly the n-6 AA (C20:4n-6) and the n-3 DHA (C22:6n-3). DHA accounts for 10-15% of FA in the brain and may account for up to 50% of brain tissue PUFA (Diau *et al.* 2005). Essential FA must be transported into the brain across the BBB from circulating plasma. In rats a daily turnover has been reported of up to 5% for esterified AA and 8% of esterified DHA replaced by unesterified PUFA from plasma, while daily AA replacement is estimated at only 0.3% in humans (Rapoport, Chang and Spector, 2001). It has been reported that the brain is a major consumer of circulating PUFA, where the levels of uptake from plasma into PPL mimics the consumption rates in the brain (Chen *et al.*, 2008). It has been shown in rat studies that unesterified forms of plasma FA rather than esterified forms are incorporated into the brain (Chen *et al.*, 2015; Sublette *et al.*, 2007; Spector, 2001; Purdon *et al.*, 1997). Esterified forms of circulating FA include TAG, FAG, CE and PPL while unesterified are counted as FFA. Furthermore, reports show that the brain concentration of DHA is kept at a steady-state even in brain injury (Kim, 2014; DeMar *et al.*, 2004), and as DHA synthesis from lower n-3 FA such as ALA (C18:3n-3) is low in the brain, it is agreed that the brain supply of DHA predominantly comes from plasma (DeMar *et al.*, 2005). AA and DHA are crucial for cell signalling and are used to produce oxylipins such as eicosanoids mediated by COX, LOX and cytochrome P450 (CYP) enzymes (Melissa Gabbs *et al.*, 2015; Bazinet, 2014). An increase in

the dietary LA/ALA ratio has been found to reduce DHA and increase AA levels in the rat brain (Lands, Morris and Libelt 1990).

The brain consumes high levels of energy compared to other organs, mostly in the form of glucose. As discussed in the Chapter 1, a typical human brain consumes approximately 120 g of glucose daily, which is transported across the permeably restrictive blood brain barrier (BBB) mediated by astrocytes and a large family of sodium independent glucose transporters (GLUTs) and sodium-dependent glucose co-transporters (SGLT) (Shah, DeSilva and Abbruscato, 2012). Most glucose in the brain is consumed *via* mitochondrial oxidative phosphorylation, converted to ATP and used to maintain normal neural function (Hall *et al.*, 2012). Normal glucose metabolism is rate limited by the enzyme cytochrome C oxidase and results in naturally occurring reactive oxygen species (ROS) which, when in excess, leads to exacerbated OS (Perez-Pardo *et al.*, 2017; Nilsson and Busto, 1976). With age comes the decline in the efficiency of the highly regulated mitochondrial enzymatic process leading to increasing levels of ROS and OS (Ahmad *et al.*, 2017; Pérez-Gracia, Torrejón-Escribano and Ferrer, 2008) supported by the finding of increased OS biomarkers in brain and peripheral blood tissues of MND patients such as seen in AD (Sultana and Butterfield, 2010). A metabolic feature regularly seen in AD is a decline of approximately 50% in glucose based-ATP production, which tends to deteriorate as the disease progresses (Hoyer 1992) with impaired glucose transport and ATP production correlated with increased levels of A β protein (Gella *et al.*, 2009). Decreased levels of both GLUT-1 and GLUT-3 transporters have been reported in AD (Liu *et al.*, 2008; Mooradian, Chung and Shah, 1997; Harr, Simonian and Hyman, 1995; Simpson *et al.*, 1994) with each transporter respectively responsible for glucose transport across the BBB (Brockmann 2009) and into neurons (Augustin 2010; Shepherd *et al.* 1992). With decreased levels of these transporters correlating to abnormal hyperphosphorylation of tau (Liu *et al.*, 2008), it is believed that such perturbations in GLUT levels disrupts brain glucose homeostasis and mitochondrial function which increases OS, neuro-inflammation and eventually neurodegeneration (Cong *et al.*, 2011; Cunnane *et al.*, 2011; Hoyer, 2004). In contrast, increased levels of GLUT-2 (Liu *et al.*, 2008) and GLUT-12 (Pujol-Gimenez *et al.*, 2014) have been recently found in AD and is thought to be a compensation mechanism to continue glucose supply to neural tissue. Glucose transported *via* GLUT-12 however enters anaerobic glycolytic metabolism, which further augments OS (Zawacka-Pankau *et al.* 2011). Recent, compelling evidence has associated AD with T2DM due to similar shared clinical, biochemical and pathophysiological manifestations (Chen and Zhong, 2013) particularly OS (Rosales-Corral *et al.*, 2015).

LCFA are also a source of energy for the body and are required for the synthesis of structural lipids (e.g., phospholipids and sphingolipids) (Schäffler and Schölmerich, 2010) which are essential to reproduction, cell differentiation, inflammation, and cognition (Clarke and Nakamura, 2013; Harbige, 2003). As discussed under Section 1.15, where glucose is not available, β -oxidation of lipids occurs within the mitochondria. In times of energy demand, the protein kinase AMPK is activated, which phosphorylates both ACC1 and ACC2, inactivating them, leading to a decrease in fatty acid synthesis and an increase in fatty acid β -oxidation. Similarly, as discussed under Section 1.15, PPAR receptors are responsible for triggering gene transcription of lipid metabolism mediators involved in adipogenesis and β -oxidation, and contribute to the regulation of oxidative stress, inflammation, and neuroprotection (Han *et al.*, 2017; Duvall and Levy, 2016; Echeverría *et al.*, 2016; Motojima *et al.*, 1998; Martin *et al.*, 1997). PPAR is predominantly expressed in tissues that undergo high rates of fatty acid catabolism, including the digestive tract, liver, heart, skeletal muscle, kidneys and brain tissue, particularly in neurons and astrocytes (Tahri-Joutey *et al.*, 2021). A wide variety of lipophilic molecules/ ligands activate PPAR α , which when bound, undergo conformational changes and trigger gene transcription involved in lipid metabolism and oxidation (Tahri-Joutey *et al.*, 2021). Within the β -oxidation system VLCFA are shortened to LCFA in the peroxisome which participates in cellular thermogenesis and produces H₂O₂ (Cherkaoui-Malki *et al.*, 2012) while shortened LCFA are further metabolised by mitochondrial β -oxidation for ATP synthesis (Tahri-Joutey *et al.*, 2021).

PPAR ligands include SFA, UFA and PUFA as well as their metabolites (Chen *et al.*, 2020; Forman *et al.*, 1997; Kliewer *et al.*, 1997). LC-PUFA are the natural ligands of PPAR α/γ , where n-3 PUFA, namely EPA (C20:5n-3) and DHA (C22:6n-3) bind with high affinity for activation (Duszka *et al.*, 2020; Kosgei *et al.*, 2020; Laleh *et al.*, 2019; Kersten *et al.*, 2017; Pawar *et al.*, 2003). n-6 LC-PUFA such as LA (C18:2n-6) and AA (C20:4n-6), n-3 DPA (C22:5n-3) and ω -9 erucic acid (C22:1n-9) have also been shown to stimulate PPAR activity (Chen *et al.*, 2020; Laleh *et al.*, 2019; Duvall *et al.*, 2016; Echeverría *et al.*, 2016; Hostetler *et al.*, 2006; Pawar *et al.*, 2003). Endogenous FA metabolites also act as PPAR ligands including acyl CoAs, oxidised fatty acids, hydroxylated fatty acids, PPL, eicosanoids, endocannabinoid-like molecules and lipoprotein lipolytic products (Liput *et al.* 2021). Exogenous PPAR activators include dietary PUFA such as EPA and DHA and plant extracts such as GbE and other polyphenolic flavonoids, isoflavonoids, terpenes, steroids, carotenoids, coumarins, lignans, and tannins (Tahri-Joutey *et al.*, 2021; Grygiel-Górniak, 2014). PPAR α activators and PPAR γ agonists are used for treating dyslipidemia and T2DM with PPAR β/δ overexpression is shown to prevent obesity

in a HFD and increase glucose metabolism while protecting against ischemia-reperfusion injury (Yu *et al.*, 2008).

To explore the effect of a HFD on brain lipid profiles, in this study both the hippocampus and hypothalamus tissue were collected from NFD, HFD-S, HFD-PF and HFD-GbE treated rats. Total fatty acids were extracted, subjected to acid-catalysed esterification to produce FAMES and analysed by GC-FID spectrometry and reported as mean $\% \pm \text{SEM}$. Differences between NFD and HFD-S feeding was statistically analysed by Student's T test, while HFD-fed subsets were analysed by one-way ANOVA with Tukey's *post hoc* test. The level of statistical significance was set at $*p < 0.05$.

6.2 Hypothalamus

In total hypothalamus fatty acids profiles, few changes occurred FA percentage levels when comparing a NFD to an HFD-S diet. Those of note are a 7.5% increase in C18:0 in the HFD-S (C18:0; NFD, 18.45±0.14%; HFD-S, 19.83±0.57%, p=0.05) and a 3% increase in total SFA levels (Σ SFA; NFD, 44.56±0.46%; HFD-S, 46.17±0.52%, p=0.04) (Table 72). Total MUFA levels also decreased by 4.6% in the HFD-S compared to the NFD (Σ MUFA; NFD, 25.83±0.44%; HFD-S, 24.64±0.29%, p=0.03) (Table 72). Although no significant changes were seen in the Σ MUFA/ Σ SFA ratio and Σ UFA/ Σ SFA ratio, a decreasing trend was seen in both. Likewise, an increasing trend was seen in the C18:1n-7/C18:0 ratio, along with a significant increase in the C22:5n-3/C18:3n-3 ratio (C22:5n-3/C18:3n-3; NFD, 0.01±0.01; HFD-S, 0.07±0.01, p=0.002) (Table 73).

When comparing the HFD subsets a decreasing trend in C16:1n-7 was seen in HFD-PF (p=0.06) and significant decrease in HFD-GbE (p=0.01) compared to the HFD-S group (Table 74). This affected the $\Sigma\omega$ 7 level in a similar way where a decreasing trend in was seen in HFD-PF (p=0.09) and significant decrease in HFD-GbE (p=0.01) compared to the HFD-S group ($\Sigma\omega$ 7; HFD-S, 3.34±0.09; HFD-PF, 3.06±0.10; HFD-GbE, 2.95±0.09) (Table 74). This was also reflected in the C18:1n-9/C16:1n-7 ratio that significantly increase in the HFD-GbE group compared to HFD-S (p=0.02) (C18:1n-9/C16:1n-7; HFD-S, 70.45±9.20; HFD-PF, 97.50±9.59; HFD-GbE, 108.54±8.24) (Table 75). Finally, a C22:5n-3 levels decreased 2-fold in the HFD-PF group compared to HFD-S (p=0.002) while a decreasing trend was seen in HFD-GbE compared to HFD-S (p=0.08) (C22:5n-3; HFD-S, 0.14±0.02; HFD-PF, 0.07±0.01; HFD-GbE, 0.10±0.01). This change in C22:5n-3 was reflected in the C22:5n-3/C18:3n-3 ratio where both HFD-PF (p=0.002) and HFD-GbE (p=0.005) decreased approximately 2-fold for each group compared to HFD-S (C22:5n-3/C18:3n-3; HFD-S, 0.07±0.01; HFD-PF, 0.03±0.01; HFD-GbE, 0.04±0.01) (Table 75). The C22:6n-3/C22:5n-3 ratio was increased significantly in the HFD-PF group compared to both the HFD-S group (p=0.004), and the HFD-GbE group (p=0.02), although no significant difference was seen between HFD-S and HFD-GbE (C22:6n-3/C22:5n-3; HFD-S, 89.26±14.56; HFD-PF, 140.75±9.10; HFD-GbE, 98.12±3.47). Finally, the C22:6n-3/C18:3n-3 ratio showed a decreasing trend between the HFD-S and HFD-GbE groups (p=0.06) (C22:6n-3/C18:3n-3; HFD-S, 5.74±0.62; HFD-PF, 4.11±0.68; HFD-GbE, 3.61±0.52) indicating a relative increase in C18:3n-3 and decrease in C22:6n-3 levels (Table 68).

Table 72. Hypothalamus total fatty acid methyl esters (FAME) for normal fat diet (NFD) and high fat diet (HFD-S) (N=10 per group). Fatty acid results are presented as area % percentage mean and standard error of the mean (SEM), and statistically analysed by Students t-test. The level of statistical significance was set at * $p < 0.05$.

	NFD			HFD-S			p value
	MEAN %	±	SEM	MEAN %	±	SEM	
C14:0	0.06	±	0.01	0.11	±	0.02	0.12
C16:0	19.52	±	0.62	20.14	±	0.22	0.32
C17:0	0.13	±	0.01	0.13	±	0.02	0.98
C18:0	18.45	±	0.14	19.83	±	0.57	0.05
C20:0	0.74	±	0.05	0.64	±	0.04	0.12
C22:0	0.35	±	0.03	0.34	±	0.03	0.85
C23:0	0.16	±	0.01	0.15	±	0.01	0.41
DMA 16:0	1.10	±	0.09	1.10	±	0.10	0.97
DMA 18:0	4.05	±	0.06	3.73	±	0.23	0.25
ΣSFA DMA	5.15	±	0.14	4.83	±	0.30	0.40
ΣSFA	44.56	±	0.46	46.17	±	0.52	0.04
C16:1n-7	0.23	±	0.02	0.27	±	0.03	0.41
C18:1n-7	3.06	±	0.05	3.04	±	0.08	0.84
C18:1n-9t	0.09	±	0.02	0.08	±	0.03	0.90
C18:1n-9	17.02	±	0.27	16.56	±	0.17	0.15
C20:1n-9	1.27	±	0.07	1.27	±	0.09	0.99
C22:1n-9	0.25	±	0.01	0.21	±	0.01	0.04
C24:1n-9	1.05	±	0.08	0.91	±	0.06	0.16
DMA 18:1	1.42	±	0.04	1.17	±	0.12	0.10
C18:1 Total	20.14	±	0.26	19.65	±	0.21	0.15
Σω7	3.30	±	0.06	3.34	±	0.09	0.72
Σω9	19.65	±	0.36	18.97	±	0.23	0.12
ΣMUFA	25.83	±	0.44	24.64	±	0.29	0.03
C18:2n-6	0.81	±	0.14	0.78	±	0.06	0.84
C18:3n-6	0.07	±	0.01	0.08	±	0.01	0.77
C20:2n-6	0.11	±	0.01	0.10	±	0.01	0.78
C20:3n-6	0.28	±	0.01	0.28	±	0.01	0.89
C20:4n-6	7.39	±	0.10	7.87	±	0.33	0.22
C22:4n-6	3.99	±	0.06	3.98	±	0.07	0.93
Σn-6 PUFA	12.64	±	0.13	13.08	±	0.35	0.31
Σn-6metabolites	11.84	±	0.05	12.30	±	0.38	0.30
C18:3n-3	2.43	±	0.25	2.02	±	0.23	0.25
C20:3n-3	0.17	±	0.01	0.19	±	0.02	0.32
C22:5n-3	0.08	±	0.02	0.14	±	0.02	0.14
C22:6n-3	10.18	±	0.23	10.51	±	0.34	0.47
Σn-3 PUFA	12.81	±	0.25	12.81	±	0.46	>0.99
Σn-3 metabolites	10.38	±	0.22	10.79	±	0.34	0.36
ΣPUFA	25.45	±	0.17	25.88	±	0.59	0.53
ΣUFA	51.29	±	0.39	50.53	±	0.53	0.28

Table 73. Hypothalamus total fatty acid methyl esters (FAME) ratios for normal fat diet (NFD) and high fat diet (HFD-S) (N=10 per group). Results presented as mean an (SEM), and statistically analysed by one-way ANOVA with Tukey's Post-hoc test. The level of statistical significance was set at *p < 0.05.

	NFD			HFD-S			p value
	MEAN %	±	SEM	MEAN %	±	SEM	
ΣMUFA/ΣPUFA	1.02	±	0.02	0.96	±	0.03	0.16
ΣMUFA/ΣSFA	0.58	±	0.01	0.53	±	0.01	0.008
ΣPUFA/ΣSFA	0.99	±	0.02	1.05	±	0.03	0.13
ΣUFA/ΣSFA	1.15	±	0.02	1.10	±	0.02	0.09
C18:0/C16:0	6.22	±	1.15	5.37	±	0.52	0.48
C16:1n-7/C16:0	1.82	±	0.15	2.30	±	0.34	0.26
C18:1n-9/C16:0	137.03	±	14.28	144.34	±	17.26	0.76
C18:1n-9/C16:1n-7	76.68	±	6.37	70.45	±	9.20	0.60
C18:1n-7/C18:0	4.24	±	0.22	4.87	±	0.22	0.06
C18:1/C18:0	27.99	±	1.61	31.77	±	1.76	0.14
n-6/n-3	0.99	±	0.03	1.03	±	0.05	0.49
C20:4n-6/C18:2n-6	11.39	±	2.03	10.85	±	1.19	0.81
C20:4n-6/C20:3n6	27.30	±	1.69	28.42	±	0.81	0.53
C20:4n-6/C22:6n3	0.73	±	0.01	0.75	±	0.04	0.54
C20:4n-6/C18:2n6	11.39	±	2.03	10.85	±	1.19	0.81
C20:4n-6/C18:3n3	3.30	±	0.37	4.50	±	0.78	0.22
C20:3n-3/C18:3n-3	0.08	±	0.01	0.09	±	0.03	0.63
C22:5n-3/C18:3n-3	0.01	±	0.01	0.07	±	0.01	0.002
C22:6n-3/C18:3n-3	4.56	±	0.52	5.74	±	0.62	0.18
C22:6n-3/C22:5n-3	137.00	±	38.14	89.26	±	14.56	0.17
1 (% monoenoics)	25.83	±	0.44	24.64	±	0.29	0.03
2 (% dienoics)	0.92	±	0.15	0.87	±	0.06	0.76
3 (% trienoics)	2.95	±	0.26	2.52	±	0.22	0.23
4 (% tetraenoics)	11.38	±	0.07	11.86	±	0.37	0.27
5 (% pentaenoics)	0.03	±	0.02	0.13	±	0.02	0.005
6 (% hexaenoics)	10.18	±	0.23	10.51	±	0.34	0.47
Unsaturation Index	51.29	±	0.39	50.53	±	0.53	0.28

Table 74. Hypothalamus total fatty acid methyl esters (FAME) for high fat diet groups; High fat diet with-saline (HFD-S), High fat diet -pair-fed (HFD-PF) and High fat diet- Ginkgo biloba (HFD-GbE) (N=10 per group). Fatty acid results are presented as area % percentage mean and standard error of the mean (SEM), and statistically analysed by one-way ANOVA with Tukey's Post-hoc test. The level of statistical significance was set at * $p < 0.05$.

	HFD-S			HFD-PF			HFD-GbE			S Vs PF	S Vs GbE	PF Vs GbE
	MEAN %	SEM		MEAN %	SEM		MEAN %	SEM				
C14:0	0.11	±	0.02	0.06	±	0.01	0.06	±	0.01	0.09	0.11	>0.99
C16:0	20.14	±	0.22	19.49	±	0.63	19.83	±	0.62	>0.99	0.64	0.64
C17:0	0.13	±	0.02	0.15	±	0.06	0.09	±	0.02	0.89	0.91	0.91
C18:0	19.83	±	0.57	18.70	±	0.44	18.52	±	0.30	0.20	0.14	0.96
C20:0	0.64	±	0.04	0.83	±	0.16	0.71	±	0.05	0.37	0.87	0.70
C22:0	0.34	±	0.03	0.30	±	0.02	0.35	±	0.03	0.61	0.91	0.39
C23:0	0.15	±	0.01	0.15	±	0.01	0.15	±	0.01	>0.99	0.81	0.83
DMA 16:0	1.10	±	0.10	0.96	±	0.04	>0.99	±	0.04	0.30	0.56	0.90
DMA 18:0	3.73	±	0.23	3.59	±	0.22	3.53	±	0.22	0.90	0.81	0.98
ΣSFA DMA	4.83	±	0.30	4.55	±	0.24	4.53	±	0.23	0.72	0.70	>0.99
ΣSFA	46.17	±	0.52	44.18	±	0.94	44.24	±	0.80	0.17	0.21	>0.99
C16:1n-7	0.27	±	0.03	0.19	±	0.02	0.16	±	0.02	0.06	0.01	0.69
C18:1n-7	3.04	±	0.08	2.89	±	0.08	2.79	±	0.08	0.41	0.10	0.66
C18:1n-9	16.56	±	0.17	16.53	±	0.77	16.25	±	0.36	>0.99	0.91	0.92
C20:1n-9	1.27	±	0.09	1.30	±	0.06	1.34	±	0.14	0.97	0.90	0.97
C22:1n-9	0.21	±	0.01	0.21	±	0.02	0.25	±	0.02	0.98	0.31	0.24
C24:1n-9	0.91	±	0.06	0.92	±	0.04	0.96	±	0.08	0.99	0.84	0.91
DMA 18:1	1.17	±	0.12	1.56	±	0.08	1.63	±	0.15	0.06	0.03	0.89
C18:1 Total	19.65	±	0.21	19.42	±	0.84	19.04	±	0.42	0.96	0.74	0.89
Σω7	3.34	±	0.09	3.06	±	0.10	2.95	±	0.09	0.09	0.01	0.67
Σω9	18.97	±	0.23	18.83	±	0.71	18.79	±	0.34	0.98	0.96	>0.99
ΣMUFA	24.64	±	0.29	25.01	±	0.75	25.02	±	0.32	0.87	0.86	>0.99
C18:2n-6	0.78	±	0.06	1.03	±	0.30	0.92	±	0.18	0.66	0.88	0.93
C18:3n-6	0.08	±	0.01	0.12	±	0.03	0.27	±	0.18	0.95	0.40	0.57
C20:2n-6	0.10	±	0.01	0.11	±	0.01	0.10	±	0.01	0.78	>0.99	0.75
C20:3n-6	0.28	±	0.01	0.28	±	0.03	0.27	±	0.01	>0.99	0.95	0.92
C20:4n-6	7.87	±	0.33	7.18	±	0.26	7.26	±	0.17	0.17	0.26	0.98
C22:4n-6	3.98	±	0.07	3.83	±	0.13	3.85	±	0.06	0.47	0.59	0.99
Σn-6 PUFA	13.08	±	0.35	12.53	±	0.43	12.68	±	0.27	0.52	0.72	0.95
Σn-6metabol	12.30	±	0.38	11.50	±	0.37	11.75	±	0.14	0.21	0.49	0.85
C18:3n-3	2.02	±	0.23	3.91	±	1.29	3.25	±	0.45	0.24	0.56	0.84
C20:3n-3	0.19	±	0.02	0.15	±	0.01	0.14	±	0.01	0.09	0.07	0.98
C22:5n-3	0.14	±	0.02	0.07	±	0.01	0.10	±	0.01	0.002	0.08	0.24
C22:6n-3	10.51	±	0.34	9.84	±	0.41	9.97	±	0.19	0.34	0.51	0.96
Σn-3 PUFA	12.81	±	0.46	13.94	±	0.96	13.48	±	0.39	0.46	0.78	0.89
Σn-3 metabolites	10.79	±	0.34	10.03	±	0.42	10.23	±	0.20	0.27	0.52	0.92
ΣPUFA	25.88	±	0.59	26.46	±	0.67	26.28	±	0.48	0.76	0.89	0.98
ΣUFA	50.53	±	0.53	51.47	±	0.44	51.14	±	0.43	0.33	0.65	0.88

Table 75. Hypothalamus total fatty acid methyl esters (FAME) ratios for high fat diet groups; High fat diet with-saline (HFD-S), High fat diet -pair-fed (HFD-PF) and High fat diet- Ginkgo biloba (HFD-GbE) (N=10 per group). Results presented as mean \pm (SEM), and statistically analysed by one-way ANOVA with Tukey's Post-hoc test. The level of statistical significance was set at * $p < 0.05$.

	HFD-S		HFD-PF		HFD-GbE		S Vs PF	S Vs GbE	PF Vs GbE
	MEAN	SEM	MEAN	SEM	MEAN	SEM			
Σ MUFA/ Σ PUFA	0.96	\pm 0.03	0.95	\pm 0.05	0.95	\pm 0.02	>0.99	0.98	0.99
Σ MUFA/ Σ SFA	0.53	\pm 0.01	0.57	\pm 0.10	0.57	\pm 0.01	0.13	0.12	>0.99
Σ PUFA/ Σ SFA	1.05	\pm 0.03	1.08	\pm 0.07	1.06	\pm 0.03	0.94	>0.99	0.97
Σ UFA/ Σ SFA	1.10	\pm 0.02	1.17	\pm 0.03	1.16	\pm 0.04	0.16	0.28	0.97
C18:0/C16:0	5.37	\pm 0.52	7.36	\pm 1.33	9.65	\pm 1.87	0.51	0.06	0.51
C16:1n-7/C16:0	2.30	\pm 0.34	1.99	\pm 0.35	1.94	\pm 0.19	0.76	0.70	0.76
C18:1n-9/C16:0	144.3	\pm 17.26	184.6	\pm 33.84	220.5	\pm 33.29	0.56	0.14	0.56
C18:1n-9/C16:1n-7	70.45	\pm 9.20	97.50	\pm 9.59	108.54	\pm 8.24	0.10	0.02	0.10
C18:1n-7/C18:0	0.15	\pm 0.01	0.15	\pm 0.01	0.15	\pm 0.01	0.99	0.82	0.76
C18:1/C18:0	31.77	\pm 1.76	28.86	\pm 3.49	28.01	\pm 2.24	0.71	0.58	0.71
n-6/n-3	1.03	\pm 0.05	0.94	\pm 0.07	0.95	\pm 0.03	0.43	0.59	0.43
C20:4n-6/C18:2n-6	10.85	\pm 1.19	9.97	\pm 1.40	9.99	\pm 1.52	0.89	0.90	>0.99
C20:3n-3/C18:3n-3	0.09	\pm 0.03	0.05	\pm 0.01	0.04	\pm 0.01	0.21	0.08	0.81
C22:5n-3/C18:3n-3	0.07	\pm 0.01	0.03	\pm 0.01	0.04	\pm 0.01	0.002	0.005	0.89
C22:6n-3/C18:3n-3	5.74	\pm 0.62	4.11	\pm 0.68	3.61	\pm 0.52	0.16	0.06	0.84
C22:6n-3/C22:5n-3	89.26	\pm 14.56	140.75	\pm 9.10	98.12	\pm 3.47	0.004	0.81	0.02
1 (% monoenoics)	24.64	\pm 0.29	25.01	\pm 0.75	25.02	\pm 0.32	0.87	0.86	>0.99
2 (% dienoics)	0.87	\pm 0.06	1.13	\pm 0.30	1.02	\pm 0.18	0.64	0.86	0.93
3 (% trienoics)	2.52	\pm 0.22	4.42	\pm 1.30	3.90	\pm 0.57	0.26	0.50	0.90
4 (% tetraenoics)	11.86	\pm 0.37	11.01	\pm 0.38	11.11	\pm 0.21	0.19	0.28	0.98
5 (% pentaenoics)	0.13	\pm 0.02	0.07	\pm 0.01	0.10	\pm 0.01	0.002	0.08	0.24
6 (% hexaenoics)	10.51	\pm 0.34	9.84	\pm 0.41	9.97	\pm 0.19	0.34	0.51	0.96
Unsaturation Index	50.53	\pm 0.53	51.47	\pm 0.44	51.13	\pm 0.38	0.32	0.63	0.86

6.3 Hippocampus

In total hippocampus fatty acids profiles, no significant changes in FA percentage levels occurred in the hippocampus when comparing the NFD or HFD-S groups. While no significant differences occurred in the C18:2n-6 ($p=0.97$) and C20:4n-6 ($p=0.27$) fatty acids between the groups (Table 76), a 28% decrease in the C20:4n-6/C18:2n-6 ratio for the HFD-S group indicates a shift in the balance between the n-6 with C18:2n-6 increasing as C20:4n-6 decreasing (C20:4n-6/C18:2n-6; NFD, $26.71\pm 1.06\%$; HFD-S, $19.18\pm 2.12\%$, $p=0.01$). Similarly while neither C22:6n-3 ($p=0.17$) or C22:5n-3 ($p=0.26$) (Table 76) significantly changed between the NFD and HFD-S group, a 12% decrease in the C22:6n-3/C22:5n-3 ratio (Table 77) indicates that a shift in the balance between the n-3 FA occurred, where C22:6n-3 decreased more in the HFD-S group (C22:6n-3/C22:5n-3; NFD, $93.20\pm 3.83\%$; HFD-S, $81.68\pm 2.82\%$, $p=0.03$). When comparing the 3 HFD subsets, only a significant decrease in C22:0 was seen in the GbE group ($p=0.03$) compared to the HFD-S group (Table 78) and no changes in FA ratios (Table 79).

Table 76. Hippocampus total fatty acid methyl esters (FAME) for normal fat diet (NFD) and high fat diet (HFD-S) (N=10 per group). Fatty acid results are presented as area % percentage mean and standard error of the mean (SEM), and statistically analysed by Students t-test. The level of statistical significance was set at * $p < 0.05$.

	NFD			HFD-S			p value
	MEAN %		SEM	MEAN %		SEM	
C14:0	0.05	±	0.01	0.07	±	0.01	0.07
C16:0	20.20	±	0.21	20.21	±	0.20	0.97
C18:0	19.31	±	0.16	18.91	±	0.28	0.22
C20:0	0.49	±	0.02	0.49	±	0.02	0.88
C22:0	0.41	±	0.02	0.42	±	0.02	0.51
C23:0	0.20	±	0.01	0.19	±	0.01	0.41
DMA 16:0	1.99	±	0.04	2.08	±	0.08	0.34
DMA 18:0	3.35	±	0.05	3.27	±	0.08	0.42
ΣSFA.DMA	5.33	±	0.08	5.34	±	0.16	0.95
ΣSFA	46.21	±	0.14	45.90	±	0.52	0.57
C16:1n-7	0.17	±	0.01	0.20	±	0.02	0.24
C18:1n-7t	0.03	±	0.01	0.04	±	0.01	0.31
C18:1n-7	2.56	±	0.03	2.50	±	0.06	0.38
C18:1n-9	15.12	±	0.22	15.27	±	0.31	0.70
C20:1n-9	0.92	±	0.03	0.98	±	0.04	0.26
C22:1n-9	0.18	±	0.01	0.21	±	0.02	0.18
C24:1n-9	1.21	±	0.04	1.21	±	0.04	0.97
DMA 18:1	1.16	±	0.04	1.13	±	0.04	0.57
DMA 18:1 Total	1.16	±	0.04	1.13	±	0.04	0.57
C18:1 Total	17.71	±	0.23	17.81	±	0.35	0.81
Σω7	2.76	±	0.04	2.74	±	0.07	0.84
Σω9	17.43	±	0.28	17.68	±	0.32	0.58
ΣMUFA	21.35	±	0.33	21.55	±	0.36	0.70
C18:2n-6	0.41	±	0.01	1.03	±	0.52	0.25
C18:3n-6	0.04	±	0.01	0.04	±	0.01	0.97
C20:2n-6	0.09	±	0.01	0.10	±	0.01	0.26
C20:3n-6	0.23	±	0.01	0.24	±	0.01	0.21
C20:4n-6	10.79	±	0.14	10.24	±	0.46	0.27
C22:2n-6	0.02	±	0.01	0.02	±	0.01	0.74
C22:4n-6	4.09	±	0.04	3.99	±	0.07	0.25
Σn-6 PUFA	15.66	±	0.14	15.67	±	0.08	0.98
Σn-6 metabolites	15.25	±	0.15	14.63	±	0.52	0.26
C18:3n-3	0.76	±	0.18	0.77	±	0.13	0.97
C20:3n-3	0.08	±	0.01	0.11	±	0.01	0.13
C22:5n-3	0.12	±	0.01	0.13	±	0.01	0.26
C22:6n-3	10.93	±	0.23	10.38	±	0.31	0.17
Σn-3 PUFA	11.89	±	0.28	11.38	±	0.33	0.26
Σn-3 metabolites	11.13	±	0.23	10.61	±	0.32	0.20
ΣPUFA	27.55	±	0.29	27.05	±	0.33	0.26
ΣUFA	48.91	±	0.17	48.59	±	0.26	0.33

Table 77. Hippocampus total fatty acid methyl esters (FAME) ratios for normal fat diet (NFD) and high fat diet (HFD-S) (N=10 per group). Results presented as mean an (SEM), and statistically analysed by one-way ANOVA with Tukey's Post-hoc test. The level of statistical significance was set at *p < 0.05

	NFD			HFD-S			p value
	MEAN %	±	SEM	MEAN %	±	SEM	
ΣMUFA/ΣPUFA	0.78	±	0.02	0.80	±	0.02	0.46
ΣMUFA/ΣSFA	0.46	±	0.01	0.47	±	0.01	0.93
ΣPUFA/ΣSFA	1.29	±	0.03	1.26	±	0.03	0.47
ΣUFA/ΣSFA	1.06	±	0.01	1.06	±	0.02	0.93
C18:0/C16:0	4.97	±	0.23	4.88	±	0.25	0.80
C16:1n-7/C16:0	1.74	±	0.07	2.03	±	0.30	0.36
C18:1n-9/C16:0	155.56	±	7.64	153.00	±	9.53	0.84
C18:1n-9/C16:1n-7	89.69	±	3.62	82.35	±	7.05	0.37
C18:1n-7/C18:0	5.37	±	0.26	5.14	±	0.21	0.51
C18:1/C18:0	37.07	±	1.72	36.62	±	1.45	0.84
n-6/n-3	1.32	±	0.03	1.39	±	0.04	0.26
C18:2n-6/C18:3n-3	0.65	±	0.06	1.35	±	0.59	0.25
C20:4n-6/C18:2n-6	26.71	±	1.06	19.18	±	2.12	0.01
C20:4n-6/C20:3n6	48.09	±	2.07	42.52	±	2.03	0.07
C20:4n-6/C22:6n3	0.99	±	0.02	0.99	±	0.04	0.98
C20:4n-6/C18:3n3	17.52	±	1.85	15.30	±	1.61	0.38
C20:3n-3/C18:3n-3	0.13	±	0.02	0.16	±	0.03	0.39
C22:5n-3/C18:3n-3	0.19	±	0.02	0.19	±	0.02	0.82
C22:6n-3/C18:3n-3	17.64	±	1.85	15.47	±	1.57	0.38
C22:6n-3/C22:5n-3	93.20	±	3.83	81.68	±	2.82	0.03
1 (% monoenoics)	21.35	±	0.33	21.55	±	0.36	0.70
2 (% dienoics)	0.51	±	0.02	1.15	±	0.52	0.24
3 (% trienoics)	1.12	±	0.18	1.16	±	0.12	0.83
4 (% tetraenoics)	14.88	±	0.16	14.23	±	0.51	0.24
5 (% pentaenoics)	0.12	±	0.01	0.13	±	0.01	0.26
6 (% hexaenoics)	10.93	±	0.23	10.38	±	0.31	0.17
Unsaturation Index	48.91	±	0.17	48.59	±	0.26	0.33

Table 78. Hippocampus total fatty acid methyl esters (FAME) for high fat diet groups; High fat diet with-saline (HFD-S), High fat diet -pair-fed (HFD-PF) and High fat diet- Ginkgo biloba (HFD-GbE) (N=10 per group). Fatty acid results are presented as area % percentage mean and standard error of the mean (SEM), and statistically analysed by one-way ANOVA with Tukey's Post-hoc test. The level of statistical significance was set at *p < 0.05.

	HFD-S		HFD-PF		HFD-GbE		S Vs PF	S Vs GbE	PF Vs GbE
	MEAN %	SEM	MEAN %	SEM	MEAN %	SEM			
C14:0	0.07 ± 0.01	0.05 ± 0.01	0.06 ± 0.01	0.07 ± 0.01	0.72	0.18	0.54		
C16:0	20.21 ± 0.20	20.09 ± 0.19	20.07 ± 0.33	0.50	>0.99	>0.99	>0.99		
C18:0	18.91 ± 0.28	19.28 ± 0.15	18.90 ± 0.22	0.99	>0.99	0.99			
C20:0	0.49 ± 0.02	0.48 ± 0.01	0.50 ± 0.07	0.97	>0.99	0.99			
C21:0	0.04 ± 0.01	0.04 ± 0.01	0.01 ± 0.01	0.97	0.38	0.27			
C22:0	0.42 ± 0.02	0.21 ± 0.07	0.10 ± 0.05	0.56	0.03	0.20			
C23:0	0.19 ± 0.01	0.21 ± 0.01	0.21 ± 0.01	0.88	0.89	>0.99			
DMA 16:0	2.08 ± 0.08	2.19 ± 0.03	2.23 ± 0.02	0.94	0.93	>0.99			
DMA 18:0	3.27 ± 0.08	3.35 ± 0.02	3.28 ± 0.02	>0.99	0.84	0.83			
ΣSFA.DMA	5.34 ± 0.16	5.54 ± 0.03	5.51 ± 0.04	0.99	0.90	0.84			
ΣSFA	45.90 ± 0.52	46.09 ± 0.21	45.59 ± 0.27	>0.99	>0.99	0.99			
C16:1n-7	0.20 ± 0.02	0.23 ± 0.02	0.21 ± 0.01	0.94	0.80	0.95			
C18:1n-7	2.50 ± 0.06	2.52 ± 0.07	2.54 ± 0.13	0.95	>0.99	0.92			
C18:1n-9	15.27 ± 0.31	15.31 ± 0.23	15.20 ± 0.31	>0.99	0.98	>0.99			
C20:1n-9	0.98 ± 0.04	0.95 ± 0.03	>0.99 ± 0.06	>0.99	0.99	0.99			
C22:1n-9	0.21 ± 0.02	0.19 ± 0.01	0.20 ± 0.02	0.97	0.75	0.61			
C24:1n-9	1.21 ± 0.04	1.31 ± 0.06	1.33 ± 0.08	0.89	0.88	>0.99			
DMA 18:1	1.13 ± 0.04	1.22 ± 0.05	1.22 ± 0.06	0.94	0.94	>0.99			
C18:1 Total	17.81 ± 0.35	17.89 ± 0.26	17.79 ± 0.31	>0.99	0.76	0.77			
Σω7	2.74 ± 0.07	2.80 ± 0.07	2.78 ± 0.14	0.94	>0.99	0.94			
Σω9	17.68 ± 0.32	17.77 ± 0.30	17.75 ± 0.42	>0.99	0.99	>0.99			
ΣMUFA	21.55 ± 0.36	21.79 ± 0.37	21.74 ± 0.50	>0.99	>0.99	0.99			
C18:2n-6	1.03 ± 0.52	0.47 ± 0.02	0.61 ± 0.07	0.59	0.55	>0.99			
C18:3n-6	0.04 ± 0.01	0.05 ± 0.01	0.08 ± 0.03	0.88	>0.99	0.85			
C20:2n-6	0.10 ± 0.01	0.10 ± 0.01	0.09 ± 0.01	0.99	0.80	0.74			
C20:3n-6	0.24 ± 0.01	0.26 ± 0.01	0.25 ± 0.01	0.85	0.99	0.90			
C20:4n-6	10.24 ± 0.46	10.63 ± 0.12	10.51 ± 0.18	0.96	0.99	0.99			
C22:2n-6	0.02 ± 0.01	0.01 ± 0.01	0.02 ± 0.01	0.88	0.39	0.67			
C22:4n-6	3.99 ± 0.07	4.15 ± 0.07	4.13 ± 0.08	0.98	>0.99	0.99			
Σn-6 PUFA	15.67 ± 0.08	15.66 ± 0.11	15.72 ± 0.18	>0.99	>0.99	0.99			
Σn-6metabolites	14.63 ± 0.52	15.19 ± 0.13	15.07 ± 0.17	0.96	0.99	0.99			
C18:3n-3	0.77 ± 0.13	0.50 ± 0.02	0.67 ± 0.17	0.57	0.76	0.96			
C20:3n-3	0.11 ± 0.01	0.12 ± 0.01	0.08 ± 0.03	0.86	0.97	0.96			
C22:5n-3	0.13 ± 0.01	0.12 ± 0.01	0.12 ± 0.01	0.93	0.82	0.97			
C22:6n-3	10.38 ± 0.31	10.36 ± 0.28	10.05 ± 0.36	0.98	0.94	0.99			
Σn-3 PUFA	11.38 ± 0.33	11.10 ± 0.28	10.93 ± 0.39	0.96	0.63	0.79			
Σn-3 metabolites	10.61 ± 0.32	10.60 ± 0.27	10.26 ± 0.34	0.98	0.67	0.78			
ΣPUFA	27.05 ± 0.33	26.76 ± 0.33	26.64 ± 0.44	0.99	0.73	0.79			
ΣUFA	48.59 ± 0.26	48.55 ± 0.21	48.39 ± 0.19	>0.99	0.76	0.78			

Table 79. Hippocampus total fatty acid methyl esters (FAME) ratios for high fat diet groups; High fat diet with-saline (HFD-S), High fat diet -pair-fed (HFD-PF) and High fat diet- Ginkgo biloba (HFD-GbE) (N=10 per group). Results presented as mean an (SEM), and statistically analysed by one-way ANOVA with Tukey's Post-hoc test. The level of statistical significance was set at * $p < 0.05$.

	HFD-S		HFD-PF		HFD-GbE		S Vs PF	S Vs GbE	PF Vs GbE
	MEAN %	SEM	MEAN %	SEM	MEAN %	SEM			
Σ MUFA/ Σ PUFA	0.80	± 0.02	0.82	± 0.02	0.82	± 0.03	0.80	0.48	0.85
Σ MUFA/ Σ SFA	0.47	± 0.01	0.47	± 0.01	0.48	± 0.01	0.99	0.39	0.43
Σ PUFA/ Σ SFA	1.26	± 0.03	1.23	± 0.03	1.23	± 0.05	0.73	0.47	0.89
Σ UFA/ Σ SFA	1.06	± 0.02	1.05	± 0.01	1.06	± 0.01	0.60	0.88	0.89
C18:0/C16:0	4.88	± 0.25	4.74	± 0.12	5.25	± 0.97	0.95	0.99	0.98
C16:1n-7/C16:0	2.03	± 0.30	2.29	± 0.13	2.19	± 0.24	0.53	0.46	0.99
C18:1n-9/C16:0	153.00	± 9.53	153.93	± 6.12	157.12	± 8.46	0.99	0.99	0.96
C18:1n-9/C16:1n-7	82.35	± 7.05	68.94	± 3.86	74.58	± 3.99	0.53	0.37	0.95
C18:0/C18:1n-7	0.20	± 0.01	0.19	± 0.01	0.19	± 0.02	0.47	0.47	>0.99
C18:1n-7/C18:0	5.14	± 0.21	5.34	± 0.19	5.53	± 0.47	0.56	0.47	0.98
C18:1/C18:0	36.62	± 1.45	37.82	± 0.79	40.07	± 4.80	0.90	0.67	0.90
n-6/n-3	1.39	± 0.04	1.42	± 0.04	1.45	± 0.05	0.96	0.95	>0.99
C18:2n-6/C18:3n-3	1.35	± 0.59	0.96	± 0.05	1.11	± 0.16	0.99	0.85	0.91
C20:4n-6/C18:2n-6	19.18	± 2.12	22.85	± 1.06	18.34	± 1.58	0.53	0.38	0.96
C20:4n-6/C18:3n-3	15.30	± 1.61	21.66	± 1.07	19.53	± 2.38	0.11	0.05	0.84
C20:3n-3/C18:3n-3	0.16	± 0.03	0.26	± 0.02	0.14	± 0.04	0.55	0.40	0.95
C22:5n-3/C18:3n-3	0.19	± 0.02	0.24	± 0.01	0.22	± 0.02	0.82	0.70	0.97
C22:6n-3/C18:3n-3	15.47	± 1.57	21.04	± 1.01	18.64	± 2.44	0.74	0.43	0.85
C22:6n-3/C22:5n-3	81.68	± 2.82	88.35	± 3.42	85.01	± 5.72	0.96	0.53	0.69
1 (% monoenoics)	21.55	± 0.36	21.79	± 0.37	21.74	± 0.50	>0.99	0.80	0.78
2 (% dienoics)	1.15	± 0.52	0.58	± 0.02	0.75	± 0.09	0.59	0.48	0.98
3 (% trienoics)	1.16	± 0.12	0.93	± 0.03	1.07	± 0.17	0.76	0.59	0.96
4 (% tetraenoics)	14.23	± 0.51	14.77	± 0.14	14.64	± 0.18	0.97	0.89	0.77
5 (% pentaenoics)	0.13	± 0.01	0.12	± 0.01	0.12	± 0.01	0.94	0.53	0.73
6 (% hexaenoics)	10.38	± 0.31	10.36	± 0.28	10.05	± 0.36	0.98	0.67	0.78
Unsaturation Index	48.59	± 0.26	48.55	± 0.21	48.39	± 0.19	>0.99	0.75	0.77

6.4 Discussion

The hypothalamus is a key regulator of food intake and has been shown to be influenced by dietary intake (McLean *et al.*, 2019). Leptin and insulin signalling are crucial within the hypothalamic signalling system for the regulation and maintenance of glucose processing, overall energy homeostasis and adiposity (Thon, Hosoi and Ozawa, 2016). The hypothalamus exhibits a high level of plasticity to allow for quick changes in the environment particularly around fuel sensing and neuronal firing (Dietrich and Horvath, 2009, 2011, 2013). Three major peripheral hormones, leptin, ghrelin and insulin induce acute responses in the melanocortin system of the hypothalamus in an opposing manner (Dietrich and Horvath, 2013). Obesity has been shown to disrupt leptin and ghrelin signalling and insulin receptor function, leading to IR, hyperphagia and hyperleptinemia (Hucik *et al.*, 2021; Obradovic *et al.*, 2021; Cervone *et al.*, 2020; Gruzdeva *et al.*, 2019; Izquierdo *et al.*, 2019; Zanetti *et al.*, 2019; Briggs *et al.*, 2013; Nazarians-Armavil, Menchella and Belsham, 2013; Gomez *et al.*, 2012; Reed *et al.*, 2010; Ernst *et al.*, 2009; Handjjeva-Darlenka and Boyadjieva, 2009; Morrison, 2009; Morton *et al.*, 2006; Cheng *et al.*, 2002; Hileman *et al.*, 2002).

The adipocyte-derived hormone leptin enhances anorexigenic POMC/ α -MSH-expressing neuronal firing and decreases orexigenic NPY/AgRP neuronal firing (Izquierdo *et al.*, 2019; Moulton and Harvey, 2011). The stomach-derived hormone ghrelin enhances NPY/AgRP neuronal firing and decreases POMC cell firing (Lin *et al.*, 2016; Ueberberg *et al.*, 2009; Jianhua Liu *et al.*, 2008; Kohno *et al.*, 2008; Gauna *et al.*, 2004; Kojima *et al.*, 1999). The pancreas-derived hormone insulin also affects ARC neuronal firing and has been shown to disrupt leptin mediated neuronal control (Nazarians-Armavil, Menchella and Belsham, 2013) while ghrelin has been shown to improve insulin sensitivity as well as neurogenesis (Chung *et al.*, 2013; Li *et al.*, 2013; Gauna *et al.*, 2004). Leptin works predominantly by inducing the JAK-STAT3 pathway (Guo *et al.* 2008). Insulin predominantly induces the PI3K–Akt pathway (Hoy *et al.*, 2009; Liu *et al.*, 2009; Vestergaard *et al.*, 2008), while ghrelin induces JAK2/STAT3, PI3K–Akt and ERK1/2 pathways (Eid *et al.*, 2018; Chung *et al.*, 2008, 2013; Li *et al.*, 2013). Leptin, a product of the obese (*ob*) gene, is an anorexigenic adipocyte-secreted hormone responsible for regulating appetite, bodyweight and energy expenditure and homeostasis in the CNS as well as playing a role in proinflammatory immune responses, angiogenesis and lipolysis (Obradovic *et al.*, 2021). As adipocyte volume increases, leptin levels also increase. As circulating leptin levels increase and cross the blood brain barrier (BBB), a reduction in appetite ensues to control and regulate body weight *via* a negative feedback mechanism between adipose tissue and the hypothalamus. Leptin

binds to the transmembrane leptin receptor (LEP-R) (a cognate receptor) and through a negative feedback loop between adipose tissue and the hypothalamus, inhibits the synthesis and release of neuropeptide-Y (NPY) in the arcuate nucleus (ARC) (Stephens *et al.*, 1995) and the dorsomedial hypothalamic nucleus (DMH) (Fei *et al.* 1997). LEP-Rb inhibits the expression of neuropeptide agouti-related peptide (AgRP), an appetite stimulating protein. LEP-Rb also stimulates the expression of POMC, an appetite suppressing protein (Obradovic *et al.*, 2021) which stimulates the expression of alpha-melanocyte-stimulating hormone (α -MSH) which binds to the melanocortin receptor (MCR) (Münzberg, Flier and Bjørnbæk, 2004; Cowley *et al.*, 2001; Elias *et al.*, 1999). This leads to appetite-suppression, inhibiting food intake and increasing energy expenditure (Obradovic *et al.*, 2021; Papathanasiou *et al.*, 2019; Stern *et al.*, 2016; Park *et al.*, 2015). Meanwhile leptin deficiency is associated with hyperglycemia and IR (Obradovic *et al.*, 2021).

Leptin also modulates lipid metabolism and lipolysis, proinflammatory immune responses and insulin sensitivity in several tissues (Stern, Rutkowski and Scherer, 2016; Farr, Gavrieli and Mantzoros, 2015). Circulating leptin serum levels strongly correlate to adiposity and body fat percentage. In a fasting state, plasma leptin levels decrease, promoting food intake, with feeding and overfeeding increasing *ob* gene expression and leptin levels (Kolaczynski *et al.*, 1996; de Vos *et al.*, 1995). Leptin secretion displays a pulsatile-like circadian rhythm, with levels highest at midnight, and lowest in mid-afternoon, with a higher pulse amplitude in obesity where fat mass acts as an amplifier for leptin secretion (Koutkia *et al.*, 2003; Licinio *et al.*, 1997, 1998). This mechanism is dysfunctional in obesity however, where despite increased circulating levels of leptin, high levels of leptin resistance occur, negating the proactive effects attributed to leptin on energy homeostasis (Enriori *et al.*, 2007; Münzberg, Flier and Bjørnbæk, 2004; Heymsfield *et al.*, 1999). It has been reported that women are more susceptible to resistance than men (Licinio *et al.*, 1998). Leptin resistance occurs due to a defective leptin pathway including disruptions to leptin synthesis, decreased LEP-R expression and defective intracellular leptin receptor (LEP-R) signalling leading to a decrease in leptin transport across the BBB (di Spiezio *et al.*, 2018; Haddad-Tóvolli *et al.*, 2017; Burguera *et al.*, 2000). Furthermore, excessive serum leptin levels may contribute to decreased BBB permeability (di Spiezio *et al.*, 2018; Haddad-Tóvolli *et al.*, 2017; Burguera *et al.*, 2000). This negates the hypothalamic-induced anorexic effects of leptin, leading to reduced satiety and appetite suppression leading to over-consumption of nutrients and increased total body mass. Due to leptin-resistance, exogenous leptin treatment is limited in terms of effect. Consequently, leptin sensitisers are now being explored instead (Obradovic *et al.*, 2021).

Long term consumption of a HFD can lead to leptin resistance in the ARC of the hypothalamus and ventral tegmental area (VTA) of the midbrain (Enriori *et al.*, 2007; Münzberg, Flier and Bjørbæk, 2004; Heymsfield *et al.*, 1999). A HFD is shown to stimulate SOCS3 expression and activation of STAT3 resistance by leptin in POMC, ARC and AgRP neurons in rodents although some compensatory mechanisms to leptin resistance may occur in both ARC and VTA regions (Banin *et al.*, 2021; Gamber *et al.*, 2012; Münzberg, Flier and Bjørbæk, 2004; El-Haschimi *et al.*, 2000). The orexigenic hormone ghrelin is released from the stomach prior to and in anticipation of a meal and decreases immediately after feeding. Circulating ghrelin levels stimulates food intake and growth hormone secretion and helps regulate adipose tissue lipolysis and fatty acid β -oxidation (Hucik *et al.*, 2021; Cervone *et al.*, 2018, 2020; Kraft, Cervone and Dyck, 2019; Cervone and Dyck, 2017; Gomez *et al.*, 2012; Vestergaard *et al.*, 2008; Barazzoni *et al.*, 2005; Wren *et al.*, 2000). Through the suppression of hormone-sensitive lipase (HSL) possibly by the blunting in the phosphorylation of HSL activation sites, Ser660 and 563 (Kraft, Cervone and Dyck, 2019), it has been shown that ghrelin reduces β adrenoreceptor-stimulated lipolysis and fatty acid re-esterification in adipocytes in both SAT and VAT adipose tissues, thus regulating TAG hydrolysis (Kraft, Cervone and Dyck, 2019; Muccioli *et al.*, 2004). Ghrelin has also been shown to attenuate neuroinflammation and demyelination (Liu *et al.*, 2019; Andrews *et al.*, 2008) and facilitates neuronal repair following injury restoring plasticity (Stoyanova and Lutz 2021). Specifically, ghrelin has been shown to mediate spinal cord neurogenesis in the foetus (Sato *et al.*, 2006) and hippocampal neurogenesis (Davies, 2022; Buntwal *et al.*, 2019; Kunath and Dresler, 2014; Chung *et al.*, 2013). Obesity and metabolic syndrome are also associated with decreased fasting ghrelin levels (FGL) where FGL reflect insulin sensitivity recovery and VAT reduction and lowered body weight (Tsaban *et al.*, 2022). A chronic HFD has been shown to have persistent inhibitory effects on plasma ghrelin levels (Hucik *et al.*, 2021; Briggs *et al.*, 2013; Gomez *et al.*, 2012; Cano *et al.*, 2009; Handjjeva-Darlenska and Boyadjieva, 2009; Poppitt *et al.*, 2005) with ghrelin resistance seen in NPY and AgRP neurons of the hypothalamus (Briggs *et al.*, 2013).

Of the hypothalamic results seen between a NFD and HFD-S, one of the most notable changes was the 1.4% increase in C18:0 in the HFD-S (C18:0; NFD, 18.45 \pm 0.14%; HFD-S, 19.83 \pm 0.57%, $p=0.05$) and a 1.6% increase in total SFA levels (Σ SFA; NFD, 44.56 \pm 0.46%; HFD-S, 46.17 \pm 0.52%, $p=0.04$). The increase in SFA levels affected the total MUFA levels which decreased by 1.2% in the HFD-S compared to the NFD (Σ MUFA; NFD, 25.83 \pm 0.44%; HFD-S, 24.64 \pm 0.29%, $p=0.03$) and while no significant changes were seen in the Σ MUFA/ Σ SFA ratio (Σ MUFA/ Σ SFA; NFD, 0.58 \pm 0.01; HFD-S, 0.53 \pm 0.01, $p=0.008$) and Σ UFA/ Σ SFA ratio (Σ UFA/ Σ SFA; NFD, 1.15 \pm 0.02; HFD-S, 1.10 \pm 0.02, $p=0.09$) a decreasing

trend was seen in both. Likewise, an increasing trend in the C18:1n-7/C18:0 ratio (C18:1n-7/C18:0; NFD, 4.24 ± 0.22 ; HFD-S, 4.87 ± 0.22 , $p=0.06$) suggests that comparatively larger amounts of C18:1n-7 are being incorporated into the phospholipid membrane compared to C18:0. Similarly, a significant increase in the C22:5n-3/C18:3n-3 ratio (C22:5n-3/C18:3n-3; NFD, 0.01 ± 0.01 ; HFD-S, 0.07 ± 0.01 , $p=0.002$) suggests that comparatively, the higher n-3 FA C22:5n-3 is being incorporated more into the membrane than C18:3n-3 in the HFD. Each of these last results suggest a potential shift in DNL.

A high fat diet (HFD) is also associated with disruptions to the normal daily pattern of plasma insulin, adiponectin, IL-1, IL-6, TNF α , leptin, ghrelin, and MCP-1 (Hucik *et al.*, 2021; Malesza *et al.*, 2021; Cervone *et al.*, 2020; Gomez *et al.*, 2012; Cano *et al.*, 2009; Poppitt *et al.*, 2005). In HFD obese models, high-fat consumption produces hypothalamic inflammation in the central nervous system. Hypothalamic inflammation is associated with toll like receptor 4 (TLR4) activation of astrocytes and microglia, and increased expressions of TNF α , IL-1 β , and IL-6, along with activation of the IKK β /NF- κ B inflammatory pathway and mitochondrial dysfunction which can lead to insulin and leptin resistance and metabolic syndrome (Bhusal, Rahman and Suk, 2022; Benomar and Taouis, 2019; Rogero and Calder, 2018; Baufeld *et al.*, 2016; Masson *et al.*, 2015; Schneeberger *et al.*, 2013; Shechter *et al.*, 2013; Cai and Liu, 2012; Milanski *et al.*, 2009, 2012; Thaler *et al.*, 2012; Williams, 2012; Velloso and Schwartz, 2011; Tuncman *et al.*, 2006; Zhang *et al.*, 2005; Awad, Gagnon and Messier, 2004). A HFD has been shown to increase pro-inflammatory genes in as little as 3 days but takes as much as 8 weeks for CNS resident microglia to appear (Baufeld *et al.*, 2016). The link between hypothalamic inflammation and diet-induced leptin-resistance, glucose intolerance and obesity and has also been shown in studies looking at TLR4 and TNF α . These studies showed amelioration of glucose intolerance, leptin resistance and subsequently reduced food intake (Benzler *et al.*, 2013; Cai and Liu, 2012; Milanski *et al.*, 2012; Tuncman *et al.*, 2006).

A high-fat diet has been shown to induce rapid changes in the mouse hypothalamic proteome (McLean *et al.*, 2018; Zahid *et al.*, 2014; Bubber *et al.*, 2005). Of the changes reported by Mclean and colleagues (2019), protein changes were associated with the cytoskeleton and synaptic plasticity, cellular stress responses, glucose metabolism and mitochondrial function, many associated with the development of AD (McLean *et al.*, 2019). Pathological alterations such as IR, inflammation or mitochondrial dysfunction associated with obesity, are also related to AD pathological processes (Mínguez-Olaondo, Irimia and Frühbeck, 2017; O'Brien *et al.*, 2017). Milanski and colleagues (2009, 2012) have shown that five days of intracerebroventricular injection of SFA stearic acid (C18:0), which is shown to be increased in this study in the HFD-S Group, induces hypothalamic

inflammation but does not affect systemic inflammatory markers (Milanski *et al.*, 2009, 2012). While control mice exhibited hepatic IR following 5 days of intracerebroventricular C18:0 treatment, TLR4 loss-of-function mutants and TNF- α receptor 1 (TNFRp55 $^{-/-}$ mice) knockout mice did not and exhibited protection from diet-induced hepatic IR (Milanski *et al.*, 2012). Further to this, Milanski and colleagues (2012) also showed that following hypothalamic TLR4 or TNF α signalling inhibition, improved insulin signalling through IR, IRS1 and Akt signalling reduced hepatic steatosis in HFD-fed Wistar rats, however these improvements were not seen in LDL receptor knockout mice (Milanski *et al.*, 2012). A chronic HFD has been shown to have persistent inhibitory effects on plasma ghrelin levels (Hucik *et al.*, 2021; Briggs *et al.*, 2013; Gomez *et al.*, 2012; Cano *et al.*, 2009; Handjieva-Darlenska and Boyadjieva, 2009; Poppitt *et al.*, 2005) with ghrelin resistance seen in NPY and AgRP neurons of the hypothalamus (Briggs *et al.*, 2013). Relatively higher values of ghrelin seen at night due to overnight fasting following a normal diet, are no longer observed in high-fat fed rats (Gomez *et al.*, 2012; Cano *et al.*, 2009).

Under the same experimental conditions as this study, previous work from our group have shown that a HFD promotes a loss of insulin sensitivity and significantly increased glucose levels in retroperitoneal tissue and gastrocnemius muscle of rats along with increasing body adiposity and plasma triacylglycerol levels (Hirata *et al.*, 2015; Banin *et al.*, 2014). Some of the hypothalamic proteins reported as changed following a HFD by McLean and colleagues (2019) and linked to AD include phosphoglucomutase-1 (PGM1) responsible for regulating glucose-1-phosphate and glucose-6-phosphate involved in glucose metabolism which has also been shown to be dysregulated in AD (Minjarez *et al.*, 2016). Similarly, triosephosphate isomerase, phosphoglycerate mutase 1 and Isocitrate dehydrogenase involved in regulating the glycolytic pathway were also altered and have been shown to be reduced in AD in response to OS (Zahid *et al.*, 2014; Mamelak, 2012; Perluigi *et al.*, 2010). Excess glucose in the brain is associated with toxic AGES, increased inflammation, microglia activity and cellular degradation (Hsieh *et al.*, 2019). The changes in both glucose metabolism and glycolytic pathway protein may have been in response to the increase in circulating glucose levels seen after 3 days of a HFD, that crosses the BBB by the non-insulin dependent GLUT1 transporter (Devraj *et al.*, 2011).

McLean and colleagues (2019) also reported changes in proteins related to neurogenesis, synaptogenesis, neurite outgrowth and axonal and dendritic cytoskeletal, suggesting synaptic remodelling. Many actin-related proteins were altered that are responsible for dendritic spine formation and structure (McLean *et al.*, 2019). Changes of note were the proteins DRP1 and DRP2

that had several post-translational modifications (McLean *et al.*, 2019), and are responsible for the regulation of Schwann cell myelination, microtubule assembly, axonal differentiation, and dendritic spine formation (McLean *et al.*, 2019; Sherman *et al.*, 2001; Roberts *et al.*, 1996). Dendritic cells in the hypothalamus are required for AgRP-activating in response to fasting (Liu *et al.*, 2012). McLean and colleagues (2019) also found in that N42 hypothalamic neurons challenged with PA (C18:0) had 38% lower DRP-2 protein which was unaffected by oleic acid (OA). They also found that in PA-challenged cells, areas occupied by mitochondria were decreased, appeared rounded, and isolated compared to elongated and branched mitochondria seen in both OA challenged and control groups. OA challenges in contrast increased mitochondrial cellular area (McLean *et al.*, 2019). Horvath and colleagues, (2010) found when comparing Sprague-Dawley rats selectively bred for either high weight gain (DIO) or obesity-resistant low weight gain (DR) rats on a 12-week HFD, DIO rats gained significantly more weight and fat mass, and experienced hyperinsulinaemia, increased plasma leptin levels and decreased circulating ghrelin levels (Horvath *et al.*, 2010). In DIO rats, a HFD was associated with synaptic reorganisation of the ARC melanocortin system. HFD fed DIO rats experienced increased number of excitatory contacts but decreased number of synaptic connections in anorexigenic POMC neurons. This was accompanied by significantly increased glial ensheathment of the DIO POMC perikarya compared to DR rats, which may produce inflammation and cellular stress. Horvath and colleagues (2010) suggest that increased gliosis may occur in response to daily cycles of synaptic plasticity caused by shifting hormone levels such as leptin and ghrelin, where leptin causes ROS generation in POMC neurons triggering further glial proliferation and cellular stress (Horvath *et al.*, 2010). McLean and colleagues (2019) have also demonstrated that within 3 days of a HFD the hypothalamic proteome changes indicating cellular stress, mitochondrial function and altered synaptic plasticity (McLean *et al.*, 2019).

Given the body of research mentioned above linking a high- fat diet, specifically C18:0 to increased inflammation, OS, neuronal damage and de-sensitisation to leptin, insulin and ghrelin in the hypothalamus and connected peripheral tissue responsible for regulating energy homeostasis, a partial causal link to the increased C18:0 reported here in the HFD-S may be inferred. This may contribute to inflammation, insulin, energy and appetite dysregulation as seen other previous studies under similar conditions

Next when comparing the HFD subsets of the hypothalamus, no stand-out significant differences occurred when comparing all HFD groups. A decreasing trend in C16:1n-7 was seen in HFD-PF ($p=0.06$) and significant decrease in HFD-GbE ($p=0.01$) compared to the HFD-S group (Table 74). This

affected the $\Sigma\omega7$ level in a similar way where a decreasing trend in was seen in HFD-PF ($p=0.09$) and significant decrease in HFD-GbE ($p=0.01$) compared to the HFD-S group ($\Sigma\omega7$; HFD-S, 3.34 ± 0.09 ; HFD-PF, 3.06 ± 0.10 ; HFD-GbE, 2.95 ± 0.09). This was also reflected in the C18:1n-9/C16:1n-7 ratio that significantly increase in the HFD-GbE group compared to HFD-S ($p=0.02$) (C18:1n-9/C16:1n-7; HFD-S, 70.45 ± 9.20 ; HFD-PF, 97.50 ± 9.59 ; HFD-GbE, 108.54 ± 8.24) (Table 75).

The changes in C22:5n-3 levels showed a 2-fold decrease in the HFD-PF group compared to HFD-S ($p=0.002$) but only a trending decrease in the HFD-GbE group compared to HFD-S ($p=0.08$) (C22:5n-3; HFD-S, 0.14 ± 0.02 ; HFD-PF, 0.07 ± 0.01 ; HFD-GbE, 0.10 ± 0.01) (Table 74). This may suggest that either less C22:5n-3 is being produced by DNL, or that it may be liberated and utilized in another metabolic pathway such being converted to C22:6n-3 or liberated for oxylipin inflammatory mediation. The idea that C22:5n-3 is being utilized elsewhere is supported by changes in C22:5n-3/C18:3n-3 ratio where both HFD-PF ($p=0.002$) and HFD-GbE ($p=0.005$) decreased approximately 2-fold for each group compared to HFD-S (C22:5n-3/C18:3n-3; HFD-S, 0.07 ± 0.01 ; HFD-PF, 0.03 ± 0.01 ; HFD-GbE, 0.04 ± 0.01) (Table 75).

Reports show that the brain concentration of DHA is kept at a steady state even in brain injury (Kim, 2014; DeMar *et al.*, 2004). DHA synthesis from other n-3 FA such as ALA (C18:3n-3) is low in the brain, while the predominant brain supply of DHA is thought to come from plasma (DeMar *et al.*, 2005). It has been reported that ALA to DHA conversion is inefficient in human but is higher in women than men due to oestrogen (Greupner *et al.*, 2018; Goyens *et al.*, 2006; Burdge, 2004; Giltay *et al.*, 2004) and is influenced by the amounts of ALA and LA in the diet, rather than LA/ALA ratios (Goyens *et al.*, 2006). The C22:6n-3/C18:3n-3 ratio showed a decreasing trend between the HFD-S and HFD-GbE groups ($p=0.06$) (C22:6n-3/C18:3n-3; HFD-S, 5.74 ± 0.62 ; HFD-PF, 4.11 ± 0.68 ; HFD-GbE, 3.61 ± 0.52) (Table 75) indicating a relative increase in C18:3n-3 and decrease in C22:6n-3 levels in the groups. In comparison, however, the C22:6n-3/C22:5n-3 ratio showed that while overall levels of C22:6n-3 decreased compared to C18:3n-3, the relative amount of C22:5n-3 was lower than C22:6n-3 for both the HFD-PF group ($p=0.004$), and the HFD-GbE group ($p=0.02$) compared to the HFD-S group (C22:6n-3/C22:5n-3; HFD-S, 89.26 ± 14.56 ; HFD-PF, 140.75 ± 9.10 ; HFD-GbE, 98.12 ± 3.47) (Table 75). This suggests a need for C22:6n-3 rather than from C18:3n-3 to maintain the DHA steady-state to be significantly similar in all three high fat groups despite caloric restriction in HFD-PF and HFD-GbE (Hypothalamus C22:6n-3; HFD-S; $10.51\pm0.34\%$; HFD-PF, $9.84\pm0.41\%$; HFD-GbE, $9.97\pm0.19\%$) (Table 75). As illustrated in Figure 4 the conversion from C22:5n-3 to C22:6n-3 requires much less enzymatic steps and is therefore less energetically costly than converted from C18:3n-3.

This is in keeping with Dornellas and colleagues (2015) that have found that rat hypothalamic total PUFA levels remained steady in an 8-week lard-enriched diet and experienced increased amounts of C20:5n-3 and C20:3n-6, the precursors of C22:6n-3 and C20:4n-6. This finding suggested that peripheral tissues may be acting as a buffer and provided a continued supply of higher PUFA to maintain the brain FA profile (Dornellas *et al.*, 2015). More recent work from our group has shown that 35-day old Wistar rats fed either a high- fish-oil or high-soybean-oil diet, the fish oil group did not experience obesity, but the soybean oil group did. Furthermore, soybean oil fed rats experienced an imbalance in the n-6/ n-3 ratios in peripheral tissues, but not in the hypothalamus, which experienced an increase in n-3 (Watanabe *et al.*, 2022). Together these findings along with our group further support the concept that the body uses FA from peripheral tissues to maintain preferential FA uptake of the brain.

Alternatively, PPAR ligands include SFA, UFA and PUFA as well as their metabolites (Chen, Shang, *et al.*, 2020; Forman, Chen, *et al.*, 1997; Kliewer, Sundseth, *et al.*, 1997). PPAR receptors are responsible for triggering gene transcription of lipid metabolism mediators involved in FA β -oxidation, and contribute to the regulation of oxidative stress, inflammation, and neuroprotection (Han, Shen, *et al.*, 2017; Duvall and Levy, 2016; Echeverría, Ortiz, *et al.*, 2016; Motojima, Passilly, *et al.*, 1998; Martin, Schoonjans, *et al.*, 1997). LC-PUFA are the natural ligands of PPAR α/γ , where n-3 PUFA, C22:5n-3 (Hostetler, Kier, *et al.*, 2006) as well as EPA (C20:5n-3) and DHA (C22:6n-3) bind with high affinity for activation (Duszka, Gregor, *et al.*, 2020; Kosgei, Coelho, *et al.*, 2020; Laleh, Yaser, *et al.*, 2019; Kersten and Stienstra, 2017; Pawar and Jump, 2003). As well as the significant results discussed above, C18:0 percentage levels in the HFD-GbE group returned to levels like that in the NFD group (C18:0; NFD, 18.45 \pm 0.14%; HFD-GbE, 19.52 \pm 0.3%). This may indicate that any C18:0-mitigated inflammation induced by elevated levels in HFD-S, may be ameliorated by GbE treatment.

GbE has been shown to possess antioxidant, anti-inflammatory, and anti-obesogenic properties. It has been shown to reduce visceral adiposity, weight gain and food intake and reduce adipocyte hypertrophy in WAT. Recently work from our group have shown that have shown that GbE improves the hypothalamic anorexigenic effectors in rats after a single dose by inducing hypothalamic POMC, CART (anorexigenic), and 5-HT_{2C} (leptin/serotonin receptor) gene expression but not the orexigenic (AgRP/NPY) neuropeptides (Machado, Pereira, *et al.*, 2021). Banin and colleagues (2017) have also showed that 14 days of GbE treatment attenuated obesity in ovariectomized (OVX) rats by stimulating the hypothalamic serotonergic system. Research has also shown that GbE plays an antioxidative role in the hippocampus of ovariectomized rats and restore serotonin and leptin

receptor levels (Machado, Banin, *et al.*, 2021). Machado and colleagues (2021) hypothesised that the restoration of serotonin and leptin receptor levels were related to the restoration of serotonin levels in the ventro-medial hypothalamus, which in turn ameliorated the anorexigenic -serotonin response impaired by ovariectomy (Machado, Banin, *et al.*, 2021). Ovariectomy-induced menopause increased resistance to serotonin hypophagia, resulting in increased food intake and body weight and consequent obesity, while GbE treatment attenuated it (Banin *et al.*, 2017). Furthermore, GbE treatment significantly increased 5-HT microdialysate levels in OVX rats but not sham-operated rats after 60-80 minutes of treatment, although levels of 5-HT were found to be increased in the Sham+GbE group at 20-40 mins treatment compared to the OVX group. While they found not differences in protein levels of 5-HT_{1A} and 5-HT_{2C} a significant 60% reduction 5-HTT protein levels were seen in OVX + GbE rats compared to the Sham group (Banin *et al.*, 2017). Furthermore, work from our group have shown that GbE has been shown to modulate lipid metabolism, adipogenesis, inflammation and OS and improve insulin signalling and sensitivity (Hirata *et al.*, 2015, 2019, 2022; Machado, Banin *et al.*, 2021; Machado, Pereira *et al.*, 2021, Hirata *et al.*, 2019; Banin *et al.*, 2014). Work from our group has shown that GbE ameliorated decreased IRS-1 levels and reduced the phosphorylation of NF- κ B p65 by 60% along with TNF- α levels, while increasing the gene expression of the anti-inflammatory cytokine IL-10 in comparison to the nontreated obese rats (Hirata, Banin, *et al.*, 2015). Other reports also indicate improvements to glycaemia, insulin levels, IR and reduced glycosylated HbA_{1c} levels with GbE supplementation in both animal and clinical studies (Aziz, Hussain, *et al.*, 2018; Hirata, Banin, *et al.*, 2015; Banin, Hirata, *et al.*, 2014; Lasaite, Spadiene, *et al.*, 2014; Siegel, Ermilov, *et al.*, 2014; Zhou, Meng, *et al.*, 2011; Kudolo, Wang, *et al.*, 2006)

As previously mentioned, hypothalamic inflammation is associated with toll like receptor 4 (TLR4) activation of astrocytes and microglia, and increased expressions of TNF α , IL-1 β , and IL-6, along with activation of the IKK β /NF- κ B inflammatory pathway and mitochondrial dysfunction which can lead to insulin and leptin resistance and metabolic syndrome 2 (Bhusal, Rahman, *et al.*, 2022; Benomar and Taouis, 2019; Rogero and Calder, 2018; Baufeld, Osterloh, *et al.*, 2016; Masson, Nair, *et al.*, 2015; Schneeberger, Dietrich, *et al.*, 2013; Shechter, London, *et al.*, 2013; Cai and Liu, 2012; Milanski, Arruda, *et al.*, 2012; Thaler, Yi, *et al.*, 2012; Williams, 2012; Velloso and Schwartz, 2011; Tuncman, Hirosumi, *et al.*, 2006; Zhang, Dong, *et al.*, 2005; Awad, Gagnon, *et al.*, 2004).

The link with hypothalamic inflammation and diet-induced leptin-resistance, glucose intolerance and obesity and has also been shown in TLR4 and TNF α inhibition studies that showed amelioration of glucose intolerance, leptin resistance and subsequently reduced food intake following inhibition of

TLR4 and TNF α (Benzler, Ganjam, *et al.*, 2013; Cai and Liu, 2012; Milanski, Arruda, *et al.*, 2012; Tuncman, Hirosumi, *et al.*, 2006). Previous research under similar experimental conditions as this study, ameliorated glucose tolerance, leptin resistance and reduced food intake is also seen following GbE treatment (Machado, Pereira, *et al.*, 2021). Additionally, research has also shown that GbE treatment ameliorates decreased IRS-1 levels and reduced the phosphorylation of TNF- α levels, while increasing the gene expression of the anti-inflammatory cytokine IL-10 in comparison to the nontreated obese rats (Hirata, Banin, *et al.*, 2015). GbE also improves the hypothalamic anorexigenic effectors in rats after a single dose by inducing hypothalamic POMC, CART (anorexigenic), and 5-HT2C (leptin/serotonin receptor) gene expression (Machado, Pereira, *et al.*, 2021). Significant decreases in OS and inflammatory markers such as hs-CRP, TNF- α , IL-6 and malondialdehyde levels have also been attributed to GbE supplementation (Yan, Li, *et al.*, 2020; Aziz, Hussain, *et al.*, 2018; Hirata, Banin, *et al.*, 2015; Siegel, Ermilov, *et al.*, 2014; Thanoon, Abdul-Jabbar, *et al.*, 2012; Kudolo, Wang, *et al.*, 2006) while GSH and SOD increased (Yan, Li, *et al.*, 2020; Thanoon, Abdul-Jabbar, *et al.*, 2012; Bridi, Crossetti, *et al.*, 2001). It has also been shown that both resveratrol and GbE have been shown to modulation of the Akt insulin signalling pathway (Yan, Li, *et al.*, 2020; Lejri, Grimm, *et al.*, 2019; Brasnyó, Molnár, *et al.*, 2011). Akt activation requires a fine balance to moderate fluctuations between cell survival and apoptosis. Increased Akt phosphorylation (p-Akt) have modulating actions on the apoptotic/cell survival PI3K/Akt/mTOR and IGF-1R/Akt/Wnt signalling pathways (Park, Lim, *et al.*, 2010; Vanamala, Reddivari, *et al.*, 2010).

Previous studies under similar conditions have shown that GbE plays an antioxidative role in the hippocampus of ovariectomized rats and restore serotonin and leptin receptor levels (Machado, Banin, *et al.*, 2021). Machado and colleagues (2021) also hypothesised that the restoration of serotonin and leptin receptor levels by GbE treatment were related to the restoration of serotonin levels in the ventro-medial hypothalamus (Machado, Pereira, *et al.*, 2021) which in turn ameliorated the anorexigenic-serotonin response impaired by ovariectomy (Banin, Machado, *et al.*, 2017). In a 90-day clinical trial, patients with metabolic syndrome already on metformin were given GbE (120 mg capsule/day) or placebo. In patients with metabolic syndrome GbE supplementation significantly decreased HbA1c, fasting serum glucose and insulin levels. BMI, waist circumference and visceral adiposity index were also all improved. Serum leptin, lipid profiles and inflammatory markers (hsCRP, TNF- α and IL-6) also improved compared to baseline values (Aziz, Hussain, *et al.*, 2018).

Furthermore, in relation to the effects of caloric restriction, Briggs and colleagues (2013) have reported that after 12 weeks of HFD, DIO mice underwent calorie-restricted (CR) weight loss (-40%

calories) until they matched lean control animal weight. CR weight loss resulted in increased total plasma ghrelin, restored ghrelin sensitivity, and increased hypothalamic NPY and AgRP mRNA expression with both NPY and AgRP neurons having shown ghrelin resistance before starting CR (Briggs, Lockie, *et al.*, 2013). From their results they also proposed that following DIO, a higher body weight set-point may be set, and that CR-based weight loss may cause the brain to protect the new higher set-point and result in rebound weight gain once regular feeding commences. They proposed that the increase in peripheral ghrelin concentrations and the amelioration of ghrelin resistance in neuronal populations in the hypothalamic ARC could be a mechanism to promote a return to the previous weight set-point. This was supported by work in DIO ghrelin-knockout mice that had reduced body weight gain after CR compared to wild-type mice (Briggs, Lockie, *et al.*, 2013).

6.5 Summary

In summary, no significant changes in FA percentage levels occurred in the total hippocampus fatty acids profiles, although a decreased shift in the ratio between n-6 FA levels (increased HFD-S C18:2n-6 and decreased C20:4n-6) and n-3 FA levels (decreased HFD-S C22:6n-3) did occur in the HFD-S group compared to the NFD group. The main result from total hypothalamus fatty acids analysis showed that a HFD increased the levels of C18:0. Both a HFD and increased C18:0 levels are linked to disruptions to insulin, ghrelin and leptin signalling associated with appetite regulation, which are ameliorated by GbE treatment. Furthermore, GbE treatment altered C16:1n-7 levels known to improve insulin signalling, while changes in n-3 PUFA may be associated with maintaining DHA steady-state levels in the hypothalamus.

Chapter 7 – PC12 rat pheochromocytoma cell neuronal model

7.1 Introduction

Following the results of a NFD, HFD and GbE phytotherapy in hippocampus and hypothalamus tissue, we set out to investigate similar FA and phytotherapy treatments in an *in vitro* cellular model. *In vitro* models allow for higher throughput of research, reduced animal-use and thereby often reducing costs. It also allows for a more precise control over experimental conditions (Graudejus *et al.*, 2018). PC12 rat pheochromocytoma cells are an established cell culture model for neuronal experimentation and ATCC CRL-1721 PC12 cells were used for this present study, hereafter referred to as PC12 cells. When cultured in the presence of NGF, PC12 cells differentiate into a sympathetic neuron phenotype of ganglion neurons both in morphology with neurite outgrowth and functionality whereby they are electrically excitable and synthesise and store dopamine (Hu *et al.*, 2018; Mullenbrock, Shah and Cooper, 2011; Das, Freudenrich and Mundy, 2004; Greene and Tischler, 1976). As P12 cells growing protocols and neuronal differentiation methods had not yet been established in the biology department in the School of Science and the Environment at the University of Worcester, these were optimized first.

When PC12 cells are grown in suspension they form round grape-like clusters with cells around 6-14µm in diameter and can form large aggregates at high density. To differentiate PC12 cells, they must first adhere to a culture vessel surface. As PC12 cells do not adhere to plastic surfaces, several different culture vessel coating protocols exist including coatings of Type I and IV collagen, poly-L-lysine (PLL), poly-D-lysine (PDL), fibronectin and laminin (Wiatrak *et al.*, 2020; Orłowska *et al.*, 2018; Kinarivala *et al.*, 2017; Das, Freudenrich and Mundy, 2004; Keshmirian, Bray and Carbonetto, 1989). It is reported that PC12 cells tend to detach during differentiation (Kinarivala *et al.*, 2017b), therefore an initial screening process was conducted between PLL, type I and type IV collagen coating and NGF with 1% horse serum media (data not shown). This screening identified that cells grown on both type I and type IV collagen showed better adherence over time compared to PLL. This is in keeping with the report of Wiakrak and colleagues (2020) that also identified collagen as a preferred surface coating compared to PPL (Wiatrak *et al.*, 2020). For this study, Type I collagen (10µg/cm²) was selected as the coating method for further experiments.

Initial morphological observations were also conducted comparing PC12 cells grown in suspension (Figure 15) and as adherent cells coated tissue culture plates (Figure 16). Cells in suspension grew as small irregularly shaped cells floating in multi-cell aggregates with a propensity to form larger aggregates at higher densities (Figure 15) but showed little adherence to plastic. When grown on type I collagen-coated ($10\mu\text{g}/\text{cm}^2$) tissue culture vessels they exhibited a varied profile of small epithelial-shaped cells, some stellate-shaped cells, some elongated cells and some rounded but attached cells (Figure 16) after 24 hours of incubation. This is in keeping with other reports of PC12 adherent growth (Kinarivala *et al.*, 2017).

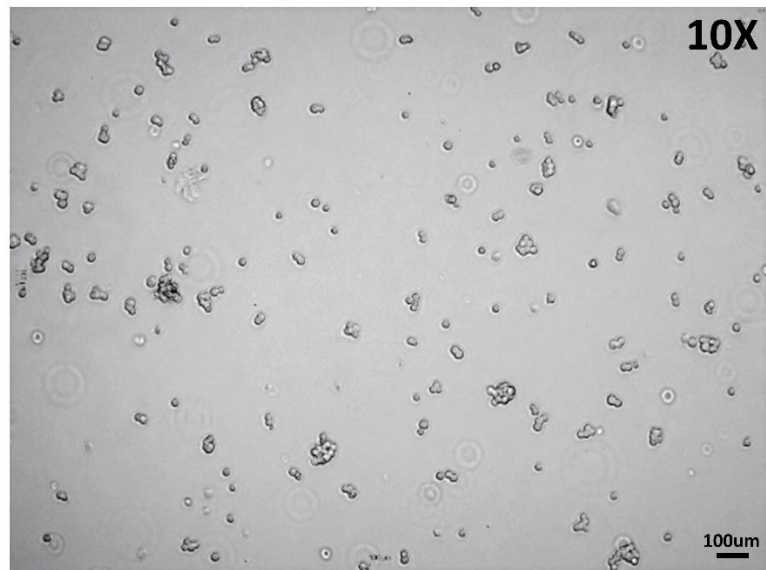
7.2 Growth curve

An initial cell growth curve was conducted on PC12 cells grown in suspension and on type I collagen ($10\mu\text{g}/\text{cm}^2$). Following the cell culture subculture guidelines outlined in Type I collagen solution (Corning™ Collagen I, Rat 100mg, Cat no#11563550) was purchased from Fisher Scientific. Poly-L-lysine solution (0.01%, sterile-filtered, BioReagent, Cat no.#P4707) and type IV Collagen (from human placenta, Bornstein and Traub Type IV, powder, Cat no.#C5533) was purchased from Merck-Sigma-Aldrich. Type IV collagen solution was made up to a final solution of 1mg/ml (0.1% w/v collagen solution) in 0.1M glacial acetic acid stirred at room temperature for 1-3 hours as per Merck PC12 collagen coating protocol (Merck, 2020a). The solution was sterilised by incubating overnight at 4°C with 10% v/v chloroform. The top collagen layer was aseptically removed, aliquoted and stored at -20°C for up to 6 months. Aliquots were subsequently defrosted and diluted 10 times to obtain at 0.01% solution as needed.

Table 8. cells were initially seeded at 1×10^4 cells/cm² in 96 well plates and grown in 100µl of RPMI complete media, with media replaced every 2 days. Cells were counted every two days *via* haemocytometer using trypan blue staining for a viable cell count. Cells grown in suspension were aspirated directly from the wells, centrifuged, stained, and counted. Adherent cells were trypsinized briefly to release cells from the plate surface, washed, centrifuged, stained, and counted. As shown in Figure 17 cells grown in cell suspension continued to double approximately every 48 hours up to and including Day 10, in keeping with previous reports of PC12 cell growth (Merck, 2020; Thermo-Fisher, 2020; ATCC, 2014). Similarly, cells grown as adherent cells on type I collagen doubled approximately every 96 hours (Day 0, 3200 cells Vs Day 4; 7121 cells; Day 8, 16,090 cells) in line with ATCC guidelines (Type I collagen solution (Corning™ Collagen I, Rat 100mg, Cat no#11563550) was purchased from Fisher Scientific. Poly-L-lysine solution (0.01%, sterile-filtered, BioReagent, Cat no.#P4707) and type IV Collagen (from human placenta, Bornstein and Traub Type IV, powder, Cat no.#C5533) was purchased from Merck-Sigma-Aldrich. Type IV collagen solution was made up to a final solution of 1mg/ml (0.1% w/v collagen solution) in 0.1M glacial acetic acid stirred at room temperature for 1-3 hours as per Merck PC12 collagen coating protocol (Merck, 2020a). The solution was sterilised by incubating overnight at 4°C with 10% v/v chloroform. The top collagen layer was aseptically removed, aliquoted and stored at -20°C for up to 6 months. Aliquots were subsequently defrosted and diluted 10 times to obtain at 0.01% solution as needed.

Table 8). Confluency of adherent cells is reported to be $4-5 \times 10^4$ cells/cm². On Day 8, the adherent cell count was approximately 5.2×10^4 cells/cm². After day 8, the adherent cells having reached confluency on the plate surface, began to detach, and form additional aggregates in suspension. Only cells that remained attached to the cell surface were counted on day 10, which is indicated by the plateau of cell growth for day 10 adherent cells (Figure 17).

PC12 - Low density suspension



PC12 - High density suspension

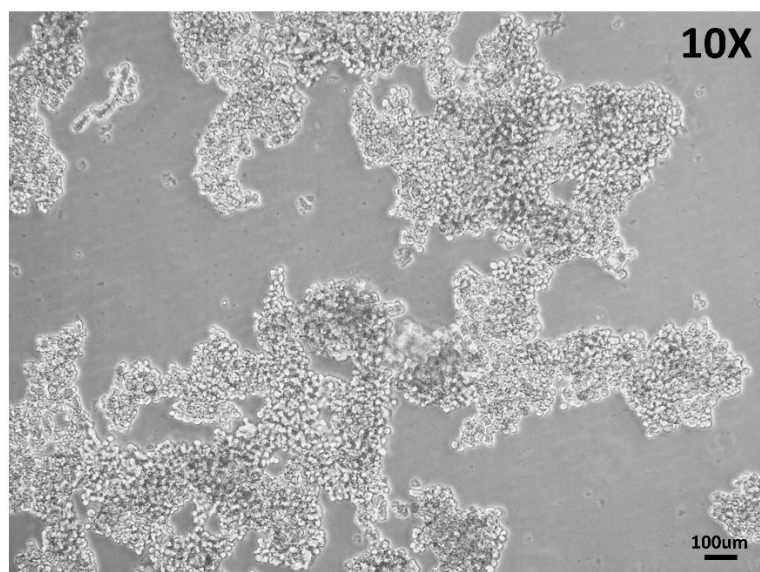


Figure 15. Microphotograph of PC12 cells grown in suspension in RPMI complete media (15% serum) at low and high density. Cells in suspension grew as small irregularly shaped cells floating in multi-cell aggregates with a propensity to form larger aggregates at higher densities and showed little adherence to plastic

PC12 - Adherent on Type I Collagen – 24 hours

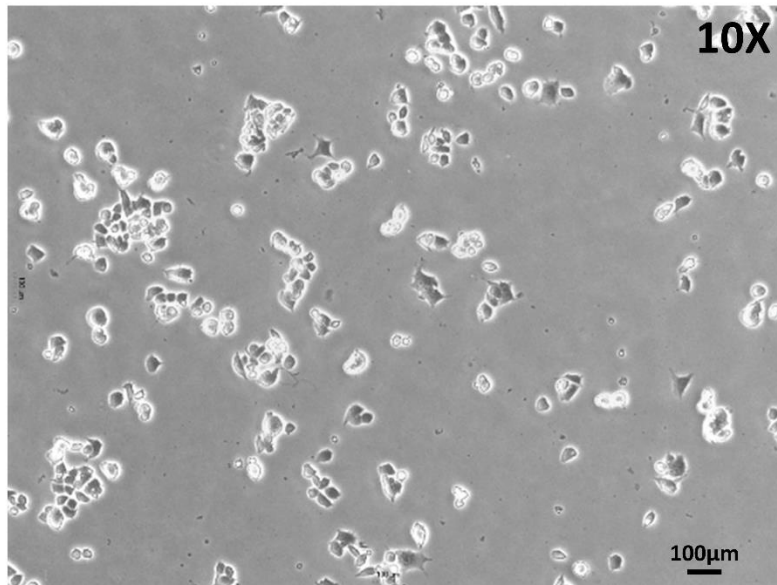


Figure 16. Microphotograph of PC12 cells grown as adherent cells on Type I collagen ($10\mu\text{g}/\text{cm}^2$) in RPMI complete media (15% serum). Cells exhibited a varied profile of small epithelial-shaped cells, some stellate-shaped cells, some elongated cells and some rounded but attached cells

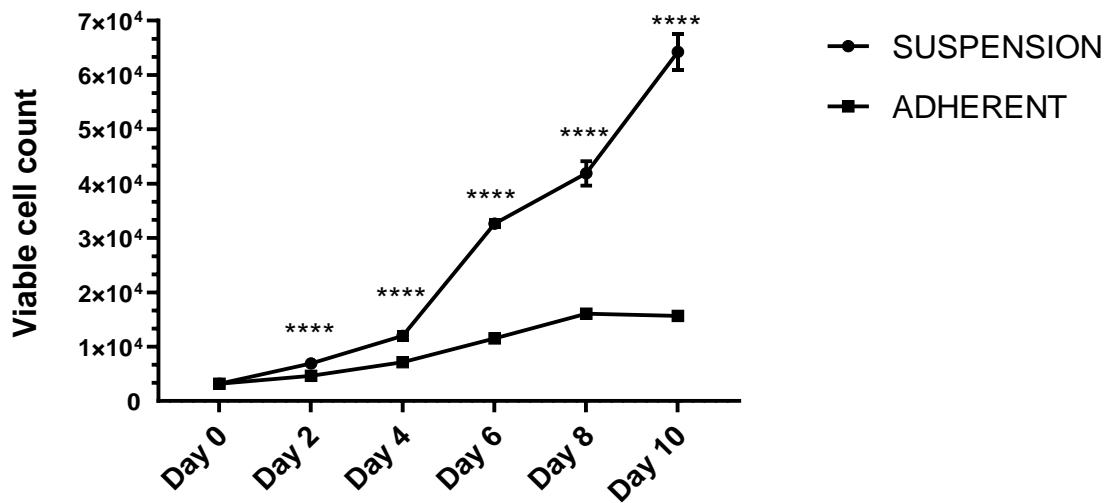


Figure 17. Growth curve of PC12 cells grown in suspension and on type I collagen (10 μ g/cm²) (adherent). Suspension cells experienced exponential growth up to and including day 10, doubling approximately every 48 hours. Adherent cells approximately doubled every 96 hours up until day 8, with growth plateauing by day 10 whereby cells began to detach into suspension. Data presented as mean \pm SEM. Data analysed by Two-way repeat measures ANOVA with Šídák post hoc test, **** $p < 0.0001$).

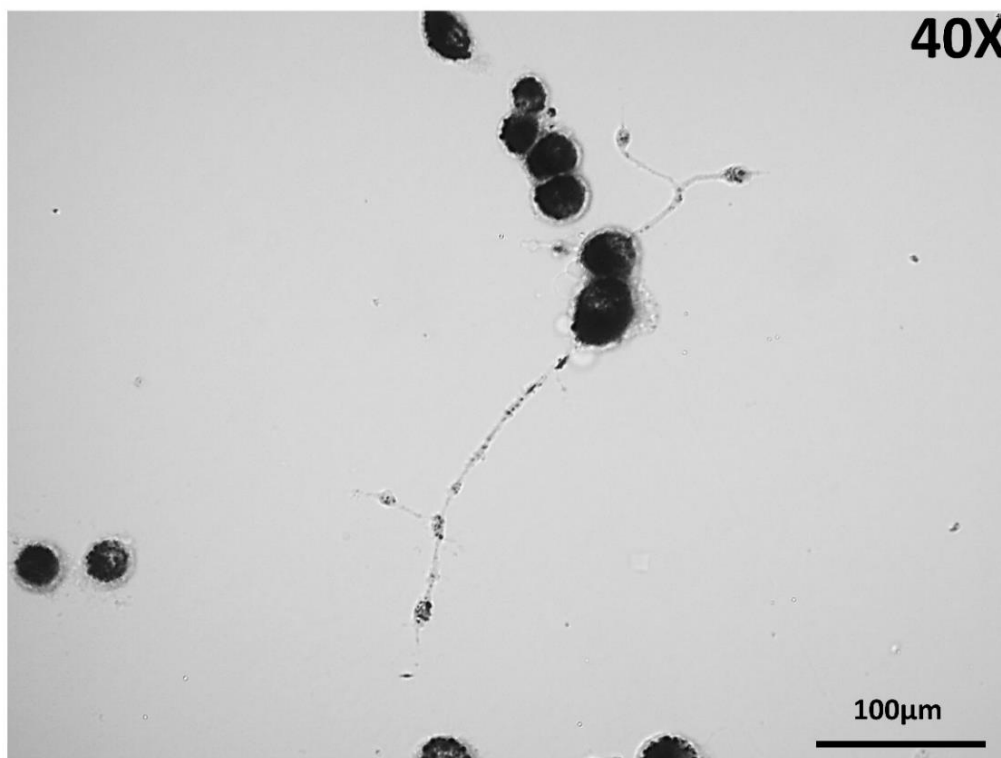


Figure 18. Formazan accumulation (dark colouration) in undifferentiated (round cells) and differentiated (cells with neurite outgrowth) PC12 cells following incubation with MTT (3-[4,5-dimethylthiazol-2-yl]-2,5-diphenyltetrazolium bromide).

7.3 NGF neuronal differentiation

Nerve growth factor (NGF) supports the survival, differentiation, and maintenance of neurons (Mitra, Behbahani and Eriksdotter, 2019). PC12 NGF differentiation occurs through the activation of the receptor-tyrosine kinase, TrkA receptor which in turn activates the Raf/MEK/ERK/MAP kinase pathway (Mullenbrock, Shah and Cooper, 2011; Das, Freudenrich and Mundy, 2004), PI3K/Akt pathway (Higuchi *et al.*, 2003; Jeon *et al.*, 2010) and PLCg/PKC pathway (Greene and Tischler, 1976; Segal, 2003) which causes a decrease in cell proliferation and increase in neurite outgrowth (Mullenbrock, Shah and Cooper, 2011; Das, Freudenrich and Mundy, 2004). Neurite outgrowth encompasses two differing growths from the cell body. The first is a long thin axon that is utilized for signal transmission. The second outgrowth is shorter dendrites that function to receive signals. Together they allow for signal transmission and connectivity between different neurons (Sierra-Fonseca *et al.*, 2014). Over time, NGF-treated PC12 cells experience an increase in neuronal markers including axonal growth-associated protein 43 (GAP-43) (Chung, Shum and Caraveo, 2020; Holahan, 2015), synaptic protein synapsin-1 (Hu *et al.*, 2018; Das, Freudenrich and Mundy, 2004; Romano *et al.*, 1987), neurofilaments (light (NF-L), medium (NF-M) and heavy (NF-H)) (Schimmelpfeng, Weibezahn and Dertinger, 2004; Lee and Cleveland, 1994) and β -Tubulin III (Maioli *et al.*, 2015; Sadri *et al.*, 2014; Ohuchi *et al.*, 2002; Caceres, Banker and Binder, 1986). Cytoskeletal structures such as neurofilaments, tubulin and actin are essential for neuronal signalling within neurite extensions (Miller and Suter, 2018; Sierra-Fonseca *et al.*, 2014).

In contradiction to the cessation of proliferation following NGF treatment NGF stimulation may also promote proliferation through the MAPK pathway (Santos, Verveer and Bastiaens, 2007; Klesse *et al.*, 1999; Rudkin *et al.*, 1989). This has contributed to issues with PC12 differentiation with low differentiation rates, limited neurite outgrowths and continued proliferation rates observed (Hu *et al.*, 2018). With this in mind, to further aid PC12 cell differentiation and reduce cell proliferation, a variety of reduced-serum media protocols have been reported in the literature to aid in the differentiation of PC12 cells into their neuronal type including 1%, 0.5% and 0.1% horse serum media and 1% BSA media (Hu *et al.*, 2018; Mei *et al.*, 2013; Hahn, Jones and Meyer, 2009; Das, Freudenrich and Mundy, 2004; Marszalek *et al.*, 2004; Rudkin *et al.*, 1989). Various concentrations of NGF have also been reportedly used in PC12 differentiation generally ranging from 25-100ng/ml of media (Merck, 2020; Wiatrak *et al.*, 2020; Dikmen, 2017; Kinarivala *et al.*, 2017; ATCC, 2014; Schimmelpfeng, Weibezahn and Dertinger, 2004; Pang *et al.*, 1995). To initially evaluate cell proliferation and viability during PC12 cell differentiation in each reduced-serum media (1%, 0.5% and 0.1% horse serum media

and 1% BSA media), MTT assays were conducted on Day 0, 2, 4 and 6 for each group. MTT is a yellow tetrazolium salt that when endocytosed by viable cells is subsequently reduced to purple formazan and accumulated in endosomal and lysosomal compartments. It is transported to the cell surface for exocytosis in the form of needle-like crystals (Isobe, Yanagisawa and Michikawa, 2001; Liu and Schubert, 1997). A representative image of formazan accumulation in PC12 cells is shown in Figure 18. Cell morphology is shown and data is graphically represented as mean±SEM and analysed by two-way ANOVA with either Šídák (15% Vs 1% serum groups) or Tukey (1% serum Vs NGF or GbE) *post hoc* tests (Figure 19 - Figure 22). Data from 0.5% media and 0.1% media can be found in Appendix 6. To further optimize the differentiation of PC12 cells into a neuronal-type morphology, varying concentrations of NGF (25, 50 and 100ng/ml) were also screened for in conjunction with differing reduced-serum media to identify an optimal differentiation method. All experiments were conducted on cells from passages 9-13 only. This was based on the previous findings and recommendations from Kinarivala and colleagues (2017) that found better accuracy and invariability in PC12 differentiation in conjunction with the testing of neuro-protective/damaging compounds. PC12 cells with lower or higher passages became inconsistently susceptible to injury and apoptosis from serum deprivation and external treatments (Kinarivala *et al.*, 2017). PC12 cells were plated on 96-well plates at 5×10^4 cells/cm² per well in RPMI complete (15% serum) media and allowed to adhere for 24 hours before media was replaced with indicated reduced-serum differentiation media. Subsequent morphological observations were made on cells in a variety of reduced serum media supplemented with NGF (15,50 and 100ng/ml) to induce differentiation.

Treatment with 50 and 100µg/ml of GbE was also assessed in a reduced-serum media owing to its reported antioxidant capacity and its potential in reducing neurotoxicity (Mango, Weisz and Nisticò, 2016; Shi *et al.*, 2009; Smith and Luo, 2003; Bastianetto *et al.*, 2000), amyloidogenesis and fibril formation (Ramassamy, 2006; Colciaghi *et al.*, 2004; Luo *et al.*, 2002). It is also reported to support proliferation, differentiation, and growth of cells (Peng *et al.*, 2009; Pierre *et al.*, 1999; Scott *et al.*, 1995) through the up-regulated expression of growth hormone and nerve growth factor (Ahlemeyer and Kriegstein, 2003; Watanabe *et al.*, 2001; Pierre *et al.*, 1999).

7.4 1% Horse Serum (HS) media differentiation

Despite the 1% HS reduced-serum media (1% HS), cell viability continued over the 6-day incubation period (Figure 19.A), with cell number doubling compared to Day 0 (191%) although significantly less than proliferation in RPMI complete media (269% Vs 0 Hrs, $p < 0.0001$), although cells started to detach from the collagen coating into suspension after 72 hours in the 1% HS group. No significant difference in viability was seen in vehicle only treatment compared to 1% HS across all time points. Forty-eight hours of cell treatment with 50ng/ml NGF resulted in significantly increased cell viability (321% Vs 0 Hrs, $p = 0.04$) but not for 25ng/ml (309%, $p = 0.076$) or 100ng/ml NGF (178%, $p > 0.99$) when compared to 1% HS cells (160% Vs 0 Hrs) (Figure 19.B). After 96 hours of treatment, viability significantly increased further for 25ng/ml (363% Vs 0 Hrs, $p = 0.038$) and 50ng/ml NGF treatment (428% Vs 0 Hrs, $p = 0.0008$) but not in 100ng/ml NGF treatment (218% Vs 0 Hrs, $p > 0.99$) compared to 1% HS (198% Vs 0 Hrs) (Figure 19.B.). After 144 hours of treatment, viability across all NGF treatments (25ng/ml-231%; 50ng/ml-211%, 100ng/ml-165% Vs 0 Hrs) decreased to a level comparable to 1% HS only treatment (191% Vs 0 Hrs). This result is in keeping with the findings of Greene (1978) that reported that under serum-free conditions, NGF treatment resulted in approximately one doubling of cells that remaining viable for up to 4 weeks with continued NGF treatment (Greene, 1978). Morphologically, as shown in Figure 20, after 144 hours of NGF treatment, neurite outgrowths were observed in all three NGF (25, 50 and 100ng/ml) treatments, with outgrowths appearing more abundant and longer in 50 and 100 ng/ml treatments. Rounded non-differentiated cells were also observed interspersed throughout differentiated cells. Treatment with 50 and 100 μ g/ml of GbE did not significantly increase viability compared to 1% HS alone across all timepoints (Figure 19.C.). Morphologically cells appeared rounded without neurite outgrowths (Figure 21) like that of 1% HS low serum treated cells.

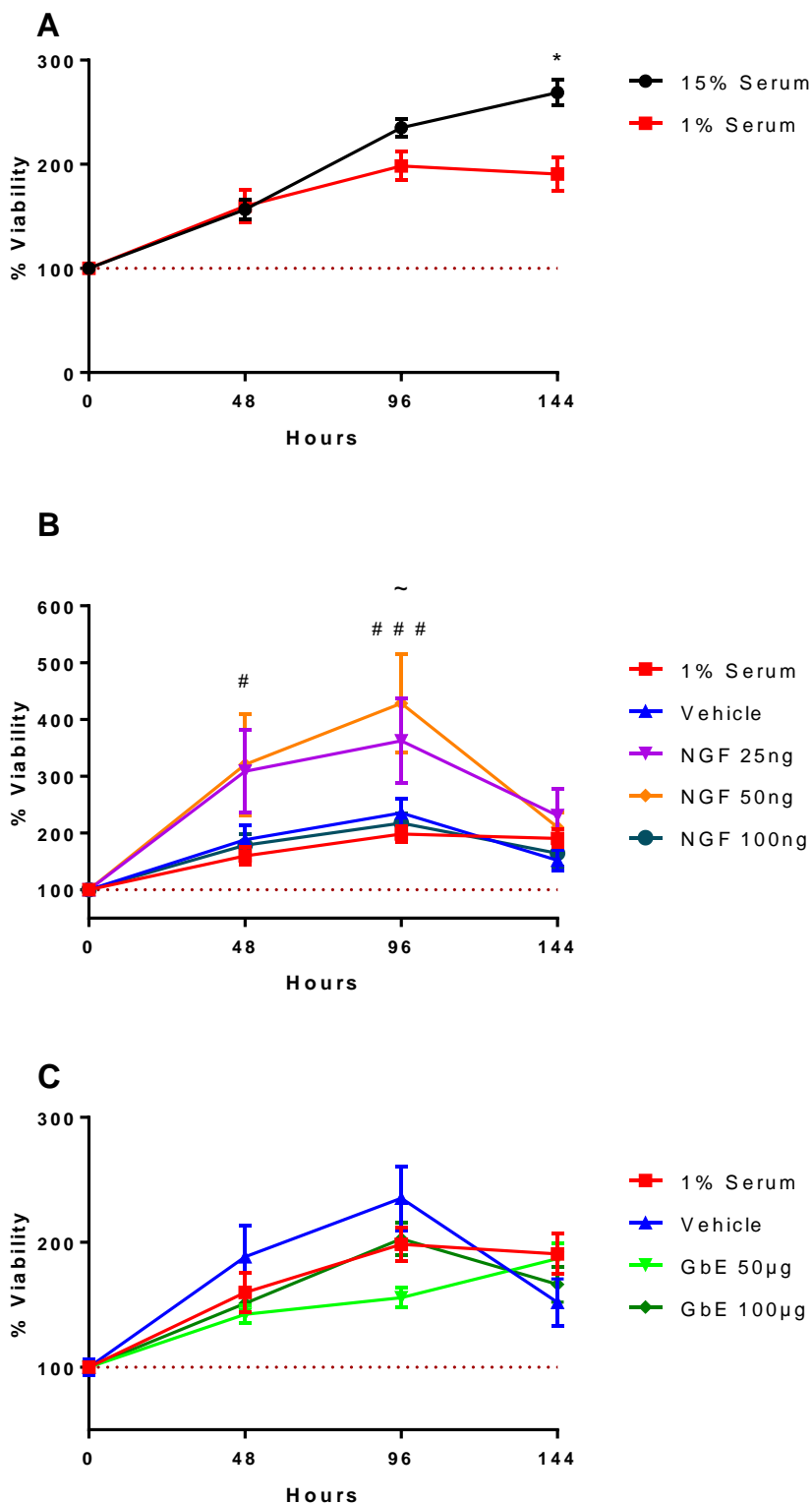


Figure 19. Viability (%) of PC12 cells after six days incubation with 1% horse serum (1% HS) media. A). 15% complete serum media (10% horse serum+ 5% foetal bovine serum) Vs 1% HS. B). 1% HS media Vs Vehicle (0.085% saline) and nerve growth factor 2.5s (NGF 25,50 and 100ng/ml) C. 1% HS Vs Ginkgo biloba (GbE, 50 and 100ug/ml). * $p < 0.05$, ** $p < 0.01$, *** $p < 0.001$, **** $p < 0.0001$ vs 1% serum. ~ p =Vs 25ng/ml NGF, # p = Vs NGF 50ng/ml, & p = Vs NGF 100ng/ml vs 1% serum. Data presented as mean±SEM. Data analysed by Two-way ANOVA with Šídák (A.) or Tukey (B. and C.) post hoc test).

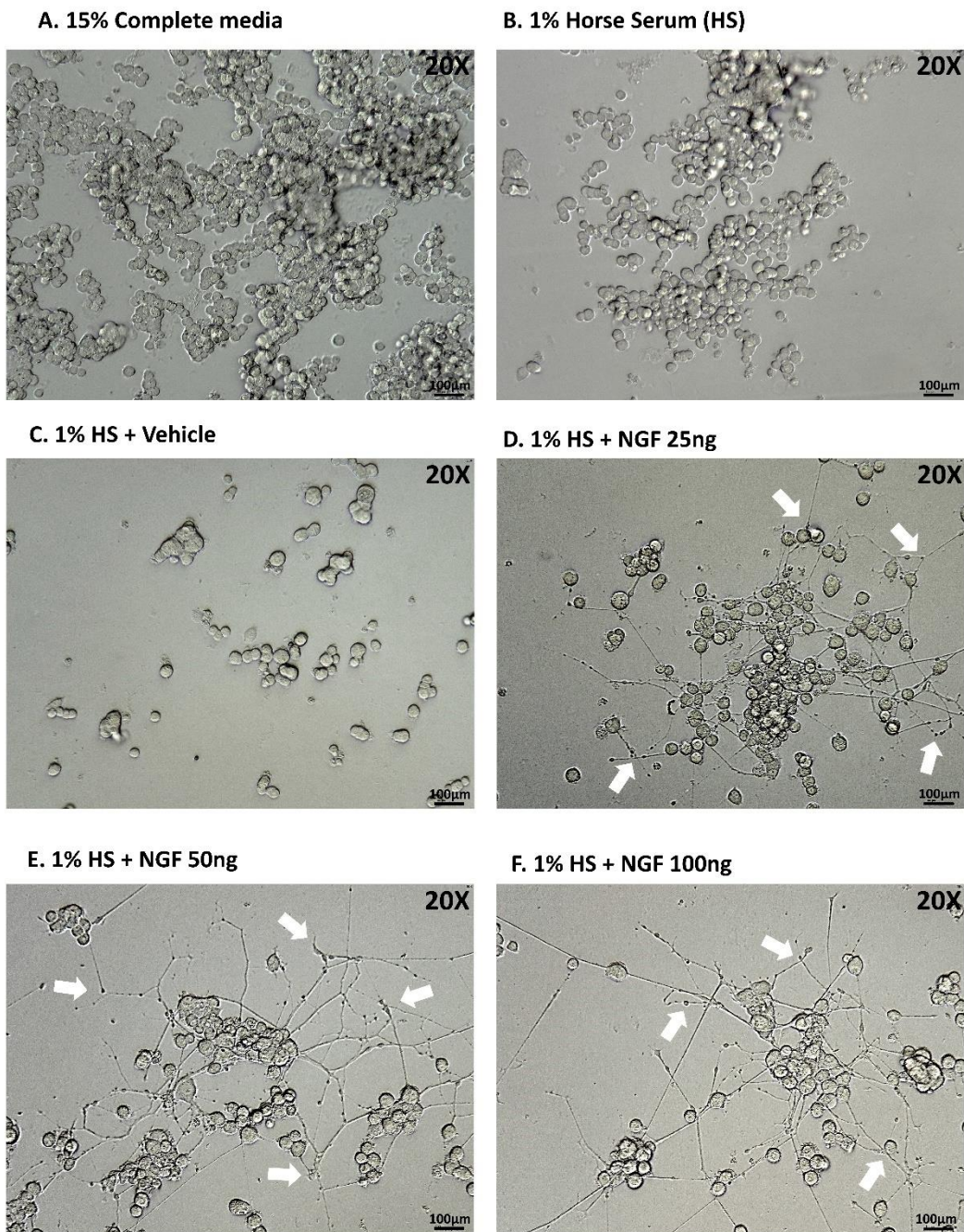
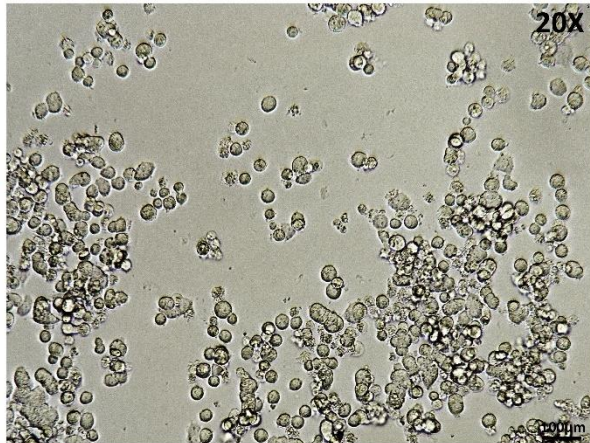
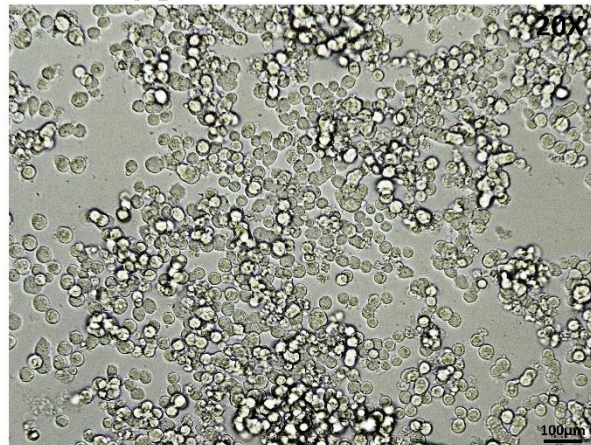


Figure 20. Microphotographs of PC12 cell differentiation with RPMI media supplemented with 1% horse serum (1% HS) and nerve growth factor (NGF) for 144 hours. A.) PC12 cells incubated in complete media (RPMI + 15% serum. B.) Cells incubated in 1% HS. C.) Cells incubated in 1% HS and 0.85% Saline (Vehicle). D.) Cells incubated in 1% HS and 25ng/ml NGF. E.) Cells incubated in 1% HS and 50ng/ml NGF. F.) Cells incubated in 1% HS and 100ng/ml NGF. Media was replaced every 48 hours. Increased neurite outgrowth was observed in all NGF treatments (D-F) but not with 0.85% saline (C). White arrows indicate representative long neurite outgrowth.

1% Horse serum (HS) media



GbE 50 μg/ml in 1% HS media



GbE 100 μg/ml in 1% HS media

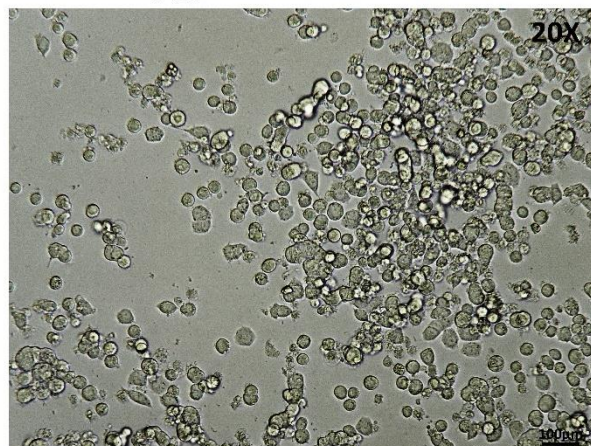


Figure 21. Microphotographs of PC12 cells treated with 50 and 100 μg/ml GbE in 1% horse serum (HS) media for 144 hours. Little neurite outgrowths were observed in both 1% HS only cells as well as cells treated with 50 and 100 μg/ml GbE.

7.5 1% BSA media differentiation

After 96 hours of 1% BSA media incubation, there was 96.4% less proliferation (138.8% Vs 0 Hrs, $p < 0.0001$) than in RPMI complete media (235.2% Vs 0 Hrs) although at 144hrs proliferation increased to 172% (compared to 0 Hrs) in 1% BSA reduced serum media, but was still significantly less than that RPMI complete media (269.8% Vs 0 Hrs, $p < 0.00001$) (Figure 22). With regards to NGF treatment, no significant difference in viability was seen in either vehicle or NGF treatment compared to 1% BSA only incubated cells across all time points (Figure 22 Figure 22.B). After 144 hours of treatment, viability across all NGF treatments (25ng/ml-122%; 50ng/ml-129%, 100ng/ml-135% Vs 0 Hrs) was less but not significantly so, compared to 1% BSA only treatment (172% Vs 0 Hrs).

As shown in Figure 23, after 144hours of NGF treatment, neurite outgrowths were observed in all NGF treatment groups with neurite outgrowth appearing longer and more abundant with increasing NGF concentrations. Some neurite outgrowth was also observed in both the 1% BSA only (Figure 23 and Figure 24), and vehicle only groups, indicating the 1% BSA media contributed to neurite outgrowth somewhat regardless of NGF treatment. Comparing viability percentages, incubating with 1% BSA and NGF resulted in less cell proliferation. This was apparent when 1% HS serum cells were compared to 1% BSA were compared. After 144 hours of treatment, most non-differentiated cells (without visible neurite outgrowth) in the 1% BSA cells appeared visually to be undergoing apoptosis in the form of cytoplasmic condensation, cellular fragmentation, or membrane rupturing, while 1% HS cells appeared rounded with little apoptosis. At 96 hours of GbE treatment, viability was higher in 50 $\mu\text{g/ml}$ GbE (210.6% Vs 0 Hrs) compared to 1% BSA only treatment (138.8% Vs 0 Hrs, $p = 0.002$) but not in 100 $\mu\text{g/ml}$ GbE (167.6%, $p = 0.47$). Similarly, at 144 hrs, viability remained higher in 50 $\mu\text{g/ml}$ GbE (228.6% Vs 0 Hrs, $p = 0.02$) treatment compared to 1% BSA only (172% Vs 0 Hrs) but not for 100 $\mu\text{g/ml}$ GbE (197.1%, $p = 0.58$). Morphologically, after 144hrs of treatment both 50 and 100 $\mu\text{g/ml}$ GbE treatments displayed shorter neurite outgrowths comparable to that of 1% BSA only treatment (Figure 24.).

Owing to the observable neurite outgrowth and viability of cells following 1% BSA media-NGF differentiation, and the compatibility of BSA as the vehicle of choice for stable fatty acid delivery to cells *in vitro* (Liu *et al.*, 2008), 1% BSA differentiation media was chosen as the method of choice for subsequent differentiation and experiments. All cells for further experimentation were differentiated on T75-type I coated flasks for 7 days with 25ng/ml NGF with media changed every 2 days. For experimentation, differentiated cells were trypsinized, counted and replated onto appropriate collagen coated culture plates, as details in section 2.17 in Chapter 2 - Methods. Differentiated cells

were allowed to adhere and re-establish neurite outgrowth for 24 hours before further experimentation. Representative images of replated 1% BSA media differentiated cells ready for treated can be seen in Figure 25. Replated differentiated P12 cells form a dense network of overlapping neurites which can be seen in Figure 25.C.

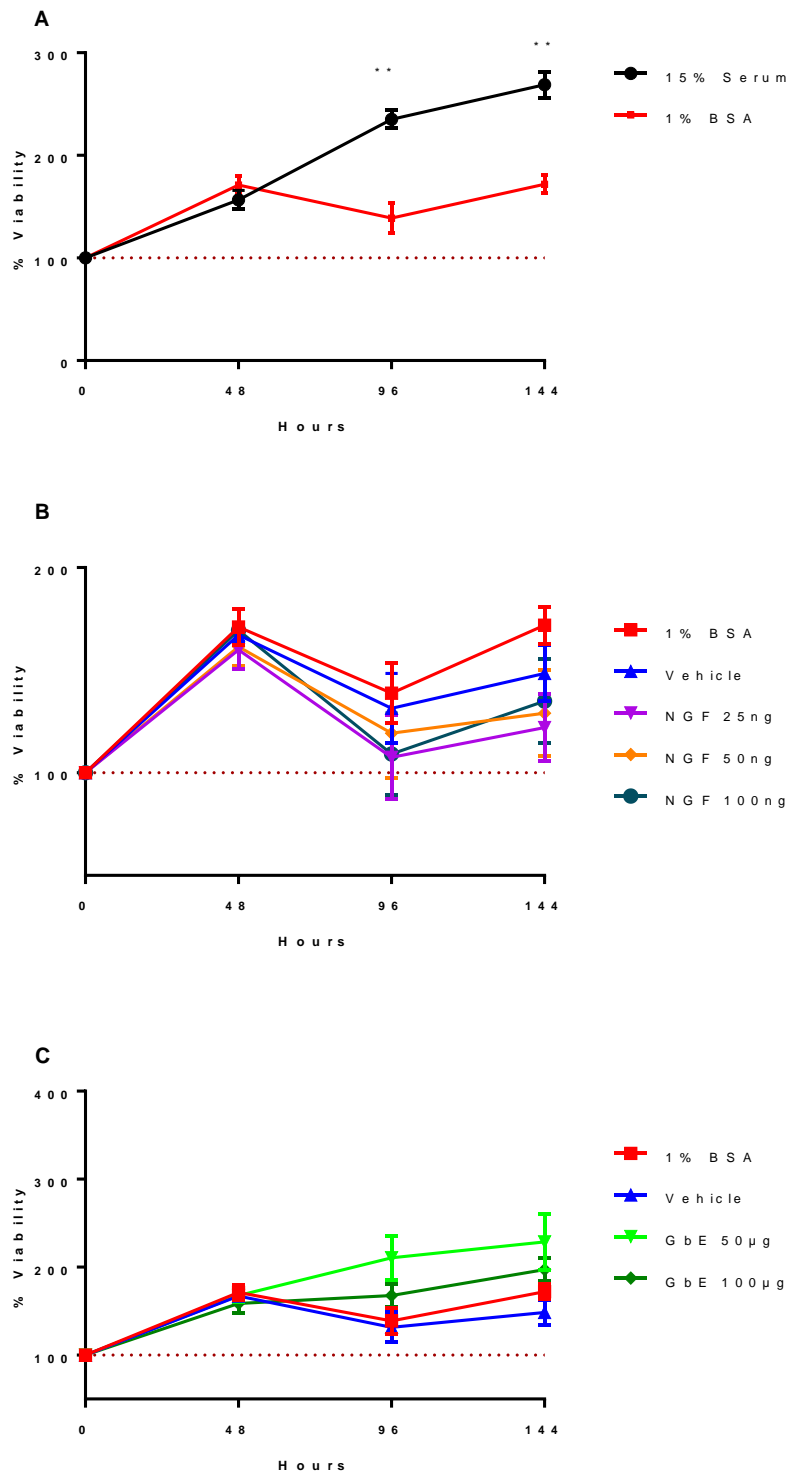


Figure 22. Viability (%) of PC12 cells after six days incubation with 1% bovine serum albumin (1% BSA) media. A). 15% complete serum media (10% horse serum+ 5% foetal bovine serum) Vs 1% BSA. B). 1% BSA media Vs Vehicle (0.085% saline) and nerve growth factor 2.5s (NGF 25,50 and 100ng/ml) C. 1% BSA Vs Ginkgo biloba (GbE, 50 and 100ug/ml). * $p < 0.05$, ** $p < 0.01$, *** $p < 0.001$, **** $p < 0.0001$ vs 1% serum. ~ p =Vs 25ng/ml NGF, # p = Vs NGF 50ng/ml, & p = Vs NGF 100ng/ml vs 1% serum. Data presented as mean±SEM. Data analysed by Two-way ANOVA with Šídák (A.) or Tukey (B. and C.) post hoc test).

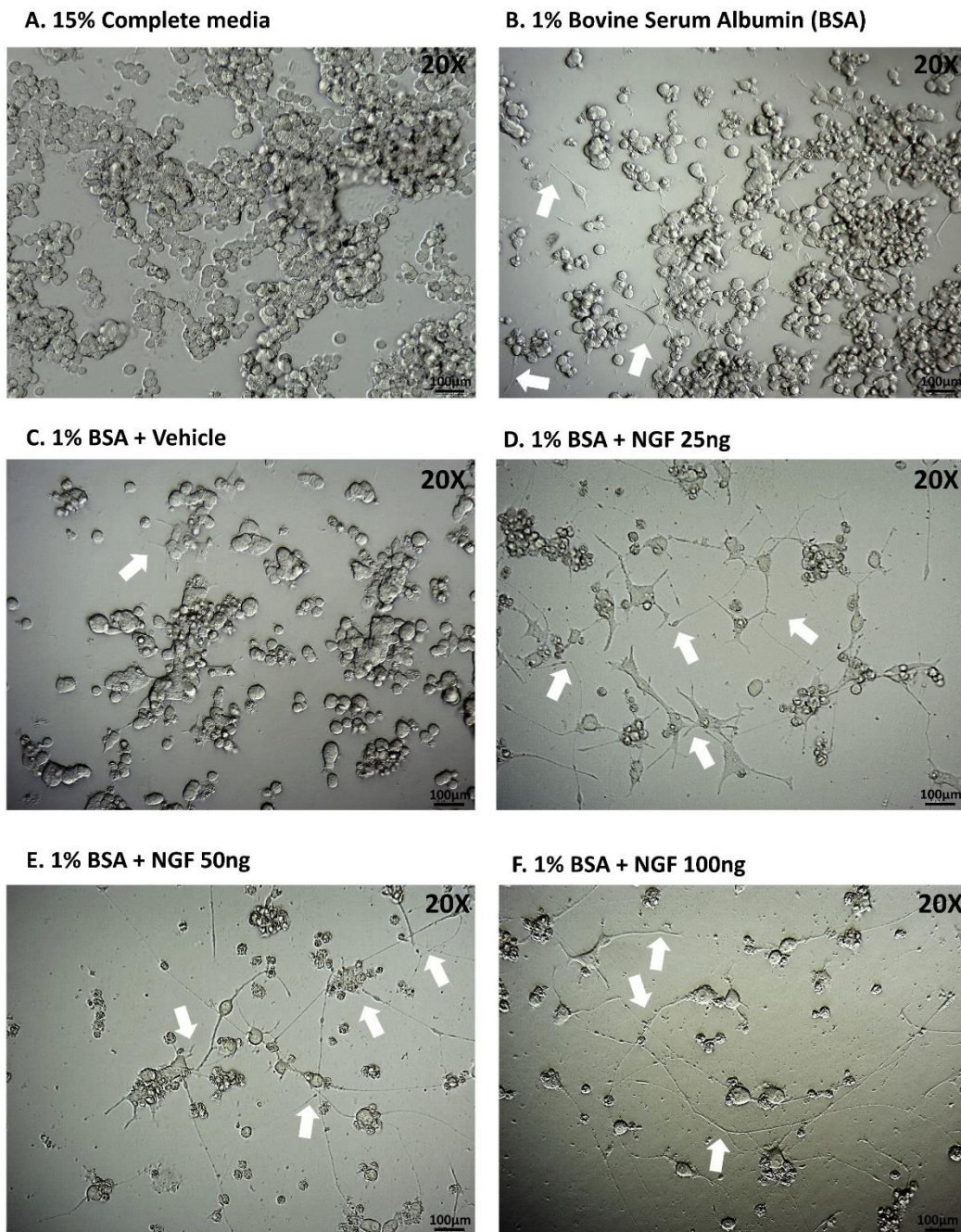
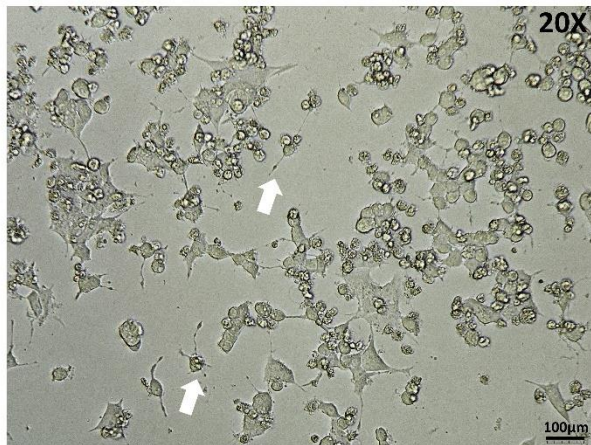
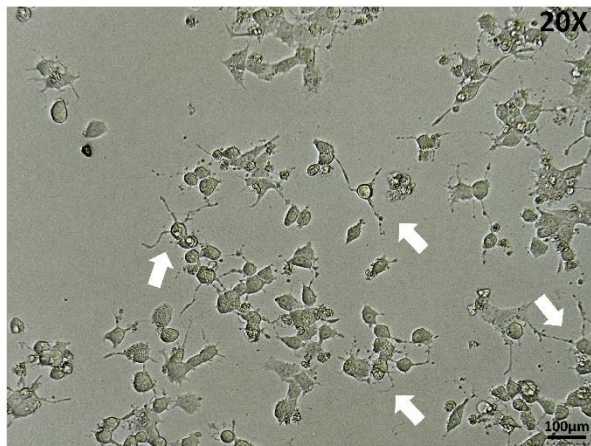


Figure 23. Microphotographs of PC12 cell differentiation with RPMI media supplemented with 1% bovine serum albumin (1% BSA) and nerve growth factor (NGF) for 7 days. A.) PC12 cells incubated in complete media (RPMI + 15% serum. B.) Cells incubated in 1% BSA. C.) Cells incubated in 1% BSA and 0.85% Saline (Vehicle). D.) Cells incubated in 1% BSA and 25ng/ml NGF. E.) Cells incubated in 1% BSA and 50ng/ml NGF. F.) Cells incubated in 1% BSA and 100ng/ml NGF. Media was replaced every 48 hours. Increased neurite outgrowth was observed in all NGF treatments (D-F) but not with 0.85% saline (C). White arrows indicate representative long neurite outgrowth.

1% BSA media



GbE 50µg/ml in 1% BSA media



GbE 100µg/ml in 1% BSA media

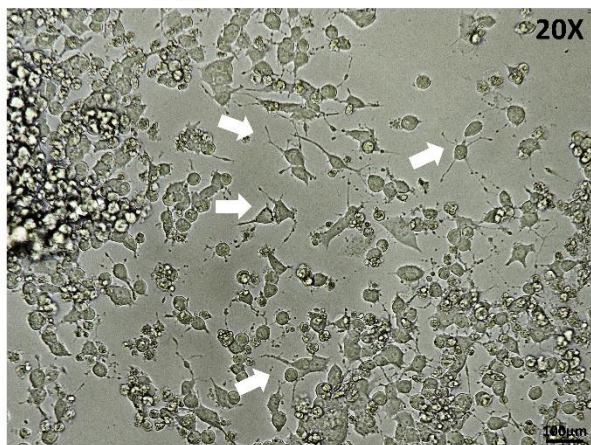


Figure 24. Microphotographs of PC12 cells treated with 50 and 100µg/ml GbE in 1% BSA media for 144 hours. Short neurite outgrowths were observed in 1% BSA only cells as well as cells treated with 50 and 100µg/ml GbE. White arrows indicate representative long neurite outgrowth.

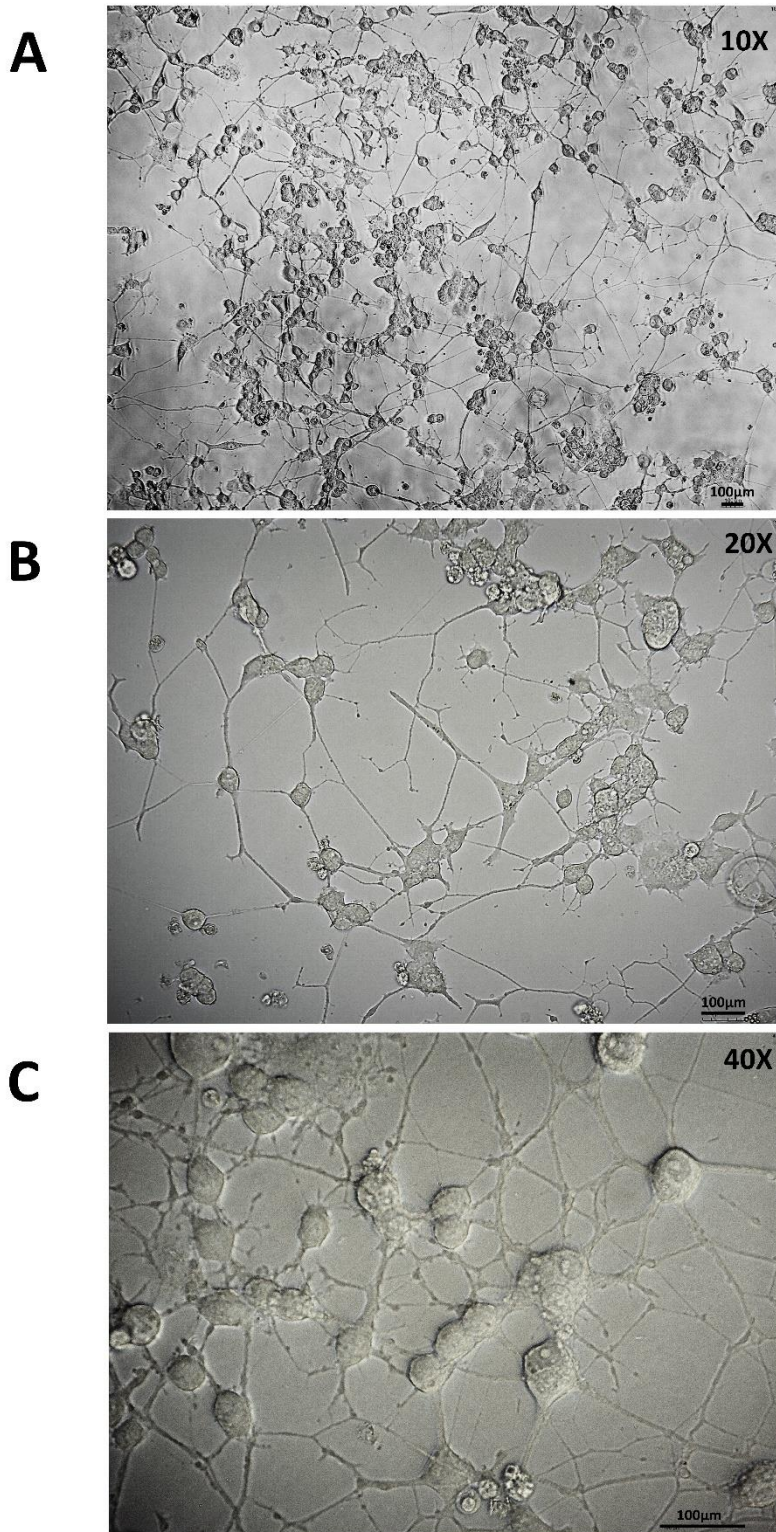


Figure 25. Microphotographs of replated differentiated PC12 cells. PC12 cells were differentiated for 7 days with 25ng/ml NGF followed by trypsinization, replating onto Type I collagen coated plates and an additional 24 hours of NGF treatment in low-serum (1% bovine serum albumin (BSA)) media. PC12 cells photographed at A.) 10X B.) 20X. C.) 40X. Differentiated P12 cells form a dense network of overlapping neurites.

7.6 Differentiation – β -Tubulin III

To determine the effect of 1% BSA-NGF treatment on PC12 differentiation, levels of β -tubulin III were analysed by flow cytometry. β -tubulin III is a main component of microtubules and is primarily expressed in neurons and is an established and commonly used neuronal marker with levels increasing during PC12 cell differentiation (Maioli *et al.*, 2015; Sadri *et al.*, 2014; Ohuchi *et al.*, 2002; Caceres, Banker and Binder, 1986).

PC12 cells were treated for 7 days with 1% BSA media supplemented with 25ng/ml NGF. After 7 days cells were harvested followed by fixation and permeabilization with Biolegend Cyto-Fast™ Fix/Perm buffer set as per manufacturer's instructions. Cells were analysed from 3 different passages (n=3) with a minimum of 4 replicates per passage. Cells were labelled with either Biolegend PE anti-Tubulin β 3 (TUBB3) Antibody or PE Mouse IgG2a, κ Isotype Ctrl Antibody as per manufacturer's instructions. As illustrated in Figure 26, Panel C, β -tubulin III levels increased significantly by 5-fold in NGF-treated PC12 cells compared to non-treated (RPMI) cells ($p < 0.0001$). This is in keeping with morphology observations that also showed increased neurite outgrowth in NGF-treated cells (Figure 23 and Figure 24). Owing to the limitations of the flow cytometer machine, cells fluorescing over 10^5 (log scale) were unable to be captured on a representative graph.

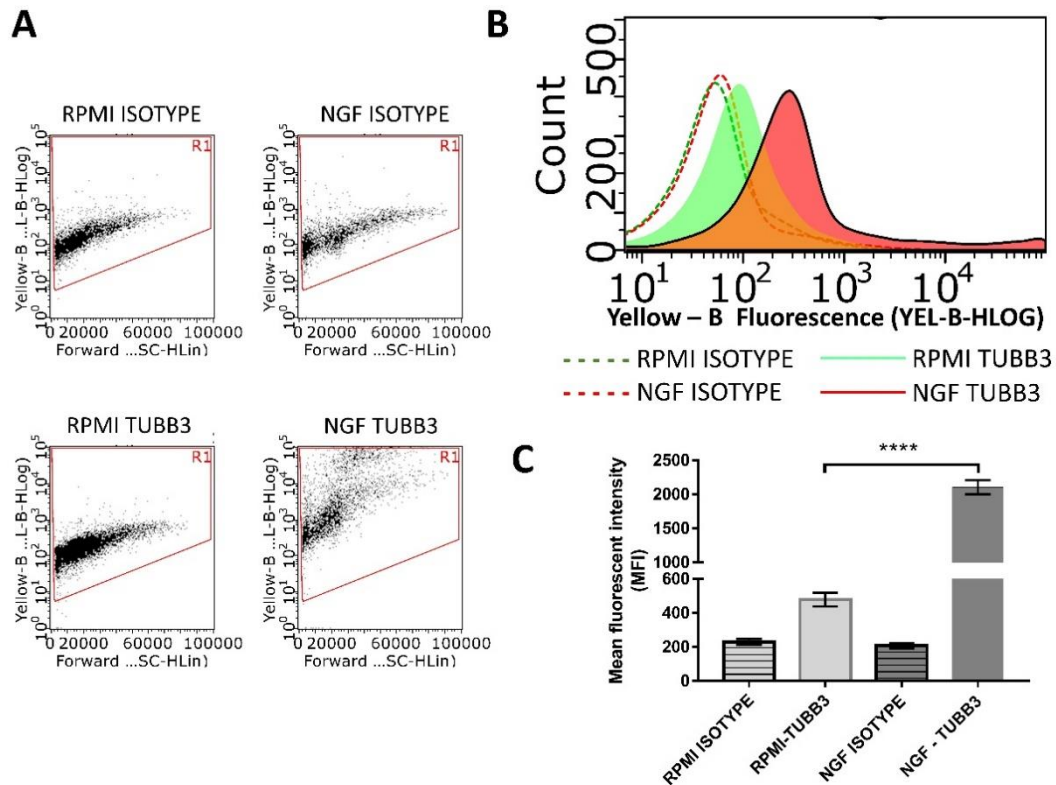


Figure 26. Effect of NGF treatment on Tubulin- β 3 levels in PC12 cells. A). Representative dot plot profiles of Tubulin- β 3 or isotype-control PC12 labelled cells treated with 25ng NGF in 1% BSA media for 7 days (NGF) or no treatment (RPMI). Acquisition of 20,000 events. B). Representative yellow/blue (FL2) overlay histogram showing fixed and permeabilized cells intracellularly stained with anti-Tubulin- β 3 (TUBB3) (clone TUJ1) PE (green (RPMI) and red (NGF) filled histograms) or with mouse IgG2a, κ PE isotype control (clone MOPC-173 (green (RPMI) and red (NGF) open histograms). C). Bar chart displaying mean PE signal (yellow/blue mean fluorescent intensity (MFI)) that equates to intracellular TUBB3 levels. NGF-treated cells (Red) displayed significantly increased levels of TUBB3 compared to RPMI non-treated (Green) cells. Data presented as mean \pm SEM (n=3) analysed by one-way ANOVA with Tukey post-hoc test (****p<0.001).

7.7 Neurofilament protein levels in NGF differentiation

Neurofilament proteins are another established neuronal marker for PC12 differentiation (Schimmelpfeng, Weibezahn and Dertinger, 2004; Clark and Lee, 1991; Lindenbaum, Carbonetto and Mushynski, 1987; Lee, 1985; Lee and Page, 1984; Lee, Trojanowski and Schlaepfer, 1982). Neurofilaments are major cytoskeletal proteins in myelinated nerves, with a linear relationship associated with levels of neurofilaments and axonal diameter and radial growth (Schimmelpfeng, Weibezahn and Dertinger, 2004; Cleveland *et al.*, 1991; Lee, Trojanowski and Schlaepfer, 1982). Neurofilaments, particularly neurofilament light chain (NF-L), are also used as biomarkers in diseases involved in cognitive decline including ALS, AD, frontotemporal dementia and Huntington's disease (Lee *et al.*, 2022; Behzadi *et al.*, 2021; Ingannato *et al.*, 2021; Moscoso *et al.*, 2021; Verde, Otto and Silani, 2021; Benedet *et al.*, 2020; Forgrave *et al.*, 2019; Gille *et al.*, 2019; Kern *et al.*, 2019; Gaiani *et al.*, 2017; Deng *et al.*, 2009).

To determine if levels of neurofilaments increased in NGF-treated PC12 cells, 10 μ g of whole cell lysates (N=6, taken from 3 separate passages) was loaded and run on to SDS-PAGE gels, transferred to nitrocellulose paper and incubated with monoclonal antibodies. PC12 Cells treated for 7 days with 1% BSA media and 25ng/ml NGF showed increased expression of Neurofilament medium chain (NF-M) and NF-L, as shown by western blotting and illustrated in Figure 27. This is in keeping with other previous reports of PC12 differentiation (Schimmelpfeng, Weibezahn and Dertinger, 2004; Clark and Lee, 1991; Lindenbaum, Carbonetto and Mushynski, 1987; Lee, 1985; Lee and Page, 1984; Lee, Trojanowski and Schlaepfer, 1982).

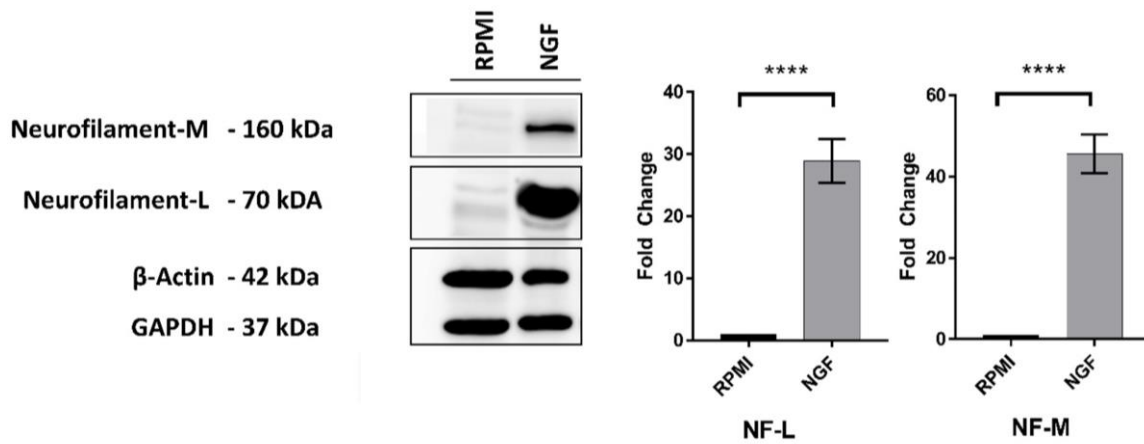


Figure 27. Detection of Neurofilament-L and Neurofilament-M by western blot analysis in undifferentiated (RPMI) PC12 cells and 7-Day NGF-differentiated (NGF) PC12 cells. Blots were incubated with monoclonal antibodies for Neurofilament-L (1:2000), Neurofilament-M (1:2000), β -Actin (1:10000) and GAPDH (1:10000) followed by HRP-conjugated secondary antibody (1:1000). 10 μ g of whole cell lysate was loaded per lane. Data analysed by t-test. **** p <0.0001, n =6.

7.8 Cell apoptosis in PC12 differentiation

To further identify the health of 1% BSA-NGF differentiated cells, cell apoptosis was analysed by Annexin-7AAD flow cytometry. Annexin V is an intracellular protein that binds to phosphatidylserine (PS) in a calcium-dependent manner (Biolegend, 2020; Suzuki *et al.*, 2010; Wang *et al.*, 2007). PS, an anionic phospholipid normally only found on the inner cytosolic leaflet of the cell membrane translocates to the outer leaflet during early apoptosis (Shlomovitz, Speir and Gerlic, 2019; Kay *et al.*, 2012; Kay and Grinstein, 2011; Leventis and Grinstein, 2010; Yeung *et al.*, 2008). To identify whether cells are apoptotic or necrotic, 7-amino-actinomycin (7-AAD) is used. Late apoptotic cells stain positively with 7-AAD as it binds to nuclear DNA, while early apoptotic cells can exclude the 7-AAD dye (Biolegend, 2020).

As discussed in the introduction (1.13) the plasma membrane serves as a barrier and facilitator of ionic exchange and molecular transport in and out of the cell (Hulbert *et al.*, 2005, 2007). The phospholipids PC and SM are predominantly found on the outer leaflet of the cell membrane, while PS, PI and PE are primarily found on the inner leaflet in healthy cells (Mariño and Kroemer, 2013). Phospholipid asymmetry in the mammalian cellular membrane is maintained by the translocation of phospholipids either from the outer to the inner leaflet, or *vice versa*, by flippase, floppase and scramblase ATP-dependent enzymes (Shlomovitz, Speir and Gerlic, 2019; Hankins *et al.*, 2015; Kay *et al.*, 2012; Leventis and Grinstein, 2010). This lipid asymmetry is responsible for electrochemical properties of the cellular membrane and acts as an important mediator in cell signalling (van Meer, 2011; van Meer, Voelker and Feigenson, 2008). For example, PI operates as a secondary messenger when located on the inner leaflet while PS translocated on the outer leaflet instigates platelet activation in blood clotting as well as acting as a phagocytic signal for engulfment in apoptotic cells (Hankins *et al.*, 2015; Suzuki *et al.*, 2013; van Meer, 2011; van Meer, Voelker and Feigenson, 2008). Briefly, differentiated PC12 cells were trypsinized for 5 minutes to release them from the plate surface. The trypsin was neutralized with RPMI-complete media, and the cell sample gently centrifuged (100xg) to pellet the cells, with supernatant discarded. The cell pellet was washed with 1X PBS and centrifuged again, and the supernatant discarded. To 1×10^5 cells, 100 μ l of binding buffer was added and 5 μ l each of Annexin+ 7AAD mix (1:1 ratio). Cells were gently vortexed and incubated for 15 minutes at room temperature in the dark. A further 100 μ l of binding buffer was added to each sample and the sample vortexed immediately prior to running on the flow cytometer. Data is graphically depicted in Figure 28.

Healthy cells

Comparing both RPMI and 1% BSA media, no significant differences in healthy cell levels were seen between cells incubated in RPMI complete (15% serum) media and 1% BSA reduced serum media ($p=0.75$) after 7 days of incubation. Comparing cells incubated in 1% BSA media, treatment with vehicle only (0.85% Saline) for 7 days resulted in an 8% decrease in healthy cells compared to 1% BSA media alone ($p=0.02$) (Figure 28.A). After 7 days of 25ng/ml NGF treatment 52% of cells were identified as healthy, a 26% decrease compared to the 1% BSA media only group ($p<0.0001$). Upon the trypsinization and replating of NGF-differentiated PC12 cells (Day 8) for further treatments, the number of cells identified as healthy increased to 76%, a 24% increase compared to the non-replated NGF-differentiated cells (Day 7) ($p<0.0001$).

Early apoptosis

Incubation with 1% BSA media for 7 days resulted in 14% more cells in early apoptosis (19%) compared to complete media (5%) ($p<0.0001$) (Figure 28.B). Treatment with vehicle only resulted in 6% more cells in early apoptosis (25%, $p=0.02$) compared to the 19% seen with 1% BSA media only ($p=0.02$). No significant difference between vehicle control and in NGF treated cells (21%, $p=0.66$) were seen for early apoptotic cells. Following replating of NGF differentiated cells, 15% of cells were identified as early apoptotic, a significant decrease of 4% compared to non-replated NGF differentiated cells (21%, $p=0.0006$).

Late apoptosis

Cells incubated with 1% BSA media for 7 days resulted in 7% less cells (1.9%) in late apoptosis than 15% complete media (9.1%) ($p=0.004$) (Figure 28.C). Cells incubated with 1% BSA media had approximately 1.9% of cells in late apoptosis with no significant difference seen when compared to 1% BSA media + vehicle (0.85% saline) (3.1%) ($p=0.98$). Treatment with NGF resulted in 22% more cells in late apoptosis (24.3%) than 1% BSA media alone ($p<0.0001$). Replating NGF differentiated cells after day 7 resulted in 19.6% less cells in late apoptosis (4.7%) compared to non-replated differentiated cells ($p<0.0001$).

Dead

1% BSA media had significantly fewer dead cells (0.4%) than complete media (4%) ($p<0.0001$) (Figure 28.D). No significant differences in dead cell percentages occurred between 1% BSA media (0.4%) and treatment in vehicle alone (0.9%) ($p=0.97$). While not significant, treatment with NGF resulted in 2.4% more dead cells (2.5%) compared to 1% BSA media only ($p=0.07$). No significant differences in

dead cell percentages were seen between non-replated and replated NGF differentiated cells ($p=0.98$).

In summary, following 7 days of 25ng/ml NGF treatment, approximately 52% of cells were healthy, and a further 19% in early apoptosis. Following trypsinisation, washing and re-plating of differentiated cells, the percentage of healthy cells in the sample increased to 76%, while cells in early apoptosis decreased to 15%. Replating NGF differentiated cells after 7 days of differentiation resulted in 19.6% less cells in late apoptosis (4.7%) compared to non-replated differentiated cells ($p<0.0001$).

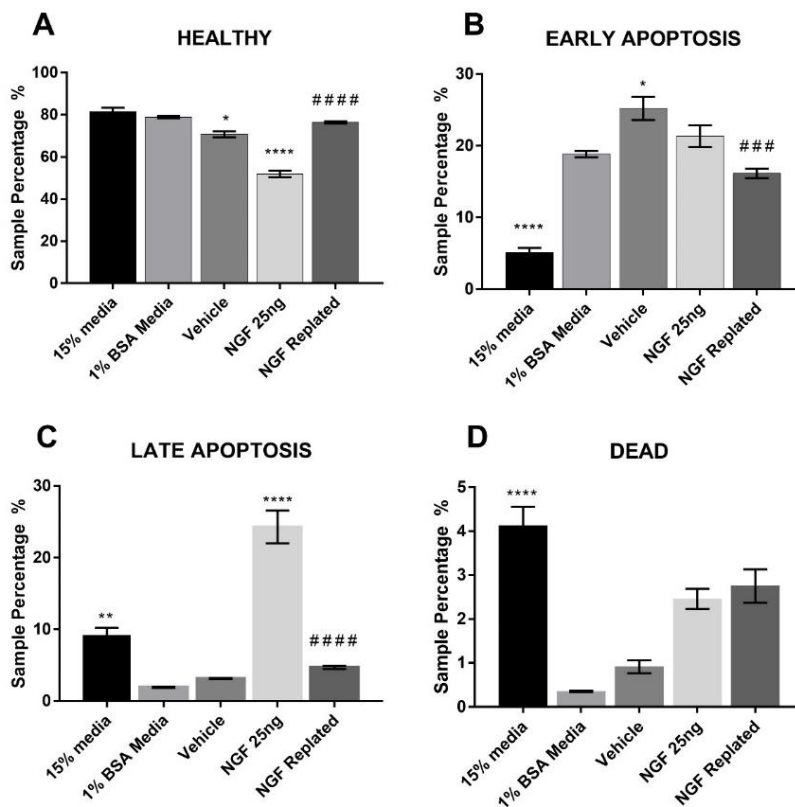
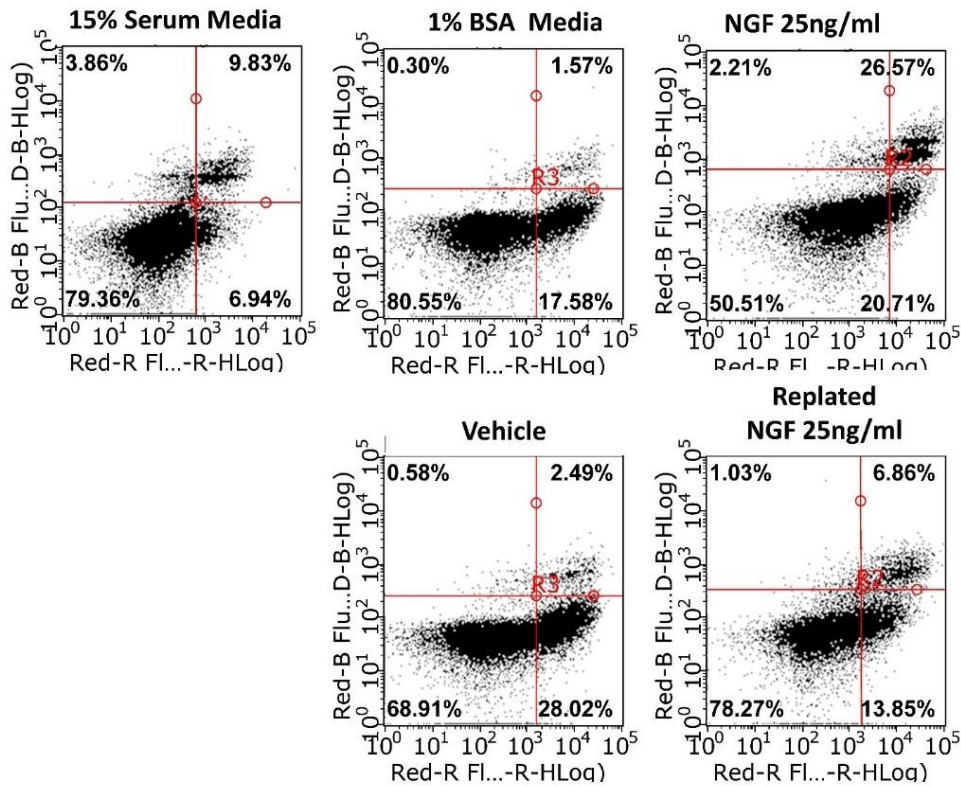


Figure 28. Annexin-V/7-AAD FACS analysis of PC12 cell differentiation. Cells treated for 7 days with either complete media (15% serum)(n=27), 1% BSA media (n=10) or 1% BSA media with vehicle control (0.85% saline) (n=10), 25ng/ml NGF-2.5s (n=22) or replated NGF differentiated PC12 cells (n=49). **A**). Healthy cells **B**). Early apoptosis **C**). Late apoptosis **D**). Dead. * $p < 0.05$, ** $p < 0.01$, *** $p < 0.001$, **** $p < 0.0001$ vs 1% BSA media. # $p < 0.05$, ## $p < 0.01$, ### $p < 0.001$, #### $p < 0.0001$ NGF 25ng Vs NGF replated. One-way ANOVA with Tukey post hoc test.

7.9 *In vitro* model of oxidative stress injury in PC12 cells

Biological tissue consumes oxygen in energy production producing cellular-damaging free radicals and reactive oxygen species (ROS) such as hydrogen peroxide (H_2O_2), hydroxyl radical ($\text{HO}\cdot$) and superoxide anion radical ($\text{O}_2^{\cdot-}$) (Dunn *et al.*, 2015). Neuronal cells are highly susceptible to oxidative stress and ROS damage, particularly with regards to peroxidizable compartments including the phospholipid cell membrane, lipoproteins as well as contributing to DNA damage. Cellular ROS production is a major contributor to neuronal tissue injury with increased levels associated with neurodegeneration (Goldsteins *et al.*, 2022; Hajam *et al.*, 2022; A. Singh *et al.*, 2019; Li *et al.*, 2013; Gandhi and Abramov, 2012). ROS stimulates the release of pro-apoptotic proteins and cytochrome C (Cyt C) which induce cell apoptosis by activating caspase family members (Dunn *et al.*, 2015). For this study, H_2O_2 was used to establish an *in vitro* model of OS injury in PC12 cells. H_2O_2 is a major producer of cellular ROS and causes DNA damage and lipid peroxidation which can lead to cell membrane disturbances (Gough and Cotter, 2011).

Both undifferentiated and differentiated cells were incubated with H_2O_2 at increasing concentrations of 0, 12.5, 25, 40, 100, 200 and 400 μM (Figure 29). Viability was determined by MTT assay. MTT (5 mg/ml, 10 μl) was added into each well and cultured at 37°C for 4 hrs to produce formazan crystals and dissolved with 100 μL of solubilization solution (10% SDS in 0.01M HCL) per well. Viability was measured against non-treated cells. n=12 was taken from a minimum of 3 passages. In undifferentiated PC12 cells (Figure 29.A), a significant decrease in viability was seen between the control group and 24 hr H_2O_2 treatment at 200 μM (~75%; p=0.0001) and 400 μM (~62%; p=0.0001). This is consistent with other published reports that show that PC12 viability decreases significantly from ~80% at 200 μM H_2O_2 treatment (Liu *et al.*, 2017) to ~60% at 500 μM H_2O_2 (Lee *et al.*, 2018). In differentiated PC12 cells (Figure 29.B), a significant decrease in viability was also seen at 50 μM (~84%, p=0.03), 100 μM (~81%, p<0.0001), 200 μM (~77%, p<0.0001) and 400 μM (~68%, p<0.0001) H_2O_2 treatment compared to the control group after 24 hours. The increase in viability in differentiated cells at 400 μM H_2O_2 treatment is likely due to the NGF treatment which as has been shown to protect against damage from H_2O_2 as well as serum, oxygen and glucose deprivation (Kinarivala *et al.*, 2017; Sun *et al.*, 2017). Similarly, differentiated PC12 cells have been also shown to be more resistant to drug-induced neurotoxicity than undifferentiated cells (Sakagami *et al.*, 2018). 400 μM of H_2O_2 was chosen for subsequent experiments to induce toxicity.

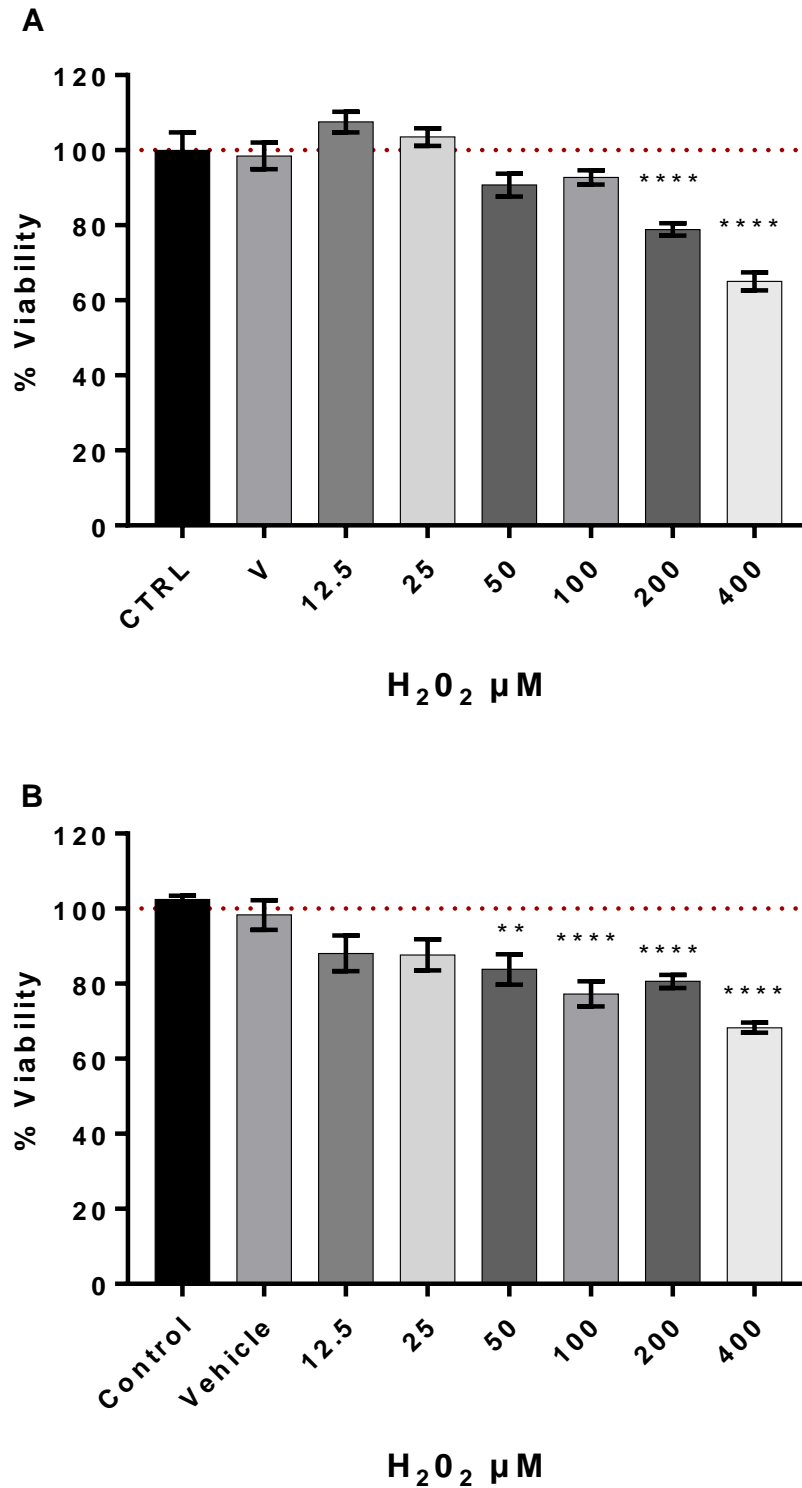


Figure 29. Cell viability of PC12 cells incubated with H₂O₂ (0-400 μM) (A) Undifferentiated PC12 cells were incubated with H₂O₂ (0-400 μM) or 0.85% Saline (vehicle control) for 24 h, then the cell viability was determined by the MTT assay. (B) Differentiated PC12 cells were incubated with H₂O₂ (0-400 μM) or 0.85% Saline (vehicle control) for 24 h, then the cell viability was determined by the MTT assay. Data represented means±SEM, **p* < 0.05, ***p* < 0.01, ****p* < 0.001, *****p* < 0.0001 vs control group, One-Way ANOVA with Tukey post hoc test. N=12 taken from a minimum 3 passages.

7.10 GbE treatment in undifferentiated and differentiated PC12 cells

GbE has been shown to possess antioxidant, anti-inflammatory and neuroprotective properties (Isah, 2015; Diamond and Bailey, 2013; Christen, 2004; Smith and Luo, 2004; Ahlemeyer and Krieglstein, 2003; Kuribara *et al.*, 2003; Ponto and Schultz, 2003; Tendi *et al.*, 2002; Luo, 2001; Janssens *et al.*, 1995).

PC12 cells were seeded at confluency (5×10^4 cells/cm²) in 96 well plates and allowed to adhere for 24 hours. Undifferentiated cells were incubated with RPMI complete media, while differentiated cells were incubated with 1% BSA+ 25ng/ml NGF media. After 24 hours, cells were incubated with increasing concentrations of GbE (0, 12.5, 25, 40, 100, 200 and 400 μ M) for a further 24 h. Viability was determined by MTT assay. MTT (5 mg/ml, 10 μ l) was added into each well and cultured at 37°C for 4 hrs to produce formazan crystals and dissolved with 100 μ L of solubilization solution (10% SDS in 0.01M HCL) per well. Viability was measured against non-treated cells. n=12 was taken from a minimum of 3 passages.

As shown in Figure 30, all tested concentrations of GbE were found to be non-toxic. In undifferentiated PC12 cells (Figure 30.A), no significant differences were seen between the control group and any of the GbE treatments after 24 hours although an increase in viability was seen in both the 200 μ g/ml (107%) and 400 μ g/ml (108%) GbE-treated groups. In differentiated PC12 cells (Figure 30.B), when compared to non-treated cells, a significant increase in viability was seen in both 200 μ g/ml (111%, $p=0.03$) and 400 μ g/ml (117%, $p=0.0003$) GbE-treated groups. The increase in viability is in keeping with the findings of Tchantchou and colleagues (2009) that found bilobalide (5, 10, and 15 μ M) and quercetin (5, 7, and 10 μ M), both components of GbE, significantly increased cell proliferation in hippocampal neurons in a dose-dependent manner (Tchantchou *et al.*, 2009). Eckert and colleagues (2005) found that GbE (0.5, 10, 100 μ g/ml) significantly improved the mitochondrial membrane potential of PC12 cells and ameliorated the decrease in ATP production significantly and in a dose dependent manner, following mitochondrial damage (Eckert *et al.*, 2005). Similarly, Abdel-Kader and colleagues (2007) reported that GbE treatment in PC12 cells also alleviated mitochondrial functions at concentrations as low as 10 μ g/ml (Abdel-Kader *et al.*, 2007). (Rhein and colleagues (2010) also reported the significant beneficial effects of GbE in wild-type human neuroblastoma SH-SY5Y cells or SH-SY5Y cells transfected with human wild-type APP to induce increased A β levels. They found that GbE treatment reduced ROS levels, enhanced of respiratory control ratio, and increased in ATP levels (Rhein *et al.*, 2010).

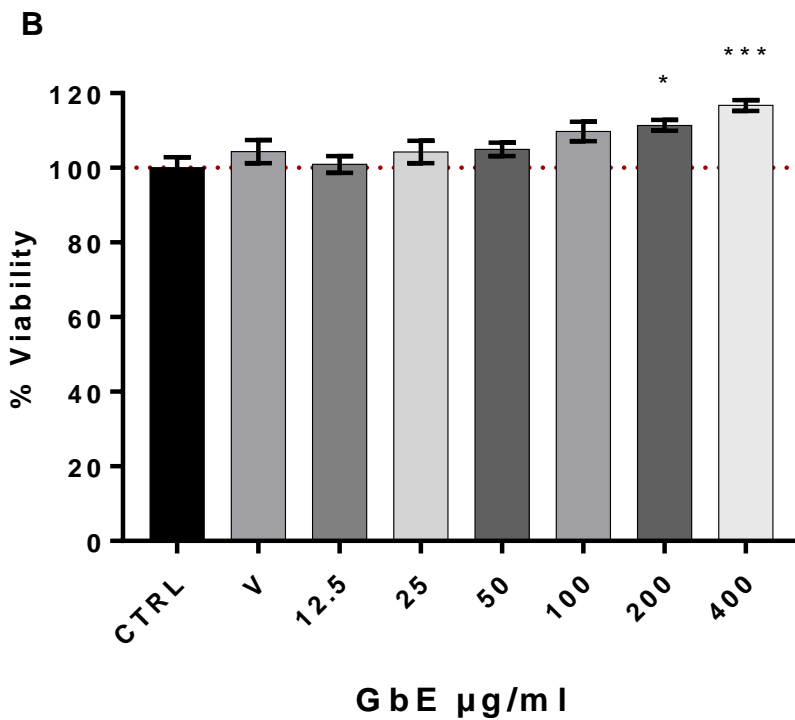
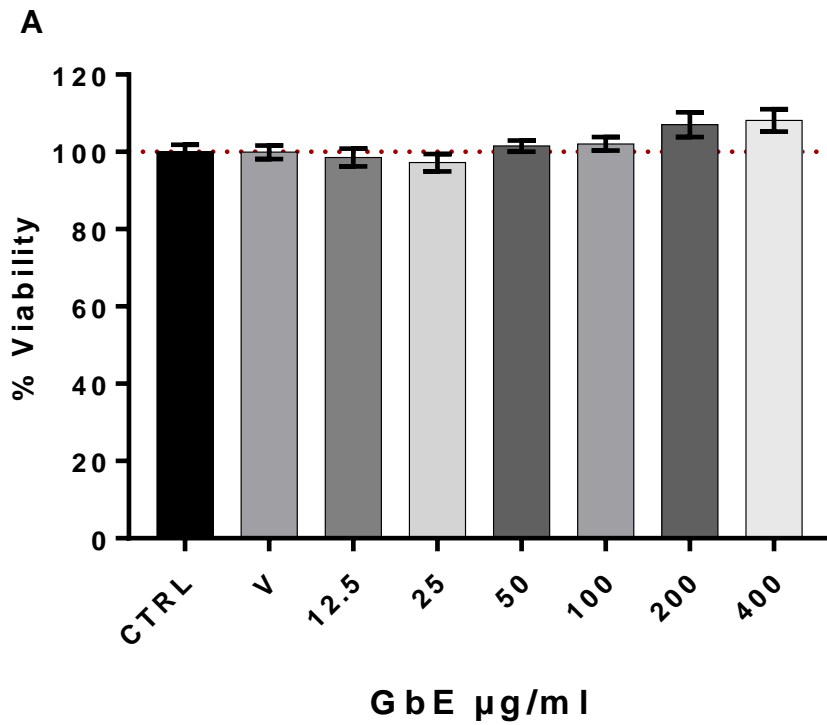


Figure 30. Cell viability of PC12 cells incubated with Ginkgo biloba (GbE) (12.5–400 $\mu\text{g/ml}$) (A) Undifferentiated PC12 cells were incubated with GbE (12.5–400 $\mu\text{g/ml}$) or 0.85% Saline vehicle control (V) for 24 h, then the cell viability was determined by the MTT assay. (B) Differentiated PC12 cells were incubated with GbE (12.5–400 $\mu\text{g/ml}$) or 0.85% Saline vehicle control (V) for 24 h, then the cell viability was determined by the MTT assay. Data represented means \pm SEM, * $p < 0.05$, ** $p < 0.01$, *** $p < 0.001$, **** $p < 0.0001$ vs control group, One-way ANOVA with Tukey post hoc test. $N=12$ taken from a minimum 3 passages.

7.11 Cell viability of GbE treatments in oxidative stress induced neuronal injury

Considering that increased ROS levels can cause cell membrane injury, inhibiting OS-induced neuronal injury is considered valuable in the treatment of neurological diseases (Hajam *et al.*, 2022; Singh *et al.*, 2019; Jia *et al.*, 2016; Li *et al.*, 2013; Eckert *et al.*, 2005). This includes the use of antioxidant therapeutics that can protect against H₂O₂ damage (Shin *et al.*, 2021; Gao *et al.*, 2018; Lv *et al.*, 2017; Cheong *et al.*, 2016; Jia *et al.*, 2016; Li and Li, 2015; Chen *et al.*, 2010; Lu *et al.*, 2010; Rhein *et al.*, 2010).

To explore the effect of GbE pre-treatment on H₂O₂-induced PC12 neuronal injury, differentiated PC12 cells were pre-treated for 24 hours with GbE at indicated concentrations (0-400 µg/ml). The media was changed, and cells were then incubated with or without 400 µM H₂O₂ or vehicle control for a further 24 hours. As shown in Figure 31 in non-pre-treated cells and cells pre-treated with vehicle only (0.85% saline) and subsequent treatment with 400 µM H₂O₂ caused viability to reduce to 68% (p<0.0001) compared to control cells. GbE pre-treatments at all concentrations (12.5, 25, 50, 100, 200, 400 µg/ml) attenuated the decrease in cell viability induced by 400 µM H₂O₂ (GbE; 12.5, 25, 10, 200, 400 µg/ml, p<0.0001) with similar viability profiles seen between corresponding GbE pre-treatments with and without H₂O₂ treatment. In an SH-SY5Y cell model, GbE has been shown to ameliorates oxidative phosphorylation (OXPHOS) performance and restored Aβ-induced mitochondria failure (Rhein *et al.*, 2010). This is in keeping with reports by Rhein and colleagues (2010) that found significant beneficial effects of GbE in wild-type human neuroblastoma SH-SY5Y cells or SH-SY5Y cells transfected with human wild-type APP to induce increased Aβ levels. They found that GbE treatment reduced ROS levels, enhanced the respiratory control ratio, and increased ATP levels (Rhein *et al.*, 2010). Similarly, Abdel-Kader and colleagues (2007) and Eckert and colleagues (2005) both found that GbE as low as 10µg/ml significantly improved the mitochondrial membrane potential of PC12 cells following mitochondrial damage (Abdel-Kader *et al.*, 2007; Eckert *et al.*, 2005). 50µg/ml and 100µg/ml concentrations of GbE was used in subsequent experiments.

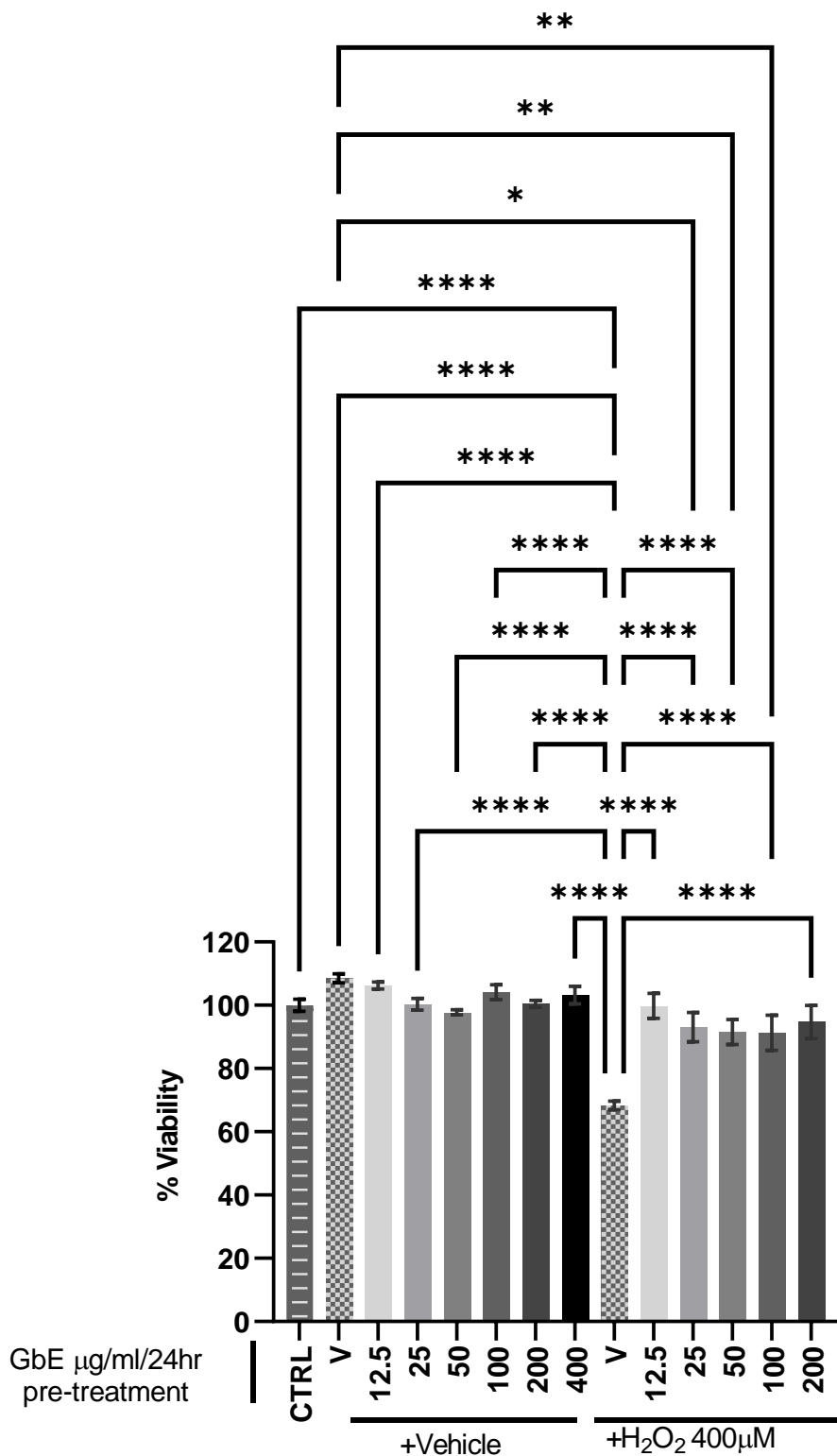


Figure 31. GbE attenuated the decrease in cell viability induced by H₂O₂ in PC12 cells. Cells were pre-treated for 24 hours with GbE at indicated concentrations, then incubated with or without 400 μM H₂O₂ or vehicle control for a further 24 hours. Viability % compared to control. Data analysed by two-way ANOVA with Tukey *post hoc* test. Data represented as mean \pm SEM, **p* < 0.05, ***p* < 0.01, *****p* < 0.0001.

7.12 Cell viability of NFD, HFD and GbE treatments

To identify the viability and apoptosis rate of PC12 cell treatments with NFD and HFD FA mixes, in isolation or combined with GbE treatment, Annexin V-7AAD cell apoptosis assays were conducted as described in section 2.22. All cell samples were treated for 24 hours with either 100 μ M of NFD or HFD FA mix, GbE treatments at GbE-50 μ g/ml (GbE50) and GbE-100 μ g/ml (GbE100), or a combination of NFD or HFD with GbE. n=18 collected from a minimum of 3 passages. Data is graphically depicted in Figure 32.A.

Healthy cells

Illustrated in Figure 32.B, differentiated PC12 (PC12-Diff) cells had 7% less healthy cells, compared to undifferentiated cells (PC12-Undiff vs. PC12-Diff; 79.71% vs 72.65%, $p=0.01$). No significant difference was seen between PC12-Diff cells and vehicle only treated cells (PC12-Diff vs. Vehicle 72.65% vs 69.69%, $p=0.89$). Compared to PC12-Diff cells (72.65%) while not significant different, viability decreased by 5% in cells treated with either NFD 100 μ M (NFD, 67.36, $p=0.16$) and 2% in HFD 100 μ M (HFD, 70.7, $p=0.99$). Similarly, compared to PC12-Diff cells, no significant differences in viability were seen in cells treated with either GbE 50 μ g/ml (GbE50, 73.81%, $p>0.99$) or GbE 100 μ g/ml (GbE100, 75.61%, $p>0.89$). When cells were treated with NFD + GbE50, viability reduced by 6.6% to 66% ($p=0.03$) compared to PC12-Diff cells, with a similar 6.5% decrease seen in HFD + GbE50 (66.2%, $p=0.06$) while no significant changes were seen in cells treated with either NFD + GbE100 (70.67%, $p=0.99$) or HFD + GbE100 (70.98%, $p=>0.99$) compared to PC12-Diff baseline. A further decrease of approximately 7.7% and 7.8%, respectively, was also seen in cells treated with a combination of NFD + GbE50 ($p=0.01$) and HFD + GbE50 ($p=0.02$) compared to just GbE50 treated cells. Interestingly, the decrease in viability seen in NFD treated cells was ameliorated when cells were additionally treated with GbE100 (NFD + GbE100; 70.67% viable, $p=0.99$), while no changes were seen in with HFD + GbE100 treatment (70.98%, $p>0.99$) compared to non-treated PC12-Diff cells.

Early Apoptosis

Illustrated in Figure 32.C, 16.3% more PC12-Diff cells were identified in early apoptosis compared to PC12-undiff cells (PC12-Undiff vs. PC12-Diff, 5.7% Vs 21.99%, $p < 0.0001$) Treatment with vehicle alone resulted in 4% less cells in early apoptosis (17.93%, $p = 0.05$) compared to PC12-Diff cells alone. While no differences in early-apoptosis were seen in GbE50 treatment (18.44%, $p = 0.24$) compared to PC12-Diff (21.99%), a 6% decrease in early apoptosis was seen in GbE100 treatment (15.95%, $p = 0.0001$). While no changes in NFD (21.63%) were seen compared to PC12-Diff, cells treated with both NFD+GbE100 had a 4.75% decrease in early apoptosis (17.24%, $p = 0.01$) while NFD+GbE50 only resulted in a partial decrease of 3.5% (18.44%, $p = 0.24$). No differences in early apoptosis were seen in cells treated with HFD (19.7%, $p = 0.77$), HFD + GbE50 (21.2%, $p > 0.99$) or HFD + GbE100 (20.32%, $p = 0.96$). Treatment with HFD + GbE100 increased early apoptosis by 4.4% compared to GbE100 treatment alone ($p = 0.02$). Similarly, NFD+GbE100 treatment increased early apoptosis by 4.4% compared to NFD treatment alone ($p = 0.02$). while treatment with NFD + GbE100 (22.5%) resulted in 5.3% less cells in early apoptosis compared to NFD + GbE50 (17.24%) treatment ($p = 0.003$).

Late Apoptosis

Illustrated in Figure 32.D, 6.3% less PC12-Diff cells were identified in late apoptosis compared to PC12-undiff cells (PC12-Undiff vs. PC12-Diff, 10.23% Vs 3.9%, $p < 0.0001$). No differences were seen between vehicle alone compared other treatments, although vehicle treated cells experienced a 5.1% increase in late apoptosis (9%, $p = 0.001$) compared to PC12-Diff alone. This might suggest that the increased percentages in late apoptotic cells in most treatment groups compared to PC12-Diff alone may be a consequence of the vehicle. Both GbE50 and GbE100 treatment appeared to partially ameliorate the effect of the vehicle as no statistical difference was seen between GbE50 (6.6%, $p = 0.59$) and GbE100 (7.4%, $p = 0.13$) compared to PC12-Diff cells, with levels between both GbE50 and GbE100 being statistically similar ($p > 0.99$). Both NFD or HFD treatment had a similar late apoptotic cell percentage of 9% and 7.4% respectively ($p = 0.95$), with levels like that of the vehicle alone treatment (NFD, $p > 0.99$; HFD, $p = 0.94$) although NFD levels were statistically increased compared to PC12-Diff ($p = 0.002$) but not in the HFD group ($p = 0.14$). Similarly, NFD + GbE50 (10.8%, $p < 0.0001$) and NFD + GbE100 (9%, $p = 0.002$) treatments showed higher amounts of cells in late apoptosis compared to PC-Diff cells. Interestingly, while the combined treatment of HFD + GbE100 resulted in 7.2% of late apoptosis cells, it did not significantly increase late apoptosis compared to PC12-Diff ($p = 0.19$), HFD treatment alone ($p > 0.99$), or GbE100 treatment alone ($p > 0.99$). HFD + GbE50 treatment however

resulted in 11.7% of cells in late apoptosis significantly higher than that of PC12-Diff cells ($p < 0.0001$), HFD treatment ($p = 0.03$) GbE50 treatment ($p = 0.01$), and HFD + GbE100 ($p = 0.02$).

Dead

Illustrated in Figure 32.E, PC12-Diff cells had 2.9% less dead cells compared to PC12-undifferentated cells (PC12-Undiff vs. PC12-Diff, 4.4% Vs 1.45%, $p < 0.0001$). An increase of 1.9% in dead cells was seen in vehicle alone treated cells (3.3%) compared to PC12-Diff cells ($p = 0.0002$). Compared to vehicle treatment, both GbE50 and GbE100 treatments ameliorated the effect of vehicle on cells (GbE50, 1.1%, $p < 0.0001$; GbE, 1.06%, $p < 0.0001$) and with the levels of dead cells for both GbE treatments comparable to that of PC12-Diff cells (GbE50, 1.1%, $p = > 0.99$; GbE100, 0.4%, $p = > 0.99$). Similarly, NFD and HFD treatments were also like that of PC12-Diff cells (NFD, 2.02%, $p = 0.94$; HFD, 2.2%, $p = 0.67$). NFD + GbE100 treatment increased the level of dead cells by 1.7% compared to PC12-Diff cells (NFD + GbE100, 3.1%, $p = 0.002$) and was similar to that of vehicle treatment alone ($p > 0.99$), while NFD + GbE50 (1.1%), HFD + GbE50 (0.92%) and HFD + GbE100 (1.5%) treatment levels remained similar to that of PC12-Diff cells, and significantly less than that of vehicle alone (NFD, $p = 0.05$, HFD, $p = 0.18$, NFD + GbE50, $p < 0.0001$; HFD + GbE50, $p < 0.0001$; HFD + GbE100, $p = 0.0004$). The combination of NFD + GbE100 also resulted in significantly more dead cells than just GbE100 treatment (GbE100, 1.06%; NFD + GbE100, 3.1%, $p < 0.0001$) which was not seen in HFD + GbE100 treatment (1.5%, $p > 0.99$). NFD + GbE100 produced significantly more dead cells than NFD + GbE50 (1.1%, $p = 0.0001$) and HFD + GbE100 (1.5%, $p = 0.003$).

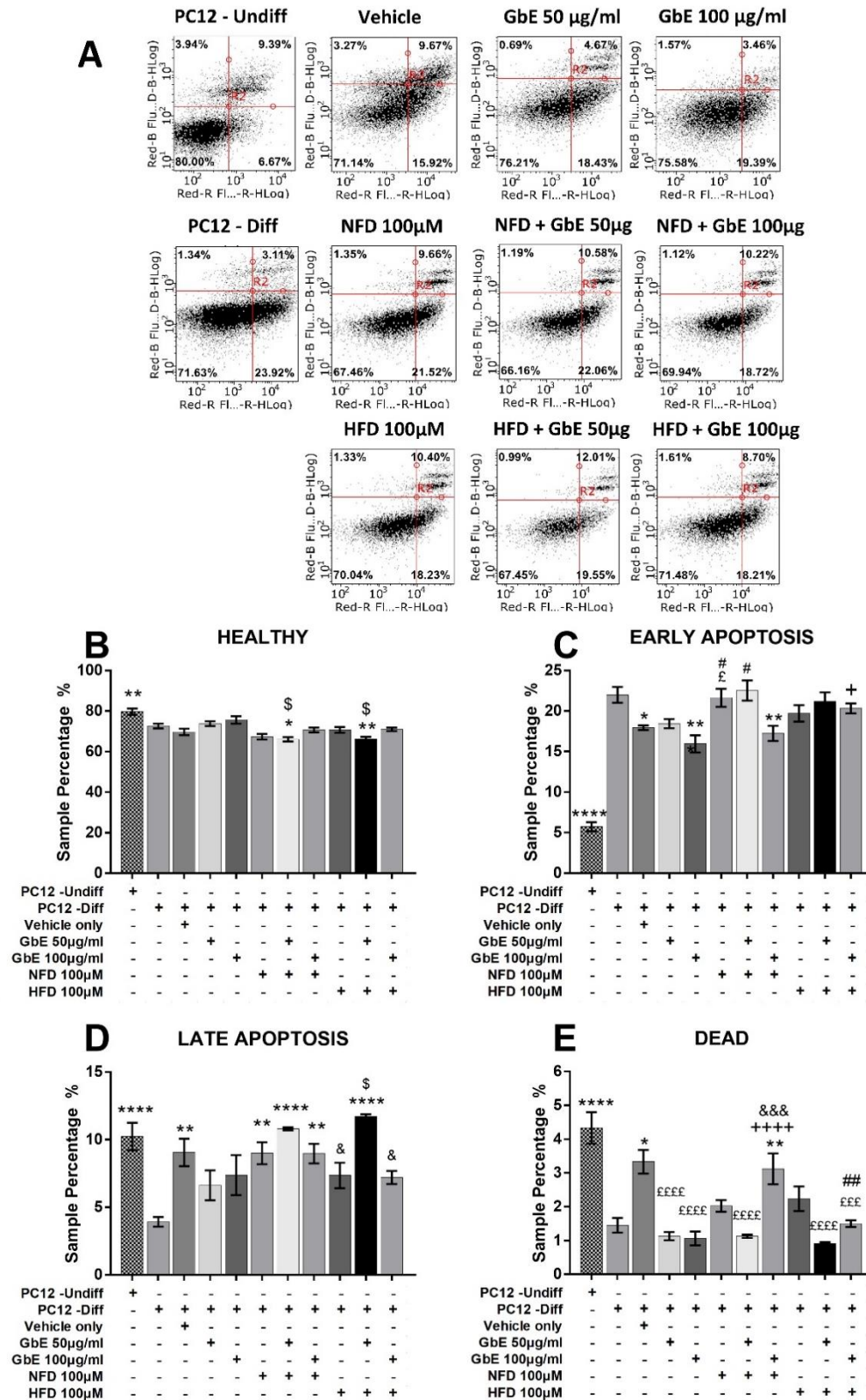


Figure 32. Annexin-V/7-AAD FACS analysis of PC12 cells. Undifferentiated (PC12 Undiff) and differentiated (PC12 diff) cells treated for 24 hours with either vehicle control (0.85% saline), Ginkgo biloba (GbE) (50 and 100ug/ml), normal fat diet fatty acid mix (NFD) or high fat diet fatty acid mix (HFD) (100uM) or various combinations. A). Representative Red/Blue (FL3) vs Red/Red (FL4) bivariate analysis after 24 hrs of treatment. Bar charts display sample percentage (%) identified as B). Healthy cells C). Early apoptosis D). Late apoptosis E). Dead. Data analysed by one-way ANOVA with Tukey post hoc test. Significance identified as * $p < 0.05$, ** $p < 0.01$, *** $p < 0.001$, **** $p < 0.0001$ vs non-treated differentiated PC12 cells; £ = Vs Vehicle; \$ = Vs GbE 50ug; + = Vs GbE 100ug; ^ = Vs HFD 100µM; & = Vs HFD + GbE 50µg; # = Vs NFD + GbE 100µg; • = Vs NFD + GbE 50µg

7.13 Cell viability of NFD, HFD and GbE treatments in H₂O₂ neuronal injury

To identify any protective effect of the pre-treatment of PC12 cell treatments with NFD and HFD FA mixes, in isolation or combined with GbE treatment, on cellular toxicity caused by 400 μ M H₂O₂ for 24 hours, Annexin V-7AAD Cell apoptosis assays were conducted as described in section 2.22. All cell samples were treated for 24 hours with either 100 μ M of NFD or HFD FA mix, GbE treatments at GbE-50 μ g/ml (GbE50) and GbE-100 μ g/ml (GbE100), or a combination of NFD or HFD with GbE, followed by a wash and media change with 24 hr treatment with 400 μ M H₂O₂. n=18 collected from a minimum of 3 passages. Representative dot plots are shown in Figure 33.A.

Healthy

As illustrated in Figure 33.B, treatment with H₂O₂-vehicle alone (H₂O) had no effect on healthy cell levels (p=0.99). Treatment with 400 μ M H₂O₂ decreased the levels of PC12-Diff healthy cells by 17.4% from 74% down to 56.6% (p<0.0001). All pre-treatments ameliorated the effect of 400 μ M H₂O₂, including vehicle control (63%, p=0.02) but to a lesser degree than other treatments including GbE50 (82%, p>0.0001), GbE100 (74.9%, p>0.0001), NFD (75%, p>0.0001), NFD+GbE50 (82.2%, p>0.0001), NFD+GbE100 (74%, p>0.0001), HFD (75.9%, p>0.0001), HFD GbE50 (80%, p>0.0001) and HFD + GbE100 (76.8%, p>0.0001). In contrast to GbE50 and HFD+GbE50 treatment which provided the most protection, NFD + GbE50 (67.3%) provided less protection against the effects of H₂O₂ treatment compared to GbE50 alone (82.2%, p>0.0001) or NFD + GbE100 (74%, p=0.0005) but not significantly less than NFD alone (75%, p=0.32).

Early Apoptosis

As illustrated in Figure 33.C, following 400 μ M H₂O₂ treatment, 18.7% of non-pre-treated PC-Diff cells were in early apoptosis compared to cells treated with 0.85% saline (Vehicle; 13.1%; p<0.0001). In contrast, cells pre-treated with 0.85% saline following by H₂O₂ experienced 21.4% of cells in early apoptosis (p=0.0001). Levels of cells in early apoptosis were comparable between non-pre-treated and vehicle-pre-treated cells treated with by H₂O₂ (p=0.99). Cells pre-treated with GbE50 ameliorated the effects of H₂O₂ treatment on early apoptosis compared to non-pre-treated PC12-Diff cells (18.7%, p<0.0001), vehicle pre-treatment (21.36%, p<0.0001) and GbE100 (18.5%, p=0.01) or NFD+GbE50 (21.2%, p=0.001). A similar amelioration of effects caused by H₂O₂ treatment was seen with HFD+GbE50 pre-treatment (12.9%, p=0.0001) which reduced cells in early apoptosis by 7.3% compared to H₂O₂ treatment alone and NFD + GbE50 (12.9%, p=0.003), with both GbE50 and HFD + GbE50 having a similar reducing effect to each other (p=0.99).

Late Apoptosis

As illustrated in Figure 33.D, cells treated with 400 μ M H₂O₂ resulted in 15.9% more cells in late apoptosis (20.1%) than no treatment (5.6%, p<0.0001). All 24 hour pre-treated cell showed a reduced percentage of late apoptosis cells compared to H₂O₂ treatment alone including vehicle (6.9%, p<0.0001), GbE50 (3.8%, p<0.0001), GbE100 (5.4%, p<0.0001), NFD (5.6%, p<0.0001), NFD + GbE50 (8.9%, p<0.0001), NFD + GbE100 (6.1%, p<0.0001), HFD (5.4%, p<0.0001), HFD + GbE50 (4%, p<0.0001), HFD + GbE100 (4.2%, p<0.0001). Except for NFD + GbE50 (p=0.53), all pre-treatments significantly reduced the number of cells in late apoptosis further following H₂O₂ treatment compared to vehicle pre-treatment alone (p<0.0001).

Dead

As illustrated in Figure 33.E, H₂O₂ treatment resulted in 1.4% more cell death (3.1%) than no treatment (1.7%, p<0.03). Following H₂O₂ treatment in pre-treated cells, less cell death was experienced compared to H₂O₂ treatment alone in the following groups: GbE100 (1.2%, p=0.01), NFD (0.91%, p=0.001), NFD + GbE100 (0.95, p=0.0004), HFD (1.3%, p=0.02), HFD + GbE50 (0.69%, p=0.001) and HFD + GbE100 (0.63%, p<0.0001). Cells pre-treated with vehicle (0.85% saline) followed by H₂O₂ vehicle (H₂O₂) experienced 3.7% more cell death than H₂O₂ treatment alone (3.1%, p<0.0001).

Overall, supplementation with the NFD-FA mixture led to a decrease in healthy cells, and increase in apoptosis, with the effects enhanced by additional supplementation of GbE50, and ameliorated with GbE100 supplementation. Less cells experienced early and late apoptosis and cell death with HFD treatments than that of NFD, respectively. This is an interesting finding considering that the HFD treatment contains more SFA. Alternatively, as the HFD mix contained more MUFA and less n-6 PUFA, this may have had some ameliorating properties around n-6 pro-inflammatory responses in the cell. To investigate this possibility further, lipid profiles following H₂O₂ treatment could be explored. Following up in these Annexin-V/7-AAD FACS analysis results which indicates a shift in phosphatidylserine orientation in the lipid membrane, the effect on NFD, HFD and GbE treatments on Akt (protein kinase B) was evaluated. Akt is also involved in the regulation of apoptosis and OS resistance.

Pre-treatments

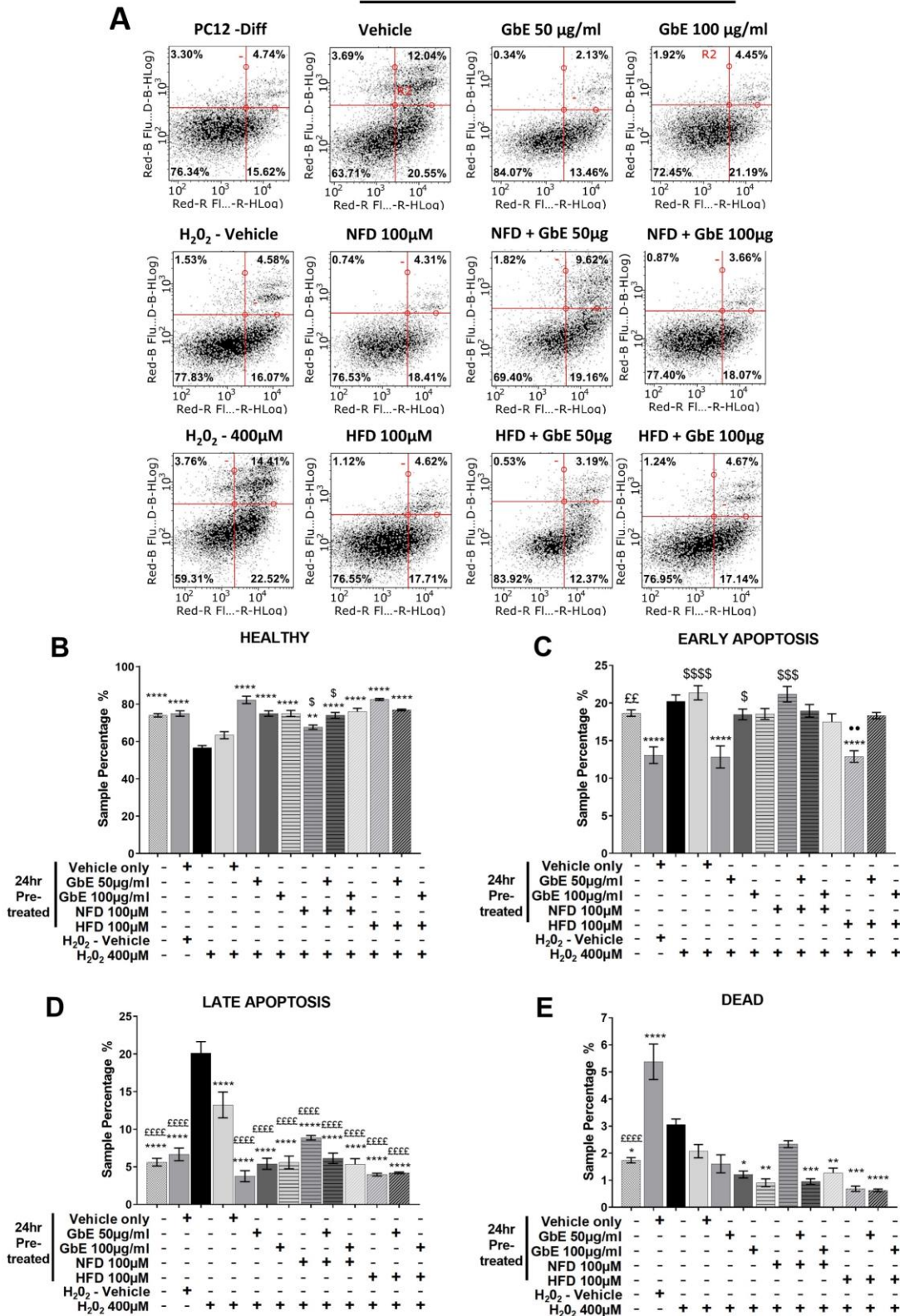


Figure 33. Annexin-V/7-AAD FACS analysis of PC12 cells treated with 400µM H₂O₂ for 24 hours. Differentiated (PC12-Diff) cells were pre-treated for 24 hours with vehicle (0.85% saline), Ginkgo biloba (GbE) (50 and 100µg/ml), normal fat diet fatty acid mix (NFD) or high fat diet fatty acid mix (HFD) (100µM) and combinations. A). Representative Red/Blue (FL3) Vs Red/Red (FL4) bivariate analysis of 24 hr treatment with 400µM H₂O₂. Bar charts display sample percentage (%) identified as B). Healthy cells C). Early apoptosis D). Late apoptosis E). Dead. Data analysed by one-way ANOVA with Tukey post hoc test. Significance identified as *p < 0.05, **p < 0.01, ***p < 0.001, ****p < 0.0001 vs non-treated differentiated PC12 cells; £ = Vs Vehicle; \$ = Vs GbE 50µg; + = Vs GbE 100µg; • = Vs NFD + GbE 50µg

7.14 NFD, HFD and GbE treatments and Akt activation

Phosphoinositides derived from the phospholipid PI are membrane phospholipids modulated by PI kinases and PI phosphatases (Sasaki *et al.*, 2009). Phosphoinositides function as both secondary messengers in signalling pathways and as docking lipids for the regulation of cellular homeostasis including cellular transport, metabolism, growth and cell death (Tariq and Luikart, 2021; Phan *et al.*, 2019). Within the nervous system, phosphatidylinositol 4,5-bisphosphate (PIP₂), and phosphatidylinositol 3,4,5-trisphosphate (PIP₃), generated from the membrane-bound phospholipid phosphatidylinositol (PI) and are predominantly found in the inner cytoplasmic leaflet of plasma membrane (di Paolo and de Camilli, 2006). Both PIP₂ and PIP₃ are involved in neuronal morphogenesis, synaptic plasticity and signal transduction. PIP₃ is generated from PIP₂ by phosphatidylinositol 3-kinase (PI3-K) induced phosphorylation at position 3 hydroxyl residue. Phosphatidylinositol 3-kinase (PI3-K) activation is stimulated by growth factors including insulin-like growth factor (IGF) and NGF (Tariq and Luikart, 2021). The activation of PIP₃ by PI3-K recruits Akt (protein kinase B) and phosphoinositide-dependent protein kinase (PDK), both pleckstrin homology (PH) domain containing proteins, to the plasma membrane (Risso *et al.*, 2015). PDK localizes to cholesterol-rich membrane rafts (Gao *et al.*, 2011) and phosphorylates Akt at threonine-308 (p-Akt(T308)) which stabilizes and initially causes renders Akt active (Kim and Chung, 2002). p-Akt(T308) is subsequently phosphorylated at serine-473 by mammalian target of rapamycin complex 2 (mTORC2) to maximal activation (Sarbasov *et al.*, 2005). mTORC2 is associated with the control of cell survival (Laplanche and Sabatini, 2012).

Akt activation is a positive regulator of PC12 cell differentiation (Kim *et al.*, 2004). It has been reported that phosphorylated Akt is localized at the tips of growth cones in NGF-treated PC12 cells (Higuchi *et al.*, 2003) with active Akt associated with increased axon calibre and branching (Markus, Zhong and Snider, 2002). Akt regulates cell growth through inhibitory GSK3 phosphorylation (Hermida, Dinesh Kumar and Leslie, 2017). Akt also indirectly activates mTORC1 through the inhibitory phosphorylation of TSC. mTORC1 is involved in cell growth, metabolism and cellular stress responses, including dendritic protein synthesis, neuronal cellular growth, synaptic plasticity (McCabe *et al.*, 2020; Takei and Nawa, 2014; Hoeffler and Klann, 2010; Jaworski and Sheng, 2006). mTORC1 is also associated with regulating lipid synthesis, storage, release and metabolism through sterol responsive element binding protein (SRBEP) (Ricoult and Manning, 2013).

Akt is also involved in the regulation of apoptosis, OS resistance through the targeting of transcription factors of forkhead box class O (FOXO) family. FOXO activity has been associated with aged-related

diseases including T2DM, AD and PD that can lead to axonal degeneration (Du and Zheng, 2021; Maiese, 2015; Zhan *et al.*, 2010). H₂O₂, a ROS and by-product of cellular metabolism and is regulated by cellular antioxidant defence mechanisms. An imbalance in ROS regulation leads to oxidative stress. Exogenous H₂O₂ is commonly used for neuronal oxidative-stress preconditioning (Lee, He and Liou, 2021; Chadwick *et al.*, 2010; Wang and Michaelis, 2010). H₂O₂, activates phosphatidylinositol-3 kinase (PI3K) and its downstream target Akt, and may promote cell survival or apoptosis (Kim *et al.*, 2011).

To begin with, we looked that baseline levels of Akt activation in differentiated PC12 cells compared to non-differentiated cells. Shown in Figure 34 the activation of Akt, shown as the ratio between phosphorylated Akt (serine 473) and total Akt is 4.2 times higher in differentiated PC12 cells (NGF) that have been treated with NGF for 7 days compared to undifferentiated cells (RPMI) ($p < 0.0001$) that received no NGF treatment. This is in keeping with previous reports that NGF stimulates Akt activation through the NGF-mediation of PI3-K on PIP₃, an upstream regulator of Akt (Tariq and Luikart, 2021; Phan *et al.*, 2019; Risso *et al.*, 2015; Gao *et al.*, 2011; Sasaki *et al.*, 2009; di Paolo and de Camilli, 2006; Sarbassov *et al.*, 2005; Kim and Chung, 2002).

In differentiated PC12 cells, Akt activation (p-Akt(S473)/Akt total) was measured following 24 hours of GbE (100 µg), NFD (100µM), GbE+NFD, HFD (100µM) and GbE+HFD pre-treatments (Figure 35) as well as pre-treated cells treated with 400 µM H₂O₂ for 24 hours and (Figure 36). As shown in Figure 35, no significant changes in Akt activation were seen after 24 hours between non-treated cells (NGF CTRL) and vehicle control ($p = 0.99$), GbE ($p = 0.49$), NFD ($p = 0.6$) or GbE+NFD ($p = 0.99$) groups. Treatment with HFD however shown in Figure 36, resulted in a significant increase of 118% ($p = 0.0001$) in p-Akt(S473)/Akt total ratio levels compared to no treatment (NGF-CTRL) which was partially ameliorated when combined with 100µg of GbE (HFD+GbE100) which showed a lesser, but still significant 55% increase ($p = 0.0001$) in p-Akt levels compared to CTRL.

After 24 hours of pre-treatment containing media was replaced with fresh media followed by 400 µM H₂O₂ for an additional 24 hours. Akt activation significantly decreased by 33% in differentiated PC12 cells following 24 hours of treatment with H₂O₂ (NGF+ H₂O₂, $p < 0.0008$) compared to no H₂O₂ treatment (NGF-CTRL). Decreases in Akt activation after H₂O₂ treatment was also seen in the vehicle control group which decreased by 24% (Vehicle+ H₂O₂, $p = 0.018$), GbE pre-treatment which decreased by 28% (GbE100 + H₂O₂, $p = 0.0004$), NFD pre-treatment which decreased by 32% (NFD+ H₂O₂, $p < 0.0005$), and GbE+NFD which decreased by 34% (GbE+ H₂O₂, $p = 0.0004$). Interestingly, p-Akt(S473)/Akt total ratio levels decreased in the HFD+H₂O₂ to 77%, comparable to levels seen in the

no-treatment group (NGF-CTRL, $p=0.37$), which equates to a 141% decrease between HFD treatment alone, and HFD+H₂O₂ ($p<0.0001$). While HFD+GbE100 p-Akt(S473)/Akt total ratio levels were higher than no-treatment, following H₂O₂ treatment (HFD+GbE100+ H₂O₂) the ratio levels decreased to 55% of levels seen in no-treatment, which equated to a 100% ($p<0.0001$) decrease between pre-treatment (HFD+GbE100) and post treatment (HFD+GbE100+ H₂O₂). No significant differences were seen between p-Akt/Akt-total ratio levels between any of the H₂O₂ treated groups.

GbE is known to increase the phosphorylation of phosphorylated IGF1R, Akt (Ser473), mTOR, PTEN and GSK3 β (Tan, 2020, Lejri, 2019). GbE has also been shown to inhibit H₂O₂-induced cell apoptosis in SH-SY5Y cells *via* inactivation of AKT, JNK, and caspase-3 (Shi *et al.*, 2009). GbE has also been shown to enhance hippocampal neurogenesis by restoring impaired phosphorylation of the transcription factor CREB and BDNF expression in β -amyloid-expressing neuroblastoma cells in a transgenic mouse model of AD (Xu *et al.*, 2007). CREB is phosphorylated by Akt, and in turn increases expression of BDNF (Esvald *et al.*, 2020; Dong *et al.*, 2018). One issue with the utilisation of exogenously produced H₂O₂ *in vitro* is the need to use one high micromolar concentration to produce OS and cellular damage which may not directly reflect endogenous low micromolar concentration produced continuously from metabolic processes. Ransy and colleagues demonstrated in Chinese hamster ovary (CHO) cells convert exogenous H₂O₂ into O₂ within a few minutes (Ransy *et al.*, 2020). The data here, which were collected after 24 hours, may have missed the initial effects of NFD, HFD and GbE treatments on Akt activity. What is interesting however, is that in the HFD treated groups, Akt activation remains elevated beyond that of the control group, despite being taken after 24 hours of treatment. As discussed in Section 1.17 a complication of obesity includes disturbed IR signalling. This has also been positively correlated with T2DM, hyperglycaemia and decreased cognition in an ageing population (Cunnane *et al.*, 2011) and with the pathogenesis of AD (Baker *et al.*, 2011; Matsuzaki *et al.*, 2010; Okereke *et al.*, 2008). IR appears to contribute to abnormal brain glucose metabolism, with upregulation of insulin receptors in AD (Frölich *et al.*, 1998; Hoyer, 1992). Microvascular complications of hyperglycaemia include low perfusion rates and increased vascular permeability attributed to abnormal proliferation of endothelial cells which can affect the BBB (Prasad *et al.*, 2014). These disturbances can also lead to an overproduction of mitochondrial superoxide and exaggerated activation of intracellular signalling cascades, including PI3-K and Akt (Huang *et al.*, 2018). This can also be accompanied with lipid peroxidation and increased formation of AGEs (Dias and Griffiths, 2014).

Future work on this would include investigating the effects of NFD, HFD and GbE treatments time-response experiments over 24 hours. Similarly, exposure of cells to more continuous sources of OS may also provide more information on overall Akt activity within the cell. Treating cells with β -amyloid to mimic AD could also be investigated in relation to the NFD, HFD and GbE treatments used here. Lipid peroxidation could also be investigated.

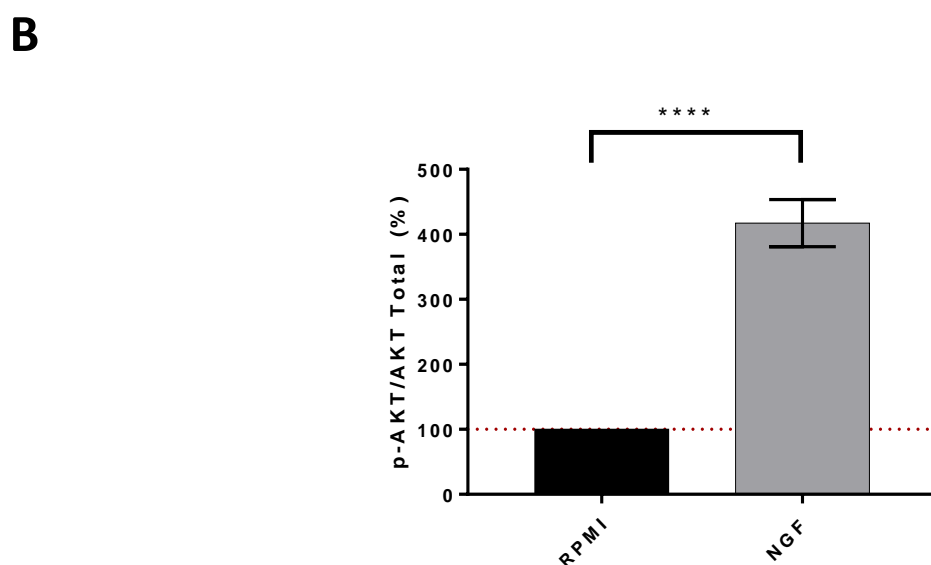
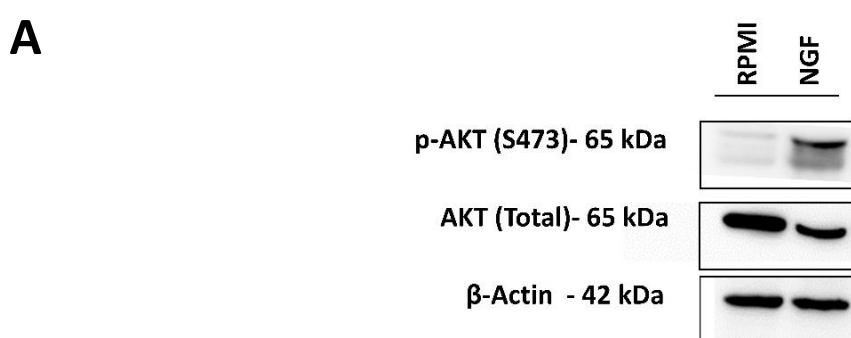
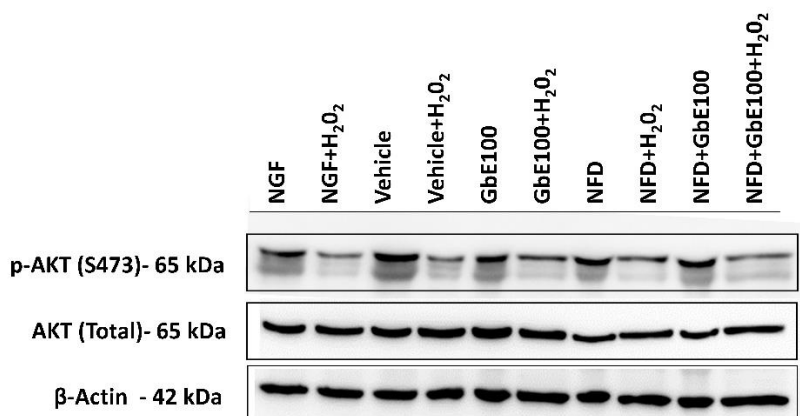


Figure 34. Effect of NGF treatment on expression of phosphorylated-Akt (Ser473) and Akt-Total in PC12 cells. A). Western blot detection of p-Akt(S473) and Akt (Total) in undifferentiated (RPMI) and NGF-differentiated (NGF, 25ng/ml for 7 days) PC12 cells. B). Semi-quantitative results of the p-Akt(S473)/Akt (Total) protein level ratio between undifferentiated and differentiated PC12 cells. Data are represented as mean \pm SEM (N=10) and analysed by two-tailed students t-test C). * $p < 0.05$, ** $p < 0.01$, *** $p < 0.001$, **** $p < 0.0001$.

A



B

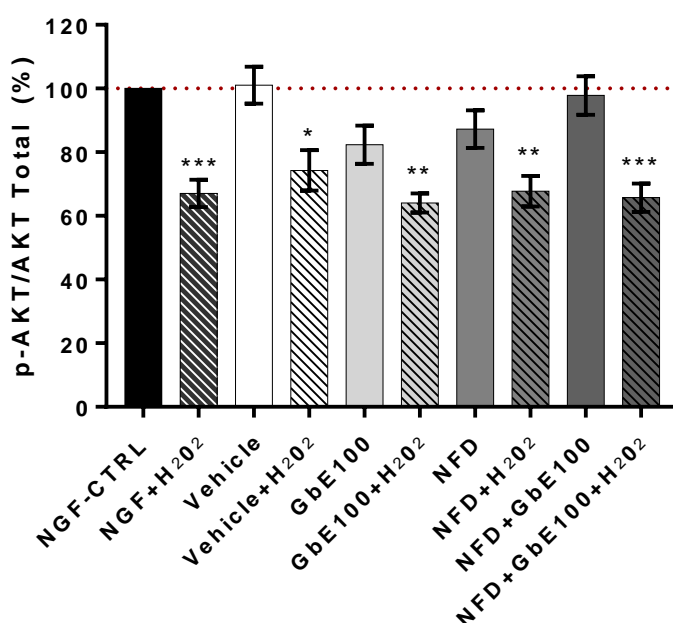


Figure 35. Effect of normal fat diet (NFD) fatty acid supplementation and standardised Ginkgo biloba (GbE) treatment on expression of phosphorylated-Akt (Ser473) and Akt-Total. A). Western blot detection of p-Akt (S473) and Akt (Total) in undifferentiated (RPMI) and NGF-differentiated (NGF, 25ng/ml for 7 days) PC12 cells, and differentiated PC12 cells pre-treated for 24 hours with vehicle (0.85% saline), GbE (100ug/ml) and/or normal fat diet fatty acid mix (NFD, 100uM) and subsequently treated for 24 hours with 400µM H₂O₂. B). Semi-quantitative results of the p-Akt(S473)/Akt (Total) protein level ratio for differentiated PC12 cells with pre-treatments and H₂O₂ exposure. Data are represented as mean±SEM (N=5). Data analysed by one-way ANOVA with Tukey Post Hoc test. **p* < 0.05, ***p* < 0.01, ****p* < 0.001, *****p* < 0.0001 vs non-treated differentiated PC12 cells (NGF-CTRL).

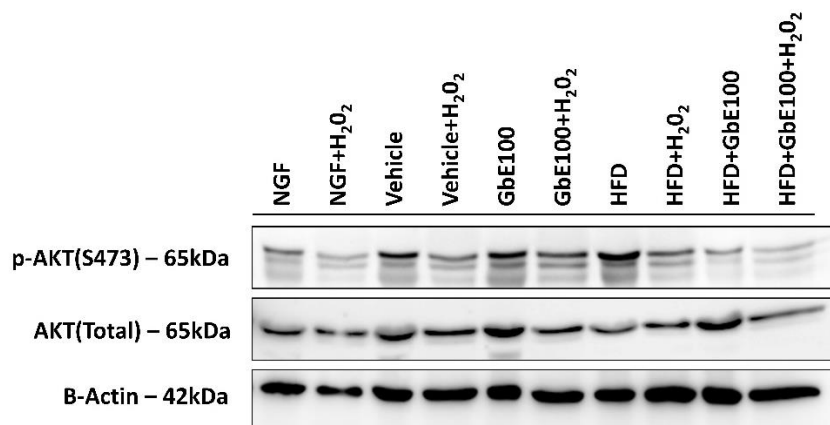
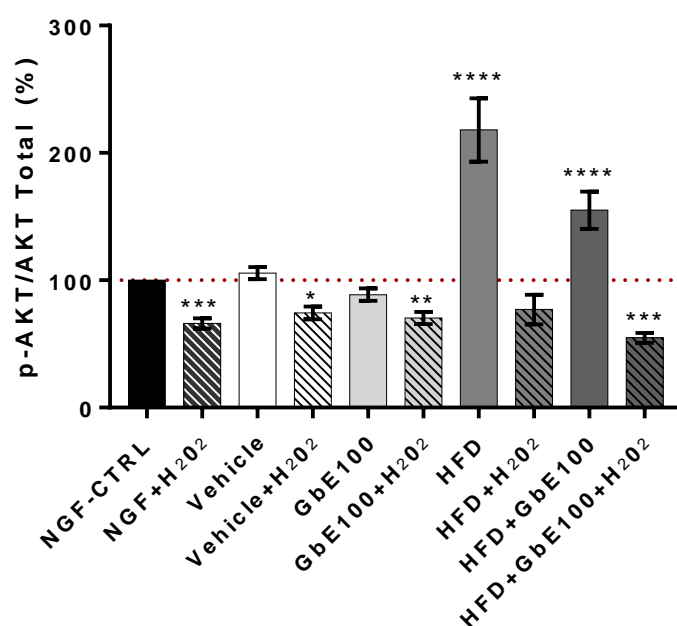
A**B**

Figure 36. Effect of high fat diet (HFD) fatty acid supplementation and standardised Ginkgo biloba (GbE) treatment on expression of phosphorylated-Akt (Ser473) and Akt-Total. A). Western blot detection of p-Akt (S473) and Akt (Total) in undifferentiated (RPMI) and NGF-differentiated (NGF, 25ng/ml for 7 days) PC12 cells, and differentiated PC12 cells pre-treated for 24 hours with vehicle (0.85% saline), GbE (100ug/ml) and/or HFD fatty acid mix (HFD, 100uM) and subsequently treated for 24 hours with 400µM H₂O₂. B). Semi-quantitative results of the p-Akt(S473)/Akt (Total) protein level ratio for differentiated PC12 cells with pre-treatments and H₂O₂ exposure. Data are represented as mean±SEM (N=2). Data analysed by one-way ANOVA with Tukey Post Hoc test. * $p < 0.05$, ** $p < 0.01$, *** $p < 0.001$, **** $p < 0.0001$ vs non-treated differentiated PC12 cells (NGF-CTRL).

7.15 NFD, HFD and GbE treatments and Nrf2 protein expression

Other downstream metabolic switches have all been recently implicated in AD, including the mTOR, GSK3 and the antioxidant Nrf2 and the predominantly pro-inflammatory molecule NF- κ B (Ahmed *et al.*, 2017; Mazzanti and Di Giacomo, 2016; Shen *et al.*, 2016; Csiszár *et al.*, 2015). Nrf2 modulates cellular responses to OS, with levels moderated by the intensity of OS experienced. Nrf2 is activated by OS, allowing its translocation to the nucleus where it facilitates the transcription of antioxidant and Phase 2 detoxifying enzymes that combat OS (Villeneuve, Lau and Zhang, 2010). Nrf2 is a major regulator in cellular and organismal defence by regulating stress-inducible activation of multiple cytoprotective genes (Liu, Locascio and Doré, 2019; Cuadrado *et al.*, 2018; Yamamoto, Kensler and Motohashi, 2018; Ma, 2013). Nrf2 is involved in regulating the transcription of detoxifying and antioxidant enzymes that counteract OS, and binds to the ARE region of DNA, a binding region it competes against the pro-inflammatory NF- κ B molecule for.

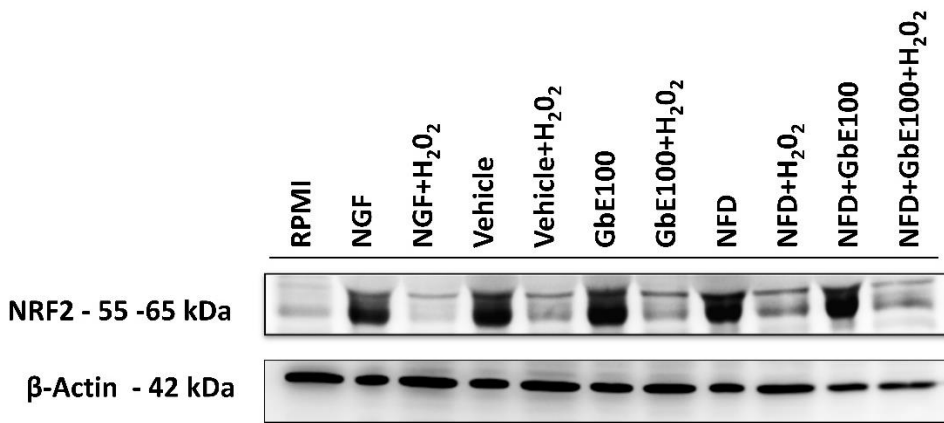
Nrf2 may be upregulated by multiple polyphenols and has been shown to reduce activity of pro-inflammatory NF- κ B which is regulated by the Akt signalling pathways (Wagner, Terschluesen and Rimbach, 2013). Research has shown that both resveratrol and GbE are both capable of upregulating the expression of Nrf2 (Liu, Locascio and Doré, 2019; Hsu *et al.*, 2009; Liu *et al.*, 2007; Yao *et al.*, 2007; Andreadi *et al.*, 2006; Ishunina, Kamphorst and Swaab, 2004). GbE specifically has been shown to activate the Nrf2-Keap1-ARE antioxidant cell defence signalling pathway (Singh *et al.*, 2019; Ahmed *et al.*, 2017; Huang *et al.*, 2013; Serrano-García *et al.*, 2013; Hsu *et al.*, 2009; Liu *et al.*, 2007; Andreadi *et al.*, 2006; Ishunina, Kamphorst and Swaab, 2004). Resveratrol, a structurally similar compound to numerous chemicals found in GbE, has similarly shown to restore Nrf2 levels in the brain (Kumar *et al.*, 2011). Resveratrol has also been shown to attenuate cytotoxicity from A β 1-42 by upregulating Heme Oxygenase-1 *via* the PI3K/Akt/Nrf2 Pathway (Hui *et al.*, 2018).

To build on the previous findings Nrf2 protein expression was investigated in NFD, HFD and GbE treatments. To begin with, a baseline of Nrf2 levels between undifferentiated and differentiated PC12 cells was investigated. As shown in Figure 37.A and Figure 37.B, following PC12 differentiation for 7 days with NGF, Nrf2 protein expression increased 3.7 fold ($p < 0.0001$). In differentiated PC12 cells, Nrf2 expression was compared against non-treated differentiated cells (RPMI) and after 24 hours of treatment with GbE (100 μ g), NFD (100 μ M) and GbE+NFD pre-treatments (Figure 37.C) as well as pre-treated cells additionally treated with 400 μ M H₂O₂ for 24 hours. As shown in Figure 37.C, no significant change in Nrf2 expression was seen after 24 hrs of treatment between the non-treated

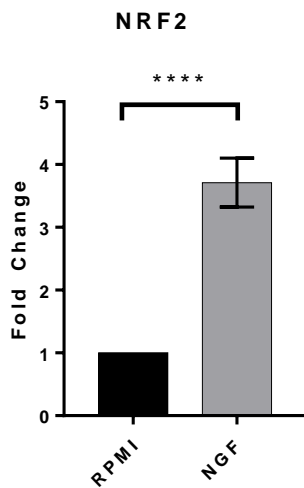
cells (NGF CTRL), vehicle control ($p > 0.99$), GbE ($p > 0.99$), NFD ($p > 0.99$) and GbE+NFD ($p > 0.99$) treated groups. Significant decrease of 69.5% in Nrf2 protein expression was seen in differentiated PC12 cells following 400 μM H_2O_2 treatment for 24 hours (NGF+ H_2O_2 , $p = 0.009$) compared to no treatment (NGF-CTRL). This decrease was similarly observed in the 66% decrease in vehicle control+ H_2O_2 ($p < 0.0001$), and the 66% decrease in GbE+ H_2O_2 ($p < 0.0001$) (Figure 37.C). In cells treated with a NFD and HFD compared to non-treated cells (NGF-CTRL) a decrease of 64% was seen in the HFD+ H_2O_2 ($p < 0.0001$, (Figure 38.C) while GbE+NFD+ H_2O_2 ($p < 0.0001$, (Figure 37.C) decreased by 56%. NFD treatment showed partial amelioration of the effects H_2O_2 on Nrf2 protein expression with a lesser decrease of 39% (NFD+ H_2O_2 , $p = 0.03$) and 38% (GbE+NFD+ H_2O_2 , $p = 0.04$) respectively (Figure 37.C), compared to non-treated control cells. This resulted in a significant difference between Nrf2 levels between non-pre-treated PC12 cells following H_2O_2 treatment and that of both NFD+ H_2O_2 ($p = 0.005$) and GbE+NFD+ H_2O_2 ($p = 0.004$) treated groups (Figure 37.C).

Like that discussed regarding Akt activation, as this data was collected from cells after 24 hours of treatment, future work on Nrf2 could include investigating the effects of NFD, HFD and GbE treatments time-response experiments over 24 hours. Subtle changes in Nrf2 levels may be more apparent closer to the initial treatment time. Phosphorylated levels of Nrf2 could also be explored, to show its effect of treatments on activation. Similarly, exposure of cells to more continuous sources of OS may also provide more information on overall Nrf2 activity within the cell and the effects of NFD, HFD and GbE treatments. The effect of β -amyloid on Nrf2 activity could also be investigated in relation to the NFD, HFD and GbE treatments.

A



B



C

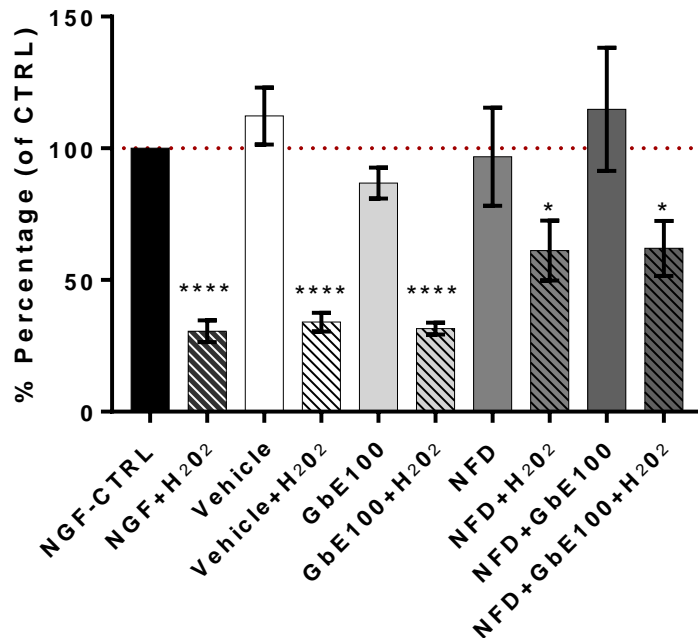
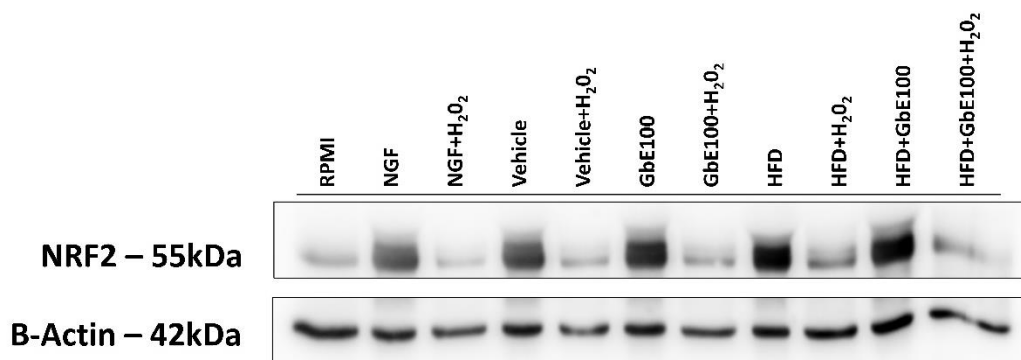
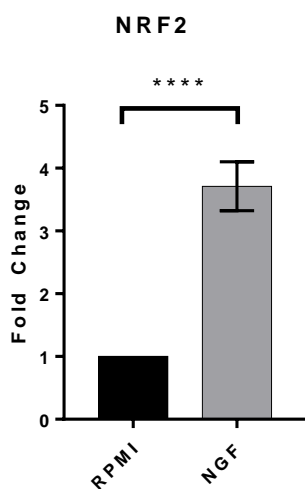


Figure 37. Effect of normal fat diet (NFD) fatty acid supplementation and standardised Ginkgo biloba (GbE) treatment on expression of NF-E2-related factor 2 (Nrf2). A). Western blot detection of Nrf2 in undifferentiated (RPMI) and NGF-differentiated (NGF, 25ng/ml) PC12 cells, and differentiated PC12 cells pre-treated for 24 hours with vehicle (0.85% saline), GbE (100ug/ml) and/or normal fat diet fatty acid mix (NFD, 100uM) and subsequently treated for 24 hours with 400 μ M H₂O₂. B). Semi-quantitative results of Nrf2 protein levels between undifferentiated and differentiated PC12 cells. C). Semi-quantitative results of Nrf2 protein levels for differentiated PC12 cells with pre-treatments and H₂O₂ exposure. Data are represented as mean \pm SEM from six experiments. Data analysed by One-way ANOVA with Tukey Post Hoc test. ****P < 0.0001 vs control group (NGF-CTRL).

A



B



C

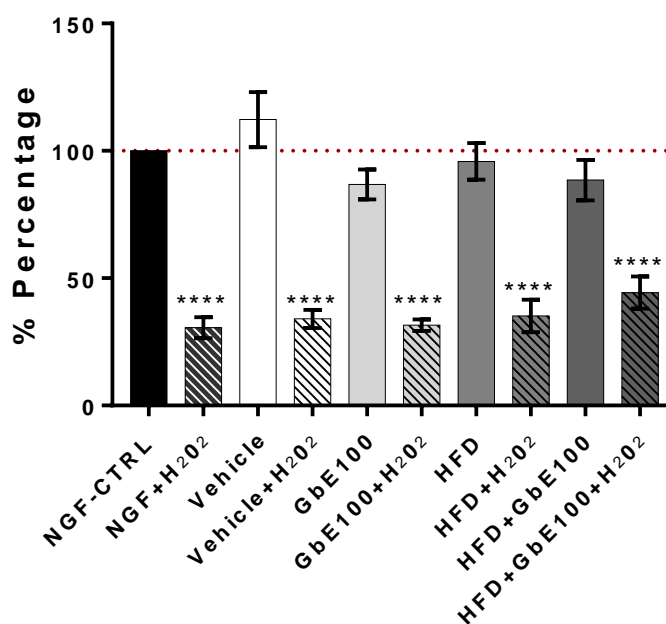


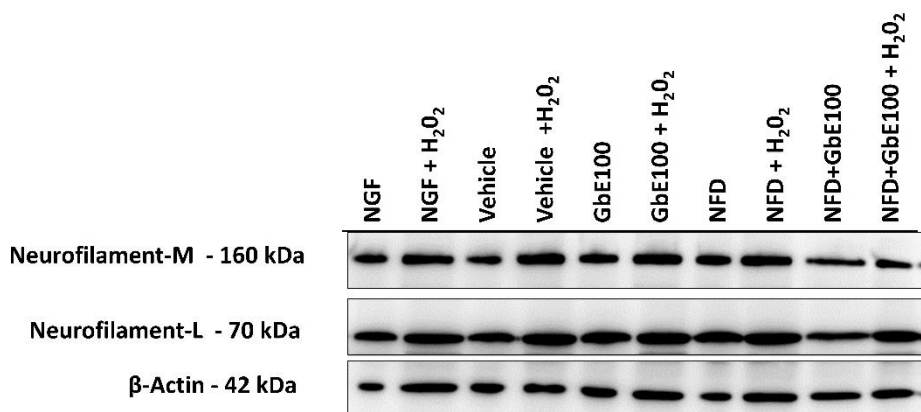
Figure 38. Effect of high fat diet (HFD) fatty acid supplementation and standardised Ginkgo biloba (GbE) treatment on expression of NF-E2-related factor 2 (Nrf2). A). Western blot detection of Nrf2 in undifferentiated (RPMI) and NGF-differentiated (NGF, 25ng/ml) PC12 cells, and differentiated PC12 cells pre-treated for 24 hours with vehicle (0.85% saline), GbE (100ug/ml) and/or high fat diet fatty acid mix (HFD, 100uM) and subsequently treated for 24 hours with 400µM H₂O₂. B). Semi-quantitative results of Nrf2 protein levels between undifferentiated and differentiated PC12 cells. C). Semi-quantitative results of Nrf2 protein levels for differentiated PC12 cells with pre-treatments and H₂O₂ exposure. Data are represented as mean±SEM from six experiments. Data analysed by One-way ANOVA with Tukey Post Hoc test. ****P < 0.0001 vs control group (NGF-CTRL).

7.16 Effect of NFD, HFD and GbE treatment on neurofilament levels

Fatty acid-binding proteins (FABPs) reversibly bind FAs and facilitate their transport intracellularly to compartments such as the nucleus, mitochondria, peroxisomes, and the ER. Epidermal FABP (E-FABP/FABP5) is expressed in embryonic stages and stem cell differentiation into motor neurons (Falomir-Lockhart *et al.*, 2019; Liu *et al.*, 2010) and facilitates PPL synthesis by transporting LCFA (Falomir-Lockhart *et al.*, 2019). E-FABP also facilitates differentiation and neuronal survival after injury (Wang *et al.*, 2021; Figueroa *et al.*, 2016; Yu *et al.*, 2012) through FA transport and its high affinity to retinoic acid that activates PPAR β/δ (Falomir-Lockhart *et al.*, 2019; Senga *et al.*, 2018; Yu *et al.*, 2012; Schug *et al.*, 2007). Liu and colleagues (2008) reported that Epidermal FABP (E-FABP/FABP5), controlled by mitogen-activated protein kinase kinase (MEK), is highly expressed in NGF-treated differentiating P12 cells. They found that cells treated with DHA, EPA and AA exhibited increased neurite length, but not increased E-FABP mRNA levels (Liu *et al.*, 2008). This may somewhat explain the increase in NF-L in both NFD and HFD treated cells compared to control cells as shown in Figure 39 and Figure 40.

A single treatment of 400 μ M hydrogen peroxide did not significantly decrease neurofilament levels compared to controls. As previously mentioned, neurofilaments such as NF-L, are used as biomarkers in diseases involved in cognitive decline including ALS, AD, frontotemporal dementia and Huntington's disease, with increased levels associated with severity of disease (Lee *et al.*, 2022; Behzadi *et al.*, 2021; Ingannato *et al.*, 2021; Moscoso *et al.*, 2021; Verde, Otto and Silani, 2021; Benedet *et al.*, 2020; Forgrave *et al.*, 2019; Gille *et al.*, 2019; Kern *et al.*, 2019; Gaiani *et al.*, 2017; Deng *et al.*, 2009). For future experiments, longer more consistent exposure to hydrogen peroxide, consistent with *in vivo* low-grade inflammation could be explored in a time-dependent manner to further evaluate the effect of NFD, HFD and GbE treatments on neurofilament levels during times of oxidative stress.

A



B

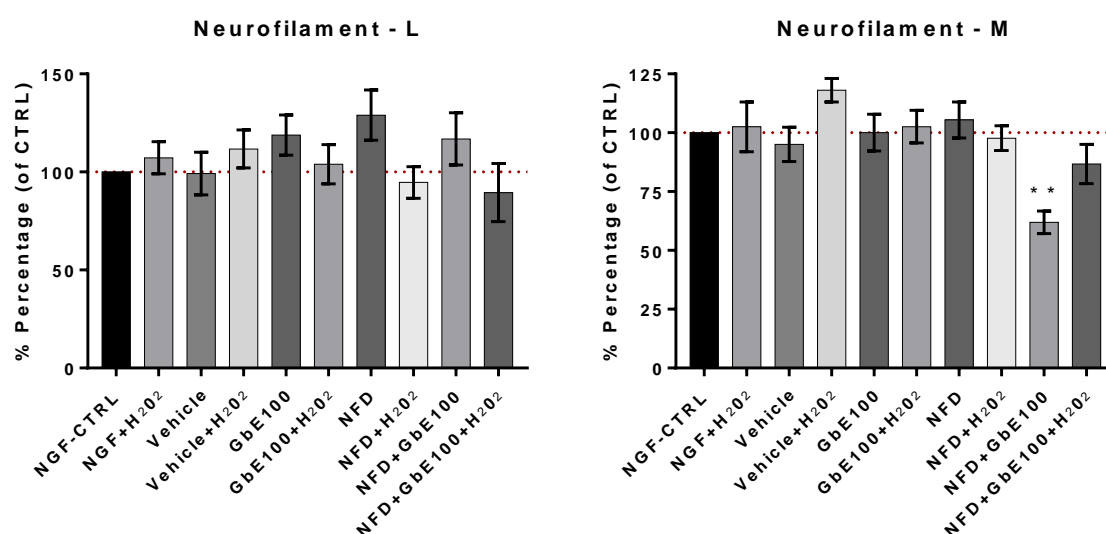
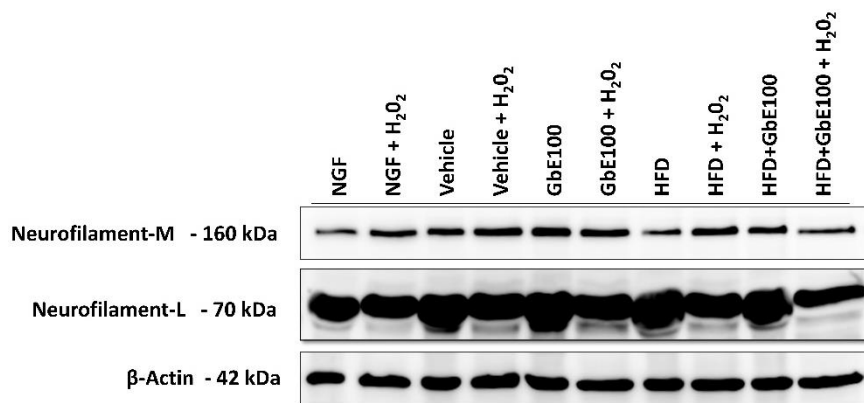


Figure 39. Effect of normal fat diet (NFD) fatty acid supplementation and standardised Ginkgo biloba (GbE) treatment on expression of neurofilament-L (NF-L) and neurofilament-M (NF-M). A). Western blot detection of Nrf2 in undifferentiated (RPMI) and NGF-differentiated (NGF, 25ng/ml) PC12 cells, and differentiated PC12 cells pre-treated for 24 hours with vehicle (0.85% saline), GbE (100ug/ml) and/or normal fat diet fatty acid mix (NFD, 100uM) and subsequently treated for 24 hours with 400 μ M H₂O₂. B). Semi-quantitative results of NF-L and NF-M protein levels between undifferentiated and differentiated PC12 cells. C). Semi-quantitative results of NF-L and NF-M protein levels for differentiated PC12 cells with pre-treatments and H₂O₂ exposure. Data are represented as mean \pm SEM from six experiments. Data analysed by One-way ANOVA with Tukey Post Hoc test, ** $p < 0.01$, vs non-treated differentiated PC12 cells (NGF-CTRL).

A



B

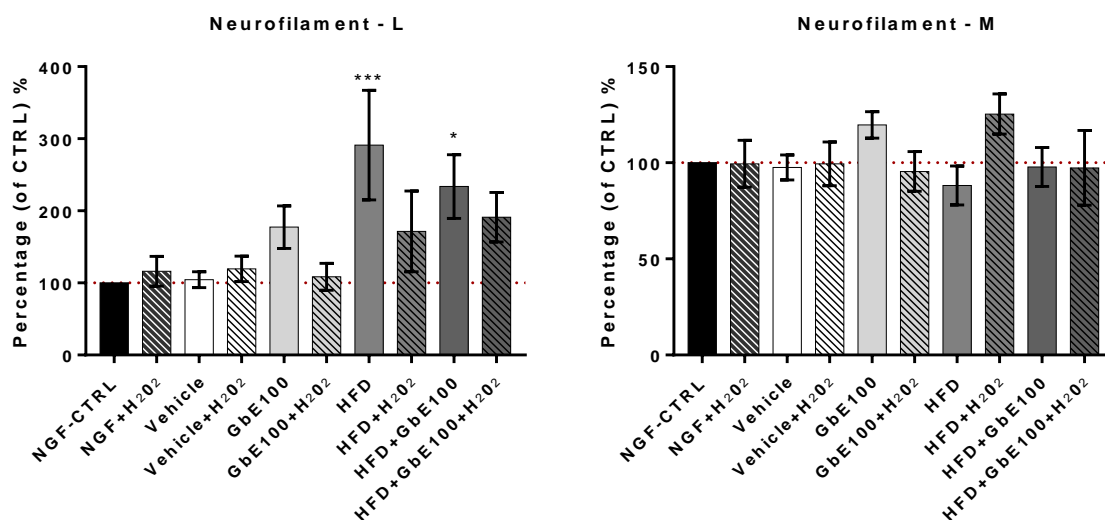


Figure 40. Effect of high fat diet (NFD) fatty acid supplementation and standardised Ginkgo biloba (GbE) treatment on expression of neurofilament-L (NF-L) and neurofilament-M (NF-M). A). Western blot detection of NF-L and NF-M in undifferentiated (RPMI) and NGF-differentiated (NGF, 25ng/ml) PC12 cells, and differentiated PC12 cells pre-treated for 24 hours with vehicle (0.85% saline), GbE (100ug/ml) and/or normal fat diet fatty acid mix (NFD, 100uM) and subsequently treated for 24 hours with 400µM H₂O₂. B). Semi-quantitative results of NF-L and NF-M protein levels between undifferentiated and differentiated PC12 cells. C). Semi-quantitative results of NF-L and NF-M protein levels for differentiated PC12 cells with pre-treatments and H₂O₂ exposure. Data are represented as mean±SEM from six experiments. Data analysed by One-way ANOVA with Tukey Post Hoc test. * $p < 0.05$, *** $p < 0.001$ vs non-treated differentiated PC12 cells (NGF-CTRL).

7.17 The effect of PC12 differentiation on cellular total lipid profiles

PC12 cells (1×10^5) were treated for 7 days with either RPMI (15% serum/complete) media (RPMI), 1% BSA media (BSA) or 1% BSA media with 25ng NGF (BSA+NGF) for 7 days. Following 7 days of NGF treatment and total cellular lipids extracted by Folch method as previously described in Chapter 2, methylated and the total FA profile analysed by GC-FID. Data is shown in Table 80 and Table 81.

The data in Table 80 shows that SFA percentage levels decreased from 47.8% seen in RPMI to 39.1% in BSA ($p=0.004$ vs RPMI) but increased to 57.2% in BSA-NGF ($p<0.0001$ vs RPMI) treatment, largely due to the significant increase of C18:0 to 57% ($p<0.0001$) in the BSA+NGF groups compared to the 13.1 and 13.6% seen in the RPMI and BSA groups respectively. In an opposite fashion, MUFA levels increased from 34.2% in RPMI samples to 43.6% in BSA samples ($p=0.02$ vs RPMI) but decreased to 29.4% in BSA+NGF samples ($p=0.31$ vs RPMI, $p=0.001$ vs BSA). Of particular interest, PUFA levels decreased from 5.4% in RPMI cells to 13.5% in BSA ($p=0.02$ vs RPMI) and 9.9% in BSA+NGF ($p<0.0001$ vs RPMI; $p=0.02$ vs BSA) (Table 80).

While n-6 PUFA levels nearly halved from 11.4% in RPMI samples, to 6.8% in BSA ($p=0.001$ vs RPMI) and 6.6% in BSA+NGF ($p=0.0001$ vs RPMI) samples, this was largely due to the decreases in LA (C18:2n-6) in both BSA and BSA+NGF groups but also decreased AA (C20:4n-6) in the BSA+NGF group. Interestingly, C18:3n-3 increased from 3.1% in RPMI to 5.6% in BSA samples ($p=0.003$ vs RPMI), but not in BSA+NGF samples (2.8%, $p=0.92$ vs RPMI). n-3 metabolites decreased from 2.3% in RPMI to 1.2% in BSA ($p=0.002$ vs RPMI) and 0.5% in BSA+NGF ($p<0.0001$ vs RPMI; $p=0.0001$ vs BSA) largely due to changes in DHA (C22:6n-3) which decreased from 1.8% in RPMI to 1.2% in BSA ($p=0.02$ vs RPMI) and 0.5% in BSA+NGF ($p<0.0001$ vs RPMI; $p=0.02$ vs BSA). Overall while UFA increased from 51% in RPMI samples to 57.1% in BSA samples ($p<0.12$ vs RPMI), levels decreased to 39.3% in BSA+NGF ($p=0.003$ vs RPMI) (Table 80).

This data is consistent with the work of Msika and colleagues (2012), that found when PC12 cells under normal proliferating conditions in 15% serum media, both ALA and LA metabolic conversion differs. They found that ALA conversion to EPA and DHA was much more active than that of LA to AA in proliferating cells. PC12 cells undergoing NGF differentiation however are unable to perform this conversion to higher PUFA (Msika *et al.*, 2012). Msika and colleagues reported that PUFA deficiency may occur due to a lack of fatty acids present in the media. Despite this they found that PUFA deficiency did not affect NGF differentiation, with neural outgrowth and morphology unaffected, even when additional supplementation of LA or ALA was added to the media. Furthermore, they also

reported that when NGF-treated cells were supplemented with ALA, the cells were unable to elongate and desaturate past 20-hydrocarbon-long to EPA to DHA. This was also corroborated with EPA and LA supplementation that also showed no further elongation/desaturation past C20 hydrocarbon chains (Msika *et al.*, 2012). Together this suggested a change in elongase 2 (ELOVL2) regulation due to NGF treatment, which has also been shown to be involved in DHA regulation in the peroxisome (Igarashi *et al.*, 2008; Wang *et al.*, 2005), while Msika and colleagues also reported ELOVL5 upregulation by NGF (Msika *et al.*, 2012).

Table 80. PC12 fatty acid methyl esters (FAME) for RPMI complete media, 1% BSA media and 1% BSA media supplemented with nerve growth factor (NGF). N=8 per group. Fatty acid results are presented as area % percentage mean and standard error of the mean (SEM), and statistically analysed by one-way ANOVA with Tukey's Post-hoc test. The level of statistical significance was set at * $p < 0.05$.

	RPMI complete		1% BSA Media		1% BSA Media + NGF		RPMI VS BSA	RPMI VS NGF	BSA vs NGF
	MEAN %	SEM	MEAN %	SEM	MEAN %	SEM	p value	p value	p value
C16:0	24.4	± 1.0	21.3	± 0.2	21.9	± 1.0	0.03	0.11	0.86
C17:0	0.2	± <0.1	0.2	± <0.1	0.3	± <0.1	0.9	0.2	0.1
C18:0	13.6	± 0.4	13.1	± 0.4	30.2	± 1.3	0.89	<0.0001	<0.0001
C20:0	0.8	± 0.1	0.7	± 0.2	2.0	± 0.2	0.97	0.001	0.0003
C22:0	0.5	± 0.1	0.2	± 0.1	0.8	± 0.1	0.009	0.03	<0.0001
ΣSFA.DMA	3.8	± 0.1	2.1	± <0.1	2.0	± 0.2	<0.0001	<0.0001	0.85
ΣSFA	47.8	± 2.0	39.1	± 0.6	57.2	± 2.1	0.004	0.003	<0.0001
C16:1n-7	1.0	± 0.2	1.7	± 0.0	0.3	± <0.1	0.0003	0.001	<0.0001
C18:1n7	5.6	± 0.7	7.8	± 0.2	2.9	± 0.3	0.008	0.003	<0.0001
C18:1n-9	21.6	± 0.9	24.2	± 0.6	16.0	± 1.3	0.16	0.001	<0.0001
C20:1n-9	1.0	± <0.1	1.2	± 0.1	2.0	± 0.4	0.82	0.03	0.08
C20:1n-11	1.1	± 0.2	2.2	± 0.5	2.3	± 0.8	0.38	0.35	0.99
C20:3n-9	1.8	± 0.4	4.0	± 0.1	1.2	± 0.3	0.0001	0.31	<0.0001
C24:1n-9	1.0	± 0.1	1.6	± <0.1	0.8	± 0.1	0.001	0.32	0.0001
DMA 18:1	0.5	± 0.3	0.4	± 0.2	3.9	± 0.5	0.97	<0.0001	<0.0001
DMA 18:1 Total	1.5	± 0.4	1.9	± 0.2	4.8	± 0.5	0.67	<0.0001	0.0001
C18:1 Total	27.2	± 1.6	32.0	± 0.7	18.9	± 1.6	0.045	0.0009	<0.0001
ω7	6.5	± 0.9	9.6	± 0.2	3.2	± 0.3	0.004	0.002	<0.0001
ω9	27.2	± 1.5	33.6	± 1.1	22.3	± 2.0	0.02	0.09	0.0001
ΣMUFA	34.2	± 2.7	43.6	± 1.2	29.4	± 2.6	0.02	0.31	0.001
C18:2n-6	5.8	± 0.8	1.0	± 0.3	1.8	± 0.1	<0.0001	0.0001	0.53
C18:3n-6	0.1	± 0.1	0.8	± 0.3	1.3	± 0.4	0.20	0.02	0.38
C20:3n-6	1.6	± 0.1	0.7	± 0.1	0.7	± 0.4	0.04	0.04	0.99
C20:4n-6	3.6	± 0.8	3.4	± 0.1	1.4	± 0.2	0.96	0.02	0.04
C22:4n-6	0.2	± 0.2	0.9	± 0.1	0.8	± 0.2	0.01	0.03	0.96
n-6 PUFA	11.4	± 1.1	6.8	± 0.3	6.6	± 0.7	0.001	0.001	0.99
Σ6 metabolites	5.6	± 0.8	5.8	± 0.2	4.8	± 0.7	0.98	0.65	0.53
C18:3n-3	3.1	± 0.4	5.6	± 0.5	2.8	± 0.5	0.003	0.92	0.002
C20:5n-3	0.2	± <0.1	-	± -	-	± -			
C22:5n-3	0.3	± 0.1	-	± -	-	± -			
C22:6n-3	1.8	± 0.2	1.2	± 0.2	0.5	± 0.1	0.02	<0.0001	0.02
n-3 PUFA	5.4	± 0.3	6.8	± 0.5	3.3	± 0.5	0.08	0.01	0.0001
Σn-3 metabolites	2.3	± 0.3	1.2	± 0.2	0.5	± 0.1	0.002	<0.0001	0.11
ΣPUFA	16.8	± 1.1	13.5	± 0.4	9.9	± 0.9	0.02	<0.0001	0.02
ΣUFA	51.0	± 2.0	57.1	± 1.1	39.3	± 3.1	0.12	0.003	<0.0001

Table 81. PC12 fatty acid methyl ester (FAME) ratios for RPMI complete media, 1% BSA media and 1%BSA media supplemented with nerve growth factor (NGF) (N=8 per group). Results are presented as mean and standard error of the mean (SEM), and statistically analysed by one-way ANOVA with Tukey's Post-hoc test. The level of statistical significance was set at * $p < 0.05$.

	RPMI complete			1% BSA Media			1% BSA Media + NGF			RPMI VS BSA	RPMI VS NGF	BSA vs NGF
	MEAN %	SEM		MEAN %	SEM		MEAN %	SEM		p value	p value	p value
MUFA/PUFA	2.2	±	0.3	3.3	±	0.2	3.0	±	0.3	0.01	0.05	0.84
MUFA/SFA	2.9	±	0.2	2.9	±	0.1	6.1	±	0.7	>0.99	<0.0001	<0.0001
PUFA/SFA	0.4	±	<0.1	0.3	±	<0.1	0.2	±	<0.1	0.95	<0.0001	<0.0001
UFA/SFA	1.1	±	0.1	1.5	±	<0.1	0.7	±	0.1	0.008	0.007	<0.0001
C18:0/C16:0	0.6	±	<0.1	0.6	±	<0.1	1.4	±	<0.1	0.36	<0.0001	<0.0001
C16:1n-7/C16:0	<0.1	±	<0.1	0.1	±	<0.1	<0.1	±	<0.1	0.002	0.006	<0.0001
C18:1n-9/C16:0	0.9	±	0.1	1.1	±	<0.1	0.8	±	0.1	0.07	0.31	0.003
C18:1n-9/C16:1n-7	25.3	±	2.4	14.0	±	0.4	54.3	±	4.5	0.02	<0.0001	<0.0001
C18:1n-7/C18:0	0.4	±	0.1	0.6	±	<0.1	0.1	±	<0.1	0.02	0.0003	<0.0001
C18:1/C18:0	2.0	±	0.2	2.5	±	0.1	0.6	±	0.1	0.07	<0.0001	<0.0001
n6/n3	2.2	±	0.3	1.1	±	0.1	2.6	±	0.8	0.17	0.81	0.06
C18:3n-6/C18:2n-6	0.1	±	<0.1	0.4	±	0.5	0.8	±	0.3	0.74	0.24	0.61
C20:3n-6/C18:3n-6	2.4	±	0.7	0.6	±	0.3	0.3	±	0.2	0.01	0.005	0.83
C22:4n-6/C20:4n-6	3.8	±	0.1	3.9	±	0.3	2.1	±	0.4	0.97	0.045	0.001
1 (% monoenoics)	34.2	±	2.7	43.6	±	1.2	29.4	±	2.6	0.02	0.31	0.0007
2 (% dienoics)	11.7	±	1.7	1.9	±	0.5	4.7	±	0.3	<0.0001	0.0005	0.20
3 (% trienoics)	5.3	±	0.3	4.5	±	0.6	6.0	±	2.4	0.89	0.93	0.70
4 (% tetraenoics)	15.3	±	3.4	17.2	±	0.5	9.1	±	1.7	0.83	0.16	0.05
5 (% pentaenoics)	2.3	±	0.6	<0.1	±	<0.1	0.4	±	0.2	0.0003	0.002	0.74
6 (% hexaenoics)	11.0	±	1.1	7.0	±	1.1	2.8	±	0.7	0.02	<0.0001	0.02
Unsaturation Index	79.9	±	3.2	74.2	±	2.4	52.3	±	3.9	0.42	<0.0001	0.0003

7.18 The effect of NFD, HFD and GbE treatments on cellular total lipid profiles

PC12 cells were treated with either NFD100 or HFD100, GbE50 or GbE100 or a mixture of both for 24 hours. Total, cellular lipids extracted by the Folch method as previously described in Chapter 2, methylated and the total FA profile analysed by GC-FID.

As shown in Table 82 and Table 83, when compared to non-treated control cells (CTRL), total SFA decreased by at least 10% in all treatment groups except the vehicle control groups. MUFA levels increased in GbE50 and GbE100 treated cells, but not in any other treatment groups. This was largely seen in the form of C18:1n-9 (oleic acid) and C20:3n-9 (mead acid). In contrast to the MUFA data, total PUFA increased in all FA treated cells (NFD, NFD+GbE50, NFD+GbE100, HFD, HFD+GbE50, HFD+GbE100) but not in the GbE-only treated groups. This was largely due to the increase in n-6 PUFA in the NFD and HFD treated groups.

Interestingly, the collective total UFA (MUFA+ PUFA) significantly increased across all treatment groups. In turn the UI of the samples significantly increased for all treatment groups, although GbE50 and GbE100 cells increased less than that of the NFD and HFD only groups. Except for NFD+GbE100, cells treated with NFD or HFD with GbE experienced a further increase in the unsaturation index, compared to just NFD or HFD treatment alone. Interestingly, NFD and HFD cells treated with GbE50 experienced larger increases in PUFA, compared to GbE100 treatments, which may indicate GbE dosage effects on FA metabolism.

As discussed in section 1.8, DNL MUFA occurs through the conversion of C16:0 (Palmitic acid) to either C16:1n-7 (palmitoleic acid) or C18: -7 (vaccenic acid) or the conversion of C16:0 to C18:0 (stearic acid) and C18:1n-9 (oleic acid). Also discussed in section 1.7 and section 1.12 the fluidity and flexibility of the cell membrane depends on the type of lipid incorporated into the membrane, where unsaturated fatty acids increase fluidity (Pilon, 2016). The membrane fluidity can affect protein enrichment and localisation throughout the membrane, potentially affecting cellular function (van Meer and de Kroon, 2011; Hulbert *et al.*, 2005). For example, decreased membrane fluidity impairs insulin receptors and disrupts dispersion of GLUT4 glucose transporters throughout the cell membrane, contributing to IR (Pilon, 2016).

This present study corroborates with the findings of Msika and colleagues (2012) that found differentiated PC12 cells experienced PUFA deficiency due in part to the effect of NGF on several genes involved in FA metabolism (ELOVL5, ELOVL2, SCD1 (D9D) and PPAR α). They reported that LA (C18:2n-6) upregulated all these genes, but ALA (alpha linolenic acid) regulated the genes for FADs

and ELOVL5 (Msika *et al.*, 2012). Together these findings would suggest that GbE may influence DNL from SFA to MUFA. This may explain the decrease in SFA and increase in MUFA seen across the GbE50 and GbE100 groups. Furthermore, oleic acid (C18:1n-9) and mead acid (C20:3n-9) was significantly increased in both GbE50 and GbE100 cells, with the latter being an indicator for PUFA deficiency (Ichi *et al.*, 2014). As GbE and GbE100 experienced an increase in UI compared to non-treated control cells, this might suggest a protective effect of GbE on membrane fluidity, where the double bonds found in oleic acid and mead acid will provide additional flexibility to the membrane, helping to buffer against OS and facilitating protein transport in the membrane.

Interestingly, when comparing the total FA profiles in PC12 cells to the hippocampus and hypothalamus total FA profiles in NFD, HFD and HFD+GbE groups (Chapter 6), similar percentage levels of SFA (around 45%) are seen across all groups in the total FA profile. MUFA and PUFA levels however vary in PC12 cells compared to the rat brain tissue samples. This may be due to the protective compensatory mechanism found within the body designed to protect the brain whereby peripheral tissues may provide supplementary PUFA to maintain homeostasis and cellular plasticity. As PC12 cells lack the *in vivo* buffering capacity from peripheral tissues to maintain cellular plasticity and rely on the FA contents of cell culture media to provide adequate FA supply, particularly essential FA, the effect of cell culture media and additional FA supplementation, as recommended by Msika *et al.*, (2010) should be investigated further on differentiating PC12 cells.

Table 82. Fatty acid methyl esters of PC12 cells treated with either NFD or HFD fatty acids, GbE (50µg/ml or 100µg/ml) or a combination of NFD, HFD and GbE (N=8 per group). Results are presented as mean % of the total sample, and statistically analysed by one-way ANOVA with Tukey's Post-hoc test. The level of statistical significance was set at *p < 0.05.

	CTRL	Vehicle	GbE 50	GbE 100	NFD	NFD+ GbE50	NFD+ GbE100	HFD	HFD+ GbE 50	HFD+ GbE 100	CTRL Vs Vehicle	CTRL Vs GbE50	CTRL Vs GbE 100	CTRL Vs NFD	CTRL Vs NFD+ GbE50	CTRL Vs NFD+ GbE100	CTRL Vs HFD	CTRL Vs HFD+ GbE50	CTRL Vs HFD+ GbE100
	MEAN %										p value								
C16:0	21.9	19.5	19.0	18.0	17.7	18.7	19.1	19.7	14.7	13.0	0.63	0.35	0.06	0.03	0.22	0.41	0.71	<0.0001	<0.0001
C18:0	30.2	27.4	21.5	22.1	20.2	21.0	24.1	22.6	20.3	26.9	0.98	0.03	0.05	0.01	0.02	0.33	0.09	0.01	0.95
C20:0	2.0	1.7	1.2	1.1	1.2	1.0	1.6	1.4	1.6	1.5	0.97	0.06	0.01	0.05	0.005	0.86	0.33	0.85	0.56
C22:0	0.8	0.5	0.6	0.5	0.5	0.5	0.5	0.5	0.5	0.6	0.001	0.07	0.001	0.001	0.002	0.03	0.001	0.04	0.14
C24:0	-	0.2	0.4	0.2	0.4	0.7	-	0.1	0.7	-	>0.99	0.79	>0.99	0.85	0.15	>0.99	>0.99	0.09	>0.99
DMA18:0	0.7	0.8	1.1	1.1	1.1	1.0	1.0	1.0	1.1	1.3	>0.99	0.92	0.95	0.96	>0.99	0.98	0.98	0.96	0.56
ΣSFA	57.2	50.2	44.1	43.1	41.3	43.0	46.7	45.5	39.2	43.4	0.21	0.0002	<0.0001	<0.0001	<0.0001	0.01	0.001	<0.0001	0.0001
C16:1n-7	0.3	1.4	0.5	0.8	0.3	0.3	0.2	0.4	0.4	0.5	0.25	>0.99	0.96	>0.99	>0.99	>0.99	>0.99	>0.99	>0.99
C18:1n7	2.9	2.9	5.0	4.8	3.5	3.6	3.2	3.7	3.7	2.3	>0.99	<0.0001	<0.0001	0.34	0.16	0.98	0.14	0.14	0.48
C18:1n-9	16.0	16.6	26.0	24.7	18.0	19.0	18.9	22.3	18.0	15.3	>0.99	<0.0001	<0.0001	0.74	0.19	0.23	<0.0001	0.72	>0.99
C20:1n-9	2.0	0.3	1.2	1.0	1.6	1.0	0.9	1.2	1.1	0.3	<0.0001	0.08	0.003	0.91	0.01	0.002	0.10	0.03	<0.0001
C20:1n-11	2.3	2.7	0.8	1.8	1.4	1.6	1.7	1.4	3.4	3.9	>0.99	0.91	>0.99	>0.99	>0.99	>0.99	>0.99	0.98	0.87
C20:3n-9	1.2	1.7	2.8	2.7	1.4	1.5	1.7	1.9	1.6	1.3	0.17	<0.0001	<0.0001	>0.99	0.76	0.14	0.01	0.60	>0.99
C22:1n-9	-	2.7	2.7	3.2	6.7	2.3	2.4	2.2	3.1	5.2	0.03	0.03	0.005	<0.0001	0.12	0.08	0.15	0.01	<0.0001
C24:1n-9	0.8	1.0	0.7	0.7	0.6	0.6	0.5	0.5	0.8	0.4	>0.99	>0.99	>0.99	>0.99	>0.99	0.98	0.99	>0.99	0.94
DMA 18:1	4.8	4.9	2.8	3.0	3.0	3.0	3.6	2.9	3.7	3.9	>0.99	0.29	0.48	0.47	0.43	0.89	0.38	0.95	0.98
C18:1 Total	18.9	19.5	31.1	29.5	21.5	22.7	22.1	26.0	21.7	17.6	>0.99	<0.0001	<0.0001	0.64	0.16	0.35	0.001	0.55	0.99
ω7	3.2	4.3	5.6	5.6	3.9	4.0	3.4	4.0	4.1	2.8	0.58	0.001	0.001	0.96	0.92	>0.99	0.86	0.83	>0.99
ω9	22.3	25.0	34.2	34.0	29.6	26.1	26.2	29.6	28.0	26.2	0.90	<0.0001	<0.0001	0.01	0.60	0.55	0.009	0.09	0.53
ΣMUFA	29.4	33.2	41.9	42.1	35.9	32.4	32.7	36.0	35.0	32.7	0.80	<0.0001	<0.0001	0.13	0.94	0.90	0.12	0.29	0.90
C18:2n-6	1.8	1.7	2.1	1.9	9.5	10.4	5.3	5.4	8.7	4.2	>0.99	>0.99	>0.99	<0.0001	<0.0001	0.001	0.0004	<0.0001	0.06
C18:3n-6	1.3	1.9	1.0	0.7	0.9	0.9	1.4	0.9	0.8	1.4	0.82	0.96	0.58	0.94	0.88	>0.99	0.95	0.83	>0.99
C20:3n-6	0.7	0.5	0.4	0.4	0.8	0.8	0.5	0.6	0.8	0.5	>0.99	0.99	0.98	>0.99	>0.99	>0.99	>0.99	>0.99	>0.99
C20:4n-6	1.4	1.5	2.5	2.4	3.5	4.0	2.5	2.6	3.3	2.5	>0.99	0.02	0.05	<0.0001	<0.0001	0.04	0.01	<0.0001	0.02
C22:2n-6	0.5	0.2	0.1	0.1	0.2	0.1	0.2	0.2	0.2	0.1	0.0001	<0.0001	<0.0001	0.0001	<0.0001	0.0001	0.0002	0.002	<0.0001
C22:4n-6	0.8	0.9	0.5	0.9	0.4	0.4	0.9	0.7	0.8	0.9	>0.99	0.99	>0.99	0.96	0.96	>0.99	>0.99	>0.99	>0.99
n-6 PUFA	6.6	6.6	6.6	6.4	15.5	16.9	10.8	10.5	16.1	9.6	>0.99	>0.99	>0.99	<0.0001	<0.0001	<0.0001	0.0001	<0.0001	0.005
Σ6metabolites	4.8	4.9	4.5	4.5	5.9	6.5	5.5	5.1	7.4	5.4	>0.99	>0.99	>0.99	0.72	0.16	0.98	>0.99	0.003	0.99
C18:3n-3	2.8	4.4	2.9	2.6	2.6	2.4	3.8	2.8	4.2	3.6	0.16	>0.99	>0.99	>0.99	>0.99	0.78	>0.99	0.34	0.98
C20:5n-3	-	-	0.1	0.1	0.1	0.1	0.1	0.1	0.2	0.1	>0.99	0.17	0.99	0.08	>0.99	0.06	0.58	0.005	0.99
C22:5n-3	0.1	0.3	0.1	0.2	0.3	0.3	0.2	0.2	0.3	0.2	0.59	>0.99	0.97	0.43	0.12	0.83	0.95	0.31	0.71
C22:6n-3	0.5	0.3	0.8	0.8	0.7	0.8	0.5	0.6	0.6	0.4	0.67	0.03	0.06	0.29	0.04	>0.99	0.87	0.81	>0.99
n-3 PUFA	3.3	7.7	5.8	7.2	6.0	6.4	8.1	6.4	8.0	4.3	0.10	0.79	0.23	0.71	0.51	0.06	0.51	0.06	<0.0001
Σ3metabolites	0.5	0.6	1.0	1.0	1.1	1.2	0.9	0.9	1.1	0.7	>0.99	0.02	0.06	0.01	0.001	0.40	0.28	0.01	0.91
ΣPUFA	9.9	14.3	12.4	13.5	21.5	23.4	18.8	16.9	24.1	22.3	0.11	0.79	0.31	<0.0001	<0.0001	<0.0001	0.0004	<0.0001	<0.0001
ΣUFA	39.3	47.5	54.3	55.6	57.4	55.8	51.5	52.9	59.2	55.0	0.18	0.0002	<0.0001	<0.0001	<0.0001	0.004	0.001	<0.0001	<0.0001
Unsaturation Index	52.3	64.8	74.4	79.1	89.7	92.1	78.0	78.6	91.4	95.2	0.65	0.03	0.004	<0.0001	<0.0001	0.01	0.005	<0.0001	<0.0001

Table 83. Fatty acid methyl ester ratios of PC12 cells treated with either NFD or HFD fatty acids, GbE (50µg/ml or 100µg/ml) or a combination of NFD, HFD and GbE (N=8 per group). Results are presented as mean % of the total sample, and statistically analysed by one-way ANOVA with Tukey's Post-hoc test. The level of statistical significance was set at *p < 0.05.

	CTRL	Vehicle	GbE 50	GbE 100	NFD	NFD+ GbE50	NFD+ GbE100	HFD	HFD+ GbE 50	HFD+ GbE 100	CTRL Vs Vehicle	CTRL Vs GbE 50	CTRL Vs GbE 100	CTRL Vs NFD	CTRL Vs NFD+ GbE50	CTRL Vs NFD+ GbE100	CTRL Vs HFD	CTRL Vs HFD+ GbE50	CTRL Vs HFD+ GbE100
	MEAN %										p value								
n-6/ n-3	2.6	1.1	1.3	1.0	3.1	3.1	1.4	1.8	2.2	0.8	0.07	0.18	0.06	0.99	0.99	0.33	0.86	>0.99	0.02
MUFA/PUFA	3.0	2.5	3.4	3.2	1.7	1.4	1.8	2.1	1.5	1.5	0.25	0.89	>0.99	<0.0001	<0.0001	<0.0001	0.005	<0.0001	<0.0001
MUFA/SFA	6.1	3.8	3.6	3.3	1.9	1.9	2.6	2.7	1.7	2.0	<0.0001	<0.0001	<0.0001	<0.0001	<0.0001	<0.0001	<0.0001	<0.0001	<0.0001
PUFA/SFA	0.2	0.3	0.3	0.3	0.5	0.5	0.4	0.4	0.6	0.5	0.62	0.73	0.39	<0.0001	<0.0001	0.01	<0.05	<0.0001	<0.0001
UFA/SFA	0.7	1.0	1.2	1.3	1.4	1.3	1.1	1.2	1.6	1.3	0.64	0.01	0.003	0.0003	0.004	0.11	0.05	<0.0001	0.004
C18:0/C16:0	1.4	1.4	1.1	1.2	1.1	1.1	1.3	1.1	1.6	2.2	>0.99	0.98	>0.99	0.98	0.98	>0.99	0.99	>0.99	0.01
C16:1n-7/C16:0	-	0.1	-	-	-	-	-	-	-	-	0.42	>0.99	0.97	>0.99	>0.99	>0.99	>0.99	>0.99	0.97
C18:1n-9/C16:0	0.8	0.9	1.4	1.4	1.0	1.0	1.0	1.1	1.3	1.2	0.99	0.0001	0.0001	0.48	0.49	0.53	0.06	0.002	0.005
C18:1n-9/C16:1n-7	54.3	36.3	48.8	40.6	56.6	54.8	136.7	61.0	72.4	219.9	>0.99	>0.99	>0.99	>0.99	>0.99	0.97	>0.99	>0.99	0.41
C18:1n-7/C18:0	0.1	0.1	0.2	0.2	0.2	0.2	0.1	0.2	0.2	0.1	>0.99	<0.0001	<0.0001	0.002	0.002	0.60	0.02	<0.05	>0.99
C18:1/C18:0	0.6	0.7	1.5	1.4	1.1	1.1	0.9	1.2	0.9	0.7	0.99	<0.0001	<0.0001	0.003	0.001	0.14	0.0001	0.13	>0.99
C20:4n-6/C20:3n-6	-974.2	7.6	6.6	6.6	4.2	4.7	4.7	4.6	4.0	5.2	0.35	0.31	0.31	0.31	0.31	0.31	0.31	0.31	0.31
C20:4n-6/C22:6n-3	3.6	4.5	3.3	3.2	5.0	5.5	4.9	4.3	4.5	4.9	0.72	>0.99	>0.99	0.09	0.01	0.14	0.88	0.68	0.24
C20:4n-6/C20:5n-3	20.8	18.1	21.5	21.4	23.8	27.8	14.5	17.8	33.8	17.4	>0.99	>0.99	>0.99	>0.99	>0.99	>0.99	>0.99	>0.99	>0.99
C20:4n-6/C18:2n-6	0.8	0.9	1.2	1.3	0.4	0.4	0.5	0.5	0.4	0.6	0.86	<0.0001	<0.0001	<0.0001	<0.0001	0.002	0.004	<0.0001	0.19
C22:6n-3/C22:5n-3	2.4	3.0	5.7	4.8	2.5	2.2	2.5	3.3	2.1	3.3	>0.99	0.90	0.99	>0.99	>0.99	>0.99	>0.99	>0.99	>0.99
C18:3n-6/C18:2n-6	0.8	1.1	0.4	0.4	0.1	0.1	0.3	0.2	0.1	0.4	0.59	0.35	0.17	0.001	0.0004	0.03	0.003	0.001	0.10
C20:3n-6/C18:3n-6	0.3	0.4	0.6	0.5	0.9	0.9	0.6	0.8	1.0	0.3	>0.99	0.99	>0.99	0.34	0.49	>0.99	0.75	0.22	>0.99
C22:5n-3/C20:5n-3	1.1	1.4	1.2	1.2	1.9	2.3	1.1	1.2	1.7	0.4	>0.99	>0.99	>0.99	0.68	0.19	>0.99	>0.99	0.93	0.81
C22:4n-6/C20:4n-6	2.1	1.8	3.8	2.5	2.8	3.4	3.3	2.8	2.1	2.9	>0.99	0.23	>0.99	>0.99	0.86	0.62	0.98	>0.99	0.96
1 (% monoenoics)	29.4	33.2	41.9	42.1	35.9	32.4	32.7	36.0	35.0	32.7	0.80	<0.0001	<0.0001	0.13	0.94	0.90	0.12	0.29	0.90
2 (% dienoics)	4.7	3.7	4.4	3.9	19.6	21.6	11.0	11.2	20.7	8.6	0.99	>0.99	>0.99	<0.0001	<0.0001	<0.0001	<0.0001	<0.0001	0.01
3 (% trienoics)	6.0	15.3	9.8	14.1	12.3	13.7	16.0	13.0	13.3	35.9	0.64	>0.99	0.80	0.95	0.84	0.54	0.91	0.88	<0.0001
4 (% tetraenoics)	9.1	9.4	12.3	13.3	15.7	17.7	13.5	13.4	16.4	13.9	>0.99	0.43	0.11	0.001	<0.0001	0.08	0.09	0.0001	0.04
5 (% pentaenoics)	0.4	1.4	1.3	1.1	2.1	2.0	1.8	1.4	2.3	1.5	0.64	0.77	0.92	0.08	0.09	0.24	0.68	0.02	0.55
6 (% hexaenoics)	2.8	1.7	4.7	4.6	4.2	4.6	3.0	3.7	3.7	2.6	0.66	0.03	0.06	0.29	0.04	>0.99	0.85	0.81	>0.99

7.19 Summary

In summary, PC12 cells undergoing NGF differentiation experience increases in β -Tubulin III, Neurofilaments (NF-L and NF-M) increased Akt activation and Nrf2 protein expression. HFD treatment increases Akt activation and NF-L protein expression levels, which is not seen in NFD treatment. NFD treatment seem to partially ameliorate the decrease in Nrf2 protein expression following OS caused by hydrogen peroxide, while HFD treatment does not. Total FA profile analysis indicates that following NFD-differentiation, cells appear to experience FA deficiency, which is ameliorated with NFD and HFD FA treatment. GbE treatment appears to stimulate compensatory FA metabolic pathways by increasing oleic acid and mead acid, which can help counteract FA deficiency by increasing the UI of the cell membrane. Future PC12 neuronal studies should consider FA supplementation in the media during or after differentiation and before additional treatments take place to negate FA deficiency.

Chapter 8 - Final conclusions

An HFD, typical of a “western-style” diet, is high in lipids such as SFA and cholesterol and is associated with an increased risk of developing metabolic disorders including obesity, diabetes, cardiovascular disease as well as brain-related disorders related to hypothalamus-pituitary-adrenocortical axis dysregulation including cognitive impairment, anxiety, stress, and depression (López-Taboada *et al.*, 2020). Dietary lipids are utilized for energy or stored in the body primarily in the form of TAG in adipose tissues. They are transported around the body in the form of very low-density lipids (VLDL-TAG), cholesterol, CE and PPL and incorporated into cellular membranes in the form of phospholipids or stored in adipocytes as TAG (Bhutia and Ganapathy, 2021).

Complications from obesity include a variety of non-communicable diseases such as coronary heart disease, hypertension, hypercholesterolemia, steatosis, cirrhosis, severe pancreatitis, and cancer. Higher incidences of metabolic disorders associated with obesity include IR (a major co-morbidity), metabolic syndrome, T2DM and atherogenic dyslipidaemia (Abdullah *et al.*, 2010; Salamone and Bugianesi, 2010) and an increased risk ratio of developing dementia in later years (Pugazhenthii, Qin and Reddy, 2017). Obesity also affects appetite regulating hormones including adiponectin, leptin, ghrelin, and insulin (Forny-Germano, de Felice and do Nascimento Vieira, 2019; Wang and Scherer, 2016; Abizaid *et al.*, 2006).

GbE has been shown to possess antioxidant, anti-inflammatory, and anti-obesogenic properties. It has been shown to reduce visceral adiposity, weight gain and food intake and reduce adipocyte hypertrophy in WAT. Furthermore, previous research has shown that GbE modulates obesity and weight gain, lipid metabolism, adipogenesis, inflammation and OS and improve insulin signalling and sensitivity (Banin *et al.*, 2014, 2017, 2021; Machado, Banin, *et al.*, 2021; Machado, Pereira, *et al.*, 2021; Hirata *et al.*, 2019; Hirata *et al.*, 2015, 2019).

In this study, it has been shown that analysing just total lipid profiles of tissues may mask the more subtle changes in the different lipid classes found within the FA depot of tissues. Overall, this study has found that total fatty acid profiles largely represent the TAG profile of tissues, particularly in adipose tissue. This study has shown that in both RET and MES adipose tissue a HFD causes increased SFA and MUFA levels and decreased PUFA in the adipocyte total fatty acid profiles and TAG. Both adipose tissue profiles for all lipid classes (TAG, CE, MAG+DAG and

PPL) had similar profiles, most likely due to being supplied by the same abdominal lymphatics delivering dietary fats (Williams and Rabbani, 2011). The changes in SFA, MUFA and PUFA levels affected the UI of the tissues, and therefore the buffering capacity of the cell.

Following an HFD, both RET and MES adipose tissues an increased ω -6/ ω -3 PUFA ratios, which can influence and increase pro-inflammatory oxylipins. An unbalanced n-6 /n-3-ratio over of 20+:1 is commonly found in WSD (Husted and Bouzinova, 2016; Deckelbaum, 2010; Schmitz and Ecker, 2008; Harbige, 2003; Simopoulos, 2002; Broughton *et al.*, 1991).

The n-6 /n-3-ratio in NFD-VAT -RET total fatty acid profiles showing a ratio of 17:1, while the HFD total fatty acid profiles were double this at 34:1. Leng and colleagues (2017) have demonstrated that when a diet with a high n-6/n-3-ratio of approximate 18:1 LA/ALA, as seen in this study in the HFD-chow, this resulted in an increase in n-6/n-3 oxylipins in the liver compared to a lower ratio diet (approx. 8:1) (Leng, Winter and Aukema, 2017). Extrapolating from the results of Leng and colleagues (2017), it is possible that an increase in n-6/n-3 oxylipins may also occur between our two baseline diet groups (NFD and HFD) favouring a more pro-inflammatory environment, particularly with the two-fold increase following an HFD.

Of the lipid classes explored in both adipose tissue and the liver, the greatest differences were seen in the PPL fraction. PPL are responsible for the fluidity and stability of the cell membrane, which is dependent of the type of FA incorporated into the PPL structure (Weijers, 2012, 2015a, 2015b; Hulbert *et al.*, 2005, 2007). PPL make up the bulk of the cell membrane and serves as a barrier and facilitator of ionic exchange and molecular transport in and out of the cell (Hulbert *et al.*, 2005, 2007). Cell membrane function is influenced by the fluidity and stability of the cell membrane, which is dependent of the type of fatty acids incorporated into the phospholipid structure, and the amount of cholesterol-rich microdomains. Increased cell membrane fluidity is associated with higher amounts of unsaturated fatty acids and decreased fluidity is associated with higher saturated fatty acids and cholesterol (Pilon, 2016a). A high SFA-HFD diet therefore may not only contribute to increased enlargement of fat depots but may also modulate tissue and cell membrane lipid signatures. Altered membrane fluidity may also contribute to altered protein enrichment and localisation throughout the membrane, potentially affecting cellular function. Decreased membrane fluidity is associated with impaired insulin signalling and glucose uptake due to impaired insulin receptors and disrupted dispersion of GLUT4 glucose transporters respectively,

throughout the cell membrane. This in turn may contribute to IR and the development of metabolic syndrome and diabetes, both co-morbidities of obesity (Pilon, 2016).

In both adipose tissues (RET and MES) and the liver, increases in SFA and decreases in PUFA were seen in the HFD obese group compared to rats fed an NFD. In both adipose tissues, when HFD fed obese rats were supplemented with GbE for 14 days, SFA increased further in the PPL fraction of RET adipocytes. GbE has been shown to decrease food intake in animals. As such the pair-fed group (HFD-PF) that was used as a control for the calorie restriction, showed different changes in PPL than that of GbE, where MUFA levels significantly increased and PUFA decreased following caloric restriction. Comparing both groups, GbE treatment MUFA levels decreased in contrast to the PF group, while PUFA levels also decreased in GbE but not to the extent seen in the PF group. These findings may suggest changes in enzyme activity involved in DNL and lipogenesis such as HSL, PLIN1, FAS and ELOVL6 and/or CAV related lipid trafficking and oxylipin production associated with inflammation mediation. This would need to be investigated further in future studies. Interestingly, in the PPL fraction of the liver, both caloric restriction (HFD-PF) and GbE treatment (HFD-GbE) resulted in a significant increase in n-3 PUFA in total FA profiles, TAG and PPL profiles. In contrast, n-3 PUFA decreased in the CE fraction following GbE treatment. This finding indicates the mobilization of PUFA from peripheral tissues back towards the liver could occur, or some additional protection against PUFA utilization for inflammation mitigation. This would need to be investigated more in future studies.

A high-fat diet has been shown to induce rapid changes in the mouse hypothalamic proteome (McLean *et al.*, 2019; McLean *et al.*, 2018; Zahid *et al.*, 2014; Bubber *et al.*, 2005). Changes including changes in cytoskeleton and synaptic plasticity, cellular stress responses, glucose metabolism and mitochondrial function with many of these associated with the development of AD (McLean *et al.* 2019). Pathological alterations such as IR, inflammation or mitochondrial dysfunction associated with obesity, are also related to AD pathological processes (Mínguez-Olaondo, Irimia and Frühbeck, 2017; O'Brien *et al.*, 2017). Long term consumption of high fat diet (HFD) can lead to leptin resistance in the ARC of the hypothalamus and ventral tegmental area (VTA) of the midbrain. This can affect appetite regulation and energy expenditure (Enriori *et al.*, 2007; Münzberg, Flier and Bjørbæk, 2004; Heymsfield *et al.*, 1999). It was found in the hypothalamus total fatty acids of HFD obese rats that levels of C18:0 were increased. Milanski and colleagues (2009, 2012) have shown that five days of intracerebroventricular

injection of SFA stearic acid (C18:0), induces hypothalamic inflammation but does not affect systemic inflammatory markers (Milanski *et al.*, 2009, 2012). This study also showed that hepatic IR occurred following 5 days of intracerebroventricular C18:0 treatment (Milanski *et al.*, 2012). Both caloric restriction (HFD-PF) and GbE treatment both ameliorated the elevated levels of C18:0. In this study, hippocampus total fatty acids profiles showed no significant changes in FA percentage levels between NFD or HFD-S groups, or those treated with GbE or calorie restricted (HFD-PF). As no other significant changes in MUFA or PUFA occurred in either hippocampus or hypothalamus tissue, these findings suggest that peripheral tissues may be acting as a buffer and provided a continued supply of higher PUFA to main the brain FA profile, as shown in other studies (Watanabe *et al.*, 2022; Dornellas *et al.*, 2015). This might explain the changes in PUFA levels in the adipose tissues, but should be investigated further in future studies, including the fatty acid profiles in circulating plasma.

Future work relating to this male Wistar rat study include bigger groups and longer treatment times to mimic long-term supplementation. Further proteome analysis on the tissues analysed here, specifically looking at fatty acid metabolism related genes and those related to OS and glucose signalling. Other polyphenols such as resveratrol, or singular molecules found in GbE would also be explored to see if similar results could be found.

Finally, from the development of an in-house PC12 neuronal model, it was seen in PC12 cells undergrowing NGF differentiation experience increases in β -Tubulin III, NF-L and NF-M increased Akt activation and Nrf2 protein expression. HFD FA treatments increased Akt activation and neurofilament-L protein expression levels, which was not seen in NFD FA treatment. NFD treatment seem to partially ameliorate the decrease in Nrf2 protein expression following OS caused by hydrogen peroxide, while HFD treatment does not. Total FA profile analysis indicates that following NFD-differentiation, cells appear to experience FA deficiency, which is ameliorated with NFD and HFD FA treatment. GbE treatment appears to stimulate compensatory FA metabolic pathways by increasing oleic acid and mead acid, which can help counteract FA deficiency by increasing the unsaturation index of the cell membrane. Future PC12 neuronal studies should consider FA supplementation in the media during or after differentiation and before additional treatments take place to negate FA deficiency. More time-response studies would also be beneficial to investigate the acute responses to FA and GbE treatments. Use of amyloid- β to induce an AD like phenotype could also be explored in relation to the effects of a HFD and the effects of GbE treatments.

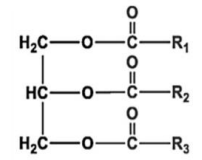
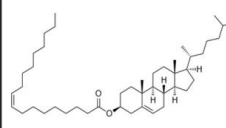
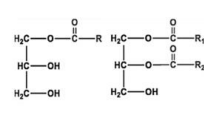
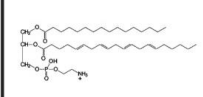

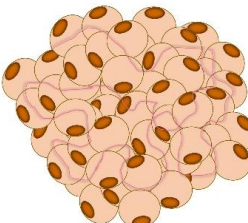
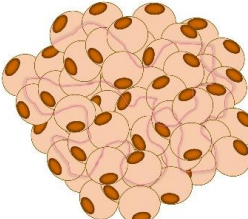
		 TAG		 CE		 MAG+DAG		 PPL		
	↑ increased Vs NFD ↓ Decreased Vs NFD	NFD	HFD	NFD	HFD	NFD	HFD	NFD	HFD	
 Liver		ΣSFA %	28	26	17	26	38	41	43	66
		ΣMUFA %	21	29	11	16	16	22	5	4
		ΣPUFA %	49	34	67	59	44	36	50	18
		Σn-6 PUFA %	46	32	52	48	11	11	44	14
		Σn-3PUFA %	3	2	16	11	5	7	6	4
		n-6/n-3	14	19	3	5	8	5	8	3
 Retroperitoneal Adipose tissue		ΣSFA %	23	28	21	25	24	26	38	49
		ΣMUFA %	29	48	25	44	26	47	24	25
		ΣPUFA %	46	23	52	30	48	26	34	24
		Σn-6 PUFA %	44	23	48	28	45	25	30	19
		Σn-3PUFA %	2	1	1	0.1	3	1	4	5
		n-6/n-3	37	38	12	19	17	31	11	6
 Mesenteric Adipose tissue		ΣSFA %	22	28	15	22	44	29	60	50
		ΣMUFA %	30	48	23	43	21	45	10	19
		ΣPUFA %	48	23	60	34	30	26	29	29
		Σn-6 PUFA %	46	23	55	32	28	25	27	28
		Σn-3PUFA %	2	1	5	2	2	2	2	3
		n-6/n-3	21	41	12	20	16	20	17	27

Figure 41. Summary of changes in liver, retroperitoneal and mesenteric tissue following 8 weeks of a HFD compared to a NFD analysed by GC-FID. NFD= normal fat diet; HFD = high fat diet; TAG= Triglycerides; CE = Cholesteryl Esters, MAG+DAG= Monoglycerides + Diglycerides; PPL = Phospholipids; SFA=saturated fatty acid, MUFA=monounsaturated fatty acid, PUFA =polyunsaturated fatty acid

↑ increased Vs S
↓ Decreased Vs S

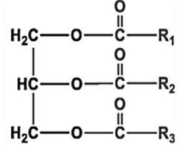
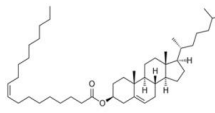
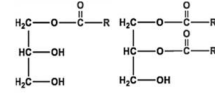
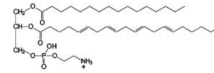

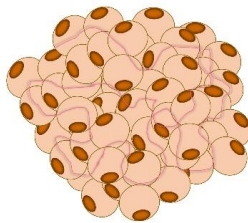
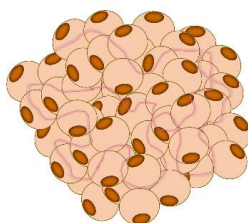
		 TAG	 CE	 MAG+DAG	 PPL
		S PF GbE	S PF GbE	S PF GbE	S PF GbE
 Liver	ΣSFA %	26 29 27	26 25 26	41 36 36	66 40 40
	ΣMUFA %	29 31 27	16 17 23	21 26 27	4 4 4
	ΣPUFA %	34 38 34	59 55 47	36 37 36	18 44 44
	Σn-6 PUFA %	32 35 32	48 45 40	29 33 32	14 38 37
	Σn-3PUFA %	2 2 2	11 10 6	7 5 4	4 6 6
	n-6/n-3	19 17 14	5 5 8	4 8 8	3 5 5
 Retroperitoneal Adipose tissue	ΣSFA %	28 28 28	25 25 23	26 29 26	49 46 59
	ΣMUFA %	48 48 48	44 43 44	47 44 46	25 35 20
	ΣPUFA %	23 23 23	30 31 31	26 24 26	24 15 20
	Σn-6 PUFA %	23 22 23	28 29 30	25 23 25	19 12 15
	Σn-3PUFA %	1 1 1	2 2 1	1 1 1	5 4 5
	n-6/n-3	38 35 38	19 21 20	31 30 32	6 3 3
 Mesenteric Adipose tissue	ΣSFA %	28 28 27	22 23 22	29 30 28	50 33 61
	ΣMUFA %	48 49 49	43 44 43	45 44 45	32 33 14
	ΣPUFA %	23 23 23	34 33 33	26 25 23	30 10 18
	Σn-6 PUFA %	23 23 23	32 31 32	25 24 21	28 9 18
	Σn-3PUFA %	1 1 1	2 2 2	2 2 2	2 0.3 0.4
	n-6/n-3	41 41 45	20 20 20	20 19 18	41 24 60

Figure 42. Summary of changes in liver, retroperitoneal and mesenteric tissue in rats fed a HFD and treated with Saline (S), pair-feeding (PF) and Ginkgo biloba (GbE) for 14 days and analysed by GC-FID. NFD= normal fat diet; HFD = high fat diet; TAG= Triglycerides; CE = Cholesteryl Esters, MAG+DAG= Monoglycerides + Diglycerides; PPL = Phospholipids; SFA=saturated fatty acid, MUFA=monounsaturated fatty acid, PUFA =polyunsaturated fatty acid

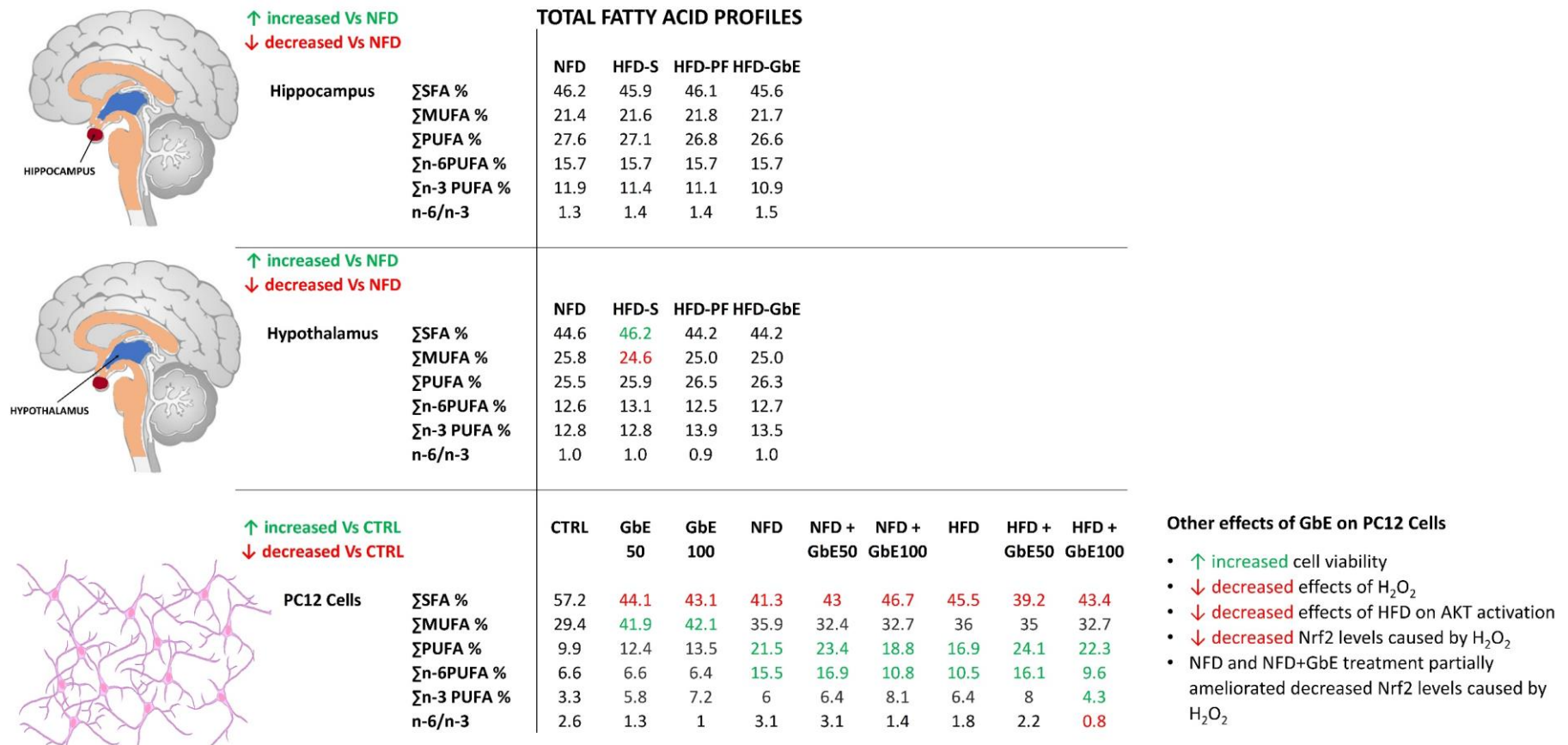


Figure 43. Summary of changes in total fatty acid profiles of hippocampus, hypothalamus and differentiated PC12 (rat pheochromocytoma) cells. Hippocampus and hypothalamus total fatty acid profiles were compared following 8 weeks of a NFD or HFD. HFD-fed rats were subsequently treated with HFD- Saline (S), pair-feeding (PF) or Ginkgo biloba (GbE) for 14 days and total fatty acid profiles compared. Differentiated PC12 cells were treated with NFD, HFD, GbE or combinations for 24 hours and total fatty acid profiles compared. NFD= normal fat diet; HFD = high fat diet; SFA=saturated fatty acid, MUFA=monounsaturated fatty acid, PUFA =polyunsaturated fatty acid; H₂O₂ = hydrogen peroxide; AKT= protein kinase B; Nrf2= nuclear factor erythroid 2-related factor 2.

Publications and conferences

ORCID; 0000-0002-2595-2898

Papers

Boldarine, V.T., **Joyce, E.**, Pedroso, A.P., Telles, M.M., Oyama, L.M., Bueno, A.A. and Ribeiro, E.B., 2021. Oestrogen replacement fails to fully revert ovariectomy-induced changes in adipose tissue monoglycerides, diglycerides and cholesteryl esters of rats fed a lard-enriched diet. *Scientific Reports*, 11(1), pp.1-11. <https://doi.org/10.1038/s41598-021-82837-6> (Attached in Appendix 3).

Submitted and awaiting review:

Hirata, B. K. S., Aono, A. H., Machado, M. M. F., **Joyce, E. C.**, Bueno, A. A., Kuroshu, R. M., Oyama, L. M., Ribeiro, E. B., Niero, C. V., & Telles, M. M. (2022). *Ginkgo biloba* extract (GbE) restores gut microbiota dysbiosis in diet-induced obese rats independently of high-fat diet energy intake.

Conference presentations and posters

“*Ginkgo biloba* extract supplementation differently alters fatty acid composition in neutral lipid classes of the liver in obese rats fed a high-fat diet”. UK Congress on Obesity (UKCO) 2022, 7-8th September 2022, Lancaster, UK

Virtual conference talk- Joint talk with Dr Allain Bueno (1 ½ hours)

“Lipid classes: Exploring the intricacies of fatty acid storage and usage in the body”
Congresso UNIFESP 2021, Brazil on 27th October 2021

“*Ginkgo biloba* extract (GbE) modifies phospholipid fatty acid profiles of mesenteric adipose tissue of obese rats fed a high-fat diet”; EP1-27; European Congress on Obesity (ECO Online 2021). 28th Congress, 10-13 May 2021. ABSTRACTS (2021) Obesity Facts, 14(suppl 1(1), pp. 1–154. <https://doi.org/10.1159/000515911>

“*Ginkgo biloba* extract supplementation differently alters fatty acid composition in neutral lipid classes of mesenteric adipose tissue of obese rats fed a high-fat diet”; EP1-25; European Congress on Obesity (ECO Online 2021). 28th Congress, 10-13 May 2021. ABSTRACTS (2021) Obesity Facts, 14(suppl 1(1), pp. 1–154. <https://doi.org/10.1159/000515911>

"*Ginkgo biloba* extract alters polyunsaturated fatty acids in the hippocampus of high-fat diet obese rats". ISSFAL 14th International Congress, 10-14 May 2021

"*Ginkgo biloba* extract supplementation alters ω 7 MUFA, ω 6 and ω 3 PUFA ratios in hypothalamus tissue of obese rats fed a high fat diet". ISSFAL 14th International Congress, 10-14 May 2021

"*Ginkgo biloba* extract decreases saturated and monounsaturated fatty acid content in the cholesterol ester fraction of lipids extracted from visceral adipose tissue of obese rats fed a lard-rich diet". Obesity Reviews. 2020; 21(S1): e13118. <https://doi.org/10.1111/obr.13118>

"Ovariectomy-induced menopause influences the cholesterol ester fatty acid composition of retroperitoneal adipose tissue in diet-induced obese rats, partially reverted by hormone replacement therapy"; EP-188. Obesity Reviews. 2020; 21(S1): e13118. <https://doi.org/10.1111/obr.13118>

"*Ginkgo biloba* extract supplementation decreases energy intake in high fat diet obese rats and modifies tissue fatty acid composition"; 26th European Congress on Obesity, April 29th - May 1st, 2019. P01.030 page 92 <https://www.karger.com/Article/Pdf/497797>

References

Abate, G., Marziano, M., Rungratanawanich, W., Memo, M., & Uberti, D. (2017). Nutrition and AGE-ing: Focusing on Alzheimer' s Disease. 2017.

Abbott, K. A., Burrows, T. L., Thota, R. N., Acharya, S., & Garg, M. L. (2016). Do ω -3 PUFAs affect insulin resistance in a sex-specific manner? A systematic review and meta-analysis of randomized controlled trials. *The American Journal of Clinical Nutrition*, 104(5), 1470–1484.

Abdel-Kader, Reham, Hauptmann, S., Keil, U., Scherping, I., Leuner, K., Eckert, A., & Müller, W. E. (2007). Stabilization of mitochondrial function by Ginkgo biloba extract (EGb 761). *Pharmacol Res*, 56(6), 493–502. <https://doi.org/10.1016/j.phrs.2007.09.011>

Abdullah, A., Peeters, A., de Courten, M., & Stoelwinder, J. (2010). The magnitude of association between overweight and obesity and the risk of diabetes: A meta-analysis of prospective cohort studies. *Diabetes Research and Clinical Practice*, 89(3), 309–319. <https://doi.org/10.1016/J.DIABRES.2010.04.012>

Abete, I., Goyenechea, E., Zulet, M. A., & Martínez, J. A. (2011). Obesity and metabolic syndrome: Potential benefit from specific nutritional components. *Nutrition, Metabolism and Cardiovascular Diseases*, 21(Suppl 2), B1–B15. <https://doi.org/10.1016/j.numecd.2011.05.001>

Abizaid, A., Liu, Z. W., Andrews, Z. B., Shanabrough, M., Borok, E., Elsworth, J. D., Roth, R. H., Sleeman, M. W., Picciotto, M. R., Tschöp, M. H., Gao, X. B., & Horvath, T. L. (2006). Ghrelin modulates the activity and synaptic input organization of midbrain dopamine neurons while promoting appetite. *Journal of Clinical Investigation*, 116(12), 3229–3239. <https://doi.org/10.1172/JCI29867>

Abo-Salem, O. M. (2014a). Kaempferol Attenuates the Development of Diabetic Neuropathic Pain in Mice: Possible Anti-Inflammatory and Antioxidant Mechanisms. *Open Access Macedonian Journal of Medical Sciences*, 2(3), 424–430. <https://doi.org/10.3889/oamjms.2014.073>

Abu-Elheiga, L., Brinkley, W. R., Zhong, L., Chirala, S. S., Woldegiorgis, G., & Wakil, S. J. (2000). The subcellular localization of acetyl-CoA carboxylase 2. *Proceedings of the National Academy of Sciences*, 97(4), 1444–1449. <https://doi.org/10.1073/PNAS.97.4.1444>

Abu-Elheiga, L., Wu, H., Gu, Z., Bressler, R., & Wakil, S. J. (2012). Acetyl-CoA carboxylase 2 $-/-$ mutant mice are protected against fatty liver under high-fat, high-carbohydrate dietary and *De novo* lipogenic conditions. *Journal of Biological Chemistry*, 287(15), 12578–12588. <https://doi.org/10.1074/jbc.M111.309559>

Adlof, R. O. (2003). *Advances in Lipid Methodology*. Elsevier.

Ahlemeyer, B., & Krieglstein, J. (2003a). Neuroprotective effects of Ginkgo biloba extract. *Cellular and Molecular Life Sciences CMLS*, 60(9), 1779–1792. <https://doi.org/10.1007/s00018-003-3080-1>

Ahlemeyer, B., & Krieglstein, J. (2003b). Pharmacological studies supporting the therapeutic use of Ginkgo biloba extract for Alzheimer's disease. *Pharmacopsychiatry*, 36(SUPPL. 1). <https://doi.org/10.1055/s-2003-40454>

Ahmad, W., Ijaz, B., Shabbiri, K., Ahmed, F., & Rehman, S. (2017). Oxidative toxicity in diabetes and Alzheimer's disease: mechanisms behind ROS/RNS generation. *Journal of Biomedical Science*, 24(1), 76.

Ahme, O. S., Galano, J. M., Pavlickova, T., Revol-Cavalier, J., Vigor, C., Lee, J. C. Y., Oger, C., & Durand, T. (2020). Moving forward with isoprostanes, neuroprostanes and phytoprostanes: where are we now? *Essays in Biochemistry*, 64(3), 463–484. <https://doi.org/10.1042/EBC20190096>

Ahmed, T., Javed, S., Javed, S., Tariq, A., Šamec, D., Tejada, S., Nabavi, S. F., Braidly, N., & Nabavi, S. M. (2017). Resveratrol and Alzheimer's Disease: Mechanistic Insights. *Molecular Neurobiology*, 54(4), 2622–2635. <https://doi.org/10.1007/s12035-016-9839-9>

Ajuwon, K. M., & Spurlock, M. E. (2005). Adiponectin inhibits LPS-induced NF- κ B activation and IL-6 production and increases PPAR γ 2 expression in adipocytes. *American Journal of Physiology-Regulatory, Integrative and Comparative Physiology*, 288(5), R1220–R1225.

Akter, K., Lanza, E. A., Martin, S. A., Myronyuk, N., Rua, M., & Raffa, R. B. (2011). Diabetes mellitus and Alzheimer's disease: Shared pathology and treatment? *British Journal of Clinical Pharmacology*, 71(3), 365–376. <https://doi.org/10.1111/j.1365-2125.2010.03830.x>

Albert, B. B., Derraik, J. G. B., Brennan, C. M., Biggs, J. B., Smith, G. C., Garg, M. L., Cameron-Smith, D., Hofman, P. L., & Cutfield, W. S. (2014). Higher omega-3 index is associated with increased insulin sensitivity and more favourable metabolic profile in middle-aged overweight men. *Scientific Reports*, 4, 6697.

Alberts, B., Johnson, A., Lewis, J., Raff, M., Roberts, K., & Walter, P. (2002). *The Lipid Bilayer*. <https://www.ncbi.nlm.nih.gov/books/NBK26871/>

Aldrovandi, M., Hammond, V. J., Podmore, H., Hornshaw, M., Clark, S. R., Marnett, L. J., Slatter, D. A., Murphy, R. C., Collins, P. W., & O'Donnell, V. B. (2013). Human platelets generate phospholipid-esterified prostaglandins via cyclooxygenase-1 that are inhibited by low dose aspirin supplementation. *Journal of Lipid Research*, 54(11), 3085–3097. <https://doi.org/10.1194/jlr.M041533>

Alkhoury, N., Dixon, L. J., & Feldstein, A. E. (2009). Lipotoxicity in nonalcoholic fatty liver disease: not all lipids are created equal. *Expert Rev Gastroenterol Hepatol*, 3(4), 445–451. <https://doi.org/10.1586/egh.09.32>

Al-Numair, K. S., Chandramohan, G., Veeramani, C., & Alsaif, M. A. (2015a). Ameliorative effect of kaempferol, a flavonoid, on oxidative stress in streptozotocin-induced diabetic rats. *Redox Report: Communications in Free Radical Research*, 20(5), 198–209. <https://doi.org/10.1179/1351000214Y.0000000117>

Alonso, C., Nouredin, M., Lu, S. C., & Mato, J. M. (2019). Biomarkers and subtypes of deranged lipid metabolism in non-alcoholic fatty liver disease. *World Journal of Gastroenterology*, 25(24), 3009. <https://doi.org/10.3748/WJG.V25.I24.3009>

Al-Sari, N., Suvitaival, T., Mattila, I., Ali, A., Ahonen, L., Trost, K., Henriksen, T. F., Pociot, F., Dragsted, L. O., & Legido-Quigley, C. (2020). Lipidomics of human adipose tissue reveals diversity between body areas. *PLOS ONE*, 15(6), e0228521. <https://doi.org/10.1371/JOURNAL.PONE.0228521>

Alves, M. A., Lamichhane, S., Dickens, A., McGlinchey, A., Ribeiro, H. C., Sen, P., Wei, F., Hyötyläinen, T., & Orešič, M. (2021). Systems biology approaches to study lipidomes in health and disease. *Biochimica et Biophysica Acta (BBA) - Molecular and Cell Biology of Lipids*, 1866(2), 158857. <https://doi.org/10.1016/j.bbailip.2020.158857>

Alves-Bezerra, M., & Cohen, D. E. (2017). Triglyceride metabolism in the liver. *Comprehensive Physiology*, 8(1), 1. <https://doi.org/10.1002/CPHY.C170012>

Alzahrani, N. S., Alshammari, G. M., El-Ansary, A., Yagoub, A. E. A., Amina, M., Saleh, A., & Yahya, M. A. (2022). Anti-Hyperlipidemia, Hypoglycemic, and Hepatoprotective Impacts of Pearl Millet (*Pennisetum glaucum* L.) Grains and Their Ethanol Extract on Rats Fed a High-Fat Diet. *Nutrients*, 14(9). <https://doi.org/10.3390/NU14091791>

Ameer, F., Scanduzzi, L., Hasnain, S., Kalbacher, H., & Zaidi, N. (2014). *De novo* lipogenesis in health and disease. *Metabolism - Clinical and Experimental*, 63(7), 895–902. <https://doi.org/10.1016/j.metabol.2014.04.003>

Amiri, M., Yousefnia, S., Seyed Forootan, F., Peymani, M., Ghaedi, K., & Nasr Esfahani, M. H. (2018). Diverse roles of fatty acid binding proteins (FABPs) in development and pathogenesis of cancers. *Gene*, 676, 171–183. <https://doi.org/10.1016/j.gene.2018.07.035>

Anagnostopoulou, A., Camargo, L. L., Rodrigues, D., Montezano, A. C., & Touyz, R. M. (2020). Importance of cholesterol-rich microdomains in the regulation of Nox isoforms and redox signaling in human vascular smooth muscle cells. *Scientific Reports* 2020 10:1, 10(1), 1–20. <https://doi.org/10.1038/s41598-020-73751-4>

Anderson, J. W., Baird, P., Davis, R. H., Ferreri, S., Knudtson, M., Koraym, A., Waters, V., & Williams, C. L. (2009). Health benefits of dietary fiber. *Nutrition Reviews*, 67(4), 188–205. <https://doi.org/10.1111/j.1753-4887.2009.00189.x>

André, C., Dinel, A. L., Ferreira, G., Layé, S., & Castanon, N. (2014). Diet-induced obesity progressively alters cognition, anxiety-like behavior and lipopolysaccharide-induced depressive-like behavior: Focus on brain indoleamine 2,3-dioxygenase activation. *Brain, Behavior, and Immunity*, 41(1), 10–21. <https://doi.org/10.1016/j.bbi.2014.03.012>

Andreadi, C. K., Howells, L. M., Atherfold, P. A., & Manson, M. M. (2006). Involvement of Nrf2, p38, B-Raf, and nuclear factor- κ B, but not phosphatidylinositol 3-kinase, in induction of hemoxygenase-1 by dietary polyphenols. *Molecular Pharmacology*, 69(3), 1033–1040.

Andreoletti, P., Raas, Q., Gondcaille, C., Cherkaoui-Malki, M., Trompier, D., & Savary, S. (2017). Predictive Structure and Topology of Peroxisomal ATP-Binding Cassette (ABC) Transporters. *International Journal of Molecular Sciences*, 18(7), 1593. <https://doi.org/10.3390/IJMS18071593>

Andrews, Z. B., & al., et. (2008). UCP2 mediates ghrelin's action on NPY/AgRP neurons by lowering free radicals. *Nature*, 454, 846–851.

Anstey, K. J., Cherbuin, N., Budge, M., & Young, J. (2011). Body mass index in midlife and late-life as a risk factor for dementia: a meta-analysis of prospective studies. *Obesity Reviews : An Official Journal of the International Association for the Study of Obesity*, 12(5). <https://doi.org/10.1111/J.1467-789X.2010.00825.X>

APA. (2013). American Psychiatric Association - Diagnostic and statistical manual of mental disorders: DSM-5. Arlington, VA.

Arab, L., & Akbar, J. (2002). Biomarkers and the measurement of fatty acids. *Public Health Nutrition*, 5(6a), 865–871. <https://doi.org/10.1079/phn2002391>

Araya, J., Rodrigo, R., Videla, L. A., Thielemann, L., Orellana, M., Pettinelli, P., & Poniachik, J. (2004). Increase in long-chain polyunsaturated fatty acid n - 6/n - 3 ratio in relation to hepatic steatosis in patients with non-alcoholic fatty liver disease. *Clin Sci (Lond)*, 106(6), 635–643. <https://doi.org/10.1042/cs20030326>

Arenaza-Urquijo, E. M., Wirth, M., & Chételat, G. (2015). Cognitive reserve and lifestyle: Moving towards preclinical Alzheimer's disease. *Frontiers in Aging Neuroscience*, 7(JUN), 134. <https://doi.org/10.3389/FNAGI.2015.00134/BIBTEX>

Astarita, G., Kendall, A. C., Dennis, E. A., & Nicolaou, A. (2015a). Targeted lipidomic strategies for oxygenated metabolites of polyunsaturated fatty acids. *Biochimica et Biophysica Acta (BBA) - Molecular and Cell Biology of Lipids*, 1851(4), 456–468. <https://doi.org/10.1016/J.BBALIP.2014.11.012>

Astorg, P., Bertrais, S., Laporte, F., Arnault, N., Estaquio, C., Galan, P., Favier, A., & Hercberg, S. (2008). Plasma n-6 and n-3 polyunsaturated fatty acids as biomarkers of their dietary intakes: A cross-sectional study within a cohort of middle-aged French men and women. *European Journal of Clinical Nutrition*, 62(10), 1155–1161. <https://doi.org/10.1038/sj.ejcn.1602836>

ATCC. (2014). PC-12 Cells: ATCC® CRL-1721 vs. ATCC® CRL-1721.1. https://www.lgcstandards-atcc.org/Global/FAQs/2/E/PC12_Cells__ATCC_CRL1721_vs_ATCC_CRL1721-783.aspx?geo_country=gb

Augustin, R. (2010). The protein family of glucose transport facilitators: It's not only about glucose after all. *IUBMB Life*, 62(5), 315–333.

Awad, A., Araby, I. E. El, & Albaiomy, R. (2021). The influence of Ginkgo Biloba on hepatic gene expression of (PGC1- α , PPAR- α and GLUT-2), liver, kidney functions, hematological and lipid

profile in type I diabetic rats. *Zagazig Veterinary Journal*, 44511(3), 270–282. <https://Doi.org/10.21608/zvjz.2021.86000.1149>

Awad, N., Gagnon, M., & Messier, C. (2004). The relationship between impaired glucose tolerance, type 2 diabetes, and cognitive function. *J Clin Exp Neuropsychol*, 26(8), 1044–1080. <https://Doi.org/10.1080/13803390490514875>

Aydos, L. R., Amaral, L. A. do, Souza, R. S. de, Jacobowski, A. C., Santos, E. F. dos, & Macedo, M. L. R. (2019). Nonalcoholic Fatty Liver Disease Induced by High-Fat Diet in C57bl/6 Models. *Nutrients*, 11(12). <https://Doi.org/10.3390/NU11123067>

Aziz, T. A., Hussain, S. A., Mahwi, T. O., & Ahmed, Z. A. (2018). Efficacy and safety of Ginkgo biloba extract as an ‘add-on’ treatment to metformin for patients with metabolic syndrome: a pilot clinical study. *Therapeutics and Clinical Risk Management*, 14, 1219–1226. <https://Doi.org/10.2147/TCRM.S169503>

Aziz, T. A., Hussain, S. A., Mahwi, T. O., Ahmed, Z. A., Rahman, H. S., & Rasedee, A. (2018). The efficacy and safety of Ginkgo biloba extract as an adjuvant in type 2 diabetes mellitus patients ineffectively managed with metformin: A double-blind, randomized, placebo-controlled trial. *Drug Design, Development and Therapy*, 12, 735. <https://Doi.org/10.2147/DDDT.S157113>

Babio, N., Bulló, M., Basora, J., Martínez-González, M. A., Fernández-Ballart, J., Márquez-Sandoval, F., Molina, C., & Salas-Salvadó, J. (2009). Adherence to the Mediterranean diet and risk of metabolic syndrome and its components. *Nutrition, Metabolism and Cardiovascular Diseases*, 19(8), 563–570. <https://Doi.org/10.1016/j.numecd.2008.10.007>

Bailén, M., Bressa, C., Martínez-López, S., González-Soltero, R., Montalvo Lominchar, M. G., San Juan, C., & Larrosa, M. (2020). Microbiota Features Associated With a High-Fat/Low-Fiber Diet in Healthy Adults. *Frontiers in Nutrition*, 7, 583608. <https://Doi.org/10.3389/fnut.2020.583608>

Baker. (2019). Obesity Statistics.

Baker, L. D., Cross, D. J., Minoshima, S., Belongia, D., Watson, G. S., & Craft, S. (2011). Insulin resistance and Alzheimer-like reductions in regional cerebral glucose metabolism for cognitively normal adults with prediabetes or early type 2 diabetes. *Archives of Neurology*, 68(1), 51–57.

Balasubramanian, P., Kiss, T., Tarantini, S., Nyúl-Tóth, Á., Ahire, C., Yabluchanskiy, A., ... & Ungvari, Z. (2021). Obesity-induced cognitive impairment in older adults: a microvascular perspective. *American Journal of Physiology-Heart and Circulatory Physiology*, 320(2), H740-H761. <https://Doi.org/10.1152/AJPHEART.00736.2020>

Banin, R. M., de Andrade, I. S., Cerutti, S. M., Oyama, L. M., Telles, M. M., & Ribeiro, E. B. (2017). Ginkgo biloba Extract (GbE) stimulates the hypothalamic serotonergic system and attenuates obesity in ovariectomized rats. *Frontiers in Pharmacology*, 8(SEP). <https://Doi.org/10.3389/FPHAR.2017.00605/PDF>

Banin, R. M., Hirata, B. K. S., Andrade, I. S., Zemdegs, J. C. S., Clemente, A. P. G., Dornellas, A. P. S., Boldarine, V. T., Estadella, D., Albuquerque, K. T., Oyama, L. M., Ribeiro, E. B., & Telles, M. M. (2014a). Beneficial effects of Ginkgo biloba extract on insulin signaling cascade, dyslipidemia, and body adiposity of diet-induced obese rats. *Brazilian Journal of Medical and Biological Research = Revista Brasileira de Pesquisas Medicas e Biologicas*, 47(9), 780–788. <https://Doi.org/10.1590/1414-431x20142983>

Banin, R. M., Machado, M. M. F., de Andrade, I. S., Carvalho, L. O. T., Hirata, B. K. S., de Andrade, H. M., Júlio, V. da S., Ribeiro, J. de S. F. B., Cerutti, S. M., Oyama, L. M., Ribeiro, E. B., & Telles, M. M. (2021). Ginkgo biloba extract (GbE) attenuates obesity and anxious/depressive-like behaviours induced by ovariectomy. *Scientific Reports*, 11(1). <https://Doi.org/10.1038/s41598-020-78528-3>

Banin, R. M., Machado, M. M. F., & Telles, M. M. (2017). A Bi-Directional Relation between Menopause and Obesity: Focus on the Main Causes and Associated Metabolic Diseases. *Current Research in Diabetes & Obesity Journal*, 3(2), 41–43. <https://Doi.org/10.19080/CRDOJ.2017.03.555609>

Bansal, S., Buring, J. E., Rifai, N., Mora, S., Sacks, F. M., & Ridker, P. M. (2007). Fasting compared with nonfasting triglycerides and risk of cardiovascular events in women. *Journal of the American Medical Association*, 298(3), 309–316. <https://Doi.org/10.1001/JAMA.298.3.309>

Barazzoni, R., Bosutti, A., Stebel, M., Cattin, M. R., Roder, E., Visintin, L., Cattin, L., Biolo, G., Zanetti, M., & Guarnieri, G. (2005). Ghrelin regulates mitochondrial-lipid metabolism gene expression and tissue fat distribution in liver and skeletal muscle. *American Journal of Physiology. Endocrinology and Metabolism*, 288(1). <https://Doi.org/10.1152/AJPENDO.00115.2004>

Barber, M. C., Price, N. T., & Travers, M. T. (2005). Structure and regulation of acetyl-CoA carboxylase genes of metazoa. *Biochimica et Biophysica Acta - Molecular and Cell Biology of Lipids*, 1733(1), 1–28. <https://Doi.org/10.1016/J.BBALIP.2004.12.001>

Barile, C. J., Tse, E. C. M., Li, Y., Gewargis, J. P., Kirchsclager, N. A., Zimmerman, S. C., & Gewirth, A. A. (2016). The Flip-Flop Diffusion Mechanism across Lipids in a Hybrid Bilayer Membrane. *Biophysical Journal*, 110(11), 2451–2462. <https://Doi.org/10.1016/J.BPJ.2016.04.041>

Barone, R., Rizzo, R., Tabbí, G., Malaguarnera, M., Frye, R. E., & Bastin, J. (2019). Nuclear Peroxisome Proliferator-Activated Receptors (PPARs) as Therapeutic Targets of Resveratrol for Autism Spectrum Disorder. *International Journal of Molecular Sciences* 2019, Vol. 20, Page 1878, 20(8), 1878. <https://Doi.org/10.3390/IJMS20081878>

Barrea, L., Muscogiuri, G., Pugliese, G., de Alteriis, G., Colao, A., & Savastano, S. (2021). Metabolically Healthy Obesity (MHO) vs. Metabolically Unhealthy Obesity (MUO) Phenotypes in PCOS: Association with Endocrine-Metabolic Profile, Adherence to the Mediterranean Diet, and Body Composition. *Nutrients*, 13(11). <https://Doi.org/10.3390/NU13113925>

Barrows, B. R., & Parks, E. J. (2006). Contributions of different fatty acid sources to very low-density lipoprotein-triacylglycerol in the fasted and fed states. *The Journal of Clinical Endocrinology and Metabolism*, 91(4), 1446–1452. <https://doi.org/10.1210/JC.2005-1709>

Bartrés-Faz, D., & Arenaza-Urquijo, E. M. (2011). Structural and functional imaging correlates of cognitive and brain reserve hypotheses in healthy and pathological aging. *Brain Topography*, 24(3–4), 340–357. <https://doi.org/10.1007/S10548-011-0195-9>

Bastianetto, S., Ramassamy, C., Doré, S., Christen, Y., Poirier, J., & Quirion, R. (2000). The ginkgo biloba extract (EGb 761) protects hippocampal neurons against cell death induced by β -amyloid. *European Journal of Neuroscience*, 12(6), 1882–1890.

Bastin, J., & Djouadi, F. (2016). Resveratrol and Myopathy. *Nutrients*, 8(5). <https://doi.org/10.3390/NU8050254>

Baufeld, C., Osterloh, A., Prokop, S., Miller, K. R., & Heppner, F. L. (2016). High-fat diet-induced brain region-specific phenotypic spectrum of CNS resident microglia. *Acta Neuropathol.*, 132, 361–375.

Baur, J. A., & Sinclair, D. A. (2006). Therapeutic potential of resveratrol: The in vivo evidence. In *Nature Reviews Drug Discovery* (Vol. 5, Issue 6, pp. 493–506). <https://doi.org/10.1038/nrd2060>

Baylin, A., Kabagambe, E. K., Siles, X., & Campos, H. (2002). Adipose tissue biomarkers of fatty acid intake. *American Journal of Clinical Nutrition*, 76(4), 750–757. <https://doi.org/10.1093/ajcn/76.4.750>

Bazinet, R. P., & Layé, S. (2014). Polyunsaturated fatty acids and their metabolites in brain function and disease. *Nature Reviews Neuroscience*, 15(12), 771–785. <https://doi.org/10.1038/nrn3820>

Beaulac, J., & Sandre, D. (2017). Critical review of bariatric surgery, medically supervised diets, and behavioural interventions for weight management in adults. *Perspectives in Public Health*, 137(3), 162–172. <https://doi.org/10.1177/1757913916653425>

Beaven, S. W., Matveyenko, A., Wroblewski, K., Chao, L., Wilpitz, D., Hsu, T. W., Lentz, J., Drew, B., Hevener, A. L., & Tontonoz, P. (2013). Reciprocal Regulation of Hepatic and Adipose Lipogenesis by Liver X Receptors in Obesity and Insulin Resistance. *Cell Metabolism*, 18(1), 106. <https://doi.org/10.1016/J.CMET.2013.04.021>

Behzadi, A., Pujol-Calderón, F., Tjust, A. E., Wuolikainen, A., Höglund, K., Forsberg, K., Portelius, E., Blennow, K., Zetterberg, H., & Andersen, P. M. (2021). Neurofilaments can differentiate ALS subgroups and ALS from common diagnostic mimics. *Scientific Reports*, 11(1). <https://doi.org/10.1038/s41598-021-01499-6>

Benedet, A. L., Leuzy, A., Pascoal, T. A., Ashton, N. J., Mathotaarachchi, S., Savard, M., Therriault, J., Kang, M. S., Chamoun, M., Schöll, M., Zimmer, E. R., Gauthier, S., Labbe, A., Zetterberg, H., Rosa-Neto, P., & Blennow, K. (2020). Stage-specific links between plasma

neurofilament light and imaging biomarkers of Alzheimer's disease. *Brain*, 143(12), 3793–3804. <https://doi.org/10.1093/brain/awaa342>

Benomar, Y., & Taouis, M. (2019). Molecular mechanisms underlying obesity-induced hypothalamic inflammation and insulin resistance: Pivotal role of resistin/tlr4 pathways. *Frontiers in Endocrinology*, 10(MAR), 140. <https://doi.org/10.3389/FENDO.2019.00140/BIBTEX>

Benzler, J., Ganjam, G. K., Legler, K., Stöhr, S., Krüger, M., Steger, J., & Tups, A. (2013a). Acute inhibition of central c-Jun N-terminal kinase restores hypothalamic insulin signalling and alleviates glucose intolerance in diabetic mice. *J Neuroendocrinol*, 25(5), 446–454. <https://doi.org/10.1111/jne.12018>

Berthiaume, M., Laplante, M., Festuccia, W., Gélinas, Y., Poulin, S., Lalonde, J., Joanisse, D. R., Thieringer, R., & Deshaies, Y. (2007). Depot-specific modulation of rat intraabdominal adipose tissue lipid metabolism by pharmacological inhibition of 11beta-hydroxysteroid dehydrogenase type 1. *Endocrinology*, 148(5), 2391–2397. <https://doi.org/10.1210/EN.2006-1199>

Bhusal, A., Rahman, M. H., & Suk, K. (2022). Hypothalamic inflammation in metabolic disorders and aging. *Cellular and Molecular Life Sciences*, 79(1). <https://doi.org/10.1007/S00018-021-04019-X>

Bhutia, Y. D., & Ganapathy, V. (2015). Short, but smart: SCFAs train T cells in the gut to fight autoimmunity in the brain. *Immunity*, 43(4), 629–631. <https://doi.org/10.1016/j.immuni.2015.09.014>

Bhutia, Y. D., & Ganapathy, V. (2021). Digestion and absorption of carbohydrate, protein, and fat. *Sleisenger & Fordtran's Gastrointestinal and Liver Disease*. 11th Ed. Philadelphia, PA: Elsevier.

Bigornia, S. J., Farb, M. G., Mott, M. M., Hess, D. T., Carmine, B., Fiscale, A., Joseph, L., Apovian, C. M., & Gokce, N. (2012). Relation of depot-specific adipose inflammation to insulin resistance in human obesity. *Nutrition and Diabetes*, 2(MARCH). <https://doi.org/10.1038/NUTD.2012.3>

Biolegend. (2018). Cyto-Fast Fix-Perm Buffer Set. <https://www.biolegend.com/nl-nl/products/cyto-fast-fix-perm-buffer-set-16765>

Biolegend. (2020). APC Annexin V Apoptosis Detection Kit with 7-AAD, Version: 2. <https://www.biolegend.com/fr-lu/products/apc-annexin-v-apoptosis-detection-kit-with-7-aad-9754>

Birkenfeld, A. L., & Shulman, G. I. (2014). Nonalcoholic fatty liver disease, hepatic insulin resistance, and type 2 diabetes. *Hepatology (Baltimore, Md.)*, 59(2), 713–723. <https://doi.org/10.1002/HEP.26672>

Björkhem, I. (2006). Crossing the barrier: oxysterols as cholesterol transporters and metabolic modulators in the brain. *Journal of Internal Medicine*, 260(6), 493–508. <https://doi.org/10.1111/J.1365-2796.2006.01725.X>

Björkhem, I., Leoni, V., & Meaney, S. (2010). Genetic connections between neurological disorders and cholesterol metabolism. *Journal of Lipid Research*, 51(9), 2489–2503. <https://doi.org/10.1194/JLR.R006338>

Björkhem, I., Lövgren-Sandblom, A., Leoni, V., Meaney, S., Brodin, L., Salveson, L., Winge, K., Pålhagen, S., & Svenningsson, P. (2013). Oxysterols and Parkinson's disease: evidence that levels of 24S-hydroxycholesterol in cerebrospinal fluid correlates with the duration of the disease. *Neuroscience Letters*, 555, 102–105. <https://doi.org/10.1016/J.NEULET.2013.09.003>

Björkhem, I., Meaney, S., & Fogelman, A. M. (2004). Brain cholesterol: long secret life behind a barrier. *Arteriosclerosis, Thrombosis, and Vascular Biology*, 24(5), 806–815. <https://doi.org/10.1161/01.ATV.0000120374.59826.1B>

Bjorntorp, P. (1990). 'Portal' adipose tissue as a generator of risk factors for cardiovascular disease and diabetes. *Arteriosclerosis*, 10(4), 493–496. <https://doi.org/10.1161/01.ATV.10.4.493>

Bligh, E. G., & Dyer, W. J. (1959). A rapid method of total lipid extraction and purification. *Canadian Journal of Biochemistry and Physiology*, 37(8), 911–917.

Bodovitz, S., & Klein, W. L. (1996). Cholesterol modulates-secretase cleavage of amyloid precursor protein. *Journal of Biological Chemistry*, 271(8), 4436–4440.

Bogl, L. H., Kaprio, J., & Pietiläinen, K. H. (2020). Dietary n-6 to n-3 fatty acid ratio is related to liver fat content independent of genetic effects: Evidence from the monozygotic co-twin control design. *Clinical Nutrition*, 39(7), 2311–2314. <https://doi.org/10.1016/J.CLNU.2019.10.011>

Boldarine, V. T., Joyce, E., Pedroso, A. P., Telles, M. M., Oyama, L. M., Bueno, A. A., & Ribeiro, E. B. (2021). Oestrogen replacement fails to fully revert ovariectomy-induced changes in adipose tissue monoglycerides, diglycerides and cholesteryl esters of rats fed a lard-enriched diet. *Scientific Reports* 2021 11:1, 11(1), 1–11. <https://doi.org/10.1038/s41598-021-82837-6>

Bondia-Pons, I., Ryan, L., & Martinez, J. A. (2012). Oxidative stress and inflammation interactions in human obesity. *Journal of Physiology and Biochemistry*, 68(4), 701–711. <https://doi.org/10.1007/S13105-012-0154-2>

Booth, A., Magnuson, A., & Foster, M. (2014). Detrimental and protective fat: Body fat distribution and its relation to metabolic disease. *Hormone Molecular Biology and Clinical Investigation*, 17(1), 13–27. <https://doi.org/10.1515/HMBCI-2014-0009>

Börgeeson, E., Johnson, A. M. F., Lee, Y. S., Till, A., Syed, G. H., Ali-Shah, S. T., Guiry, P. J., Dalli, J., Colas, R. A., Serhan, C. N., Sharma, K., & Godson, C. (2015). Lipoxin A4 attenuates obesity-induced adipose inflammation and associated liver and kidney disease. *Cell Metabolism*, 22(1), 125. <https://doi.org/10.1016/J.CMET.2015.05.003>

Borra, M. T., Smith, B. C., & Denu, J. M. (2005). Mechanism of human SIRT1 activation by resveratrol. *Journal of Biological Chemistry*, 280(17), 17187–17195. <https://doi.org/10.1074/jbc.M501250200>

Bosviel, R., Joumard-Cubizolles, L., Chinetti-Gbaguidi, G., Bayle, D., Copin, C., Hennuyer, N., Duplan, I., Staels, B., Zanoni, G., Porta, A., Balas, L., Galano, J. M., Oger, C., Mazur, A., Durand, T., & Gladine, C. (2017). DHA-derived oxylipins, neuroprostanes and protectins, differentially and dose-dependently modulate the inflammatory response in human macrophages: Putative mechanisms through PPAR activation. *Free Radical Biology & Medicine*, 103, 146–154. <https://doi.org/10.1016/j.freeradbiomed.2016.12.018>

Braet, G. C. (2003). Cognitive interference due to food cues in childhood obesity. *J Clin Child Adolesc*, 32, 32–39.

Brasnyó, P., Molnár, G. A. G. A., Mohás, M., Markó, L., Laczy, B., Cseh, J., Mikolás, E., Szijártó, I. A., Mérei, Á., Halmai, R., Mészáros, L. G., Sümegi, B., Wittmann, I., Mérei, A., & Halmai, R. (2011). Resveratrol improves insulin sensitivity, reduces oxidative stress and activates the Akt pathway in type 2 diabetic patients. *British Journal of Nutrition*, 106(3), 383–389. <https://doi.org/10.1017/S0007114511000316>

Bray, G. A., & Popkin, B. M. (1998). Dietary fat intake does affect obesity! *The American Journal of Clinical Nutrition*, 68(6), 1157–1173. <https://doi.org/10.1093/AJCN/68.6.1157>

Breen, M. R., Camps, M., Carvalho-Simoes, F., Zorzano, A., & Pilch, P. F. (2012). Cholesterol Depletion in Adipocytes Causes Caveolae Collapse Concomitant with Proteosomal Degradation of Cavin-2 in a Switch-Like Fashion. *PLOS ONE*, 7(4), e34516. <https://doi.org/10.1371/JOURNAL.PONE.0034516>

Breil, C., Abert Vian, M., Zemb, T., Kunz, W., & Chemat, F. (2017). “Bligh and Dyer” and Folch methods for solid–liquid–liquid extraction of lipids from microorganisms. Comprehension of solvation mechanisms and towards substitution with alternative solvents. *International Journal of Molecular Sciences*, 18(4), 708.

Bridi, R., Crossetti, F. P., Steffen, V. M., & Henriques, A. T. (2001). The antioxidant activity of standardized extract of *Ginkgo biloba* (EGb 761) in rats. *Phytotherapy Research*, 15(5), 449–451.

Briggs, D. I., Lockie, S. H., Wu, Q., Lemus, M. B., Stark, R., & Andrews, Z. B. (2013). Calorie-Restricted Weight Loss Reverses High-Fat Diet-Induced Ghrelin Resistance, Which Contributes to Rebound Weight Gain in a Ghrelin-Dependent Manner. *Endocrinology*, 154(2), 709–717. <https://doi.org/10.1210/EN.2012-1421>

Brockmann, K. (2009). The expanding phenotype of GLUT1-deficiency syndrome. *Brain and Development*, 31(7), 545–552.

Broughton, K. S., Whelan, J., Hardardottir, I., & Kinsella, J. E. (1991). Effect of Increasing the Dietary (n-3) to (n-6) Polyunsaturated Fatty Acid Ratio on Murine Liver and Peritoneal Cell Fatty Acids and Eicosanoid Formation. *The Journal of Nutrition*, 121(2), 155–164. <https://doi.org/10.1093/JN/121.2.155>

Bruce, K. D., Zsombok, A., & Eckel, R. H. (2017). Lipid processing in the brain: A key regulator of systemic metabolism. *Frontiers in Endocrinology*, 8(APR), 60. <https://doi.org/10.3389/FENDO.2017.00060/BIBTEX>

Bruss, M. D., Khambatta, C. F., Ruby, M. A., Aggarwal, I., & Hellerstein, M. K. (2010). Calorie restriction increases fatty acid synthesis and whole body fat oxidation rates. *American Journal of Physiology. Endocrinology and Metabolism*, 298(1). <https://doi.org/10.1152/AJPENDO.00524.2009>

Bubber, P., Haroutunian, V., Fisch, G., Blass, J. P., & Gibson, G. E. (2005). Mitochondrial abnormalities in Alzheimer brain: mechanistic implications. *Ann Neurol*, 57(5), 695–703. <https://doi.org/10.1002/ana.20474>

Budson, A. E., & Solomon, P. R. (2021). *Memory Loss, Alzheimer's Disease, and Dementia-E-Book: A Practical Guide for Clinicians*. Elsevier Health Sciences.

Bueno, A. A., Brand, A., Neville, M. M., Lehane, C., Brierley, N., & Crawford, M. A. (2015). Erythrocyte phospholipid molecular species and fatty acids of Down syndrome children compared with non-affected siblings. *British Journal of Nutrition*, 113(1), 72–81.

Bueno, A. A., Habitante, C. A., Oyama, L. M., Estadella, D., Ribeiro, E. B., & Oller Do Nascimento, C. M. (2011). White adipose tissue re-growth after partial lipectomy in high fat diet induced obese Wistar rats. *Journal of Physiological Sciences*, 61(1), 55–63. <https://doi.org/10.1007/s12576-010-0122-y>

Bueno, A. A., Oyama, L. M., de Oliveira, C., Pisani, L. P., Ribeiro, E. B., Silveira, V. L. F., & Oller Do Nascimento, C. M. (2008). Effects of different fatty acids and dietary lipids on adiponectin gene expression in 3T3-L1 cells and C57BL/6J mice adipose tissue. *Pflugers Archiv European Journal of Physiology*, 455(4), 701–709. <https://doi.org/10.1007/s00424-007-0330-3>

Buettner, R., Schölmerich, J., & Bollheimer, L. C. (2007). High-fat diets: Modeling the metabolic disorders of human obesity in rodents. *Obesity*, 15(4), 798–808. <https://doi.org/10.1038/OBY.2007.608>

Buie, J. J., Watson, L. S., Smith, C. J., & Sims-Robinson, C. (2019). Obesity-related cognitive impairment: The role of endothelial dysfunction. *Neurobiology of Disease*, 132, 104580. <https://doi.org/10.1016/J.NBD.2019.104580>

Buntwal, L., Sassi, M., Morgan, A. H., Andrews, Z. B., & Davies, J. S. (2019). Ghrelin-Mediated Hippocampal Neurogenesis: Implications for Health and Disease. *Trends in Endocrinology and Metabolism*, 30(11), 844–859. <https://doi.org/10.1016/J.TEM.2019.07.001>

Burdge, G. (2004). Alpha-linolenic acid metabolism in men and women: nutritional and biological implications. *Current Opinion in Clinical Nutrition and Metabolic Care*, 7(2), 137–144. <https://doi.org/10.1097/00075197-200403000-00006>

Burdge, G. C., & Calder, P. C. (2005). Conversion of α -linolenic acid to longer-chain polyunsaturated fatty acids in human adults. In *Reproduction Nutrition Development* (Vol. 45, Issue 5, pp. 581–597). <https://doi.org/10.1051/rnd:2005047>

Burdge, G. C., Wright, P., Jones, A. E., & Wootton, S. A. (2000). A method for separation of phosphatidylcholine, triacylglycerol, non-esterified fatty acids and cholesterol esters from plasma by solid-phase extraction. *British Journal of Nutrition*, 84(5), 781–787.

Burguera, B., Couce, M. E., Curran, G. L., Jensen, M. D., Lloyd, R. v., Cleary, M. P., & Poduslo, J. F. (2000). Obesity is associated with a decreased leptin transport across the blood-brain barrier in rats. *Diabetes*, 49(7), 1219–1223. <https://doi.org/10.2337/DIABETES.49.7.1219>

Burns, J., Yokota, T., Ashihara, H., Lean, M. E. J., & Crozier, A. (2002). Plant foods and herbal sources of resveratrol. *Journal of Agricultural and Food Chemistry*, 50(11), 3337–3340.

Byrnes, K. G., Walsh, D., Walsh, L. G., Coffey, D. M., Ullah, M. F., Mirapeix, R., Hikspoors, J., Lamers, W., Wu, Y., Zhang, X. Q., Zhang, S. X., Brama, P., Dunne, C. P., O'Brien, I. S., Peirce, C. B., Shelly, M. J., Scanlon, T. G., Luther, M. E., Brady, H. D., ... Coffey, J. C. (2021). The development and structure of the mesentery. *Communications Biology*, 4(1). <https://doi.org/10.1038/S42003-021-02496-1>

Caceres, A., Banker, G. A., & Binder, L. (1986). Immunocytochemical localization of tubulin and microtubule-associated protein 2 during the development of hippocampal neurons in culture. *Journal of Neuroscience*, 6(3), 714–722. <https://doi.org/10.1523/JNEUROSCI.06-03-00714.1986>

Cadena-Obando, D., Ramírez-Rentería, C., Ferreira-Hermosillo, A., Albarrán-Sanchez, A., Sosa-Eroza, E., Molina-Ayala, M., & Espinosa-Cárdenas, E. (2020). Are there really any predictive factors for a successful weight loss after bariatric surgery? *BMC Endocrine Disorders*, 20(1), 1–8. <https://doi.org/10.1186/S12902-020-0499-4/FIGURES/1>

Cai, D., & Liu, T. (2012). Inflammatory cause of metabolic syndrome via brain stress and NF- κ B. *Aging*, 4(2), 98–115. <https://doi.org/10.18632/AGING.100431>

Calder, P. C., & Grimble, R. F. (2002). Polyunsaturated fatty acids, inflammation and immunity. *European Journal of Clinical Nutrition*, 56(SUPPL. 3). <https://doi.org/10.1038/sj.ejcn.1601478>

Caligiuri, S. P. B., Love, K., Winter, T., Gauthier, J., Taylor, C. G., Blydt-Hansen, T., Zahradka, P., & Aukema, H. M. (2013). Dietary Linoleic Acid and α -Linolenic Acid Differentially Affect Renal Oxylipins and Phospholipid Fatty Acids in Diet-Induced Obese Rats. *The Journal of Nutrition*, 143(9), 1421–1431. <https://doi.org/10.3945/JN.113.177360>

Calle, E. E., Rodriguez, C., Walker-Thurmond, K., & Thun, M. J. (2003). Overweight, obesity, and mortality from cancer in a prospectively studied cohort of U.S. adults. *The New England Journal of Medicine*, 348(17), 1625–1638. <https://doi.org/10.1056/NEJM0A021423>

Calle, E. E., Thun, M. J., Petrelli, J. M., Rodriguez, C., & Heath, C. W. (1999). Body-mass index and mortality in a prospective cohort of U.S. adults. *The New England Journal of Medicine*, 341(15), 1097–1105. <https://doi.org/10.1056/NEJM199910073411501>

Calvin Coffey, J., Walsh, D., Byrnes, K. G., Hohenberger, W., & Heald, R. J. (2020). Mesentery - a 'New' organ. *Emerging Topics in Life Sciences*, 4(2), 191–206. <https://doi.org/10.1042/ETLS20200006>

Campillo, M., Medina, S., Fanti, F., Gallego-Gómez, J. I., Simonelli-Muñoz, A., Bultel-Poncé, V., Durand, T., Galano, J. M., Tomás-Barberán, F. A., Gil-Izquierdo, Á., & Domínguez-Perles, R. (2021). Phytosteranes and phytofurans modulate COX-2-linked inflammation markers in LPS-stimulated THP-1 monocytes by lipidomics workflow. *Free Radical Biology & Medicine*, 167, 335–347. <https://doi.org/10.1016/j.freeradbiomed.2021.03.002>

Canevelli, M., Adali, N., Kelaiditi, E., Cantet, C., Ousset, P.-J., & Cesari, M. (2014). Effects of Ginkgo biloba supplementation in Alzheimer's disease patients receiving cholinesterase inhibitors: data from the ICTUS study. *Phytomedicine*, 21(6), 888–892.

Canfora, E. E., Meex, R. C. R., Venema, K., & Blaak, E. E. (2019). Gut microbial metabolites in obesity, NAFLD and T2DM. *Nat. Rev. Endocrinol.*, 15(5), 261–273. <https://doi.org/10.1038/s41574-019-0156-z>

Cano, P., Cardinali, D. P., Ríos-Lugo, M. J., Fernández-Mateos, M. P., Reyes Toso, C. F., & Esquifino, A. I. (2009). Effect of a high-fat diet on 24-hour pattern of circulating adipocytokines in rats. *Obesity (Silver Spring, Md.)*, 17(10), 1866–1871. <https://doi.org/10.1038/OBY.2009.200>

Cao, H., Gerhold, K., Mayers, J. R., Wiest, M. M., Watkins, S. M., & Hotamisligil, G. S. (2008). Identification of a Lipokine, a Lipid Hormone Linking Adipose Tissue to Systemic Metabolism. *Cell*, 134(6), 933. <https://doi.org/10.1016/j.cell.2008.07.048>

Carapelle, E., Mundi, C., Cassano, T., & Avolio, C. (2020). Interaction between Cognitive Reserve and Biomarkers in Alzheimer Disease. *International Journal of Molecular Sciences* 2020, Vol. 21, Page 6279, 21(17), 6279. <https://doi.org/10.3390/IJMS21176279>

Caricilli, A. M., Nascimento, P. H., Pauli, J. R., Tsukumo, D. M. L., Velloso, L. A., Carnevali, J. B., & Saad, M. J. A. (2008). Inhibition of toll-like receptor 2 expression improves insulin sensitivity and signaling in muscle and white adipose tissue of mice fed a high-fat diet. *Journal of Endocrinology*, 199(3), 399–406. <https://doi.org/10.1677/JOE-08-0354>

Carpentier, A. C., Blondin, D. P., Virtanen, K. A., Richard, D., Haman, F., & Turcotte, É. E. (2018). Brown adipose tissue energy metabolism in humans. *Frontiers in Endocrinology*, 9(AUG), 447. <https://doi.org/10.3389/FENDO.2018.00447/BIBTEX>

Castrejón-Tellez, V., Rodríguez-Pérez, J. M., Pérez-Torres, I., Pérez-Hernández, N., Cruz-Lagunas, A., Guarner-Lans, V., Vargas-Alarcón, G., & Rubio-Ruiz, M. E. (2016). The Effect of Resveratrol and Quercetin Treatment on PPAR Mediated Uncoupling Protein (UCP-) 1, 2, and 3 Expression in Visceral White Adipose Tissue from Metabolic Syndrome Rats. *International Journal of Molecular Sciences* 2016, Vol. 17, Page 1069, 17(7), 1069. <https://doi.org/10.3390/IJMS17071069>

Catalano, K. J., Stefanovski, D., & Bergman, R. N. (2010). Critical role of the mesenteric depot versus other intra-abdominal adipose depots in the development of insulin resistance in young rats. *Diabetes*, 59(6), 1416–1423. <https://doi.org/10.2337/DB08-0675>

Caussy, C., Aubin, A., & Loomba, R. (2021). The Relationship Between Type 2 Diabetes, NAFLD, and Cardiovascular Risk. *Current Diabetes Reports*, 21(5). <https://doi.org/10.1007/S11892-021-01383-7>

Cazarolli, L. H., Folador, P., Pizzolatti, M. G., & Silva, F. R. M. B. (2009). Signaling pathways of kaempferol-3-neohesperidoside in glycogen synthesis in rat soleus muscle. *Biochimie*, 91(7), 843–849. <https://doi.org/10.1016/j.biochi.2009.04.004>

Ceddia, R. P., Liu, D., Shi, F., Crowder, M. K., Mishra, S., Kass, D. A., & Collins, S. (2021). Increased Energy Expenditure and Protection From Diet-Induced Obesity in Mice Lacking the cGMP-Specific Phosphodiesterase PDE9. *Diabetes*, 70(12), 2823–2836. <https://doi.org/10.2337/DB21-0100>

Cervone, D. T., & Dyck, D. J. (2017). Acylated and unacylated ghrelin do not directly stimulate glucose transport in isolated rodent skeletal muscle. *Physiological Reports*, 5(13). <https://doi.org/10.14814/PHY2.13320>

Cervone, D. T., Hucik, B., Lovell, A. J., & Dyck, D. J. (2020). Unacylated ghrelin stimulates fatty acid oxidation to protect skeletal muscle against palmitate-induced impairment of insulin action in lean but not high-fat fed rats. *Metabolism Open*, 5, 100026. <https://doi.org/10.1016/J.METOP.2020.100026>

Cervone, D. T., Sheremeta, J., Kraft, E. N., & Dyck, D. J. (2019). Acylated and unacylated ghrelin directly regulate β -3 stimulated lipid turnover in rodent subcutaneous and visceral adipose tissue *ex vivo* but not *in vivo*. *Adipocyte*, 8(1), 1-15. <https://doi.org/10.1080/21623945.2018.1528811>

Chadwick, W., Zhou, Y., Park, S. S., Wang, L., Mitchell, N., Stone, M. D., Becker, K. G., Martin, B., & Maudsley, S. (2010). Minimal Peroxide Exposure of Neuronal Cells Induces Multifaceted Adaptive Responses. *PLOS ONE*, 5(12), e14352. <https://doi.org/10.1371/JOURNAL.PONE.0014352>

Chait, A., & den Hartigh, L. J. (2020). Adipose Tissue Distribution, Inflammation and Its Metabolic Consequences, Including Diabetes and Cardiovascular Disease. *Frontiers in Cardiovascular Medicine*, 7, 22. <https://doi.org/10.3389/FCVM.2020.00022/BIBTEX>

Chajès, V., Jenab, M., Romieu, I., Ferrari, P., Dahm, C. C., Overvad, K., Egeberg, R., Tjønneland, A., Clavel-Chapelon, F., Boutron-Ruault, M. C., Engel, P., Teucher, B., Kaaks, R., Floegel, A., Boeing, H., Trichopoulou, A., Dilis, V., Karapetyan, T., Mattiello, A., ... González, C. A. (2011). Plasma phospholipid fatty acid concentrations and risk of gastric adenocarcinomas in the European Prospective Investigation into Cancer and Nutrition (EPIC-EURGAST). *The American Journal of Clinical Nutrition*, 94(5), 1304–1313. <https://doi.org/10.3945/AJCN.110.005892>

Chang, E., Varghese, M., & Singer, K. (2018). Gender and Sex Differences in Adipose Tissue. *Current Diabetes Reports*, 18(9), 69. <https://doi.org/10.1007/S11892-018-1031-3>

Chang, T. T., Chen, Y. A., Li, S. Y., & Chen, J. W. (2021). Nrf-2 mediated heme oxygenase-1 activation contributes to the anti-inflammatory and renal protective effects of Ginkgo biloba

extract in diabetic nephropathy. *Journal of Ethnopharmacology*, 266, 113474. <https://doi.org/10.1016/J.JEP.2020.113474>

Chapman, K., Holmes, M., & Seckl, J. (2013). 11β -Hydroxysteroid Dehydrogenases: Intracellular Gate-Keepers of Tissue Glucocorticoid Action. *Physiological Reviews*, 93(3), 1139. <https://doi.org/10.1152/PHYSREV.00020.2012>

ChemicalBook. (2017). Nervonic acid methyl ester CAS#: 2733-88-2. https://www.chemicalbook.com/ProductChemicalPropertiesCB9104242_EN.htm

Chen, C. T., Green, J. T., Orr, S. K., & Bazinet, R. P. (2008). Regulation of brain polyunsaturated fatty acid uptake and turnover. *Prostaglandins, Leukotrienes, and Essential Fatty Acids*, 79(3–5), 85–91. <https://doi.org/10.1016/J.PLEFA.2008.09.003>

Chen, C. T., Kitson, A. P., Hopperton, K. E., Domenichiello, A. F., Trépanier, M. O., Lin, L. E., Ermini, L., Post, M., Thies, F., & Bazinet, R. P. (2015). Plasma non-esterified docosahexaenoic acid is the major pool supplying the brain. *Scientific Reports* 2015 5:1, 5(1), 1–12. <https://doi.org/10.1038/srep15791>

Chen, L., Duan, Y., Wei, H., Ning, H., Bi, C., Zhao, Y., Qin, Y., & Li, Y. (2019). Acetyl-CoA carboxylase (ACC) as a therapeutic target for metabolic syndrome and recent developments in ACC1/2 inhibitors. *Expert Opinion on Investigational Drugs*, 28(10), 917–930. <https://doi.org/10.1080/13543784.2019.1657825>

Chen, L., Xu, B., Liu, L., Luo, Y., Yin, J., Zhou, H., Chen, W., Shen, T., Han, X., & Huang, S. (2010). Hydrogen peroxide inhibits mTOR signaling by activation of AMPK α leading to apoptosis of neuronal cells. *Laboratory Investigation* 2010 90:5, 90(5), 762–773. <https://doi.org/10.1038/labinvest.2010.36>

Chen, L. Y., Liu, L. K., Peng, L. N., Lin, M. H., Chen, L. K., Lan, C. F., & Chang, P. L. (2014). Identifying residents at greater risk for cognitive decline by Minimum Data Set in long-term care settings. *Journal of Clinical Gerontology and Geriatrics*, 5(4), 122–126. <https://doi.org/10.1016/J.JCGG.2014.05.006>

Chen, X., Shang, L., Deng, S., Li, P., Chen, K., Gao, T., Zhang, X., Chen, Z., & Zeng, J. (2020). Peroxisomal oxidation of erucic acid suppresses mitochondrial fatty acid oxidation by stimulating malonyl-CoA formation in the rat liver. *Journal of Biological Chemistry*, 295(30), 10168–10179. <https://doi.org/10.1074/JBC.RA120.013583>

Chen, Y., Yu, K., Hu, Y., & Chang, Y. (2019). Ginkgo biloba Extract Protects Mesenteric Arterioles of Old Rats via Improving Vessel Elasticity through Akt/FoxO3a Signaling Pathway. *Annals of Vascular Surgery*, 57, 220–228. <https://doi.org/10.1016/j.avsg.2019.01.001>

Chen, Z., & Zhong, C. (2013). Decoding Alzheimer's disease from perturbed cerebral glucose metabolism: implications for diagnostic and therapeutic strategies. *Progress in Neurobiology*, 108, 21–43.

Cheng, A., Uetani, N., Simoncic, P. D., Chaubey, V. P., Lee-Loy, A., McGlade, C. J., Kennedy, B. P., & Tremblay, M. L. (2002). Attenuation of leptin action and regulation of obesity by protein

tyrosine phosphatase 1B. *Developmental Cell*, 2(4), 497–503. [https://doi.org/10.1016/S1534-5807\(02\)00149-1](https://doi.org/10.1016/S1534-5807(02)00149-1)

Cheng, D., Liang, B., & Li, Y. (2012). Antihyperglycemic effect of Ginkgo biloba extract in streptozotocin-induced diabetes in rats. *BioMed Research International*, 2013.

Cheong, C. U., Yeh, C. S., Hsieh, Y. W., Lee, Y. R., Lin, M. Y., Chen, C. Y., & Lee, C. H. (2016). Protective Effects of Costunolide against Hydrogen Peroxide-Induced Injury in PC12 Cells. *Molecules* 2016, Vol. 21, Page 898, 21(7), 898. <https://doi.org/10.3390/MOLECULES21070898>

Cherkaoui-Malki, M., Surapureddi, S., I. El Hajj, H., Vamecq, J., & Andreoletti, P. (2012). Hepatic steatosis and peroxisomal fatty acid beta-oxidation. *Current Drug Metabolism*, 13(10), 1412–1421. <https://doi.org/10.2174/138920012803762765>

Chiang, J. Y. L., & Ferrell, J. M. (2018). Bile Acid Metabolism in Liver Pathobiology. *Gene Expression*, 18(2), 71. <https://doi.org/10.3727/105221618X15156018385515>

Chien, K. R. (2004). Molecular Basis of Cardiovascular Disease: A Companion to Braunwald's Heart Disease. *Molecular Basis of Cardiovascular Disease: A Companion to Braunwald's Heart Disease*, 1–713. <https://doi.org/10.1016/B978-0-7216-9428-3.X5001-X>

Chirala, S. S., Chang, H., Matzuk, M., Abu-Elheiga, L., Mao, J., Mahon, K., Finegold, M., & Wakil, S. J. (2003). Fatty acid synthesis is essential in embryonic development: Fatty acid synthase null mutants and most of the heterozygotes die in utero. *Proceedings of the National Academy of Sciences of the United States of America*, 100(11), 6358. <https://doi.org/10.1073/PNAS.0931394100>

Chiu, S., Williams, P. T., & Krauss, R. M. (2017). Effects of a very high saturated fat diet on LDL particles in adults with atherogenic dyslipidemia: A randomized controlled trial. *PLoS One*, 12(2). <https://doi.org/10.1371/JOURNAL.PONE.0170664>

Chiu, Y. L., Tsai, W. C., Wu, C. H., Wu, C. H., Cheng, C. C., Lin, W. S., Tsai, T. N., & Wu, L. S. (2020). Ginkgo biloba Induces Thrombomodulin Expression and Tissue-Type Plasminogen Activator Secretion via the Activation of Krüppel-Like Factor 2 within Endothelial Cells. *American Journal of Chinese Medicine*, 48(2), 357–372. <https://doi.org/10.1142/S0192415X20500184>

Cho, Y. L., Park, J. G., Kang, H. J., Kim, W., Cho, M. J., Jang, J. H., Kwon, M. G., Kim, S., Lee, S. H., Lee, J., Kim, Y. G., Park, Y. J., Kim, W. K., Bae, K. H., Kwon, B. M., Chung, S. J., & Min, J. K. (2019). Ginkgetin, a biflavone from Ginkgo biloba leaves, prevents adipogenesis through STAT5-mediated PPAR γ and C/EBP α regulation. *Pharmacological Research*, 139, 325–336. <https://doi.org/10.1016/J.PHRS.2018.11.027>

Choe, S. S., Huh, J. Y., Hwang, I. J., Kim, J. I., & Kim, J. B. (2016). Adipose Tissue Remodeling: Its Role in Energy Metabolism and Metabolic Disorders. *Frontiers in Endocrinology*, 7(APR), 1. <https://doi.org/10.3389/FENDO.2016.00030>

Choque, B., Catheline, D., Rioux, V., & Legrand, P. (2014). Linoleic acid: between doubts and certainties. *Biochimie*, 96(1), 14–21. <https://doi.org/10.1016/J.BIOCHI.2013.07.012>

Christen, Y. (2004). Ginkgo biloba and neurodegenerative disorders. *Front Biosci*, 9(1–3), 3091–3104.

Christie, W. (2006). Prostanoids—prostaglandins, prostacyclins, and thromboxanes. LIPIDMAPS. https://www.lipidmaps.org/resources/lipidweb/lipidweb_html/lipids/fa-eic/eicprost/index.htm#:~:text=In%20the%20approved%20nomenclature%2C%20each,the%20substituents%20on%20the%20ring.

Christie, W. (2021). Fatty Acids: Straight-Chain Saturated. In LipidMaps. https://www.lipidmaps.org/resources/lipidweb/lipidweb_html/lipids/fa-eic/fa-sat/index.htm

Christie, W. W. (1993). Preparation of lipid extracts from tissues. *Advances in Lipid Methodology*, 2(1), 195–213.

Chuang, C. C., Martinez, K., Xie, G., Kennedy, A., Bumrungpert, A., Overman, A., Jia, W., & McIntosh, M. K. (2010). Quercetin is equally or more effective than resveratrol in attenuating tumor necrosis factor- α -mediated inflammation and insulin resistance in primary human adipocytes. *The American Journal of Clinical Nutrition*, 92(6), 1511–1521. <https://doi.org/10.3945/AJCN.2010.29807>

Chung, D., Shum, A., & Caraveo, G. (2020). GAP-43 and BASP1 in Axon Regeneration: Implications for the Treatment of Neurodegenerative Diseases. *Frontiers in Cell and Developmental Biology*, 8, 890. <https://doi.org/10.3389/FCELL.2020.567537/BIBTEX>

Chung, H., Li, E., Kim, Y., Kim, S., & Park, S. (2013). Multiple signaling pathways mediate ghrelin-induced proliferation of hippocampal neural stem cells. *Journal of Endocrinology*, 218(1), 49–59. <https://doi.org/10.1530/JOE-13-0045>

Chung, H., Seo, S., Moon, M., & Park, S. (2008). Phosphatidylinositol-3-kinase/Akt/glycogen synthase kinase-3 β and ERK1/2 pathways mediate protective effects of acylated and unacylated ghrelin against oxygen-glucose deprivation-induced apoptosis in primary rat cortical neuronal cells. *Journal of Endocrinology*, 198(3), 511–521. <https://doi.org/10.1677/JOE-08-0160>

Chung, S., Yao, H., Caito, S., Hwang, J., Arunachalam, G., & Rahman, I. (2010). Regulation of SIRT1 in cellular functions: role of polyphenols. *Archives of Biochemistry and Biophysics*, 501(1), 79–90.

Chusyd, D. E., Wang, D., Huffman, D. M., & Nagy, T. R. (2016). Relationships between Rodent White Adipose Fat Pads and Human White Adipose Fat Depots. *Frontiers in Nutrition*, 3. <https://doi.org/10.3389/FNUT.2016.00010/PDF>

Cisbani, G., & Bazinet, R. P. (2021). The role of peripheral fatty acids as biomarkers for Alzheimer's disease and brain inflammation. *Prostaglandins, Leukotrienes and Essential Fatty Acids*, 164, 102205. <https://doi.org/10.1016/J.PLEFA.2020.102205>

Clark, E. A., & Lee, V. M. -Y. (1991). The Differential Role of Protein Kinase C Isozyme in the Rapid Induction of Neurofilament Phosphorylation by Nerve Growth Factor and Phorbol Esters in PC12 Cells. *Journal of Neurochemistry*, 57(3), 802–810. <https://doi.org/10.1111/j.1471-4159.1991.tb08222.x>

Clarke, S. D., & Nakamura, M. T. (2013). Fatty Acid Structure and Synthesis. *Encyclopedia of Biological Chemistry: Second Edition*, 285–289. <https://doi.org/10.1016/B978-0-12-378630-2.00038-4>

Cleveland, D. W., Monteiro, M. J., Wong, P. C., Gill, S. R., Gearhart, J. D., & Hoffman, P. N. (1991). Involvement of neurofilaments in the radial growth of axons. *Journal of Cell Science*, 100(SUPPL. 15), 85–95. https://doi.org/10.1242/jcs.1991.supplement_15.12

Cohen, D. E., & Fisher, E. A. (2013). Lipoprotein Metabolism, Dyslipidemia and Nonalcoholic Fatty Liver Disease. *Seminars in Liver Disease*, 33(4), 380. <https://doi.org/10.1055/S-0033-1358519>

Cohen-Mansfield, J., Taylor, L., McConnell, D., & Horton, D. (1999). Estimating the cognitive ability of nursing home residents from the minimum data set. *Outcomes Management for Nursing Practice*, 3(1), 43–46. <https://europepmc.org/article/med/9934198>

Colciaghi, F., Borroni, B., Zimmermann, M., Bellone, C., Longhi, A., Padovani, A., Cattabeni, F., Christen, Y., & Di Luca, M. (2004). Amyloid precursor protein metabolism is regulated toward alpha-secretase pathway by Ginkgo biloba extracts. *Neurobiology of Disease*, 16(2), 454–460.

Cole, R. M., Puchala, S., Ke, J. Y., Abdel-Rasoul, M., Harlow, K., O'Donnell, B., Bradley, D., Andridge, R., Borkowski, K., Newman, J. W., & Belury, M. A. (2020). Linoleic Acid-Rich Oil Supplementation Increases Total and High-Molecular-Weight Adiponectin and Alters Plasma Oxylipins in Postmenopausal Women with Metabolic Syndrome. *Current Developments in Nutrition*, 4(9). <https://doi.org/10.1093/CDN/NZAA136>

Colizzi, C. (2019). The protective effects of polyphenols on Alzheimer's disease: A systematic review. *Alzheimer's & Dementia: Translational Research & Clinical Interventions*, 5, 184–196.

Cong, W., Tao, R., Tian, J., Zhao, J., Liu, Q., & Ye, F. (2011). EGb761, an extract of Ginkgo biloba leaves, reduces insulin resistance in a high-fat-fed mouse model. *Acta Pharmaceutica Sinica B*, 1(1), 14–20.

Connor, W. E., Lin, D. S., & Colvis, C. (1996). Differential mobilization of fatty acids from adipose tissue. *Journal of Lipid Research*, 37(2), 290–298. [https://doi.org/10.1016/S0022-2275\(20\)37616-1](https://doi.org/10.1016/S0022-2275(20)37616-1)

Corder, E. H., Saunders, A. M., Risch, N. J., Strittmatter, W. J., Schmechel, D. E., Gaskell, P. C., Rimmler, J. B., Locke, P. A., Conneally, P. M., & Schmechel, K. E. (1994). Protective effect of apolipoprotein E type 2 allele for late onset Alzheimer disease. *Nature Genetics*, 7(2), 180–184.

Corning. (2019). Corning® Collagen IV, Human, 0.25mg. <https://ecatalog.corning.com/life-sciences/b2b/UK/en/Cell-Culture/Growth-Factors-and-Cytokines/Corning®-Collagen/p/354245>

Costa, R. R. S., Villela, N. R., Souza, M. das G. C., Boa, B. C. S., Cyrino, F. Z. G. A., Silva, S. V, Lisboa, P. C., Moura, E. G., Barja-Fidalgo, T. C., & Bouskela, E. (2011). High fat diet induces central obesity, insulin resistance and microvascular dysfunction in hamsters. *Microvascular Research*, 82(3), 416–422. <https://doi.org/10.1016/j.mvr.2011.08.007>

Cowley, M. A., et Al., Smart, J. L., Rubinstein, M., Cerdán, M. G., Diano, S., Horvath, T. L., Cone, R. D., & Low, M. J. (2001). Leptin activates anorexigenic POMC neurons through a neural network in the arcuate nucleus. *Nature*, 411(6836), 480–484. <https://doi.org/10.1038/35078085>

Craig, M., Yarrarapu, S. N. S., & Dimri, M. (2021). *Biochemistry, Cholesterol*. <https://www.ncbi.nlm.nih.gov/books/NBK513326/>

Crawford, M. A. (1992). The role of dietary fatty acids in biology: their place in the evolution of the human brain. *Nutrition Reviews*, 50(4), 3–11.

Crovesy, L., Masterson, D., & Rosado, E. L. (2020). Profile of the gut microbiota of adults with obesity: a systematic review. *European Journal of Clinical Nutrition* 2020 74:9, 74(9), 1251–1262. <https://doi.org/10.1038/s41430-020-0607-6>

Csiszár, A., Csiszar, A., Pinto, J. T., Gautam, T., Kleusch, C., Hoffmann, B., Tucsek, Z., Toth, P., Sonntag, W. E., & Ungvari, Z. (2015). Resveratrol encapsulated in novel fusogenic liposomes activates Nrf2 and attenuates oxidative stress in cerebromicrovascular endothelial cells from aged rats. *Journals of Gerontology Series A: Biomedical Sciences and Medical Sciences*, 70(3), 303–313.

Cuadrado, A., Manda, G., Hassan, A., Alcaraz, M. J., Barbas, C., Daiber, A., Ghezzi, P., León, R., López, M. G., & Oliva, B. (2018a). Transcription factor NRF2 as a therapeutic target for chronic diseases: a systems medicine approach. *Pharmacological Reviews*, 70(2), 348–383.

Cui, J., Li, L., Ren, L., Sun, J., Zhao, H., & Sun, Y. (2021). Dietary n-3 and n-6 fatty acid intakes and NAFLD: A cross-sectional study in the United States. *Asia Pac J Clin Nutr*, 30(1), 87–98. [https://doi.org/10.6133/apjcn.202103_30\(1\).0011](https://doi.org/10.6133/apjcn.202103_30(1).0011)

Cui, W., Chen, S. L., & Hu, K. Q. (2010). Quantification and mechanisms of oleic acid-induced steatosis in HepG2 cells. *American Journal of Translational Research*, 2(1), 95. <https://pmc/articles/PMC2826826/>

Cunnane, S., Nugent, S., Roy, M., Courchesne-Loyer, A., Croteau, E., Tremblay, S., Castellano, A., Pifferi, F., Bocti, C., & Paquet, N. (2011a). Brain fuel metabolism, aging, and Alzheimer's disease. In *Nutrition* (Vol. 27, Issue 1). Elsevier. <https://doi.org/10.1016/j.nut.2010.07.021.BRAIN>

Cypess, A. M., Lehman, S., Williams, G., Tal, I., Rodman, D., Goldfine, A. B., Kuo, F. C., Palmer, E. L., Tseng, Y.-H., Doria, A., Kolodny, G. M., & Kahn, C. R. (2009). Identification and Importance

of Brown Adipose Tissue in Adult Humans. *New England Journal of Medicine*, 360(15), 1509–1517. https://doi.org/10.1056/NEJMOA0810780/SUPPL_FILE/NEJM_CYPRESS_1509SA1.PDF

Cypess, A. M., Weiner, L. S., Roberts-Toler, C., Elia, E. F., Kessler, S. H., Kahn, P. A., English, J., Chatman, K., Trauger, S. A., Doria, A., & Kolodny, G. M. (2015). Activation of human brown adipose tissue by a β 3-adrenergic receptor agonist. *Cell Metabolism*, 21(1), 33–38. <https://doi.org/10.1016/j.cmet.2014.12.009>

da Silva, H. E., Arendt, B. M., Noureldin, S. A., Therapondos, G., Guindi, M., & Allard, J. P. (2014). A cross-sectional study assessing dietary intake and physical activity in Canadian patients with nonalcoholic fatty liver disease vs healthy controls. *J Acad Nutr Diet*, 114(8), 1181–1194. <https://doi.org/10.1016/j.jand.2014.01.009>

Das, Freudenrich, & Mundy. (2004). Assessment of PC12 cell differentiation and neurite growth: a comparison of morphological and neurochemical measures. *Neurotoxicology and Teratology*, 26(3), 397–406. <https://doi.org/10.1016/j.ntt.2004.02.006>

Davies, J. M. S., Cillard, J., Friguet, B., Cadenas, E., Cadet, J., Cayce, R., Fishmann, A., Liao, D., Bulteau, A. L., Derbré, F., Rébillard, A., Burstein, S., Hirsch, E., Kloner, R. A., Jakowec, M., Petzinger, G., Sauce, D., Sennlaub, F., Limon, I., ... Davies, K. J. A. (2017). The Oxygen Paradox, the French Paradox, and age-related diseases. *GeroScience*, 39(5–6), 499. <https://doi.org/10.1007/S11357-017-0002-Y>

Davies, J. S. (2022). Ghrelin mediated hippocampal neurogenesis. *Vitamins and Hormones*. <https://doi.org/10.1016/bs.vh.2021.12.003>

De Aguilar, J. L. G. (2019). Lipid biomarkers for amyotrophic lateral sclerosis. *Frontiers in Neurology*, 10(APR), 284. <https://doi.org/10.3389/fneur.2019.00284/BIBTEX>

DeMar, J. C., Ma, K., Bell, J. M., & Rapoport, S. I. (2004). Half-lives of docosahexaenoic acid in rat brain phospholipids are prolonged by 15 weeks of nutritional deprivation of n-3 polyunsaturated fatty acids. *Journal of Neurochemistry*, 91(5), 1125–1137. <https://doi.org/10.1111/j.1471-4159.2004.02789.x>

DeMar, J. C., Ma, K., Chang, L., Bell, J. M., & Rapoport, S. I. (2005). α -Linolenic acid does not contribute appreciably to docosahexaenoic acid within brain phospholipids of adult rats fed a diet enriched in docosahexaenoic acid. *Journal of Neurochemistry*, 94(4), 1063–1076. <https://doi.org/10.1111/j.1471-4159.2005.03258.x>

de Santis, A., Varela, Y., Sot, J., D'Errico, G., Goñi, F. M., & Alonso, A. (2018). Omega-3 polyunsaturated fatty acids do not fluidify bilayers in the liquid-crystalline state. *Scientific Reports* 2018 8:1, 8(1), 1–13. <https://doi.org/10.1038/s41598-018-34264-3>

de Vos, P., Saladin, R., Auwerx, J., & Staels, B. (1995). Induction of ob gene expression by corticosteroids is accompanied by body weight loss and reduced food intake. *The Journal of Biological Chemistry*, 270(27), 15958–15961. <https://doi.org/10.1074/JBC.270.27.15958>

Deckelbaum, R. J. (2010). n-6 and n-3 fatty acids and atherosclerosis: Ratios or amounts? *Arteriosclerosis, Thrombosis, and Vascular Biology*, 30(12), 2325–2326. <https://doi.org/10.1161/ATVBAHA.110.214353>

Del Gobbo, L. C., Imamura, F., Aslibekyan, S., Marklund, M., Virtanen, J. K., Wennberg, M., Yakoob, M. Y., Chiuve, S. E., Dela Cruz, L., Frazier-Wood, A. C., Fretts, A. M., Guallar, E., Matsumoto, C., Prem, K., Tanaka, T., Wu, J. H. Y., Zhou, X., Helmer, C., Ingelsson, E., ... Mozaffarian, D. (2016). ω -3 Polyunsaturated fatty acid biomarkers and coronary heart disease: Pooling project of 19 cohort studies. *JAMA Internal Medicine*, 176(8), 1155–1166. <https://doi.org/10.1001/jamainternmed.2016.2925>

den Besten, G., Bleeker, A., Gerding, A., van Eunen, K., Havinga, R., van Dijk, T. H., Oosterveer, M. H., Jonker, J. W., Groen, A. K., Reijngoud, D. J., & Bakker, B. M. (2015). Short-chain fatty acids protect against high-fat diet-induced obesity via a PPAR γ -dependent switch from lipogenesis to fat oxidation. *Diabetes*, 64(7), 2398–2408. <https://doi.org/10.2337/db14-1213>

Deng, Y., Li, B., Liu, Y., Iqbal, K., Grundke-Iqbal, I., & Gong, C. X. (2009). Dysregulation of insulin signaling, glucose transporters, O-GlcNAcylation, and phosphorylation of tau and neurofilaments in the brain: Implication for Alzheimer's disease. *American Journal of Pathology*, 175(5), 2089–2098. <https://doi.org/10.2353/AJPATH.2009.090157>

De-Santis, A., Varela, Y., Sot, J., D'Errico, G., Goñi, F. M., & Alonso, A. (2018). Omega-3 polyunsaturated fatty acids do not fluidify bilayers in the liquid-crystalline state. *Scientific Reports* 2018 8:1, 8(1), 1–13. <https://doi.org/10.1038/s41598-018-34264-3>

Devraj, K., Klinger, M. E., Myers, R. L., Mokashi, A., Hawkins, R. A., & Simpson, I. A. (2011). GLUT-1 glucose transporters in the blood-brain barrier: differential phosphorylation. *Journal of Neuroscience Research*, 89(12), 1913–1925. <https://doi.org/10.1002/JNR.22738>

Di Miceli, M., Bosch-Bouju, C., & Layé, S. (2020). PUFA and their derivatives in neurotransmission and synapses: a new hallmark of synaptopathies. *Proceedings of the Nutrition Society*, 79(4), 388–403. <https://doi.org/10.1017/S0029665120000129>

di Paolo, G., & de Camilli, P. (2006). Phosphoinositides in cell regulation and membrane dynamics. *Nature*, 443(7112), 651–657. <https://doi.org/10.1038/NATURE05185>

di Spiezio, A., Sandin, E. S., Dore, R., Müller-Fielitz, H., Storck, S. E., Bernau, M., Mier, W., Oster, H., Jöhren, O., Pietrzik, C. U., Lehnert, H., & Schwaninger, M. (2018). The LepR-mediated leptin transport across brain barriers controls food reward. *Molecular Metabolism*, 8, 13–22. <https://doi.org/10.1016/J.MOLMET.2017.12.001>

Diamond, B. J., & Bailey, M. R. (2013). Ginkgo biloba: indications, mechanisms, and safety. *Psychiatric Clinics*, 36(1), 73–83.

Dias, I. H. K., & Griffiths, H. R. (2014). *Oxidative stress in diabetes—circulating advanced glycation end products, lipid oxidation and vascular disease*. SAGE Publications Sage UK: London, England.

- Diau, G. Y., Hsieh, A. T., Sarkadi-Nagy, E. A., Wijendran, V., Nathanielsz, P. W., & Brenna, J. T. (2005). The influence of long chain polyunsaturate supplementation on docosahexaenoic acid and arachidonic acid in baboon neonate central nervous system. *BMC Medicine*, 3. <https://doi.org/10.1186/1741-7015-3-11>
- Dietrich, M. O., & Horvath, T. L. (2009). Feeding signals and brain circuitry. *Eur. J. Neurosci.*, 30, 1688–1696.
- Dietrich, M. O., & Horvath, T. L. (2011). Synaptic plasticity of feeding circuits: hormones and hysteresis. *Cell*, 146, 863–865.
- Dietrich, M. O., & Horvath, T. L. (2013). Hypothalamic control of energy balance: insights into the role of synaptic plasticity. *Trends in Neurosciences*, 36(2), 65–73. <https://doi.org/10.1016/J.TINS.2012.12.005>
- Dikmen, M. (2017). Comparison of the effects of curcumin and rg108 on ngf-induced pc-12 adh cell differentiation and neurite outgrowth. *Journal of Medicinal Food*, 20(4), 376–384. <https://doi.org/10.1089/jmf.2016.3889>
- Ditano-Vázquez, P., Torres-Peña, J. D., Galeano-Valle, F., Pérez-Caballero, A. I., Demelo-Rodríguez, P., Lopez-Miranda, J., Katsiki, N., Delgado-Lista, J., & Alvarez-Sala-Walther, L. A. (2019). The fluid aspect of the mediterranean diet in the prevention and management of cardiovascular disease and diabetes: The role of polyphenol content in moderate consumption of wine and olive oil. *Nutrients*, 11(11). <https://doi.org/10.3390/nu11112833>
- Djuric, Z., Bassis, C. M., Plegue, M. A., Sen, A., Turgeon, D. K., Herman, K., Young, V. B., Brenner, D. E., & Ruffin, M. T. (2019). Increases in colonic bacterial diversity after ω -3 fatty acid supplementation predict decreased colonic prostaglandin E2 concentrations in healthy adults. *Journal of Nutrition*, 149(7), 1170–1179. <https://doi.org/10.1093/jn/nxy255>
- Djuric, Z., Turgeon, D. K., Sen, A., Ren, J., Herman, K., Ramaswamy, D., Zhao, L., Ruffin, M. T., Normolle, D. P., Smith, W. L., & Brenner, D. E. (2017). The Anti-inflammatory Effect of Personalized Omega-3 Fatty Acid Dosing for Reducing Prostaglandin E 2 in the Colonic Mucosa Is Attenuated in Obesity. *Cancer Prevention Research (Philadelphia, Pa.)*, 10(12), 729–737. <https://doi.org/10.1158/1940-6207.CAPR-17-0091>
- Dong, Y., Pu, K., Duan, W., Chen, H., Chen, L., & Wang, Y. (2018). Involvement of Akt/CREB signaling pathways in the protective effect of EPA against interleukin-1 β -induced cytotoxicity and BDNF down-regulation in cultured rat hippocampal neurons. *BMC Neuroscience*, 19(1), 1–8.
- Donmez, G. (2012). The neurobiology of sirtuins and their role in neurodegeneration. *Trends in Pharmacological Sciences*, 33(9), 494–501.
- Dornellas, A. P. S., Watanabe, R. L. H., Pimentel, G. D., Boldarine, V. T., Nascimento, C. M. O., Oyama, L. M., Ghebremeskel, K., Wang, Y., Bueno, A. A., & Ribeiro, E. B. (2015). Deleterious effects of lard-enriched diet on tissues fatty acids composition and hypothalamic insulin actions. *Prostaglandins Leukotrienes and Essential Fatty Acids*, 102–103, 21–29. <https://doi.org/10.1016/j.plefa.2015.10.003>

Dozsa, A., Dezso, B., Toth, B. I., Bacsı, A., Poliska, S., Camera, E., Picardo, M., Zouboulis, C. C., Bıró, T., Schmitz, G., Liebisch, G., Rühl, R., Remenyik, E., & Nagy, L. (2014). PPAR γ -mediated and arachidonic acid-dependent signaling is involved in differentiation and lipid production of human sebocytes. *Journal of Investigative Dermatology*, 134(4), 910–920. <https://doi.org/10.1038/jid.2013.413>

Du, S., & Zheng, H. (2021). Role of FoxO transcription factors in aging and age-related metabolic and neurodegenerative diseases. *Cell & Bioscience* 2021 11:1, 11(1), 1–17. <https://doi.org/10.1186/S13578-021-00700-7>

Ducrot, P., Méjean, C., Bellisle, F., Allès, B., Hercberg, S., & Péneau, S. (2018). Adherence to the French Eating Model is inversely associated with overweight and obesity: results from a large sample of French adults. *British Journal of Nutrition*, 120(2), 231–239. <https://doi.org/10.1017/S0007114518000909>

Dugo, P., Fawzy, N., Cichello, F., Cacciola, F., Donato, P., & Mondello, L. (2013). Stop-flow comprehensive two-dimensional liquid chromatography combined with mass spectrometric detection for phospholipid analysis. *Journal of Chromatography A*, 1278, 46–53.

Duivenvoorde, L. P. M., van Schothorst, E. M., Bunschoten, A., & Keijer, J. (2011). Dietary restriction of mice on a high-fat diet induces substrate efficiency and improves metabolic health. *Journal of Molecular Endocrinology*, 47(1), 81–97. <https://doi.org/10.1530/JME-11-0001>

Dunn, J. D., Alvarez, L. A. J., Zhang, X., & Soldati, T. (2015). Reactive oxygen species and mitochondria: A nexus of cellular homeostasis. *Redox Biology*, 6, 472–485. <https://doi.org/10.1016/J.REDOX.2015.09.005>

Duszka, K., Gregor, A., Guillou, H., König, J., & Wahli, W. (2020). Peroxisome Proliferator-Activated Receptors and Caloric Restriction—Common Pathways Affecting Metabolism, Health, and Longevity. *Cells* 2020, Vol. 9, Page 1708, 9(7), 1708. <https://doi.org/10.3390/CELLS9071708>

Duvall, M. G., & Levy, B. D. (2016). DHA- and EPA-derived resolvins, protectins, and maresins in airway inflammation. *European Journal of Pharmacology*, 785, 144. <https://doi.org/10.1016/J.EJPBAR.2015.11.001>

Dyall, S. C. (2015). Long-chain omega-3 fatty acids and the brain: A review of the independent and shared effects of EPA, DPA and DHA. *Frontiers in Aging Neuroscience*, 7(APR), 1–15. <https://doi.org/10.3389/fnagi.2015.00052>

Dye, L., Boyle, N. B., Champ, C., & Lawton, C. (2017). The relationship between obesity and cognitive health and decline. *Proceedings of the Nutrition Society*, 76(4), 443–454. <https://doi.org/10.1017/S0029665117002014>

Eccleston, H. B., Andringa, K. K., Betancourt, A. M., King, A. L., Mantena, S. K., Swain, T. M., Tinsley, H. N., Nolte, R. N., Nagy, T. R., Abrams, G. A., & Bailey, S. M. (2011). Chronic Exposure to a High-Fat Diet Induces Hepatic Steatosis, Impairs Nitric Oxide Bioavailability, and Modifies

the Mitochondrial Proteome in Mice. *Antioxidants & Redox Signaling*, 15(2), 447. <https://doi.org/10.1089/ARS.2010.3395>

Echeverría, F., Ortiz, M., Valenzuela, R., & Videla, L. A. (2016). Long-chain polyunsaturated fatty acids regulation of PPARs, signaling: Relationship to tissue development and aging. *Prostaglandins, Leukotrienes, and Essential Fatty Acids*, 114, 28–34. <https://doi.org/10.1016/j.plefa.2016.10.001>

Eckert, A., Keil, U., Scherping, I., Hauptmann, S., & Müller, W. E. (2005). Stabilization of mitochondrial membrane potential and improvement of neuronal energy metabolism by Ginkgo biloba extract Egb 761. *Annals of the New York Academy of Sciences*, 1056, 474–485. <https://doi.org/10.1196/ANNALS.1352.023>

Edith, O., Janius, R. B., & Yunus, R. (2012). Factors affecting the cold flow behaviour of biodiesel and methods for improvement—a review. *Pertanika J. Sci. Technol*, 20(1), 1–14.

Edmond, J., Higa, T. A., Korsak, R. A., Bergner, E. A., & Lee, W. N. P. (1998). Fatty acid transport and utilization for the developing brain. *Journal of Neurochemistry*, 70(3), 1227–1234. <https://doi.org/10.1046/j.1471-4159.1998.70031227.x>

EFSA Panel on Dietetic Products and Allergies. (2010). Scientific opinion on dietary reference values for fats, including saturated fatty acids, polyunsaturated fatty acids, monounsaturated fatty acids, trans fatty acids, and cholesterol. *EFSA Journal*, 8(3), 1461.

Eid, R. A., Alkhateeb, M. A., Eleawa, S., Al-Hashem, F. H., Al-Shraim, M., El-kott, A. F., Zaki, M. S. A., Dallak, M. A., & Aldera, H. (2018). Cardioprotective effect of ghrelin against myocardial infarction-induced left ventricular injury via inhibition of SOCS3 and activation of JAK2/STAT3 signaling. *Basic Research in Cardiology*, 113(2). <https://doi.org/10.1007/s00395-018-0671-4>

El-Haschimi, K., Pierroz, D. D., Hileman, S. M., Bjørnbæk, C., & Flier, J. S. (2000). Two defects contribute to hypothalamic leptin resistance in mice with diet-induced obesity. *The Journal of Clinical Investigation*, 105(12), 1827–1832. <https://doi.org/10.1172/JCI9842>

Elias, C. F., Aschkenasi, C., Lee, C., Kelly, J., Ahima, R. S., Bjørnbæk, C., Flier, J. S., Saper, C. B., Elmquist, J. K., et al., Aschkenasi, C., Lee, C., Kelly, J., Ahima, R. S., Bjørnbæk, C., Flier, J. S., Saper, C. B., & Elmquist, J. K. (1999). Leptin differentially regulates NPY and POMC neurons projecting to the lateral hypothalamic area. *Neuron*, 23(4), 775–786. [https://doi.org/10.1016/S0896-6273\(01\)80035-0](https://doi.org/10.1016/S0896-6273(01)80035-0)

Emre, M. (2009). Classification and diagnosis of dementia: a mechanism-based approach. *European Journal of Neurology*, 16(2), 168–173. <https://doi.org/10.1111/j.1468-1331.2008.02379.x>

Endo, J., & Arita, M. (2016). Cardioprotective mechanism of omega-3 polyunsaturated fatty acids. *Journal of Cardiology*, 67(1), 22–27. <https://doi.org/10.1016/j.jjcc.2015.08.002>

Enos, R. T., Velázquez, K. T., & Murphy, E. A. (2014). Insight into the impact of dietary saturated fat on tissue-specific cellular processes underlying obesity-related diseases. *The*

Journal of Nutritional Biochemistry, 25(6), 600–612.
<https://doi.org/10.1016/J.JNUTBIO.2014.01.011>

Enriori, P. J., Evans, A. E., Sinnayah, P., Jobst, E. E., Tonelli-Lemos, L., Billes, S. K., Glavas, M. M., Grayson, B. E., Perello, M., Nilni, E. A., Grove, K. L., & Cowley, M. A. (2007). Diet-induced obesity causes severe but reversible leptin resistance in arcuate melanocortin neurons. *Cell Metabolism*, 5(3), 181–194. <https://doi.org/10.1016/J.CMET.2007.02.004>

Ernst, M. B., Wunderlich, C. M., Hess, S., Paehler, M., Mesaros, A., Koralov, S. B., Kleinridders, A., Husch, A., Münzberg, H., Hampel, B., Alber, J., Kloppenburg, P., Brüning, J. C., & Wunderlich, F. T. (2009). Enhanced Stat3 activation in POMC neurons provokes negative feedback inhibition of leptin and insulin signaling in obesity. *Journal of Neuroscience*, 29(37), 11582–11593. <https://doi.org/10.1523/JNEUROSCI.5712-08.2009>

Escobedo, N., Proulx, S. T., Karaman, S., Dillard, M. E., Johnson, N., Detmar, M., & Oliver, G. (2016). Restoration of lymphatic function rescues obesity in Prox1-haploinsufficient mice. *JCI Insight*, 1(2). <https://doi.org/10.1172/JCI.INSIGHT.85096>

Esmaili, S., Hemmati, M., & Karamian, M. (2020). Physiological role of adiponectin in different tissues: a review. *Archives of physiology and biochemistry*, 126(1), 67-73. <https://doi.org/10.1080/13813455.2018.1493606>

Estruch, R., & Salas-Salvadó, J. (2013). “Towards an even healthier mediterranean diet”. *Nutrition, Metabolism and Cardiovascular Diseases*, 23(12), 1163–1166. <https://doi.org/10.1016/J.NUMECD.2013.09.003>

Esvald, E.-E., Tuvikene, J., Sirp, A., Patil, S., Bramham, C. R., & Timmusk, T. (2020). CREB family transcription factors are major mediators of BDNF transcriptional autoregulation in cortical neurons. *Journal of Neuroscience*, 40(7), 1405–1426.

Eurostat. (2021). Body mass index (BMI) by sex, age and educational attainment level | European Health Interview Survey (EHIS) | Statistics | Eurostat. https://ec.europa.eu/eurostat/databrowser/view/HLTH_EHIS_BM1E__custom_1162105/bookmark/table?lang=en&bookmarkId=6f21bd9e-cbe6-4467-9821-2050435af363

Evangelista, E. A., Cho, C. W., Aliwarga, T., & Totah, R. A. (2020). Expression and Function of Eicosanoid-Producing Cytochrome P450 Enzymes in Solid Tumors. *Frontiers in Pharmacology*, 11, 828. <https://doi.org/10.3389/FPHAR.2020.00828/BIBTEX>

Fahy, E., Cotter, D., Sud, M., & Subramaniam, S. (2011). Lipid classification, structures and tools. *Biochimica et Biophysica Acta*, 1811(11), 637. <https://doi.org/10.1016/J.BBALIP.2011.06.009>

Fahy, E., Sud, M., Cotter, D., & Subramaniam, S. (2007). LIPID MAPS online tools for lipid research. *Nucleic Acids Research*, 35(SUPPL.2). <https://doi.org/10.1093/nar/gkm324>

Falomir-Lockhart, L. J., Cavazzutti, G. F., Giménez, E., & Toscani, A. M. (2019). Fatty acid signaling mechanisms in neural cells: Fatty acid receptors. *Frontiers in Cellular Neuroscience*, 13, 162. <https://doi.org/10.3389/FNCEL.2019.00162/BIBTEX>

- Fan, Y. Y., Davidson, L. A., Callaway, E. S., Goldsby, J. S., & Chapkin, R. S. (2014). Differential effects of 2- and 3-series E-prostaglandins on in vitro expansion of Lgr5+ colonic stem cells. *Carcinogenesis*, 35(3), 606–612. <https://doi.org/10.1093/CARCIN/BGT412>
- Fang, C. X., Dong, F., Thomas, D. P., Ma, H., He, L., & Ren, J. (2008). Hypertrophic cardiomyopathy in high-fat diet-induced obesity: Role of suppression of forkhead transcription factor and atrophy gene transcription. *American Journal of Physiology - Heart and Circulatory Physiology*, 295(3). <https://doi.org/10.1152/AJPHEART.00319.2008>
- Fang, W., Li, H., Zhou, L., Su, L., Liang, Y., & Mu, Y. (2010). Effect of prostaglandin E1 on TNF-induced vascular inflammation in human umbilical vein endothelial cells. *Canadian Journal of Physiology and Pharmacology*, 88(5), 576–583. <https://doi.org/10.1139/Y10-028>
- FAO (Food and Agriculture organisation) (2010). Fats and fatty acids in human nutrition. Report of an expert consultation, 10-14 November 2008, Geneva.
- Farr, O. M., Gavrieli, A., & Mantzoros, C. S. (2015). Leptin applications in 2015: What have we learned about leptin and obesity? *Current Opinion in Endocrinology, Diabetes and Obesity*, 22(5), 353–359. <https://doi.org/10.1097/MED.000000000000184>
- Fei, H., Okano, H. J., Li, C., Lee, G. H., Zhao, C., Darnell, R., & Friedman, J. M. (1997). Anatomic localization of alternatively spliced leptin receptors (Ob-R) in mouse brain and other tissues. *Proceedings of the National Academy of Sciences of the United States of America*, 94(13), 7001–7005. <https://doi.org/10.1073/PNAS.94.13.7001>
- Feingold, K. R., & Grunfeld, C. (2021). Introduction to Lipids and Lipoproteins. Endotext. <https://www.ncbi.nlm.nih.gov/books/NBK305896/>
- Ferramosca, A., & Zara, V. (2014). Modulation of hepatic steatosis by dietary fatty acids. *World Journal of Gastroenterology*, 20(7), 1746–1755. <https://doi.org/10.3748/wjg.v20.i7.1746>
- Ferrières, J. (2004). The French paradox: lessons for other countries. *Heart (British Cardiac Society)*, 90(1), 107–111. <https://doi.org/10.1136/HEART.90.1.107>
- Fiala, M., Kooij, G., Wagner, K., Hammock, B., & Pellegrini, M. (2017). Modulation of innate immunity of patients with Alzheimer’s disease by omega-3 fatty acids. *FASEB Journal*, 31(8), 3229–3239. <https://doi.org/10.1096/fj.201700065R>
- Figueroa, J. D., Serrano-Illan, M., Licero, J., Cordero, K., Miranda, J. D., & de Leon, M. (2016). Fatty Acid Binding Protein 5 Modulates Docosahexaenoic Acid-Induced Recovery in Rats Undergoing Spinal Cord Injury. <https://Home.Liebertpub.Com/Neu>, 33(15), 1436–1449. <https://doi.org/10.1089/NEU.2015.4186>
- Filhoulaud, G., Guilmeau, S., Dentin, R., Girard, J., & Postic, C. (2013). Novel insights into ChREBP regulation and function. *Trends in Endocrinology and Metabolism: TEM*, 24(5), 257–268. <https://doi.org/10.1016/J.TEM.2013.01.003>

Fitzpatrick, A. L., Kuller, L. H., Lopez, O. L., Diehr, P., O'Meara, E. S., Longstreth, W. T., & Luchsinger, J. A. (2009). Midlife and late-life obesity and the risk of dementia: cardiovascular health study. *Archives of Neurology*, 66(3), 336–342. <https://doi.org/10.1001/ARCHNEUROL.2008.582>

Folch, J., Ascoli, I., Lees, M., Meath, J. A., & LeBaron, F. N. (1951). Preparation of lipide extracts from brain tissue. *J Biol Chem*, 191(2), 833–841.

Folch, J., Lees, M., & Stanley, G. H. S. (1957). A simple method for the isolation and purification of total lipides from animal tissues. *Journal of Biological Chemistry*, 226(1), 497–509.

Forgrave, L. M., Ma, M., Best, J. R., & DeMarco, M. L. (2019). The diagnostic performance of neurofilament light chain in CSF and blood for Alzheimer's disease, frontotemporal dementia, and amyotrophic lateral sclerosis: A systematic review and meta-analysis. *Alzheimer's & Dementia* (Amsterdam, Netherlands), 11, 730–743. <https://doi.org/10.1016/j.dadm.2019.08.009>

Forman, B. M., Chen, J., & Evans, R. M. (1997). Hypolipidemic drugs, polyunsaturated fatty acids, and eicosanoids are ligands for peroxisome proliferator-activated receptors α and δ . *Proceedings of the National Academy of Sciences*, 94(9), 4312–4317. <https://doi.org/10.1073/PNAS.94.9.4312>

Forny-Germano, L., de Felice, F. G., & do Nascimento Vieira, M. N. (2019). The role of leptin and adiponectin in obesity-associated cognitive decline and Alzheimer's disease. *Frontiers in Neuroscience*, 13(JAN), 1027. <https://doi.org/10.3389/FNINS.2018.01027/BIBTEX>

Foster, M. T., & Pagliassotti, M. J. (2012). Metabolic alterations following visceral fat removal and expansion. *Adipocyte*, 1(4), 192–199. <https://doi.org/10.4161/ADIP.21756>

Foster, M. T., Shi, H., Seeley, R. J., & Woods, S. C. (2011). Removal of intra-abdominal visceral adipose tissue improves glucose tolerance in rats: Role of hepatic triglyceride storage. *Physiology and Behavior*, 104(5), 845–854. <https://doi.org/10.1016/J.PHYSBEH.2011.04.064>

Fraser, T., Tayler, H., & Love, S. (2010). Fatty acid composition of frontal, temporal and parietal neocortex in the normal human brain and in Alzheimer's disease. *Neurochemical Research*, 35(3), 503–513. <https://doi.org/10.1007/s11064-009-0087-5>

Frayn, K. N., & Karpe, F. (2013). Regulation of human subcutaneous adipose tissue blood flow. *International Journal of Obesity* 2014 38:8, 38(8), 1019–1026. <https://doi.org/10.1038/ijo.2013.200>

Freeman, L. A., & Remaley, A. T. (2016). Discovery of High-Density Lipoprotein Gene Targets from Classical Genetics to Genome-Wide Association Studies. *Translational Cardiometabolic Genomic Medicine*, 119–159. <https://doi.org/10.1016/B978-0-12-799961-6.00006-8>

Fridolfsson, H. N., Roth, D. M., Insel, P. A., & Patel, H. H. (2014). Regulation of intracellular signaling and function by caveolin. *The FASEB Journal*, 28(9), 3823–3831. <https://doi.org/10.1096/FJ.14-252320>

Friedli, O., & Freigang, S. (2017). Cyclopentenone-containing oxidized phospholipids and their isoprostanes as pro-resolving mediators of inflammation. *Biochimica et Biophysica Acta. Molecular and Cell Biology of Lipids*, 1862(4), 382–392. <https://doi.org/10.1016/j.bbali.2016.07.006>

Frölich, L., Blum-Degen, D., Bernstein, H.-G., Engelsberger, S., Humrich, J., Laufer, S., Muschner, D., Thalheimer, A., Türk, A., & Hoyer, S. (1998). Brain insulin and insulin receptors in aging and sporadic Alzheimer's disease. *Journal of Neural Transmission*, 105(4–5), 423–438.

Fruhwürth, S., Vogel, H., Schürmann, A., & Williams, K. J. (2018). Novel insights into how overnutrition disrupts the hypothalamic actions of leptin. *Frontiers in Endocrinology*, 9(MAR), 89. <https://doi.org/10.3389/fendo.2018.00089>/BIBTEX

Fryar, C. D., Carroll, M. D., & Afful, J. (2020). Prevalence of overweight, obesity, and severe obesity among adults aged 20 and over: United States, 1960–1962 through 2017–2018. *NCHS Health E-Stats*.

Fu, X., Yin, H. H., Wu, M. J., He, X., Jiang, Q., Zhang, L. T., & Liu, J. Y. (2022). High Sensitivity and Wide Linearity LC-MS/MS Method for Oxylipin Quantification in Multiple Biological Samples. *Journal of Lipid Research*, 63(12), 100302. <https://doi.org/10.1016/j.jlr.2022.100302>

Fujiwara, S. I., & Amisaki, T. (2013). Fatty acid binding to serum albumin: Molecular simulation approaches. In *Biochimica et Biophysica Acta - General Subjects* (Vol. 1830, Issue 12, pp. 5427–5434). Elsevier B.V. <https://doi.org/10.1016/j.bbagen.2013.03.032>

Furukawa, S., Fujita, T., Shimabukuro, M., Iwaki, M., Yamada, Y., Nakajima, Y., Nakayama, O., Makishima, M., Matsuda, M., & Shimomura, I. (2004). Increased oxidative stress in obesity and its impact on metabolic syndrome. *Journal of Clinical Investigation*, 114(12), 1752–1761. <https://doi.org/10.1172/JCI200421625>

Gabbs, M., Leng, S., Devassy, J. G., Monirujjaman, M., & Aukema, H. M. (2015). Advances in Our Understanding of Oxylipins Derived from Dietary PUFAs. *Advances in Nutrition*, 6(5), 513–540. <https://doi.org/10.3945/AN.114.007732>

Gaiani, A., Martinelli, I., Bello, L., Querin, G., Puthenparampil, M., Ruggero, S., Toffanin, E., Cagnin, A., Briani, C., Pegoraro, E., & Soraru, G. (2017). Diagnostic and prognostic biomarkers in amyotrophic lateral sclerosis: Neurofilament light chain levels in definite subtypes of disease. *JAMA Neurology*, 74(5), 525–532. <https://doi.org/10.1001/jamaneurol.2016.5398>

Galano, J. M., Lee, Y. Y., Oger, C., Vigor, C., Vercauteren, J., Durand, T., Giera, M., & Lee, J. C. Y. (2017). Isoprostanes, neuroprostanes and phytoprostanes: An overview of 25 years of research in chemistry and biology. *Progress in Lipid Research*, 68, 83–108. <https://doi.org/10.1016/j.plipres.2017.09.004>

Gamber, K. M., Huo, L., Ha, S., Hairston, J. E., Greeley, S., & Bjørnbæk, C. (2012). Overexpression of leptin receptors in hypothalamic POMC neurons increases susceptibility to diet-induced obesity. *PloS One*, 7(1). <https://doi.org/10.1371/journal.pone.0030485>

Gómez-Ruiz, A., Milagro, F. I., Campián, J., Martínez, J. A., & De Miguel, C. (2011). High-fat diet feeding alters metabolic response to fasting/non fasting conditions. Effect on caveolin expression and insulin signalling. *Lipids in Health and Disease*, 10, 55. <https://doi.org/10.1186/1476-511X-10-55>

Gandhi, S., & Abramov, A. Y. (2012). Mechanism of oxidative stress in neurodegeneration. *Oxidative Medicine and Cellular Longevity*, 2012. <https://doi.org/10.1155/2012/428010>

Gao, J., Liu, S., Xu, F., Liu, Y., Lv, C., Deng, Y., Shi, J., & Gong, Q. (2018). Trilobatin Protects Against Oxidative Injury in Neuronal PC12 Cells Through Regulating Mitochondrial ROS Homeostasis Mediated by AMPK/Nrf2/Sirt3 Signaling Pathway. *Frontiers in Molecular Neuroscience*, 11, 267. <https://doi.org/10.3389/fnmol.2018.00267/BIBTEX>

Gao, X., Lowry, P. R., Zhou, X., Depry, C., Wei, Z., Wong, G. W., & Zhang, J. (2011). PI3K/Akt signaling requires spatial compartmentalization in plasma membrane microdomains. *Proceedings of the National Academy of Sciences of the United States of America*, 108(35), 14509–14514. <https://doi.org/10.1073/pnas.1019386108/-/DCSUPPLEMENTAL>

Gao, Y., Zhang, W., Zeng, L. Q., Bai, H., Li, J., Zhou, J., Zhou, G. Y., Fang, C. W., Wang, F., & Qin, X. J. (2020). Exercise and dietary intervention ameliorate high-fat diet-induced NAFLD and liver aging by inducing lipophagy. *Redox Biology*, 36. <https://doi.org/10.1016/j.redox.2020.101635>

Gardener, S., Gu, Y., Rainey-Smith, S. R., Keogh, J. B., Clifton, P. M., Mathieson, S. L., Taddei, K., Mondal, A., Ward, V. K., & Scarmeas, N. (2012). Adherence to a Mediterranean diet and Alzheimer's disease risk in an Australian population. *Translational Psychiatry*, 2(10), e164–e164–e164–e164.

Gariballa, S., Alkaabi, J., Yasin, J., & al Essa, A. (2019). Total adiponectin in overweight and obese subjects and its response to visceral fat loss. *BMC Endocrine Disorders*, 19(1), 1–6.

Gathercole, L. L., Morgan, S. A., Bujalska, I. J., Hauton, D., Stewart, P. M., & Tomlinson, J. W. (2011). Regulation of Lipogenesis by Glucocorticoids and Insulin in Human Adipose Tissue. *PLoS ONE*, 6(10), 26223. <https://doi.org/10.1371/JOURNAL.PONE.0026223>

Gatz, M., Reynolds, C. A., Fratiglioni, L., Johansson, B., Mortimer, J. A., Berg, S., Fiske, A., & Pedersen, N. L. (2006). Role of genes and environments for explaining Alzheimer disease. *Archives of General Psychiatry*, 63(2), 168–174.

Gauna, C., Meyler, F. M., Janssen, J. A. M. J. L., Delhanty, P. J. D., Abribat, T., Koetsveld, P. Van, Hofland, L. J., Broglio, F., Ghigo, E., & Lely, A. J. Van Der. (2004). Administration of acylated ghrelin reduces insulin sensitivity, whereas the combination of acylated plus unacylated ghrelin strongly improves insulin sensitivity. *Journal of Clinical Endocrinology and Metabolism*, 89(10), 5035–5042. <https://doi.org/10.1210/JC.2004-0363>

Gavin, K. M., Cooper, E. E., Raymer, D. K., & Hickner, R. C. (2013). Estradiol effects on subcutaneous adipose tissue lipolysis in premenopausal women are adipose tissue depot specific and treatment dependent. *American Journal of Physiology - Endocrinology and Metabolism*, 304(11). <https://doi.org/10.1152/AJPENDO.00023.2013>

Gealekman, O., Guseva, N., Hartigan, C., Apotheker, S., Gorgoglione, M., & Gurav, K. (2011). Depot-specific differences and insufficient subcutaneous adipose tissue angiogenesis in human obesity. *CIRC J*, 123.

Gella, A., & Durany, N. (2009). Oxidative stress in Alzheimer disease. *Cell Adhesion & Migration*, 3(1), 88–93.

Georgescu, A., Popov, D., Constantin, A., Nemezc, M., Alexandru, N., Cochior, D., & Tudor, A. (2011). Dysfunction of human subcutaneous fat arterioles in obesity alone or obesity associated with Type 2 diabetes. *Clinical Science (London, England : 1979)*, 120(10), 463–472. <https://doi.org/10.1042/CS20100355>

Ghosh, S., DeCoffe, D., Brown, K., Rajendiran, E., Estaki, M., Dai, C., Yip, A., & Gibson, D. L. (2013). Fish oil attenuates omega-6 polyunsaturated fatty acid-induced dysbiosis and infectious colitis but impairs LPS dephosphorylation activity causing sepsis. *PLoS One*, 8(2).

Gille, B., de Schaepdryver, M., Goossens, J., Dedeene, L., de Vocht, J., Oldoni, E., Goris, A., van den Bosch, L., Depreitere, B., Claeys, K. G., Tournoy, J., van Damme, P., & Poesen, K. (2019). Serum neurofilament light chain levels as a marker of upper motor neuron degeneration in patients with Amyotrophic Lateral Sclerosis. *Neuropathology and Applied Neurobiology*, 45(3), 291–304. <https://doi.org/10.1111/nan.12511>

Giltay, E. J., Gooren, L. J. G., Toorians, A. W. F. T., Katan, M. B., & Zock, P. L. (2004). Docosahexaenoic acid concentrations are higher in women than in men because of estrogenic effects. *The American Journal of Clinical Nutrition*, 80(5), 1167–1174. <https://doi.org/10.1093/AJCN/80.5.1167>

Giroli, M. G., Werba, J. P., Risé, P., Porro, B., Sala, A., Amato, M., Tremoli, E., Bonomi, A., & Veglia, F. (2021). Effects of mediterranean diet or low-fat diet on blood fatty acids in patients with coronary heart disease. A randomized intervention study. *Nutrients*, 13(7). <https://doi.org/10.3390/nu13072389>

Giudetti, A. M., Romano, A., Lavecchia, A. M., & Gaetani, S. (2016). The Role of Brain Cholesterol and its Oxidized Products in Alzheimer's Disease. *Current Alzheimer Research*, 13(2), 198–205. <https://doi.org/10.2174/1567205012666150921103426>

Glatz, J. F. C., & Luiken, J. J. F. P. (2018). Dynamic role of the transmembrane glycoprotein CD36 (SR-B2) in cellular fatty acid uptake and utilization. *Journal of Lipid Research*, 59(7), 1084–1093. <https://doi.org/10.1194/JLR.R082933>

Goate, A., Chartier-Harlin, M.-C., Mullan, M., Brown, J., Crawford, F., Fidani, L., Giuffra, L., Haynes, A., Irving, N., & James, L. (1991). Segregation of a missense mutation in the amyloid precursor protein gene with familial Alzheimer's disease. *Nature*, 349(6311), 704–706.

Godessart, N., Camacho, M., López-Belmonte, J., Antón, R., García, M., De Moragas, J. M., & Vila, L. (1996). Prostaglandin H-synthase-2 is the main enzyme involved in the biosynthesis of octadecanoids from linoleic acid in human dermal fibroblasts stimulated with interleukin-1beta. *The Journal of Investigative Dermatology*, 107(5), 726–732. <https://doi.org/10.1111/1523-1747.EP12365616>

Goedecke, J. H., Wake, D. J., Levitt, N. S., Lambert, E. v., Collins, M. R., Morton, N. M., Andrew, R., Seckl, J. R., & Walker, B. R. (2006). Glucocorticoid metabolism within superficial subcutaneous rather than visceral adipose tissue is associated with features of the metabolic syndrome in South African women. *Clinical Endocrinology*, 65(1), 81–87. <https://doi.org/10.1111/J.1365-2265.2006.02552.X>

Goldstein, J. L., & Brown, M. S. (2015). A century of cholesterol and coronaries: From plaques to genes to statins. *Cell*, 161(1), 161–172. <https://doi.org/10.1016/J.CELL.2015.01.036>

Goldsteins, G., Hakosalo, V., Jaronen, M., Keuters, M. H., Lehtonen, Š., & Koistinaho, J. (2022). CNS Redox Homeostasis and Dysfunction in Neurodegenerative Diseases. *Antioxidants (Basel, Switzerland)*, 11(2). <https://doi.org/10.3390/antiox11020405>

Gomes, A. C., Hoffmann, C., Mota, J. F., & Mota, C. H. A. C. G. J. F. (2018). The human gut microbiota: metabolism and perspective in obesity. *Gut Microbes*, 9(4), 308. <https://doi.org/10.1080/19490976.2018.1465157>

Gomez, G., Han, S., Englander, E. W., & Greeley, G. H. (2012). Influence of a long-term high-fat diet on ghrelin secretion and ghrelin-induced food intake in rats. *Regulatory Peptides*, 173(1–3), 60–63. <https://doi.org/10.1016/J.REGPEP.2011.09.006>

González-Gross, M., Marcos, A., & Pietrzik, K. (2001). Nutrition and cognitive impairment in the elderly. *British Journal of Nutrition*, 86(3), 313–321.

Gosmain, Y., Dif, N., Berbe, V., Loizon, E., Rieusset, J., Vidal, H., & Lefai, E. (2005). Regulation of SREBP-1 expression and transcriptional action on HKII and FAS genes during fasting and refeeding in rat tissues. *Journal of Lipid Research*, 46(4), 697–705. <https://doi.org/10.1194/JLR.M400261-JLR200>

Gough, D. R., & Cotter, T. G. (2011). Hydrogen peroxide: a Jekyll and Hyde signalling molecule. *Cell Death & Disease* 2011 2:10, 2(10), e213–e213. <https://doi.org/10.1038/cddis.2011.96>

Goyens, P. L. L., Spilker, M. E., Zock, P. L., Katan, M. B., & Mensink, R. P. (2006). Conversion of α -linolenic acid in humans is influenced by the absolute amounts of α -linolenic acid and linoleic acid in the diet and not by their ratio. *The American Journal of Clinical Nutrition*, 84(1), 44–53. <https://doi.org/10.1093/AJCN/84.1.44>

Graudejus, O., Ponce Wong, R., Varghese, N., Wagner, S., & Morrison, B. (2018). Bridging the gap between in vivo and in vitro research: Reproducing in vitro the mechanical and electrical environment of cells in vivo. *Frontiers in Cellular Neuroscience*, 12. https://doi.org/10.3389/FNCEL.2018.38.00069/EVENT_ABSTRACT

Greene, L. A. (1978). Nerve growth factor prevents the death and stimulates the neuronal differentiation of clonal PC12 pheochromocytoma cells in serum-free medium. *The Journal of Cell Biology*, 78(3), 747–755. <https://doi.org/10.1083/JCB.78.3.747>

Greene, L. A., & Tischler, A. S. (1976). Establishment of a noradrenergic clonal line of rat adrenal pheochromocytoma cells which respond to nerve growth factor. *Proceedings of the*

National Academy of Sciences of the United States of America, 73(7), 2424–2428. <https://doi.org/10.1073/pnas.73.7.2424>

Greenhill, C. (2018). Mechanisms of insulin resistance. *Nat. Rev. Endocrinol.*, 14(10), 565. <https://doi.org/10.1038/s41574-018-0083-4>

Greupner, T., Kutzner, L., Nolte, F., Strangmann, A., Kohrs, H., Hahn, A., Schebb, N. H., & Schuchardt, J. P. (2018). Effects of a 12-week high- α -linolenic acid intervention on EPA and DHA concentrations in red blood cells and plasma oxylipin pattern in subjects with a low EPA and DHA status. *Food & Function*, 9(3), 1587–1600. <https://doi.org/10.1039/C7FO01809F>

Grimaldi, P. A. (2010). Metabolic and nonmetabolic regulatory functions of peroxisome proliferator-activated receptor beta. *Current Opinion in Lipidology*, 21(3), 186–191. <https://doi.org/10.1097/MOL.0B013E32833884A4>

Gropper, S. S., Smith, J. L., & Groff, J. L. (2009). *Advanced Nutrition and Human Metabolism Fifth Edition*.

Grouleff, J., Irudayam, S. J., Skeby, K. K., & Schiøtt, B. (2015). The influence of cholesterol on membrane protein structure, function, and dynamics studied by molecular dynamics simulations. *Biochimica et Biophysica Acta (BBA) - Biomembranes*, 1848(9), 1783–1795. <https://doi.org/10.1016/j.bbamem.2015.03.029>

Gruzdeva, O., Borodkina, D., Uchasova, E., Dyleva, Y., & Barbarash, O. (2019). Leptin resistance: underlying mechanisms and diagnosis. *Diabetes, Metabolic Syndrome and Obesity: Targets and Therapy*, 12, 191. <https://doi.org/10.2147/DMSO.S182406>

Grygiel-Górniak, B. (2014). Peroxisome proliferator-activated receptors and their ligands: Nutritional and clinical implications - A review. *Nutrition Journal*, 13(1), 1–10. <https://doi.org/10.1186/1475-2891-13-17/FIGURES/7>

Grzybek, M., Palladini, A., Alexaki, V. I., Surma, M. A., Simons, K., Chavakis, T., Klose, C., & Coskun, Ü. (2019). Comprehensive and quantitative analysis of white and brown adipose tissue by shotgun lipidomics. *Molecular Metabolism*, 22, 12–20.

Gu, X., Xie, Z., Wang, Q., Liu, G., Qu, Y., Zhang, L., Pan, J., Zhao, G., & Zhang, Q. (2009). Transcriptome profiling analysis reveals multiple modulatory effects of Ginkgo biloba extract in the liver of rats on a high-fat diet. *The FEBS Journal*, 276(5), 1450–1458.

Guan, M., Qu, L., Tan, W., Chen, L., & Wong, C. W. (2011). Hepatocyte nuclear factor-4 alpha regulates liver triglyceride metabolism in part through secreted phospholipase A₂ GXIIB. *Hepatology (Baltimore, Md.)*, 53(2), 458–466. <https://doi.org/10.1002/HEP.24066>

Gunstone, F. D. (1996). *Fatty Acid and Lipid Chemistry*. *Fatty Acid and Lipid Chemistry*. <https://doi.org/10.1007/978-1-4615-4131-8>

Guo, Z., Jiang, H., Xu, X., Duan, W., & Mattson, M. P. (2008). Leptin-mediated cell survival signaling in hippocampal neurons mediated by JAK STAT3 and mitochondrial stabilization.

Journal of Biological Chemistry, 283(3), 1754–1763.
<https://doi.org/10.1074/JBC.M703753200>

Gustavsson, J., Parpal, S., Karlsson, M., Ramsing, C., Thorn, H., Borg, M., Lindroth, M., Peterson, K. H., Magnusson, K., & Strålfors, P. (1999). Localization of the insulin receptor in caveolae of adipocyte plasma membrane. *The FASEB Journal*, 13(14), 1961–1971.

Haczeyni, F., Bell-Anderson, K. S., & Farrell, G. C. (2018). Causes and mechanisms of adipocyte enlargement and adipose expansion. *Obesity Reviews : An Official Journal of the International Association for the Study of Obesity*, 19(3), 406–420. <https://doi.org/10.1111/OBR.12646>

Haddad-Tóvolli, R., Dragano, N. R. V., Ramalho, A. F. S., & Velloso, L. A. (2017). Development and function of the blood-brain barrier in the context of metabolic control. *Frontiers in Neuroscience*, 11(APR), 224. <https://doi.org/10.3389/FNINS.2017.00224/BIBTEX>

Hahn, A. T., Jones, J. T., & Meyer, T. (2009). Cell Cycle Quantitative analysis of cell cycle phase durations and PC12 differentiation using fluorescent biosensors. *Cell Cycle*, 8(7). <https://doi.org/10.4161/cc.8.7.8042>

Hajam, Y. A., Rani, R., Ganie, S. Y., Sheikh, T. A., Javaid, D., Qadri, S. S., Pramodh, S., Alsulimani, A., Alkhanani, M. F., Harakeh, S., Hussain, A., Haque, S., & Reshi, M. S. (2022). Oxidative Stress in Human Pathology and Aging: Molecular Mechanisms and Perspectives. *Cells*, 11(3). <https://doi.org/10.3390/cells11030552>

Hajeyah, A. A., Griffiths, W. J., Wang, Y., Finch, A. J., & O'Donnell, V. B. (2020). The Biosynthesis of Enzymatically Oxidized Lipids. *Frontiers in Endocrinology*, 11, 910. <https://doi.org/10.3389/FENDO.2020.591819/BIBTEX>

Hall, C. N., Klein-Flügge, M. C., Howarth, C., & Attwell, D. (2012). Oxidative phosphorylation, not glycolysis, powers presynaptic and postsynaptic mechanisms underlying brain information processing. *Journal of Neuroscience*, 32(26), 8940–8951.

Hamilton, J. A. (2007). New insights into the roles of proteins and lipids in membrane transport of fatty acids. *Prostaglandins, Leukotrienes, and Essential Fatty Acids*, 77(5–6), 355–361. <https://doi.org/10.1016/J.PLEFA.2007.10.020>

Hamilton, J. A., Hillard, C. J., Spector, A. A., & Watkins, P. A. (2007). Brain uptake and utilization of fatty acids, lipids and lipoproteins: Application to neurological disorders. *Journal of Molecular Neuroscience*, 33(1), 2–11. <https://doi.org/10.1007/S12031-007-0060-1>

Hammarstedt, A., Syed, I., Vijayakumar, A., Eliasson, B., Gogg, S., Kahn, B. B., & Smith, U. (2018). Adipose tissue dysfunction is associated with low levels of the novel Palmitic Acid Hydroxystearic Acids. *Scientific Reports* 2018 8:1, 8(1), 1–11. <https://doi.org/10.1038/s41598-018-34113-3>

Hammond, V. J., & O'Donnell, V. B. (2012). Esterified eicosanoids: Generation, characterization and function. *Biochimica et Biophysica Acta - Biomembranes*, 1818(10), 2403–2412. <https://doi.org/10.1016/J.BBAMEM.2011.12.013>

Han, L., Shen, W. J., Bittner, S., Kraemer, F. B., & Azhar, S. (2017). PPARs: regulators of metabolism and as therapeutic targets in cardiovascular disease. Part I: PPAR- α . *Future cardiology*, 13(3), 259-278. <https://doi.org/10.2217/FCA-2016-0059>

Hancock, C. R., Han, D. H., Chen, M., Terada, S., Yasuda, T., Wright, D. C., & Holloszy, J. O. (2008). High-fat diets cause insulin resistance despite an increase in muscle mitochondria. *Proceedings of the National Academy of Sciences of the United States of America*, 105(22), 7815. <https://doi.org/10.1073/PNAS.0802057105>

Handjieva-Darlenska, T., & Boyadjieva, N. (2009). The effect of high-fat diet on plasma ghrelin and leptin levels in rats. *Journal of Physiology and Biochemistry* 2009 65:2, 65(2), 157–164. <https://doi.org/10.1007/BF03179066>

Hankins, H. M., Baldrige, R. D., Xu, P., & Graham, T. R. (2015). Role of flippases, scramblases and transfer proteins in phosphatidylserine subcellular distribution. *Traffic (Copenhagen, Denmark)*, 16(1), 35–47. <https://doi.org/10.1111/TRA.12233>

Harbige, L. S. (2003). Fatty acids, the immune response, and autoimmunity: a question of n-6 essentiality and the balance between n-6 and n-3. *Lipids*, 38(4), 323–341. <https://doi.org/10.1007/S11745-003-1067-Z>

Hardy, J., & Selkoe, D. J. (2002). The amyloid hypothesis of Alzheimer's disease: progress and problems on the road to therapeutics. *Science*, 297(5580), 353–356.

Hariri, N., & Thibault, L. (2010). High-fat diet-induced obesity in animal models. *Nutrition research reviews*, 23(2), 270-299.

Harms, M., & Seale, P. (2013). Brown and beige fat: Development, function and therapeutic potential. *Nature Medicine*, 19(10), 1252–1263. <https://doi.org/10.1038/NM.3361>

Harr, S. D., Simonian, N. A., & Hyman, B. T. (1995). Functional alterations in Alzheimer's disease: decreased glucose transporter 3 immunoreactivity in the perforant pathway terminal zone. *Journal of Neuropathology & Experimental Neurology*, 54(1), 38–41.

Harris, D. C. (2010). *Quantitative chemical analysis*. Macmillan.

Harris, W. S., Mozaffarian, D., Rimm, E., Kris-Etherton, P., Rudel, L. L., Appel, L. J., Engler, M. M., Engler, M. B., & Sacks, F. (2009). Omega-6 fatty acids and risk for cardiovascular disease: A science advisory from the American Heart Association nutrition subcommittee of the council on nutrition, physical activity, and metabolism; council on cardiovascular nursing; and council on epidemiology and prevention. *Circulation*, 119(6), 902–907. <https://doi.org/10.1161/CIRCULATIONAHA.108.191627>

He, J., Cui, Z., & Zhu, Y. (2021). The role of caveolae in endothelial dysfunction. *Medical Review*, 1(1), 78–91. <https://doi.org/10.1515/MR-2021-0005>

Hebbard, L., & George, J. (2011). Animal models of nonalcoholic fatty liver disease. *Nat Rev Gastroenterol Hepatol*, 8(1), 35–44. <https://doi.org/10.1038/nrgastro.2010.191>

Heinritz, S. N., Weiss, E., Eklund, M., Aumiller, T., Heyer, C. M. E., Messner, S., Rings, A., Louis, S., Bischoff, S. C., & Mosenthin, R. (2016). Impact of a High-Fat or High-Fiber Diet on Intestinal Microbiota and Metabolic Markers in a Pig Model. *Nutrients*, 8(5). <https://doi.org/10.3390/NU8050317>

Heiss, C. N., Mannerås-Holm, L., Lee, Y. S., Serrano-Lobo, J., Gladh, A. H., Seeley, R. J., Drucker, D. J., Bäckhed, F., Olofsson, L. E., Gladh, A. H., Seeley, R. J., Drucker, D. J., Bäckhed, F., & Olofsson, L. E. (2021). The gut microbiota regulates hypothalamic inflammation and leptin sensitivity in Western diet-fed mice via a GLP-1R-dependent mechanism. *Cell Reports*, 35(8). <https://doi.org/10.1016/j.celrep.2021.109163>

Henis, Y. I., Rimonl, G., & Felderl, S. (1982). Lateral mobility of phospholipids in turkey erythrocytes. Implications for adenylate cyclase activation. *Journal of Biological Chemistry*, 257(3), 1407–1411. [https://doi.org/10.1016/S0021-9258\(19\)68207-4](https://doi.org/10.1016/S0021-9258(19)68207-4)

Heras-Molina, A., Pesantez-Pacheco, J. L., Vazquez-Gomez, M., Garcia-Contreras, C., Astiz, S., Isabel, B., & Gonzalez-Bulnes, A. (2020). Short-Term Effects of Early Menopause on Adiposity, Fatty Acids Profile and Insulin Sensitivity of a Swine Model of Female Obesity. *Biology*, 9(9), 1–16. <https://doi.org/10.3390/biology9090284>

Hermida, M. A., Dinesh Kumar, J., & Leslie, N. R. (2017). GSK3 and its interactions with the PI3K/AKT/mTOR signalling network. *Advances in Biological Regulation*, 65, 5–15. <https://doi.org/10.1016/j.jbior.2017.06.003>

Hewawasam, E., Liu, G., Jeffery, D. W., Muhlhausler, B. S., & Gibson, R. A. (2018). A stable method for routine analysis of oxylipins from dried blood spots using ultra-high performance liquid chromatography–tandem mass spectrometry. *Prostaglandins, Leukotrienes and Essential Fatty Acids*, 137, 12–18. <https://doi.org/10.1016/j.plefa.2018.08.001>

Heymsfield, S. B., Greenberg, A. S., Fujioka, K., Dixon, R. M., Kushner, R., Hunt, T., Lubina, J. A., Patane, J., Self, B., Hunt, P., & McCamish, M. (1999). Recombinant leptin for weight loss in obese and lean adults: a randomized, controlled, dose-escalation trial. *JAMA*, 282(16), 1568–1575. <https://doi.org/10.1001/JAMA.282.16.1568>

Higdon, J. V., & Frei, B. (2003). Obesity and oxidative stress: A direct link to CVD? *Arteriosclerosis, Thrombosis, and Vascular Biology*, 23(3), 365–367. <https://doi.org/10.1161/01.ATV.0000063608.43095.E2>

Higuchi, M., Onishi, K., Masuyama, N., & Gotoh, Y. (2003). The phosphatidylinositol-3 kinase (PI3K)-Akt pathway suppresses neurite branch formation in NGF-treated PC12 cells. *Genes to Cells: Devoted to Molecular & Cellular Mechanisms*, 8(8), 657–669. <https://doi.org/10.1046/j.1365-2443.2003.00663.x>

Hileman, S. M., Pierroz, D. D., Masuzaki, H., Björnk, C., El-Haschimi, K., Banks, W. A., & Flier, J. S. (2002). Characterization of Short Isoforms of the Leptin Receptor in Rat Cerebral Microvessels and of Brain Uptake of Leptin in Mouse Models of Obesity. *Endocrinology*, 143(3), 775–783. <https://doi.org/10.1210/endo.143.3.8669>

Hinz, C., Liggi, S., Mocciaro, G., Jung, S., Induruwa, I., Pereira, M., Bryant, C. E., Meckelmann, S. W., O'Donnell, V. B., Farndale, R. W., Fjeldsted, J., & Griffin, J. L. (2019). A Comprehensive UHPLC Ion Mobility Quadrupole Time-of-Flight Method for Profiling and Quantification of Eicosanoids, Other Oxylipins, and Fatty Acids. *Analytical Chemistry*, 91(13), 8025–8035. https://doi.org/10.1021/ACS.ANALCHEM.8B04615/SUPPL_FILE/AC8B04615_SI_006.XLSX

Hirata, B. K. S., Banin, R. M., Dornellas, A. P. S., de Andrade, I. S., Zemdegs, J. C. S., Caperuto, L. C., Oyama, L. M., Ribeiro, E. B., & Telles, M. M. (2015). Ginkgo biloba extract improves insulin signaling and attenuates inflammation in retroperitoneal adipose tissue depot of obese rats. *Mediators of Inflammation*, 2015.

Hirata, B. K. S., Cruz, M. M., de Sá, R. D. C. C., Farias, T. S. M., Machado, M. M. F., Bueno, A. A., Alonso-Vale, M. I. C., & Telles, M. M. (2019). Potential anti-obesogenic effects of Ginkgo biloba observed in epididymal white adipose tissue of obese rats. *Frontiers in Endocrinology*, 10(MAY), 284. <https://doi.org/10.3389/FENDO.2019.00284/BIBTEX>

Hirata, B. K. S., Pedroso, A. P., Machado, M. M. F., Neto, N. I. P., Perestrelo, B. O., de Sá, R. D. C. C., Alonso-Vale, M. I. C., Nogueira, F. N., Oyama, L. M., Ribeiro, E. B., Tashima, A. K., & Telles, M. M. (2019). Ginkgo biloba extract modulates the retroperitoneal fat depot proteome and reduces oxidative stress in diet-induced obese rats. *Frontiers in Pharmacology*, 10(JUN). <https://doi.org/10.3389/FPHAR.2019.00686/PDF>

Ho, L., Chen, L. H., Wang, J., Zhao, W., Talcott, S. T., Ono, K., Teplow, D., Humala, N., Cheng, A., & Percival, S. S. (2009). Heterogeneity in red wine polyphenolic contents differentially influences Alzheimer's disease-type neuropathology and cognitive deterioration. *Journal of Alzheimer's Disease*, 16(1), 59–72.

Ho, L., Ferruzzi, M. G., Janle, E. M., Wang, J., Gong, B., Chen, T.-Y., Lobo, J., Cooper, B., Wu, Q. L., & Talcott, S. T. (2013). Identification of brain-targeted bioactive dietary quercetin-3-O-glucuronide as a novel intervention for Alzheimer's disease. *The FASEB Journal*, 27(2), 769–781.

Hovens, I.B., Dalenberg, J.R. and Small, D.M., 2019. A brief neuropsychological battery for measuring cognitive functions associated with obesity. *Obesity*, 27(12), pp.1988-1996.

Hochberg, Z. (2018). An Evolutionary Perspective on the Obesity Epidemic. *Trends in Endocrinology and Metabolism: TEM*, 29(12), 819–826. <https://doi.org/10.1016/J.TEM.2018.09.002>

Hoeffler, C. A., & Klann, E. (2010). mTOR Signaling: At the Crossroads of Plasticity, Memory, and Disease. *Trends in Neurosciences*, 33(2), 67. <https://doi.org/10.1016/J.TINS.2009.11.003>

Holahan, M. R. (2015). GAP-43 in synaptic plasticity: molecular perspectives. *Research and Reports in Biochemistry*, 5, 137–146. <https://doi.org/10.2147/RRBC.S73846>

Holloway, C. J., Cochlin, L. E., Emmanuel, Y., Murray, A., Codreanu, I., Edwards, L. M., Szmigielski, C., Tyler, D. J., Knight, N. S., Saxby, B. K., Lambert, B., Thompson, C., Neubauer, S., & Clarke, K. (2011). A high-fat diet impairs cardiac high-energy phosphate metabolism and

cognitive function in healthy human subjects. *American Journal of Clinical Nutrition*, 93(4), 748–755. <https://doi.org/10.3945/AJCN.110.002758>

Horton, J. D., Bashmakov, Y., Shimomura, I., & Shimano, H. (1998). Regulation of sterol regulatory element binding proteins in livers of fasted and re-fed mice. *Proceedings of the National Academy of Sciences of the United States of America*, 95(11), 5987. <https://doi.org/10.1073/PNAS.95.11.5987>

Horton, J. D., Goldstein, J. L., & Brown, M. S. (2002). SREBPs: activators of the complete program of cholesterol and fatty acid synthesis in the liver. *The Journal of Clinical Investigation*, 109(9), 1125–1131. <https://doi.org/10.1172/JCI15593>

Horvath, T. L., Sarman, B., García-Cáceres, C., Enriori, P. J., Sotonyi, P., Shanabrough, M., Borok, E., Argente, J., Chowen, J. A., Perez-Tilve, D., Pfuger, P. T., Brönneke, H. S., Levin, B. E., Diano, S., Cowley, M. A., & Tschöp, M. H. (2010). Synaptic input organization of the melanocortin system predicts diet-induced hypothalamic reactive gliosis and obesity. *Proceedings of the National Academy of Sciences of the United States of America*, 107(33), 14875–14880. <https://doi.org/10.1073/PNAS.1004282107/ASSET/13F66EB8-4D43-4DC9-A609-CD49E00D3944/ASSETS/GRAPHIC/PNAS.1004282107FIG04.JPEG>

Hostetler, H. A., Kier, A. B., & Schroeder, F. (2006). Very-Long-Chain and Branched-Chain Fatty Acyl-CoAs Are High Affinity Ligands for the Peroxisome Proliferator-Activated Receptor α (PPAR α)†. *Biochemistry*, 45(24), 7669–7681. <https://doi.org/10.1021/BI060198L>

Hou, J., Chong, Z. Z., Shang, Y. C., & Maiese, K. (2010). Early Apoptotic Vascular Signaling is Determined by Sirt1 Through Nuclear Shuttling, Forkhead Trafficking, Bad, and Mitochondrial Caspase Activation. *Current Neurovascular Research*, 7(2), 95–112. <https://doi.org/10.2174/156720210791184899>

Hou, T. Y., McMurray, D. N., & Chapkin, R. S. (2016). Omega-3 fatty acids, lipid rafts, and T cell signaling. *European Journal of Pharmacology*, 785, 2–9. <https://doi.org/10.1016/J.EJP.2015.03.091>

Hovens, I.B., Dalenberg, J.R. and Small, D.M., 2019. A brief neuropsychological battery for measuring cognitive functions associated with obesity. *Obesity*, 27(12), pp.1988-1996.

Howland, D. S., Trusko, S. P., Savage, M. J., Reaume, A. G., Lang, D. M., Hirsch, J. D., Maeda, N., Siman, R., Greenberg, B. D., & Scott, R. W. (1998). Modulation of secreted β -amyloid precursor protein and amyloid β -peptide in brain by cholesterol. *Journal of Biological Chemistry*, 273(26), 16576–16582.

Hoy, A. J., Brandon, A. E., Turner, N., Watt, M. J., Bruce, C. R., Cooney, G. J., & Kraegen, E. W. (2009). Lipid and insulin infusion-induced skeletal muscle insulin resistance is likely due to metabolic feedback and not changes in IRS-1, Akt, or AS160 phosphorylation. *American Journal of Physiology - Endocrinology and Metabolism*, 297(1). <https://doi.org/10.1152/AJPENDO.90945.2008>

Hoyer, S. (1992). Oxidative energy metabolism in Alzheimer brain. *Molecular and Chemical Neuropathology*, 16(3), 207–224.

Hoyer, S. (2004). Glucose metabolism and insulin receptor signal transduction in Alzheimer disease. *European Journal of Pharmacology*, 490(1–3), 115–125.

Hsieh, C. F., Liu, C. K., Lee, C. T., Yu, L. E., & Wang, J. Y. (2019). Acute glucose fluctuation impacts microglial activity, leading to inflammatory activation or self-degradation. *Scientific Reports*, 9(1). <https://doi.org/10.1038/S41598-018-37215-0>

Hsu, C.-L., Wu, Y.-L., Tang, G.-J., Lee, T.-S., & Kou, Y. R. (2009). Ginkgo biloba extract confers protection from cigarette smoke extract-induced apoptosis in human lung endothelial cells: role of heme oxygenase-1. *Pulmonary Pharmacology & Therapeutics*, 22(4), 286–296.

Hu, N., Yu, J.-T., Tan, L., Wang, Y.-L., Sun, L., & Tan, L. (2013). Nutrition and the risk of Alzheimer's disease. *BioMed Research International*, 2013.

Hu, R., Cao, Q., Sun, Z., Chen, J., Zheng, Q., & Xiao, F. (2018). A novel method of neural differentiation of PC12 cells by using Opti-MEM as a basic induction medium. *International Journal of Molecular Medicine*, 41(1), 195–201. <https://doi.org/10.3892/IJMM.2017.3195/DOWNLOAD>

Huang, C.-H., Yang, M.-L., Tsai, C.-H., Li, Y.-C., Lin, Y.-J., & Kuan, Y.-H. (2013). Ginkgo biloba leaves extract (EGb 761) attenuates lipopolysaccharide-induced acute lung injury via inhibition of oxidative stress and NF- κ B-dependent matrix metalloproteinase-9 pathway. *Phytomedicine*, 20(3–4), 303–309.

Huang, J., Zhu, R., & Shi, D. (2021). The role of FATP1 in lipid accumulation: a review. *Molecular and Cellular Biochemistry* 2021 476:4, 476(4), 1897–1903. <https://doi.org/10.1007/S11010-021-04057-W>

Huang, X., Liu, G., Guo, J., & Su, Z. (2018). The PI3K/AKT pathway in obesity and type 2 diabetes. *International Journal of Biological Sciences*, 14(11), 1483–1496. <https://doi.org/10.7150/ijbs.27173>

Huang, Y., & Mahley, R. W. (2014). Apolipoprotein E: Structure and function in lipid metabolism, neurobiology, and Alzheimer's diseases. *Neurobiology of Disease*, 72(Part A), 3–12. <https://doi.org/10.1016/J.NBD.2014.08.025>

Hucik, B., Lovell, A. J., Hoecht, E. M., Cervone, D. T., Mutch, D. M., & Dyck, D. J. (2021). Regulation of adipose tissue lipolysis by ghrelin is impaired with high-fat diet feeding and is not restored with exercise. *Adipocyte*, 10(1), 338–349. <https://doi.org/10.1080/21623945.2021.1945787>

Hughes, K. A., Reynolds, R. M., Andrew, R., Critchley, H. O. D., & Walker, B. R. (2010). Glucocorticoids Turn Over Slowly in Human Adipose Tissue in Vivo. *The Journal of Clinical Endocrinology and Metabolism*, 95(10), 4696. <https://doi.org/10.1210/JC.2010-0384>

Hui, Y., Chengyong, T., Cheng, L., Haixia, H., Yuanda, Z., & Weihua, Y. (2018). Resveratrol attenuates the cytotoxicity induced by amyloid- β 1–42 in PC12 cells by upregulating heme oxygenase-1 via the PI3K/Akt/Nrf2 pathway. *Neurochemical Research*, 43(2), 297–305. <https://doi.org/10.1007/s11064-017-2421-7>

Hulbert, A. J. (2010). Metabolism and longevity: is there a role for membrane fatty acids? *Integrative and Comparative Biology*, 50(5), 808–817. <https://doi.org/10.1093/ICB/ICQ007>

Hulbert, A. J., Pamplona, R., Buffenstein, R., & Buttemer, W. A. (2007a). Life and death: Metabolic rate, membrane composition, and life span of animals. *Physiological Reviews*, 87(4), 1175–1213. <https://doi.org/10.1152/PHYSREV.00047.2006/ASSET/IMAGES/LARGE/Z9J0040724420010.JPEG>

Hulbert, A. J., Turner, N., Storlien, L. H., & Else, P. L. (2005a). Dietary fats and membrane function: implications for metabolism and disease. *Biological Reviews*, 80(1), 155–169.

Hung, C. S., Lee, J. K., Yang, C. Y., Hsieh, H. R., Ma, W. Y., Lin, M. S., Liu, P. H., Shih, S. R., Liou, J. M., Chuang, L. M., Chen, M. F., Lin, J. W., Wei, J. N., & Li, H. Y. (2014). Measurement of Visceral Fat: Should We Include Retroperitoneal Fat? *PLOS ONE*, 9(11), e112355–e112355. <https://doi.org/10.1371/JOURNAL.PONE.0112355>

Hussain, M. M. (2014). Intestinal lipid absorption and lipoprotein formation. *Current Opinion in Lipidology*, 25(3), 200–206. <https://doi.org/10.1097/MOL.0000000000000084>

Hussey, B., Lindley, M., & Mastana, S. (2017). Omega 3 fatty acids, inflammation and DNA methylation: an overview. <https://doi.org/10.1080/17584299.2017.1319454>

Husted, K. S., & Bouzinova, E. V. (2016). The importance of n-6/n-3 fatty acids ratio in the major depressive disorder. *Medicina*, 52(3), 139–147. <https://doi.org/10.1016/J.MEDICI.2016.05.003>

Iacobini, C., Pugliese, G., Blasetti Fantauzzi, C., Federici, M., & Menini, S. (2019a). Metabolically healthy versus metabolically unhealthy obesity. *Metabolism: Clinical and Experimental*, 92, 51–60. <https://doi.org/10.1016/J.METABOL.2018.11.009>

Ibrahim, M., Anishetty, S., & Ibrahim, S. A. M. (2012). A meta-metabolome network of carbohydrate metabolism: interactions between gut microbiota and host. *Biochemical and Biophysical Research Communications*, 428(2), 278–284. <https://doi.org/10.1016/J.BBRC.2012.10.045>

Ibrahim, M. M. (2010). Subcutaneous and visceral adipose tissue: Structural and functional differences. In *Obesity Reviews* (Vol. 11, Issue 1, pp. 11–18). Blackwell Publishing Ltd. <https://doi.org/10.1111/j.1467-789X.2009.00623.x>

Ichi, I., Kono, N., Arita, Y., Haga, S., Arisawa, K., Yamano, M., Nagase, M., Fujiwara, Y., & Arai, H. (2014). Identification of genes and pathways involved in the synthesis of Mead acid (20:3n – 9), an indicator of essential fatty acid deficiency. *Biochimica et Biophysica Acta (BBA) - Molecular and Cell Biology of Lipids*, 1841(1), 204–213. <https://doi.org/10.1016/J.BBALIP.2013.10.013>

Igarashi, M., Ma, K., Chang, L., Bell, J. M., & Rapoport, S. I. (2008). Rat heart cannot synthesize docosahexaenoic acid from circulating α -linolenic acid because it lacks elongase-2. *Journal of Lipid Research*, 49(8), 1735–1745. <https://doi.org/10.1194/JLR.M800093-JLR200>

Ingalls, S. T., Kriaris, M. S., Xu, Y., DeWulf, D. W., Tserng, K.-Y., & Hoppel, C. L. (1993). Method for isolation of non-esterified fatty acids and several other classes of plasma lipids by column chromatography on silica gel. *Journal of Chromatography B: Biomedical Sciences and Applications*, 619(1), 9–19.

Ingannato, A., Bagnoli, S., Mazzeo, S., Bessi, V., Matà, S., del Mastio, M., Lombardi, G., Ferrari, C., Sorbi, S., & Nacmias, B. (2021). Neurofilament Light Chain and Intermediate HTT Alleles as Combined Biomarkers in Italian ALS Patients. *Frontiers in Neuroscience*, 15, 695049. <https://doi.org/10.3389/fnins.2021.695049>

Inoue, M., Gotoh, K., Seike, M., Masaki, T., Honda, K., Kakuma, T., & Yoshimatsu Prof., H. (2012). Role of the spleen in the development of steatohepatitis in high-fat-diet-induced obese rats. *Exp. Biol. Med. (Maywood)*, 237(4), 461–470. <https://doi.org/10.1258/ebm.2011.011230>

Isah, T. (2015). Rethinking Ginkgo biloba L.: Medicinal uses and conservation. *Pharmacognosy Reviews*, 9(18), 140. <https://doi.org/10.4103/0973-7847.162137>

Ishunina, T. A., Kamphorst, W., & Swaab, D. F. (2004). Metabolic alterations in the hypothalamus and basal forebrain in vascular dementia. *Journal of Neuropathology and Experimental Neurology*, 63(12), 1243–1254. <https://doi.org/10.1093/jnen/63.12.1243>

Islam, M. M., Hlushchenko, I., & Pfisterer, S. G. (2022). Low-Density Lipoprotein Internalization, Degradation and Receptor Recycling Along Membrane Contact Sites. *Frontiers in Cell and Developmental Biology*, 10, 33. <https://doi.org/10.3389/fcell.2022.826379/BIBTEX>

Isobe, I., Yanagisawa, K., & Michikawa, M. (2001). 3-(4,5-Dimethylthiazol-2-yl)-2,5-diphenyltetrazolium bromide (MTT) causes Akt phosphorylation and morphological changes in intracellular organelles in cultured rat astrocytes. *Journal of Neurochemistry*, 77(1), 274–280. <https://doi.org/10.1046/J.1471-4159.2001.T01-1-00237.X>

Iverson, S. J., Lang, S. L. C., & Cooper, M. H. (2001). Comparison of the Bligh and Dyer and Folch methods for total lipid determination in a broad range of marine tissue. *Lipids*, 36(11), 1283–1287.

Izquierdo, A. G., Crujeiras, A. B., Casanueva, F. F., & Carreira, M. C. (2019). Leptin, Obesity, and Leptin Resistance: Where Are We 25 Years Later? *Nutrients*, 11(11). <https://doi.org/10.3390/NU11112704>

Janssens, D., Michiels, C., Delaive, E., Eliaers, F., & Drieu, K. (1995). Protection of hypoxia-induced ATP decrease in endothelial cells by ginkgo biloba extract and bilobalide. *Biochem Pharmacol*, 50.

Jaworski, J., & Sheng, M. (2006). The growing role of mTOR in neuronal development and plasticity. *Molecular Neurobiology*, 34(3), 205–219. <https://doi.org/10.1385/MN:34:3:205>

Jennings, B. C., & Linder, M. E. (2010). Regulation of G Proteins by Covalent Modification. *Handbook of Cell Signaling*, 2/e, 2, 1629–1633. <https://doi.org/10.1016/B978-0-12-374145-5.00200-X>

Jensen, V. S., Hvid, H., Damgaard, J., Nygaard, H., Ingvorsen, C., Wulff, E. M., Lykkesfeldt, J., & Fledelius, C. (2018). Dietary fat stimulates development of NAFLD more potently than dietary fructose in Sprague-Dawley rats. *Diabetology and Metabolic Syndrome*, 10(1), 1–13. <https://doi.org/10.1186/S13098-018-0307-8/FIGURES/5>

Jensen-Urstad, A. P. L., & Semenkovich, C. F. (2012). Fatty acid synthase and liver triglyceride metabolism: housekeeper or messenger? *Biochimica et Biophysica Acta (BBA)-Molecular and Cell Biology of Lipids*, 1821(5), 747–753.

Jeon, S., Park, J. K., Bae, C. D., & Park, J. (2010). NGF-induced moesin phosphorylation is mediated by the PI3K, Rac1 and Akt and required for neurite formation in PC12 cells. *Neurochemistry International*, 56(6–7), 810–818. <https://doi.org/10.1016/j.neuint.2010.03.005>

Jeong, D. W., Jang, H., Choi, S. Q., & Choi, M. C. (2016). Enhanced stability of freestanding lipid bilayer and its stability criteria. *Scientific Reports*, 6(December), 1–7. <https://doi.org/10.1038/srep38158>

Jeong, H.-S., Kim, K.-H., Lee, I.-S., Park, J. Y., Kim, Y., Kim, K.-S., & Jang, H.-J. (2017). Ginkgolide A ameliorates non-alcoholic fatty liver diseases on high fat diet mice. *Biomedicine & Pharmacotherapy*, 88, 625–634.

Jia, J., Zhang, L., Shi, X., Wu, M., Zhou, X., Liu, X., & Huo, T. (2016). SOD2 Mediates Amifostine-Induced Protection against Glutamate in PC12 Cells. *Oxidative Medicine and Cellular Longevity*, 2016. <https://doi.org/10.1155/2016/4202437>

Jia, L., Betters, J. L., & Yu, L. (2011). Niemann-pick C1-like 1 (NPC1L1) protein in intestinal and hepatic cholesterol transport. *Annual Review of Physiology*, 73, 239–259. <https://doi.org/10.1146/ANNUREV-PHYSIOL-012110-142233>

Jialal, I., Kaur, H., & Devaraj, S. (2014). Toll-like Receptor Status in Obesity and Metabolic Syndrome: A Translational Perspective. *J Clin Endocrinol Metab*, 99(1), 39–48. <https://doi.org/10.1210/jc.2013-3092>

Jorge, A. P., Horst, H., Sousa, E. De, Pizzolatti, M. G., & Silva, F. R. M. B. (2004). Insulinomimetic effects of kaempferitrin on glycaemia and on 14C-glucose uptake in rat soleus muscle. *Chemico-Biological Interactions*, 149(2–3), 89–96. <https://doi.org/10.1016/J.CBI.2004.07.001>

Jou, J., Choi, S. S., & Diehl, A. M. (2008). Mechanisms of disease progression in nonalcoholic fatty liver disease. *Seminars in Liver Disease*, 28(4), 370–379. <https://doi.org/10.1055/S-0028-1091981>

Jové, M., Mota-Martorell, N., Pradas, I., Galo-Licon, J. D., Martín-Gari, M., Obis, È., Sol, J., & Pamplona, R. (2020). The Lipidome Fingerprint of Longevity. *Molecules* 2020, Vol. 25, Page 4343, 25(18), 4343. <https://doi.org/10.3390/MOLECULES25184343>

Ju, H., Zou, R., Venema, V. J., & Venema, R. C. (1997). Direct interaction of endothelial nitric-oxide synthase and caveolin-1 inhibits synthase activity. *Journal of Biological Chemistry*, 272(30), 18522–18525. <https://doi.org/10.1074/JBC.272.30.18522>

Jump, D. B. (2011). Fatty acid regulation of hepatic lipid metabolism. *Current Opinion in Clinical Nutrition and Metabolic Care*, 14(2), 115. <https://doi.org/10.1097/MCO.0B013E328342991C>

Kahle, M., Schäfer, A., Seelig, A., Schultheiß, J., Wu, M., Aichler, M., Leonhardt, J., Rathkolb, B., Rozman, J., Sarioglu, H., Hauck, S. M., Ueffing, M., Wolf, E., Kastenmueller, G., Adamski, J., Walch, A., Hrabé de Angelis, M., & Neschen, S. (2015). High fat diet-induced modifications in membrane lipid and mitochondrial-membrane protein signatures precede the development of hepatic insulin resistance in mice. *Molecular Metabolism*, 4(1), 39. <https://doi.org/10.1016/J.MOLMET.2014.11.004>

Kalra, A., Yetiskul, E., Wehrle, C. J., & Tuma, F. (2022). *Physiology, Liver*. StatPearls. <https://www.ncbi.nlm.nih.gov/books/NBK535438/>

Kamp, F., & Hamilton, J. A. (2006). How fatty acids of different chain length enter and leave cells by free diffusion. *Prostaglandins, Leukotrienes, and Essential Fatty Acids*, 75(3), 149–159. <https://doi.org/10.1016/J.PLEFA.2006.05.003>

Kandimalla, R., Thirumala, V., & Reddy, P. H. (2017). Is Alzheimer's disease a type 3 diabetes? A critical appraisal. *Biochimica et Biophysica Acta (BBA)-Molecular Basis of Disease*, 1863(5), 1078–1089.

Kang, J. X. (2003). The importance of omega-6/omega-3 fatty acid ratio in cell function. *Omega-6/Omega-3 Essential Fatty Acid Ratio: The Scientific Evidence*, 92, 23–36.

Kanoski, S. E., & Davidson, T. L. (2011). Western diet consumption and cognitive impairment: Links to hippocampal dysfunction and obesity. *Physiology and Behavior*, 103(1), 59–68. <https://doi.org/10.1016/J.PHYSBEH.2010.12.003>

Karch, C. M., & Goate, A. M. (2015). Alzheimer's disease risk genes and mechanisms of disease pathogenesis. *Biological Psychiatry*, 77(1), 43. <https://doi.org/10.1016/J.BIOPSYCH.2014.05.006>

Karlsson, M., Thorn, H., Parpal, S., Strålfors, P., & Gustavsson, J. (2002). Insulin induces translocation of glucose transporter GLUT4 to plasma membrane caveolae in adipocytes. *The FASEB Journal : Official Publication of the Federation of American Societies for Experimental Biology*, 16(2), 249–251. <https://doi.org/10.1096/fj.01-0646fje>

Karunathilaka, N., & Rathnayake, S. (2021). Screening for mild cognitive impairment in people with obesity: a systematic review. *BMC Endocrine Disorders*, 21(1), 230. <https://doi.org/10.1186/s12902-021-00898-0>

Karuppagounder, S. S., Pinto, J. T., Xu, H., Chen, H.-L., Beal, M. F., & Gibson, G. E. (2009). Dietary supplementation with resveratrol reduces plaque pathology in a transgenic model of Alzheimer's disease. *Neurochemistry International*, 54(2), 111–118.

Kashiwagi, S., Atochin, D. N., Li, Q., Schleicher, M., Pong, T., Sessa, W. C., & Huang, P. L. (2013). eNOS phosphorylation on serine 1176 affects insulin sensitivity and adiposity. *Biochemical and Biophysical Research Communications*, 431(2), 284–290. <https://doi.org/10.1016/J.BBRC.2012.12.110>

Katsiki, N., Mikhailidis, D. P., & Mantzoros, C. S. (2016). Non-alcoholic fatty liver disease and dyslipidemia: an update. *Metabolism*, 65(8), 1109–1123. <https://doi.org/10.1016/j.metabol.2016.05.003>

Kaur, S., Chhabra, R., & Nehru, B. (2013). Ginkgo biloba extract attenuates hippocampal neuronal loss and cognitive dysfunction resulting from trimethyltin in mice. *Phytomedicine: International Journal of Phytotherapy and Phytopharmacology*, 20(2), 178–186. <https://doi.org/10.1016/J.PHYMED.2012.10.003>

Kawaguchi, K., & Morita, M. (2016). ABC Transporter Subfamily D: Distinct Differences in Behavior between ABCD1-3 and ABCD4 in Subcellular Localization, Function, and Human Disease. *BioMed Research International*, 2016. <https://doi.org/10.1155/2016/6786245>

Kawahara, K., Hohjoh, H., Inazumi, T., Tsuchiya, S., & Sugimoto, Y. (2015). Prostaglandin E2-induced inflammation: Relevance of prostaglandin E receptors. *Biochimica et Biophysica Acta*, 1851(4), 414–421. <https://doi.org/10.1016/J.BBALIP.2014.07.008>

Kawano, Y., Nakae, J., Watanabe, N., Kikuchi, T., Tateya, S., Tamori, Y., Kaneko, M., Abe, T., Onodera, M., & Itoh, H. (2016). Colonic Pro-inflammatory Macrophages Cause Insulin Resistance in an Intestinal Ccl2/Ccr2-Dependent Manner. *Cell Metabolism*, 24(2), 295–310. <https://doi.org/10.1016/J.CMET.2016.07.009>

Kawashima, H. (2019). Intake of arachidonic acid-containing lipids in adult humans: Dietary surveys and clinical trials. *Lipids in Health and Disease*, 18(1), 1–9. <https://doi.org/10.1186/S12944-019-1039-Y/FIGURES/2>

Kay, J. G., & Grinstein, S. (2011). Sensing phosphatidylserine in cellular membranes. *Sensors (Basel, Switzerland)*, 11(2), 1744–1755. <https://doi.org/10.3390/S110201744>

Kay, J. G., Koivusalo, M., Ma, X., Wohland, T., & Grinstein, S. (2012). Phosphatidylserine dynamics in cellular membranes. *Molecular Biology of the Cell*, 23(11), 2198–2212. <https://doi.org/10.1091/MBC.E11-11-0936>

Kellerer, T., Kleigrewe, K., Brandl, B., Hofmann, T., Hauner, H., & Skurk, T. (2021). Fatty Acid Esters of Hydroxy Fatty Acids (FAHFAs) Are Associated With Diet, BMI, and Age. *Frontiers in Nutrition*, 8, 436. <https://doi.org/10.3389/FNUT.2021.691401/BIBTEX>

Kennedy, A., Martinez, K., Chuang, C. C., Lapoint, K., & McIntosh, M. (2009). Saturated fatty acid-mediated inflammation and insulin resistance in adipose tissue: mechanisms of action and implications. *The Journal of Nutrition*, 139(1), 1–4. <https://doi.org/10.3945/JN.108.098269>

Kern, S., Syrjanen, J. A., Blennow, K., Zetterberg, H., Skoog, I., Waern, M., Hagen, C. E., van Harten, A. C., Knopman, D. S., Jack, C. R., Petersen, R. C., & Mielke, M. M. (2019). Association

of Cerebrospinal Fluid Neurofilament Light Protein with Risk of Mild Cognitive Impairment among Individuals Without Cognitive Impairment. *JAMA Neurology*, 76(2), 187–193. <https://doi.org/10.1001/jamaneurol.2018.3459>

Kersten, S., & Stienstra, R. (2017). The role and regulation of the peroxisome proliferator activated receptor alpha in human liver. *Biochimie*, 136, 75–84. <https://doi.org/10.1016/j.biochi.2016.12.019>

Keshmirian, J., Bray, G., & Carbonetto, S. (1989). The extracellular matrix modulates the response of PC12 cells to nerve growth factor: cell aggregation versus neurite outgrowth on 3-dimensional laminin substrata. *Journal of Neurocytology*, 18(4), 491–504. <https://doi.org/10.1007/BF01474545>

Khalili, L., Valdes-Ramos, R., & Harbige, L. S. (2021). Effect of n-3 (Omega-3) Polyunsaturated Fatty Acid Supplementation on Metabolic and Inflammatory Biomarkers and Body Weight in Patients with Type 2 Diabetes Mellitus: A Systematic Review and Meta-Analysis of RCTs. *Metabolites* 2021, Vol. 11, Page 742, 11(11), 742. <https://doi.org/10.3390/METABO11110742>

Kim, D., & Chung, J. (2002). Akt: versatile mediator of cell survival and beyond. *Journal of Biochemistry and Molecular Biology*, 35(1), 106–115. <https://doi.org/10.5483/BMBREP.2002.35.1.106>

Kim, G. W., Jo, H. K., & Chung, S. H. (2018). Ginseng seed oil ameliorates hepatic lipid accumulation in vitro and in vivo. *Journal of Ginseng Research*, 42(4), 419–428. <https://doi.org/10.1016/j.jgr.2017.04.010>

Kim, H. Y. (2014). Neuroprotection by docosahexaenoic acid in brain injury. *Military Medicine*, 179(11), 106–111. <https://doi.org/10.7205/milmed-d-14-00162>

Kim, S. Y., Bae, S., Choi, K. H., & An, S. (2011). Hydrogen peroxide controls Akt activity via ubiquitination/degradation pathways. *Oncology Reports*, 26(6), 1561–1566. <https://doi.org/10.3892/OR.2011.1439/HTML>

Kim, Y., Seger, R., Suresh Babu, C. v, Hwang, S.-Y., & Yoo, Y. S. (2004). A positive role of the PI3-K/Akt signaling pathway in PC12 cell differentiation. *Molecules & Cells (Springer Science & Business Media BV)*, 18(3).

Kinarivala, Shah, Abbruscato, & Trippier. (2017). Passage Variation of PC12 Cells Results in Inconsistent Susceptibility to Externally Induced Apoptosis. *ACS Chemical Neuroscience*, 8(1), 82–88. <https://doi.org/10.1021/ACSCHEMNEURO.6B00208>

King, M. W. (2014). Lipids: Triglyceride and Phospholipid Synthesis. In *Integrative Medical Biochemistry Examination and Board Review*. McGraw-Hill Education. accesspharmacy.mhmedical.com/content.aspx?aid=1122103817

Kiriyama, Y., & Nochi, H. (2021). Physiological Role of Bile Acids Modified by the Gut Microbiome. *Microorganisms*, 10(1), 68. <https://doi.org/10.3390/microorganisms10010068>

- Kishida, K., Kim, K. K., Funahashi, T., Matsuzawa, Y., Kang, H. C., & Shimomura, I. (2011). Relationships between circulating adiponectin levels and fat distribution in obese subjects. *Journal of Atherosclerosis and Thrombosis*, 18(7), 592–595. <https://doi.org/10.5551/JAT.7625>
- Klesse, L., Meyers, K., Marshall, C., & Parada, L. (1999). Nerve growth factor induces survival and differentiation through two distinct signaling cascades in PC12 cells. *Oncogene*, 18(12), 2055–2068. <https://doi.org/10.1038/sj.onc.1202524>
- Kliwer, S. A., Sundseth, S. S., Jones, S. A., Brown, P. J., Wisely, G. B., Koble, C. S., Devchand, P., Wahli, W., Willson, T. M., Lenhard, J. M., & Lehmann, J. M. (1997). Fatty acids and eicosanoids regulate gene expression through direct interactions with peroxisome proliferator-activated receptors α and γ . *Proceedings of the National Academy of Sciences*, 94(9), 4318–4323. <https://doi.org/10.1073/PNAS.94.9.4318>
- Knothe, G., & Dunn, R. O. (2009). A Comprehensive Evaluation of the Melting Points of Fatty Acids and Esters Determined by Differential Scanning Calorimetry. *Journal of the American Oil Chemists' Society*, 86(9), 843–856. <https://doi.org/10.1007/S11746-009-1423-2>
- Knuth, N. D., & Horowitz, J. F. (2006). The elevation of ingested lipids within plasma chylomicrons is prolonged in men compared with women. *Journal of Nutrition*, 136(6), 1498–1503. <https://doi.org/10.1093/JN/136.6.1498>
- Ko, J. K., Lee, S. S., & Martin, H. (2010). Phytochemicals as modulators of PPARs and RXRs. *PPAR Research*. <https://doi.org/10.1155/2010/407650>
- Koch, M., Furtado, J. D., DeKosky, S. T., Fitzpatrick, A. L., Lopez, O. L., Kuller, L. H., Mukamal, K. J., & Jensen, M. K. (2020). Plasma phospholipid fatty acids, cognitive function, and risk of dementia among older adults. *Alzheimer's & Dementia*, 16(S4), e046369–e046369. <https://doi.org/10.1002/ALZ.046369>
- Koenen, M., Hill, M. A., Cohen, P., & Sowers, J. R. (2021). Obesity, Adipose Tissue and Vascular Dysfunction. *Circulation Research*, 951–968. <https://doi.org/10.1161/CIRCRESAHA.121.318093>
- Kohlmeier, M. (2015). Nutrient Metabolism: Structures, Functions, and Genes. *Nutrient Metabolism: Structures, Functions, and Genes*, 1–898.
- Kohno, D., Sone, H., Minokoshi, Y., & Yada, T. (2008). Ghrelin raises $[Ca^{2+}]_i$ via AMPK in hypothalamic arcuate nucleus NPY neurons. *Biochemical and biophysical research communications*, 366(2), 388–392.
- Kojima, M., Hosoda, H., Date, Y., Nakazato, M., Matsuo, H., & Kangawa, K. (1999). Ghrelin is a growth-hormone-releasing acylated peptide from stomach. *Nature*, 402(6762), 656–660. <https://doi.org/10.1038/45230>
- Kojima, M., & Kangawa, K. (2005). Ghrelin: Structure and function. *Physiological Reviews*, 85(2), 495–522. <https://doi.org/10.1152/PHYSREV.00012.2004>

Kolaczynski, J. W., Considine, R. V, Ohannesian, J., Marco, C., Opentanova, I., Nyce, M. R., Myint, M., & Caro, J. F. (1996). Responses of leptin to short-term fasting and refeeding in humans: a link with ketogenesis but not ketones themselves. *Diabetes*, 45(11), 1511–1515. <https://doi.org/10.2337/DIAB.45.11.1511>

Kolaczynski, J. W., Ohannesian, J. P., Considine, R. V, Marco, C. C., & Caro, J. F. (1996). Response of leptin to short-term and prolonged overfeeding in humans. *The Journal of Clinical Endocrinology and Metabolism*, 81(11), 4162–4165. <https://doi.org/10.1210/JCEM.81.11.8923877>

Koltermann, A., Hartkorn, A., Koch, E., Fürst, R., Vollmar, A. M., & Zahler, S. (2007). Ginkgo biloba extract EGb 761 increases endothelial nitric oxide production in vitro and in vivo. *Cellular and Molecular Life Sciences: CMLS*, 64(13), 1715–1722. <https://doi.org/10.1007/S00018-007-7085-Z>

Konrad, D., & Wueest, S. (2014). The gut-adipose-liver axis in the metabolic syndrome. *Physiology*, 29(5), 304–313. <https://doi.org/10.1152/PHYSIOL.00014.2014>

Kosgei, V. J., Coelho, D., Guéant-Rodriguez, R. M., & Guéant, J. L. (2020). Sirt1-PPARS Cross-Talk in Complex Metabolic Diseases and Inherited Disorders of the One Carbon Metabolism. *Cells* 2020, Vol. 9, Page 1882, 9(8), 1882. <https://doi.org/10.3390/CELLS9081882>

Koster, A., Murphy, R. A., Eiriksdottir, G., Aspelund, T., Sigurdsson, S., Lang, T. F., Gudnason, V., Launer, L. J., & Harris, T. B. (2015). Fat distribution and mortality: the AGES-Reykjavik Study. *Obesity (Silver Spring, Md.)*, 23(4), 893–897. <https://doi.org/10.1002/OBY.21028>

Koutkia, P., Canavan, B., Johnson, M. L., DePaoli, A., & Grinspoon, S. (2003). Characterization of leptin pulse dynamics and relationship to fat mass, growth hormone, cortisol, and insulin. *American Journal of Physiology. Endocrinology and Metabolism*, 285(2). <https://doi.org/10.1152/AJPENDO.00097.2003>

Kraft, E. N., Cervone, D. T., & Dyck, D. J. (2019). Ghrelin stimulates fatty acid oxidation and inhibits lipolysis in isolated muscle from male rats. *Physiological Reports*, 7(7), e14028. <https://doi.org/10.14814/PHY2.14028>

Kris-Etherton, P. M., Petersen, K., & van Horn, L. (2018). Convincing evidence supports reducing saturated fat to decrease cardiovascular disease risk. *BMJ Nutrition, Prevention & Health*, 1(1), 23–26. <https://doi.org/10.1136/BMJNPH-2018-000009>

Kudolo, G. B. (2001). The Effect of 3-Month Ingestion of Ginkgo biloba Extract (EGb 761) on Pancreatic β -Cell Function in Response to Glucose Loading in Individuals with Non-Insulin-Dependent Diabetes Mellitus. *The Journal of Clinical Pharmacology*, 41(6), 600–611.

Kudolo, G. B., Wang, W., Javors, M., & Blodgett, J. (2006). The effect of the ingestion of Ginkgo biloba extract (EGb 761) on the pharmacokinetics of metformin in non-diabetic and type 2 diabetic subjects—A double blind placebo-controlled, crossover study. *Clinical Nutrition*, 25(4), 606–616. <https://doi.org/https://doi.org/10.1016/j.clnu.2005.12.012>

Kuk, J. L., Katzmarzyk, P. T., Nichaman, M. Z., Church, T. S., Blair, S. N., & Ross, R. (2006). Visceral fat is an independent predictor of all-cause mortality in men. *Obesity (Silver Spring, Md.)*, 14(2), 336–341. <https://doi.org/10.1038/OBY.2006.43>

Kumar, A., & Singh, A. (2015). A review on Alzheimer's disease pathophysiology and its management: an update. *Pharmacological Reports*, 67(2), 195–203.

Kumar, A., Singh, C. K., LaVoie, H. A., DiPette, D. J., & Singh, U. S. (2011). Resveratrol restores Nrf2 level and prevents ethanol-induced toxic effects in the cerebellum of a rodent model of fetal alcohol spectrum disorders. *Molecular Pharmacology*, 80(3), 446–457.

Kumar, A., Sundaram, K., Mu, J., Dryden, G. W., Sriwastva, M. K., Lei, C., Zhang, L., Qiu, X., Xu, F., Yan, J., Zhang, X., Park, J. W., Merchant, M. L., Bohler, H. C. L., Wang, B., Zhang, S., Qin, C., Xu, Z., Han, X., ... Zhang, H. G. (2021). High-fat diet-induced upregulation of exosomal phosphatidylcholine contributes to insulin resistance. *Nature Communications* 2021 12:1, 12(1), 1–21. <https://doi.org/10.1038/s41467-020-20500-w>

Kunath, N., & Dresler, M. (2014). Ghrelin and memory. *Central Functions of the Ghrelin Receptor*, 167–175. https://doi.org/10.1007/978-1-4939-0823-3_10

Kuribara, H., Weintraub, S. T., Yoshihama, T., & Maruyama, Y. (2003). An Anxiolytic-Like Effect of Ginkgo biloba Extract and Its Constituent, Ginkgolide-A, in Mice. *Journal of Natural Products*, 66(10), 1333–1337. <https://doi.org/10.1021/NP030122F>

Kurin, E., Fakhrudin, N., & Nagy, M. (2013). ENOS promoter activation by red wine polyphenols: An interaction study. *Acta Facultatis Pharmaceuticae Universitatis Comeniana*, 60(1), 27–33. <https://doi.org/10.2478/AFPUC-2013-0013>

Kwok, K. H. M., Lam, K. S. L., & Xu, A. (2016). Heterogeneity of white adipose tissue: Molecular basis and clinical implications. *Experimental and Molecular Medicine*, 48(3). <https://doi.org/10.1038/EMM.2016.5>

Kyriazi, E., Tsiotra, P. C., Boutati, E., Ikonomidis, I., Fountoulaki, K., Maratou, E., Lekakis, J., Dimitriadis, G., Kremastinos, D. T., & Raptis, S. A. (2011). Effects of adiponectin in TNF- α , IL-6, and IL-10 cytokine production from coronary artery disease macrophages. *Hormone and Metabolic Research = Hormon- Und Stoffwechselforschung = Hormones et Metabolisme*, 43(8), 537–544. <https://doi.org/10.1055/S-0031-1277227>

Lackey, D. E., & Olefsky, J. M. (2016). Regulation of metabolism by the innate immune system. *Nature Reviews. Endocrinology*, 12(1), 15–20. <https://doi.org/10.1038/NREND0.2015.189>

LaFoya, B., Munroe, J. A., & Albig, A. R. (2019). A comparison of resveratrol and other polyphenolic compounds on Notch activation and endothelial cell activity. *PLoS ONE*, 14(1). <https://doi.org/10.1371/JOURNAL.PONE.0210607>

Lagouge, M., Argmann, C., Gerhart-Hines, Z., Meziane, H., Lerin, C., Daussin, F., Messadeq, N., Milne, J., Lambert, P., Elliott, P., Geny, B., Laakso, M., Puigserver, P., & Auwerx, J. (2006). Resveratrol Improves Mitochondrial Function and Protects against Metabolic Disease by

Activating SIRT1 and PGC-1 α . *Cell*, 127(6), 1109–1122. <https://doi.org/10.1016/j.cell.2006.11.013>

Laleh, P., Yaser, K., & Alireza, O. (2019). Oleoylethanolamide: A novel pharmaceutical agent in the management of obesity-an updated review. *Journal of Cellular Physiology*, 234(6), 7893–7902. <https://doi.org/10.1002/JCP.27913>

Lam, Y. Y., Ha, C. W. Y., Campbell, C. R., Mitchell, A. J., Dinudom, A., Oscarsson, J., Cook, D. I., Hunt, N. H., Caterson, I. D., Holmes, A. J., & Storlien, L. H. (2012). Increased gut permeability and microbiota change associate with mesenteric fat inflammation and metabolic dysfunction in diet-induced obese mice. *PLoS ONE*, 7(3). <https://doi.org/10.1371/JOURNAL.PONE.0034233>

Lam, Y. Y., Ha, C. W. Y., Hoffmann, J. M. A., Oscarsson, J., Dinudom, A., Mather, T. J., Cook, D. I., Hunt, N. H., Caterson, I. D., Holmes, A. J., & Storlien, L. H. (2015). Effects of dietary fat profile on gut permeability and microbiota and their relationships with metabolic changes in mice. *Obesity (Silver Spring, Md.)*, 23(7), 1429–1439. <https://doi.org/10.1002/OBY.21122>

Lands, W. E. M., Morris, A., & Libelt, B. (1990). Quantitative effects of dietary polyunsaturated fats on the composition of fatty acids in rat tissues. *Lipids*, 25(9), 505–516. <https://doi.org/10.1007/BF02537156>

Laplante, M., & Sabatini, D. M. (2012). mTOR Signaling in Growth Control and Disease. *Cell*, 149(2), 274–293. <https://doi.org/10.1016/J.CELL.2012.03.017>

Lasaitte, L., Spadiene, A., Savickiene, N., Skesters, A., & Silova, A. (2014). The effect of Ginkgo biloba and Camellia sinensis extracts on psychological state and glycemic control in patients with type 2 diabetes mellitus. *Natural Product Communications*, 9(9), 1934578X1400900931–1934578X1400900931.

Le Lay, S., & Kurzchalia, T. V. (2005). Getting rid of caveolins: Phenotypes of caveolin-deficient animals. *Biochimica et Biophysica Acta (BBA) - Molecular Cell Research*, 1746(3), 322–333. <https://doi.org/10.1016/J.BBAMCR.2005.06.001>

Ledesma, M. D., Martin, M. G., & Dotti, C. G. (2012). Lipid changes in the aged brain: effect on synaptic function and neuronal survival. *Progress in Lipid Research*, 51(1), 23–35.

Lee, A. G. (1991). Lipids and their effects on membrane proteins: evidence against a role for fluidity. *Progress in Lipid Research*, 30(4), 323–348. [https://doi.org/10.1016/0163-7827\(91\)90002-M](https://doi.org/10.1016/0163-7827(91)90002-M)

Lee, C. Y. J., Seet, R. C. S., Huang, S. H., Long, L. H., & Halliwell, B. (2009). Different patterns of oxidized lipid products in plasma and urine of dengue fever, stroke, and Parkinson's disease patients: cautions in the use of biomarkers of oxidative stress. *Antioxidants & Redox Signaling*, 11(3), 407–420. <https://doi.org/10.1089/ARS.2008.2179>

Lee, E. H., Kwon, H. S., Koh, S. H., Choi, S. H., Jin, J. H., Jeong, J. H., Jang, J. W., Park, K. W., Kim, E. J., Kim, H. J., Hong, J. Y., Yoon, S. J., Yoon, B., Kang, J. H., Lee, J. M., Park, H. H., & Ha, J.

(2022). Serum neurofilament light chain level as a predictor of cognitive stage transition. *Alzheimer's Research and Therapy*, 14(1). <https://doi.org/10.1186/s13195-021-00953-x>

Lee, J. M., Lee, H., Kang, S. B., & Park, W. J. (2016). Fatty Acid Desaturases, Polyunsaturated Fatty Acid Regulation, and Biotechnological Advances. *Nutrients*, 8(1). <https://doi.org/10.3390/NU8010023>

Lee, J., Song, K., Huh, E., Oh, M. S., & Kim, Y. S. (2018). Neuroprotection against 6-OHDA toxicity in PC12 cells and mice through the Nrf2 pathway by a sesquiterpenoid from *Tussilago farfara*. *Redox Biology*, 18, 6. <https://doi.org/10.1016/J.REDOX.2018.05.015>

Lee, M. J., Wu, Y., & Fried, S. K. (2013). Adipose tissue heterogeneity: implication of depot differences in adipose tissue for obesity complications. *Molecular Aspects of Medicine*, 34(1), 1–11. <https://doi.org/10.1016/J.MAM.2012.10.001>

Lee, M. K., & Cleveland, D. W. (1994). Neurofilament function and dysfunction: involvement in axonal growth and neuronal disease. *Current Opinion in Cell Biology*, 6(1), 34–40. [https://doi.org/10.1016/0955-0674\(94\)90113-9](https://doi.org/10.1016/0955-0674(94)90113-9)

Lee, V. M. Y. (1985). Neurofilament protein abnormalities in PC12 cells: Comparison with neurofilament proteins of normal cultured rat sympathetic neurons. *Journal of Neuroscience*, 5(11), 3039–3046. <https://doi.org/10.1523/jneurosci.05-11-03039.1985>

Lee, V. M. Y., & Page, C. (1984). The dynamics of nerve growth factor-induced neurofilament and vimentin filament expression and organization in PC12 cells. *Journal of Neuroscience*, 4(7), 1705–1714. <https://doi.org/10.1523/jneurosci.04-07-01705.1984>

Lee, V., Trojanowski, J. Q., & Schlaepfer, W. W. (1982). Induction of neurofilament triplet proteins in PC12 cells by nerve growth factor. *Brain Research*, 238(1), 169–180. [https://doi.org/10.1016/0006-8993\(82\)90779-X](https://doi.org/10.1016/0006-8993(82)90779-X)

Lee, Y., Lai, H. T. M., de Oliveira Otto, M. C., Lemaitre, R. N., McKnight, B., King, I. B., Song, X., Huggins, G. S., Vest, A. R., Siscovick, D. S., & Mozaffarian, D. (2020). Serial Biomarkers of *De novo* Lipogenesis Fatty Acids and Incident Heart Failure in Older Adults: The Cardiovascular Health Study. *Journal of the American Heart Association*, 9(4). <https://doi.org/10.1161/JAHA.119.014119>

Lee, Y. M., He, W., & Liou, Y. C. (2021). The redox language in neurodegenerative diseases: oxidative post-translational modifications by hydrogen peroxide. *Cell Death & Disease* 2021 12:1, 12(1), 1–13. <https://doi.org/10.1038/s41419-020-03355-3>

Lejri, I., Grimm, A., & Eckert, A. (2019). Ginkgo biloba extract increases neurite outgrowth and activates the Akt/mTOR pathway. *PLoS ONE*, 14(12). <https://doi.org/10.1371/JOURNAL.PONE.0225761>

Lemaitre, R. N., King, I. B., Mozaffarian, D., Kuller, L. H., Tracy, R. P., & Siscovick, D. S. (2003). n-3 polyunsaturated fatty acids, fatal ischemic heart disease, and nonfatal myocardial infarction in older adults: The Cardiovascular Health Study. *American Journal of Clinical Nutrition*, 77(2), 319–325. <https://doi.org/10.1093/ajcn/77.2.319>

- Leng, S., Winter, T., & Aukema, H. M. (2017). Dietary LA and sex effects on oxylipin profiles in rat kidney, liver, and serum differ from their effects on PUFAs. *Journal of Lipid Research*, 58(8), 1702–1712. <https://doi.org/10.1194/jlr.M078097>
- Leoni, V., & Caccia, C. (2011). Oxysterols as biomarkers in neurodegenerative diseases. *Chemistry and Physics of Lipids*, 164(6), 515–524.
- Leventis, P. A., & Grinstein, S. (2010). The distribution and function of phosphatidylserine in cellular membranes. *Annual Review of Biophysics*, 39(1), 407–427. <https://doi.org/10.1146/ANNUREV.BIOPHYS.093008.131234>
- Li, E., Chung, H., Kim, Y., Kim, D. H., Ryu, J. H., Sato, T., Kojima, M., & Park, S. (2013). Ghrelin directly stimulates adult hippocampal neurogenesis: implications for learning and memory. *Endocrine Journal*, 60(6), 781–789. <https://doi.org/10.1507/ENDOCRJ.EJ13-0008>
- Li, J., Wang, T., Liu, P., Yang, F., Wang, X., Zheng, W., & Sun, W. (2021). Hesperetin ameliorates hepatic oxidative stress and inflammation via the PI3K/AKT-Nrf2-ARE pathway in oleic acid-induced HepG2 cells and a rat model of high-fat diet-induced NAFLD. *Food & Function*, 12(9), 3898–3918. <https://doi.org/10.1039/D0FO02736G>
- Li, J., Wuliji, O., Li, W., Jiang, Z. G., & Ghanbari, H. A. (2013). Oxidative stress and neurodegenerative disorders. *International Journal of Molecular Sciences*, 14(12), 24438–24475. <https://doi.org/10.3390/ijms141224438>
- Li, M. Y., Chang, C. T., Han, Y. T., Liao, C. P., Yu, J. Y., & Wang, T. W. (2018). Ginkgolide B promotes neuronal differentiation through the Wnt/ β -catenin pathway in neural stem cells of the postnatal mammalian subventricular zone. *Scientific Reports* 2018 8:1, 8(1), 1–10. <https://doi.org/10.1038/s41598-018-32960-8>
- Li, P., & Li, Z. (2015). Neuroprotective effect of paeoniflorin on H₂O₂-induced apoptosis in PC12 cells by modulation of reactive oxygen species and the inflammatory response. *Experimental and Therapeutic Medicine*, 9(5), 1768–1772. <https://doi.org/10.3892/ETM.2015.2360/HTML>
- Li, P., Liu, S., Lu, M., Bandyopadhyay, G., Oh, D., Imamura, T., Johnson, A. M. F., Sears, D., Shen, Z., Cui, B., Kong, L., Hou, S., Liang, X., Iovino, S., Watkins, S. M., Ying, W., Osborn, O., Wollam, J., Brenner, M., & Olefsky, J. M. (2016). Hematopoietic-Derived Galectin-3 Causes Cellular and Systemic Insulin Resistance. *Cell*, 167(4), 973–984.e12. <https://doi.org/10.1016/J.CELL.2016.10.025>
- Li, P., Oh, D. Y., Bandyopadhyay, G., Lagakos, W. S., Talukdar, S., Osborn, O., Johnson, A., Chung, H., Mayoral, R., Maris, M., Ofrecio, J. M., Taguchi, S., Lu, M., & Olefsky, J. M. (2015). LTB₄ promotes insulin resistance in obese mice by acting on macrophages, hepatocytes and myocytes. *Nature Medicine*, 21(3), 239–247. <https://doi.org/10.1038/NM.3800>
- Li, S., Zhang, X., Fang, Q., Zhou, J., Zhang, M., Wang, H., Chen, Y., Xu, B., Wu, Y., Qian, L., & Xu, Y. (2017). Ginkgo biloba extract improved cognitive and neurological functions of acute ischaemic stroke: a randomised controlled trial. *Stroke and Vascular Neurology*, 2(4), 189–197. <https://doi.org/10.1136/SVN-2017-000104>

Liakh, I., Pakiet, A., Sledzinski, T., & Mika, A. (2020). Methods of the Analysis of Oxylipins in Biological Samples. *Molecules*, 25(2). <https://doi.org/10.3390/MOLECULES25020349>

Lian, C. Y., Zhai, Z. Z., Li, Z. F., & Wang, L. (2020). High fat diet-triggered non-alcoholic fatty liver disease: A review of proposed mechanisms. *Chemico-Biological Interactions*, 330. <https://doi.org/10.1016/J.CBI.2020.109199>

Liao, C. C., Ou, T. T., Huang, H. P., & Wang, C. J. (2014). The inhibition of oleic acid induced hepatic lipogenesis and the promotion of lipolysis by caffeic acid via up-regulation of AMP-activated kinase. *J Sci Food Agric*, 94(6), 1154–1162. <https://doi.org/10.1002/jsfa.6386>

LiCausi, F., & Hartman, N. W. (2018). Role of mTOR complexes in neurogenesis. *International Journal of Molecular Sciences*, 19(5), 1544.

Licinio, J., Mantzoros, C., Negrão, A. B., Cizza, G., Wong, M. L. I., Bongiorno, P. B., Chrousos, G. P., Karp, B., Allen, C., Flier, J. S., & Gold, P. W. (1997). Human leptin levels are pulsatile and inversely related to pituitary-adrenal function. *Nature Medicine*, 3(5), 575–579. <https://doi.org/10.1038/NM0597-575>

Licinio, J., Negrão, A. B., Mantzoros, C., Kaklamani, V., Wong, M.-L., Bongiorno, P. B., Negro, P. P., Mulla, A., Veldhuis, J. D., Cernal, L., Flier, J. S., & Gold, P. W. (1998). Sex differences in circulating human leptin pulse amplitude: clinical implications. *The Journal of Clinical Endocrinology and Metabolism*, 83(11), 4140–4147. <https://doi.org/10.1210/JCEM.83.11.5291>

Lin, B., Hasegawa, Y., Takane, K., Koibuchi, N., Cao, C., & Kim-Mitsuyama, S. (2016). High-fat-diet intake enhances cerebral amyloid angiopathy and cognitive impairment in a mouse model of alzheimer's disease, independently of metabolic disorders. *Journal of the American Heart Association*, 5(6). <https://doi.org/10.1161/JAHA.115.003154>

Lindenbaum, M. H., Carbonetto, S., & Mushynski, W. E. (1987). Nerve growth factor enhances the synthesis, phosphorylation, and metabolic stability of neurofilament proteins in PC12 cells. *Journal of Biological Chemistry*, 262(2), 605–610. [https://doi.org/10.1016/s0021-9258\(19\)75826-8](https://doi.org/10.1016/s0021-9258(19)75826-8)

Lindenboim, L., Diamond, R., Rothenberg, E., & Stein, R. (1995). Apoptosis Induced by Serum Deprivation of PC 12 Cells Is Not Preceded by Growth Arrest and Can Occur at Each Phase of the Cell Cycle. *Cancer Research*, 55, 1242–1247.

Liou, C. J., Lai, X. Y., Chen, Y. L., Wang, C. L., Wei, C. H., & Huang, W. C. (2015). Ginkgolide C suppresses adipogenesis in 3T3-L1 adipocytes via the AMPK signaling pathway. *Evidence-Based Complementary and Alternative Medicine*, 2015. <https://doi.org/10.1155/2015/298635>

Lipid-Maps. (2022). LIPID MAPS. <https://www.lipidmaps.org/>

Liput, K. P., Lepczyński, A., Ogłuszka, M., Nawrocka, A., Poławska, E., Grzesiak, A., Ślaska, B., Pareek, C. S., Czarnik, U., & Pierzchała, M. (2021). Effects of Dietary n–3 and n–6

Polyunsaturated Fatty Acids in Inflammation and Cancerogenesis. *International Journal of Molecular Sciences*, 22(13), 6965. <https://doi.org/10.3390/IJMS22136965>

Listenberger, L. L., Han, X., Lewis, S. E., Cases, S., Farese, R. v., Ory, D. S., & Schaffer, J. E. (2003). Triglyceride accumulation protects against fatty acid-induced lipotoxicity. *Proceedings of the National Academy of Sciences of the United States of America*, 100(6), 3077–3082. <https://doi.org/10.1073/PNAS.0630588100>

Liu, C., Wang, C., Guan, S., Liu, H., Wu, X., Zhang, Z., Gu, X., Zhang, Y., Zhao, Y., Tse, L. A., & Fang, X. (2019). The Prevalence of Metabolically Healthy and Unhealthy Obesity according to Different Criteria. *Obesity Facts*, 12(1), 78–90. <https://doi.org/10.1159/000495852>

Liu, F., Li, Z., He, X., Yu, H., & Feng, J. (2019). Ghrelin attenuates neuroinflammation and demyelination in experimental autoimmune encephalomyelitis involving NLRP3 inflammasome signaling pathway and pyroptosis. *Frontiers in Pharmacology*, 10, 1320. <https://doi.org/10.3389/FPHAR.2019.01320/BIBTEX>

Liu, H. Y., Hong, T., Wen, G. B., Han, J., Zuo, D., Liu, Z., & Cao, W. (2009). Increased basal level of Akt-dependent insulin signaling may be responsible for the development of insulin resistance. *American Journal of Physiology - Endocrinology and Metabolism*, 297(4). <https://doi.org/10.1152/AJPENDO.00374.2009>

Liu, J., García-Cardena, G., & Sessa, W. C. (1996). Palmitoylation of endothelial nitric oxide synthase is necessary for optimal stimulated release of nitric oxide: implications for caveolae localization. *Biochemistry*, 35(41), 13277–13281.

Liu, J. W., Almaguel, F. G., Bu, L., de Leon, D. D., & de Leon, M. (2008). Expression of E-FABP in PC12 cells increases neurite extension during differentiation: Involvement of n-3 and n-6 fatty acids. *Journal of Neurochemistry*, 106(5), 2015–2029. <https://doi.org/10.1111/j.1471-4159.2008.05507.x>

Liu, L., Locascio, L. M., & Doré, S. (2019). Critical role of Nrf2 in experimental ischemic stroke. *Frontiers in Pharmacology*, 10, 153.

Liu, L., Zeng, Z., Gaur, U., Fang, J., Little, P. J., & Zheng, W. (2017). Berberine Protects against Hydrogen Peroxide-Induced Oxidative Damage in PC12 Cells through Activation of ERK1/2 Pathway. *Clin Exp Pharmacol*, 7(236), 1459–2161.

Liu, M., Shen, L., Yang, Q., Nauli, A. M., Bingamon, M., Wang, D. Q. H., Ulrich-Lai, Y. M., & Tso, P. (2021). Sexual dimorphism in intestinal absorption and lymphatic transport of dietary lipids. *The Journal of Physiology*, 599(22), 5015–5030. <https://doi.org/10.1113/JP281621>

Liu, R. Z., Mita, R., Beaulieu, M., Gao, Z., & Godbout, R. (2010). Fatty acid binding proteins in brain development and disease. *International Journal of Developmental Biology*, 54(8–9), 1229–1239. <https://doi.org/10.1387/IJDB.092976RL>

Liu, T., Kong, D., Shah, B. P., Ye, C., Koda, S., Saunders, A., Ding, J. B., Yang, Z., Sabatini, B. L., & Lowell, B. B. (2012). Fasting activation of AgRP neurons requires NMDA receptors and

involves spinogenesis and increased excitatory tone. *Neuron*, 73(3), 511–522. <https://doi.org/10.1016/j.neuron.2011.11.027>

Liu, X.-P., Goldring, C. E. P., Copple, I. M., Wang, H.-Y., Wei, W., Kitteringham, N. R., & Park, B. K. (2007). Extract of Ginkgo biloba induces phase 2 genes through Keap1-Nrf2-ARE signaling pathway. *Life Sciences*, 80(17), 1586–1591.

Liu, Y., Liu, F., Iqbal, K., Grundke-Iqbal, I., & Gong, C. X. (2008). Decreased glucose transporters correlate to abnormal hyperphosphorylation of tau in Alzheimer disease. *FEBS Letters*, 582(2), 359. <https://doi.org/10.1016/j.febslet.2007.12.035>

Liu, Y., & Schubert, D. (1997). Cytotoxic amyloid peptides inhibit cellular 3-(4,5-dimethylthiazol-2-yl)-2,5-diphenyltetrazolium bromide (MTT) reduction by enhancing MTT formazan exocytosis. *Journal of Neurochemistry*, 69(6), 2285–2293. <https://doi.org/10.1046/j.1471-4159.1997.69062285.x>

Livingstone, D. E. W., & Walker, B. R. (2003). Is 11 β -hydroxysteroid dehydrogenase type 1 a therapeutic target? Effects of carbenoxolone in lean and obese Zucker rats. *The Journal of Pharmacology and Experimental Therapeutics*, 305(1), 167–172. <https://doi.org/10.1124/jpet.102.044842>

Lodhi, I. J., Wei, X., & Semenkovich, C. F. (2011). Lipoexpediency: *De novo* lipogenesis as a metabolic signal transmitter. *Trends in Endocrinology and Metabolism: TEM*, 22(1), 1–8. <https://doi.org/10.1016/j.tem.2010.09.002>

Longpré, F., Garneau, P., & Ramassamy, C. (2006). Protection by EGb 761 against β -amyloid-induced neurotoxicity: involvement of NF- κ B, SIRT1, and MAPKs pathways and inhibition of amyloid fibril formation. *Free Radical Biology and Medicine*, 41(12), 1781–1794.

Loomba, R., Quehenberger, O., Armando, A., & Dennis, E. A. (2015). Polyunsaturated fatty acid metabolites as novel lipidomic biomarkers for noninvasive diagnosis of nonalcoholic steatohepatitis. *Journal of Lipid Research*, 56(1), 185–192. <https://doi.org/10.1194/jlr.P055640>

Lopes, H. F., Corrêa-Giannella, M. L., Consolim-Colombo, F. M., & Egan, B. M. (2016). Visceral adiposity syndrome. *Diabetology and Metabolic Syndrome*, 8(1), 1–8. <https://doi.org/10.1186/s13098-016-0156-2/tables/1>

López, M., Tovar, S., Vázquez, M. J., Nogueiras, R., Señarís, R., & Diéguez, C. (2005). Sensing the fat: Fatty acid metabolism in the hypothalamus and the melanocortin system. *Peptides*, 26(10), 1753–1758. <https://doi.org/10.1016/j.peptides.2004.11.025>

López-Gómez, C., Santiago-Fernández, C., García-Serrano, S., García-Escobar, E., Gutiérrez-Repiso, C., Rodríguez-Díaz, C., Ho-Plágaro, A., Martín-Reyes, F., Garrido-Sánchez, L., Valdés, S., Rodríguez-Cañete, A., Rodríguez-Pacheco, F., & García-Fuentes, E. (2020). Oleic Acid Protects Against Insulin Resistance by Regulating the Genes Related to the PI3K Signaling Pathway. *Journal of Clinical Medicine*, 9(8), 1–14. <https://doi.org/10.3390/jcm9082615>

López-Taboada, I., González-Pardo, H., & Conejo, N. M. (2020). Western Diet: Implications for Brain Function and Behavior. *Frontiers in Psychology*, 11, 2895. <https://doi.org/10.3389/fpsyg.2020.564413>/BIBTEX

Lorent, J. H., Levental, K. R., Ganesan, L., Rivera-Longworth, G., Sezgin, E., Doktorova, M., Lyman, E., & Levental, I. (2020). Plasma membranes are asymmetric in lipid unsaturation, packing and protein shape. *Nature Chemical Biology* 2020 16:6, 16(6), 644–652. <https://doi.org/10.1038/s41589-020-0529-6>

Lu, L., Wang, S., Fu, L., Liu, D., Zhu, Y., & Xu, A. (2016). Bilobalide protection of normal human melanocytes from hydrogen peroxide-induced oxidative damage via promotion of antioxidase expression and inhibition of endoplasmic reticulum stress. *Clinical and Experimental Dermatology*, 41(1), 64–73. <https://doi.org/10.1111/CED.12664>

Lu, Y., Gwee, X., Chua, D. Q., Lee, T. S., Lim, W. S., Chong, M. S., Yap, P., Yap, K. B., Rawtaer, I., Liew, T. M., Pan, F., & Ng, T. P. (2021). Nutritional Status and Risks of Cognitive Decline and Incident Neurocognitive Disorders: Singapore Longitudinal Ageing Studies. *The Journal of Nutrition, Health & Aging*, 25(5), 660–667. <https://doi.org/10.1007/S12603-021-1603-9>

Lu, Y. hua, Su, M. yuan, Huang, H. ya, Lin-Li, & Yuan, C. gen. (2010). Protective effects of the citrus flavanones to PC12 cells against cytotoxicity induced by hydrogen peroxide. *Neuroscience Letters*, 484(1), 6–11. <https://doi.org/10.1016/J.NEULET.2010.07.078>

Luck, H., Tsai, S., Chung, J., Clemente-Casares, X., Ghazarian, M., Revelo, X. S., Lei, H., Luk, C. T., Shi, S. Y., Surendra, A., Copeland, J. K., Ahn, J., Prescott, D., Rasmussen, B. A., Chng, M. H. Y., Engleman, E. G., Girardin, S. E., Lam, T. K. T., Croitoru, K., ... Winer, D. A. (2015). Regulation of obesity-related insulin resistance with gut anti-inflammatory agents. *Cell Metabolism*, 21(4), 527–542. <https://doi.org/10.1016/J.CMET.2015.03.001>

Luo, H. H., Zhao, M. di, Feng, X. F., Gao, X. Q., Hong, M., Liu, M. L., Li, Y. P., Liu, W. Q., Liu, Y. M., Yu, C. C., Cao, Y. F., Yang, X. L., Fang, Z. Z., & Zhang, P. (2021). Decreased plasma n6 : n3 polyunsaturated fatty acids ratio interacting with high C-peptide promotes non-alcoholic fatty liver disease in type 2 diabetes patients. *Journal of Diabetes Investigation*, 12(7), 1263. <https://doi.org/10.1111/JDI.13469>

Luo, Y. (2001). Ginkgo biloba neuroprotection: Therapeutic implications in Alzheimer's disease. *Journal of Alzheimer's Disease*, 3(4), 401–407.

Luo, Y., Smith, J. V., Paramasivam, V., Burdick, A., Curry, K. J., Buford, J. P., Khan, I., Netzer, W. J., Xu, H., & Butko, P. (2002). Inhibition of amyloid- β aggregation and caspase-3 activation by the Ginkgo biloba extract EGb761. *Proceedings of the National Academy of Sciences*, 99(19), 12197–12202.

Lütjohann, D., Papassotiropoulos, A., Björkhem, I., Locatelli, S., Bagli, M., Oehring, R. D., Schlegel, U., Jessen, F., Rao, M. L., Bergmann, K. Von, & Heun, R. (2000). Plasma 24S-hydroxycholesterol (cerebrosterol) is increased in Alzheimer and vascular demented patients. *Journal of Lipid Research*, 41(2), 195–198. [https://doi.org/10.1016/s0022-2275\(20\)32052-6](https://doi.org/10.1016/s0022-2275(20)32052-6)

Lv, R., Du, L., Lu, C., Wu, J., Ding, M., Wang, C., Mao, N., & Shi, Z. (2017). Allicin protects against H₂O₂-induced apoptosis of PC12 cells via the mitochondrial pathway. *Experimental and Therapeutic Medicine*, 14(3), 2053–2059. <https://doi.org/10.3892/ETM.2017.4725>/DOWNLOAD

Ma, Q. (2013). Role of nrf2 in oxidative stress and toxicity. *Annual Review of Pharmacology and Toxicology*, 53, 401–426.

Ma, Y., Ajnakina, O., Steptoe, A., & Cadar, D. (2020a). Higher risk of dementia in English older individuals who are overweight or obese. *International Journal of Epidemiology*, 49(4), 1353–1365. <https://doi.org/10.1093/IJE/DYAA099>

Ma, Y., Nenkov, M., Chen, Y., Press, A. T., Kaemmerer, E., & Gassler, N. (2021). Fatty acid metabolism and acyl-CoA synthetases in the liver-gut axis. *World Journal of Hepatology*, 13(11), 1512. <https://doi.org/10.4254/WJH.V13.I11.1512>

MacÁšek, J., Zeman, M., Zák, A., Staňková, B., & Vecka, M. (2021). Altered Indices of Fatty Acid Elongases ELOVL6, ELOVL5, and ELOVL2 Activities in Patients with Impaired Fasting Glycemia. [https://Home.Liebertpub.Com/Met](https://home.liebertpub.com/met), 19(7), 386–392. <https://doi.org/10.1089/MET.2021.0012>

Machado, M. M. F., Banin, R. M., Thomaz, F. M., de Andrade, I. S., Boldarine, V. T., de Souza Figueiredo, J., Hirata, B. K. S., Oyama, L. M., Lago, J. H. G., Ribeiro, E. B., & Telles, M. M. (2021). Ginkgo biloba Extract (GbE) Restores Serotonin and Leptin Receptor Levels and Plays an Antioxidative Role in the Hippocampus of Ovariectomized Rats. *Molecular Neurobiology*, 58(6), 2692–2703. <https://doi.org/10.1007/S12035-021-02281-5>

Machado, M. M. F., Pereira, J. P., Hirata, B. K. S., Júlio, V. S., Banin, R. M., Andrade, H. M., Ribeiro, E. B., Cerutti, S. M., & Telles, M. M. (2021a). A Single Dose of Ginkgo biloba Extract Induces Gene Expression of Hypothalamic Anorexigenic Effectors in Male Rats. *Brain Sciences*, 11(12). <https://doi.org/10.3390/BRAINSCI11121602>

Maeda, K., Cao, H., Kono, K., Gorgun, C. Z., Furuhashi, M., Uysal, K. T., Cao, Q., Atsumi, G., Malone, H., Krishnan, B., Minokoshi, Y., Kahn, B. B., Parker, R. A., & Hotamisligil, G. S. (2005). Adipocyte/macrophage fatty acid binding proteins control integrated metabolic responses in obesity and diabetes. <https://doi.org/10.1016/j.cmet.2004.12.008>

Magnuson, A. M., Fouts, J. K., Regan, D. P., Booth, A. D., Dow, S. W., & Foster, M. T. (2018). Adipose Tissue Extrinsic Factor: Obesity-Induced Inflammation and the Role of the Visceral Lymph Node. *Physiology & Behavior*, 190, 71. <https://doi.org/10.1016/J.PHYSBEH.2018.02.044>

Maiese, K. (2015). FoxO proteins in the nervous system. *Analytical Cellular Pathology*, 2015. <https://doi.org/10.1155/2015/569392>

Maioli, M., Rinaldi, S., Migheli, R., Pigliaru, G., Rocchitta, G., Santaniello, S., Basoli, V., Castagna, A., Fontani, V., Ventura, C., & Serra, P. A. (2015). Neurological morphofunctional differentiation induced by REAC technology in PC12. A neuro protective model for Parkinson's disease OPEN. Nature Publishing Group. <https://doi.org/10.1038/srep10439>

Mäkelä, T. N. K., Tuomainen, T.-P., Hantunen, S., & Virtanen, J. K. (2022). Associations of serum n-3 and n-6 polyunsaturated fatty acids with prevalence and incidence of nonalcoholic fatty liver disease. *The American Journal of Clinical Nutrition*. <https://doi.org/10.1093/AJCN/NQAC150>

Malesza, I. J., Malesza, M., Walkowiak, J., Mussin, N., Walkowiak, D., Aringazina, R., Bartkowiak-Wieczorek, J., & Mądry, E. (2021). High-fat, western-style diet, systemic inflammation, and gut microbiota: A narrative review. *Cells*, 10(11). <https://doi.org/10.3390/cells10113164>

Malik, V. S., Chiuve, S. E., Campos, H., Rimm, E. B., Mozaffarian, D., Hu, F. B., & Sun, Q. (2015). Circulating Very-Long-Chain Saturated Fatty Acids and Incident Coronary Heart Disease in US Men and Women. *Circulation*, 132(4), 260–268. <https://doi.org/10.1161/CIRCULATIONAHA.114.014911>

Mamelak, M. (2012). Sporadic Alzheimer's disease: the starving brain. *J Alzheimers Dis*, 31(3), 459–474. <https://doi.org/10.3233/jad-2012-120370>

Mango, D., Weisz, F., & Nisticò, R. (2016). Ginkgolic Acid Protects against A β -Induced Synaptic Dysfunction in the Hippocampus. *Frontiers in Pharmacology*, 7, 401. <https://doi.org/10.3389/fphar.2016.00401>

Marambaud, P., Zhao, H., & Davies, P. (2005). Resveratrol promotes clearance of Alzheimer's disease amyloid- β peptides. *Journal of Biological Chemistry*, 280(45), 37377–37382. <https://doi.org/10.1074/JBC.M508246200>

Mårin, P., Lönn, L., Andersson, B., Odén, B., Olbe, L., Bengtsson, B. A., & Björntorp, P. (1996). Assimilation of triglycerides in subcutaneous and intraabdominal adipose tissues in vivo in men: effects of testosterone. *The Journal of Clinical Endocrinology and Metabolism*, 81(3), 1018–1022. <https://doi.org/10.1210/JCEM.81.3.8772568>

Mariño, G., & Kroemer, G. (2013). Mechanisms of apoptotic phosphatidylserine exposure. *Cell Research*, 23(11), 1247. <https://doi.org/10.1038/CR.2013.115>

Marion-Letellier, R., Savoye, G., & Ghosh, S. (2016). Fatty acids, eicosanoids and PPAR gamma. *European Journal of Pharmacology*, 785, 44–49. <https://doi.org/10.1016/j.ejphar.2015.11.004>

Marklund, M., Wu, J. H. Y., Imamura, F., Del Gobbo, L. C., Fretts, A., De Goede, J., Shi, P., Tintle, N., Wennberg, M., Aslibekyan, S., Chen, T. A., De Oliveira Otto, M. C., Hirakawa, Y., Eriksen, H. H., Kröger, J., Laguzzi, F., Lankinen, M., Murphy, R. A., Prem, K., ... Risérus, U. (2019). Biomarkers of Dietary Omega-6 Fatty Acids and Incident Cardiovascular Disease and Mortality: An Individual-Level Pooled Analysis of 30 Cohort Studies. *Circulation*, 139(21), 2422–2436. <https://doi.org/10.1161/CIRCULATIONAHA.118.038908>

Markus, A., Zhong, J., & Snider, W. D. (2002). RAF and AKT mediate distinct aspects of sensory axon growth. *Neuron*, 35(1), 65–76. [https://doi.org/10.1016/S0896-6273\(02\)00752-3](https://doi.org/10.1016/S0896-6273(02)00752-3)

- Marszalek, J. R., Kitidis, C., Dararutana, A., & Lodish, H. F. (2004). Acyl-CoA synthetase 2 overexpression enhances fatty acid internalization and neurite outgrowth. *Journal of Biological Chemistry*, 279(23), 23882–23891. <https://doi.org/10.1074/jbc.M313460200>
- Martin, C. R. (2015). Lipids and Fatty Acids in the Preterm Infant, Part 1: Basic Mechanisms of Delivery, Hydrolysis, and Bioavailability. *NeoReviews*, 16(3), e160–e168. <https://doi.org/10.1542/NEO.16-3-E160>
- Martin, G., Schoonjans, K., Lefebvre, A. M., Staels, B., & Auwerx, J. (1997). Coordinate Regulation of the Expression of the Fatty Acid Transport Protein and Acyl-CoA Synthetase Genes by PPAR α and PPAR γ Activators *. *Journal of Biological Chemistry*, 272(45), 28210–28217. <https://doi.org/10.1074/JBC.272.45.28210>
- Martin, L. F., Klim, C. M., Vannucci, S. J., Dixon, L. B., Landis, J. R., & LaNoue, K. F. (1990). Alterations in adipocyte adenylate cyclase activity in morbidly obese and formerly morbidly obese humans. *Surgery*, 108(2), 228–234; discussion 234. <https://europepmc.org/article/med/2166354>
- Martin, T. F., & Grishanin, R. N. (2003). PC12 cells as a model for studies of regulated secretion in neuronal and endocrine cells. *Methods Cell Biol*, 71(34), 267–286.
- Martinez-Lopez, N., & Singh, R. (2015). Autophagy and Lipid Droplets in the Liver. *Annual Review of Nutrition*, 35(1), 215–237. <https://doi.org/10.1146/annurev-nutr-071813-105336>
- Massaad, C. A. (2011). Neuronal and vascular oxidative stress in Alzheimer's disease. *Current Neuropharmacology*, 9(4), 662–673.
- Massey, J. B., Bick, D. H., & Pownall, H. J. (1997). Spontaneous transfer of monoacyl amphiphiles between lipid and protein surfaces. *Biophysical Journal*, 72(4), 1732–1743. [https://doi.org/10.1016/S0006-3495\(97\)78819-2](https://doi.org/10.1016/S0006-3495(97)78819-2)
- Masson, G. S., Nair, A. R., Dange, R. B., Silva-Soares, P. P., Michelini, L. C., & Francis, J. (2015). Toll-like receptor 4 promotes autonomic dysfunction, inflammation and microglia activation in the hypothalamic paraventricular nucleus: role of endoplasmic reticulum stress. *PloS One*, 10(3). <https://doi.org/10.1371/JOURNAL.PONE.0122850>
- Matsuzaka, T., Shimano, H., Yahagi, N., Kato, T., Atsumi, A., Yamamoto, T., Inoue, N., Ishikawa, M., Okada, S., Ishigaki, N., Iwasaki, H., Iwasaki, Y., Karasawa, T., Kumadaki, S., Matsui, T., Sekiya, M., Ohashi, K., Hastay, A. H., Nakagawa, Y., ... Yamada, N. (2007). Crucial role of a long-chain fatty acid elongase, Elovl6, in obesity-induced insulin resistance. *Nature Medicine*, 13(10), 1193–1202. <https://doi.org/10.1038/NM1662>
- Matsuzaki, T., Sasaki, K., Tanizaki, Y., Hata, J., Fujimi, K., Matsui, Y., Sekita, A., Suzuki, S. O., Kanba, S., & Kiyohara, Y. (2010). Insulin resistance is associated with the pathology of Alzheimer disease: the Hisayama study. *Neurology*, 75(9), 764–770.
- Mattace Raso, G., Simeoli, R., Russo, R., Iacono, A., Santoro, A., Paciello, O., Ferrante, M. C., Canani, R. B., Calignano, A., & Meli, R. (2013). Effects of sodium butyrate and its synthetic

amide derivative on liver inflammation and glucose tolerance in an animal model of steatosis induced by high fat diet. *PLoS One*, 8(7). <https://doi.org/10.1371/journal.pone.0068626>

Matyash, V., Liebisch, G., Kurzchalia, T. V, Shevchenko, A., & Schwudke, D. (2008). Lipid extraction by methyl-tert-butyl ether for high-throughput lipidomics. *Journal of Lipid Research*, 49(5), 1137–1146.

Mayeux, R., & Stern, Y. (2012). Epidemiology of Alzheimer Disease. *Cold Spring Harbor Perspectives in Medicine*, 2(8). <https://doi.org/10.1101/CSHPERSPECT.A006239>

Mazza, M., Capuano, A., Bria, P., & Mazza, S. (2006). Ginkgo biloba and donepezil: a comparison in the treatment of Alzheimer's dementia in a randomized placebo-controlled double-blind study. *European Journal of Neurology*, 13(9), 981–985. <https://doi.org/10.1111/j.1468-1331.2006.01409.x>

Mazzanti, G., & Di Giacomo, S. (2016). Curcumin and resveratrol in the management of cognitive disorders: What is the clinical evidence? *Molecules*, 21(9), 1–27. <https://doi.org/10.3390/molecules21091243>

McCabe, M. P., Cullen, E. R., Barrows, C. M., Shore, A. N., Tooke, K. I., Laprade, K. A., Stafford, J. M., & Weston, M. C. (2020). Genetic inactivation of mTORC1 or mTORC2 in neurons reveals distinct functions in glutamatergic synaptic transmission. *ELife*, 9. <https://doi.org/10.7554/ELIFE.51440>

McGirr, S., Venegas, C., & Swaminathan, A. (2020). Alzheimers Disease: A Brief Review. *Journal of Experimental Neurology*, 1(3).

McLean, F. H., Campbell, F. M., Langston, R. F., Sergi, D., Resch, C., Grant, C., Morris, A. C., Mayer, C. D., & Williams, L. M. (2019). A high-fat diet induces rapid changes in the mouse hypothalamic proteome. *Nutrition and Metabolism*, 16(1), 1–16. <https://doi.org/10.1186/S12986-019-0352-9/FIGURES/3>

McLean, F. H., Grant, C., Morris, A. C., Horgan, G. W., Polanski, A. J., Allan, K., Campbell, F. M., Langston, R. F., & Williams, L. M. (2018). Rapid and reversible impairment of episodic memory by a high-fat diet in mice. *Scientific Reports*, 8(1), 11976. <https://doi.org/10.1038/s41598-018-30265-4>

Medina, S., Gil-Izquierdo, Á., Durand, T., Ferreres, F., & Domínguez-Perles, R. (2018). Structural/Functional Matches and Divergences of Phytoprostanes and Phytofurans with Bioactive Human Oxylipins. *Antioxidants (Basel, Switzerland)*, 7(11). <https://doi.org/10.3390/ANTIOX7110165>

Mei, C., Han, X., Zhang, J., Gao, L., Liu, H., Mei, C., Han, X., Zhang, J., Gao, L., & Liu, H. (2013). Neuroprotective Effects of Ginkgo Biloba Extract (GbE) on Oxygen-Glucose Deprivation (OGD) in PC12 Cells. *Engineering*, 5(10), 142–145. <https://doi.org/10.4236/ENG.2013.510B030>

Melissa Gabbs, Leng, S., Devassy, J. G., Monirujjaman, M., & Aukema, H. M. (2015). Advances in Our Understanding of Oxylipins Derived from Dietary PUFAs. *Advances in Nutrition*, 6(5), 513–540. <https://doi.org/10.3945/AN.114.007732>

Mells, J. E., Fu, P. P., Kumar, P., Smith, T., Karpen, S. J., & Anania, F. A. (2015). Saturated fat and cholesterol are critical to inducing murine metabolic syndrome with robust nonalcoholic steatohepatitis. *J Nutr Biochem*, 26(3), 285–292. <https://doi.org/10.1016/j.jnutbio.2014.11.002>

Mendez, M. F. (2017). Early-Onset Alzheimer Disease. *Neurologic Clinics*, 35(2), 263–281. <https://doi.org/10.1016/j.ncl.2017.01.005>

Menotti, A., & Puddu, P. E. (2015). How the Seven Countries Study contributed to the definition and development of the Mediterranean diet concept: A 50-year journey. *Nutrition, Metabolism and Cardiovascular Diseases*, 25(3), 245–252. <https://doi.org/10.1016/j.NUMECD.2014.12.001>

Merck. (2020a). PC-12 Cell Line from rat. https://www.sigmaaldrich.com/catalog/product/sigma/cb_88022401?lang=en®ion=GB

Merck. (2020b). Protocol - Collagen Coating. <https://www.sigmaaldrich.com/technical-documents/articles/biofiles/collagen-product-protocols.html>

Mesquita, T. R. R., de Jesus, I. C. G., dos Santos, J. F., de Almeida, G. K. M., de Vasconcelos, C. M. L., Guatimosim, S., Macedo, F. N., dos Santos, R. v., de Menezes-Filho, J. E. R., Miguel-dos-Santos, R., Matos, P. T. D., Scalzo, S., Santana-Filho, V. J., Albuquerque-Júnior, R. L. C., Pereira-Filho, R. N., & Lauton-Santos, S. (2017). Cardioprotective action of Ginkgo biloba extract against sustained β -adrenergic stimulation occurs via activation of M2/NO pathway. *Frontiers in Pharmacology*, 8(MAY). <https://doi.org/10.3389/FPHAR.2017.00220/PDF>

Michel, J. B., Feron, O., Sacks, D., & Michel, T. (1997). Reciprocal regulation of endothelial nitric-oxide synthase by Ca²⁺-calmodulin and caveolin. *The Journal of Biological Chemistry*, 272(25), 15583–15586. <https://doi.org/10.1074/JBC.272.25.15583>

Michel, T., & Feron, O. (1997). Nitric oxide synthases: which, where, how, and why? *The Journal of Clinical Investigation*, 100(9), 2146–2152.

Milanski, M., Arruda, A. P., Coope, A., Ignacio-Souza, L. M., Nunez, C. E., Roman, E. A., Romanatto, T., Pascoal, L. B., Caricilli, A. M., Torsoni, M. A., Prada, P. O., Saad, M. J., & Velloso, L. A. (2012). Inhibition of hypothalamic inflammation reverses diet-induced insulin resistance in the liver. *Diabetes*, 61(6), 1455–1462. <https://doi.org/10.2337/DB11-0390>

Milanski, M., Degasperi, G., Coope, A., Morari, J., Denis, R., Cintra, D. E., Tsukumo, D. M. L., Anhe, G., Amaral, M. E., Takahashi, H. K., Curi, R., Oliveira, H. C., Carvalheira, J. B. C., Bordin, S., Saad, M. J., & Velloso, L. A. (2009). Saturated Fatty Acids Produce an Inflammatory Response Predominantly through the Activation of TLR4 Signaling in Hypothalamus: Implications for the Pathogenesis of Obesity. *Journal of Neuroscience*, 29(2), 359–370. <https://doi.org/10.1523/JNEUROSCI.2760-08.2009>

Miller, A. A., & Spencer, S. J. (2014). Obesity and neuroinflammation: A pathway to cognitive impairment. *Brain, Behavior, and Immunity*, 42, 10–21. <https://doi.org/10.1016/j.BBI.2014.04.001>

Miller, K. E., & Suter, D. M. (2018). An integrated cytoskeletal model of neurite outgrowth. *Frontiers in Cellular Neuroscience*, 12, 447. <https://doi.org/10.3389/FNCEL.2018.00447/BIBTEX>

Milne, G. L. (2017). Classifying oxidative stress by F 2-Isoprostane levels in human disease: The re-imagining of a biomarker. *Redox Biology*, 12, 897–898. <https://doi.org/10.1016/J.REDOX.2017.04.028>

Min, S.-W., Sohn, P. D., Cho, S.-H., Swanson, R. A., & Gan, L. (2013). Sirtuins in neurodegenerative diseases: an update on potential mechanisms. *Frontiers in Aging Neuroscience*, 5, 53.

Mínguez-Olaondo, A., Irimia, P., & Frühbeck, G. (2017). Obesity and the nervous system: more questions. *The Lancet Neurology*, 16(10), 773. [https://doi.org/10.1016/S1474-4422\(17\)30292-2](https://doi.org/10.1016/S1474-4422(17)30292-2)

Minjarez, B., Calderón-González, K. G., Rustarazo, M. L. V., Herrera-Aguirre, M. E., Labra-Barrios, M. L., Rincon-Limas, D. E., del Pino, M. M. S., Mena, R., & Luna-Arias, J. P. (2016). Identification of proteins that are differentially expressed in brains with Alzheimer's disease using iTRAQ labeling and tandem mass spectrometry. *J Proteome*, 139, 103–121. <https://doi.org/10.1016/j.jprot.2016.03.022>

Minville-Walz, M., Gresti, J., Pichon, L., Bellenger, S., Bellenger, J., Narce, M., & Riolland, M. (2012). Distinct regulation of stearoyl-CoA desaturase 1 gene expression by cis and trans C18:1 fatty acid in human aortic smooth muscle cells. *Genes & Nutrition*, 7(2), 209–216. <https://doi.org/10.1007/S12263-011-0258-2>

Mishra, A., Chaudhary, A., & Sethi, S. (2004). Oxidized omega-3 fatty acids inhibit NF-kappaB activation via a PPARalpha-dependent pathway. *Arteriosclerosis, Thrombosis, and Vascular Biology*, 24(9), 1621–1627. <https://doi.org/10.1161/01.ATV.0000137191.02577.86>

Mitra, S., Behbahani, H., & Eriksson, M. (2019). Innovative therapy for Alzheimer's disease with focus on biodelivery of NGF. *Frontiers in Neuroscience*, 13(FEB), 38. <https://doi.org/10.3389/FNINS.2019.00038/BIBTEX>

Mittal, B. (2019a). Subcutaneous adipose tissue & visceral adipose tissue. In *Indian Journal of Medical Research* (Vol. 149, Issue 5, pp. 571–573). Wolters Kluwer Medknow Publications. https://doi.org/10.4103/ijmr.IJMR_1910_18

Mittendorfer, B. (2011). Origins of metabolic complications in obesity: Adipose tissue and free fatty acid trafficking. In *Current Opinion in Clinical Nutrition and Metabolic Care* (Vol. 14, Issue 6, pp. 535–541). <https://doi.org/10.1097/MCO.0b013e32834ad8b6>

Mlinar, B., Marc, J., Jensterle, M., Bokal, E. V., Jerin, A., & Pfeifer, M. (2011). Expression of 11 β -hydroxysteroid dehydrogenase type 1 in visceral and subcutaneous adipose tissues of patients with polycystic ovary syndrome is associated with adiposity. *The Journal of Steroid Biochemistry and Molecular Biology*, 123(3–5), 127–132. <https://doi.org/10.1016/J.JSBMB.2010.12.002>

- Moloney, A. M., Griffin, R. J., Timmons, S., O'Connor, R., Ravid, R., & O'Neill, C. (2010). Defects in IGF-1 receptor, insulin receptor and IRS-1/2 in Alzheimer's disease indicate possible resistance to IGF-1 and insulin signalling. *Neurobiology of Aging*, 31(2), 224–243. <https://doi.org/10.1016/j.neurobiolaging.2008.04.002>
- Moreno-Fernández, S., Garcés-Rimón, M., Vera, G., Astier, J., Landrier, J. F., & Miguel, M. (2018). High fat/high glucose diet induces metabolic syndrome in an experimental rat model. *Nutrients*, 10(10), 1502.
- Monteiro, J., Leslie, M., Moghadasian, M. H., Arendt, B. M., Allard, J. P., & Ma, D. W. L. (2014). The role of n - 6 and n - 3 polyunsaturated fatty acids in the manifestation of the metabolic syndrome in cardiovascular disease and non-alcoholic fatty liver disease. *Food Funct*, 5(3), 426–435. <https://doi.org/10.1039/c3fo60551e>
- Mooradian, A. D., Chung, H. C., & Shah, G. N. (1997). GLUT-1 expression in the cerebra of patients with Alzheimer's disease. *Neurobiology of Aging*, 18(5), 469–474.
- Morrison, C. D. (2009). Leptin signaling in brain: A link between nutrition and cognition? *Biochimica et Biophysica Acta (BBA) - Molecular Basis of Disease*, 1792(5), 401–408. <https://doi.org/10.1016/j.bbadis.2008.12.004>
- Morton, G. J., Cummings, D. E., Baskin, D. G., Barsh, G. S., & Schwartz, M. W. (2006). Central nervous system control of food intake and body weight. *Nature*, 443(7109), 289–295. <https://doi.org/10.1038/NATURE05026>
- Moscoso, A., Grothe, M. J., Ashton, N. J., Karikari, T. K., Lantero Rodríguez, J., Snellman, A., Suárez-Calvet, M., Blennow, K., Zetterberg, H., & Schöll, M. (2021). Longitudinal Associations of Blood Phosphorylated Tau181 and Neurofilament Light Chain with Neurodegeneration in Alzheimer Disease. *JAMA Neurology*, 78(4), 396–406. <https://doi.org/10.1001/jamaneurol.2020.4986>
- Motojima, K., Passilly, P., Peters, J. M., Gonzalez, F. J., & Latruffe, N. (1998). Expression of putative fatty acid transporter genes are regulated by peroxisome proliferator-activated receptor alpha and gamma activators in a tissue- and inducer-specific manner. *The Journal of Biological Chemistry*, 273(27), 16710–16714. <https://doi.org/10.1074/JBC.273.27.16710>
- Moult, P. R., & Harvey, J. (2011). NMDA receptor subunit composition determines the polarity of leptin-induced synaptic plasticity. *Neuropharmacology*, 61(5–6), 924–936. <https://doi.org/10.1016/j.neuropharm.2011.06.021>
- Mozaffarian, D., Lemaitre, R. N., King, I. B., Song, X., Huang, H., Sacks, F. M., Rimm, E. B., Wang, M., & Siscovick, D. S. (2013). Plasma phospholipid long-chain ω -3 fatty acids and total and cause-specific mortality in older adults, a cohort study. *Annals of Internal Medicine*, 158(7), 515–525. <https://doi.org/10.7326/0003-4819-158-7-201304020-00003>
- Msika, O., Brand, A., Crawford, M. A., & Yavin, E. (2012). NGF blocks polyunsaturated fatty acids biosynthesis in n-3 fatty acid-supplemented PC12 cells. *Biochimica et Biophysica Acta*, 1821(7), 1022–1030. <https://doi.org/10.1016/j.bbailip.2012.04.007>

- Muccioli, G., Pons, N., Ghè, C., Catapano, F., Granata, R., & Ghigo, E. (2004). Ghrelin and des-acyl ghrelin both inhibit isoproterenol-induced lipolysis in rat adipocytes via a non-type 1a growth hormone secretagogue receptor. *European Journal of Pharmacology*, 498(1–3), 27–35. <https://doi.org/10.1016/J.EJPHAR.2004.07.066>
- Mueller, M., & Jungbauer, A. (2009). Culinary plants, herbs and spices – A rich source of PPAR γ ligands. *Food Chemistry*, 117(4), 660–667. <https://doi.org/10.1016/J.FOODCHEM.2009.04.063>
- Mullenbrock, S., Shah, J., & Cooper, G. M. (2011). Global Expression Analysis Identified a Preferentially Nerve Growth Factor-induced Transcriptional Program Regulated by Sustained Mitogen-activated Protein Kinase/Extracellular Signal-regulated Kinase (ERK) and AP-1 Protein Activation during PC12 Cell Differentiation. *Journal of Biological Chemistry*, 286(52), 45131–45145. <https://doi.org/10.1074/JBC.M111.274076>
- Munday, M. R. (2002). Regulation of mammalian acetyl-CoA carboxylase. *Biochemical Society Transactions*, 30(6), 1059–1064. <https://doi.org/10.1042/BST0301059>
- Münzberg, H., Flier, J. S., & Bjørnbæk, C. (2004). Region-specific leptin resistance within the hypothalamus of diet-induced obese mice. *Endocrinology*, 145(11), 4880–4889. <https://doi.org/10.1210/EN.2004-0726>
- Murugesan, S., Ulloa-Martínez, M., Martínez-Rojano, H., Galván-Rodríguez, F. M., Miranda-Brito, C., Romano, M. C., Piña-Escobedo, A., Pizano-Zárate, M. L., Hoyo-Vadillo, C., & García-Mena, J. (2015). Study of the diversity and short-chain fatty acids production by the bacterial community in overweight and obese Mexican children. *European Journal of Clinical Microbiology and Infectious Diseases*, 34(7), 1337–1346. <https://doi.org/10.1007/S10096-015-2355-4>
- Nagpal, R., Newman, T. M., Wang, S., Jain, S., Lovato, J. F., & Yadav, H. (2018). Obesity-Linked Gut Microbiome Dysbiosis Associated with Derangements in Gut Permeability and Intestinal Cellular Homeostasis Independent of Diet. *Journal of Diabetes Research*, 2018. <https://doi.org/10.1155/2018/3462092>
- Nagy, K., & Tiuca, I.-D. (2017). Importance of Fatty Acids in Physiopathology of Human Body. *Fatty Acids*. <https://doi.org/10.5772/67407>
- Nakamura, Y., Kotite, L., Gan, Y., Spencer, T. A., Fielding, C. J., & Fielding, P. E. (2004). Molecular Mechanism of Reverse Cholesterol Transport: Reaction of Pre- β -Migrating High-Density Lipoprotein with Plasma Lecithin/Cholesterol Acyltransferase \dagger . *Biochemistry*, 43(46), 14811–14820. <https://doi.org/10.1021/BI0485629>
- Nauli, A. M., & Matin, S. (2019). Why Do Men Accumulate Abdominal Visceral Fat? *Frontiers in Physiology*, 10, 1486. <https://doi.org/10.3389/FPHYS.2019.01486/BIBTEX>
- Nazarians-Armavil, A., Menchella, J. A., & Belsham, D. D. (2013). Cellular insulin resistance disrupts leptin-mediated control of neuronal signaling and transcription. *Molecular Endocrinology*, 27(6), 990–1003. <https://doi.org/10.1210/ME.2012-1338>

Nemes, K., Åberg, F., Gylling, H., & Isoniemi, H. (2016). Cholesterol metabolism in cholestatic liver disease and liver transplantation: From molecular mechanisms to clinical implications. *World Journal of Hepatology*, 8(22), 924. <https://doi.org/10.4254/WJH.V8.I22.924>

Neth, B. J., Graff-Radford, J., Mielke, M. M., Przybelski, S. A., Lesnick, T. G., Schwarz, C. G., Reid, R. I., Senjem, M. L., Lowe, V. J., Machulda, M. M., Petersen, R. C., Jr, C. R. J., Knopman, D. S., & Vemuri, P. (2020). Relationship Between Risk Factors and Brain Reserve in Late Middle Age: Implications for Cognitive Aging. *Frontiers in Aging Neuroscience*, 11, 355. <https://doi.org/10.3389/FNAGI.2019.00355/BIBTEX>

Netto, J. D., Wong, S., & Ritchie, M. (2013). High Resolution Separation of Phospholipids Using a Novel Orthogonal Two-Dimensional UPLC / QToF MS System Configuration. *Untargeted Metabolomics And Lipidomics*, 1–8.

Neuman, M. G., Cohen, L. B., & Nanau, R. M. (2014). Biomarkers in nonalcoholic fatty liver disease. *Canadian Journal of Gastroenterology and Hepatology*, 28(11), 607–618. <https://doi.org/10.1155/2014/757929>

Ng, F., Wijaya, L., & Tang, B. L. (2015). SIRT1 in the brain—connections with aging-associated disorders and lifespan. *Frontiers in Cellular Neuroscience*, 9(March), 64. <https://doi.org/10.3389/fncel.2015.00064>

Ng, S. C., Shi, H. Y., Hamidi, N., Underwood, F. E., Tang, W., Benchimol, E. I., Panaccione, R., Ghosh, S., Wu, J. C. Y., Chan, F. K. L., Sung, J. J. Y., & Kaplan, G. G. (2017). Worldwide incidence and prevalence of inflammatory bowel disease in the 21st century: a systematic review of population-based studies. *Lancet (London, England)*, 390(10114), 2769–2778. [https://doi.org/10.1016/S0140-6736\(17\)32448-0](https://doi.org/10.1016/S0140-6736(17)32448-0)

Ngoc, L. P., Yen Man, H., Besselink, H., Cam, H. D. T., Brouwer, A., & van der Burg, B. (2019). Identification of PPAR-activating compounds in herbal and edible plants and fungi from Vietnam. *Industrial Crops and Products*, 129, 195–200. <https://doi.org/10.1016/J.INDCROP.2018.12.003>

Nguyen, J. C. D., Killcross, A. S., & Jenkins, T. A. (2014). Obesity and cognitive decline: role of inflammation and vascular changes. *Frontiers in Neuroscience*, 8(OCT). <https://doi.org/10.3389/FNINS.2014.00375>

Nguyen, P., Leray, V., Diez, M., Serisier, S., le Bloc'H, J., Siliart, B., & Dumon, H. (2008). Liver lipid metabolism. *Journal of Animal Physiology and Animal Nutrition*, 92(3), 272–283. <https://doi.org/10.1111/J.1439-0396.2007.00752.X>

Ni, Y., Zhao, L., Yu, H., Ma, X., Bao, Y., Rajani, C., Loo, L. W. M., Shvetsov, Y. B., Yu, H., Chen, T., Zhang, Y., Wang, C., Hu, C., Su, M., Xie, G., Zhao, A., Jia, W., & Jia, W. (2015). Circulating Unsaturated Fatty Acids Delineate the Metabolic Status of Obese Individuals. *EBioMedicine*, 2(10), 1513–1522. <https://doi.org/10.1016/J.EBIOM.2015.09.004>

Nielsen, T. S., Jessen, N., Jørgensen, J. O. L., Møller, N., & Lund, S. (2014). Dissecting adipose tissue lipolysis: molecular regulation and implications for metabolic disease. *Journal of Molecular Endocrinology*, 52(3), R199–R222. <https://doi.org/10.1530/JME-13-0277>

Nilsson, L., & Busto, R. (1976). Brain energy metabolism during the process of dying and after cardiopulmonary resuscitation. *Acta Anaesthesiologica Scandinavica*, 20(1), 57–64.

Node, K., Huo, Y., Ruan, X., Yang, B., Spiecker, M., Ley, K., Zeldin, D. C., & Liao, J. K. (1999). Anti-inflammatory Properties of Cytochrome P450 Epoxygenase-Derived Eicosanoids. *Science (New York, N.Y.)*, 285(5431), 1276. <https://doi.org/10.1126/science.285.5431.1276>

Noeman, S. A., Hamooda, H. E., & Baalash, A. A. (2011). Biochemical study of oxidative stress markers in the liver, kidney and heart of high fat diet induced obesity in rats. *Diabetology and Metabolic Syndrome*, 3(1). <https://doi.org/10.1186/1758-5996-3-17>

Riggs, N.R., Spruijt-Metz, D., Chou, C.P. and Pentz, M.A. (2012). Relationships between executive cognitive function and lifetime substance use and obesity-related behaviors in fourth grade youth. *Child Neuropsychol*, 18, 1–11.

Obradovic, M., Sudar-Milovanovic, E., Soskic, S., Essack, M., Arya, S., Stewart, A. J., Gojobori, T., & Isenovic, E. R. (2021). Leptin and Obesity: Role and Clinical Implication. *Frontiers in Endocrinology*, 12, 563. <https://doi.org/10.3389/FENDO.2021.585887/BIBTEX>

Obrenovich, M., Siddiqui, B., McCloskey, B., & Reddy, V. P. (2020). The Microbiota–Gut–Brain Axis Heart Shunt Part I: The French Paradox, Heart Disease and the Microbiota. *Microorganisms* 2020, Vol. 8, Page 490, 8(4), 490. <https://doi.org/10.3390/MICROORGANISMS8040490>

Obrenovich, M., Tabrez, S., Siddiqui, B., McCloskey, B., & Perry, G. (2020). The Microbiota–Gut–Brain Axis–Heart Shunt Part II: Prosaic Foods and the Brain–Heart Connection in Alzheimer Disease. *Microorganisms* 2020, Vol. 8, Page 493, 8(4), 493. <https://doi.org/10.3390/MICROORGANISMS8040493>

O’Brien, P. D., Hinder, L. M., Callaghan, B. C., & Feldman, E. L. (2017). Neurological consequences of obesity. *The Lancet. Neurology*, 16(6), 465–477. [https://doi.org/10.1016/S1474-4422\(17\)30084-4](https://doi.org/10.1016/S1474-4422(17)30084-4)

O’Donnell, V. B., & Murphy, R. C. (2012). New families of bioactive oxidized phospholipids generated by immune cells: identification and signaling actions. *Blood*, 120(10), 1985. <https://doi.org/10.1182/BLOOD-2012-04-402826>

O’Donnell, V. B., & Murphy, R. C. (2017). Directing eicosanoid esterification into phospholipids. *Journal of Lipid Research*, 58(5), 837. <https://doi.org/10.1194/JLR.C075986>

O’Flanagan, C. H., Morais, V. A., Wurst, W., de Strooper, B., & O’Neill, C. (2014). The Parkinson’s gene PINK1 regulates cell cycle progression and promotes cancer-associated phenotypes. *Oncogene* 2015 34:11, 34(11), 1363–1374. <https://doi.org/10.1038/onc.2014.81>

Ogunbona, O. B., & Claypool, S. M. (2019). Emerging Roles in the Biogenesis of Cytochrome c Oxidase for Members of the Mitochondrial Carrier Family. *Frontiers in Cell and Developmental Biology*, 7, 3. <https://doi.org/10.3389/FCELL.2019.00003>

Ohira, M., Watanabe, Y., Yamaguchi, T., Onda, H., Yamaoka, S., Abe, K., Nakamura, S., Tanaka, S., Kawagoe, N., Nabekura, T., Oshiro, T., Nagayama, D., Tatsuno, I., & Saiki, A. (2021). Decreased Triglyceride and Increased Serum Lipoprotein Lipase Levels Are Correlated to Increased High-Density Lipoprotein-Cholesterol Levels after Laparoscopic Sleeve Gastrectomy. *Obesity Facts*, 14(6), 633–640. <https://doi.org/10.1159/000519410>

Ohuchi, T., Maruoka, S., Sakudo, A., & Arai, T. (2002). Assay-based quantitative analysis of PC12 cell differentiation. *Journal of Neuroscience Methods*, 118(1), 1–8. [https://doi.org/10.1016/S0165-0270\(02\)00116-4](https://doi.org/10.1016/S0165-0270(02)00116-4)

Okereke, O. I., Kang, J. H., Cook, N. R., Gaziano, J. M., Manson, J. E., Buring, J. E., & Grodstein, F. (2008). Type 2 diabetes mellitus and cognitive decline in two large cohorts of community-dwelling older adults. *Journal of the American Geriatrics Society*, 56(6), 1028–1036.

Omar, B., Banke, E., Ekelund, M., Frederiksen, S., & Degerman, E. (2011). Alterations in cyclic nucleotide phosphodiesterase activities in omental and subcutaneous adipose tissues in human obesity. *Nutrition & Diabetes*, 1(8), e13. <https://doi.org/10.1038/NUTD.2011.9>

Oni-Orisan, A., Edin, M. L., Lee, J. A., Wells, M. A., Christensen, E. S., Vendrov, K. C., Lih, F. B., Tomer, K. B., Bai, X., Taylor, J. M., Stouffer, G. A., Zeldin, D. C., & Lee, C. R. (2016). Cytochrome P450-derived epoxyeicosatrienoic acids and coronary artery disease in humans: A targeted metabolomics study. *Journal of Lipid Research*, 57(1), 109–119. <https://doi.org/10.1194/JLR.M061697/ATTACHMENT/EA40C0F6-7285-4145-B82F-1ADEC861EC8E/MMC1.PDF>

Ono, K., Condron, M. M., Ho, L., Wang, J., Zhao, W., Pasinetti, G. M., & Teplow, D. B. (2008). Effects of grape seed-derived polyphenols on amyloid β -protein self-assembly and cytotoxicity. *Journal of Biological Chemistry*, 283(47), 32176–32187.

Orlowska, A., Perera, P. T., Al Kobaisi, M. A., Dias, A., Nguyen, H. K. D., Ghanaati, S., Baulin, V., Crawford, R. J., & Ivanova, E. P. (2017). The effect of coatings and nerve growth factor on attachment and differentiation of pheochromocytoma cells. *Materials (Basel, Switzerland)*, 11(1), 60. <https://doi.org/10.3390/MA11010060>

Orly, J., & Schramm, M. (1975). Fatty acids as modulators of membrane functions: Catecholamine-activated adenylate cyclase of the turkey erythrocyte (fi-adrenergic receptor/membrane fluidity/transition temperature/GTP site/guanylyl imidodiphosphate). *Journal of Biological Chemistry*, 250(9), 3437–3483.

Overby, H. B., & Ferguson, J. F. (2021). Gut Microbiota-Derived Short-Chain Fatty Acids Facilitate Microbiota:Host Cross talk and Modulate Obesity and Hypertension. *Current Hypertension Reports*, 23(2). <https://doi.org/10.1007/S11906-020-01125-2>

Pachikian, B. D., Neyrinck, A. M., Cani, P. D., Portois, L., Deldicque, L., de Backer, F. C., Bindels, L. B., Sohet, F. M., Malaisse, W. J., Francaux, M., Carpentier, Y. A., & Delzenne, N. M. (2008). Hepatic steatosis in n-3 fatty acid depleted mice: Focus on metabolic alterations related to tissue fatty acid composition. *BMC Physiology*, 8(1). <https://doi.org/10.1186/1472-6793-8-21>

Pacholec, M., Bleasdale, J. E., Chrnyk, B., Cunningham, D., Flynn, D., Garofalo, R. S., Griffith, D., Griffor, M., Loulakis, P., & Pabst, B. (2010). SRT1720, SRT2183, SRT1460, and resveratrol are not direct activators of SIRT1. *Journal of Biological Chemistry*, 285(11), 8340–8351.

Palmieri, E. M., Spera, I., Menga, A., Infantino, V., Porcelli, V., Iacobazzi, V., Pierri, C. L., Hooper, D. C., Palmieri, F., & Castegna, A. (2015). Acetylation of human mitochondrial citrate carrier modulates mitochondrial citrate/malate exchange activity to sustain NADPH production during macrophage activation. *Biochimica et Biophysica Acta*, 1847(8), 729–738. <https://doi.org/10.1016/j.bbabi.2015.04.009>

Palmieri, F. (2004). The mitochondrial transporter family (SLC25): physiological and pathological implications. *Pflügers Archiv: European Journal of Physiology*, 447(5), 689–709. <https://doi.org/10.1007/S00424-003-1099-7>

Palmisano, B. T., Zhu, L., Eckel, R. H., & Stafford, J. M. (2018). Sex differences in lipid and lipoprotein metabolism. *Molecular Metabolism*, 15, 45–55. <https://doi.org/10.1016/j.molmet.2018.05.008>

Palosaari, P. M., & Hiltunen, J. K. (1990). Peroxisomal bifunctional protein from rat liver is a trifunctional enzyme possessing 2-enoyl-CoA hydratase, 3-hydroxyacyl-CoA dehydrogenase, and delta 3, delta 2-enoyl-CoA isomerase activities. *Journal of Biological Chemistry*, 265(5), 2446–2449. [https://doi.org/10.1016/S0021-9258\(19\)39819-9](https://doi.org/10.1016/S0021-9258(19)39819-9)

Pamplona, R., Barja, G., & Portero-Otín, M. (2002). Membrane fatty acid unsaturation, protection against oxidative stress, and maximum life span: a homeoviscous-longevity adaptation? *Annals of the New York Academy of Sciences*, 959, 475–490. <https://doi.org/10.1111/J.1749-6632.2002.TB02118.X>

Panagiotakos, D. B., Pitsavos, C., Yannakoulia, M., Chrysohoou, C., & Stefanadis, C. (2005). The implication of obesity and central fat on markers of chronic inflammation: The ATTICA study. *Atherosclerosis*, 183(2), 308–315. <https://doi.org/10.1016/j.atherosclerosis.2005.03.010>

Pang, L., Sawada, T., Decker, S. J., & Saltiel, A. R. (1995). Inhibition of MAP kinase kinase blocks the differentiation of PC-12 cells induced by nerve growth factor. *Journal of Biological Chemistry*, 270(23), 13585–13588. <https://doi.org/10.1074/jbc.270.23.13585>

Panickar, K. S., & Bhatena, S. J. (2010). Control of Fatty Acid Intake and the Role of Essential Fatty Acids in Cognitive Function and Neurological Disorders. 463–484. <https://doi.org/10.1201/9781420067767-c18>

Papathanasiou, A. E., Nolen-Doerr, E., Farr, O. M., & Mantzoros, C. S. (2019). GEOFFREY HARRIS PRIZE LECTURE 2018: Novel pathways regulating neuroendocrine function, energy homeostasis and metabolism in humans. *European journal of endocrinology*, 180(2), R59-R71. <https://doi.org/10.1530/EJE-18-0847>

Park, E.-S. S., Lim, Y., Hong, J.-T. T., Yoo, H.-S. S., Lee, C.-K. K., Pyo, M.-Y. Y., & Yun, Y.-P. P. (2010). Pterostilbene, a natural dimethylated analog of resveratrol, inhibits rat aortic vascular smooth muscle cell proliferation by blocking Akt-dependent pathway. *Vascular Pharmacology*, 53(1–2), 61–67. <https://doi.org/10.1016/j.vph.2010.04.001>

Park, H. G., Kothapalli, K. S. D., Park, W. J., DeAllie, C., Liu, L., Liang, A., Lawrence, P., & Brenna, J. T. (2016). Palmitic acid (16:0) competes with omega-6 linoleic and omega-3 α -linolenic acids for FADS2 mediated Δ 6-desaturation. *Biochimica et Biophysica Acta*, 1861(2), 91–97. <https://doi.org/10.1016/j.bbali.2015.11.007>

Park, H. K., & Ahima, R. S. (2015). Physiology of leptin: energy homeostasis, neuroendocrine function and metabolism. *Metabolism: Clinical and Experimental*, 64(1), 24–34. <https://doi.org/10.1016/j.metabol.2014.08.004>

Park, H. S., Lim, J. H., Kim, M. Y., Kim, Y., Hong, Y. A., Choi, S. R., Chung, S., Kim, H. W., Choi, B. S., Kim, Y. S., Chang, Y. S., & Park, C. W. (2016). Resveratrol increases AdipoR1 and AdipoR2 expression in type 2 diabetic nephropathy. *Journal of Translational Medicine*, 14(1), 1–13. <https://doi.org/10.1186/s12967-016-0922-9/figures/7>

Park, S., Park, N.-Y., Valacchi, G., & Lim, Y. (2012). Calorie Restriction with a High-Fat Diet Effectively Attenuated Inflammatory Response and Oxidative Stress-Related Markers in Obese Tissues of the High Diet Fed Rats. *Mediators of Inflammation*, 2012, 11. <https://doi.org/10.1155/2012/984643>

Parrish, C. C., Myher, J. J., Kuksis, A., & Angel, A. (1997). Lipid structure of rat adipocyte plasma membranes following dietary lard and fish oil. *Biochimica et Biophysica Acta (BBA) - Biomembranes*, 1323(2), 253–262. [https://doi.org/10.1016/S0005-2736\(96\)00192-7](https://doi.org/10.1016/S0005-2736(96)00192-7)

Parry, S. A., Rosqvist, F., Peters, S., Young, R. K., Cornfield, T., Dyson, P., & Hodson, L. (2021). The influence of nutritional state on the fatty acid composition of circulating lipid fractions: Implications for their use as biomarkers of dietary fat intake. *Upsala Journal of Medical Sciences*, 126(1). <https://doi.org/10.48101/ujms.v126.7649>

Parton, R.G., 2018. Caveolae: structure, function, and relationship to disease. *Annual review of cell and developmental biology*, 34, pp.111-136 <https://doi.org/10.1146/annurev-cellbio-100617-062737>

Pasinetti, G. M. M. aria, Wang, J., Ho, L., Zhao, W., & Dubner, L. (2015). Roles of resveratrol and other grape-derived polyphenols in Alzheimer's disease prevention and treatment. *Biochimica et Biophysica Acta*, 1852(6), 1202–1208. <https://doi.org/10.1016/j.bbadis.2014.10.006>

Paulmyer-Lacroix, O., Boullu, S., Oliver, C., Alessi, M.-C., & Grino, M. (2002). Expression of the mRNA coding for 11 β -hydroxysteroid dehydrogenase type 1 in adipose tissue from obese patients: an in-situ hybridization study. *The Journal of Clinical Endocrinology and Metabolism*, 87(6), 2701–2705. <https://doi.org/10.1210/JCEM.87.6.8614>

Paulsen, S. K., Pedersen, S. B., Fisker, S., & Richelsen, B. (2007). 11 β -HSD type 1 expression in human adipose tissue: impact of gender, obesity, and fat localization. *Obesity (Silver Spring, Md.)*, 15(8), 1954–1960. <https://doi.org/10.1038/OBY.2007.233>

Pawar, A., & Jump, D. B. (2003). Unsaturated fatty acid regulation of peroxisome proliferator-activated receptor α activity in rat primary hepatocytes. *The Journal of Biological Chemistry*, 278(38), 35931–35939. <https://doi.org/10.1074/JBC.M306238200>

Peckett, A. J., Wright, D. C., & Riddell, M. C. (2011). The effects of glucocorticoids on adipose tissue lipid metabolism. *Metabolism*, 60(11), 1500–1510. <https://doi.org/10.1016/j.metabol.2011.06.012>

Pegueroles, J., Jiménez, A., Vilaplana, E., Montal, V., Carmona-Iragui, M., Pané, A., Alcolea, D., Videla, L., Casajoana, A., Clarimón, J., Ortega, E., Vidal, J., Blesa, R., Lleó, A., & Fortea, J. (2018). Obesity and Alzheimer's disease, does the obesity paradox really exist? A magnetic resonance imaging study. *Oncotarget*, 9(78), 34691. <https://doi.org/10.18632/oncotarget.26162>

Peng, S., Garzon, D. J., Marchese, M., Klein, W., Ginsberg, S. D., Francis, B. M., Mount, H. T. J., Mufson, E. J., Salehi, A., & Fahnstock, M. (2009). Decreased brain-derived neurotrophic factor depends on amyloid aggregation state in transgenic mouse models of Alzheimer's disease. *Journal of Neuroscience*, 29(29), 9321–9329.

Pérez-Gracia, E., Torrejón-Escribano, B., & Ferrer, I. (2008). Dystrophic neurites of senile plaques in Alzheimer's disease are deficient in cytochrome c oxidase. *Acta Neuropathologica*, 116(3), 261–268.

Perez-Matute, P., Neville, M. J., Tan, G. D., Frayn, K. N., & Karpe, F. (2009). Transcriptional control of human adipose tissue blood flow. *Obesity (Silver Spring, Md.)*, 17(4), 681–688. <https://doi.org/10.1038/oby.2008.606>

Perez-Pardo, P., Kliet, T., Dodiya, H. B., Broersen, L. M., Garssen, J., Keshavarzian, A., & Kraneveld, A. D. (2017). The gut-brain axis in Parkinson's disease: Possibilities for food-based therapies. *European Journal of Pharmacology*, 817(May), 86–95. <https://doi.org/10.1016/j.ejphar.2017.05.042>

Perluigi, M., di Domenico, F., Giorgi, A., Schininà, M. E., Coccia, R., Cini, C., Bellia, F., Cambria, M. T., Cornelius, C., Butterfield, D. A., & Calabrese, V. (2010). Redox proteomics in aging rat brain: involvement of mitochondrial reduced glutathione status and mitochondrial protein oxidation in the aging process. *J Neurosci Res*, 88(16), 3498–3507. <https://doi.org/10.1002/jnr.22500>

Perry, R. J., Camporez, J. P. G., Kursawe, R., Titchenell, P. M., Zhang, D., Perry, C. J., Jurczak, M. J., Abudukadier, A., Han, M. S., Zhang, X. M., Ruan, H. Bin, Yang, X., Caprio, S., Kaech, S. M., Sul, H. S., Birnbaum, M. J., Davis, R. J., Cline, G. W., Petersen, K. F., & Shulman, G. I. (2015). Hepatic acetyl CoA links adipose tissue inflammation to hepatic insulin resistance and type 2 diabetes. *Cell*, 160(4), 745–758. <https://doi.org/10.1016/j.cell.2015.01.012>

Petković, M., Vocks, A., Müller, M., Schiller, J., & Arnhold, J. (2005). Comparison of different procedures for the lipid extraction from HL-60 cells: a MALDI-TOF mass spectrometric study. *Zeitschrift Für Naturforschung C*, 60(1–2), 143–152.

Petrus, P., Rosqvist, F., Edholm, D., Mejhert, N., Arner, P., Dahlman, I., Rydén, M., Sundbom, M., & Risérus, U. (2015). Saturated fatty acids in human visceral adipose tissue are associated with increased 11- β -hydroxysteroid-dehydrogenase type 1 expression. *Lipids in Health and Disease*, 14(1), 1–5. <https://doi.org/10.1186/s12944-015-0042-1/figures/3>

Phan, T. K., Williams, S. A., Bindra, G. K., Lay, F. T., Poon, I. K. H., & Hulett, M. D. (2019). Phosphoinositides: multipurpose cellular lipids with emerging roles in cell death. *Cell Death and Differentiation*, 26(5), 781. <https://doi.org/10.1038/S41418-018-0269-2>

Phenomex. (2017). Kinetex HPLC/UHPLC Columns Tips for Care and Use.

Piccinin, E., Cariello, M., de Santis, S., Ducheix, S., Sabbà, C., Ntambi, J. M., & Moschetta, A. (2019). Role of Oleic Acid in the Gut-Liver Axis: From Diet to the Regulation of Its Synthesis via Stearoyl-CoA Desaturase 1 (SCD1). *Nutrients*, 11(10). <https://doi.org/10.3390/NU11102283>

Pierre, S., Jamme, I., Droy-Lefaix, M.-T., Nouvelot, A., & Maixent, J.-M. (1999). Ginkgo biloba extract (EGb 761) protects Na, K-ATPase activity during cerebral ischemia in mice. *Neuroreport*, 10(1), 47–51.

Pilon, M. (2016). Revisiting the membrane-centric view of diabetes. *Lipids in Health and Disease*, 15(1), 1–6. <https://doi.org/10.1186/S12944-016-0342-0>

Plácido, J., Ferreira, J. V., Araújo, J., Silva, F. D. O., Ferreira, R. B., Guimarães, C., de Carvalho, A. N., Laks, J., & Deslandes, A. C. (2021). Beyond the Mini-Mental State Examination: The Use of Physical and Spatial Navigation Tests to Help to Screen for Mild Cognitive Impairment and Alzheimer's Disease. *Journal of Alzheimer's Disease*, 81(3), 1243–1252. <https://doi.org/10.3233/JAD-210106>

Pond, C. M., & Mattacks, C. A. (2003). The source of fatty acids incorporated into proliferating lymphoid cells in immune-stimulated lymph nodes. *The British Journal of Nutrition*, 89(3), 375–382. <https://doi.org/10.1079/BJN2002784>

Ponto, L. L. B., & Schultz, S. K. (2003). Ginkgo biloba extract: review of CNS effects. *Annals of Clinical Psychiatry*, 15(2), 109–119.

Popović, T. B., Borozan, S. Z., Takić, M. M., Kojadinović, M. J., Rankovic, S., Ranić, M., & de Luka, S. R. (2014). Fatty acid composition and oxidative stress parameters in plasma after fish oil supplementation in aging. *Croatica Chemica Acta*, 87(3), 207–212. <https://doi.org/10.5562/CCA2405>

Poppitt, S. D., Leahy, F. E., Keogh, G. F., Wang, Y., Mulvey, T. B., Stojkovic, M., Chan, Y. K., Choong, Y. S., McArdle, B. H., & Cooper, G. J. S. (2005). Effect of high-fat meals and fatty acid saturation on postprandial levels of the hormones ghrelin and leptin in healthy men. *European Journal of Clinical Nutrition* 2006 60:1, 60(1), 77–84. <https://doi.org/10.1038/sj.ejcn.1602270>

Postic, C., Dentin, R., Denechaud, P. D., & Girard, J. (2007). ChREBP, a transcriptional regulator of glucose and lipid metabolism. *Annual Review of Nutrition*, 27, 179–192. <https://doi.org/10.1146/ANNUREV.NUTR.27.061406.093618>

Prabhakar, P., Cheng, V., & Michel, T. (2000). A chimeric transmembrane domain directs endothelial nitric-oxide synthase palmitoylation and targeting to plasmalemmal caveolae. *Journal of Biological Chemistry*, 275(25), 19416–19421.

Prakash, J., Wang, V., Quinn, & Mitchell, C. S. (2021). Unsupervised Machine Learning to Identify Separable Clinical Alzheimer's Disease Sub-Populations. *Brain Sciences*, 11(8). <https://doi.org/10.3390/BRAINSCI11080977>

Pranger, I. G., Corpeleijn, E., Muskiet, F. A. J., Kema, I. P., Singh-Povel, C., & Bakker, S. J. L. (2019). Circulating fatty acids as biomarkers of dairy fat intake: data from the lifelines biobank and cohort study. *Biomarkers: Biochemical Indicators of Exposure, Response, and Susceptibility to Chemicals*, 24(4), 360–372. <https://doi.org/10.1080/1354750X.2019.1583770>

Prasad, S., Sajja, R. K., Naik, P., & Cucullo, L. (2014). Diabetes mellitus and blood-brain barrier dysfunction: an overview. *Journal of Pharmacovigilance*, 2(2), 125.

Prickett, C., Brennan, L., & Stolwyk, R. (2015). Examining the relationship between obesity and cognitive function: A systematic literature review. *Obesity Research and Clinical Practice*, 9(2), 93–113. <https://doi.org/10.1016/j.orcp.2014.05.001>

Prince, M., Ali, G. C., Guerchet, M., Prina, A. M., Albanese, E., & Wu, Y. T. (2016). Recent global trends in the prevalence and incidence of dementia, and survival with dementia. *Alzheimer's Research & Therapy*, 8(1). <https://doi.org/10.1186/S13195-016-0188-8>

Prince, M., Comas-Herrera, A., Knapp, M., Guerchet, M., & Karagiannidou, M. (2016). World Alzheimer report 2016: improving healthcare for people living with dementia: coverage, quality and costs now and in the future Report Improving healthcare for people living with dementia coverage, Quality and costs now and In the future.

Prince, M. J., Wimo, A., Guerchet, M. M., Ali, G. C., Wu, Y.-T., & Prina, M. (2015). World Alzheimer Report 2015 - The Global Impact of Dementia: An analysis of prevalence, incidence, cost and trends. *Alzheimer's Disease International*.

Pugazhenthii, S., Qin, L., & Reddy, P. H. (2017). Common neurodegenerative pathways in obesity, diabetes, and Alzheimer's disease. *Biochimica et Biophysica Acta (BBA)-Molecular Basis of Disease*, 1863(5), 1037–1045.

Pujol-Gimenez, J., Martisova, E., Perez-Mediavilla, A., Lostao, M. P., & Ramirez, M. J. (2014). Expression of the glucose transporter GLUT12 in Alzheimer's disease patients. *Journal of Alzheimer's Disease*, 42(1), 97–101.

Purdon, D., Arai, T., research, S. R.-J. of lipid, & 1997, undefined. (1997). No evidence for direct incorporation of esterified palmitic acid from plasma into brain lipids of awake adult rat. *ASBMB*. [https://doi.org/10.1016/S0022-2275\(20\)37260-6](https://doi.org/10.1016/S0022-2275(20)37260-6)

Pyrina, I., Chung, K. J., Michailidou, Z., Koutsilieris, M., Chavakis, T., & Chatzigeorgiou, A. (2020). Fate of Adipose Progenitor Cells in Obesity-Related Chronic Inflammation. *Frontiers in Cell and Developmental Biology*, 8, 644. <https://doi.org/10.3389/FCCELL.2020.00644/BIBTEX>

Qiu, W., Wu, H., Hu, Z., Wu, X., Tu, M., Fang, F., Zhu, X., Liu, Y., Lian, J., Valverde, P., van Dyke, T., Steffensen, B., Dong, L. Q., Tu, Q., Zhou, X., & Chen, J. (2021). Identification and

characterization of a novel adiponectin receptor agonist adipo anti-inflammation agonist and its anti-inflammatory effects in vitro and in vivo. *British Journal of Pharmacology*, 178(2), 280–297. <https://doi.org/10.1111/BPH.15277>

R Cserjesi, O. L. A. P. L. L. (2009). Altered executive function in obesity. Exploration of the role of affective states on cognitive abilities. *Appetite*, 52, 535–539.

Raclot, T. (2003). Selective mobilization of fatty acids from adipose tissue triacylglycerols. *Progress in Lipid Research*, 42(4), 257–288. [https://doi.org/10.1016/S0163-7827\(02\)00066-8](https://doi.org/10.1016/S0163-7827(02)00066-8)

Radhakrishnan, A., Goldstein, J. L., McDonald, J. G., & Brown, M. S. (2008). Switch-like control of SREBP-2 transport triggered by small changes in ER cholesterol: a delicate balance. *Cell Metabolism*, 8.

Radhakrishnan, S., Yeung, S. F., Ke, J.-Y., Antunes, M. M., & Pellizzon, M. A. (2022). Considerations When Choosing High-Fat, High-Fructose, and High-Cholesterol Diets to Induce Experimental Nonalcoholic Fatty Liver Disease in Laboratory Animal Models. *Current Developments in Nutrition*, 5(12). <https://doi.org/10.1093/CDN/NZAB138>

Rafiei, H., Omidian, K., & Bandy, B. (2019). Dietary Polyphenols Protect Against Oleic Acid-Induced Steatosis in an in Vitro Model of NAFLD by Modulating Lipid Metabolism and Improving Mitochondrial Function. *Nutrients*, 11(3). <https://doi.org/10.3390/NU11030541>

Rahat-Rozenbloom, S., Gloor, G., Wolever, T., & Fernandes, J. (2014). Evidence for greater production of colonic short-chain fatty acids in overweight than lean humans. *Int J Obes*, 38, 1525–1531.

Rakhshandehroo, M., Knoch, B., Müller, M., & Kersten, S. (2010). Peroxisome Proliferator-Activated Receptor Alpha Target Genes. *PPAR Research*, 2010. <https://doi.org/10.1155/2010/612089>

Ramassamy, C. (2006). Emerging role of polyphenolic compounds in the treatment of neurodegenerative diseases: A review of their intracellular targets. *European Journal of Pharmacology*, 545(1), 51–64. <https://doi.org/10.1016/j.ejphar.2006.06.025>

Ranković, S., Popović, T., Martačić, J. D., Petrović, S., Tomić, M., Ignjatović, Đ., Tovilović-Kovačević, G., & Glibetić, M. (2017). Liver phospholipids fatty acids composition in response to different types of diets in rats of both sexes. *Lipids in Health and Disease*, 16(1). <https://doi.org/10.1186/S12944-017-0483-9>

Ransy, C., Vaz, C., Lombès, A., & Bouillaud, F. (2020). Use of H₂O₂ to Cause Oxidative Stress, the Catalase Issue. *International Journal of Molecular Sciences* 2020, Vol. 21, Page 9149, 21(23), 9149. <https://doi.org/10.3390/IJMS21239149>

Rapoport, S. I., Chang, M. C. J., & Spector, A. A. (2001). Delivery and turnover of plasma-derived essential PUFAs in mammalian brain. *Journal of Lipid Research*, 42(5), 678–685. [https://doi.org/10.1016/S0022-2275\(20\)31629-1](https://doi.org/10.1016/S0022-2275(20)31629-1)

Rask, E., Walker, B. R., Söderberg, S., Livingstone, D. E. W., Eliasson, M., Johnson, O., Andrew, R., & Olsson, T. (2002). Tissue-Specific Changes in Peripheral Cortisol Metabolism in Obese Women: Increased Adipose 11 β -Hydroxysteroid Dehydrogenase Type 1 Activity. *The Journal of Clinical Endocrinology & Metabolism*, 87(7), 3330–3336. <https://doi.org/10.1210/JCEM.87.7.8661>

Rask-Andersen, M., Karlsson, T., Ek, W. E., & Johansson, Å. (2019). Genome-wide association study of body fat distribution identifies adiposity loci and sex-specific genetic effects. *Nature Communications* 2019 10:1, 10(1), 1–10. <https://doi.org/10.1038/s41467-018-08000-4>

Rauschert, S., Uhl, O., Koletzko, B., & Hellmuth, C. (2014). Metabolomic biomarkers for obesity in humans: a short review. *Annals of Nutrition & Metabolism*, 64(3–4), 314–324. <https://doi.org/10.1159/000365040>

Reed, A. S., Unger, E. K., Olofsson, L. E., Piper, M. L., Myers, M. G., & Xu, A. W. (2010). Functional role of suppressor of cytokine signaling 3 upregulation in hypothalamic leptin resistance and long-term energy homeostasis. *Diabetes*, 59(4), 894–906. <https://doi.org/10.2337/DB09-1024>

Reid, B. N., Ables, G. P., Otlivanchik, O. A., Schoiswohl, G., Zechner, R., Blaner, W. S., Goldberg, I. J., Schwabe, R. F., Chua, S. C., & Huang, L. S. (2008). Hepatic Overexpression of Hormone-sensitive Lipase and Adipose Triglyceride Lipase Promotes Fatty Acid Oxidation, Stimulates Direct Release of Free Fatty Acids, and Ameliorates Steatosis. *The Journal of Biological Chemistry*, 283(19), 13087. <https://doi.org/10.1074/JBC.M800533200>

Reis, A., Rudnitskaya, A., Blackburn, G. J., Fauzi, N. M., Pitt, A. R., & Spickett, C. M. (2013). A comparison of five lipid extraction solvent systems for lipidomic studies of human LDL. *Journal of Lipid Research*, 54(7), 1812–1824.

Reisberg, B., Ferris, S. H., de Leon, M. J., & Crook, T. (1982). The global deterioration scale for assessment of primary degenerative dementia. *American Journal of Psychiatry*, 139(9), 1136–1139. <https://doi.org/10.1176/AJP.139.9.1136>

Rett, B. S., & Whelan, J. (2011). Increasing dietary linoleic acid does not increase tissue arachidonic acid content in adults consuming Western-type diets: a systematic review. *Nutrition & Metabolism*, 8. <https://doi.org/10.1186/1743-7075-8-36>

Reyes-Quiroz, M. E., Alba, G., Saenz, J., Santa-María, C., Geniz, I., Jiménez, J., Ramírez, R., Martín-Nieto, J., Pintado, E., & Sobrino, F. (2014). Oleic acid modulates mRNA expression of liver X receptor (LXR) and its target genes ABCA1 and SREBP1c in human neutrophils. *Eur J Nutr*, 53(8), 1707–1717. <https://doi.org/10.1007/s00394-014-0677-0>

Rhee, K.-J., Lee, C. G., Kim, S. W., Gim, D.-H., Kim, H.-C., & Jung, B. D. (2015). Extract of Ginkgo biloba ameliorates streptozotocin-induced type 1 diabetes mellitus and high-fat diet-induced type 2 diabetes mellitus in mice. *International Journal of Medical Sciences*, 12(12), 987.

Rhein, V., Giese, M., Baysang, G., Meier, F., Rao, S., Schulz, K. L., Hamburger, M., & Eckert, A. (2010). Ginkgo biloba extract ameliorates oxidative phosphorylation performance and

rescues A β -induced failure. PLoS ONE, 5(8), e12359–e12359. <https://doi.org/10.1371/journal.pone.0012359>

Ricoult, S. J. H., & Manning, B. D. (2013). The multifaceted role of mTORC1 in the control of lipid metabolism. *EMBO Reports*, 14(3), 242. <https://doi.org/10.1038/EMBOR.2013.5>

Ridgway, N. D., & McLeod, R. S. (2021). *Biochemistry of lipids, lipoproteins and membranes*. Elsevier Science.

Ridlon, J. M., Kang, D. J., & Hylemon, P. B. (2006). Bile salt biotransformations by human intestinal bacteria. *Journal of Lipid Research*, 47(2), 241–259.

Ridlon, J. M., Kang, D. J., Hylemon, P. B., & Bajaj, J. S. (2014). Bile acids and the gut microbiome. *Current Opinion in Gastroenterology*, 30(3), 332–338. <https://doi.org/10.1097/MOG.0000000000000057>

Riggs, N.R., Spruijt-Metz, D., Chou, C.P. and Pentz, M.A., 2012. Relationships between executive cognitive function and lifetime substance use and obesity-related behaviors in fourth grade youth. *Child Neuropsychology*, 18(1), pp.1-11.

Risso, G., Blaustein, M., Pozzi, B., Mammi, P., & Srebrow, A. (2015). Akt/PKB: one kinase, many modifications. *The Biochemical Journal*, 468(2), 203–214. <https://doi.org/10.1042/BJ20150041>

Rivel, T., Ramseyer, C., & Yesylevskyy, S. (2019). The asymmetry of plasma membranes and their cholesterol content influence the uptake of cisplatin. *Scientific Reports* 2019 9:1, 9(1), 1–14. <https://doi.org/10.1038/s41598-019-41903-w>

Roberts, R. G., Freeman, T. C., Kendall, E., Vetrie, D. L. P., Dixon, A. K., Shaw-Smith, C., Bone, Q., & Bobrow, M. (1996). Characterization of DRP2, a novel human dystrophin homologue. *Nature Genetics*, 13(2), 223–226. <https://doi.org/10.1038/NG0696-223>

Robinson, K., Prins, J., & Venkatesh, B. (2011). Clinical review: Adiponectin biology and its role in inflammation and critical illness. *Critical Care*, 15(2), 1–9. <https://doi.org/10.1186/CC10021/TABLES/3>

Robinson, P. J., Noronha, J., DeGeorge, J. J., Freed, L. M., Nariai, T., & Rapoport, S. I. (1992). A quantitative method for measuring regional in vivo fatty-acid incorporation into and turnover within brain phospholipids: review and critical analysis. *Brain Res Brain Res Rev*, 17(3), 187–214. [https://doi.org/10.1016/0165-0173\(92\)90016-f](https://doi.org/10.1016/0165-0173(92)90016-f)

Robles, F., Vázquez, P., Emiliano, R., Amaro, G., & Briones, L. (2017). High fat diet induces alterations to intraepithelial lymphocyte and cytokine mRNA in the small intestine of C57BL/6 mice. *RSC Advances*, 7(9), 5322–5330. <https://doi.org/10.1039/C6RA24689C>

Rodríguez-Rodríguez, C., Torres, N., Gutiérrez-Urbe, J. A., Noriega, L. G., Torre-Villalvazo, I., Leal-Díaz, A. M., Antunes-Ricardo, M., Márquez-Mota, C., Ordaz, G., Chavez-Santoscoy, R. A., Serna-Saldivar, S. O., & Tovar, A. R. (2015). The effect of isorhamnetin glycosides extracted

from *Opuntia ficus-indica* in a mouse model of diet induced obesity. *Food & Function*, 6(3), 805–815. <https://doi.org/10.1039/C4FO01092B>

Rogaev, E. I., Sherrington, R., Rogaeva, E. A., Levesque, G., Ikeda, M., Liang, Y., Chi, H., Lin, C., Holman, K., & Tsuda, T. (1995). Familial Alzheimer's disease in kindreds with missense mutations in a gene on chromosome 1 related to the Alzheimer's disease type 3 gene. *Nature*, 376(6543), 775–778.

Rogero, M. M., & Calder, P. C. (2018). Obesity, Inflammation, Toll-Like Receptor 4 and Fatty Acids. *Nutrients*, 10(4). <https://doi.org/10.3390/NU10040432>

Rohr, M. W., Narasimhulu, C. A., Rudeski-Rohr, T. A., & Parthasarathy, S. (2020). Negative Effects of a High-Fat Diet on Intestinal Permeability: A Review. *Advances in Nutrition (Bethesda, Md.)*, 11(1), 77–91. <https://doi.org/10.1093/ADVANCES/NMZ061>

Román, G. C., Jackson, R. E., Gadhia, R., Román, A. N., & Reis, J. (2019). Mediterranean diet: The role of long-chain ω -3 fatty acids in fish; polyphenols in fruits, vegetables, cereals, coffee, tea, cacao and wine; probiotics and vitamins in prevention of stroke, age-related cognitive decline, and Alzheimer disease. *Revue Neurologique*, 175(10), 724–741. <https://doi.org/10.1016/j.neurol.2019.08.005>

Romano, C., Nichols, R. A., Greengard, P., & Greene, L. A. (1987). Synapsin I in PC12 cells. I. Characterization of the phosphoprotein and effect of chronic NGF treatment. *The Journal of Neuroscience: The Official Journal of the Society for Neuroscience*, 7(5), 1294–1299. <https://doi.org/10.1523/JNEUROSCI.07-05-01294.1987>

Rönnemaa, E., Zethelius, B., Vessby, B., Lannfelt, L., Byberg, L., & Kilander, L. (2012). Serum fatty-acid composition and the risk of Alzheimer's disease: a longitudinal population-based study. *European Journal of Clinical Nutrition* 2012 66:8, 66(8), 885–890. <https://doi.org/10.1038/ejcn.2012.63>

Rosales-Corral, S., Tan, D.-X., Manchester, L., & Reiter, R. J. (2015). Diabetes and Alzheimer disease, two overlapping pathologies with the same background: oxidative stress. *Oxidative Medicine and Cellular Longevity*, 2015.

Roumans, K. H. M., Sagarminaga, J. B., Peters, H. P. F., Schrauwen, P., & Schrauwen-Hinderling, V. B. (2021). Liver fat storage pathways: methodologies and dietary effects. *Current Opinion in Lipidology*, 32(1), 9–15. <https://doi.org/10.1097/MOL.0000000000000720>

Royal Society of Chemistry. (2022a). 11-Eicosenoic acid | C₂₀H₃₈O₂ | ChemSpider. <http://www.chemspider.com/Chemical-Structure.4445895.html>

Royal Society of Chemistry. (2022b). Erucic acid | C₂₂H₄₂O₂ | ChemSpider. <http://www.chemspider.com/Chemical-Structure.4444561.html?rid=5c68fca0-3b48-4e35-a402-7b0b9fdaa651>

Royal Society of Chemistry. (2022c). Methyl palmitoleate | C17H32O2 | ChemSpider. <http://www.chemspider.com/Chemical-Structure.558899.html?rid=8f960a9b-9eee-41a0-aec4-aa5ebc29ba4a>

Royal Society of Chemistry. (2022d). Nervonic acid | C24H46O2 | ChemSpider. <http://www.chemspider.com/Chemical-Structure.4444565.html?rid=d8ee9ea9-d493-4985-a5fb-e6c4ad82b8a3>

Royal Society of Chemistry. (2022e). Palmitoleic acid | C16H30O2 | ChemSpider. <http://www.chemspider.com/Chemical-Structure.393216.html?rid=08ccd8d9-28aa-4e14-855b-2bffc259e64d>

RP Bazinet, S. L. (2014). Polyunsaturated fatty acids and their metabolites in brain function and disease. *Nat Rev Neurosci*, 15, 771–785. <https://doi.org/10.1038/nrn3820>

Rudkin, B. B., Lazarovici, P., Levi, B. Z., Abe, Y., Fujita, K., & Guroff, G. (1989). Cell cycle-specific action of nerve growth factor in PC12 cells: differentiation without proliferation. *The EMBO Journal*, 8(11), 3319. <https://doi.org/10.1002/j.1460-2075.1989.tb08493.x>

Sadri, S., Khazaei, M., Ghanbari, A., Khazaei, M. R., & Shah, P. (2014). Neuronal differentiation of PC12 and embryonic stem cells in two- and three-dimensional in vitro culture. *Indian Journal of Experimental Biology*, 52, 305–311.

Sakagami, H., Hara, Y., Shi, H., Iwama, S., Nakagawa, M., Suzuki, H., Tanaka, K., Tomoyuki, A. B. E., Tamura, N., Takeshima, H., Horie, N., Kaneko, T., Shiratsuchi, H., & Kaneko, T. (2018). Change in Anticancer Drug Sensitivity During Neuronal Differentiation of PC12 Cells. *In Vivo (Athens, Greece)*, 32(4), 765–770. <https://doi.org/10.21873/INVIVO.11306>

Salama, I.I., Abdelrahman, A.H., Salama, S.I., Abdellatif, G.A., Rabah, T.M., Saleh, R.M., Elmosalami, D.M., Rabah, A.M. and Fouad, W.A., 2018. Obesity and Predictors Affecting the Occurrence of Mild Cognitive Impairment. *Research Journal Of Pharmaceutical Biological And Chemical Sciences*, 9(1), pp.748-756.

Salamone, F., & Bugianesi, E. (2010). Nonalcoholic fatty liver disease: the hepatic trigger of the metabolic syndrome. *Journal of Hepatology*, 53(6), 1146–1147.

Samovski, D., & Abumrad, N. A. (2019). Regulation of lipophagy in NAFLD by cellular metabolism and CD361. *Journal of Lipid Research*, 60(4), 755–757. <https://doi.org/10.1194/JLR.C093674>

Samuel, B. S., Shaito, A., Motoike, T., Rey, F. E., Backhed, F., Manchester, J. K., Hammer, R. E., Williams, S. C., Crowley, J., Yanagisawa, M., & Gordon, J. I. (2008). Effects of the gut microbiota on host adiposity are modulated by the short-chain fatty-acid binding G protein-coupled receptor, Gpr41. *Proceedings of the National Academy of Sciences of the United States of America*, 105(43), 16767–16772. <https://doi.org/10.1073/PNAS.0808567105>

Samuel, V. T., & Shulman, G. I. (2012). Mechanisms for insulin resistance: common threads and missing links. *Cell*, 148(5), 852–871. <https://doi.org/10.1016/J.CELL.2012.02.017>

- Samuel, V. T., & Shulman, G. I. (2016). The pathogenesis of insulin resistance: integrating signaling pathways and substrate flux. *The Journal of Clinical Investigation*, 126(1), 12–22. <https://doi.org/10.1172/JCI77812>
- Samuelson, I., & Vidal-Puig, A. (2020). Studying Brown Adipose Tissue in a Human in vitro Context. *Frontiers in Endocrinology*, 11, 629. <https://doi.org/10.3389/FENDO.2020.00629/BIBTEX>
- Sandeep, T. C., Andrew, R., Homer, N. Z. M., Andrews, R. C., Smith, K., & Walker, B. R. (2005). Increased in vivo regeneration of cortisol in adipose tissue in human obesity and effects of the 11beta-hydroxysteroid dehydrogenase type 1 inhibitor carbenoxolone. *Diabetes*, 54(3), 872–879. <https://doi.org/10.2337/DIABETES.54.3.872>
- Sansbury, B. E., Cummins, T. D., Tang, Y., Hellmann, J., Holden, C. R., Harbeson, M. A., Chen, Y., Patel, R. P., Spite, M., Bhatnagar, A., & Hil, B. G. (2012). Overexpression of endothelial nitric oxide synthase prevents diet-induced obesity and regulates adipocyte phenotype. *Circulation Research*, 111(9), 1176–1189. <https://doi.org/10.1161/CIRCRESAHA.112.266395>
- Santos, H. O., Price, J. C., & Bueno, A. A. (2020). Beyond Fish Oil Supplementation: The Effects of Alternative Plant Sources of Omega-3 Polyunsaturated Fatty Acids upon Lipid Indexes and Cardiometabolic Biomarkers—An Overview. *Nutrients*, 12(10), 1–19. <https://doi.org/10.3390/NU12103159>
- Santos, S. D. M., Verveer, P. J., & Bastiaens, P. I. H. (2007). Growth factor-induced MAPK network topology shapes Erk response determining PC-12 cell fate. *Nature Cell Biology*, 9(3), 324–330. <https://doi.org/10.1038/NCB1543>
- Saponara, R., & Bosisio, E. (1998). Inhibition of cAMP-phosphodiesterase by biflavones of *Ginkgo biloba* in rat adipose tissue. *Journal of Natural Products*, 61(11), 1386–1387. <https://doi.org/10.1021/NP970569M>
- Saragat, B., Buffa, R., Mereu, E., Succa, V., Cabras, S., Mereu, R. M., Viale, D., Putzu, P. F., & Marini, E. (2012). Nutritional and psycho-functional status in elderly patients with Alzheimer's disease. *The Journal of Nutrition, Health & Aging*, 16(3), 231–236.
- Sarbassov, D. D., Guertin, D. A., Ali, S. M., & Sabatini, D. M. (2005). Phosphorylation and regulation of Akt/PKB by the rictor-mTOR complex. *Science (New York, N.Y.)*, 307(5712), 1098–1101. <https://doi.org/10.1126/SCIENCE.1106148>
- Sasaki, T., Takasuga, S., Sasaki, J., Kofuji, S., Eguchi, S., Yamazaki, M., & Suzuki, A. (2009). Mammalian phosphoinositide kinases and phosphatases. *Progress in Lipid Research*, 48(6), 307–343. <https://doi.org/10.1016/J.PLIPRES.2009.06.001>
- Sato, M., Nakahara, K., Goto, S., Kaiya, H., Miyazato, M., Date, Y., Nakazato, M., Kangawa, K., & Murakami, N. (2006). Effects of ghrelin and des-acyl ghrelin on neurogenesis of the rat fetal spinal cord. *Biochemical and Biophysical Research Communications*, 350(3), 598–603. <https://doi.org/10.1016/J.BBRC.2006.09.088>

Sawda, C., Moussa, C., & Turner, R. S. (2017). Resveratrol for alzheimer's disease. *Annals of the New York Academy of Sciences*, 1403(1), 142–149. <https://doi.org/10.1111/nyas.13431>

Scannevin, R. H., Chollate, S., Jung, M., Shackett, M., Patel, H., Bista, P., Zeng, W., Ryan, S., Yamamoto, M., & Lukashev, M. (2012). Fumarates promote cytoprotection of central nervous system cells against oxidative stress via the nuclear factor (erythroid-derived 2)-like 2 pathway. *Journal of Pharmacology and Experimental Therapeutics*, 341(1), 274–284.

Schäffler, A., & Schölmerich, J. (2010). Innate immunity and adipose tissue biology. *Trends in Immunology*, 31(6), 228–235. <https://doi.org/10.1016/j.it.2010.03.001>

Schäffler, A., Schölmerich, J., & Büchler, C. (2005). Mechanisms of disease: Adipocytokines and visceral adipose tissue - Emerging role in intestinal and mesenteric diseases. *Nature Clinical Practice Gastroenterology and Hepatology*, 2(2), 103–111. <https://doi.org/10.1038/NCPGASTHEP0090>

Schebb, N. H., Kühn, H., Kahnt, A. S., Rund, K. M., O'Donnell, V. B., Flamand, N., Peters-Golden, M., Jakobsson, P. J., Weylandt, K. H., Rohwer, N., Murphy, R. C., Geisslinger, G., FitzGerald, G. A., Hanson, J., Dahlgren, C., Alnouri, M. W., Offermanns, S., & Steinhilber, D. (2022). Formation, Signaling and Occurrence of Specialized Pro-Resolving Lipid Mediators—What is the Evidence so far? *Frontiers in Pharmacology*, 13, 475. <https://doi.org/10.3389/fphar.2022.838782/BIBTEX>

Schimmelpfeng, J., Weibezahn, K. F., & Dertinger, H. (2004). Quantification of NGF-dependent neuronal differentiation of PC-12 cells by means of neurofilament-L mRNA expression and neuronal outgrowth. *Journal of Neuroscience Methods*, 139(2), 299–306. <https://doi.org/10.1016/j.jneumeth.2004.05.010>

Schlattner, U., Tokarska-Schlattner, M., Rousseau, D., Boissan, M., Mannella, C., Epand, R., & Lacombe, M. L. (2014). Mitochondrial cardiolipin/phospholipid trafficking: The role of membrane contacts site complexes and lipid transfer proteins. *Chemistry and Physics of Lipids*, 179, 32–41. <https://doi.org/10.1016/j.chemphyslip.2013.12.008>

Schmitz, G., & Ecker, J. (2008). The opposing effects of n-3 and n-6 fatty acids. *Progress in Lipid Research*, 47(2), 147–155. <https://doi.org/10.1016/j.plipres.2007.12.004>

Schneeberger, M., Dietrich, M. O., Sebastián, D., Imbernón, M., Castaño, C., Garcia, A., Esteban, Y., Gonzalez-Franquesa, A., Rodríguez, I. C., Bortolozzi, A., Garcia-Roves, P. M., Gomis, R., Nogueiras, R., Horvath, T. L., Zorzano, A., & Claret, M. (2013). Mitofusin 2 in POMC neurons connects ER stress with leptin resistance and energy imbalance. *Cell*, 155(1), 172–187. <https://doi.org/10.1016/j.cell.2013.09.003>

Schrader, M., Costello, J., Godinho, L. F., & Islinger, M. (2015). Peroxisome-mitochondria interplay and disease. *Journal of Inherited Metabolic Disease*, 38(4), 681–702. <https://doi.org/10.1007/S10545-015-9819-7>

Schreiner, M. (2006). Optimization of solvent extraction and direct transmethylation methods for the analysis of egg yolk lipids. *International Journal of Food Properties*, 9(3), 573–581.

Schug, T. T., Berry, D. C., Shaw, N. S., Travis, S. N., & Noy, N. (2007). Opposing Effects of Retinoic Acid on Cell Growth Result from Alternate Activation of Two Different Nuclear Receptors. *Cell*, 129(4), 723–733. <https://doi.org/10.1016/J.CELL.2007.02.050>

Schulz, V. (2003). Ginkgo extract or cholinesterase inhibitors in patients with dementia: What clinical trials and guidelines fail to consider. *Phytomedicine*, 10, 74–79. <https://doi.org/10.1078/1433-187X-00302>

Schumann, J. (2016). It is all about fluidity: Fatty acids and macrophage phagocytosis. *European Journal of Pharmacology*, 785, 18–23. <https://doi.org/10.1016/J.EJP.2015.04.057>

Schwenk, R. W., Holloway, G. P., Luiken, J. J. F. P., Bonen, A., & Glatz, J. F. C. (2010). Fatty acid transport across the cell membrane: Regulation by fatty acid transporters. *Prostaglandins, Leukotrienes and Essential Fatty Acids (PLEFA)*, 82(4–6), 149–154. <https://doi.org/10.1016/J.PLEFA.2010.02.029>

Schwingshackl, L., Morze, J., & Hoffmann, G. (2020). Mediterranean diet and health status: Active ingredients and pharmacological mechanisms. *British Journal of Pharmacology*, 177(6), 1241–1257. <https://doi.org/10.1111/BPH.14778>

Scott, S. A., Mufson, E. J., Weingartner, J. A., Skau, K. A., & Crutcher, K. A. (1995). Nerve growth factor in Alzheimer's disease: increased levels throughout the brain coupled with declines in nucleus basalis. *Journal of Neuroscience*, 15(9), 6213–6221.

Scoville, E. A., Allaman, M. M., Brown, C. T., Motley, A. K., Horst, S. N., Williams, C. S., Koyama, T., Zhao, Z., Adams, D. W., Beaulieu, D. B., Schwartz, D. A., Wilson, K. T., & Coburn, L. A. (2018). Alterations in lipid, amino acid, and energy metabolism distinguish Crohn's disease from ulcerative colitis and control subjects by serum metabolomic profiling. *Metabolomics*, 14(1). <https://doi.org/10.1007/S11306-017-1311-Y>

Sebastià, N., Montoro, A., León, Z., & Soriano, J. M. (2017). Searching trans-resveratrol in fruits and vegetables: a preliminary screening. *Journal of Food Science and Technology*, 54(3), 842. <https://doi.org/10.1007/S13197-016-2474-7>

Sebastià, N., Montoro, A., Mañes, J., & Soriano, J. M. (2012). A preliminary study of presence of resveratrol in skins and pulps of European and Japanese plum cultivars. *Journal of the Science of Food and Agriculture*, 92(15), 3091–3094. <https://doi.org/10.1002/JSFA.5759>

Segal, R. A. (2003). Selectivity in neurotrophin signaling: theme and variations. *Annual Review of Neuroscience*, 26, 299–330. <https://doi.org/10.1146/ANNUREV.NEURO.26.041002.131421>

Seifert, R., Lushington, G. H., Mou, T.-C., Gille, A., & Sprang, S. R. (2012). Inhibitors of Membranous Adenylyl Cyclases. *Trends Pharmacol Sci*, 33(2), 64–78. <https://doi.org/10.1016/j.tips.2011.10.006>

Senga, S., Kawaguchi, K., Kobayashi, N., Ando, A., & Fujii, H. (2018). A novel fatty acid-binding protein 5-estrogen-related receptor α signaling pathway promotes cell growth and energy

metabolism in prostate cancer cells. *Oncotarget*, 9(60), 31753. <https://doi.org/10.18632/oncotarget.25878>

Serhan, C. N. (2005). Lipoxins and aspirin-triggered 15-epi-lipoxins are the first lipid mediators of endogenous anti-inflammation and resolution. *Prostaglandins, Leukotrienes and Essential Fatty Acids*, 73(3), 141–162. <https://doi.org/10.1016/j.plefa.2005.05.002>

Serhan, C. N., Dalli, J., Karamnov, S., Choi, A., Park, C.-K., Xu, Z.-Z., Ji, R.-R., Zhu, M., & Petasis, N. A. (2012). Macrophage proresolving mediator maresin 1 stimulates tissue regeneration and controls pain. *The FASEB Journal*, 26(4), 1755–1765.

Serhan, C. N., & Petasis, N. A. (2011). Resolvins and Protectins in Inflammation-Resolution. *Chemical Reviews*, 111(10), 5922. <https://doi.org/10.1021/cr100396c>

Serrano-García, N., Pedraza-Chaverri, J., Mares-Sámano, J. J., Orozco-Ibarra, M., Cruz-Salgado, A., Jiménez-Anguiano, A., Sotelo, J., & Trejo-Solís, C. (2013). *Antiapoptotic effects of EGb 761. Evidence-Based Complementary and Alternative Medicine*, 2013.

Serrano-Pozo, A., Frosch, M. P., Masliah, E., & Hyman, B. T. (2011). Neuropathological alterations in Alzheimer disease. *Cold Spring Harbor Perspectives in Medicine*, 1(1), a006189.

Sethi, S., Ziouzenkova, O., Ni, H., Wagner, D. D., Plutzky, J., & Mayadas, T. N. (2002). Oxidized omega-3 fatty acids in fish oil inhibit leukocyte-endothelial interactions through activation of PPAR alpha. *Blood*, 100(4), 1340–1346. <https://doi.org/10.1182/blood-2002-01-0316>

Shafaati, M., Marutle, A., Pettersson, H., Lövgren-Sandblom, A., Olin, M., Pikuleva, I., Winblad, B., Nordberg, A., & Björkhem, I. (2011). Marked accumulation of 27-hydroxycholesterol in the brains of Alzheimer's patients with the Swedish APP 670/671 mutation. *Journal of Lipid Research*, 52(5), 1004. <https://doi.org/10.1194/jlr.M014548>

Shah, K., DeSilva, S., & Abbruscato, T. (2012). The role of glucose transporters in brain disease: Diabetes and Alzheimer's disease. *International Journal of Molecular Sciences*, 13(10), 12629–12655. <https://doi.org/10.3390/ijms131012629>

Shao, M., Wang, Q. A., Song, A., Vishvanath, L., Busbuso, N. C., Scherer, P. E., & Gupta, R. K. (2019). Cellular origins of beige fat cells revisited. *Diabetes*, 68(10), 1874–1885. <https://doi.org/10.2337/db19-0308>

Sharma, A. X., & Holland, W. L. (2017). Adiponectin and its Hydrolase-Activated Receptors. *Journal of Nature and Science*, 3(6). [/pmc/articles/PMC5531184/](https://doi.org/10.4236/jns.2017.36006)

Sharp, L. Z., Shinoda, K., Ohno, H., Scheel, D. W., Tomoda, E., Ruiz, L., Hu, H., Wang, L., Pavlova, Z., Gilsanz, V., & Kajimura, S. (2012). Human BAT Possesses Molecular Signatures That Resemble Beige/Brite Cells. *PLoS ONE*, 7(11). <https://doi.org/10.1371/journal.pone.0049452>

Shaul, P. W., Smart, E. J., Robinson, L. J., German, Z., Yuhanna, I. S., Ying, Y., Anderson, R. G. W., & Michel, T. (1996). Acylation targets endothelial nitric-oxide synthase to plasmalemmal

caveolae. *The Journal of Biological Chemistry*, 271(11), 6518–6522. <https://doi.org/10.1074/JBC.271.11.6518>

Shechter, R., London, A., Kuperman, Y., Ronen, A., Rolls, A., Chen, A., & Schwartz, M. (2013). Hypothalamic neuronal toll-like receptor 2 protects against age-induced obesity. *Scientific Reports* 2013 3:1, 3(1), 1–8. <https://doi.org/10.1038/srep01254>

Shen, C., Cheng, W., Yu, P., Wang, L., Zhou, L., Zeng, L., & Yang, Q. (2016). Resveratrol pretreatment attenuates injury and promotes proliferation of neural stem cells following oxygen-glucose deprivation/reoxygenation by upregulating the expression of Nrf2, HO-1 and NQO1 in vitro. *Molecular Medicine Reports*, 14(4), 3646–3654. <https://doi.org/10.3892/mmr.2016.5670>

Shepherd, P. R., Gould, G. W., Colville, C. A., McCoid, S. C., Gibbs, E. M., & Kahn, B. B. (1992). Distribution of GLUT3 glucose transporter protein in human tissues. *Biochemical and Biophysical Research Communications*, 188(1), 149–154.

Sherman, D. L., Fabrizi, C., Gillespie, C. S., & Brophy, P. J. (2001). Specific disruption of a schwann cell dystrophin-related protein complex in a demyelinating neuropathy. *Neuron*, 30(3), 677–687. [https://doi.org/10.1016/S0896-6273\(01\)00327-0](https://doi.org/10.1016/S0896-6273(01)00327-0)

Sherman, S. M., & Schnyer, D. M. (2016). Major and Mild Neurocognitive Disorders. *Encyclopedia of Mental Health: Second Edition*, 33–38. <https://doi.org/10.1016/B978-0-12-397045-9.00110-5>

Sherrington, R., Rogaev, E. I., Liang, Y. al, Rogaeva, E. A., Levesque, G., Ikeda, M., Chi, H., Lin, C., Li, G., & Holman, K. (1995). Cloning of a gene bearing missense mutations in early-onset familial Alzheimer's disease. *Nature*, 375(6534), 754–760.

Shi, C., Liu, J., Wu, F., & Yew, D. T. (2010). Ginkgo biloba extract in Alzheimer's disease: from action mechanisms to medical practice. *International Journal of Molecular Sciences*, 11(1), 107–123.

Shi, C., Zhao, L., Zhu, B., Li, Q., Yew, D. T., Yao, Z., & Xu, J. (2009). Dosage effects of EGb761 on hydrogen peroxide-induced cell death in SH-SY5Y cells. *Chemico-Biological Interactions*, 180(3), 389–397.

Shi, L., & Tu, B. P. (2015). Acetyl-CoA and the Regulation of Metabolism: Mechanisms and Consequences. *Current Opinion in Cell Biology*, 33, 125. <https://doi.org/10.1016/J.CEB.2015.02.003>

Shimomura, I., Bashmakov, Y., Ikemoto, S., Horton, J. D., Brown, M. S., & Goldstein, J. L. (1999). Insulin selectively increases SREBP-1c mRNA in the livers of rats with streptozotocin-induced diabetes. *Proceedings of the National Academy of Sciences of the United States of America*, 96(24), 13656–13661. <https://doi.org/10.1073/PNAS.96.24.13656>

Shin, T. (2007). Increases in the phosphorylated form of caveolin-1 in the spinal cord of rats with clip compression injury. *Brain Research, Complete* (1141), 228–234. <https://doi.org/10.1016/J.BRAINRES.2007.01.009>

Shin, Y. S., Kim, K. J., Park, H., Lee, M. G., Cho, S., Choi, S. I., Heo, H. J., Kim, D. O., & Kim, G. H. (2021). Effects of Ecklonia cava Extract on Neuronal Damage and Apoptosis in PC-12 Cells against Oxidative Stress. *J. Microbiol. Biotechnol.*, 31(4), 584–591. <https://doi.org/10.4014/JMB.2012.12013>

Shively, C. A., Appt, S. E., Vitolins, M. Z., Uberseder, B., Michalson, K. T., Silverstein-Metzler, M. G., & Register, T. C. (2019). Mediterranean versus Western Diet Effects on Caloric Intake, Obesity, Metabolism, and Hepatosteatosis in Nonhuman Primates. *Obesity (Silver Spring, Md.)*, 27(5), 777–784. <https://doi.org/10.1002/OBY.22436>

Shlomovitz, I., Speir, M., & Gerlic, M. (2019). Flipping the dogma – phosphatidylserine in non-apoptotic cell death. *Cell Communication and Signaling* 2019 17:1, 17(1), 1–12. <https://doi.org/10.1186/S12964-019-0437-0>

Sideri, A., Stavrakis, D., Bowe, C., Shih, D. Q., Fleshner, P., Arsenescu, V., Arsenescu, R., Turner, J. R., Pothoulakis, C., & Karagiannides, I. (2015). Effects of obesity on severity of colitis and cytokine expression in mouse mesenteric fat. Potential role of adiponectin receptor 1. *American Journal of Physiology - Gastrointestinal and Liver Physiology*, 308(7), G591–G604. <https://doi.org/10.1152/AJPGI.00269.2014>

Siegel, G., Ermilov, E., Knes, O., & Rodríguez, M. (2014). Combined lowering of low grade systemic inflammation and insulin resistance in metabolic syndrome patients treated with Ginkgo biloba. *Atherosclerosis*, 237(2), 584–588.

Sierra-Fonseca, J. A., Najera, O., Martinez-Jurado, J., Walker, E. M., Varela-Ramirez, A., Khan, A. M., Miranda, M., Lamango, N. S., & Roychowdhury, S. (2014). Nerve growth factor induces neurite outgrowth of PC12 cells by promoting Gβγ-microtubule interaction. *BMC Neuroscience*, 15(1), 1–19. <https://doi.org/10.1186/S12868-014-0132-4/FIGURES/8>

Sikder, K., Shukla, S. K., Patel, N., Singh, H., & Rafiq, K. (2018). High fat diet upregulates fatty acid oxidation and ketogenesis via intervention of PPAR-γ. *Cellular Physiology and Biochemistry*, 48(3), 1317-1331.

Simons, K., & Sampaio, J. L. (2011). Membrane Organization and Lipid Rafts. *Cold Spring Harbor Perspectives in Biology*, 3(10), a004697–a004697. <https://doi.org/10.1101/CSHPERSPECT.A004697>

Simons, M., Keller, P., Strooper, B. De, Beyreuther, K., Dotti, C. G., & Simons, K. (1998). Cholesterol depletion inhibits the generation of β-amyloid in hippocampal neurons. *Proceedings of the National Academy of Sciences*, 95(11), 6460–6464.

Simopoulos, A. P. (2001). Evolutionary aspects of diet and essential fatty acids. *World Review of Nutrition and Dietetics*, 88, 18–27.

Simopoulos, A. P. (2002). The importance of the ratio of omega-6/omega-3 essential fatty acids. *Biomedicine and Pharmacotherapy*, 56(8), 365–379. [https://doi.org/10.1016/S0753-3322\(02\)00253-6](https://doi.org/10.1016/S0753-3322(02)00253-6)

Simopoulos, A. P. (2008). The importance of the omega-6/omega-3 fatty acid ratio in cardiovascular disease and other chronic diseases. *Experimental Biology and Medicine*, 233(6), 674–688.

Simopoulos, A. P. (2016). An increase in the Omega-6/Omega-3 fatty acid ratio increases the risk for obesity. *Nutrients*, 8, 128.

Simpson, I. A., Chundu, K. R., Davies-Hill, T., Honer, W. G., & Davies, P. (1994). Decreased concentrations of GLUT1 and GLUT3 glucose transporters in the brains of patients with Alzheimer's disease. *Annals of Neurology: Official Journal of the American Neurological Association and the Child Neurology Society*, 35(5), 546–551.

Sims, R., Hill, M., & Williams, J. (2020). The multiplex model of the genetics of Alzheimer's disease. *Nature Neuroscience* 2020 23:3, 23(3), 311–322. <https://doi.org/10.1038/s41593-020-0599-5>

Singh, A., Kukreti, R., Saso, L., & Kukreti, S. (2019). Oxidative stress: A key modulator in neurodegenerative diseases. *Molecules*, 24(8). <https://doi.org/10.3390/molecules24081583>

Singh, B., Parsaik, A. K., Mielke, M. M., Erwin, P. J., Knopman, D. S., Petersen, R. C., & Roberts, R. O. (2014). Association of mediterranean diet with mild cognitive impairment and Alzheimer's disease: a systematic review and meta-analysis. *Journal of Alzheimer's Disease*, 39(2), 271–282.

Singh, M. (2005). Essential fatty acids, DHA human brain. In *Indian Journal of Pediatrics* (Vol. 72, Issue 3, pp. 239–242). The Indian Journal of Pediatrics. <https://doi.org/10.1007/BF02859265>

Singh, S. K., Srivastav, S., Castellani, R. J., Plascencia-Villa, G., & Perry, G. (2019). Neuroprotective and Antioxidant Effect of Ginkgo biloba Extract Against AD and Other Neurological Disorders. *Neurotherapeutics: The Journal of the American Society for Experimental NeuroTherapeutics*, 16(3), 666–674. <https://doi.org/10.1007/S13311-019-00767-8>

Skoog, I., Lernfelt, B., Landahl, S., Palmertz, B., Andreasson, L. A., Nilsson, L., Persson, G., Odén, A., & Svanborg, A. (1996). 15-year longitudinal study of blood pressure and dementia. *Lancet* (London, England), 347(9009), 1141–1145. [https://doi.org/10.1016/S0140-6736\(96\)90608-X](https://doi.org/10.1016/S0140-6736(96)90608-X)

Smith, J. V., & Luo, Y. (2003). Elevation of oxidative free radicals in Alzheimer's disease models can be attenuated by Ginkgo biloba extract EGb 761. *Journal of Alzheimer's Disease*, 5(4), 287–300.

Smith, J. v, & Luo, Y. (2004). Studies on molecular mechanisms of Ginkgo biloba extract. *Applied Microbiology and Biotechnology*, 64(4), 465–472.

Solinas, G., Borén, J., & Dulloo, A. G. (2015). *De novo* lipogenesis in metabolic homeostasis: More friend than foe? *Molecular Metabolism*, 4(5), 367–377. <https://doi.org/10.1016/J.MOLMET.2015.03.004>

Song, Y., & Jensen, M. D. (2021). Red blood cell triglycerides—a unique pool that incorporates plasma-free fatty acids and relates to metabolic health. *Journal of Lipid Research*, 62. <https://doi.org/10.1016/j.jlr.2021.100131>

Song, Z., Xiaoli, A. M., & Yang, F. (2018). Regulation and Metabolic Significance of *De novo* Lipogenesis in Adipose Tissues. *Nutrients* 2018, Vol. 10, Page 1383, 10(10), 1383. <https://doi.org/10.3390/nu10101383>

Sonnenburg, J. L., & Bäckhed, F. (2016). Diet-microbiota interactions as moderators of human metabolism. *Nature*, 535, 56–64.

Sousa, S., Teixeira, L., & Paúl, C. (2020). Assessment of major neurocognitive disorders in primary health care: Predictors of individual risk factors. *Frontiers in Psychology*, 11, 1413. <https://doi.org/10.3389/fpsyg.2020.01413>/BIBTEX

Spadiene, A., Savickiene, N., Skesters, A., Silova, A., & Rodovicius, H. (2012). The effects of Ginkgo biloba L. and Camellia sinensis L. extracts on oxidative stress in patients with type 2 diabetes. *African Journal of Pharmacy and Pharmacology*, 6(44), 3080–3085.

Spalding, K. L., Arner, E., Westermark, P. O., Bernard, S., Buchholz, B. A., Bergmann, O., Blomqvist, L., Hoffstedt, J., Näslund, E., Britton, T., Concha, H., Hassan, M., Rydén, M., Frisén, J., & Arner, P. (2008). Dynamics of fat cell turnover in humans. *Nature*, 453(7196), 783–787. <https://doi.org/10.1038/NATURE06902>

Spector, A. A. (2001). Plasma free fatty acid and lipoproteins as sources of polyunsaturated fatty acid for the brain. *Journal of Molecular Neuroscience* 2001 16:2, 16(2), 159–165. <https://doi.org/10.1385/JMN:16:2-3:159>

Stanton, M. C., Chen, S. C., Jackson, J. V., Rojas-Triana, A., Kinsley, D., Cui, L., Fine, J. S., Greenfeder, S., Bober, L. A., & Jenh, C. H. (2011). Inflammatory Signals shift from adipose to liver during high fat feeding and influence the development of steatohepatitis in mice. *Journal of Inflammation*, 8. <https://doi.org/10.1186/1476-9255-8-8>

Staprans, I., Rapp, J. H., Pan, X. M., Ong, D. L., & Feingold, K. R. (1990). Testosterone regulates metabolism of plasma chylomicrons in rats. *Arteriosclerosis (Dallas, Tex.)*, 10(4), 591–596. <https://doi.org/10.1161/01.ATV.10.4.591>

Stellaard, F., & Lütjohann, D. (2021). Dynamics of the enterohepatic circulation of bile acids in healthy humans. *American Journal of Physiology - Gastrointestinal and Liver Physiology*, 321(1), G55–G66. <https://doi.org/10.1152/AJPGI.00476.2020>/ASSET/IMAGES/LARGE/AJPGI.00476.2020_F005.JPEG

Stephens, T. W., Basinski, M., Bristow, P. K., Bue-Valleskey, J. M., Burgett, S. G., Craft, L., Hale, J., Hoffmann, J., Hsiung, H. M., Kriauciunas, A., MacKellar, W., Rosteck, P. R., Schoner, B., Smith, D., Tinsley, F. C., Zhang, X. Y., & Heiman, M. (1995). The role of neuropeptide Y in the antiobesity action of the obese gene product. *Nature*, 377(6549), 530–532. <https://doi.org/10.1038/377530A0>

Stern, J. H., Rutkowski, J. M., & Scherer, P. E. (2016). Adiponectin, Leptin, and Fatty Acids in the Maintenance of Metabolic Homeostasis Through Adipose Tissue Crosstalk. *Cell Metabolism*, 23(5), 770. <https://doi.org/10.1016/j.cmet.2016.04.011>

Stern, Y. (2012). Cognitive reserve in ageing and Alzheimer's disease. *Lancet Neurology*, 11(11), 1006. [https://doi.org/10.1016/S1474-4422\(12\)70191-6](https://doi.org/10.1016/S1474-4422(12)70191-6)

Stillwell, W., & Wassall, S. R. (2003). Docosahexaenoic acid: Membrane properties of a unique fatty acid. *Chemistry and Physics of Lipids*, 126(1), 1–27. [https://doi.org/10.1016/S0009-3084\(03\)00101-4](https://doi.org/10.1016/S0009-3084(03)00101-4)

Storlien, L. H., Jenkins, A. B., Chisholm, D. J., Pascoe, W. S., Khouri, S., & Kraegen, E. W. (1991). Influence of dietary fat composition on development of insulin resistance in rats. Relationship to muscle triglyceride and omega-3 fatty acids in muscle phospholipid. *Diabetes*, 40(2), 280–289. <https://doi.org/10.2337/diab.40.2.280>

Stoyanova, I., & Lutz, D. (2021). Ghrelin-Mediated Regeneration and Plasticity After Nervous System Injury. *Frontiers in Cell and Developmental Biology*, 9. <https://doi.org/10.3389/fcell.2021.595914>

Strike, S. C., Carlisle, A., Gibson, E. L., & Dyllal, S. C. (2016). A high omega-3 fatty acid multinutrient supplement benefits cognition and mobility in older women: A randomized, double-blind, placebo-controlled pilot study. *Journals of Gerontology Series A: Biomedical Sciences and Medical Sciences*, 71(2), 236–242.

Strittmatter, W. J., Saunders, A. M., Schmechel, D., Pericak-Vance, M., Enghild, J., Salvesen, G. S., & Roses, A. D. (1993). Apolipoprotein E: high-avidity binding to beta-amyloid and increased frequency of type 4 allele in late-onset familial Alzheimer disease. *Proceedings of the National Academy of Sciences*, 90(5), 1977–1981.

Stryer, L., Berg, J., Tymoczko, J., & Gatto, G. (2019). *Biochemistry*. Macmillan Learning. <https://books.google.ie/books?id=lyGNtwEACAAJ>

Sublette, M. E., Bosetti, F., Demar, J. C., Ma, K., Bell, J. M., Fagin-jones, S., Russ, M. J., & Rapoport, S. I. (2007). Plasma free polyunsaturated fatty acid levels are associated with symptom severity in acute mania. *Bipolar Disorders*, 9(7), 759–765. <https://doi.org/10.1111/j.1399-5618.2007.00387.x>

Sultana, R., & Butterfield, D. A. (2010). Role of oxidative stress in the progression of Alzheimer's disease. *Journal of Alzheimer's Disease*, 19(1), 341–353.

Sun, A. Y., Simonyi, A., & Sun, G. Y. (2002). The 'French Paradox' and beyond: neuroprotective effects of polyphenols. *Free Radical Biology & Medicine*, 32(4), 314–318. [https://doi.org/10.1016/S0891-5849\(01\)00803-6](https://doi.org/10.1016/S0891-5849(01)00803-6)

Sun, A. Y., Wang, Q., Simonyi, A., & Sun, G. Y. (2010). Resveratrol as a therapeutic agent for neurodegenerative diseases. *Molecular Neurobiology*, 41(2–3), 375–383. <https://doi.org/10.1007/s12035-010-8111-y>

Sun, Q., Ma, J., Campos, H., & Hu, F. B. (2007). Plasma and erythrocyte biomarkers of dairy fat intake and risk of ischemic heart disease. *The American Journal of Clinical Nutrition*, 86(4), 929–937. <https://doi.org/10.1093/AJCN/86.4.929>

Sun, X., Yamasaki, M., Katsube, T., & Shiwaku, K. (2015). Effects of quercetin derivatives from mulberry leaves: Improved gene expression related hepatic lipid and glucose metabolism in short-term high-fat fed mice. *Nutrition Research and Practice*, 9(2), 137–143. <https://doi.org/10.4162/NRP.2015.9.2.137>

Sun, Z., Hu, W., Yin, S., Lu, X., Zuo, W., Ge, S., & Xu, Y. (2017). NGF protects against oxygen and glucose deprivation-induced oxidative stress and apoptosis by up-regulation of HO-1 through MEK/ERK pathway. *Neuroscience Letters*, 641, 8–14. <https://doi.org/10.1016/j.neulet.2017.01.046>

Suzanne, M. (2014). Type 3 diabetes is sporadic Alzheimer's disease: mini review. *European Neuropsychopharmacology*, 24(12), 1954–1960.

Suzuki, J., Denning, D. P., Imanishi, E., Horvitz, H. R., & Nagata, S. (2013). Xk-related protein 8 and CED-8 promote phosphatidylserine exposure in apoptotic cells. *Science (New York, N.Y.)*, 341(6144), 403–406. <https://doi.org/10.1126/SCIENCE.1236758>

Suzuki, J., Umeda, M., Sims, P. J., & Nagata, S. (2010). Calcium-dependent phospholipid scrambling by TMEM16F. *Nature*, 468(7325), 834–840. <https://doi.org/10.1038/NATURE09583>

Suzuki, S., Numakawa, T., Shimazu, K., Koshimizu, H., Hara, T., Hatanaka, H., Mei, L., Lu, B., & Kojima, M. (2004). BDNF-induced recruitment of TrkB receptor into neuronal lipid rafts: roles in synaptic modulation. *The Journal of Cell Biology*, 167(6), 1205–1215.

Svärd, J., Røst, T. H., Sommervoll, C. E. N., Haugen, C., Gudbrandsen, O. A., Mellgren, A. E., Rødahl, E., Fernø, J., Dankel, S. N., Sagen, J. v., & Mellgren, G. (2019). Absence of the proteoglycan decorin reduces glucose tolerance in overfed male mice. *Scientific Reports* 2019 9:1, 9(1), 1–12. <https://doi.org/10.1038/s41598-018-37501-x>

Syed, I., Lee, J., Moraes-Vieira, P. M., Donaldson, C. J., Sontheimer, A., Aryal, P., Wellenstein, K., Kolar, M. J., Nelson, A. T., Siegel, D., Mokrosinski, J., Farooqi, I. S., Zhao, J. J., Yore, M. M., Peroni, O. D., Saghatelian, A., & Kahn, B. B. (2018). Palmitic Acid Hydroxy Stearic Acids Activate GPR40 Which is Involved in Their Beneficial Effects on Glucose Homeostasis. *Cell Metabolism*, 27(2), 419. <https://doi.org/10.1016/j.cmet.2018.01.001>

Szablewski, L. (2017). Glucose Transporters in Brain: In Health and in Alzheimer's Disease. *Journal of Alzheimer's Disease*, 55(4), 1307–1320. <https://doi.org/10.3233/JAD-160841>

Tahri-Joutey, M., Andreoletti, P., Surapureddi, S., Nasser, B., Cherkaoui-Malki, M., & Latruffe, N. (2021). Mechanisms Mediating the Regulation of Peroxisomal Fatty Acid Beta-Oxidation by PPAR α . *International Journal of Molecular Sciences*, 22(16). <https://doi.org/10.3390/IJMS22168969>

Takei, N., & Nawa, H. (2014). mTOR signaling and its roles in normal and abnormal brain development. *Frontiers in Molecular Neuroscience*, 7(1 APR), 28. <https://doi.org/10.3389/FNMOL.2014.00028/BIBTEX>

Takeuchi, Y., Yahagi, N., Izumida, Y., Nishi, M., Kubota, M., Teraoka, Y., Yamamoto, T., Matsuzaka, T., Nakagawa, Y., Sekiya, M., Iizuka, Y., Ohashi, K., Osuga, J. I., Gotoda, T., Ishibashi, S., Itaka, K., Kataoka, K., Nagai, R., Yamada, N., ... Shimano, H. (2010). Polyunsaturated Fatty Acids Selectively Suppress Sterol Regulatory Element-binding Protein-1 through Proteolytic Processing and Autoloop Regulatory Circuit. *The Journal of Biological Chemistry*, 285(15), 11681. <https://doi.org/10.1074/JBC.M109.096107>

Tallima, H., & Ridi, R. el. (2018). Arachidonic acid: Physiological roles and potential health benefits: A review. *Journal of Advanced Research*, 11, 33–41. <https://doi.org/10.1016/j.jare.2017.11.004>

Tan, J., McKenzie, C., Potamitis, M., Thorburn, A. N., Mackay, C. R., & Macia, L. (2014). The role of short-chain fatty acids in health and disease. *Advances in Immunology*, 121, 91–119. <https://doi.org/10.1016/B978-0-12-800100-4.00003-9>

Tan, X., Sun, Z., & Ye, C. (2020). Dietary Ginkgo biloba leaf extracts supplementation improved immunity and intestinal morphology, antioxidant ability and tight junction proteins mRNA expression of hybrid groupers (*Epinephelus lanceolatus*♂× *Epinephelus fuscoguttatus*♀) fed high lipid diets. *Fish & Shellfish Immunology*, 98, 611–618.

Tans, R., Bande, R., van Rooij, A., Molloy, B. J., Stienstra, R., Tack, C. J., Wevers, R. A., Wessels, H. J. C. T., Gloorich, J., & van Gool, A. J. (2020). Evaluation of cyclooxygenase oxylipins as potential biomarker for obesity-associated adipose tissue inflammation and type 2 diabetes using targeted multiple reaction monitoring mass spectrometry. *Prostaglandins, Leukotrienes and Essential Fatty Acids*, 160, 102157. <https://doi.org/10.1016/J.PLEFA.2020.102157>

Tapia, G., Valenzuela, R., Espinosa, A., Romanque, P., Dossi, C., Gonzalez-Mañán, D., Videla, L. A., & D'Espessailles, A. (2014). N-3 long-chain PUFA supplementation prevents high fat diet induced mouse liver steatosis and inflammation in relation to PPAR-alpha upregulation and NF-kappaB DNA binding abrogation. *Mol Nutr Food Res*, 58(6), 1333–1341. <https://doi.org/10.1002/mnfr.201300458>

Tariq, K., & Luikart, B. W. (2021). Striking a balance: PIP2 and PIP3 signaling in neuronal health and disease. *Exploration of Neuroprotective Therapy*, 1(2), 86. <https://doi.org/10.37349/ENT.2021.00008>

Tchantchou, F., Lacor, P. N., Cao, Z., Lao, L., Hou, Y., Cui, C., Klein, W. L., & Luo, Y. (2009). Stimulation of neurogenesis and synaptogenesis by bilobalide and quercetin via common final pathway in hippocampal neurons. *Journal of Alzheimer's Disease: JAD*, 18(4), 787–798. <https://doi.org/10.3233/JAD-2009-1189>

Teixeira, L. G., Leonel, A. J., Aguilar, E. C., Batista, N. v., Alves, A. C., Coimbra, C. C., Ferreira, A. V. M., de Faria, A. M. C., Cara, D. C., & Alvarez Leite, J. I. (2011). The combination of high-fat diet-induced obesity and chronic ulcerative colitis reciprocally exacerbates adipose tissue

and colon inflammation. *Lipids in Health and Disease*, 10. <https://doi.org/10.1186/1476-511X-10-204>

Tendi, E., Bosetti, F., Dasgupta, S., Stella, A., & Drieu, K. (2002). Ginkgo biloba extracts EGb 761 and bilobalide increase NADH dehydrogenase mRNA level and mitochondrial respiratory control ratio in PC12 cells. *Neurochem Res*, 27.

Terry, R. B., Stefanick, M. L., Haskell, W. L., & Wood, P. D. (1991). Contributions of regional adipose tissue depots to plasma lipoprotein concentrations in overweight men and women: Possible protective effects of thigh fat. *Metabolism*, 40(7), 733–740. [https://doi.org/10.1016/0026-0495\(91\)90093-C](https://doi.org/10.1016/0026-0495(91)90093-C)

Thaler, J. P., Yi, C. X., Schur, E. A., Guyenet, S. J., Hwang, B. H., Dietrich, M. O., Zhao, X., Sarruf, D. A., Izgur, V., Maravilla, K. R., & al., et. (2012). Obesity is associated with hypothalamic injury in rodents and humans. *J. Clin. Invest.*, 122, 153–162.

Thanoon, I. A.-J., Abdul-Jabbar, H. A., & Taha, D. A. (2012). Oxidative Stress and C-Reactive Protein in Patients with Cerebrovascular Accident (Ischaemic Stroke): The role of Ginkgo biloba extract. *Sultan Qaboos University Medical Journal*, 12(2), 197–205. <https://doi.org/10.12816/0003113>

Thermo-Fisher. (2020). Useful Numbers for Cell Culture. https://www.thermofisher.com/uk/en/home/references/gibco-cell-culture-basics/cell-culture-protocols/cell-culture-useful-numbers.html?gclid=EAlaIqobChMI1uLG47z05wIVmpntCh0OMw53EAAYASAAEgK8kPD_BwE&s_kwid=AL!3652!3!342304045410!e!!g!!useful

Thon, M., Hosoi, T., & Ozawa, K. (2016). Insulin enhanced leptin-induced STAT3 signaling by inducing GRP78. *Scientific Reports*, 6. <https://doi.org/10.1038/SREP34312>

Tian, J., Liu, Y., & Chen, K. (2017). Ginkgo biloba extract in vascular protection: molecular mechanisms and clinical applications. *Curr Vasc Pharmacol*, 15(6), 532–548.

Tini, G., Scagliola, R., Monacelli, F., La Malfa, G., Porto, I., Brunelli, C., & Rosa, G. M. (2020). Alzheimer's Disease and Cardiovascular Disease: A Particular Association. *Cardiology Research and Practice*, 2020. <https://doi.org/10.1155/2020/2617970>

Titchenell, P. M., Quinn, W. J., Lu, M., Chu, Q., Lu, W., Li, C., Chen, H., Monks, B. R., Chen, J., Rabinowitz, J. D., & Birnbaum, M. J. (2016). Direct Hepatocyte Insulin Signaling Is Required for Lipogenesis but Is Dispensable for the Suppression of Glucose Production. *Cell Metabolism*, 23(6), 1154–1166. <https://doi.org/10.1016/J.CMET.2016.04.022>

Torres-Piedra, M., Ortiz-Andrade, R., Villalobos-Molina, R., Singh, N., Medina-Franco, J. L., Webster, S. P., Binnie, M., Navarrete-Vázquez, G., & Estrada-Soto, S. (2010). A comparative study of flavonoid analogues on streptozotocin-nicotinamide induced diabetic rats: quercetin as a potential antidiabetic agent acting via 11beta-hydroxysteroid dehydrogenase type 1 inhibition. *European Journal of Medicinal Chemistry*, 45(6), 2606–2612. <https://doi.org/10.1016/J.EJMECH.2010.02.049>

Trøseid, M., Nestvold, T. K., Rudi, K., Thoresen, H., Nielsen, E. W., & Lappegård, K. T. (2013). Plasma lipopolysaccharide is closely associated with glycemic control and abdominal obesity: evidence from bariatric surgery. *Diabetes Care*, 36(11), 3627–3632. <https://doi.org/10.2337/DC13-0451>

Tsaban, G., Yaskolka Meir, A., Zelicha, H., Rinott, E., Kaplan, A., Shalev, A., Katz, A., Brikner, D., Blüher, M., Ceglarek, U., Stumvoll, M., Stampfer, M. J., & Shai, I. (2022). Diet-induced Fasting Ghrelin Elevation Reflects the Recovery of Insulin Sensitivity and Visceral Adiposity Regression. *The Journal of Clinical Endocrinology & Metabolism*, 107(2), 336–345. <https://doi.org/10.1210/CLINEM/DGAB681>

Tsai, K. L., Chang, Y. L., Huang, P. H., Cheng, Y. H., Liu, D. H., Chen, H. Y., & Kao, C. L. (2016). Ginkgo biloba extract inhibits oxidized low-density lipoprotein (oxLDL)-induced matrix metalloproteinase activation by the modulation of the lectin-like oxLDL receptor 1-regulated signaling pathway in human umbilical vein endothelial cells. *Journal of Vascular Surgery*, 63(1), 204–215.e1. <https://doi.org/10.1016/J.JVS.2014.05.098>

Tsitouras, P. D., Gucciardo, F., Salbe, A. D., Heward, C., & Harman, S. M. (2008). High omega-3 fat intake improves insulin sensitivity and reduces CRP and IL6, but does not affect other endocrine axes in healthy older adults. *Hormone and Metabolic Research*, 40(03), 199–205.

Tuncman, G., Hirosumi, J., Solinas, G., Chang, L., Karin, M., & Hotamisligil, G. S. (2006). Functional in vivo interactions between JNK1 and JNK2 isoforms in obesity and insulin resistance. *Proc Natl Acad Sci U S A*, 103(28), 10741–10746. <https://doi.org/10.1073/pnas.0603509103>

Turnbaugh, P. J., Ley, R. E., Mahowald, M. A., Magrini, V., Mardis, E. R., & Gordon, J. I. (2006). An obesity-associated gut microbiome with increased capacity for energy harvest. *Nature*, 444(7122), 1027–1031. <https://doi.org/10.1038/NATURE05414>

Turner, N., Else, P. L., & Hulbert, A. J. (2003). Docosahexaenoic acid (DHA) content of membranes determines molecular activity of the sodium pump: Implications for disease states and metabolism. *Naturwissenschaften*, 90(11), 521–523. <https://doi.org/10.1007/S00114-003-0470-Z>

Turner, R. S., Thomas, R. G., Craft, S., van Dyck, C. H., Mintzer, J., Reynolds, B. A., Brewer, J. B., Rissman, R. A., Raman, R., Aisen, P. S., & Study, A. D. C. (2015). A randomized, double-blind, placebo-controlled trial of resveratrol for Alzheimer disease. *Neurology*, 85(16), 1383–1391. <https://doi.org/10.1212/WNL.0000000000002035>

Udenwobele, D. I., Su, R. C., Good, S. V., Ball, T. B., Shrivastav, S. V., & Shrivastav, A. (2017). Myristoylation: An important protein modification in the immune response. *Frontiers in Immunology*, 8(JUN), 751. <https://doi.org/10.3389/FIMMU.2017.00751/BIBTEX>

Ueberberg, B., Unger, N., Saeger, W., Mann, K., & Petersenn, S. (2009). Expression of ghrelin and its receptor in human tissues. *Hormone and Metabolic Research*, 41(11), 814–821. <https://doi.org/10.1055/S-0029-1233462>

Ulmer, C. Z., Jones, C. M., Yost, R. A., Garrett, T. J., & Bowden, J. A. (2018). Optimization of Folch, Bligh-Dyer, and Matyash sample-to-extraction solvent ratios for human plasma-based lipidomics studies. *Analytica Chimica Acta*, 1037, 351–357.

U.S. Department of Agriculture, A. R. S. (2016). Energy intakes: percentages of energy from protein, carbohydrate, fat, and alcohol, by gender and age. What We Eat in America, NHANES 2013–2014 Dietary Data. <https://wwwn.cdc.gov/nchs/nhanes/search/DataPage.aspx?Component=Dietary&CycleBeginYear=2013>

Valenzuela, R., & Videla, L. A. (2011). The importance of the long-chain polyunsaturated fatty acid n-6/n-3 ratio in development of non-alcoholic fatty liver associated with obesity. *Food & Function*, 2(11), 644–648. <https://doi.org/10.1039/C1FO10133A>

Valerio, A., Cardile, A., Cozzi, V., Bracale, R., Tedesco, L., Pisconti, A., Palomba, L., Cantoni, O., Clementi, E., Moncada, S., Carruba, M. O., & Nisoli, E. (2006). TNF-alpha downregulates eNOS expression and mitochondrial biogenesis in fat and muscle of obese rodents. *The Journal of Clinical Investigation*, 116(10), 2791–2798. <https://doi.org/10.1172/JCI28570>

Vallim, T. Q. D.-A., Tarling, E. J., & Edwards, P. A. (2013). Pleiotropic roles of bile acids in metabolism. *Cell Metabolism*, 17(5), 657–669. <https://doi.org/10.1016/J.CMET.2013.03.013>

Vallim, T., & Salter, A. M. (2010). Regulation of hepatic gene expression by saturated fatty acids. *Prostaglandins, Leukotrienes, and Essential Fatty Acids*, 82(4–6), 211. <https://doi.org/10.1016/J.PLEFA.2010.02.016>

van der Veen, J. N., Kennelly, J. P., Wan, S., Vance, J. E., Vance, D. E., & Jacobs, R. L. (2017). The critical role of phosphatidylcholine and phosphatidylethanolamine metabolism in health and disease. *Biochimica et Biophysica Acta (BBA) - Biomembranes*, 1859(9), 1558–1572. <https://doi.org/10.1016/J.BBAMEM.2017.04.006>

van IJendoorn, S. C. D., Agnetti, J., & Gassama-Diagne, A. (2020). Mechanisms behind the polarized distribution of lipids in epithelial cells. *Biochimica et Biophysica Acta (BBA) - Biomembranes*, 1862(2), 183145. <https://doi.org/10.1016/J.BBAMEM.2019.183145>

van Loenhoud, A. C., Groot, C., Vogel, J. W., van der Flier, W. M., & Ossenkoppele, R. (2018). Is intracranial volume a suitable proxy for brain reserve? Rik Ossenkoppele. *Alzheimer's Research and Therapy*, 10(1), 1–12. <https://doi.org/10.1186/S13195-018-0408-5/FIGURES/5>

van Meer, G. (2011). Dynamic transbilayer lipid asymmetry. *Cold Spring Harbor Perspectives in Biology*, 3(5), 1–11. <https://doi.org/10.1101/CSHPERSPECT.A004671>

Van Meer, G., & de Kroon, A. I. P. M. (2011). Lipid map of the mammalian cell. *Journal of Cell Science*, 124(1), 5–8. <https://doi.org/10.1242/JCS.071233>

van Meer, G., Voelker, D. R., & Feigenson, G. W. (2008). Membrane lipids: where they are and how they behave. *Nature Reviews. Molecular Cell Biology*, 9(2), 112. <https://doi.org/10.1038/NRM2330>

van Name, M. A., Savoye, M., Chick, J. M., Galuppo, B. T., Feldstein, A. E., Pierpont, B., Johnson, C., Shabanova, V., Ekong, U., Valentino, P. L., Kim, G., Caprio, S., & Santoro, N. (2020). A Low ω -6 to ω -3 PUFA Ratio (n-6: n-3 PUFA) Diet to Treat Fatty Liver Disease in Obese Youth. *The Journal of Nutrition*, 150(9), 2314–2321. <https://doi.org/10.1093/JN/NXAA183>

Vanamala, J., Reddivari, L., Radhakrishnan, S., & Tarver, C. (2010). Resveratrol suppresses IGF-1 induced human colon cancer cell proliferation and elevates apoptosis via suppression of IGF-1R/Wnt and activation of p53 signaling pathways. *BMC Cancer*, 10(1), 238.

Vargovic, P., Ukropec, J., Laukova, M., Cleary, S., Manz, B., Pacak, K., & Kvetnansky, R. (2011). Adipocytes as a new source of catecholamine production. *FEBS Letters*, 585(14), 2279–2284. <https://doi.org/10.1016/J.FEBSLET.2011.06.001>

Vegiopoulos, A., Rohm, M., & Herzig, S. (2017). Adipose tissue: between the extremes. *The EMBO Journal*, 36(14), 1999–2017. <https://doi.org/10.15252/EMBJ.201696206>

Velloso, L. A., & Schwartz, M. W. (2011). Altered hypothalamic function in diet-induced obesity. *International Journal of Obesity* (2005), 35(12), 1455–1465. <https://doi.org/10.1038/IJO.2011.56>

Verde, F., Otto, M., & Silani, V. (2021). Neurofilament Light Chain as Biomarker for Amyotrophic Lateral Sclerosis and Frontotemporal Dementia. *Frontiers in Neuroscience*, 15, 679199. <https://doi.org/10.3389/fnins.2021.679199>

Vestergaard, E. T., Gormsen, L. C., Jessen, N., Lund, S., Hansen, T. K., Moller, N., & Jorgensen, J. O. L. (2008). Ghrelin infusion in humans induces acute insulin resistance and lipolysis independent of growth hormone signaling. *Diabetes*, 57(12), 3205–3210. <https://doi.org/10.2337/DB08-0025>

Victorio, J. A., Guizoni, D. M., Freitas, I. N., Araujo, T. R., & Davel, A. P. (2021). Effects of High-Fat and High-Fat/High-Sucrose Diet-Induced Obesity on PVAT Modulation of Vascular Function in Male and Female Mice. *Frontiers in Pharmacology*, 12, 2252. <https://doi.org/10.3389/FPHAR.2021.720224/BIBTEX>

Videla, L. A., Rodrigo, R., Araya, J., & Poniachik, J. (2004). Oxidative stress and depletion of hepatic long-chain polyunsaturated fatty acids may contribute to nonalcoholic fatty liver disease. *Free Radical Biology & Medicine*, 37(9), 1499–1507. <https://doi.org/10.1016/j.freeradbiomed.2004.06.033>

Viguerie, N., Vidal, H., Arner, P., Holst, C., Verdich, C., Avizou, S., Astrup, A., Saris, W. H. M., Macdonald, I. A., & Klimcakova, E. (2005). Adipose tissue gene expression in obese subjects during low-fat and high-fat hypocaloric diets. *Diabetologia*, 48(1), 123–131.

Villeneuve, N. F., Lau, A., & Zhang, D. D. (2010). Regulation of the Nrf2–Keap1 antioxidant response by the ubiquitin proteasome system: an insight into cullin-ring ubiquitin ligases. *Antioxidants & Redox Signaling*, 13(11), 1699–1712.

Vingtdeux, V., Dreses-Werringloer, U., Zhao, H., Davies, P., & Marambaud, P. (2008). Therapeutic potential of resveratrol in Alzheimer's disease. *BMC Neuroscience*, 9(S2), S6–S6.

Vingtdeux, V., Giliberto, L., Zhao, H., Chandakkar, P., Wu, Q., Simon, J. E., Janle, E. M., Lobo, J., Ferruzzi, M. G., & Davies, P. (2010). AMP-activated protein kinase signaling activation by resveratrol modulates amyloid- β peptide metabolism. *Journal of Biological Chemistry*, 285(12), 9100–9113.

Vinolo, M. A. R., Rodrigues, H. G., Nachbar, R. T., & Curi, R. (2011). Regulation of Inflammation by Short Chain Fatty Acids. *Nutrients* 2011, Vol. 3, Pages 858-876, 3(10), 858–876. <https://doi.org/10.3390/NU3100858>

von Frankenberg, A. D., Marina, A., Song, X., Callahan, H. S., Kratz, M., & Utzschneider, K. M. (2017). A high-fat, high-saturated fat diet decreases insulin sensitivity without changing intra-abdominal fat in weight-stable overweight and obese adults. *European Journal of Nutrition*, 56(1), 431–443. <https://doi.org/10.1007/S00394-015-1108-6>

Votruba, S. B., & Jensen, M. D. (2006). Sex-specific differences in leg fat uptake are revealed with a high-fat meal. *American Journal of Physiology. Endocrinology and Metabolism*, 291(5). <https://doi.org/10.1152/AJPENDO.00196.2006>

Votruba, S. B., Mattison, R. S., Dumesic, D. A., Koutsari, C., & Jensen, M. D. (2007). Meal fatty acid uptake in visceral fat in women. *Diabetes*, 56(10), 2589–2597. <https://doi.org/10.2337/DB07-0439>

Wagner, A. E., Terschluesen, A. M., & Rimbach, G. (2013). Health promoting effects of brassica-derived phytochemicals: from chemopreventive and anti-inflammatory activities to epigenetic regulation. *Oxidative Medicine and Cellular Longevity*, 2013.

Wajchenberg, B. L. (2000). Subcutaneous and Visceral Adipose Tissue: Their Relation to the Metabolic Syndrome. *Endocrine Reviews*, 21(6), 697–738. <https://doi.org/10.1210/ER.21.6.697>

Wali, J. A., Jarzebska, N., Raubenheimer, D., Simpson, S. J., Rodionov, R. N., & O'sullivan, J. F. (2020). Cardio-Metabolic Effects of High-Fat Diets and Their Underlying Mechanisms—A Narrative Review. *Nutrients*, 12(5). <https://doi.org/10.3390/NU12051505>

Wanders, R. J. A., Waterham, H. R., & Ferdinandusse, S. (2016). Metabolic interplay between peroxisomes and other subcellular organelles including mitochondria and the endoplasmic reticulum. *Frontiers in Cell and Developmental Biology*, 3(JAN), 83. <https://doi.org/10.3389/FCELL.2015.00083/BIBTEX>

Wang, A., Huen, S. C., Luan, H. H., Yu, S., Zhang, C., Gallezot, J. D., Booth, C. J., & Medzhitov, R. (2016). Opposing Effects of Fasting Metabolism on Tissue Tolerance in Bacterial and Viral Inflammation. *Cell*, 166(6), 1512-1525.e12. <https://doi.org/10.1016/J.CELL.2016.07.026>

Wang, J., Ho, L., Zhao, W., Ono, K., Rosensweig, C., Chen, L., Humala, N., Teplow, D. B., & Pasinetti, G. M. (2008). Grape-derived polyphenolics prevent Abeta oligomerization and attenuate cognitive deterioration in a mouse model of Alzheimer's disease. *The Journal of Neuroscience: The Official Journal of the Society for Neuroscience*, 28(25), 6388–6392. <https://doi.org/10.1523/JNEUROSCI.0364-08.2008>

Wang, J., Ho, L., Zhao, Z., Seror, I., Humala, N., Dickstein, D. L., Thiyagarajan, M., Percival, S. S., Talcott, S. T., & Pasinetti, G. M. (2006). Moderate consumption of Cabernet Sauvignon attenuates A β neuropathology in a mouse model of Alzheimer's disease. *The FASEB Journal*, 20(13), 2313–2320.

Wang, L., Waltenberger, B., Pferschy-Wenzig, E. M., Blunder, M., Liu, X., Malainer, C., Blazevic, T., Schwaiger, S., Rollinger, J. M., Heiss, E. H., Schuster, D., Kopp, B., Bauer, R., Stuppner, H., Dirsch, V. M., & Atanasov, A. G. (2014). Natural product agonists of peroxisome proliferator-activated receptor gamma (PPAR γ): a review. *Biochemical Pharmacology*, 92(1), 73. <https://doi.org/10.1016/j.bcp.2014.07.018>

Wang, L. L., Zhang, Z. C., Hassan, W., Li, Y., Liu, J., & Shang, J. (2016). Amelioration of free fatty acid-induced fatty liver by quercetin-3-O- β -D-glucuronide through modulation of peroxisome proliferator-activated receptor- α /sterol regulatory element-binding protein-1c signaling. *Hepatology Research*, 46(2), 225-238.

Wang, X., Magkos, F., & Mittendorfer, B. (2011). Update: Sex Differences in Lipid and Lipoprotein Metabolism: It's Not Just about Sex Hormones. *The Journal of Clinical Endocrinology and Metabolism*, 96(4), 885–893. <https://doi.org/10.1210/jc.2010-2061>

Wang, X., & Michaelis, E. K. (2010). Selective neuronal vulnerability to oxidative stress in the brain. *Frontiers in Aging Neuroscience*, 2(MAR), 12. <https://doi.org/10.3389/fnagi.2010.00012/bibtext>

Wang, X., Wang, J., Gengyo-Ando, K., Gu, L., Sun, C. L., Yang, C., Shi, Y., Kobayashi, T., Shi, Y., Mitani, S., Xie, X. S., & Xue, D. (2007). C. elegans mitochondrial factor WAH-1 promotes phosphatidylserine externalization in apoptotic cells through phospholipid scramblase SCRM-1. *Nature Cell Biology*, 9(5), 541–549. <https://doi.org/10.1038/NCB1574>

Wang, Y., Botolin, D., Christian, B., Busik, J., Xu, J., & Jump, D. B. (2005). Tissue-specific, nutritional, and developmental regulation of rat fatty acid elongases. *Journal of Lipid Research*, 46(4), 706–715. <https://doi.org/10.1194/jlr.M400335-jlr200>

Wang, Y., Botolin, D., Xu, J., Christian, B., Mitchell, E., Jayaprakasam, B., Nair, M., Peters, J. M., Busik, J., Olson, L. K., & Jump, D. B. (2006). Regulation of hepatic fatty acid elongase and desaturase expression in diabetes and obesity. *Journal of Lipid Research*, 47(9), 2028–2041. <https://doi.org/10.1194/jlr.M600177-jlr200>

Wang, Y., Shinoda, Y., Cheng, A., Kawahata, I., & Fukunaga, K. (2021). Epidermal Fatty Acid-Binding Protein 5 (FABP5) Involvement in Alpha-Synuclein-Induced Mitochondrial Injury under Oxidative Stress. *Biomedicines* 2021, Vol. 9, Page 110, 9(2), 110. <https://doi.org/10.3390/biomedicines9020110>

Wang, Z., Park, H. G., Wang, D. H., Kitano, R., Kothapalli, K. S. D., & Brenna, J. T. (2020). Fatty acid desaturase 2 (FADS2) but not FADS1 desaturates branched chain and odd chain saturated fatty acids. *Biochimica et Biophysica Acta. Molecular and Cell Biology of Lipids*, 1865(3). <https://doi.org/10.1016/j.bbali.2019.158572>

Wang, Z. V., & Scherer, P. E. (2016). Adiponectin, the past two decades. *Journal of molecular cell biology*, 8(2), 93-100.

Watanabe, C. M. H., Wolffram, S., Ader, P., Rimbach, G., Packer, L., Maguire, J. J., Schultz, P. G., & Gohil, K. (2001a). The in vivo neuromodulatory effects of the herbal medicine ginkgo biloba. *Proceedings of the National Academy of Sciences*, 98(12), 6577–6580.

Watanabe, R. L. H., Boldarine, V. T., Pedroso, A. P., Telles, M. M., Dornellas, A. P. S., Wang, Y., Bueno, A., & Ribeiro, E. B. (2022). Soybean oil prevents hypothalamic N3 fatty acid composition but does not prevent peripheral tissue fatty acid disturbance in rats. *Revista Argentina de Endocrinología y Metabolismo (Argentine Journal of Endocrinology and Metabolism)*, 59(2), 24–40.

Watkins, P. A., & Ellis, J. M. (2012). Peroxisomal acyl-CoA synthetases. *Biochimica et Biophysica Acta (BBA) - Molecular Basis of Disease*, 1822(9), 1411–1420. <https://doi.org/10.1016/j.bbadis.2012.02.010>

Watson, H. (2015). Biological membranes. *Essays in Biochemistry*, 59, 43. <https://doi.org/10.1042/BSE0590043>

Weijers, R. N. M. (2012). Lipid composition of cell membranes and its relevance in type 2 diabetes mellitus. *Current Diabetes Reviews*, 8(5), 390–400. <https://doi.org/10.2174/157339912802083531>

Weijers, R. N. M. (2015a). Membrane flexibility, free fatty acids, and the onset of vascular and neurological lesions in type 2 diabetes. *Journal of Diabetes & Metabolic Disorders*, 15(1), 13.

Weijers, R. N. M. (2015b). Unsaturation index and type 2 diabetes: unknown, unloved. *World Journal of Meta-Analysis*, 3(2), 89–92.

Weijers, R. N. M. (2016a). Comment on Dornellas et al., Deleterious effects of lard-enriched diet on tissues fatty acids composition and hypothalamic insulin actions, Prostaglandins, Leukot. Essent. Fat. Acids., 102-103 (2015) 21-29. Prostaglandins, Leukotrienes, and Essential Fatty Acids, 107, 22–23. <https://doi.org/10.1016/j.plefa.2016.03.002>

Weijers, R. N. M. (2016b). Membrane flexibility, free fatty acids, and the onset of vascular and neurological lesions in type 2 diabetes. *Journal of Diabetes and Metabolic Disorders*, 15(1). <https://doi.org/10.1186/s40200-016-0235-9>

Weil, Z. M. (2012). Ischemia-induced hyperglycemia: consequences, neuroendocrine regulation, and a role for RAGE. *Hormones and Behavior*, 62(3), 280–285.

Weisberg, S. P., McCann, D., Desai, M., Rosenbaum, M., Leibel, R. L., & Ferrante, A. W. (2003). Obesity is associated with macrophage accumulation in adipose tissue. *The Journal of Clinical Investigation*, 112(12), 1796–1808. <https://doi.org/10.1172/JCI19246>

Weitzman, M. D., & Wang, J. Y. J. (2013). Cell Cycle: DNA Damage Checkpoints. *Encyclopedia of Biological Chemistry: Second Edition*, 410–416. <https://doi.org/10.1016/B978-0-12-378630-2.00419-9>

- Wettstein, A. (2000). Cholinesterase inhibitors and Ginkgo extracts — are they comparable in the treatment of dementia?: Comparison of published placebo-controlled efficacy studies of at least six months' duration. *Phytomedicine*, 6(6), 393–401. [https://doi.org/10.1016/S0944-7113\(00\)80066-5](https://doi.org/10.1016/S0944-7113(00)80066-5)
- Whitwell, J. L. (2010). The protective role of brain size in Alzheimer disease. *Expert Review of Neurotherapeutics*, 10(12), 1799. <https://doi.org/10.1586/ERN.10.168>
- Wiatrak, B., Kubis-Kubiak, A., Piwovar, A., & Barg, E. (2020). PC12 Cell Line: Cell Types, Coating of Culture Vessels, Differentiation and Other Culture Conditions. *Cells*, 9(4), 958. <https://doi.org/10.3390/cells9040958>
- Wichmann, A., Allahyar, A., Greiner, T. U., Plovier, H., Lundén, G. O., Larsson, T., Drucker, D. J., Delzenne, N. M., Cani, P. D., & Bäckhed, F. (2013). Microbial modulation of energy availability in the colon regulates intestinal transit. *Cell Host Microbe*, 14, 582–590.
- Williams, L. M. (2012). Hypothalamic dysfunction in obesity. *Proc Nutr Soc*, 71(4), 521–533. <https://doi.org/10.1017/s002966511200078x>
- Williams, S. K., & Rabbani, F. (2011a). Complications of lymphadenectomy in urologic surgery. *Urologic Clinics*, 38(4), 507–518.
- Wingo, T. S., Lah, J. J., Levey, A. I., & Cutler, D. J. (2012). Autosomal recessive causes likely in early-onset Alzheimer disease. *Archives of Neurology*, 69(1), 59–64.
- Wolfe, B. M., Kvach, E., & Eckel, R. H. (2016). Treatment of Obesity: Weight Loss and Bariatric Surgery. *Circulation Research*, 118(11), 1844. <https://doi.org/10.1161/CIRCRESAHA.116.307591>
- Wolk, A., Furuheim, M., & Vessby, B. (2001). Fatty Acid Composition of Adipose Tissue and Serum Lipids Are Valid Biological Markers Of Dairy Fat Intake in Men. *The Journal of Nutrition*, 131(3), 828–833. <https://doi.org/10.1093/JN/131.3.828>
- World Health Organisation. (2021). Obesity and overweight. <https://www.who.int/news-room/fact-sheets/detail/obesity-and-overweight>
- Wren, A. M., Small, C. J., Ward, H. L., Murphy, K. G., Dakin, C. L., Taheri, S., Kennedy, A. R., Roberts, G. H., Morgan, D. G. A., Ghatei, M. A., & Bloom, S. R. (2000). The Novel Hypothalamic Peptide Ghrelin Stimulates Food Intake and Growth Hormone Secretion. *Endocrinology*, 141(11), 4325–4328. <https://doi.org/10.1210/ENDO.141.11.7873>
- Wu, Z., Zhang, J., Gu, X., Zhang, X., Shi, S., & Liu, C. (2016). Effects of the extract of Ginkgo biloba on the differentiation of bone marrow mesenchymal stem cells in vitro. *American Journal of Translational Research*, 8(7), 3032. <file:///pmc/articles/PMC4969439/>
- Wueest, S., Yang, X., Liu, J., Schoenle, E. J., & Konrad, D. (2012). Inverse regulation of basal lipolysis in perigonadal and mesenteric fat depots in mice. *American Journal of Physiology - Endocrinology and Metabolism*, 302(1). <https://doi.org/10.1152/AJPENDO.00338.2011>

- Xia, C., Fu, Z., Battaile, K. P., & Kim, J. J. P. (2019). Crystal structure of human mitochondrial trifunctional protein, a fatty acid β -oxidation metabolon. *Proceedings of the National Academy of Sciences of the United States of America*, 116(13), 6069–6074. https://doi.org/10.1073/PNAS.1816317116/SUPPL_FILE/PNAS.1816317116.SAPP.PDF
- Xu, Y., Cui, C., Pang, C., Christen, Y., & Luo, Y. (2007a). Restoration of impaired phosphorylation of cyclic AMP response element-binding protein (CREB) by EGb 761 and its constituents in A β -expressing neuroblastoma cells. *European Journal of Neuroscience*, 26(10), 2931–2939.
- Yam, D., Eliraz, A., & Berry, E. M. (1996). Diet and disease—the Israeli paradox: possible dangers of a high omega-6 polyunsaturated fatty acid diet. *Israel Journal of Medical Sciences*, 32(11), 1134–1143.
- Yamakuchi, M., & Lowenstein, C. J. (2009). MiR-34, SIRT1, and p53: the feedback loop. *Cell Cycle*, 8(5), 712–715.
- Yamamoto, M., Kensler, T. W., & Motohashi, H. (2018a). The KEAP1-NRF2 system: a thiol-based sensor-effector apparatus for maintaining redox homeostasis. *Physiological Reviews*, 98(3), 1169–1203.
- Yan, M., Li, M., Gu, S., Sun, Z., Ma, T., & Ma, X. (2020). Ginkgo biloba extract protects diabetic rats against cerebral ischemia-reperfusion injury by suppressing oxidative stress and upregulating the expression of glutamate transporter 1. *Molecular Medicine Reports*.
- Yan, Z., Fan, R., Yin, S., Zhao, X., Liu, J., Li, L., Zhang, W., & Ge, L. (2015a). Protective effects of Ginkgo biloba leaf polysaccharide on nonalcoholic fatty liver disease and its mechanisms. *International Journal of Biological Macromolecules*, 80, 573–580. <https://doi.org/https://doi.org/10.1016/j.ijbiomac.2015.05.054>
- Yancheva, S., Ihl, R., Nikolova, G., Panayotov, P., Schlaefke, S., Hoerr, R., & for the GINDON Study Group. (2009). Ginkgo biloba extract EGb 761[®], donepezil or both combined in the treatment of Alzheimer's disease with neuropsychiatric features: A randomised, double-blind, exploratory trial. *Aging & Mental Health*, 13(2), 183–190. <https://doi.org/10.1080/13607860902749057>
- Yang, D., Tan, X., Lv, Z., Liu, B., Baiyun, R., Lu, J., & Zhang, Z. (2016). Regulation of Sirt1/Nrf2/TNF- α signaling pathway by luteolin is critical to attenuate acute mercuric chloride exposure induced hepatotoxicity. *Scientific Reports*, 6(October), 1–12. <https://doi.org/10.1038/srep37157>
- Yang, N., Ying, C., Xu, M., Zuo, X., Ye, X., Liu, L., Nara, Y., & Sun, X. (2007). High-fat diet up-regulates caveolin-1 expression in aorta of diet-induced obese but not in diet-resistant rats. *Cardiovascular Research*, 76(1), 167–174. <https://doi.org/10.1016/J.CARDIORES.2007.05.028>
- Yang, P., Chan, D., Felix, E., Cartwright, C., Menter, D. G., Madden, T., Klein, R. D., Fischer, S. M., & Newman, R. A. (2004). Formation and antiproliferative effect of prostaglandin E(3) from eicosapentaenoic acid in human lung cancer cells. *Journal of Lipid Research*, 45(6), 1030–1039. <https://doi.org/10.1194/JLR.M300455-JLR200>

Yao, P., Nussler, A., Liu, L., Hao, L., Song, F., Schirmeier, A., & Nussler, N. (2007a). Quercetin protects human hepatocytes from ethanol-derived oxidative stress by inducing heme oxygenase-1 via the MAPK/Nrf2 pathways. *Journal of Hepatology*, 47(2), 253–261.

Yao, Z.-X. X., Han, Z., Drieu, K., & Papadopoulos, V. (2004). Ginkgo biloba extract (Egb 761) inhibits beta-amyloid production by lowering free cholesterol levels. *The Journal of Nutritional Biochemistry*, 15(12), 749–756. <https://doi.org/10.1016/J.JNUTBIO.2004.06.008>

Yates, C. M., Calder, P. C., & Rainger, G. E. (2014). Pharmacology and therapeutics of omega-3 polyunsaturated fatty acids in chronic inflammatory disease. *Pharmacology & Therapeutics*, 141(3), 272–282.

Ye, R., Wang, M., Wang, Q. A., & Scherer, P. E. (2015). Adiponectin-mediated antilipotoxic effects in regenerating pancreatic islets. *Endocrinology*, 156(6), 2019–2028. <https://doi.org/10.1210/EN.2015-1066>

Yeung, J., Hawley, M., & Holinstat, M. (2017). The expansive role of oxylipins on platelet biology. *Journal of Molecular Medicine* 2017 95:6, 95(6), 575–588. <https://doi.org/10.1007/S00109-017-1542-4>

Yeung, T., Gilbert, G. E., Shi, J., Silvius, J., Kapus, A., & Grinstein, S. (2008). Membrane phosphatidylserine regulates surface charge and protein localization. *Science (New York, N.Y.)*, 319(5860), 210–213. <https://doi.org/10.1126/SCIENCE.1152066>

Yim, J. E., Heshka, S., Albu, J., Heymsfield, S., Kuznia, P., Harris, T., & Gallagher, D. (2007). Intermuscular adipose tissue rivals visceral adipose tissue in independent associations with cardiovascular risk. *International Journal of Obesity*, 31(9), 1400–1405. <https://doi.org/10.1038/SJ.IJO.0803621>

Yin, Y., Zhu, Z.-X., Li, Z., Chen, Y.-S., & Zhu, W.-M. (2021). Role of mesenteric component in Crohn's disease: A friend or foe? *World Journal of Gastrointestinal Surgery*, 13(12), 1536–1549. <https://doi.org/10.4240/WJGS.V13.I12.1536>

Yore, M. M., Syed, I., Moraes-Vieira, P. M., Zhang, T., Herman, M. A., Homan, E. A., Patel, R. T., Lee, J., Chen, S., Peroni, O. D., Dhaneshwar, A. S., Hammarstedt, A., Smith, U., McGraw, T. E., Saghatelian, A., & Kahn, B. B. (2014). Discovery of a class of endogenous mammalian lipids with anti-diabetic and anti-inflammatory effects. *Cell*, 159(2), 318. <https://doi.org/10.1016/J.CELL.2014.09.035>

Yoshida, H., Miura, S., Kishikawa, H., Hirokawa, M., Nakamizo, H., Nakatsumi, R. C., Suzuki, H., Saito, H., & Ishii, H. (2001). Fatty acids enhance GRO/CINC-1 and interleukin-6 production in rat intestinal epithelial cells. *The Journal of Nutrition*, 131(11), 2943–2950. <https://doi.org/10.1093/JN/131.11.2943>

Yoshikawa, T., Shimano, H., Yahagi, N., Ide, T., Amemiya-Kudo, M., Matsuzaka, T., Nakakuki, M., Tomita, S., Okazaki, H., Tamura, Y., Iizuka, Y., Ohashi, K., Takahashi, A., Sone, H., Osuga, J. I., Gotoda, T., Ishibashi, S., & Yamada, N. (2002). Polyunsaturated fatty acids suppress sterol regulatory element-binding protein 1c promoter activity by inhibition of liver X receptor (LXR)

binding to LXR response elements. *The Journal of Biological Chemistry*, 277(3), 1705–1711. <https://doi.org/10.1074/JBC.M105711200>

Youdim, K. A., Martin, A., & Joseph, J. A. (2000). Essential fatty acids and the brain: Possible health implications. *International Journal of Developmental Neuroscience*, 18(4–5), 383–399. [https://doi.org/10.1016/S0736-5748\(00\)00013-7](https://doi.org/10.1016/S0736-5748(00)00013-7)

Yu, B. C., Chang, C. K., Ou, H. Y., Cheng, K. C., & Cheng, J. T. (2008). Decrease of peroxisome proliferator-activated receptor delta expression in cardiomyopathy of streptozotocin-induced diabetic rats. *Cardiovascular Research*, 80(1), 78–87. <https://doi.org/10.1093/CVR/CVN172>

Yu, S., Levi, L., Siegel, R., & Noy, N. (2012). Retinoic Acid Induces Neurogenesis by Activating Both Retinoic Acid Receptors (RARs) and Peroxisome Proliferator-activated Receptor β/δ (PPAR β/δ). *Journal of Biological Chemistry*, 287(50), 42195–42205. <https://doi.org/10.1074/JBC.M112.410381>

Yu, X., Su, Q., Geng, J., Liu, H., Liu, Y., Liu, J., Shi, Y., & Zou, Y. (2021). Ginkgo biloba leaf extract prevents diabetic nephropathy through the suppression of tissue transglutaminase. *Experimental and Therapeutic Medicine*, 21(4). <https://doi.org/10.3892/ETM.2021.9764>

Zahid, S., Oellerich, M., Asif, A. R., & Ahmed, N. (2014a). Differential expression of proteins in brain regions of Alzheimer's disease patients. *Neurochemical Research*, 39(1), 208–215. <https://doi.org/10.1007/S11064-013-1210-1>

Zamin, L. L., Filippi-Chiela, E. C., Dillenburg-Pilla, P., Horn, F., Salbego, C., & Lenz, G. (2009). Resveratrol and quercetin cooperate to induce senescence-like growth arrest in C6 rat glioma cells. *Cancer Science*, 100(9), 1655–1662. <https://doi.org/10.1111/J.1349-7006.2009.01215.X>

Zanetti, M., Cappellari, G. G., Graziani, A., & Barazzoni, R. (2019). Unacylated ghrelin improves vascular dysfunction and attenuates atherosclerosis during high-fat diet consumption in rodents. *International Journal of Molecular Sciences*, 20(3). <https://doi.org/10.3390/ijms20030499>

Zang, Y., Zhang, L., Igarashi, K., & Yu, C. (2015a). The anti-obesity and anti-diabetic effects of kaempferol glycosides from unripe soybean leaves in high-fat-diet mice. *Food & Function*, 6(3), 834–841. <https://doi.org/10.1039/C4FO00844H>

Zarrouk, A., Riedinger, J. M., Ahmed, S. H., Hammami, S., Chaabane, W., Debbabi, M., Ben Ammou, S., Rouaud, O., Frih, M., Lizard, G., & Hammami, M. (2015). Fatty acid profiles in demented patients: identification of hexacosanoic acid (C26:0) as a blood lipid biomarker of dementia. *Journal of Alzheimer's Disease: JAD*, 44(4), 1349–1359. <https://doi.org/10.3233/JAD-142046>

Zawacka-Pankau, J., Grinkevich, V. V., Hüntten, S., Nikulenkov, F., Gluch, A., Li, H., Enge, M., Kel, A., & Selivanova, G. (2011). Inhibition of glycolytic enzymes mediated by pharmacologically activated p53 targeting Warburg effect to fight cancer. *Journal of Biological Chemistry*, 286(48), 41600–41615.

- Zeng, X., Zhu, M., Liu, X., Chen, X., Yuan, Y., Li, L., Liu, J., Lu, Y., Cheng, J., & Chen, Y. (2020). Oleic acid ameliorates palmitic acid induced hepatocellular lipotoxicity by inhibition of ER stress and pyroptosis. *Nutrition and Metabolism*, 17(1), 1–14. <https://doi.org/10.1186/S12986-020-0434-8/FIGURES/7>
- Zhan, L., Wang, T., Li, W., Xu, Z. C., Sun, W., & Xu, E. (2010). Activation of Akt/FoxO signaling pathway contributes to induction of neuroprotection against transient global cerebral ischemia by hypoxic pre-conditioning in adult rats. *Journal of Neurochemistry*, 114(3), 897–908. <https://doi.org/10.1111/J.1471-4159.2010.06816.X>
- Zhang, H., & Tsao, R. (2016). Dietary polyphenols, oxidative stress and antioxidant and anti-inflammatory effects. *Current Opinion in Food Science*, 8, 33–42.
- Zhang, L., Chopp, M., Meier, D. H., Winter, S., Wang, L., Szalad, A., Lu, M., Wei, M., Cui, Y., & Zhang, Z. G. (2013). Sonic hedgehog signaling pathway mediates Cerebrolysin-improved neurological function after stroke. *Stroke*, 44(7), 1965–1972. <https://doi.org/10.1161/STROKEAHA.111.000831>
- Zhang, Q. J., Holland, W. L., Wilson, L., Tanner, J. M., Kearns, D., Cahoon, J. M., Pettey, D., Losee, J., Duncan, B., Gale, D., Kowalski, C. A., Deeter, N., Nichols, A., Deesing, M., Arrant, C., Ruan, T., Boehme, C., McCamey, D. R., Rou, J., ... Symons, J. D. (2012). Ceramide mediates vascular dysfunction in diet-induced obesity by PP2A-mediated dephosphorylation of the eNOS-Akt complex. *Diabetes*, 61(7), 1848–1859. <https://doi.org/10.2337/DB11-1399/-/DC1>
- Zhang, X., Dong, F., Ren, J., Driscoll, M. J., & Culver, B. (2005). High dietary fat induces NADPH oxidase-associated oxidative stress and inflammation in rat cerebral cortex. *Exp Neurol*, 191(2), 318–325. <https://doi.org/10.1016/j.expneurol.2004.10.011>
- Zhang, Y., & Liu, D. (2011). Flavonol kaempferol improves chronic hyperglycemia-impaired pancreatic beta-cell viability and insulin secretory function. *European Journal of Pharmacology*, 670(1), 325–332. <https://doi.org/10.1016/J.EJPHAR.2011.08.011>
- Zhang, Y., Zhen, W., Maechler, P., & Liu, D. (2013). Small molecule kaempferol modulates PDX-1 protein expression and subsequently promotes pancreatic β -cell survival and function via CREB. *The Journal of Nutritional Biochemistry*, 24(4), 638–646. <https://doi.org/10.1016/J.JNUTBIO.2012.03.008>
- Zheng, W. H., Kar, S., & Quirion, R. (2002). Insulin-like growth factor-1-induced phosphorylation of transcription factor FKHRL1 is mediated by phosphatidylinositol 3-kinase/Akt kinase and role of this pathway in insulin-like growth factor-1-induced survival of cultured hippocampal neurons. *Molecular Pharmacology*, 62(2), 225–233. <https://doi.org/10.1124/MOL.62.2.225>
- Zheng, Y., Wu, Z., Yi, F., Orange, M., Yao, M., Yang, B., Liu, J., & Zhu, H. (2018). By Activating Akt/eNOS Bilobalide B Inhibits Autophagy and Promotes Angiogenesis Following Focal Cerebral Ischemia Reperfusion. *Cellular Physiology and Biochemistry*, 47(2), 604–616. <https://doi.org/10.1159/000490016>

Zhou, H., & Hylemon, P. B. (2014). Bile acids are nutrient signaling hormones. *Steroids*, 86, 62–68. <https://doi.org/10.1016/J.STEROIDS.2014.04.016>

Zhou, L., Meng, Q., Qian, T., & Yang, Z. (2011). Ginkgo biloba extract enhances glucose tolerance in hyperinsulinism-induced hepatic cells. *Journal of Natural Medicines* 2010 65:1, 65(1), 50–56. <https://doi.org/10.1007/S11418-010-0456-Z>

Zhou, Y. H., Yu, J. P., Liu, Y. F., Teng, X. J., Ming, M., Lv, P., An, P., Liu, S. Q., & Yu, H. G. (2006). Effects of Ginkgo biloba extract on inflammatory mediators (SOD, MDA, TNF- α , NF- κ Bp65, IL-6) in TNBS-induced colitis in rats. *Mediators of Inflammation*, 2006(5). <https://doi.org/10.1155/MI/2006/92642>

Zhou, Y., Lin, S., Zhang, L., & Li, Y. (2016). Resveratrol prevents renal lipotoxicity in high-fat diet-treated mouse model through regulating PPAR- α pathway. *Molecular and Cellular Biochemistry*, 411(1–2), 143–150. <https://doi.org/10.1007/S11010-015-2576-Y>

Zhu, Q., Ge, F., Dong, Y., Sun, W., Wang, Z., Shan, Y., Chen, R., Sun, J., & Ge, R. S. (2018). Comparison of flavonoids and isoflavonoids to inhibit rat and human 11 β -hydroxysteroid dehydrogenase 1 and 2. *Steroids*, 132, 25–32. <https://doi.org/10.1016/J.STEROIDS.2018.01.013>

Ziamajidi, N., Khaghani, S., Hassanzadeh, G., Vardasbi, S., Ahmadian, S., Nowrouzi, A., Ghaffari, S. M., & Abdirad, A. (2013). Amelioration by chicory seed extract of diabetes- and oleic acid-induced non-alcoholic fatty liver disease (NAFLD)/non-alcoholic steatohepatitis (NASH) via modulation of PPAR α and SREBP-1. *Food and Chemical Toxicology*, 58, 198–209. <https://doi.org/10.1016/J.FCT.2013.04.018>

Zimmermann, M., Colciaghi, F., Cattabeni, F., & Di, M. L. (2002). Ginkgo biloba extract: from molecular mechanisms to the treatment of Alzheimer's disease. *Cellular and Molecular Biology (Noisy-Le-Grand, France)*, 48(6), 613–623.

Zou, J., Chassaing, B., Singh, V., Pellizzon, M., Ricci, M., Fythe, M. D., Kumar, M. V., & Gewirtz, A. T. (2018). Fiber-Mediated Nourishment of Gut Microbiota Protects against Diet-Induced Obesity by Restoring IL-22-Mediated Colonic Health. *Cell Host & Microbe*, 23(1), 41-53.e4. <https://doi.org/10.1016/J.CHOM.2017.11.003>

Appendix 1

Optimizing fatty acid extraction - Comparison of Folch extraction methods

Lipids play a critical role in biological cellular structures and metabolic function including cell signalling, transport, and biosynthetic pathways (van Meer and de Kroon 2011a; Petković *et al.* 2005). Lipids are diverse in structure, are mostly composed of hydrophobic hydrocarbon chains (fatty acids) and may contain aliphatic moieties and functional groups (Christie 1993). They may be classified into two major groups based on the polarity of their head groups (Breil *et al.* 2017):

1. Neutral lipids: Predominantly synthesized for the storage of energy. Examples within this category include free fatty acids, sterols, sterols esters, waxes, acylglycerols and hydrophobic pigments
2. Polar lipids: predominantly found within the cellular membrane. Examples within this category include phospholipids and glycolipids. Notably, sterols such as cholesterol are also found in the cellular membrane.

The ability to estimate the total lipid content of biological tissues is a valuable tool. Lipids are soluble in many organic solvents with many methods for lipid extraction existing. While the Matyash method (Matyash *et al.* 2008) have been developed in recent decades, the most frequently used and cited protocols for lipid extraction remains with the classical Folch *et al.*, methods (Folch *et al.* 1951; Folch, Lees and Stanley 1957) and Bligh-Dyer method (Bligh and Dyer 1959). Both the Folch and Bligh-Dyer methods rely on a bi-phasic lipid extract system of chloroform (CHCl₃), methanol (MeOH) and water (H₂O) in various volumes. The combination of chloroform and methanol allows for the non-selective extraction of a broad range of lipid classes, making it a good option for non-targeted extractions (Christie, 1993). Chloroform acts as a good overall solvent for lipids and methanol (an amphiphilic compound) disrupting hydrogen bonding reducing hydrophobic reactions and destabilizes micelle structures of lipid-lipid and lipid-protein molecules (Christie 1993; Reis *et al.* 2013) allowing for the extraction of hydrophobically bound lipids. The Folch method utilizes a general guideline of at least 20 volumes of CHCl₃: MeOH: H₂O, 8:4:3, v/v/v per tissue volume while the Bligh-Dyer method utilizes three volumes of CHCl₃: MeOH: H₂O 2:2:1.8 (v/v/v) per volume of tissue (Breil *et al.*

2017) taking into account water in the sample. Both methods are comparable for the isolation of lipids, free of non-lipid contaminants (Breil *et al.* 2017; Iverson, Lang and Cooper 2001; Ulmer *et al.* 2018). The Bligh-Dyer Method is an adaptation of the original Folch method and utilizes smaller volumes of chloroform and methanol (Bligh and Dyer, 1959). This makes it suitable for samples with a high-water content. The reduced number of solvents also makes it more economical and convenient. Issues may occur however between sample types of varying water content. For this reason, the Folch method was chosen for this study for consistency across tissue types. While a variety of adapted methods based on this original Folch method have been reported, they can be costly in time, labour, equipment, glassware. They also pose an environmental issue with the quantity of toxic solvent by-products that must be disposed of. Therefore, here we set out to compare two adapted versions of the Folch *et al.*, (1957) methods as published previously (Bueno *et al.* 2015c; Schreiner 2006).

Optimizing fatty acid extraction - Comparison of Folch extraction methods

Two published lipid extraction methods (Bueno *et al.*, 2015, Schreiner, 2006) based on the original Folch *et al.*, (1957) method were compared for consistency of sampling across a variety of samples, including animal brain and adipose tissue (100mg homogenised tissue), consumable culinary oils (15mg) and *in vitro* cultured cells (1×10^6 cells) (. When comparing both methods, the double pipette method (Method 2) used approximately 70 % less solution than Method 1, as well as 50 % less time (See

Table 84). When comparing the efficacy of both methods on FA extraction, both methods produced similar GC profiles and the identified fatty acid profiles of the samples were like those previously published for the type of sample analysed (Table 85).

Table 85 and Table 86 shows the fatty acid profiles of samples used to compare method 1 and method 2 for FA extraction. Table 87 show the ratio difference between the two methods based on identification of identical FA peaks. The ratio test shows when comparing both

methods that the ratio of fatty acids that contribute to a higher percentage of the sample is close to 1:1 for most samples. Variances start to occur when lower quantities of fatty acids are present in the sample, with the most discrepancy occurring in fatty acids that contribute to less than 1% of the total sample.

Table 84. Comparison of total solution volumes for method 1 or method 2 used for fatty acid (FA) extraction optimization; Method 1 (Separatory funnel Folch method (Bueno et al., 2015) and Method 2 (Double-pipette Folch method (Schreiner, 2006))).

Solutions	Fatty acid extraction	Fatty acid extraction
	Method 1	Method 2
	(ml)	
Chlorine	41	10
Methanol	43	10
0.85% Saline	15	1
Acetyl chloride	0.6	0.6
5% Saline	4	4
Petrol Spirit	4	4
2% Potassium Bicarbonate	2	2
Heptane	1	1
Total solution per sample	110	32.6
Total duration of extraction and methylation	4 days	2 days

Table 85. Fatty acid (FA) composition of animal-based products, tissues, and cells (Mean values and standard deviations of total FA %)

	Fish oil		Bovine butter		Bovine adipose tissue		Ovine adipose tissue		Ovine brain stem		Ovine grey matter		Ovine white matter		Ovine cerebellum		Leukemia HL60 cells	
	(n=6)		(n=6)		(n=6)		(n=6)		(n=6)		(n=6)		(n=6)		(n=6)		(n=3)	
	Mean	SD	Mean	SD	Mean	SD	Mean	SD	Mean	SD	Mean	SD	Mean	SD	Mean	SD	Mean	SD
C8:0	-	-	0.41	0.2	-	-	0.01	0	-	-	-	-	-	-	-	-	-	-
C10:0	-	-	2.02	0.5	0.03	0	0.13	0.01	-	-	-	-	-	-	-	-	0.25	0.23
C12:0	-	-	3.29	0.17	0.09	0.01	0.15	0.02	-	-	-	-	-	-	-	-	0.95	0.87
C13:0	-	-	0.1	0.03	-	-	0.02	0	-	-	-	-	-	-	-	-	0.25	0.08
C14:0	0.47	0.05	11.5	0.29	2.64	0.06	2.32	0.11	0.22	0.05	0.64	0.08	0.35	0.11	0.37	0.2	4.09	3.95
C14:1n7	-	-	1.15	0.14	0.95	0.1	0.04	0.01	-	-	-	-	-	-	-	-	1.05	0.45
C15:0	-	-	1.18	0.07	0.59	0.02	0.59	0.02	-	-	-	-	0.05	0.03	-	-	0.75	0.36
C16:0	12	0.23	32.85	1.35	21.04	0.29	3.79	8.43	9.68	0.93	19.2	0.67	10.56	1.45	11.4	0.92	26.58	5.8
C16:1n7	2.04	0.11	2.02	0.3	5.15	0.39	15.88	8.24	-	-	0.45	0.06	0.22	0.07	0.18	0.06	1.28	0.53
C17:0	0.24	0.06	0.54	0.03	0.82	0.05	1.79	0.05	0.18	0.05	0.27	0.11	0.22	0.12	0.23	0.04	0.36	0.11
DMA																		
C18:0	0.25	0.04	-	-	0.02	0.01	0.03	0.01	3.16	0.16	4.64	1.05	2.97	0.3	3.76	0.19	-	-
C17:1	-	-	-	-	-	-	0.19	0	2.81	0.3	0.41	0.03	2.15	0.33	2.55	0.23	0.34	0.32
DMA 18:1	-	-	-	-	0.96	0.07	-	-	1.58	0.07	0.41	0.03	1.97	0.16	1.4	0.09	-	-
C18:0	4.74	0.2	10.11	0.03	11.13	1.1	0	1.33	12.02	0.61	20.19	0.55	11.26	1.27	15.09	1.37	14.81	3.42
C18:1n9t	0	0.06	0.46	1.79	0.48	0.06	0.53	0.02	-	-	-	-	-	-	-	-	0.33	0.24
C18:1n9	19.06	0.02	22.04	0.17	39.09	1.05	28.73	0.9	18.76	1.72	13.21	2.59	16.81	1.46	17.19	1.05	21.54	3.72
C18:1n7	2.02	0.15	0.49	0.84	1.23	0.12	0.6	0.02	2.43	0.13	2.97	0.55	2.14	0.19	3.09	0.2	2.06	0.86
C18:2n6	28.7	0.13	2.04	0.11	1.02	0.12	2.01	0.18	0.79	0.72	2.15	1.7	-	-	-	-	6.34	7.6
C18:3n3	8.83	0.14	0.57	0.02	0.53	0.02	1.29	0.04	-	-	-	-	-	-	-	-	0.54	0.3
C20:0	0.46	0.14	0.14	0.04	0.09	0.01	0.13	0.01	0.7	0.09	-	-	0.37	0.06	0.49	0.09	0.26	0.05
C20:1n9	1.24	0.06	-	-	0.13	0.01	0.09	0.02	3.96	0.73	0.37	0.13	1.97	0.36	2.98	0.39	0.1	0.05
C20:2n6	-	-	-	-	-	-	0.04	0.01	0.1	0.01	-	-	-	-	0.14	0.09	-	-
C20:3n6	-	-	0.1	0.06	0.05	0.02	0.02	0	0.43	0.13	-	-	0.46	0.19	0.4	0.07	0.62	0.07
C20:4n6	0.38	0.04	0.11	0.02	0.03	0	0.06	0.01	1.88	0.3	6.54	0.5	3.2	0.48	3.6	0.67	0.61	0.33
C20:3n3	-	-	-	-	0.02	0	0.03	0	-	-	-	-	-	-	-	-	-	-
C22:0	0.28	0.03	0.07	0.06	0.03	0	0.03	0.01	2.04	0.16	-	-	1.39	0.21	1.41	0.13	0.5	0.15
C22:1n9	0.92	0.08	0.11	0.02	0.07	0.01	0.02	0.01	1.37	0.54	-	-	0.78	0.21	1.01	0.14	-	-
C20:5n3	6.42	0.07	0.06	0.01	0.04	0.02	0.03	0.01	-	-	-	-	-	-	-	-	-	-
C23:0	-	-	-	-	-	-	0.02	0	0.63	0.11	-	-	0.47	0.11	0.48	0.12	-	-
C24:0	0.23	0.05	0.05	0.03	-	-	0.01	0	2.74	0.09	-	-	1.84	0.08	1.91	0.25	0.52	0.27
C22:4n6	0.45	0.04	-	-	-	-	-	-	1.6	0.52	2.54	0.26	2.23	0.6	1.35	0.11	0.49	0.24
C24:1n9	-	-	-	-	-	-	-	-	7.27	0.19	1.17	0.67	5.23	0.42	-	-	-	-
C22:5n3	0.83	0.08	0.11	0.05	-	-	0.16	0.02	0.77	0.08	0.87	0.17	0.94	0.21	0.7	0.05	0.67	0.45
C22:6n3	4.41	-	0.05	2.23	-	-	0.03	0.01	2.71	0.69	13.26	6.38	3.27	0.6	7.31	1.44	1.19	0.93
18 : 2n-6/ 20 : 4n-6	37.31		76.17		36.61		0.42		0.33		-		-		10.34			
ΣSFA	18.41		62.26		36.46		8.98		28.21		40.3		26.52		31.38		49.32	
ΣPUFA	75.3		29.31		48.79		49.56		42.06		43.53		37.25		37.96		36.82	
ΣMUFA	25.28		26.26		47.11		45.9		33.79		18.17		27.15		24.45		26.35	
Σn-7	4.06		3.66		7.33		16.52		2.43		3.42		2.35		3.27		4.39	
Σn-6	29.52		2.25		1.1		2.12		4.8		11.23		5.89		5.5		8.05	
Σn-3	20.49		0.8		0.58		1.54		3.48		14.13		4.21		8.01		2.41	
n6/n3	1.44		2.83		1.89		1.38		1.38		0.8		1.4		0.69		3.34	
ΣDMA	-		-		0.98	0.07	-		4.74		5.05		4.94		5.17		-	

Table 86. Comparison Fatty acid (FA) composition of plant based culinary oils following two varying fatty acid extraction methods (Method 1 Vs Method 2 (Values expressed as ratio of Method 1 (M1)/ Method 2 (M2) of total FA %)

	Coconut oil	Flax oil	Ground-nut oil	Olive Oil	Rape-seed oil	Rice-bran oil
	(n=6)	(n=6)	(n=6)	(n=6)	(n=6)	(n=6)
	M1/M2	M1/M2	M1/M2	M1/M2	M1/M2	M1/M2
C8:0	N/A	-	-	-	-	-
C10:0	N/A	-	-	-	-	-
C12:0	N/A	-	-	-	-	-
C14:0	N/A	0.9	1.0	-	1.1	0.9
C16:0	N/A	0.9	0.9	1.1	1.1	0.9
C16:1n7	N/A	0.7	1.7	0.9	1.0	0.9
C17:0	N/A	0.9	-	0.9	-	-
C18:0	N/A	1.0	0.9	1.0	1.0	0.9
C18:1n9t	N/A	-	1.1	-	1.0	1.7
C18:1n9	N/A	1.0	1.0	1.0	1.0	0.9
C18:1n7	N/A	0.9	1.0	1.0	1.0	0.9
C18:2n6	N/A	1.0	1.0	1.0	1.0	0.9
C18:3n3	N/A	1.0	0.7	1.0	1.0	0.9
C20:0	N/A	1.7	0.9	1.4	1.0	0.9
C20:1n9	N/A	1.0	1.0	0.8	0.9	0.8
C22:0	N/A	0.6	1.0	1.0	1.0	1.2
C23:0	N/A	-	0.6	-	1.2	1.0
C24:0	N/A	-	1.0	-	-	1.3
C24:1n9	N/A	-	0.8	-	-	-

Table 87. Comparison of fatty acid extraction methods on animal-based tissue fatty acid (FA) composition (Method 1 (3) Vs Method 2 (4)) (Values expressed as ratio of Method 1/ Method 2 of total FA %)

	Fish oil	Bovine butter	Bovine adipose tissue	Ovine adipose tissue	Ovine brain stem	Ovine grey matter	Ovine white matter	Ovine cerebellum
	(n=6)	(n=6)	(n=6)	(n=6)	(n=6)	(n=6)	(n=6)	(n=6)
	M1/M2	M1/M2	M1/M2	M1/M2	M1/M2	M1/M2	M1/M2	M1/M2
C8:0	-	1.4	1	1	-	-	-	-
C10:0	-	1	1	1	-	-	-	-
C12:0	-	0.9	-	1	-	-	-	-
C13:0	0.9	1	1	1	0.7	1.2	1.2	0.5
C14:0	-	1	1	1.1	-	-	-	-
C14:1n7	-	1	1	1	-	-	0.9	-
C15:0	1	1	1	1	1.1	0.9	0.9	1
C16:0	0.9	0.9	1	1	-	1.1	1.2	1.5
C16:1n7	1	1.1	1	1	0.7	2.1	0.6	1.1
C17:0	1	-	0.9	0.8	1	1.4	0.9	0.9
DMA C18:0	-	-	-	1	0.9	0.9	0.9	1
C17:1	1	-	1	-	1	1.2	0.9	0.9
DMA 18:1	1.1	1	1	1	1	1	0.9	0.9
C18:0	-	1	0.9	0.1	-	-	-	-
C18:1n9t	1	0.9	1	1.5	0.9	0.7	0.9	1.1
C18:1n9	1	0.8	1	1.2	0.9	1	0.9	1
C18:1n7	1	0.6	1	1.5	0.1	0.2	1.1	0.9
C18:2n6	1	1	1	1.4	-	-	-	-
C18:3n3	1.5	1	1	1.2	0.8	-	-	-
C20:0	0.9	0.7	1	2.2	0.8	0.8	0.9	1.1
C20:1n9	-	-	-	0.7	0.9	-	-	0.6
C20:2n6	-	-	0.8	1.5	1.6	-	0.8	1
C20:3n6	0.8	0.9	0.9	1.1	1.2	1	0.9	0.9
C20:4n6	-	-	1	1.8	-	-	-	-
C20:3n3	1	1.2	0.7	1	0.9	1.1	0.8	0.9
C22:0	1.1	0.4	1.4	2	0.6	-	0.7	1.2
C22:1n9	1	1.1	1.1	0.9	-	-	-	-
C20:5n3	-	-	-	1.1	0.8	-	0.9	0.8
C23:0	0.6	0.8	-	0.6	1	-	1	0.9
C24:0	-	-	-	-	1.4	-	1.1	0.9
C22:4n6	1	-	-	-	1	-	0.9	1
C24:1n9	1	0.9	-	1	1	0.8	0.8	1.1
C22:5n3	1	0.1	-	-	1.3	1.9	0.9	1

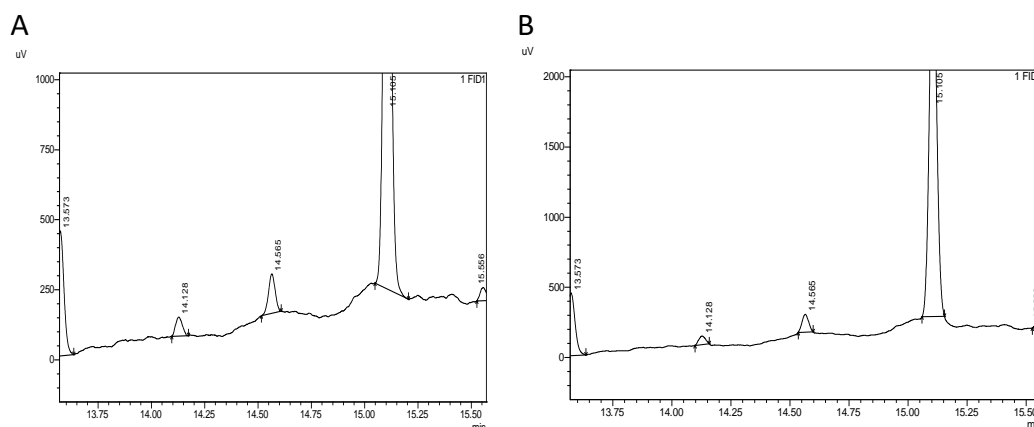
Lipid Extraction - Choosing a Folch Method

Variations of the original Folch *et al.*, (1957) method have been reported for over 60 years since its first publication. Here we compared to previously published adapted Folch methods to see if comparable fatty acid percentage (%) profiles could be achieved using small quantities of solvents following the Folch ratio of CHCl₃: MeOH: Saline.

Method 1 (Bueno *et al.*, 2015) is based more closely to the original Folch *et al.*, (1957) utilizing more than 20 volumes of the CHCl₃: MeOH: Saline solution (ratio of 8:4:3 (v/v/v)) per sample. A minor modification was made to the original method by replacing water at the initial extraction stage of 0.85% Saline solution. Using a low NaCl concentration solution provides Na⁺ and Cl⁻ ions that bind to the polar water molecules and helps force hydrophilic or amphiphilic lipids (e.g., phospholipids) with highly hydrophilic functional groups out of the aqueous phase into the organic phase, while allowing for proteins to precipitate and aggregate. This process is known as “salting out” (Christie, 1993).

Method 2, commonly known as the double pipette extraction method (Schreiner, 2006) utilizes ratio of CHCl₃: MeOH: Saline (8:4:3 (v/v/v)) but with lower quantities. Here we also utilized a 0.85% Saline solution in place of water. This method bypasses the need for filtration and a separatory funnel step, which reduces overall processing time. It also required less equipment and refrigerated storage space. When comparing the efficacy of both methods on FA extraction, both methods produced similar GC profiles and the identified fatty acid profiles of the samples. Table 87 shows the ratio difference between the two methods based on identification of identical FA peaks. The ratio test shows when comparing both methods that the ratio of fatty acids that contribute to a higher percentage of the sample is close to 1:1 for most samples of higher percentage. Variances start to occur when lower quantities of fatty acids are present in the sample, with the most discrepancy occurring in fatty acids that contribute to less than 1% of the total sample. This may be due to inconsistencies in the baseline and peak integration. Differences in the area %, area and height may occur when peaks are integrated slightly differently. Figure 44 below illustrates how minor alteration to the integration of peaks can change the numerical data in the same sample. Figure 44.A was integrated using 250µV as the y-axis r minor unit, while Figure 44.B was integrated using 500µV as the y-axis r minor unit. The resulting peak integration resulted in different area %, area and height data, and when compared against each other resulted in a close 1:1 ratio for the larger C24:0 (third peak) in all three parameters. However, because of minor changes in

peak integration a ratio difference between 1.23-1.27 occurred for both of the two smaller peaks C23:0 and C22:3n6, respectively (each representing less than 1% of the sample area percentage).



Peak	Area%		Area		Height		A/B ratio Area %	A/B ratio Area	A/B ratio Height
	Fig. A	Fig. B	Fig. A	Fig. B	Fig. A	Fig. B			
C23:0	0.041	0.033	146	119	68	60	1.24	1.23	1.13
C22:2n6	0.085	0.067	306	242	141	126	1.27	1.26	1.12
C24:0	1.697	1.625	6098	5834	2705	2666	1.04	1.05	1.01

Figure 44. Comparison of differences in area%, area and height from minor changes in peak integration of the same sample

Going forward, utilizing consistent integration techniques, and utilizing x/y axis controls will help reduce inconsistencies between peak integration. Overall, when comparing the two methods, the newer Method 2 (Double-pipette) gives consistent results to the more practiced and reported Method 1, but with the benefits of using much less solvent, time, glassware, and storage space. The double pipette method also requires less labour as it reduces the number of lengthy steps and time involved while decreasing the quantity of glassware requiring cleaning. For this study, Method 2 – Double-pipette fatty acid extraction will be the mode of extracting fatty acids for analysis as it reduces hazardous chemical usage and is more environmentally friendly, cost efficient, time efficient and less labour intensive.

Appendix 2

Solid phase extraction for isolation of lipid classes by silica gel column chromatography

A variety of methods exist for the separation of lipid classes (Adlof 2003; Burdge *et al.* 2000; Ingalls *et al.* 1993). For this study, the Ingalls *et al.*, (1993) method was selected for the separation of Cholesteryl esters, triglycerides, and phospholipids. HyperSep™ silica SPE columns (100 mg Bed Weight; 1 mL Column Volume) (code:10563985), HPLC grade Isooctane, ethyl acetate, chloroform, methanol, and glacial acetic acid were obtained from Fisher Scientific (Cleveland, OH, USA). In-house development and optimization of this method using commercially available standards was conducted in the following manner.

1. The extent of selective elution of individual lipid classes was achieved using commercially available lipid class standards purchased from Sigma –Aldrich (Merck KGaA, Darmstadt, Germany) as summarised in Table 88. 5mg of Triglycerides, Cholesteryl stearate, Erucic acid, and Heptadecanoic acid were aliquoted in triplicate. 1mg of Monoglycerides was aliquoted in triplicate. 100ug of each phospholipid was aliquoted in triplicate.
2. All solvent mixtures were made fresh before extraction at a ratio specified in the Ingalls *et al.*, (1993) method (v/v), summarized in Table 2.
3. HyperSep Columns were conditioned with 4 X 1 ml of isooctane (4 column volumes) and allowed to drain under gravity. 5 mg of sample lipid residues were extracted twice in succession with 0.5 ml of isooctane-ethyl acetate (80: 1, v/v). These extracts were applied to prepared silica gel columns under gravity. Each SPE solution (Fraction 1-6) was applied in succession as set out in Table 2 and allowed to elute under gravity. Each fraction elution was collected separately and dried under nitrogen for later analysis. Each fraction elution solution was immediately loaded on to the column after the previous solvent to avoid drying of the silica bed. Following Fraction 2 elution and collection, any solid residues remaining in the sample tubes were extracted twice in succession with 0.5 ml of isooctane-ethyl acetate (75:25, v/v), and applied to the silica gel columns, followed by elution with fraction solutions 3, 4 and 5 as per Table 2.
4. After fraction 5 elution, any solid residue remaining in the original sample tube was extracted twice with 0.5 ml of methanol and applied to the silica gel columns followed

by elution with fraction 6 solution. All elution samples were dried under OFN and stored at -20°C until needed and methylated as per the protocol outlined earlier. All methylated samples made up in 1 ml Heptane+BHT (100mg/ml). Samples were separated and analysed by GC-FID.

Table 88. Lipid standards used for testing selective elution of lipid classes by solid phase

Lipid Standards - Sigma-Aldrich (Merck KGaA, Darmstadt, Germany)	
Triglycerides in cocoa butter	IRMM801
Monoglyceride Stock Solution in pyridine	49446-U
Cholesterol	C8667
Alfa Aesar™ Cholesteryl stearate, 96%	C79409
cis-13-Docosenoic acid / Erucic acid (C22:1n9)	45629
Heptadecanoic acid (C17:0)	H3500
Phospholipids - Sigma-Aldrich (Merck KGaA, Darmstadt, Germany)	
L-alpha-Phosphatidylcholine, from egg yolk	P3556
1,2-Diacyl-sn-glycero-3-phospho-L-serine	P6641
L-α-Phosphatidylinositol from Glycine	P6636
Phosphatidylethanolamine	P7693
Sphingomyelin	S0756

Method optimisation results

Our findings using a commercially available HyperSep™ silica SPE column (100 mg Bed Weight; 1 mL Column Volume), differed to that of the original method in several ways.

It was observed that Triglycerides elute predominantly in fractions 1-3, with the majority eluting with an application of 5.5ml of Fraction 1 solution (isooctane: ethyl acetate 80:1 v/v).

An average 10-fold elution difference was observed between the Fraction 1 and Fraction 2 (Isooctane: ethyl acetate 20:1(v/v)) while an average 20-fold difference was observed between Fraction 1 and Fraction 3 (isooctane-ethyl acetate (75:25, v/v)).

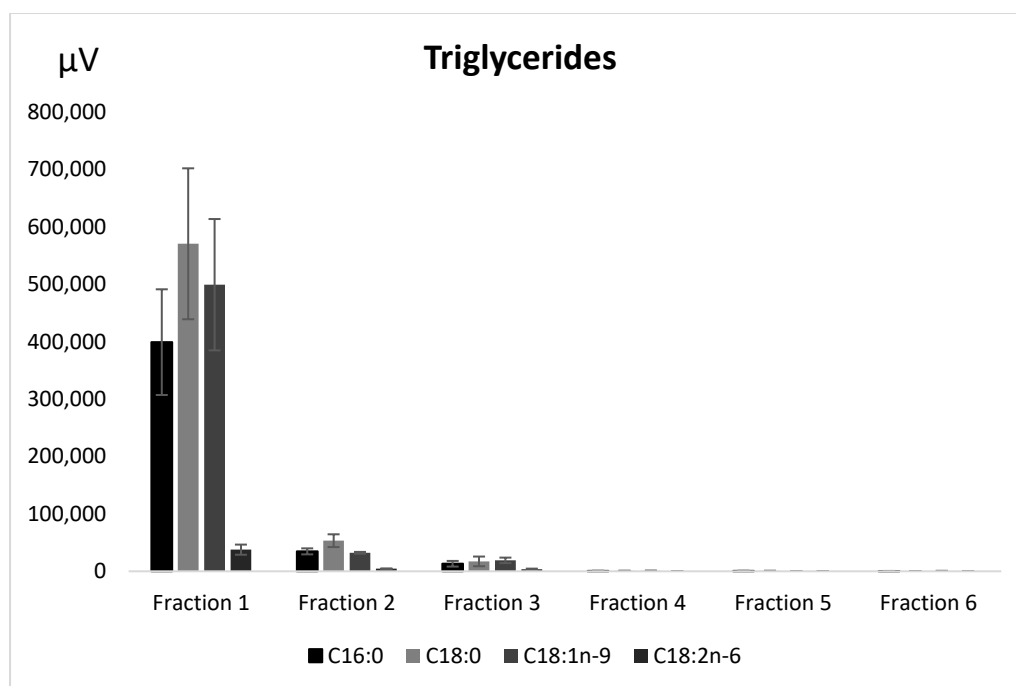


Figure 45. Silica-based solid phase extraction of triglycerides (5mg) using varying solutions, expressed in area (μV), ($n=3$). Fraction 1 - 4.5 ml of isooctane-ethyl acetate (80: 1, v/v); Fraction 2 - 5 ml of isooctane-ethyl acetate (20:1,v/v); Fraction 3 - 4.5 ml of isooctane-ethyl acetate (75:25, v/v); Fraction 4 - 4 ml of isooctane-ethyl acetate-acetic acid (75:25:2, v/v/v); Fraction 5 - 8 ml of isooctane- ethyl-acetate-acetic acid (75:25:2, v/v/v); Fraction 6 - 8 ml of Methanol.

It was observed that Cholesteryl stearate (5mg) predominantly elutes in fractions 1-3 with the highest elution observed in fraction 3 solution (4.5 ml of isooctane-ethyl acetate (75:25, v/v)). An average 2-fold elution difference was observed between the Fraction 1 and Fraction 2 while an average 1.5-fold difference was observed between Fraction 1 and Fraction 3 (Figure 46).

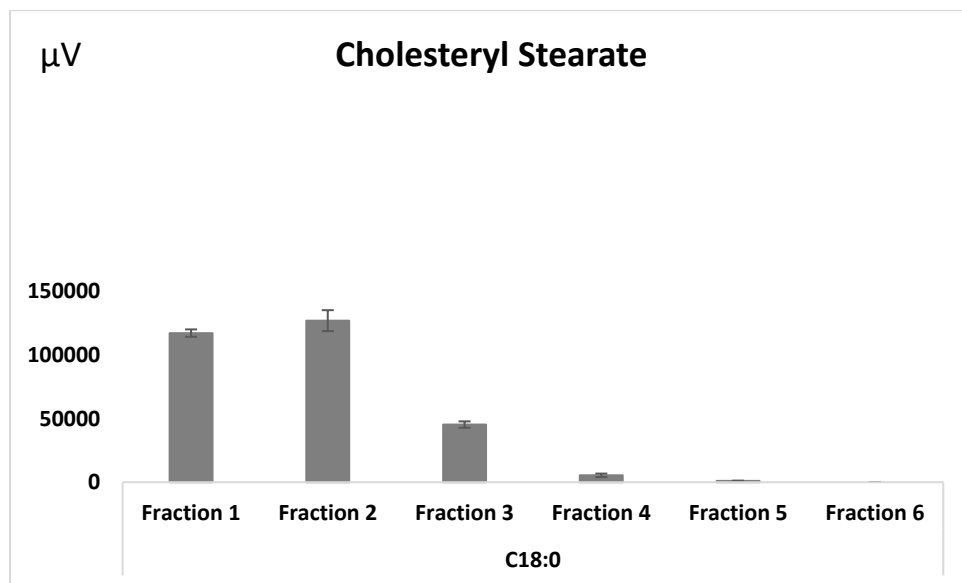


Figure 46. Silica-based solid phase extraction of Cholesteryl Stearate (5mg) using varying solutions, expressed in area (μV), (n=3). Fraction 1 - 4.5 ml of isooctane-ethyl acetate (80: 1, v/v); Fraction 2 - 5 ml of isooctane-ethyl acetate (20:1,v/v); Fraction 3 - 4.5 ml of isooctane-ethyl acetate (75:25, v/v); Fraction 4 - 4 ml of isooctane-ethyl acetate-acetic acid (75:25:2, v/v/v); Fraction 5 - 8 ml of isooctane- ethyl-acetate-acetic acid (75:25:2, v/v/v); Fraction 6 - 8 ml of Methanol.

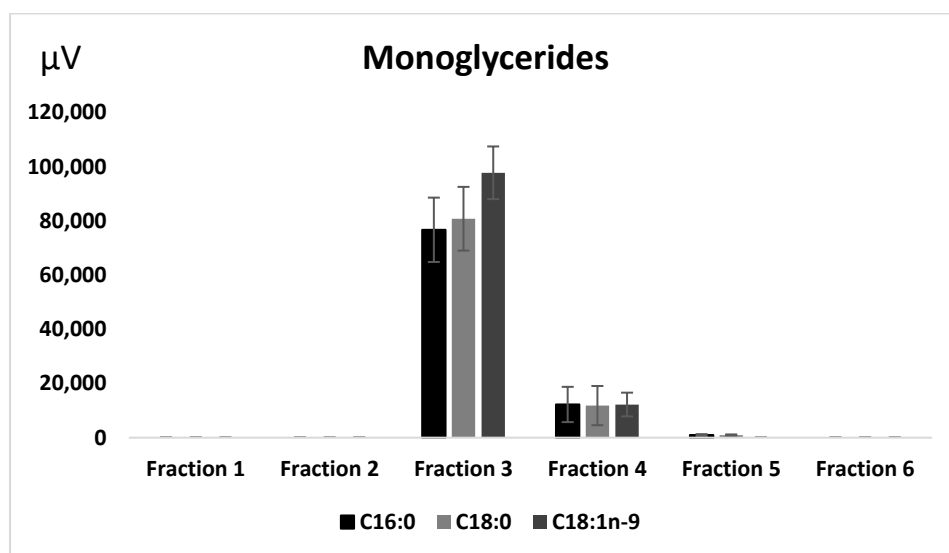


Figure 47. Silica-based solid phase extraction of monoglycerides (1mg) using varying solutions, expressed in area (μV), (n=3). Fraction 1 - 4.5 ml of isooctane-ethyl acetate (80: 1, v/v); Fraction 2 - 5 ml of isooctane-ethyl acetate (20:1,v/v); Fraction 3 - 4.5 ml of isooctane-ethyl acetate (75:25, v/v); Fraction 4 - 4 ml of isooctane-ethyl acetate-acetic acid (75:25:2, v/v/v); Fraction 5 - 8 ml of isooctane- ethyl-acetate-acetic acid (75:25:2, v/v/v); Fraction 6 - 8 ml of Methanol.

It was observed that monoglycerides (1mg) elute in fraction solutions 3-5 in varying proportions with the majority eluting with 5.5 ml of fraction 3 solution (isooctane-ethyl acetate (75:25, v/v)) (Figure 47). A 6-fold difference between fractions 3 and 4, and a 2.5-fold difference between fractions 3 and 5 was observed. It was observed that monoglycerides elute in fraction solutions 3-5 in varying proportions with the majority eluting with 5.5 ml of fraction 3 solution (isooctane-ethyl acetate (75:25, v/v)) (Figure 47). A 6-fold difference between fractions 3 and 4, and a 2.5-fold difference between fractions 3 and 5 was observed. While Fraction 4 shows promise as a representation for monoglycerides, profile for not match that of Fraction 3, which the majority of the monoglycerides fraction elutes. Additionally, there is some overlap between cholesteryls and triglycerides in fraction 3. On further analysis, however cholesteryls and triglycerides are at much lower levels compared to monglycerides when the amount of initial standard loading is taken into consideration. When the area (μV) is adjusted to represent 1mg/ml final sample rather than 5mg/ml the area for C18:0 in Cholesteryl stearate fraction 3 is 3451 μV (representing 1mg/ml) as compared to the original 14,827 μV (representing 5mg/ml) (Figure 46). When using this adjusted area of 3451 μV (representing an approximate 1mg sample) it results in a 23-fold difference favouring monoglyceride elution in fraction 3. Similarly, when triglyceride elution data is adjusted to represent a 1mg sample like that of the monoglycerides the fraction 3 elution areas are adjusted as follows: C16:0 (2629 μV), C18:0 (3451 μV) and C18:1n9 (3810 μV). The elution areas for the same fatty acids in the monoglyceride (1mg) sample are as follows: C16:0 (76683 μV), C18: zero (80752 μV) and C18:1n9 (97719 μV). When triglycerides and monoglycerides are thus compared, there is a 25-fold higher difference in favour of monoglycerides eluting in fraction 3 as compared to triglycerides. For non-esterified fatty acids testing (Heptadecanoic acid and Erucic acid), most of the elution was observed in Fraction 1. A 4-fold difference between Fraction 1 and Fraction 2 was observed for both non-esterified fatty acids, while a 60-fold and 200 fold difference was observed between fractions 1 and 3 for Heptadecanoic acid (Figure 48) and Erucic acid (Figure 49), respectively.

A 4-fold difference between Fraction 1 and Fraction 2 was observed for both non-esterified fatty acids (Heptadecanoic acid-5mg, Erucic acid – 5mg) tested while a 60-fold and 200-fold difference was observed between fractions 1 and 3 for Heptadecanoic acid and Erucic acid, respectively.

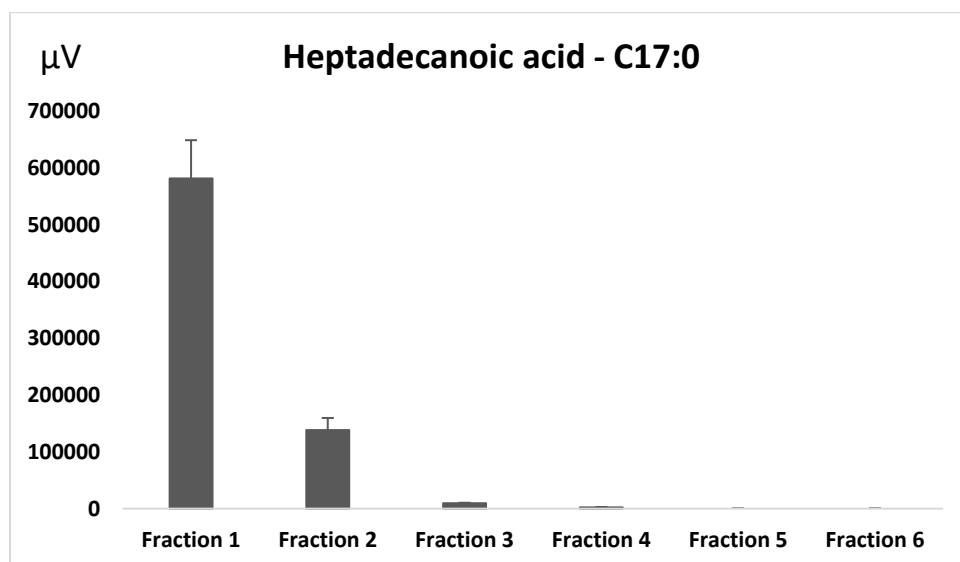


Figure 48. Silica-based solid phase extraction of Heptadecanoic acid (5mg) using varying solutions, expressed in area (μV), ($n=3$). Fraction 1 - 4.5 ml of isooctane-ethyl acetate (80: 1, v/v); Fraction 2 - 5 ml of isooctane-ethyl acetate (20:1,v/v); Fraction 3 - 4.5 ml of isooctane-ethyl acetate (75:25, v/v); Fraction 4 - 4 ml of isooctane-ethyl acetate-acetic acid (75:25:2, v/v/v); Fraction 5 - 8 ml of isooctane- ethyl-acetate-acetic acid (75:25:2, v/v/v); Fraction 6 - 8 ml of Methanol

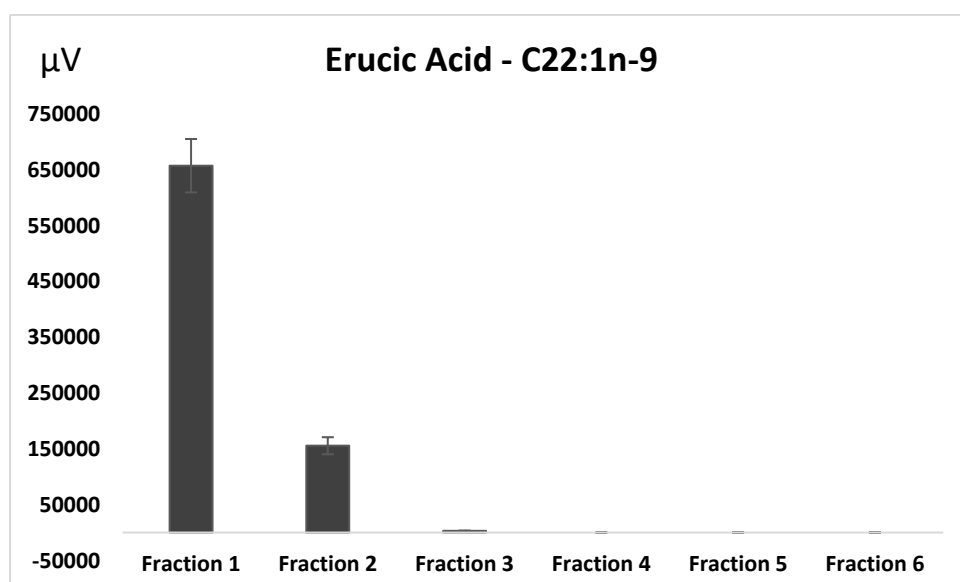


Figure 49. Silica-based solid phase extraction of Erucic acid (5mg) using varying solutions, expressed in area (μV), ($n=3$). Fraction 1 - 4.5 ml of isooctane-ethyl acetate (80: 1, v/v); Fraction 2 - 5 ml of isooctane-ethyl acetate (20:1,v/v); Fraction 3 4.5 ml of isooctane-ethyl acetate (75:25, v/v); Fraction 4 - 4 ml of isooctane-ethyl acetate-acetic acid (75:25:2, v/v/v); Fraction 5 - 8 ml of isooctane- ethyl-acetate-acetic acid (75:25:2, v/v/v); Fraction 6 - 8 ml of Methanol

For all phospholipids (100µg) tested (Phosphatidylethanolamine, Phosphatidylserine, Phosphatidylcholine, Phosphatidylinositol, Sphingomyelin) elution occurred in fraction 6 only (Figure 47 - 51).

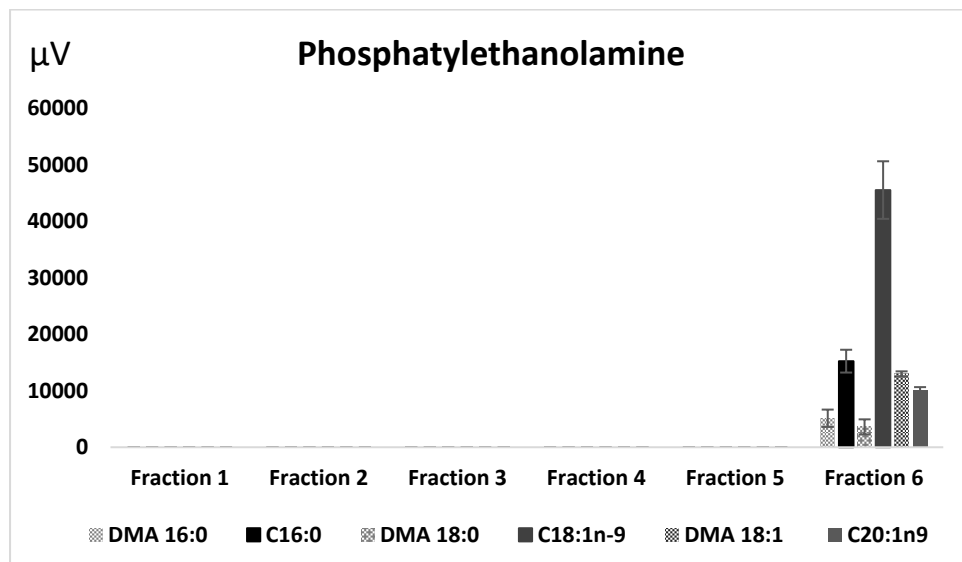


Figure 50. Silica-based solid phase extraction of Phosphatidylethanolamine (100ug) using varying solutions, expressed in area (μV), ($n=3$). Fraction 1 - 4.5 ml of isooctane-ethyl acetate (80: 1, v/v); Fraction 2 - 5 ml of isooctane-ethyl acetate (20:1,v/v); Fraction 3 - 4.5 ml of isooctane-ethyl acetate (75:25, v/v); Fraction 4 - 4 ml of isooctane-ethyl acetate-acetic acid (75:25:2, v/v/v; Fraction 5 - 8 ml of isooctane- ethyl-acetate-acetic acid (75:25:2, v/v/v); Fraction 6 - 8 ml of Methanol

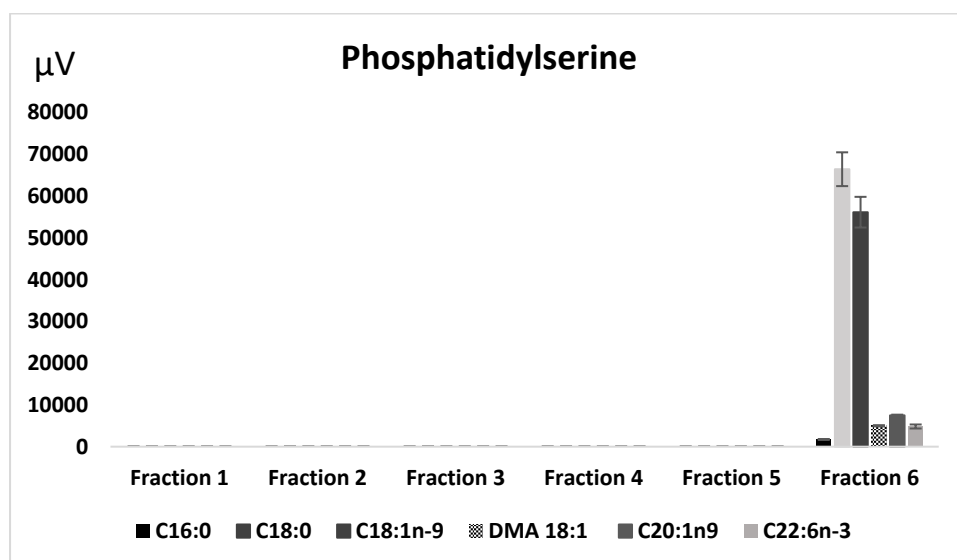


Figure 51. Silica-based solid phase extraction of Phosphatidylserine (100ug) using varying solutions, expressed in area (μV), ($n=3$). Fraction 1 - 4.5 ml of isooctane-ethyl acetate (80: 1, v/v); Fraction 2 - 5 ml of isooctane-ethyl acetate (20:1,v/v); Fraction 3 - 4.5 ml of isooctane-ethyl acetate (75:25, v/v); Fraction 4 - 4 ml of isooctane-ethyl acetate-acetic acid (75:25:2, v/v/v; Fraction 5 - 8 ml of isooctane- ethyl-acetate-acetic acid (75:25:2, v/v/v); Fraction 6 - 8 ml of Methanol.

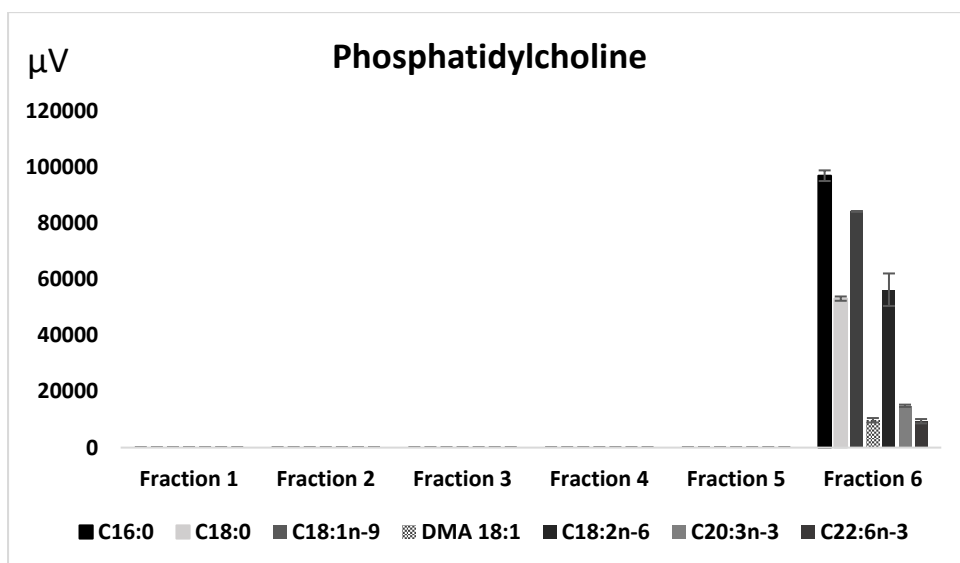


Figure 52. Silica-based solid phase extraction of Phosphatidylcholine (100ug) using varying solutions, expressed in area (μV), ($n=3$). Fraction 1 - 4.5 ml of isooctane-ethyl acetate (80: 1, v/v); Fraction 2 - 5 ml of isooctane-ethyl acetate (20:1,v/v); Fraction 3 - 4.5 ml of isooctane-ethyl acetate (75:25, v/v); Fraction 4 - 4 ml of isooctane-ethyl acetate-acetic acid (75:25:2, v/v/v; Fraction 5 - 8 ml of isooctane- ethyl-acetate-acetic acid (75:25:2, v/v/v); Fraction 6 - 8 ml of Methanol

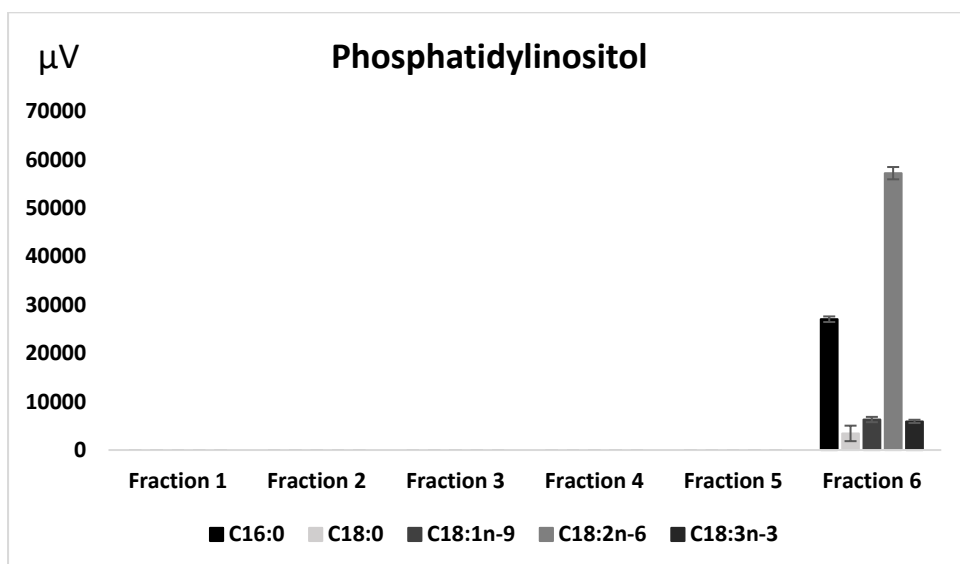


Figure 53. Silica-based solid phase extraction of Phosphatidylinositol (100ug) using varying solutions, expressed in area (μV), ($n=3$). Fraction 1 - 4.5 ml of isooctane-ethyl acetate (80: 1, v/v); Fraction 2 - 5 ml of isooctane-ethyl acetate (20:1,v/v); Fraction 3 - 4.5 ml of isooctane-ethyl acetate (75:25, v/v); Fraction 4 - 4 ml of isooctane-ethyl acetate-acetic acid (75:25:2, v/v/v; Fraction 5 - 8 ml of isooctane- ethyl-acetate-acetic acid (75:25:2, v/v/v); Fraction 6 - 8 ml of Methanol.

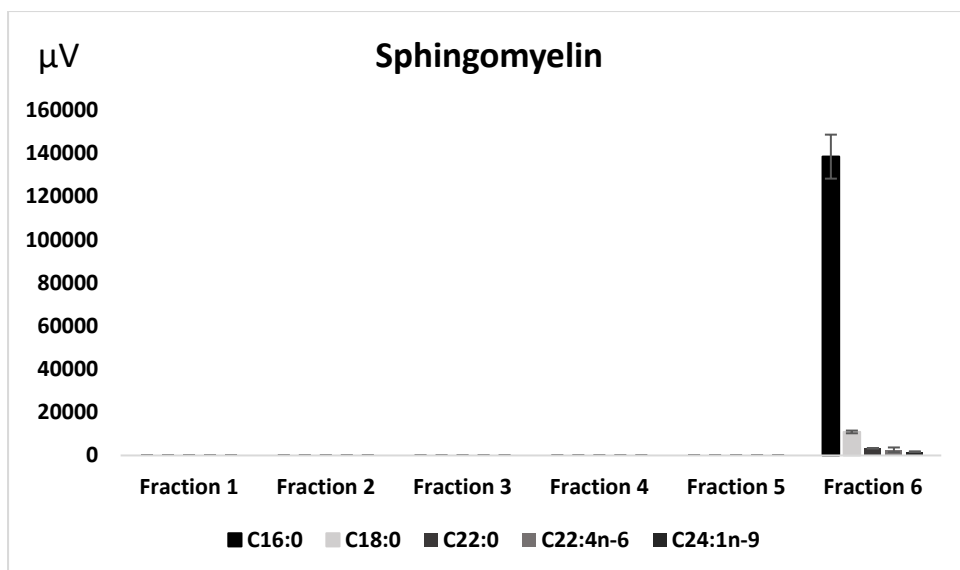


Figure 54. Silica-based solid phase extraction of Sphingomyelin (100ug) using varying solutions, expressed in area (μV), ($n=3$). Fraction 1 - 4.5 ml of isooctane-ethyl acetate (80: 1, v/v); Fraction 2 - 5 ml of isooctane-ethyl acetate (20:1, v/v); Fraction 3 - 4.5 ml of isooctane-ethyl acetate (75:25, v/v); Fraction 4 - 4 ml of isooctane-ethyl acetate-acetic acid (75:25:2, v/v/v); Fraction 5 - 8 ml of isooctane- ethyl-acetate-acetic acid (75:25:2, v/v/v); Fraction 6 - 8 ml of Methanol

When taking the selective elution test results into consideration, it was decided to use:

- Fraction 1 elution as a representation of Triglycerides
- Fraction 2 elution as a representation of Cholesteryl esters
- Fraction 3 elution as a representation of monoglycerides
- Fraction 6 elution as a representation of phospholipids

No fraction was assigned to non-esterified fatty acids owing to the overlap of elution in Fractions 1-3 with Triglycerides and Cholesteryl esters. As unbound fatty acids only make up a very small percentage of tissue lipid profiles and with TAG levels making up a large proportion of tissue lipids (Grzybek *et al.* 2019) this overlap of MAG and TAG elution with SPE separation was not considered pertinent in relation to the triglyceride profiles of Fraction 1.



OPEN **Oestrogen replacement fails to fully revert ovariectomy-induced changes in adipose tissue monoglycerides, diglycerides and cholesteryl esters of rats fed a lard-enriched diet**

Valter Tadeu Boldarine^{1,3}, Ellen Joyce², Amanda Paula Pedroso¹, Mônica Marques Telles¹, Lila Missae Oyama¹, Allain Amador Bueno² & Eliane Beraldi Ribeiro¹

Menopause may be accompanied by abdominal obesity and inflammation, conditions accentuated by high-fat intake, especially of saturated fat (SFA)-rich diets. We investigated the consequences of high-SFA intake on the fatty acid (FA) profile of monoglycerides, diglycerides and cholesteryl esters from retroperitoneal white adipose tissue (RET) of rats with ovariectomy-induced menopause, and the effect of oestradiol replacement. Wistar rats were either ovariectomized (Ovx) or sham operated (Sham) and fed either standard chow (C) or lard-enriched diet (L) for 12 weeks. Half of the Ovx rats received 17 β -oestradiol replacement (Ovx + E2). Body weight and food intake were measured weekly. RET neutral lipids were chromatographically separated and FAs analysed by gas chromatography. Ovariectomy alone increased body weight, feed efficiency, RET mass, leptin and insulin levels, leptin/adiponectin ratio, HOMA-IR and HOMA- β indexes. OvxC + E2 showed attenuation in nearly all blood markers. HOMA- β index was restored in OvxL + E2. OvxC showed significantly disturbed SFA and polyunsaturated FA (PUFA) profile in RET cholesteryl esters (CE). OvxC also showed increased monounsaturated FA (MUFA) in the monoglyceride diglyceride (Mono-Di) fraction. Similar changes were not observed in OvxL, although increased SFA and decreased PUFA was observed in Mono-Di. Overall, HRT was only partially able to revert changes induced by ovariectomy. There appears to be increased mobilization of essential FA in Ovx via CE, which is a dynamic lipid species. The same results were not found in Mono-Di, which are more inert. HRT may be helpful to preserve FA profile in visceral fat, but possibly not wholly sufficient in reverting the metabolic effects induced by menopause.

Menopause is a period in women's lives mainly characterized by the loss of ovarian hormones, during which the risk of developing central obesity is higher than in any other period¹. Menopause is associated with greater risk of other metabolic occurrences, including weight gain, and the lack of oestrogens after menopause is associated with a shift of fat distribution from subcutaneous to visceral depots, with impaired sensitivity of insulin and leptin, and subsequent predisposition to diabetes^{2,3}.

Experimentally, rodent bilateral ovariectomy has been used as a useful model for the investigation of metabolic effects induced by the lack of oestrogen^{4,5}. Our group has previously demonstrated that the intake of a lard-enriched high-fat diet by ovariectomized rats potentiated gains in body adiposity and induced metabolic alterations⁶. Saturated fat intake has been shown to induce a proinflammatory state mainly in visceral adipose tissue. In obese postmenopausal women, high saturated fat intake induced fatty acid (FA) accumulation, particularly palmitic acid^{7,8}. Diets rich in polyunsaturated fatty acids (PUFA) are also known to induce dramatic

¹Departamento de Fisiologia, Escola Paulista de Medicina, Universidade Federal de São Paulo, Rua Botucatu 862, 2º andar, Vila Clementino, São Paulo, SP 04023-062, Brasil. ²Department of Biological Sciences, College of Health, Life and Environmental Sciences, University of Worcester, Worcester, UK. [✉]email: valtertadeuboldarine@gmail.com

metabolic changes; while n-6 PUFA enriched-diets are known to increase pro-inflammatory lipid biomarkers, n-3 PUFA enriched-diets are commonly associated with anti-inflammatory or inflammation-suppressing properties⁹.

The primary function of adipocytes, the predominant cell type in white adipose tissue, is energy storage. Adipocytes also present remarkable secretory activity, through the release of a broad range of adipokines and cytokines that influence autocrine, paracrine and endocrine actions on energy metabolism, homeostasis and substrate utilization within adipose, liver and skeletal muscle tissues as well as the brain^{10–15}.

Cholesterol is an important structural component of adipocyte membranes, interacting with several steroid hormones that are produced not only in adipose tissue^{16,17}, but in other distal tissues including the adrenal and sex glands^{18,19}. Cholesterol exerts its function by preventing sterol response element-binding proteins acting as transcription factors of enzymes in the cholesterol biosynthetic pathway, thereby inhibiting sterol biosynthesis in a classical feedback mechanism²⁰.

Neutral lipids, mainly cholesteryl esters, triglycerides, diglycerides, monoglycerides and free fatty acids, are uncharged hydrophobic molecules that play a major role in energy storage^{21,22}. Cholesteryl esters (CE) are formed through ester bonds between the carboxyl group of a FA and the hydroxyl group of the cholesterol molecule, with the FA composition of CE being a direct reflection of nutritional status^{23–25}.

Given that cholesterol is found abundantly in lipid rafts within the plasma membrane, and considering its role in sterol biosynthesis in organs such as the liver, intestines and gonads^{26,27}, the influence of FA composition upon CE availability and oestrogen metabolism becomes a matter of further exploration.

Triglycerides can be conversely dismantled and reassembled to monoglycerides and diglycerides (Mono-Di) depending upon specific metabolic purposes²⁸. Furthermore, intracellular neutral lipids store essential fatty acids (EFA) during periods of abundant EFA intake, buffering EFA blood levels. Depending on physiological circumstances, EFA are mobilized for the synthesis of pro- or anti-inflammatory lipid mediators, which modulate a range of immuno-metabolic signalling pathways²⁹.

Given the detrimental consequences of metabolic disorders associated with ovarian failure and the chronic intake of energy dense diets upon quality of life of affected individuals, expanding the current knowledge on visceral adipose tissue metabolism paves the way for future, more efficient clinical and dietetic interventions. Our group has recently demonstrated that ovariectomy in control diet-fed rats favoured a disruption of the fatty acid composition of total lipid extract (which includes both polar and non-polar lipids, and most likely reflects the composition of triglycerides) obtained from retroperitoneal white adipose tissue (RET), evidencing a direct disturbance of ovariectomy upon lipid metabolism³⁰. Such findings suggest a greater than initially thought role of fatty acid composition in the development of obesity, along with the appearance of an inflammatory state, in that condition. As CE, monoglycerides and diglycerides are neutral lipid species in dynamic structural interchangeability within the white adipose tissue, the present study examined in rats the effects of ovariectomy and lard-enriched diet intake, associated or not with oestrogen replacement therapy, on the RET FA profile of CE and Mono-Di lipid fractions.

Results

High-fat diet intake further exacerbates the deleterious effects of ovariectomy. As shown in Table 1, the success of ovariectomy was confirmed by the lower uterus weight in the Ovx groups. Body weight at the beginning of the study was similar amongst the six groups, whilst the four ovariectomized groups (OvxC, OvxC + E2, OvxL, OvxL + E2) showed increased body weight, feed efficiency and RET fat mass at the end of the 12 weeks period. OvxL and OvxL + E2 showed further increased body weight and RET mass in comparison to OvxC and OvxC + E2. Ovariectomy alone or in combination with the high-fat diet significantly increased leptin and insulin levels, leptin/adiponectin ratio, HOMA-IR and HOMA- β indexes. Oestradiol replacement therapy was able to attenuate the effects of ovariectomy in the control diet group while only restoring the HOMA- β index in the lard-fed group. Total cholesterol, HDL-cholesterol and triglycerides levels did not differ significantly amongst the groups.

Ovariectomy modifies RET monoglyceride, diglyceride and cholesteryl ester FA composition, which is marginally restored by oestrogen replacement therapy. The FA composition of RET CE and Mono-Di fractions from rats fed the control diet are presented in Tables 2 and 3. Regarding the CE fraction (Table 2), the sum of SFA (Σ SFA) was significantly decreased in OvxC in comparison to ShamC, mainly as a consequence of the significantly decreased C16:0 and C18:0. OvxC + E2 showed partial restoration of the Σ SFA, but which did not reach statistical significance in relation to OvxC. The C18/C18:1 ratio was decreased in OvxC compared to ShamC, but this statistically significant difference disappeared when comparing OvxC + E2 versus ShamC. The sum of monounsaturated fatty acids (Σ MUFA) was statistically similar amongst ShamC, OvxC and OvxC + E2.

OvxC rats showed increased Σ n-3, Σ n-6 and Σ PUFA when compared to ShamC. OvxC + E2 showed a partial restoration of this change, being significantly lower than OvxC in Σ n-3, but not reaching significant differences in Σ n-6 and Σ PUFA. This phenomenon is particularly noticeable across the truly essential fatty acids alpha-linolenic acid (C18:3n-3) and linolenic acid (C18:2n-6). C18:3n-3 is higher in OvxC as compared to ShamC, whilst OvxC + E2 is found at the mid-range, being significantly different from both OvxC and ShamC. C18:2n-6 is higher in OvxC as compared to ShamC, and in OvxC + E2 it is also found at mid-range, but this time not significantly different from OvxC. C20:5n-3, C22:5n-3, C22:6n-3, C20:4n-6 and C22:4n-6 all show the same profile: increased in OvxC but only partially restored in OvxC + E2. The total amount of unsaturated fatty acids (Σ UFA = MUFA + PUFA) and the ratio Σ SFA/ Σ UFA showed similar profile: significantly different in Ovx when compared to ShamC, and only partial restoration in OvxC + E2.

	ShamC	OvxC	OvxC+E2	ShamL	OvxL	OvxL+E2
Initial body weight (g)	264.7 ± 5.2	263.0 ± 3.7	263.5 ± 5.0	266.6 ± 4.2	272.8 ± 3.7	261.5 ± 4.3
Final body weight (g)	280.8 (272.3–285.7)	338.0 (336.0–339.5)*	335.7 (325.8–337.0)*	326.3 (307.1–343.4)	410.2 (377.0–418.1)**#	381.3 (357.2–418.1)**#
Feed efficiency (g/Kcal)	2.7 ± 0.5	13.5 ± 0.6*	11.9 ± 0.8*	5.8 ± 1.0	17.3 ± 0.8**	15.2 ± 1.8**
Uterus (g)	0.4 ± 0.0	0.1 ± 0.0*	0.2 ± 0.0*	0.5 ± 0.1	0.1 ± 0.1*	0.2 ± 0.1*
RET mass (g/100 g)	1.1 ± 0.1	2.0 ± 0.2*	1.7 ± 0.1*	2.2 ± 0.1*	2.8 ± 0.2**	2.7 ± 0.2**
Leptin (ng/mL)	2.1 (1.8–2.6)	10.0 (7.8–12.5)*	5.9 (4.4–9.8)	5.2 (2.6–8.9)	12.5 (9.7–13.5)**	13.8 (10.4–14.6)**
Adiponectin (µg/mL)	5.6 (4.3–7.1)	8.0 (7.2–9.3)	7.6 (6.8–8.5)	5.8 (4.9–6.9)	7.1 (5.9–8.1)	6.2 (4.9–7.2)
Leptin/Adiponectin	0.4 (0.2–0.5)	1.4 (1.0–1.9)*	0.8 (0.6–0.9)	0.9 (0.8–1.1)	1.6 (1.4–1.8)**	1.8 (1.6–2.0)**
Glucose (mg/dL)	92.8 ± 2.9	105.7 ± 6.3	103.8 ± 6.2	107.2 ± 3.9	110.3 ± 6.3*	120.4 ± 5.2**
Insulin (ng/mL)	0.5 ± 0.0	2.3 ± 0.20*	1.3 ± 0.1	1.4 ± 0.1	2.1 ± 0.2*	2.2 ± 0.1*
HOMA-IR	3.1 (2.3–4.2)	14.37(12.0–19.0)*	7.9 (6.2–8.2)	9.4 (7.5–11.6)	16.3 (12.0–19.0)*	18.4 (6.9–22.7)**
HOMA-β	0.1 (0.1–0.2)	0.5 (0.3–0.7)*	0.2 (0.2–0.4)	0.2 (0.1–0.3)	0.5 (0.2–0.6)*	0.3 (0.2–0.4)
Total cholesterol (mg/dL)	115.4 (104.9–121.7)	140.8 (119.0–193.1)	126.3 (119.8–133.9)	102.4 (92.5–106.2)	99.5 (95.4–112.7)	110.5 (91.2–121.2)
HDL cholesterol (mg/dL)	205.7 (179.0–251.9)	163.1 (146.1–174.0)	142.3 (135.5–157.6)	190.8 (179.1–215.4)	152.3 (145.1–184.0)	149.3 (125.5–156.6)
Triglycerides (mg/dL)	99.1 (94.6–108.2)	111.2 (105.3–118.8)	122.5 (107.7–220.4)	88.61 (80.7–113.4)	105.6 (86.7–115.8)	98.8 (91.6–117.6)

Table 1. Body and serum parameters of ovariectomized (Ovx) or Sham operated rats, fed a control (C) or lard-enriched (L) diet, subjected or not to oestrogen replacement therapy (E2). Data presented as mean ± standard error (SE) for variables with normal distribution or median-interquartile range (Q1–Q3) for variables not normally distributed. n = 6 animals per group. * p < 0.05 vs. ShamC; # p < 0.05 OvxC vs. OvxL; & p < 0.05 OvxC + E2 vs. OvxL + E2; \$ p < 0.05 vs. ShamL.

The RET Mono-Di FA profile of rats fed the control diet is shown in Table 3. There were no differences in SFA amongst the three groups. The ΣMUFA was significantly higher in OvxC in comparison to ShamC, attributed to the higher levels of C18:1n-9 and C20:1n-9 observed in OvxC. Interestingly, the differences found between OvxC + E2 and ShamC were not significantly different.

Both n-3 and n-6 families were overall reduced in OvxC in comparison with ShamC, with only C22:5n-3 and C22:6n-3 reaching statistically significant reductions. Although statistically similar, Σn-3 was 19% lower in OvxC, and Σn-6 16% lower, as compared to ShamC. Following the same pattern described in the CE fraction above, OvxC + E2 rats tended to show a normalization of their Mono-Di FA levels.

Changes in monoglyceride, diglyceride and cholesteryl ester FA profile induced by the interaction of ovariectomy and lard diet are partially restored by oestrogen replacement therapy.

The FA composition of RET CE and Mono-Di fractions from rats fed the lard-enriched diet are presented in Tables 4 and 5. Regarding the FA composition of CE (Table 4), no statistically significant differences were found in SFA, except for C14:0, which was found increased in OvxL as compared to ShamL, and decreased in OvxL + E2. An identical pattern was found in the MUFA family, in which no differences was found, except for C14:1n-7. Interestingly, the differences found in the CE PUFAs of the control diet-fed group, described in Table 2, were no longer observed in the lard diet-fed groups; no statistically significant differences were found in the n-3 or n-6 families, nor in ΣPUFA, ΣUFA or the ratio ΣSFA/ΣUFA.

The RET Mono-Di FA composition of rats fed the lard diet is shown in Table 5. OvxL rats showed higher ΣSFA as compared to ShamL, result attributed to significantly higher levels of C14:0 and C18:0 in OvxL. C16:0 levels nearly reached statistical significance, with a p value of 0.08. Following the same pattern observed in previous results, OvxL + E2 rats showed a partial SFA restoration.

Within the MUFA family, the ΣMUFA content was similar across the three groups, although the levels of two FA appear to counteract each other: C16:1n-7 was significantly higher in OvxL as compared to OvxL + E2, whilst C20:1n-9 was significantly lower. The Σn-3 and Σn-6 families were statistically similar between ShamL and OvxL, but in both cases a tendency for reduction in OvxL was observed, which was found to be statistically different when both families were summed together as ΣPUFA. For both PUFA families, oestrogen replacement therapy appears to bring FA levels closer to the ShamL group. No differences were observed in ΣUFA or ΣSFA/ΣUFA across the three groups.

Fatty acid		% of total fatty acids		
		ShamC	OvxC	OvxC + E2
C14:0	Myristic acid	0.59 ± 0.15	0.59 ± 0.11	0.63 ± 0.14
C16:0	Palmitic acid	22.68 ± 2.42	14.92 ± 2.29*	18.46 ± 2.19*
C18:0	Stearic acid	7.02 ± 1.45	3.20 ± 1.04*	4.04 ± 1.34*
C20:0	Arachidic acid	0.12 ± 0.01	0.01 ± 0.01	0.05 ± 0.01
C24:0	Behenic acid	0.08 ± 0.02	0.44 ± 0.13*	0.21 ± 0.25
Σ SFA		30.37 ± 3.10	19.15 ± 3.29*	23.39 ± 1.84*
C14:1n-7	Myristoleic acid	0.03 ± 0.01	0.04 ± 0.01	0.02 ± 0.01
C16:1n-7	Palmitoleic acid	1.91 ± 0.39	2.03 ± 0.70	1.72 ± 0.60
C18:1n-9	Oleic acid	24.02 ± 4.58	21.65 ± 4.43	25.98 ± 6.42
C18:1n-7	cis-vaccenic acid	2.21 ± 0.63	1.82 ± 0.24	2.17 ± 0.26
C20:1n-9	Eicosenic acid	0.16 ± 0.10	0.10 ± 0.02	0.11 ± 0.05
C18/C18:1		0.29 ± 0.13	0.13 ± 0.02*	0.15 ± 0.07
C16:0/C16:1n-7		12.21 ± 2.46	7.73 ± 1.68	11.72 ± 4.0
Σ MUFA		28.35 ± 4.93	25.64 ± 4.92	30.01 ± 6.50
C18:3n-3	Alpha-linolenic acid (ALA)	1.06 ± 0.44	5.36 ± 1.22*	3.19 ± 1.64**
C20:5n-3	Eicosapentaenoic acid (EPA)	0.01 ± 0.02	0.15 ± 0.05*	0.10 ± 0.07
C22:5n-3	Docosapentaenoic acid (DPA)	0.11 ± 0.01	0.32 ± 0.15*	0.20 ± 0.11
C22:6n-3	Docosahexaenoic acid (DHA)	0.08 ± 0.02	0.52 ± 0.26*	0.28 ± 0.20
Σ n-3		1.22 ± 0.43	6.36 ± 1.51*	3.76 ± 1.95**
C18:2n-6	Linoleic acid (LA)	27.07 ± 5.15	44.38 ± 6.08*	40.09 ± 5.52*
C18:3n-6	Gamma-linolenic acid	0.01 ± 0.01	0.24 ± 0.07	0.12 ± 0.04
C20:2n-6	Eicosadienoic acid (EDA)	0.19 ± 0.05	0.18 ± 0.03	0.24 ± 0.11
C20:3n-6	Dihomo-gamma linolenic acid	0.56 ± 0.11	0.39 ± 0.09	0.30 ± 0.16*
C20:4n-6	Arachidonic acid (AA)	0.41 ± 0.12	1.69 ± 0.58*	1.10 ± 0.50
C22:4n-6	Docosatetraenoic acid (DTA)	0.08 ± 0.05	0.31 ± 0.15*	0.21 ± 0.05
Σ n-6		28.29 ± 5.20	47.12 ± 6.73*	42.06 ± 6.05*
Σ n-6/Σ n-3		24.31 ± 4.97	7.58 ± 1.04*	13.32 ± 5.72*
Σ PUFA		29.51 ± 2.4	53.75 ± 3.2*	45.82 ± 2.5*
Σ UFA		57.86 ± 9.22	79.11 ± 3.28*	75.83 ± 1.77*
Σ SFA/Σ UFA		0.54 ± 0.14	0.24 ± 0.05*	0.31 ± 0.03*

Table 2. Fatty acid composition of RET cholesteryl ester lipids obtained from ovariectomized (Ovx) or Sham operated rats, fed a control (C) diet, subjected or not to oestrogen replacement therapy (E2). Data presented as means ± standard error (SE) of the % of total FAs. n = 6 for each group. SFA saturated fatty acids, MUFA monounsaturated fatty acids, PUFA polyunsaturated fatty acids. *p < 0.05 vs ShamC; #p < 0.05 OvxC vs OvxC + E2.

Discussion

Menopause is an important risk factor for the development of obesity, which becomes further exacerbated when associated with the consumption of energy dense diets³³. Our group has recently demonstrated that ovariectomy modified the fatty acid profile of RET total lipid extract, which was marginally normalized by oestrogen replacement³⁰. Those results confirm that the loss of ovarian hormones, combined or not with the consumption of a lard-enriched diet, could lead to impaired lipid and fatty acid metabolism in visceral adipose tissue.

In order to further examine our hypothesis, we investigated the fatty acid composition of cholesteryl ester (CE) and monoglyceride diglyceride (Mono-Di) lipid fractions extracted from retroperitoneal white adipose tissue, firstly to determine to what extent lipids are affected by ovarian losses, and secondly to evaluate how efficient oestrogen replacement is at restoring any observed alteration.

As our most recently published results³⁰ most likely reflect the predominant triglyceride portion of the RET adipocyte fatty acid composition, in order to further examine our hypothesis, we investigated the fatty acid composition of cholesteryl ester (CE) and monoglyceride diglyceride (Mono-Di) lipid fractions extracted from retroperitoneal white adipose tissue, firstly to determine to what extent these dynamic lipid fractions are affected by ovarian losses, and secondly to evaluate how efficient oestrogen replacement is at restoring any observed alteration.

Ovariectomy alone increased body weight gain and adiposity due to increased feed efficiency, as food intake was not increased (Table 1). Insulin and leptin levels, leptin/adiponectin ratio, and HOMA indexes also increased after ovariectomy. The observed alterations were further exacerbated by high-fat diet ingestion. Our findings are consistent with the demonstration that impaired glucose homeostasis influences adipose tissue inflammation during high-fat intake³⁴. In our study, whilst oestradiol replacement was able to attenuate the serum parameters altered by ovariectomy alone, the same was not observed when in combination with high-fat diet ingestion. We

Fatty acid		% of total fatty acids		
		ShamC	OvxC	OvxC + E2
C14:0	Myristic acid	0.55 ± 0.24	0.85 ± 0.21	0.84 ± 0.46
C16:0	Palmitic acid	21.52 ± 2.44	22.29 ± 1.13	24.62 ± 2.35
C18:0	Stearic acid	5.82 ± 3.56	5.55 ± 1.10	6.36 ± 3.14
C20:0	Arachidic acid	0.08 ± 0.06	0.05 ± 0.01	0.05 ± 0.03
Σ SFA		28.63 ± 3.38	29.17 ± 1.03	32.36 ± 4.99
C14:1n-7	Myristoleic acid	0.01 ± 0.01	0.02 ± 0.01	0.02 ± 0.02
C16:1n-7	Palmitoleic acid	2.01 ± 0.46	2.23 ± 0.75	1.66 ± 0.60
C18:1n-9	Oleic acid	24.12 ± 4.14	32.55 ± 5.55*	27.50 ± 2.38
C18:1n-7	cis-vaccenic acid	2.12 ± 0.23	2.30 ± 0.29	2.44 ± 0.28
C20:1n-9	Eicosenoic acid	0.11 ± 0.02	0.20 ± 0.05*	0.13 ± 0.03*
C18:0/C18:1		0.25 ± 0.23	0.16 ± 0.03	0.22 ± 0.11
C16:0/C16:1n-7		11.13 ± 2.58	10.64 ± 2.52	16.25 ± 5.65
Σ MUFA		29.02 ± 3.03	36.82 ± 5.47*	32.02 ± 2.65
C18:3n-3	Alpha-linolenic acid (ALA)	1.58 ± 0.43	1.36 ± 0.45	1.39 ± 0.13
C20:5n-3	Eicosapentaenoic acid (EPA)	0.04 ± 0.02	0.05 ± 0.05	0.03 ± 0.02
C22:5n-3	Docosapentaenoic acid (DPA)	0.08 ± 0.03	0.02 ± 0.03*	0.06 ± 0.01*
C22:6n-3	Docosahexaenoic acid (DHA)	0.11 ± 0.04	0.05 ± 0.03*	0.07 ± 0.03
Σ n-3		1.82 ± 0.46	1.48 ± 0.54	1.55 ± 0.17
C18:2n-6	Linoleic acid (LA)	33.02 ± 6.70	28.41 ± 3.02	30.29 ± 5.01
C18:3n-6	Gamma-linolenic acid	0.03 ± 0.02	0.02 ± 0.03	0.03 ± 0.02
C20:2n-6	Eicosadienoic acid (EDA)	0.18 ± 0.02	0.19 ± 0.01	0.16 ± 0.03
C20:3n-6	Dihomo-gamma linolenic acid	0.45 ± 0.11	0.30 ± 0.20	0.27 ± 0.05
C20:4n-6	Arachidonic acid (AA)	1.21 ± 1.23	0.57 ± 0.31	0.57 ± 0.14
C22:4n-6	Docosatetraenoic acid (DTA)	0.17 ± 0.09	0.10 ± 0.08	0.09 ± 0.04
Σ n-6		35.05 ± 5.67	29.59 ± 3.55	31.40 ± 5.15
Σ n-6/Σ n-3		20.07 ± 4.41	21.57 ± 5.93	20.26 ± 3.19
Σ PUFA		36.87 ± 2.4	31.07 ± 3.2	32.95 ± 2.5
Σ UFA		65.89 ± 7.70	67.90 ± 1.78	64.97 ± 6.09
Σ SFA/Σ UFA		0.45 ± 0.11	0.43 ± 0.02	0.51 ± 0.13

Table 3. Fatty acid composition of RET monoglyceride diglyceride lipids obtained from ovariectomized (Ovx) or Sham operated rats, fed a control (C) diet, subjected or not to oestrogen replacement therapy (E2). Data presented as means ± standard error (SE) of the % of total FAs. n = 6 for each group. SFA saturated fatty acids, MUFA monounsaturated fatty acids, PUFA polyunsaturated fatty acids. *p < 0.05 vs ShamC; #p < 0.05 OvxC vs OvxC + E2.

suggest that due to the much poorer metabolic background of the lard diet-fed ovariectomized rats in comparison to the control diet-fed ovariectomized rats, the present oestradiol replacement therapy of 2.8 µg/day was possibly not sufficient to induce positive metabolic effects. Our suggestion agrees with a similar experiment in ovariectomized mice fed a lard-enriched diet, in which an oestradiol dose of 1.7 µg/day protected the mice from insulin resistance³⁵. The oestrogen dose to mice in the study of Riant was relatively much higher in comparison to our study in rats, although the oestrogen replacement dose chosen for our study appears to be compatible with the human dosage of the average transdermal replacement therapy commonly used for postmenopausal women^{36,37}.

The CE FA analyses from rats fed the control diet showed that SFA decreased in OvxC in comparison to ShamC, while both n-3 and n-6 PUFA levels increased and MUFAs remained unchanged (Table 2). However, the CE FA analyses from rats fed the lard diet showed similar SFA, MUFAs and PUFAs levels, with no further alterations than the ones caused by ovariectomy alone (Table 4). These results agree with CE being a dynamic fraction and a reflection of global metabolic status, playing a major role as an integral component of membrane lipid rafts and as vehicle for the exportation of FA stored intracellularly in adipocytes^{38,39}.

The decreased SFA levels observed in ovariectomized rats, particularly palmitic acid, was previously reported in the visceral adipose tissue of postmenopausal women, where a decreased ratio of saturation/unsaturation was identified⁴⁰. Whilst the study of Garaulet⁴⁰ suggests that dietary factors combined with the age of subjects may play an important role in this phenomenon, our results suggest that ovariectomy alone may have had an effect, once SFA content decreased from 30.37% in ShamC down to 19.15% in OvxC, whilst ShamL showed 19.04% SFA, a content similar to 19.01% in OvxL (Table 2).

Decreased levels of SFA in serum phospholipids in postmenopausal women were observed previously⁴¹, whilst another report showed increased PUFA levels in plasma CE in postmenopausal women, alongside a positive association with adiposity⁴². Our findings that CE PUFAs were significantly higher in OvxC as compared to ShamC

Fatty acid		% of total fatty acids		
		ShamL	Ovxl	Ovxl + E2
C14:0	Myristic acid	0.36 ± 0.09	0.56 ± 0.01*	0.27 ± 0.01*
C16:0	Palmitic acid	13.38 ± 3.81	13.65 ± 1.44	11.80 ± 1.81
C18:0	Stearic acid	3.49 ± 1.04	3.77 ± 1.19	3.14 ± 0.51
C20:0	Arachidic acid	0.04 ± 0.02	0.02 ± 0.03	0.03 ± 0.01
C24:0	Behenic acid	1.77 ± 1.73	1.01 ± 0.44	0.74 ± 0.45
Σ SFA		19.04 ± 4.33	19.01 ± 2.18	15.99 ± 2.05
C14:1n-7	Myristoleic acid	0.01 ± 0.01	0.03 ± 0.01*	0.01 ± 0.01*
C16:1n-7	Palmitoleic acid	1.67 ± 0.37	1.77 ± 0.32	1.46 ± 0.14
C18:1n-9	Oleic acid	29.10 ± 6.92	26.04 ± 4.22	30.32 ± 3.02
C18:1n-7	cis-vaccenic acid	2.39 ± 0.34	2.22 ± 0.19	2.09 ± 0.29
C20:1n-9	Eicosenoic acid	0.14 ± 0.08	0.09 ± 0.05	0.15 ± 0.06
C18/C18:1		0.11 ± 0.02	0.14 ± 0.05	0.10 ± 0.01
C16:0/C16:1n-7		8.82 ± 4.92	7.81 ± 0.60	8.10 ± 1.02
Σ MUFA		33.30 ± 6.98	30.14 ± 4.73	33.87 ± 2.95
C18:3n-3	Alpha-linolenic acid (ALA)	4.07 ± 2.19	4.23 ± 0.82	3.79 ± 0.60
C20:5n-3	Eicosapentaenoic acid (EPA)	0.04 ± 0.02	0.04 ± 0.02	0.04 ± 0.01
C22:5n-3	Docosapentaenoic acid (DPA)	0.13 ± 0.06	0.15 ± 0.05	0.15 ± 0.07
C22:6n-3	Docosahexaenoic acid (DHA)	0.10 ± 0.05	0.07 ± 0.06	0.14 ± 0.06
Σ n-3		4.36 ± 2.28	4.51 ± 0.84	4.13 ± 0.67
C18:2n-6	Linoleic acid (LA)	40.31 ± 8.01	43.76 ± 5.59	43.23 ± 4.33
C18:3n-6	Gamma-linolenic acid	0.10 ± 0.06	0.11 ± 0.02	0.10 ± 0.03
C20:2n-6	Eicosadienoic acid (EDA)	0.28 ± 0.07	0.21 ± 0.09	0.30 ± 0.05
C20:3n-6	Dihomo-gamma linolenic acid	0.23 ± 0.11	0.22 ± 0.02	0.25 ± 0.05
C20:4n-6	Arachidonic acid (AA)	0.99 ± 0.52	0.96 ± 0.24	0.98 ± 0.14
C22:4n-6	Docosatetraenoic acid (DTA)	0.17 ± 0.07	0.17 ± 0.04	0.21 ± 0.04
Σ n-6		42.07 ± 8.68	45.43 ± 5.73	45.07 ± 4.46
Σ n-6/Σ n-3		14.75 ± 12.99	10.23 ± 1.21	11.01 ± 0.77
Σ PUFA		46.43 ± 2.4	49.94 ± 3.2	49.20 ± 2.5
Σ UFA		79.74 ± 4.23	80.08 ± 2.38	83.06 ± 2.17
Σ SFA/Σ UFA		0.24 ± 0.07	0.24 ± 0.03	0.19 ± 0.03

Table 4. Fatty acid profile of RET cholesteryl ester lipids obtained from ovariectomized (Ovxl) or Sham operated rats, fed a lard-enriched (L) diet, subjected or not to oestrogen replacement therapy (E2). Data presented as means ± standard error (SE) of the % of total FAs. n = 6 for each group. SFA saturated fatty acids, MUFA monounsaturated fatty acids, PUFA polyunsaturated fatty acids. *p < 0.05 vs ShamL; #p < 0.05 Ovxl vs Ovxl + E2.

suggest the mobilization of intracellularly stored PUFA for utilization elsewhere, with CE deployed as a vehicle for the exportation of essential EFAs from within the cell. Our hypothesis is further corroborated by the Mono-Di findings shown in Table 3, in which DPA and DHA are significantly reduced in OvxlC as compared to ShamC, and although not statistically significant, the ΣPUFA was 15.7% lower in OvxlC (31.07% ΣPUFA) versus ShamC (36.87% ΣPUFA). We suggest that, in ovariectomised rats, adipocytes are exporting PUFAs and retaining SFAs.

The changes in CE and Mono-Di FA observed in the lard fed group were not identical to the changes observed in the control group. Whilst there was a tendency for increased ΣPUFA in CE of Ovxl (49.94% in Ovxl versus 46.43% in ShamL) (Table 4), such differences did not reach the statistical significance observed between OvxlC versus ShamC (Table 2). Nonetheless, the Mono-Di ΣPUFA content was significantly lower in Ovxl (23.46%) as compared to ShamL (31.92%) (Table 5).

The lard-fed rats in the present study were exposed to an EFA-deficient diet. The deleterious impact of saturated fat-rich diets upon peripheral tissue fatty acid profile has been previously demonstrated by us⁴³ and others^{44,45}. In a chronically deficient EFA diet, it may be possible that the biochemically harsh conditions prevented the RET CE from further adapting in ovariectomy, but it appears the Mono-Di fraction, which is located intracellularly in abundance, was able to buffer some of those unfavourable conditions, confirming the altruist role of the adipose tissue in protecting the body⁴⁶.

Oestrogen replacement was able to partially attenuate the CE FA alterations observed in ovariectomy, in which it appears to return the levels of some FA, including behenic, AA, EPA and DHA levels, to levels similar to those found in Sham rats. It has been documented that hormone replacement therapy was able to decrease the levels of behenic acid in serum phospholipids⁴¹ as well as decreased AA levels in whole blood of postmenopausal women⁴⁷. In the particular case of AA, we acknowledge the disagreement of our findings with previous studies showing that hormone replacement increase AA levels, mostly due to alterations in Δ6-desaturase activity caused

Fatty acid		% of total fatty acids		
		ShamL	OvxL	OvxL + E2
C14:0	Myristic acid	0.39 ± 0.26	0.82 ± 0.18*	0.30 ± 0.14*
C16:0	Palmitic acid	18.76 ± 5.68	24.11 ± 1.54	20.74 ± 1.83
C18:0	Stearic acid	5.46 ± 1.73	7.64 ± 0.65*	6.75 ± 0.59
C20:0	Arachidic acid	0.04 ± 0.03	0.06 ± 0.02	0.05 ± 0.02
Σ SFA		24.99 ± 7.37	32.95 ± 1.98*	28.24 ± 2.01
C14:1n-7	Myristoleic acid	0.01 ± 0.01	0.03 ± 0.02	0.01 ± 0.01
C16:1n-7	Palmitoleic acid	1.66 ± 0.36	1.94 ± 0.28	1.34 ± 0.11*
C18:1n-9	Oleic acid	32.46 ± 5.50	34.18 ± 4.67	37.64 ± 1.87
C18:1n-7	cis-vaccenic acid	2.51 ± 0.38	2.48 ± 0.16	2.24 ± 0.16
C20:1n-9	Eicosenoic acid	0.22 ± 0.09	0.14 ± 0.08	0.27 ± 0.02*
C18/C18:1		0.15 ± 0.04	0.21 ± 0.04*	0.17 ± 0.02
C16:0/C16:1n-7		11.36 ± 2.93	12.59 ± 1.48	15.55 ± 1.56*
Σ MUFA		37.14 ± 5.87	39.20 ± 4.76	41.83 ± 1.80
C18:3n-3	Alpha-linolenic acid (ALA)	1.98 ± 1.62	1.15 ± 0.31	1.07 ± 0.21
C20:5n-3	Eicosapentaenoic acid (EPA)	0.02 ± 0.01	0.06 ± 0.05	0.01 ± 0.01
C22:5n-3	Docosapentaenoic acid (DPA)	0.08 ± 0.07	0.09 ± 0.07	0.05 ± 0.03
C22:6n-3	Docosahexaenoic acid (DHA)	0.05 ± 0.06	0.12 ± 0.11	0.02 ± 0.01
Σ n-3		2.13 ± 1.75	1.41 ± 0.48	1.15 ± 0.24
C18:2n-6	Linoleic acid (LA)	28.46 ± 11.17	21.26 ± 2.94	24.06 ± 1.65
C18:3n-6	Gamma-linoleic acid	0.06 ± 0.04	0.04 ± 0.02	0.04 ± 0.04
C20:2n-6	Eicosadienoic acid (EDA)	0.25 ± 0.06	0.12 ± 0.07*	0.24 ± 0.06*
C20:3n-6	Dihomo-gamma linoleic acid	0.39 ± 0.14	0.36 ± 0.20	0.25 ± 0.11
C20:4n-6	Arachidonic acid (AA)	0.51 ± 0.31	0.30 ± 0.14	0.41 ± 0.14
C22:4n-6	Docosatetraenoic acid (DTA)	0.10 ± 0.09	0.04 ± 0.02	0.09 ± 0.04
Σ n-6		29.76 ± 11.52	22.05 ± 3.16	25.09 ± 1.85
Σ n-6/Σ n-3		16.93 ± 5.56	16.79 ± 4.67	22.36 ± 3.68
Σ PUFA		31.92 ± 2.4	23.46 ± 3.2*	26.24 ± 2.5
Σ UFA		69.03 ± 9.45	62.66 ± 2.80	68.08 ± 1.73
Σ SFA/Σ UFA		0.38 ± 0.15	0.53 ± 0.05	0.42 ± 0.03

Table 5. Fatty acid profile of RET monoglyceride diglyceride lipids obtained from ovariectomized (Ovx) or Sham operated rats, fed a lard-enriched (L) diet, subjected or not to oestrogen replacement therapy (E2). Data presented as means ± standard error (SE) of the % of FAs. n = 6 for each group. SFA saturated fatty acids, MUFA monounsaturated fatty acids, PUFA polyunsaturated fatty acids. *p < 0.05 vs ShamL; #p < 0.05 OvxL vs OvxL + E2.

by oestrogen^{41,48}. It is worth noting however that whilst those results refer to whole blood, in which there is transport of EFAs by phospholipids for the brain and other prime tissues, in our study the results were observed in retroperitoneal white adipose tissue neutral lipid species.

As compared to ShamC, the OvxC group showed in the Mono-Di fraction no differences in SFA, but the ΣMUFA was significantly increased in OvxC, mainly attributed to higher oleic acid levels (Table 3). The stearoyl-CoA desaturase, also known as Δ⁹-desaturase, is the intracellular enzyme that catalyses the rate-limiting conversion of palmitoyl-CoA and stearoyl-CoA to palmitoleic and oleic acids⁴⁹. Oleic acid is the predominant FA stored in triglycerides of adipose tissue⁵⁰, with the formation of oleic acid being a direct product of Δ⁹ desaturase activity on fatty acyl-CoA substrates⁵¹. Alessandri and colleagues⁵² reported increased Δ⁹-desaturase levels following ovariectomy in rats, whilst oestrogen has been shown to suppress its expression in liver and adipose tissue^{53,54}. Overall, such findings may explain the increased oleic acid levels in Mono-Di following ovariectomy, with subsequent tendency for reduction following oestrogen replacement.

DPA and DHA were significantly decreased in Mono-Di OvxC (Table 3), and the reduced levels of the n-6 counterparts AA and docosatetraenoic (DTA) did not reach statistically significant differences, even though a tendency was clear. Our findings that the Mono-Di fraction contained more MUFA and less PUFA agree with previous reports showing that Mono-Di molecules have an important role as intracellular storage^{55,56}, and, as opposed to CE, Mono-Di are relatively more inert. The alternate increase and decrease of PUFA levels in CE and Mono-Di respectively may suggest the transfer of PUFA from within the cell to CE for membrane utilization and exportation, resulting in Mono-Di left with higher MUFAs.

Our suggestion of increased PUFA exportation through CE, but not SFA or MUFA, in OvxC rats may be attributed to the ability of peripheral tissues to synthesise SFA and MUFA but not essential PUFA. Interestingly, Belkaid and colleagues reported that 17β-oestradiol induces stearoyl-CoA desaturase-1 expression in oestrogen-responding cancer cells⁵⁷, whilst in the opposite direction, Alessandri and colleagues⁵² reported increased hepatic Δ⁹-desaturase levels following ovariectomy in rats. In our study, the ratio C18/C18:1 was significantly decreased

in CE of OvxC as compared to ShamC (Table 2), and significantly increased in the Mono-Di fraction of OvXL versus ShamL (Table 3). We also found more MUFA in Mono-Di in OvxC as compared to ShamC, but no MUFA changes in CE between OvxC and ShamC. We have not measured stearoyl-CoA desaturase activity in our study; however, as a higher C18/C18:1 ratio denotes proportionally more saturated than monounsaturated species, we further speculate that there is transfer of fatty acids from one compartment to another.

The association of lard diet with ovariectomy (OvXL) did not trigger differences in MUFA content in the Mono-Di fraction; however, it significantly increased Σ SFA and decreased Σ PUFA in relation to ShamL (Table 5). Differently from OvxC, the Σ SFA increase in OvXL may be traced to an effect of the diet alone. Our view is corroborated by a report on rats that showed a high-fat diet regimen containing 60% of kcal from fat increased the content of diglycerides in the liver, associated with systemic insulin resistance⁵⁸. Additionally, it has been shown that a regimen of n-3 FA supplementation improved insulin sensitivity and decreased the content of diglycerides in visceral adipose tissue of rats fed a high-fat diet⁵⁹.

OvxC + E2 showed partial restoration of Σ MUFA levels in Mono-Di, whilst showing little effect in PUFA levels. Interestingly, Σ SFA and Σ PUFA were partially restored in Mono-Di in OvXL + E2. We believe oestrogen replacement may be responsible for partial attenuation of the changes observed in ovariectomy, alone or in combination with a lard diet. Our results agree with previous findings that oestrogen replacement ameliorated the overall lipid metabolism in ovariectomy alone⁶⁰ as well as in association of ovariectomy with a high-fat diet⁶¹.

The limitation of this study was to not include triglycerides, which represents a predominant fraction of neutral lipids within adipose tissue. Our choice to exclude triglycerides was based on data from our previous study where we demonstrated that ovariectomy leads to a disruption of the fatty acid composition of total lipid extract, which includes, in its majority, the triglyceride portion of neutral lipids³⁰. By choosing to focus on cholesteryl esters, monoglycerides and diglycerides we aimed to investigate the more subtle and dynamic portions of the neutral lipid synthesis pathway within the adipose tissue that would confirm any metabolic changes taking place. Nevertheless, we acknowledge that including the triglycerides in this study could add to further its relevance, and deserves attention for future studies.

In conclusion, the present study showed that ovariectomy induced dramatic changes in the cholesteryl ester and monoglyceride/diglyceride fatty acid profiles of retroperitoneal white adipose tissue. Such changes appear to have been more dramatic in rats that received the control diet, as compared to the rats that received a diet enriched with lard. The control diet-fed rats may have shown greater capacity to adapt to hormone deficiency possibly due to a better fatty acid profile and a lower mild chronic pro-inflammatory background, as compared to the rats that chronically received the lard diet. We have also found that hormone replacement therapy tended to restore the level of some of the fatty acid families, but such findings were not consistently significant across all lipid families analysed in the present study. We speculate that hormone replacement therapy alone may not be sufficient to restore fatty acid profile changes observed in ovariectomy. Further studies are necessary to investigate whether hormone replacement therapy combined with positive nutrition interventions could promote better outcomes for menopausal women, particularly those subjected to nutrient-deficient diets.

Material and methods

Experimental procedures. All experiments were conducted in accordance with the Committee in Research Ethics of the Universidade Federal de São Paulo (CEUA no.: 2172030315/2016), through the guidelines of the Conselho Nacional de Controle de Experimentação Animal (CONCEA), Ministry of Science and Technology, Brazil. Detailed experimental procedures, body composition analyses and biochemical measurements adopted in the present study have been published previously⁶.

Briefly, twelve-week-old female Wistar rats were either ovariectomized (Ovx, n = 24) or sham operated (Sham, n = 12) under ketamine/xylazine anaesthesia (66/33 mg/kg intraperitoneally). From the total of 24 OvxC rats, twelve received 17 β -oestradiol replacement (Ovx + E2 group) through the insertion of subcutaneous pellets (0.25 mg/pellet, 90-day release, Innovative Research of America, Sarasota, Florida, USA). Penicillin (60,000U intramuscularly) and ibuprofen (1 mg/kg BW orally) were administered for two days following surgery.

Rats were maintained under controlled 12 h light/dark cycle (lights on at 6:00 am) and temperature (23 \pm 1 $^{\circ}$ C) with *ad libitum* food and water for 12 weeks. Upon housing, the three above groups were randomly sub-divided six by six, according to the diet offered. ShamC, OvxC and OvxC + E2 received standard rat chow (2.87 kcal/g, 15% of energy from fat, Nuvilab CR-1, Nuvital Nutrientes SA, Colombo, PR, Brazil). The ShamL, OvXL and OvXL + E2 groups received a high-fat lard-enriched diet (3.60 kcal/g, 45% energy from fat).

The lard-enriched diet was prepared by adding to the powdered standard chow 18% lard (w/w) (Cooperativa Central Aurora de Alimentos, Chapecó, Santa Catarina, Brazil), 2% soybean oil (w/w), 10% sucrose (w/w), 20% casein (w/w) to obtain the protein content of the control diet, and 0.02% (w/w) butylated hydroxytoluene (BHT). The mixture was mechanically mixed with lukewarm water for thorough homogenization of all ingredients, passed through a milling machine to produce pellets and dried in a forced ventilation oven for 24 h at 60 $^{\circ}$ C. The diet was stored at -20 $^{\circ}$ C and offered in standardized portions. The leftovers were weighted and discarded. Body weight and 24 h food mass intake were measured weekly. Feed efficiency was calculated as (body weight gain / energy intake) \times 100.

Twelve weeks after surgery, rats were fasted for 24 h and sacrificed by decapitation under thiopental anaesthesia (80 mg/kg intraperitoneally). Trunk blood was collected. RET were dissected, weighed, snap-frozen in liquid nitrogen and stored at -80 $^{\circ}$ C. The uteri were weighed for confirmation of completeness of ovariectomy.

Bodily measurements and serum biomarkers. Initial and final body weight, uterus and RET mass, serum leptin, adiponectin, glucose, insulin, total cholesterol, HDL cholesterol and triglycerides were quantified. The HOMA index was calculated as previously described⁶. The sensitivity, intra-assay and inter-assay varia-

tions of the ELISA kits used to determine the serum levels of leptin, insulin and adiponectin were, respectively, 0.08 ng/mL; 2.49% and 3.93% for leptin; 0.1 ng/mL; 1.33% and 6.71% for insulin; 0.4 ng/mL; 1.18% and 7.34% for adiponectin.

RET lipid extraction, solid-phase chromatographic separation and fatty acid analysis. Aliquots of 1000 mg of RET was homogenized and extracted in hexane/isopropanol (3:2 v/v) containing 0.01% BHT. After addition of chloroform/methanol/water (2:1:1 v/v/v), the samples were centrifuged at 10,000g for 10 min. The organic layer was separated and evaporated to complete dryness with oxygen-free nitrogen (OFN). The lipids were partitioned again in chloroform/methanol/water (8:4:3 v/v/v), the chloroform layer was obtained, dried under OFN and kept in airtight glass vials under OFN at -20°C .

CE and Mono-Di fractions were chromatographically obtained according to a previously established protocol³¹. Briefly, sample lipid residues were extracted twice in succession with 0.5 ml of isooctane-ethyl acetate (80:1 v/v) and applied to previously prepared silica gel columns (Thermo Scientific HyperSep silica columns; 100 mg bed weight) gravimetrically. CE were eluted with 5 ml of isooctane-ethyl acetate (20:1 v/v), followed by the Mono-Di fraction elution with 4.5 ml of isooctane-ethyl acetate (75:25 v/v). The collected fractions were immediately dried under OFN and kept in airtight glass vials under OFN at -20°C until derivatization.

FA analysis was performed as previously described by our group³². Briefly, fatty acid methyl esters (FAMES) were obtained by heating lipid samples in sealed glass tubes at 70°C for 3 h with 15% acetyl chloride in dry methanol under OFN. The reaction was stopped with 5% NaCl solution at room temperature and FAMES were extracted with three washes of petroleum spirit containing 0.01% BHT. Extracted FAMES were analysed by gas chromatography with flame ionization detector (GC2010 Plus, Shimadzu, Kyoto, Japan) equipped with a Trace TR-FAME capillary column (60 m \times 0.32 mm \times 0.25 μm , Thermo Scientific, Rockford, IL, USA). FAMES were identified by comparison with the retention times of previously injected authentic standards (Sigma-Aldrich, United Kingdom). Peak areas were analysed using Shimadzu software LabSolutions (Shimadzu, Kyoto, Japan).

Statistical analyses. Body weight, RET mass and serum parameters were tested for normality (Shapiro-Wilk test) and homoscedasticity (Levene's test). Normally distributed variables (means \pm standard error of the mean) were analysed by two-way ANOVA and Tukey post hoc test. Non-parametric variables (median and interquartile range) were analysed by Kruskal-Wallis followed by multiple comparisons. Tests were performed with Statistica 12 Software (StatSoft, Tulsa, OK, USA).

CE and Mono-Di FA composition results were compared by one-way ANOVA, with groups separated according to their diet. Tests were performed by SPSS software (IBM, Chicago, IL, USA). Fatty acid results are presented as mean and standard deviation of the mean, and the level of statistical significance was set at $p < 0.05$.

Received: 8 September 2020; Accepted: 22 January 2021

Published online: 15 February 2021

References

- Donato, G. B., Fuchs, S. C., Oppermann, K., Bastos, C. & Spritzer, P. M. Association between menopause status and central adiposity measured at different cutoffs of waist circumference and waist-to-hip ratio. *Menopause* **13**(2), 280–285 (2006).
- Horber, F. F. *et al.* Effect of sex and age on bone mass, body composition and fuel metabolism in humans. *Nutrition* **13**(6), 524–534 (1997).
- Dornellas, A. P. S. *et al.* High-fat feeding improves anxiety-type behavior induced by ovariectomy in rats. *Front. Neurosci.* **12**, 557 (2018).
- Retberg, J. R., Yao, J. & Brinton, R. D. Oestrogen: A master regulator of bioenergetic systems in the brain and body. *Front. Neuroendocrinol.* **35**(1), 8–30 (2014).
- Ren, H. *et al.* Effects of combined ovariectomy with dexamethasone on rat lumbar vertebrae. *Menopause* **23**(4), 441–450 (2016).
- Boldarine, V. T. *et al.* High-fat diet intake induces depressive-like behavior in ovariectomized rats. *Sci. Rep.* **9**(1), 10551 (2019).
- Cusi, K. The role of adipose tissue and lipotoxicity in the pathogenesis of type 2 diabetes. *Curr. Diab. Rep.* **10**(4), 306–315 (2010).
- Yamatani, H., Takahashi, K., Yoshida, T., Takata, K. & Kurachi, H. Association of oestrogen with glucocorticoid levels in visceral fat in postmenopausal women. *Menopause* **20**(4), 437–442 (2013).
- Robichaud, P. P. & Surette, M. E. Polyunsaturated fatty acid-phospholipid remodeling and inflammation. *Curr. Opin. Endocrinol. Diabetes Obes.* **22**(2), 112–118 (2015).
- Bueno, A. A. *et al.* Effects of different fatty acids and dietary lipids on adiponectin gene expression in 3T3-L1 cells and C57BL/6 mice adipose tissue. *Pflügers Arch.* **455**(4), 701–709 (2008).
- Galic, S., Oakhill, J. S. & Steinberg, G. R. Adipose tissue as an endocrine organ. *Mol. Cell Endocrinol.* **316**(2), 129–139 (2010).
- Karastergiou, K. & Mohamed-Ali, V. The autocrine and paracrine roles of adipokines. *Mol. Cell Endocrinol.* **318**(1–2), 69–78 (2010).
- Makki, K., Froguel, P. & Wolowczuk, I. Adipose tissue in obesity-related inflammation and insulin resistance: Cells, cytokines, and chemokines. *ISRN Inflamm.* **2013**, 139239 (2013).
- Ahima, R. S. Adipose tissue as an endocrine organ. *Obesity (Silver Spring)* **14**(Suppl 5), 242S–249S (2006).
- Lee, T. H., Cheng, K. K., Hoo, R. L., Siu, P. M. & Yau, S. Y. The novel perspectives of adipokines on brain health. *Int. J. Mol. Sci.* **20**(22), 5638 (2019).
- Deslypere, J. P., Verdonck, L. & Vermeulen, A. Fat tissue: A steroid reservoir and site of steroid metabolism. *J. Clin. Endocrinol. Metab.* **61**(3), 564–570. <https://doi.org/10.1210/jcem-61-3-564> (1985).
- Barakat, R., Oakley, O., Kim, H., Jin, J. & Ko, C. J. Extra-gonadal sites of estrogen biosynthesis and function. *BMB Rep.* **49**(9), 488–496 (2016).
- Cerqueira, N. M. *et al.* Cholesterol biosynthesis: A mechanistic overview. *Biochemistry* **55**(39), 5483–5506 (2016).
- Bracht, J. R., Vieira-Potter, V. J., De Souza Santos, R. *et al.* The role of estrogens in the adipose tissue milieu. *Ann. N. Y. Acad. Sci.* **1461**(1), 127–143 (2020).
- Goldstein, J. L., DeBose-Boyd, R. A. & Brown, M. S. Protein sensors for membrane sterols. *Cell* **124**(1), 35–46 (2006).
- Zee, P. Lipid metabolism in the newborn II. Neutral lipids. *Pediatrics* **41**(3), 640–645 (1968).
- Hamilton, J. G. & Comai, K. Separation of neutral lipids and free fatty acids by high-performance liquid chromatography using low wavelength ultraviolet detection. *J. Lipid Res.* **25**(10), 1142–1148 (1984).

23. Moilanen, T. *et al.* Plasma cholesteryl ester fatty acids in 3- and 12-year-old Finnish children. *Atherosclerosis* **48**(1), 49–56 (1983).
24. Sandker, G. W. *et al.* Serum cholesteryl ester fatty acids and their relation with serum lipids in elderly men in Crete and The Netherlands. *Eur. J. Clin. Nutr.* **47**(3), 201–208 (1993).
25. Sanders, K., Johnson, L., O'Dea, K. & Sinclair, A. J. The effect of dietary fat level and quality on plasma lipoprotein lipids and plasma fatty acids in normocholesterolemic subjects. *Lipids* **29**(2), 129–138 (1994).
26. Pike, L. J. Lipid rafts: Bringing order to chaos. *J. Lipid Res.* **44**(4), 655–667 (2003).
27. Simons, K. & Sampaio, J. L. Membrane organization and lipid rafts. *Cold Spring Harb. Perspect. Biol.* **3**(10), a004697 (2011).
28. Athenstaedt, K. & Daum, G. The life cycle of neutral lipids: Synthesis, storage and degradation. *Cell Mol. Life Sci.* **63**(12), 1355–1369 (2006).
29. Pereira-Dutra, F. S., Teixeira, L., de Souza Costa, M. E. & Bozza, P. T. Fat, fight, and beyond: The multiple roles of lipid droplets in infections and inflammation. *J. Leukoc. Biol.* **106**(3), 563–580 (2019).
30. Boldarine, V. T. *et al.* Ovariectomy modifies lipid metabolism of retroperitoneal white fat in rats: A proteomic approach. *Am. J. Physiol. Endocrinol. Metab.* **319**(2), E427–E437 (2020).
31. Ingalls, S. T. *et al.* Method for isolation of non-esterified fatty acids and several other classes of plasma lipids by column chromatography on silica gel. *J. Chromatogr. B Biomed. Sci. Appl.* **619**(1), 9–19 (1993).
32. Bueno, A. A. *et al.* Erythrocyte phospholipid molecular species and fatty acids of Down syndrome children compared with non-affected siblings. *Br. J. Nutr.* **113**(1), 72–81 (2015).
33. Everson-Rose, S. A. *et al.* Depressive symptoms and increased visceral fat in middle-aged women. *Psychosom. Med.* **71**(4), 410–416 (2009).
34. Vatarescu, M. *et al.* Adipose tissue supports normalization of macrophage and liver lipid handling in obesity reversal. *J. Endocrinol.* **233**(3), 293–305 (2017).
35. Riant, E. *et al.* Oestrogens protect against high-fat diet-induced insulin resistance and glucose intolerance in mice. *Endocrinology* **150**(5), 2109–2117 (2009).
36. Hill, D. A., Crider, M. & Hill, S. R. Hormone therapy and other treatments for symptoms of menopause. *Am. Fam. Phys.* **94**(11), 884–889 (2016).
37. Nair, A. B. & Jacob, S. A simple practice guide for dose conversion between animals and human. *J. Basic Clin. Pharm.* **7**(2), 27–31 (2016).
38. Krause, B. R. & Hartman, A. D. Adipose tissue and cholesterol metabolism. *J. Lipid Res.* **25**(2), 97–110 (1984).
39. Sezgin, E., Levental, L., Mayor, S. & Eggeling, C. The mystery of membrane organization: Composition, regulation and roles of lipid rafts. *Nat. Rev. Mol. Cell Biol.* **18**(6), 361–374 (2017).
40. Garaulet, M., Pérez-Llamas, F., Zamora, S. & Tébar, F. J. Estudio comparativo del tipo de obesidad en mujeres pre y postmenopáusicas: relación con el tamaño adipocitario, la composición de la grasa y diferentes variables endocrinas, metabólicas, nutricionales y psicológicas (Comparative study of the type of obesity in pre- and postmenopausal women: Relationship with fat cell data, fatty acid composition and endocrine, metabolic, nutritional and psychological variables). *Med. Clin. (Barc)* **118**(8), 281–286 (2002).
41. Stark, K. D., Park, E. J. & Holub, B. J. Fatty acid composition of serum phospholipid of premenopausal women and postmenopausal women receiving and not receiving hormone replacement therapy. *Menopause* **10**(5), 448–455 (2003).
42. Lewis-Barned, N. J. *et al.* Plasma cholesteryl ester fatty acid composition, insulin sensitivity, the menopause and hormone replacement therapy. *J. Endocrinol.* **165**(3), 649–655 (2000).
43. Dornellas, A. P. *et al.* Deleterious effects of lard-enriched diet on tissues fatty acids composition and hypothalamic insulin actions. *Prostaglandins Leukot. Essent. Fatty Acids* **102–103**, 21–29 (2015).
44. Brufau, G., Canela, M. A. & Rafecas, M. A high-saturated fat diet enriched with phytosterol and pectin affects the fatty acid profile in guinea pigs. *Lipids* **41**(2), 159–168 (2006).
45. Tranchida, F. *et al.* Long-term high fructose and saturated fat diet affects plasma fatty acid profile in rats. *J. Zhejiang Univ. Sci. B* **13**(4), 307–317 (2012).
46. Flatt, J. P. Energy metabolism and the control of lipogenesis in adipose tissue. *Horm. Metab. Res.* **2**, 93–101 (1970).
47. Cybulska, A. M. *et al.* Fatty acid profile of postmenopausal women receiving, and not receiving, hormone replacement therapy. *Int. J. Environ. Res. Public Health* **16**(21), 4273 (2019).
48. Piperi, C. *et al.* Effects of hormone replacement therapy on the main fatty acids of serum and phospholipids of postmenopausal women. *In Vivo* **19**(6), 1081–1085 (2005).
49. Paton, C. M. & Ntambi, J. M. Biochemical and physiological function of stearyl-CoA desaturase. *Am. J. Physiol. Endocrinol. Metab.* **297**(1), E28–E37 (2009).
50. Jeffcoat, R. Obesity - A perspective based on the biochemical interrelationship of lipids and carbohydrates. *Med. Hypotheses* **68**(5), 1159–1171 (2007).
51. Flowers, M. T. & Ntambi, J. M. Role of stearyl-coenzyme A desaturase in regulating lipid metabolism. *Curr. Opin. Lipidol.* **19**(3), 248–256 (2008).
52. Alessandri, J. M. *et al.* Ovariectomy and 17 β -estradiol alter transcription of lipid metabolism genes and proportions of neo-formed n-3 and n-6 long-chain polyunsaturated fatty acids differently in brain and liver. *J. Nutr. Biochem.* **22**(9), 820–827 (2011).
53. Paquette, A., Wang, D., Jankowski, M., Gutkowska, J. & Lavoie, J. M. Effects of ovariectomy on PPAR α , SREBP-1c, and SCD-1 gene expression in the rat liver. *Menopause* **15**(6), 1169–1175 (2008).
54. Gao, H. *et al.* Long-term administration of estradiol decreases expression of hepatic lipogenic genes and improves insulin sensitivity in ob/ob mice: A possible mechanism is through direct regulation of signal transducer and activator of transcription 3. *Mol. Endocrinol.* **20**(6), 1287–1299 (2006).
55. Ridgway, N. D., Byers, D. M., Cook, H. W. & Storey, M. K. Integration of phospholipid and sterol metabolism in mammalian cells. *Prog. Lipid Res.* **38**(4), 337–360 (1999).
56. Baker, R. C., Nikitina, Y. & Subauste, A. R. Analysis of adipose tissue lipid using mass spectrometry. *Methods Enzymol.* **538**, 89–105 (2014).
57. Belkaid, A., Duguay, S. R., Ouellette, R. J. & Surette, M. E. 17 β -estradiol induces stearyl-CoA desaturase-1 expression in estrogen receptor-positive breast cancer cells. *BMC Cancer* **15**, 440 (2015).
58. Zabielski, P. *et al.* The effect of high fat diet and metformin treatment on liver lipids accumulation and their impact on insulin action. *Sci. Rep.* **8**(1), 7249 (2015).
59. Chacina, M. *et al.* The impact of OMEGA-3 fatty acids supplementation on insulin resistance and content of adipocytokines and biologically active lipids in adipose tissue of high-fat diet fed rats. *Nutrients* **11**(4), 835 (2019).
60. Babaei, P., Mehdizadeh, R., Ansari, M. M. & Damirchi, A. Effects of ovariectomy and oestrogen replacement therapy on visceral adipose tissue and serum adiponectin levels in rats. *Menopause Int.* **16**(3), 100–104 (2010).
61. Buniam, J. *et al.* Oestrogen and voluntary exercise attenuate cardiometabolic syndrome and hepatic steatosis in ovariectomized rats fed a high-fat high-fructose diet. *Am. J. Physiol. Endocrinol. Metab.* **316**(5), E908–E921 (2019).

Acknowledgements

The authors thank Mr Mauro Cardoso Pereira for animal care, and to Mr Nelson Inácio Pinto and Mr Noel Egginton for assistance.

Author contributions

V.T.B. performed all experiments. E.J. participated in the fatty acid analyses. A.P.P. participated in all experiments not related to fatty acid analyses. M.M.T. and L.M.O. provided essential reagents and were responsible for Elisa assays. A.A.B. supervised the fatty acid analyses and interpretation of results. E.B.R. supervised the whole project. All authors contributed to the literature review, layout and writing of the manuscript.

Funding

This study was financed by the Brazilian Agencies: Coordenação de Aperfeiçoamento de Pessoal de Nível Superior (CAPES, Finance Code 001), Conselho Nacional de Desenvolvimento Científico e Tecnológico (CNPq, Grants 453924/2014-0 and 309505/2017-8), and Fundação de Amparo à Pesquisa do Estado de São Paulo (FAPESP, Grant No. 2012/03172-4). The authors are also grateful for the University of Worcester for partial financial support.

Competing interests


The authors declare no competing interests.

Additional information

Correspondence and requests for materials should be addressed to V.T.B.

Reprints and permissions information is available at www.nature.com/reprints.

Publisher's note Springer Nature remains neutral with regard to jurisdictional claims in published maps and institutional affiliations.

 **Open Access** This article is licensed under a Creative Commons Attribution 4.0 International License, which permits use, sharing, adaptation, distribution and reproduction in any medium or format, as long as you give appropriate credit to the original author(s) and the source, provide a link to the Creative Commons licence, and indicate if changes were made. The images or other third party material in this article are included in the article's Creative Commons licence, unless indicated otherwise in a credit line to the material. If material is not included in the article's Creative Commons licence and your intended use is not permitted by statutory regulation or exceeds the permitted use, you will need to obtain permission directly from the copyright holder. To view a copy of this licence, visit <http://creativecommons.org/licenses/by/4.0/>.

© The Author(s) 2021

Appendix 4

Phospholipid molecular species separation and analysis by HPLC-MS

To further isolate, separate and characterize both the PL classes and separate and characterize the molecular species within that class a 2-dimensional (2D) LC (LC×LC) method was explored. A review of the literature resulted in two potential methods (Dugo *et al.* 2013; Netto, Wong and Ritchie 2013). Both methods reported to separate PL classes by a silica hydrophilic interaction liquid chromatography (HILIC) column in the first dimension (D1) and a by silica column in the second dimension (D2). The capability of such a system for analysis of PLs was evaluated on our equipment. The method was assessed with commercially available PL standards (Table 88) and Folch-extracted egg yolk samples. Samples were dissolved in chloroform/methanol 2:1 (v/v) and stored at $-20\text{ }^{\circ}\text{C}$ until use.

Reagents and materials

LC-MS grade reagents were purchased from Thermo Fisher Scientific, UK - water, acetonitrile, methanol, tetrahydrofuran, isopropanol, ammonium formate, and formic acid. The buffered mobile phases were adjusted to pH6.5 by adding a few drops of formic acid. The standards of phosphatidylinositol (PI), phosphatidylethanolamine (PE), phosphatidylcholine (PC), sphingomyelin (SM) and phosphatidylcholine (PC) were purchased from Sigma–Aldrich (Merck KGaA, Darmstadt, Germany) (See Table 88).

Chromatographic separations were carried out using two different core-shell columns purchased from Phenomenex, Macclesfield, UK: Phenomenex Kinetex HILIC minibore Column. $1.7\mu\text{m}$, $2.1 \times 100\text{mm}$ and Phenomenex Kinetex® $1.7\mu\text{m}$ C18 100 Å, LC Column $150 \times 2.1\text{ mm}$. All analysis was performed on a Shimadzu Nexera X2 equipped with a Shimadzu CBM-20A controller, Shimadzu LC-30ADdual-plunger pumps, Shimadzu DGU-20A5 degassing unit, Shimadzu CTO-20A column oven, Shimadzu SIL-20AC autosampler, Shimadzu SPD-M20A photo diode array detector ($2.5\mu\text{L}$ detector flow cell), Shimadzu LCMS-2020 mass spectrometer. Post run analysis was performed on Shimadzu LabSolutions (Version 5.82 SP1).

Installation of Columns

Both columns were installed and conditioned as per manufacturer's instructions (Phenomenex 2017). Briefly, each column was installed without the outlet connected to the detector. The HILIC column was initially flushed with an acetonitrile / water (85:15) solvent mixture to remove any particulate matter from the column, while the C18 column was flushed

with acetonitrile / water (65:35). An initial flow rate was set to 0.1 mL/min (for 2.1 mm ID) for 5 minutes and then increased to 0.2 mL/min (2.1mm ID) for 10 minutes with the solvent collected in a small beaker to confirm flow rate. The outlet end of column was then connected to the detector and further flushed with 30 column volumes (10ml-HILIC; 16ml-C18) at low flow (~0.2 mL/min) while monitoring the backpressure.

LC Conditions

Several flow rates and solvent combinations was assessed against commercially available standards for optimum separation (summarized in Table 89). Briefly, for HILIC separation of Phospholipid classes, Acetonitrile/ ammonium format (10 mM) (ACN/AmFm10mM) in the ratios 95:5v/v, 90:10 v/v and 85:15 v/v were assessed at flow rates of 0.05ml/min, 0.1ml/min and 0.2ml/min.

Table 89. Mobile phases and flow rates assessed for HILIC and C18 columns used for the separation of phospholipids by liquid chromatography.

	HILIC	C18
Mobile phases:	Acetonitrile/ammonium formate (10 mM) buffer pH6.5 in the ratios 95:5v/v, 90:10 v/v and 85:15 v/v	(A) ammonium formate buffer (10 mM; pH 6.5)/ isopropanol/tetrahydrofuran (30:55:15) and (B) acetonitrile Isocratic elution (40% B)
Flow Rate:	0.05ml/min - 0.2ml/min	0.1 - 0.3 ml/min
Sample injection volume:	10 µL	20 µL

MS conditions

For the identification of phospholipid molecular species MS acquisition conditions will be performed as per the Shimadzu technical report (Dugo *et al.* 2013) for a Shimadzu LCMS-2020 mass spectrometer using the ESI interface operating in both positive and negative ionization modes. The specific settings are summarized in Table 90.

Table 90. Mass spectrometry acquisition conditions for the identification of phospholipid molecular species separated on a C18 column.

Mass Spectral Range:	200–1100 <i>M/Z</i>	Desolvation Line (DI) Temperature:	250°C
Event Time:	1 Sec	DI Voltage:	–34 V
Scan Speed:	938 Amu/S	Probe Voltage:	+4.5 Kv
Nebulizing Gas (N2) Flow:	1.5 L. Min ⁻¹	Qarray Dc Voltage:	1 V
Drying Gas (N2) Flow:	15 L. Min ⁻¹	Qarray Rf Voltage:	100 V
Interface Temperature:	350°	Detection Gain:	0.8 Kv
Heat Block Temperature:	200°C		

HILIC separation of phospholipid classes

For HILIC separation of Phospholipid classes, an initial screening of solvent combinations was undertaken (data not shown) for the HILIC method screening acetonitrile: ammonium format (10 mM) (ACN: AmFm10mM) in the ratios 95:5v/v, 90:10 v/v and 85:15 v/v as per previously published methods (Dugo *et al.* 2013; Netto, Wong and Ritchie 2013). After initial screening ACN/AmFm10mM was chosen as the HILIC solvent of choice for further analysis. The pH of the solvent was also checked (data not shown) as this varied between methods from pH 5.5 – 8.0. A final pH of 6.5 was chosen as pH 5.5 interfered with detector and a pH below 7.0 was recommended for the column.

A number of flow rates (Table 89) were explored for optimum HILIC separation of phospholipids (PI, PE, PC, SM) using ACN: AmFm10mM (90:10v/v) and commercially available standards (Table 88.). Data is presented in Table 91. and Figure 55, Figure 56 and Figure 57. All flow rates adequately separated individual phospholipids into distinct fractions. 0.2ml/min allowed for the fastest separation at approx. 40 minutes; however, some overlap of PI and PE may occur with only a 0.5min difference between fractions. Better separation of PI and PE was observed when run at 0.1ml/min but still may present potential overlap of fractions with only 0.7min time difference between fractions. A final flow rate of 0.05ml/min provides a 3-minute time difference between PI and PE and will allow for distinct fraction collection between the two distinct classes. PC and SM show distinct separation at all flow rates with no overlap between them and the earlier phospholipids. A flow rate of 0.2ml/min provides the fastest separation of these two phospholipid fractions. The retention times of the phospholipid classes was tested against Folch-extracted egg yolk phospholipids (see Table 91. and Figure 55, Figure 56 and Figure 57). PE (27±0.85%), PC (72±0.9%) and SM (0.65±0.06%) were identified in the egg yolk sample (See Figure 58).

C18 separation of phospholipid molecular species

An Initial screening for separation of phospholipid molecular species by C18 liquid chromatography was undertaken using acetonitrile: ammonium formate (90:10v/v) at a flow rate of 0.3ml/min with (A) ammonium formate buffer (10 mM; pH 6.5)/isopropanol /tetrahydrofuran (30:55:15) and (B) acetonitrile; Isocratic elution (40% B). As shown in Figure 59 all standards eluted within a 25-minute run time, although PI eluted with the solvent front. PC appeared to be richest in molecular species, and appeared to have some overlapping of peaks, while PE also showed poorer peak formation. PC was further run at flow rates 0.2, 0.3 and 0.4 ml/min to explore better peak formation (Figure 60). While 0.4ml/min produced a similar peak profile to 0.3ml/min, some later peaks overlapped. 0.2ml/min produced even more overlapping.

HPLC-MS

The objective of this work was to develop an HILIC-C18-LC system in combination single quadrupole mass spectrometric detection for analysis of phospholipid molecular species in absence of a tandem mass spectrometer. Hydrophilic -interaction Chromatography (HILIC) is a technique used to separate very polar samples. It works in a similar fashion to normal-phase chromatography but with reverse-phase solvents utilizing a polar stationary phase and an organic-rich (acetonitrile) low aqueous mobile to elute analytes in order of increasing hydrophilicity. To make this separation system operate seamlessly as a 2D separation method, a quaternary solvent pump system would be required, but was not available in-house at the time of method development for use in our HPLC-MS. Due to time constraints, this method of analysis for PPL separation was reassessed and it was decided that total PPL fatty acid profiles would be examined instead. Therefore, this additional analysis was not utilized for the further sample analysis of the PPL SPE fractions but may provide a useful starting point for further method development for in-house PPL separation.

Table 91. Flow rates and retention times of commercially available standards using HILIC liquid chromatography (Acetonitrile: ammonium formate (90:10v/v) separation of phospholipids

LC Flow Rate	0.05ml/min		0.1ml/min		0.2ml/min	
	Retention time (mins)		Retention time (mins)		Retention time (mins)	
	Standard	Egg Yolk	Standard	Egg Yolk	Standard	Egg Yolk
Phosphatidylinositol (PI)	4-5	-	2 - 2.8	-	1 – 1.5	-
Phosphatidylethanol-amine (PE)	8-50	15 – 45	3.5 - 17.5	8 – 18	2 – 11	4 – 9
Phosphatidylcholine (PC)	60-85	60 – 85	30 – 40	30 – 42	13 – 20	15 – 21
Sphingomyelin (SM)	135 – 180	139 – 156	65 – 100	68 – 77	27 – 50	34 – 38

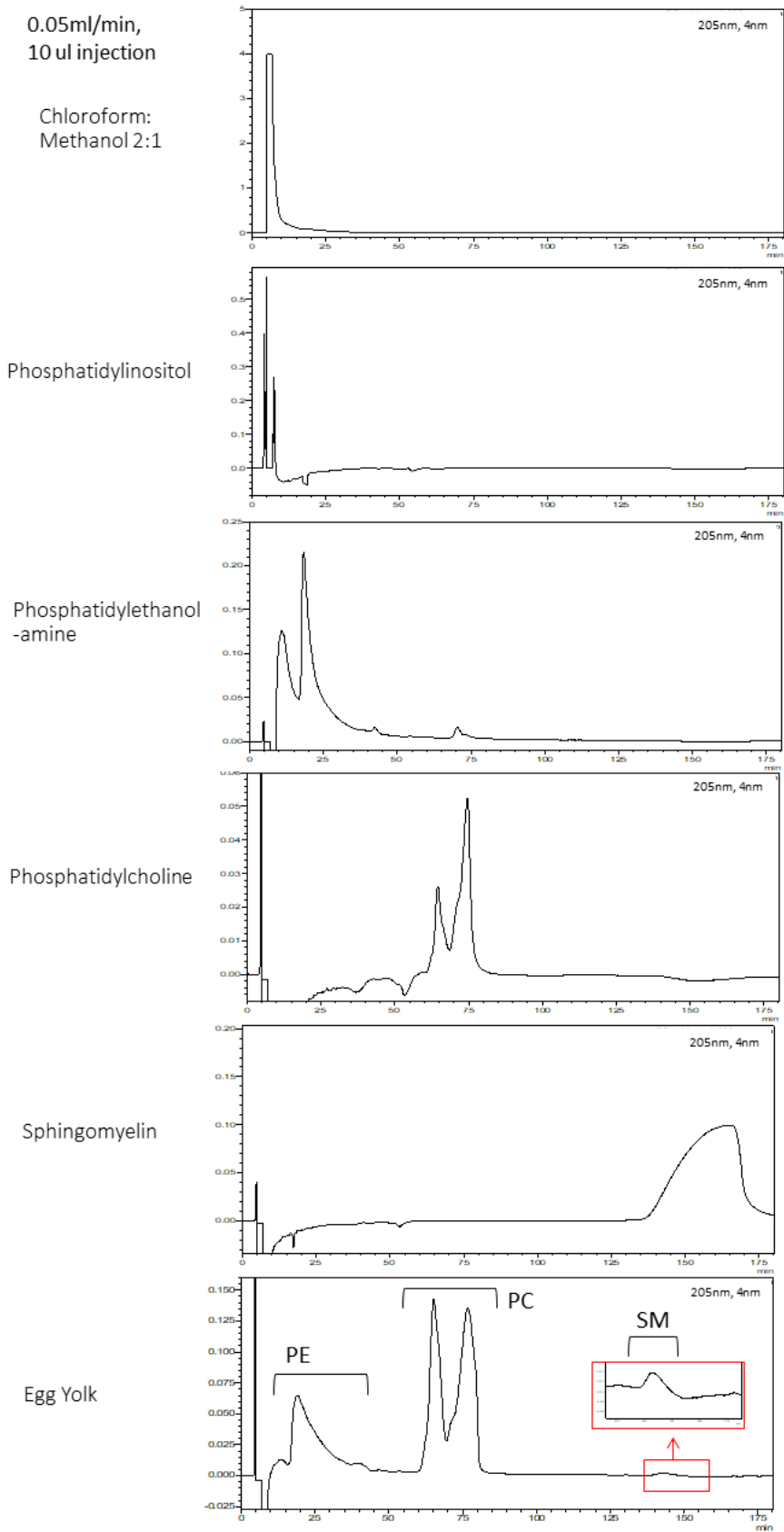


Figure 55. HILIC liquid chromatography separation of commercially available phospholipids and Folch-extracted egg yolk phospholipids using acetonitrile: ammonium formate (90:10v/v) at a flow rate of 0.05ml/min showing distinct fraction separation of lipid classes

0.1ml/min,
10 ul injection

Chloroform:
Methanol 2:1

Phosphatidylinositol

Phosphatidylethanol
-amine

Phosphatidylcholine

Sphingomyelin

Egg Yolk

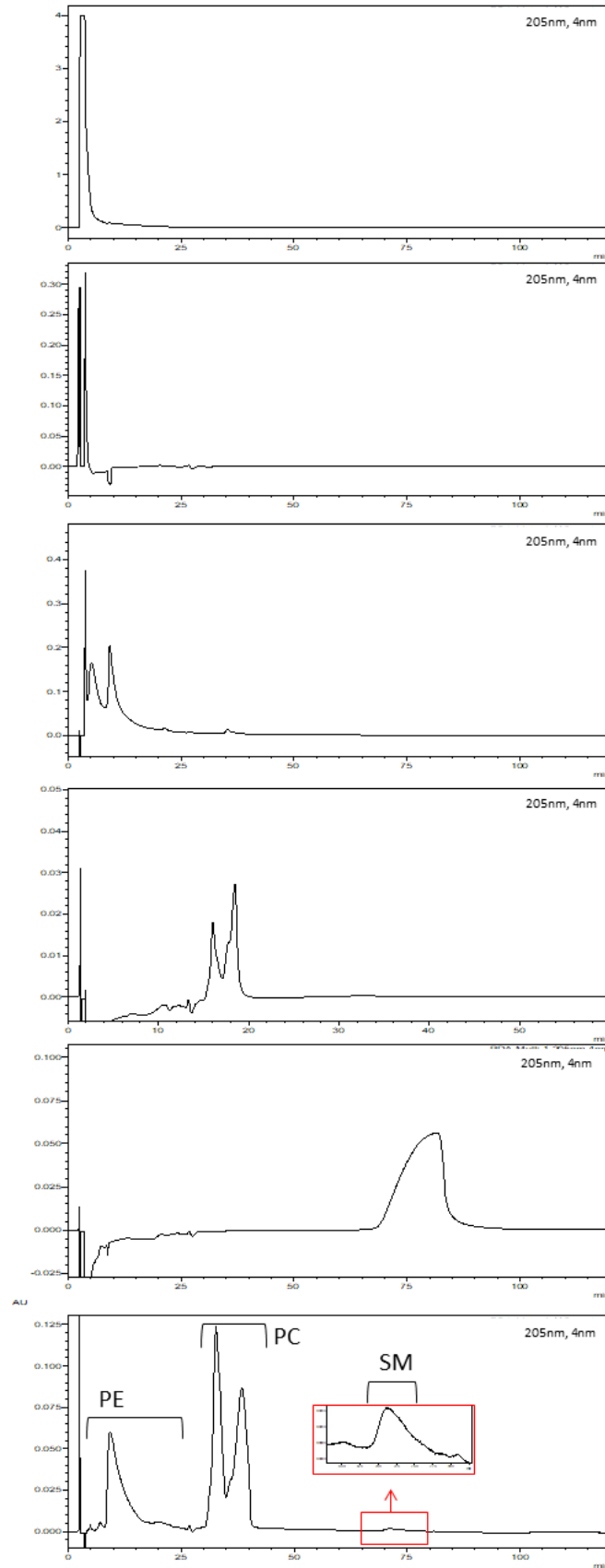
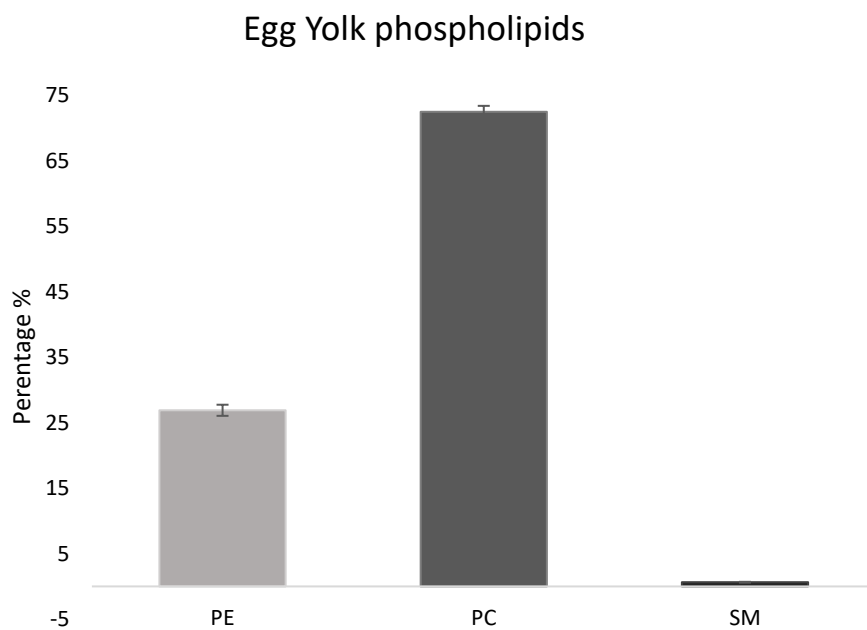


Figure 56. HILIC liquid chromatography separation of commercially available phospholipids and Folch-extracted egg yolk phospholipids using acetonitrile: ammonium formate (90:10v/v) at a flow rate of 0.1ml/min showing distinct fraction separation of lipid classes



	Sample	percentage %	SEM
			n=3
Phosphatidylethanolamine (PE)		26.89	± 0.85
Phosphatidylcholine (PC)		72.46	± 0.90
Sphingomyelin (SM)		0.65	± 0.06

Figure 58. Sample percentage (%) of phospholipids classes separated in Folch-extracted egg yolk lipids by HILIC Liquid chromatography

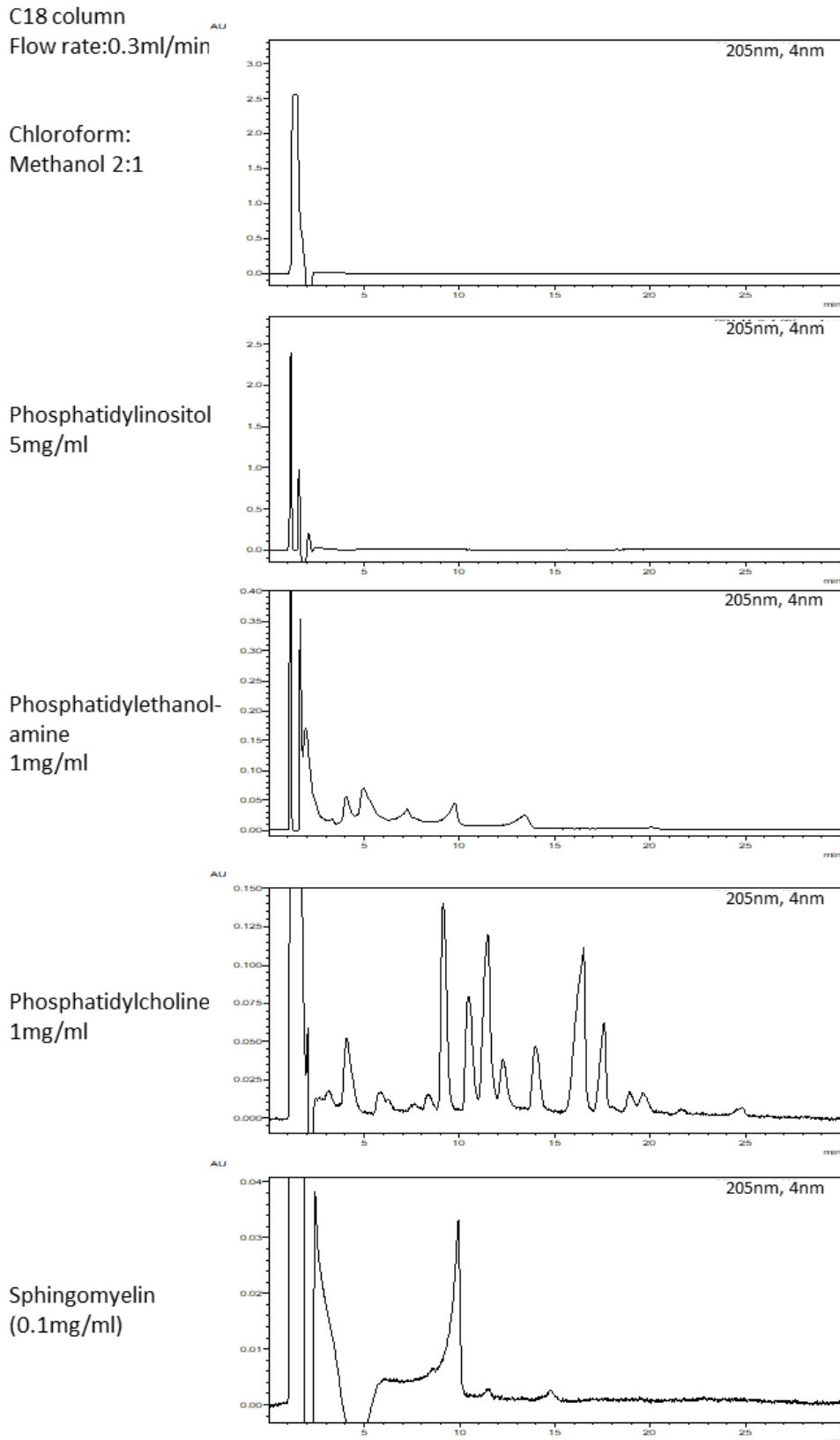


Figure 59. Separation of phospholipid molecular species by C18 liquid chromatography using acetonitrile: ammonium formate (90:10v/v) at a flow rate of 0.3ml/min with (A) ammonium formate buffer (10 mM; pH 6.5)/isopropanol/tetrahydrofuran (30:55:15) and (B) acetonitrile; Isocratic elution (40% B).

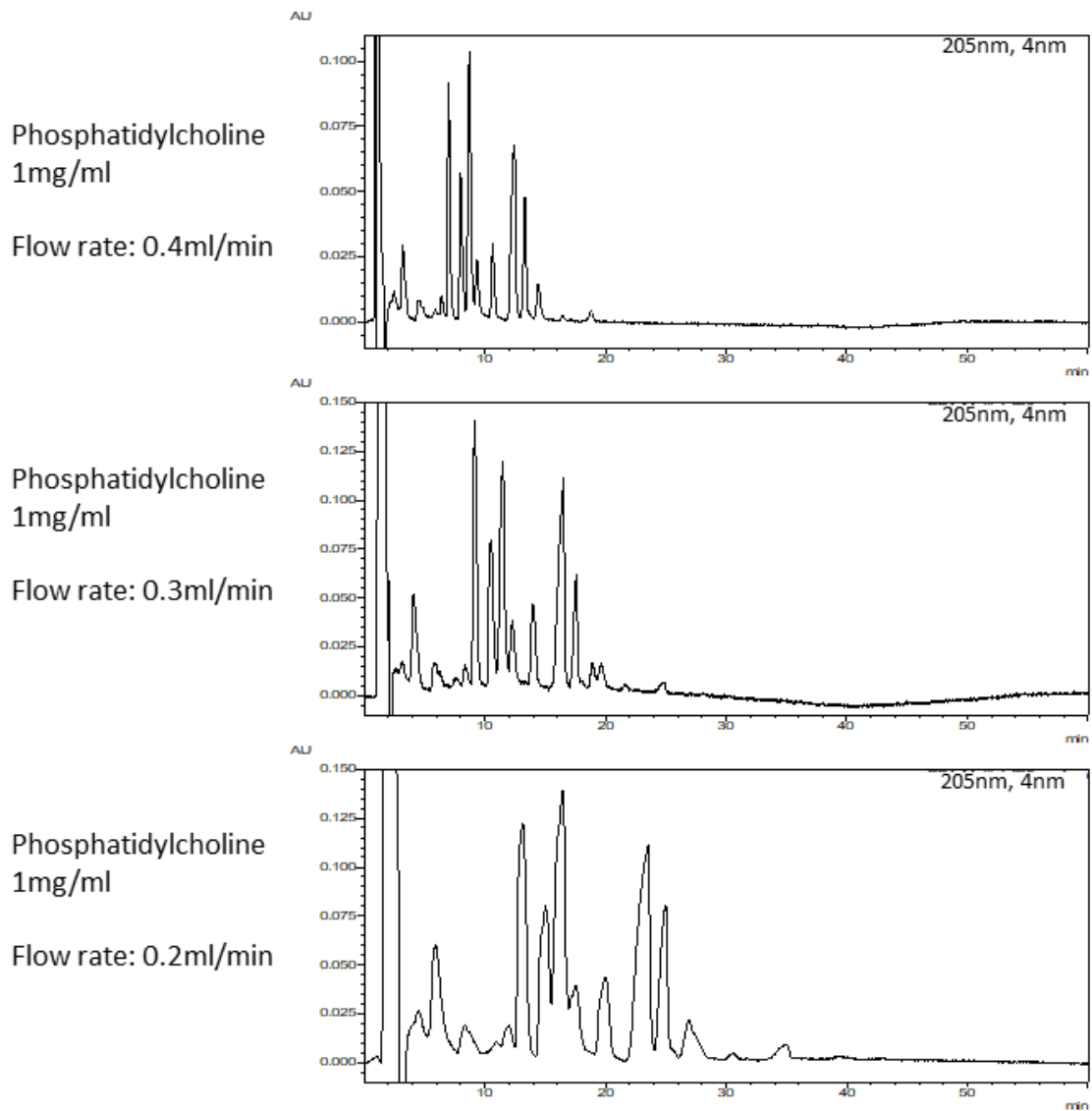


Figure 60. Separation of phospholipid molecular species by C18 liquid chromatography using acetonitrile: ammonium formate (90:10v/v) under different flow rates of 0.2, 0.3 and 0.4ml/min with (A) ammonium formate buffer (10 mM; pH 6.5)/isopropanol/tetrahydrofuran (30:55:15) and (B) acetonitrile; Isocratic elution (40% B)

Appendix 5

Table 92. Macronutrients, caloric value, and lipid profiles of normal fat diet (NFD) and high-fat diet (HFD) diet chow fed to male Wistar Rats (Taken from (Hirata Pedroso et al, 2019)).

	Standard chow	High-fat diet
Humidity (%)	9.1	1.1
Lipids (%)	4.5	31.6
Protein (%)	22.7	27.0
Carbohydrates (%)	35.9	27.5
Total fibre (%)	18.9	8.6
Fixed mineral residue (%)	8.9	4.2
Sodium chloride (%)	0.6	0.2
Calculated energy (kcal/g)	2.7	5.0
Fatty acid composition (% total)		
SATURATED FATTY ACIDS		
Myristic acid - C14:0	0.0	1.1
Palmitic acid - C16:0	14.6	21.4
Stearic acid - C18:0	3.6	11.6
Monounsaturated fatty acid		
Palmitoleic acid - C16:1n7	0.0	1.7
Vaccenic acid - C18:1n7	0.9	2.26
Oleic acid - C18:1n9	24.1	35.5
Eicosanoic acid - C20:1n9	0.3	0.6
POLYUNSATURATED FATTY ACIDS		
Linoleic acid - C18:2n6	55.4	21.4
Linolenic acid - C18:3n3	4.7	1.3

In the male Wistar rat study, rats were fed either standard rat chow (NuvilabR, Brazil, 2.7 kcal/g), or a supplemented high fat chow prepared by mixing 40% (w/w) ground standard chow with 28% (w/w) melted lard, 20% (w/w) casein powder, 10% (w/w) sucrose, 2% (w/w) soybean oil, and 0.02% (w/w) butylated hydroxytoluene (5.0 kcal/g) as standardized and used in previous studies (Banin et al. 2014b; Hirata Pedroso et al., 2019, 2015, 2019).

Appendix 6

NGF-induced differentiation

It was reported by Greene in 1978, that for PC12 cell survival and morphological differentiation in serum-free media, a minimum of 10 ng/ml 2.5S NGF was required (Greene, 1978). Under serum-free conditions up to 90% of PC12 cells become non-viable within 4-6 days but if NGF is added upon serum starvation, cells undergo one doubling and remain viable for up to 4 weeks. Additionally, if NGF is added after two or more days of serum-deprivation, NGF works to maintain surviving cells but does not stimulate cell proliferation (Greene, 1978). It is now standard protocol to use reduced serum media PC12 differentiation to limit cell proliferation and encourage cell differentiation (Rudkin *et al.*, 1989; Das, Freudenrich and Mundy, 2004; Marszalek *et al.*, 2004; Hahn, Jones and Meyer, 2009; Mei *et al.*, 2013). Reduced serum media helps to synchronize the cell cycle and arrest it in the G1 phase. G1 phase occurs at the end of mitotic division and before the commencement of DNA replication in S phase. The G1/S checkpoint prevents cells entering S phase if DNA damage is identified and triggers ubiquitin-mediated degradation and apoptosis (Weitzman and Wang, 2013). Lindenboim and colleagues (1995) also reported that upon serum starvation, RNA levels in PC12 cells decreased significantly in cells in G1, S, and G2-M phases leading to DNA damage and apoptosis (Lindenboim *et al.*, 1995). Hahn and colleagues (2009) found that NGF-treated PC12 cells predominantly arrest in G1 phase of the cell cycle compared to non-treated cells (Hahn, Jones and Meyer, 2009). Hahn and colleagues (2009) also reported that NGF-treated cells spent more time in G1 phase of the cell cycle compared to S phase. They also found that cells exposed to NGF when in G1 phase rarely proceeded into S, G2 and M phases of the cell cycle, while cells already in S, G2 and M phases, upon NGF exposure, continued through the cell cycle before arresting in G1 phase. Between 24 and 61 hours of NGF treatment, Hahn and colleagues reported that cells spent 88% of the time in G1 compared to non-NGF treated cells that spent 61% (Hahn, Jones and Meyer, 2009).

0.5% HS media differentiation

After 4 days of incubation (96 hours), cell viability of cells incubated with 0.5% HS reduced-serum media (0.5% HS) was 46% less (192 Vs 0 Hrs, $p=0.04$) than that of RPMI complete media (235% Vs 0 Hrs). At 144 hours the viability of cells grown in 0.5% HS reduced further to half (126% Vs 0 Hrs) that of RPMI complete media (269% Vs 0 Hrs, $p<0.0001$) (Figure 61.A). Like that of the 1% HS group, cells started to detach from the collagen coating into suspension after 72 hours. With regards to NGF treatment, no significant difference in viability was seen in vehicle only treatment or NGF treated groups compared to 0.5% HS across all time point (Figure 61.B). Of note however was a 104% reduction in viability in the 100ng/ml NGF group (145% Vs 0 Hrs) compared to 50ng/ml (249% Vs 0 Hrs, $p=0.002$) after 96 hours. This difference disappeared however after 144 hours of treatment with 50ng/ml NGF viability (113% Vs 0 Hrs) dropping below that of 100ng/ml NGF (143% Vs 0 Hrs), although not significantly so ($p=0.81$). At 144 hours of 0.5% HS serum deprivation, viability was found to be 126% compared to 0 Hrs, less than that of 1% HS (191%). 0.5% HS supplemented with 25ng/ml NGF resulted in 99.5% viability, 50ng/ml NGF resulted in 112.8% viability while 100ng/ml NGF resulted in 143% viability compared to 0 Hrs. 0.5% HS-NGF treated cells did not experience the approximate doubling found in the 1% HS groups (1% HS+NGF; 25ng/ml-231%; 50ng/ml-211%, 100ng/ml-165% Vs 0Hrs, Figure 61) and as reported by Greene (1978). Morphologically, as shown in Figure 62, after 144hours of NGF treatment, some long neurite outgrowths were observed in 25ng/ml NGF treatment, with observable outgrowths appearing more abundant and longer in 50 and 100 ng/ml treatments.

Treatment with 50 $\mu\text{g/ml}$ GbE (120% Vs 0 Hrs, $p=0.0003$) and 100 $\mu\text{g/ml}$ GbE (133% Vs 0 Hrs, $p=0.006$) significantly decreased cell viability compared to 0.5% HS alone (192% Vs 0 Hrs) at 96 hours (Figure 61.C.). Morphologically cells appeared rounded without neurite outgrowths (not shown), comparable to that of 0.5% HS (Figure 62).

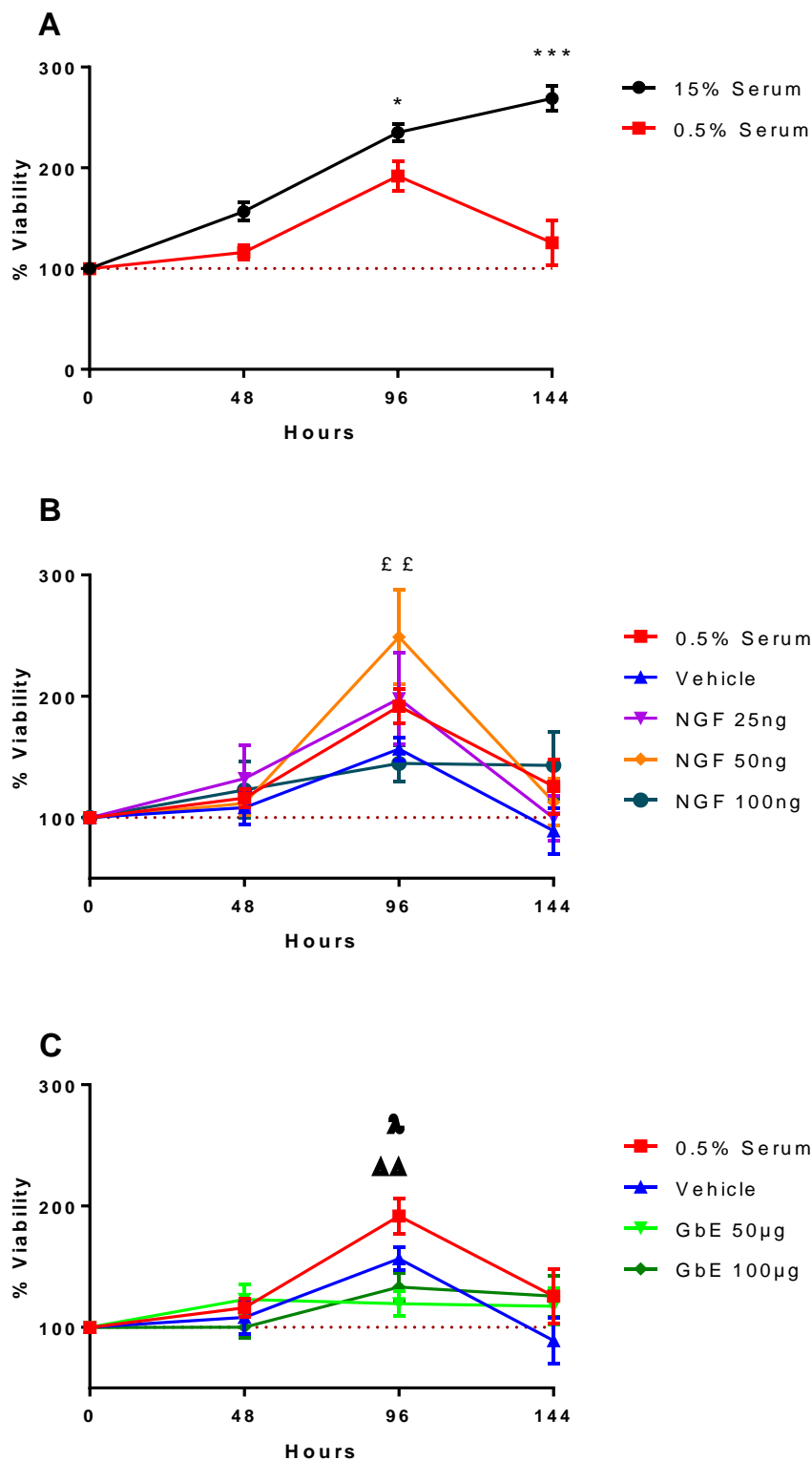
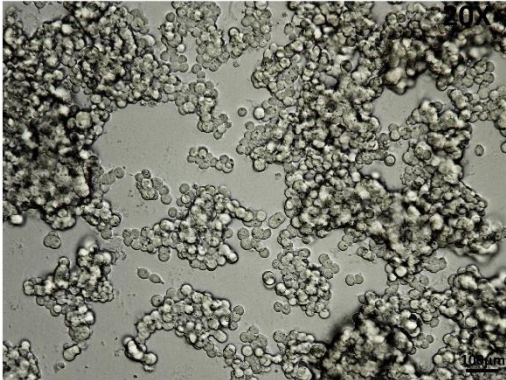
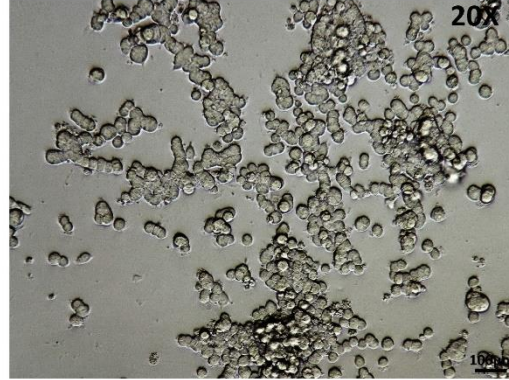


Figure 61. Viability (%) of PC12 cells after six days incubation with 1% horse serum (1% HS) media. A). 15% complete serum media (10% horse serum+ 5% foetal bovine serum) Vs 0.5% HS. B). 0.5% HS media Vs Vehicle (0.085% saline) and nerve growth factor 2.5s (NGF 25,50 and 100ng/ml) C. 0.5% HS Vs Ginkgo biloba (GbE, 50 and 100ug/ml). * $p < 0.05$, *** $p < 0.001$, ~ $p = 0.5\%$ HS Vs 25ng/ml NGF, # $p = 0.5\%$ HS Vs NGF 50ng/ml, $^{\Delta}p = 0.5\%$ HS Vs GbE50, $^{\lambda}p = 0.5\%$ HS Vs GbE100. Data presented as mean \pm SEM. Data analysed by two-way ANOVA with Šídák (A.) or Tukey (B. and C.) post hoc test.

A. 15% Complete media



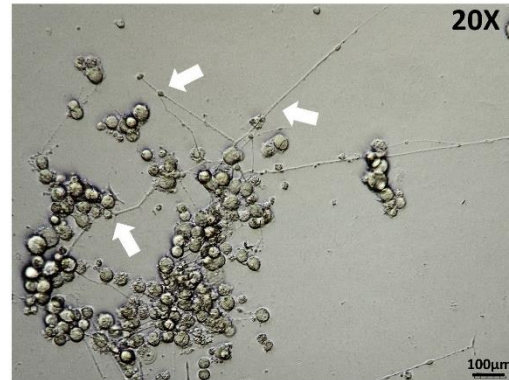
B. 0.5% Horse Serum (HS)



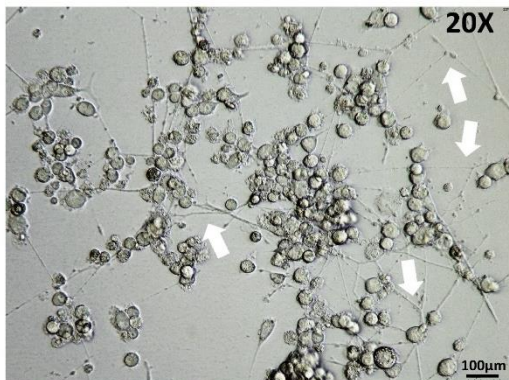
C. 0.5% HS + Vehicle



D. 0.5% HS + NGF 25ng



E. 0.5% HS + NGF 50ng



F. 0.5% HS + NGF 100ng

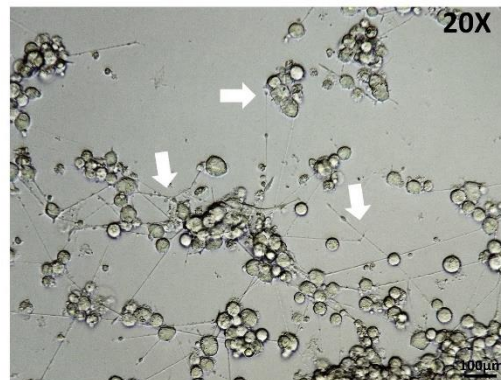


Figure 62. Microphotographs of PC12 cell differentiation with RPMI media supplemented with 0.5% horse serum (0.5% HS) and nerve growth factor (NGF) for 7 days. A.) PC12 cells incubated in complete media (RPMI + 15% serum. B.) Cells incubated in 0.5% HS. C.) Cells incubated in 0.5% HS and 0.85% Saline (Vehicle). D.) Cells incubated in 0.5% HS and 25ng/ml NGF. E.) Cells incubated in 0.5% HS and 50ng/ml NGF. F.) Cells incubated in 0.5% HS and 100ng/ml NGF. Media was replaced every 48 hours. Increased neurite outgrowth was observed in all NGF treatments (D-F) but not with 0.85% saline (C). White arrows indicate representative long neurite outgrowth.

0.1% HS media differentiation

By 48 hours of 0.1% HS incubation, cells started to detach from the collagen coating into suspension. After 96 hours of incubation, cell viability of cells incubated with 0.1% HS reduced-serum media (0.1% HS) was 92% less (153.6% Vs 0 Hrs, $p=0.04$) than that of RPMI complete media (235% Vs 0 Hrs). At 144 hours the viability of cells grown in 0.1% HS was 173.4% compared to 0 Hrs, but 95% less than the RPMI complete group (269% Vs 0 Hrs, $p<0.0001$) (Figure 63.A). With regards to NGF treatment, no significant difference in viability was seen in vehicle only treatments across all time point Figure 63.B). By 96 hours of NGF treatment, when compared to 0.1% HS alone (156% Vs 0 hrs), 25ng/ml NGF treatment (132% Vs 0hrs) was 24% less viable ($p=0.008$), 50ng/ml NGF (136.5% Vs 0 hrs) was 19.5% less viable ($p=0.047$) and 100ng/ml NGF (126.7% Vs 0 hrs) was 29% less viable ($p=0.0005$). By 144 hours of NGF treatment, viability levels significantly reduced further in all NGF treatments 25ng/ml, 94.9% Vs 0 hrs, $p<0.0001$; 50ng/ml 96.1% Vs 0 hrs, $p<0.0001$; 100ng/ml Vs 0 hrs, 102.1%, $p<0.002$) compared to 0.1% HS alone (133.7% Vs 0 hrs). Morphologically, as shown in Figure 64, after 144hours of NGF treatment, few neurite outgrowths were observed across all NGF treatments.

After 144hours of treatment with GbE, no differences in viability were observed between 0.1% HS media alone and 50 $\mu\text{g}/\text{ml}$ GbE (127.8% Vs 0 Hrs, $p=0.81$) and 100 $\mu\text{g}/\text{ml}$ GbE (127% Vs 0 Hrs, $p=0.73$) Morphologically, like that of 1% HS and 0.5% HS, cells appeared rounded without neurite outgrowths (not shown), comparable to that of 0.5% HS.

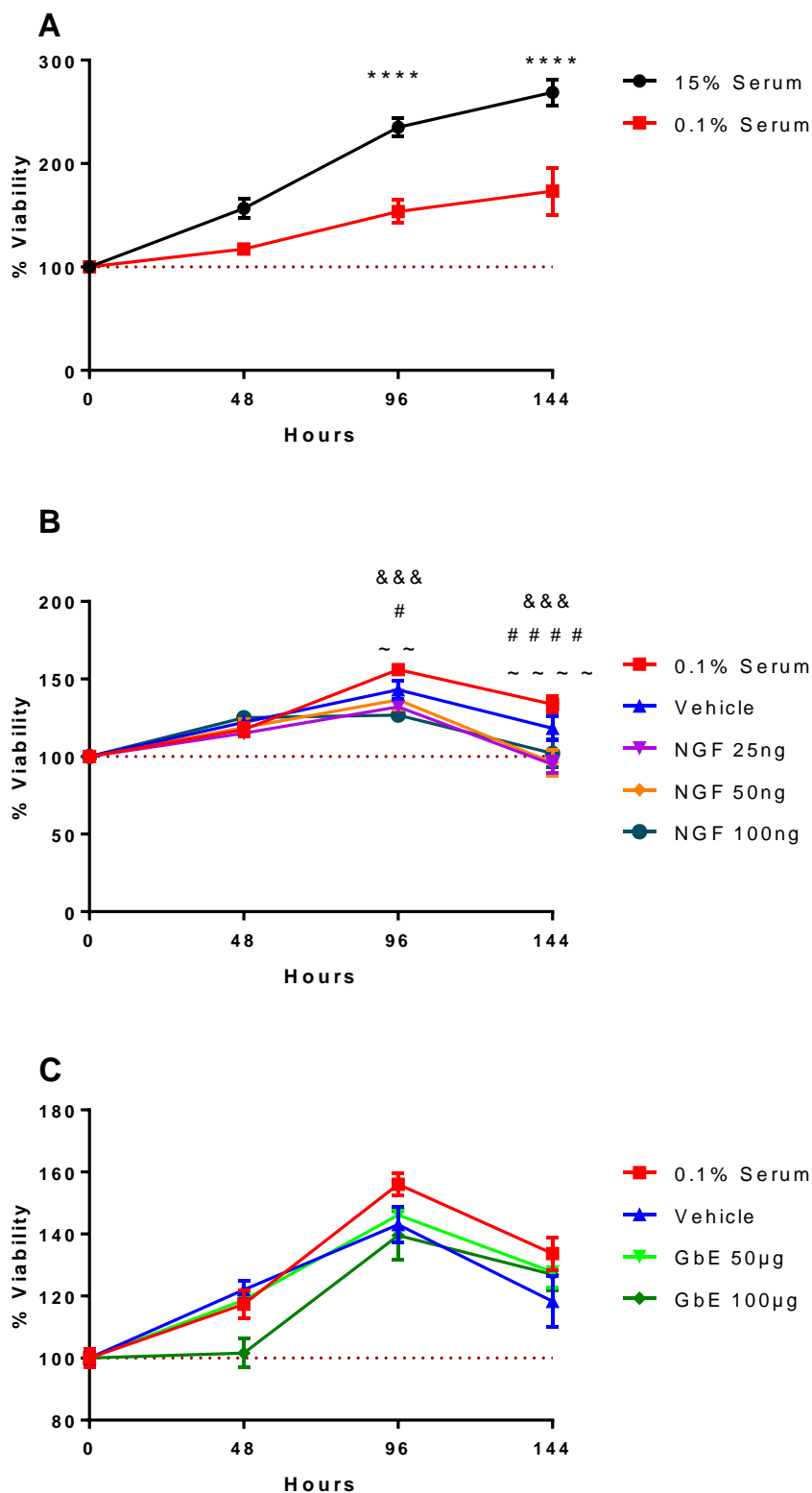
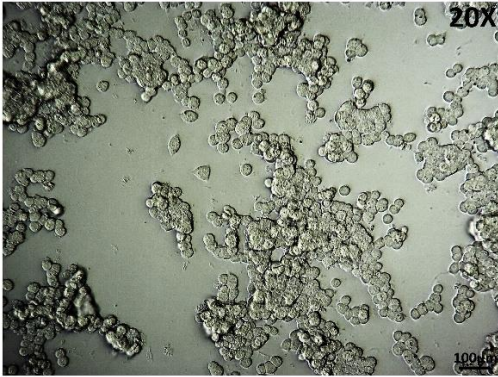


Figure 63. Viability (%) of PC12 cells after six days incubation with 0.1% horse serum (0.1% HS) media. A). 15% complete serum media (10% horse serum+ 5% foetal bovine serum) Vs 0.1% HS. B). 1% HS media Vs Vehicle (0.085% saline) and nerve growth factor 2.5s (NGF 25,50 and 100ng/ml) C. 0.1% HS Vs Ginkgo biloba (GbE, 50 and 100ug/ml). * $p < 0.05$, ** $p < 0.01$, *** $p < 0.001$, **** $p < 0.0001$ vs 1% serum. ~ p =Vs 25ng/ml NGF, # p = Vs NGF 50ng/ml, &p= Vs NGF 100ng/ml vs 0.1% serum. Data presented as mean \pm SEM. Data analysed by Two-way ANOVA with Šídák (A.) or Tukey (B. and C.) post hoc test).

A. 15% Complete media



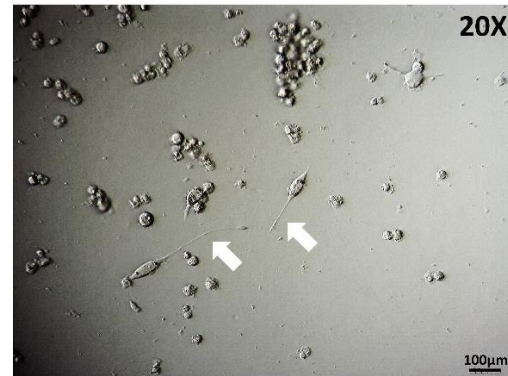
B. 0.1% Horse Serum (HS)



C. 0.1% HS + Vehicle



D. 0.1% HS + NGF 25ng



E. 0.1% HS + NGF 50ng



F. 0.1% HS + NGF 100ng

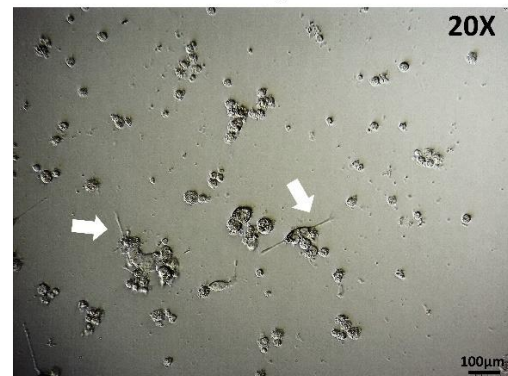


Figure 64. Microphotographs of PC12 cell differentiation with RPMI media supplemented with 0.1% horse serum (0.1% HS) and nerve growth factor (NGF) for 7 days. A.) PC12 cells incubated in complete media (RPMI + 15% serum. B.) Cells incubated in 0.1% HS. C.) Cells incubated in 0.1% HS and 0.85% Saline (Vehicle). D.) Cells incubated in 0.1% HS and 25ng/ml NGF. E.) Cells incubated in 0.1% HS and 50ng/ml NGF. F.) Cells incubated in 0.1% HS and 100ng/ml NGF. Media was replaced every 48 hours. Increased neurite outgrowth was observed in all NGF treatments (D-F) but not with 0.85% saline (C). White arrows indicate representative long neurite outgrowth.